Boron-Mediated Lignocellulose Degradation. Design, Synthesis, Properties, and
Applications of Boron-Containing Naphthoids

by

Mohd Zain Haider Kazmi

A thesis submitted in partial fulfillment of the requirements for the degree of

Doctor of Philosophy

Department of Chemistry
University of Alberta

Abstract

Lewis acidity is a molecule's tendency to accept a pair of electrons. Trivalent boron compounds are archetypical Lewis acids due to the presence of a vacant p orbital, leading to many uses in organic synthesis. For example, boron trihalides use their intrinsic Lewis acidity to accept ether oxygen electrons, facilitating ether cleavage reactions. On the other hand, organoboron compounds are commonly used in catalysis, such as in the Corey-Bakshi-Shibata reduction method. An interesting class of organoboron compounds that have recently gained prominence in the field of medicinal chemistry is boron-containing heterocycles. They are used in a number of fascinating applications and, in particular, have appeared in several FDA approved drugs. Despite the significance of boron-containing compounds, many aspects of their physicochemical properties, reactivity, and potential applications remain underexplored.

Lignocellulose is a plant biomass formed by ether and acetal linkages of phenolic and sugar monomers. Chapter 2 of this thesis describes the use of a mild method that utilizes mixed boron trihalides for processing lignocellulose into cellulose and lignin components. Such materials may offer a route to sustainable chemical production, alleviating the need for non-renewable petroleum-based feedstocks. The applicability of this method was demonstrated with a sample of white pine sawdust, followed by spectroscopic analyses and dye-staining methods.

Boron-containing heterocycles are an important motif in material science and drug discovery. As such, a comprehensive understanding of their properties is needed to enable new applications. The acidic nature of certain hemiboronic acids, such as

boron-containing naphthoids, has been a point of argument for a long time, and there has been no definite evidence regarding their aromatic character. Chapter 3 addresses these questions, along with other characteristics of boron-containing naphthoids, such as their stability and their boranol (B—OH) exchange with alcohols. Overall, this study clarifies a large body of conflicting results reported in the literature over several decades and provides important conclusions for the systematic applications of boron-containing naphthoids in the areas of catalysis and medicinal chemistry.

Chapter 4 further examines the physical properties of boron-containing naphthoids and their suitability as drug scaffolds. Moreover, new and chemoselective synthetic strategies and purification procedures are described. Small prototypical compound libraries for different boron-containing naphthoid scaffolds were produced. Many such compounds are drug bioisosteres and were subsequently evaluated in biological activity assays.

Preface

Chapter 2 (omitting Section 2.4) of this thesis was published as Kazmi, M. Z. H.; Karmakar, A.; Michaelis, V. K.; Williams, F. J. "Separation of Cellulose/Hemicellulose from Lignin in White Pine Sawdust Using Boron Trihalide Reagents" *Tetrahedron* **2019**, *75*, 1465–1470. I was responsible for the reaction optimization, data collection, analysis, and writing of the supporting information. As specified in Chapter 2, A. Karmakar, a graduate student from the Michaelis Group, performed the solid state ^{1}H NMR spectroscopy. The publication manuscript was written by F. J. Williams. F. J. Williams was the supervisory author and conceived the project. This chapter is a significantly expanded and redacted version of the manuscript. Section 2.4 corresponds to the work accomplished by me after the paper submission.

Chapter 3 (omitting Section 3.5.1) of this thesis was published as Kazmi, M. Z. H.; Rygus, J. P. G.; Ang, H. T.; Paladino, M.; Johnson, M. A.; Ferguson, M. J.; Hall, D. G. "Lewis or Brønsted? A Rectification of the Acidic and Aromatic Nature of Boranol-Containing Naphthoid Heterocycles" *J. Am. Chem. Soc.* **2021**, *143*, 10143–10156. I was responsible for the synthesis of some of the compounds relevant to Chapter 3, $H_2^{18}O$ labelling, crossover experiments in acetonitrile/water, pK_a determination by ^{11}B NMR and UV spectroscopy, data collection, and analysis. Contributions from J. P. G. Rygus, H. T. Ang, M. Paladino, M. A. Johnson, and D. G. Hall are specified in Chapter 3. M. J. Ferguson performed the X-ray crystallographic analyses on all the obtained crystals. The publication manuscript was written by D. G. Hall and some parts were written by J. P. G. Rygus. J. P. G. Rygus and I wrote the supporting information. D. G. Hall was the supervisory author and conceived the project. This chapter is a significantly expanded and redacted version of the manuscript. Section 3.5.1 describes the work on $H_2^{18}O$ labelling, that was not published.

For Chapter 4, I was responsible for the optimization of reactions and functionalization of products. I was also responsible for the development of the substrate scope, data

collection, and analysis. M. Paladino (postdoctoral researcher) and S. Li (undergraduate student) performed one preliminary reaction each, which is specified in Chapter 4. O. Schneider (labmate) and BPS Bioscience performed the biological assays, all of which are mentioned in Chapter 4. This work was performed under the supervision of D. G. Hall, who also conceived the project.

Dedicated to my beloved papa

Acknowledgements

I would like to express my deepest appreciation to everyone who contributed in some way to my PhD degree. Firstly, I am grateful to my supervisors, Dr. Dennis Hall and Dr. Florence Williams, from whom I received guidance, motivation, and knowledge. I always will remember the Monday report meetings and how they helped me grow as a chemist, as well as group meetings, which were intellectually stimulating and added to a rewarding graduate school experience. A special thanks is extended to both supervisors as well as Dr. Anna Jordan, for their help editing this thesis. I also would like to thank my committee members Dr. Rik Tykwinski and Dr. John Vederas for offering advice during my degree.

The work in this thesis would not have been possible without the service staff in the NMR, mass spectrometry, and analytical facilities. I especially would like to thank Mark Miskolzie for his help and enjoyable idiosyncratic conversations, Béla Reiz and Jing Zheng for their continued support and patience in answering all my questions, and Angie Morales for performing HRMS analyses on an almost daily basis during my thesis preparation.

I am grateful to have had such great co-workers in the Hall and Williams Groups. Many thanks to Andreas Dorian, who always made me laugh with his ridiculous sense of humor, friendship, and extraordinary support from the time I first arrived at the university, as well as for his help with editing this thesis. I also thank Khyati Gohil for being a great project partner and her kind humble nature. Thanks to Jake Blackner for reviewing one chapter of this thesis. I have had the pleasure of working with exceptional chemists, Jason Rygus, Dr. Hwee Ting Ang, and Dr. Marco Paladino, as well as Olivia Schneider, who was patient of my ignorance of biochemistry. Without their contributions, this work would not have been possible. It was a delight to work alongside lab mates Olivia Schneider, Martin Lessard, and Dawson Konowalchuk, who put up with my choice of music. The bizarre sense of

humor and peculiar giggles bestowed by Dr. Mohamad Estaitie (Momo) also made the lab an enjoyable place to be.

Beyond the lab, I enjoyed many evenings playing board games with Marco and Momo, biking in the river valley with Martin, and back packing in the mountains with Andreas and Sascha. I also would like to acknowledge various other people that I met in Edmonton and who have supported me throughout this journey. I have had great times with my dear friend, Simon Wu, playing badminton, making sushi, and partying. He was always there when I needed him. These friends have made my stay in Edmonton exhilarating and created memories I will cherish forever.

I would like to extend my deepest gratitude to my partner, Marissa MacIsaac. Her loving and caring nature and encouraging words kept me sane through my studies. I especially would like to recognize my immediate family members, my mom, Taiyaba Kazmi, my dad, Shakir Hussain, and my brother, Auon Kazmi. I would not be here without the sacrifices made by my parents and the support of my brother.

Table of Contents

List of Tables

List of Figures

List of Schemes

List of Abbreviations

Å	angstrom
AAT	Animal African Trypanosomiasis
Ac	acetyl
AcOH	acetic aid
ADP	adenosine diphoshphate
AIBN	azobisisobutyronitrile
AMP	adenosine monophosphate
app	apparent
aq.	aqueous
Ar	aryl
ARS	Alizarin Red S
BCP	bicyclo[1.1.1]pentane
Boc	*tert*-butyloxycarbonyl
br	broad
calcd.	calculated
CBS	Corey-Bakshi-Shibata
CDMT	2-chloro-4,6-dimethoxy-1,3,5-triazine
cm^{-1}	wavenumbers
DABCO	1,4-diazabicyclo[2.2.2]octane
DAPI	4′,6-diamidino-2-phenylindole
DART	direct analysis in real time
DCM	dichloromethane
dd	doublet of doublets
ddd	doublet of doublet of doublets
DDQ	2,3-dichloro-5,6-dicyano-1,4-benzoquinone
DEAM-PS	*N,N*-diethanolaminomethyl-polystyrene
DFT	Density Functional Theory
DHB	dihydroxybenzoic acid

DI	deionized
DIC	differential interference contrast
DIPEA	*N,N*-diisopropylethylamine
DMAP	4-dimethylaminopyridine
DMF	*N,N*-dimethylformamide
DMSO	dimethyl sulfoxide
DNA	deoxyribonucleic acid
dppf	1,1′-ferrocenediyl-bis(diphenylphosphine)
dt	doublet of triplets
ECN	effective carbon number
EDG	electron donating group
EI	electron impact
EML	Essential Medicines List
equiv	equivalent
ESI	electrospray ionization
ESKAPE	Enterococcus faecium, Staphylococcus aureus, Klebsiella pneumoniae, Acinetobacter baumannii, Pseudomonas aeruginosa, and Enterobacter species
Et	ethyl
Et$_2$O	diethyl ether
EtOAc	ethyl acetate
EtOH	ethanol
EWG	electron withdrawing group
FDA	Food and Drug Administration
FID	flame ionization detection
FT-IR	Fourier Transform Infrared Spectroscopy
g	gram
G	gauge
GC	gas chromatography
Glu	glutamine

Gly	glycine
h	hour
HATU	hexafluorophosphate azabenzotriazole tetramethyl uronium
His	histidine
HNE	human neutrophil elastase
HOMO	highest occupied molecular orbital
HPLC	High Performance Liquid Chromatography
HRMS	High Resolution Mass Spectrometry
IC_{50}	half maximal inhibitory concentration
*i*Pr	isopropyl
K_a	acid dissociation constant
kcal	kilocalorie
kDa	kilodaltons
LC-MS	Liquid Chromatography-Mass Spectrometry
LIFDI	liquid injection field desorption ionization
LUMO	lowest unoccupied molecular orbital
Lys	lysine
M	molarity
m	meter
m/z	mass to ion ratio
MALDI	matrix assisted laser desorption ionization
Me	methyl
MeCN	acetonitrile
MeOH	methanol
mg	milligram
MHz	megahertz
MIC	minimum inhibitory concentration
min	minute
mL	milliliter
mm	millimeter

mmol	millimole
mp	melting point
MRSA	methicillin-resistant *S. aureus*
MS	mass spectrometry
ms	millisecond
MTAP	*S*-methyl-5'-thioadenosine phosphorylase
n-Bu	normal butyl
N/A	not applicable
NAD	nicotinamide adenine dinucleotide
NBS	*N*-bromosuccinimide
NICS	Nucleus Independent Chemical Shift
nM	nanomolar
nm	nanometer
NMM	*N*-methylmorpholine
NMP	*N*-methyl-2-pyrrolidone
NMR	Nuclear Magnetic Resonance
ORTEP	Oak Ridge thermal ellipsoid plot
PARP	poly ADP-ribose polymerase
PDE4	phosphodiesterase-4
Ph	phenyl
Phe	phenylalanine
pIC_{50}	negative log of the IC_{50} value when converted to molar
pin	pinacol
PMA	phosphomolybdic acid
ppm	parts per million
psi	pound per square inch
q	quartet
quant.	quantitative
RCM	ring-closing metathesis
rpm	revolutions per minute

rt	room temperature
R_t	retention time
s	singlet
SAR	structure-activity relationship
Ser	serine
S_nAr	nucleophilic aromatic substitution
t	triplet
TAPPI	Technical Association of the Pulp and Paper Industry
TBAB	tetrabutylammonium bromide
*t*Bu	*tert*-butyl
td	triplet of doublets
Tf_2O	trifluoromethanesulfonic anhydride
TFA	trifluoroacetic acid
THF	tetrahydrofuran
TMAH	tetramethylammonium hydroxide
Trp	tryptophan
Tyr	tyrosine
UV	ultraviolet
wt.	weight
xantphos	4,5-bis(diphenylphosphino)-9,9-dimethylxanthene
XPhos	2-dicyclohexylphosphino-2′,4′,6′-triisopropylbiphenyl
XPhos-Pd-G2	chloro(2-dicyclohexylphosphino-2′,4′,6′-triisopropyl-1,1′-biphenyl)[2-(2′- amino-1,1′-biphenyl)]palladium(II)
ZOI	zone of inhibition
λ	wavelength
μ	micro
μg	microgram
μL	microliter
μM	micromolar
μm	micrometer

Chapter 1: Introduction

1.1 Lewis Acidity of Boron-Containing Compounds

Lewis acidity is defined as the ability of a molecule to accept a pair of electrons in its vacant orbital. Boron trihalides are privileged reagents, with intrinsic Lewis acidity arising due to the presence of a vacant p orbital. Their acidity increases with substitution of heavier halides as follows: $BF_3 < BCl_3 < BBr_3 < BI_3$.

Various explanations have been proposed to account for this order of Lewis acidity, such as back-bonding involving the halogen's lone pair of electrons and the boron atom's empty 2p orbital.[1] This theory of back-bonding supports the acidity order; for example, more overlap is expected between F and B (2p–2p) as compared to Cl and B (3p–2p). However, this back-bonding argument has been contradicted on the basis of the calculated overlap integral, in which BCl_3 was found to have the largest overlap (0.220), whereas BF_3 had the smallest overlap (0.187).[2] Instead, complexation energies between boron trihalides and a Lewis base ammonia give a better indication of the observed Lewis acidity trend (formation of $Cl_3B \cdot NH_3$ is favored by 4.7 kcal/mol over $F_3B \cdot NH_3$).[2] This property also is supported by the ^{1}H NMR experiments for the complex between trimethyl amine and boron trihalides, where the methyl shift increases in the order of $F_3B \cdot NMe_3 < Cl_3B \cdot NMe_3 < Br_3B \cdot NMe_3$.[3] Later, Frenking and co-workers also showed that $Cl_3B \cdot NH_3$ gives a larger bond dissociation energy (32.9 kcal/mol) as compared to $F_3B \cdot NH_3$ (24.3 kcal/mol) due to the lower energy LUMO in BCl_3.[4] Recently, Hamlin and co-workers investigated the bonding mechanism between boron trihalides and ammonia. The authors concluded that the mechanism depends on pyramidalization energy of the boron trihalide upon formation of a Lewis acid-base adducts.[5] The strain energy required for the pyramidalization is directly correlated with the bond strength (and thus electronegativity) of the attached halogens. Since, the B—I bond is weaker than the B—F bond, distortion of BI_3 from a planar to a pyramidal geometry upon Lewis base complexation is less energy demanding than the same distortion experienced by BF_3. This distortion energy postulate is considered the most accurate for explaining the observed Lewis acidity trend.

Boron trihalides have found use in an array of applications, such as BF_3 catalysis of Friedel-Crafts reactions, or the use of BBr_3 as a standard reagent for ether cleavage.[6,7] Upon combining different boron trihalides, halogen-exchange occurs, resulting in a mixture of boron species containing mixed halides (heteroleptic species).[8,9] This phenomenon has been applied for achieving a reliable regioselectivity in ether cleavage within the Williams Group.[10] The utility of such boron trihalide combinational dynamics is described in Chapter 2 for the separation of cellulose and lignin from lignocellulose (a plant biomass consisting of a variety of ether/acetal linkages).

The Lewis acidity of a boron-containing molecule can be determined by several methods, such as the Gutmann-Beckett method and the Child's method. The Gutmann-Beckett method relies on the observation of a change in the ^{31}P NMR chemical shift of triethylphosphine oxide upon coordination with the Lewis acid.[11,12] The oxygen atom of triethylphosphine oxide acts as a Lewis base, interacting with a Lewis acidic boron, resulting in deshielding of the phosphorus atom. Thus, the magnitude of the downfield chemical shift corresponds to the strength of the Lewis acid (Figure 1.1a). On the other hand, Child's method relies on the ^1H NMR downfield chemical shift observed upon Lewis acid coordination to crotonaldehyde (Figure 1.1b).[13]
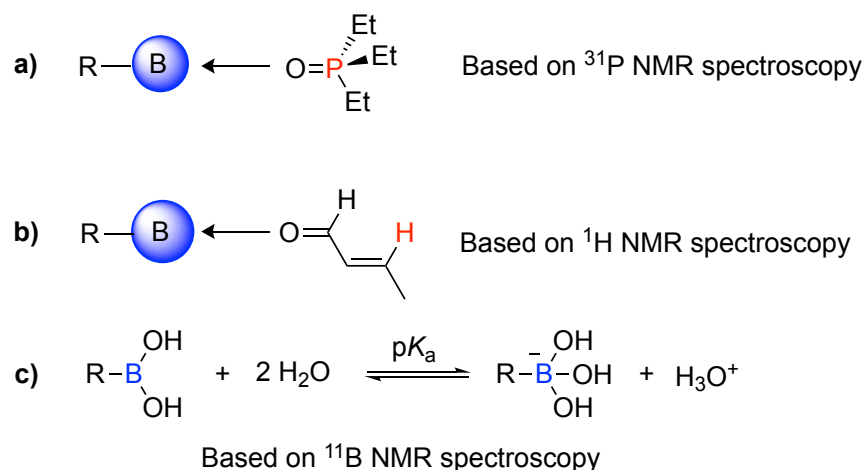
Figure 1.1. Determination of Lewis acidity by **a)** Gutmann-Beckett method, **b)** Child's method, and **c)** ^{11}B NMR spectrometry method.

Similar to boron trihalides, boronic acids, such as phenylboronic acid, are also Lewis acids. Their boranol unit (B—OH) forms a tetravalent trihydroxyborate conjugate base in a high pH environment. ^{11}B NMR spectroscopy also can give an indication of the Lewis acidity of boron-containing compounds, and can be used in the determination of their pK_a (Figure 1.1c).[14–16] Generally, a boron-containing molecule shows an upfield [11]B chemical shift (0–5 ppm) in the presence of a Lewis base, exhibiting Lewis acidity through formation of a tetrahedral boron center. The higher the pH required to achieve the tetracoordinate species (when equilibrium favors the right side), the lower the Lewis acidity of that molecule.

1.2 Applications of Boron-Containing Compounds

1.2.1 Therapeutic Potential of Boronic Acids

Taking advantage of their Lewis acidic property, boronic acids have found use in the recognition of saccharides.[17] Saccharides containing *cis*-1,2-diols or *cis*-1,3-diols can bind to a boronic acid, resulting in the formation of a five or a six membered cyclic boronate, respectively. There is a geometrical preference for *cis*-diols, as it minimizes the angle strain incurred during the boronic ester formation.[18] Since the binding of the boronic acid relies on the correct configuration of the diols, phenylboronic acid also has found use in bioconjugation chemistry.[19,20] Such interactions are measured by a method called the Alizarin Red S (ARS) displacement assay, which qualitatively assess the binding of boronic acids with sugars (see Chapter 4 for more information on the ARS displacement assay and its applications).[15,21–23]

Despite the fascinating properties of boronic acids, their use in drug discovery was rare until 2003, when the Food and Drug Administration (FDA) approved the first ever peptidomimetic boronic acid drug, bortezomib, for the treatment of multiple myeloma (Figure 1.2).[24,25] Following that, another peptidomimetic, ixazomib citrate (prodrug of ixazomib), received FDA approval in 2015.[26]
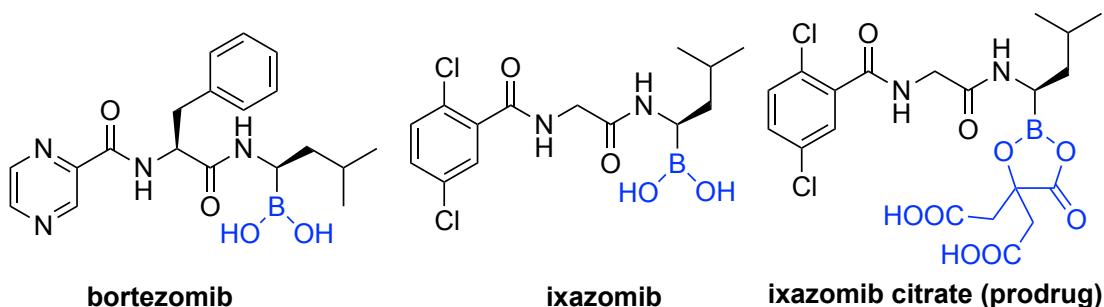
Figure 1.2. Boronic acid containing FDA approved drugs.

1.2.2 Therapeutic Potential of Cyclic Hemiboronic acids

As exemplified by benzoxaborole, hemiboronic acids have one less boranol unit compared to boronic acids (Figure 1.3). In a manner analogous to boronic acids, benzoxaborole is also a Lewis acid, and it has a strong preference to exist in its cyclic form under aqueous conditions.[27] However, the pK_a of benzoxaborole (7.4) is lower than that of phenylboronic acid (8.8).[15] The lower value for benzoxaborole is due to the angle strain arising from the presence of three sp^2 atoms (i.e., boron and two carbons) in the 5-membered cycle.[28] Upon coordination of a base, the strain is partially released, as the boron atom forms a tetrahedral boronate complex with a favorable sp^3 hybridization. Owing to these important characteristics, benzoxaboroles show exceptional properties as compared to the corresponding arylboronic acids, such as improved saccharide binding abilities. For example, at neutral pH, the association constant (K_a) for fructose binding is significantly higher for benzoxaborole (K_a = 606 M^{-1}) than for phenylboronic acid (K_a = 79 M^{-1}).[15]
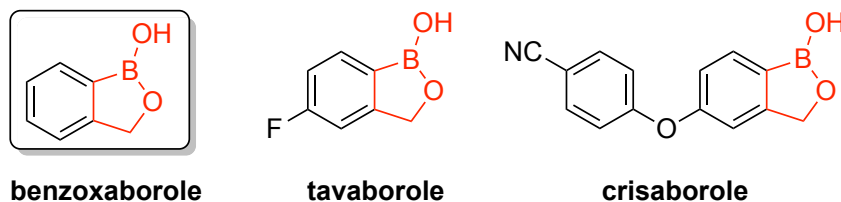
Figure 1.3. Benzoxaborole and benzoxaborole based FDA approved drugs.

A 5-fluoro substituted derivative of benzoxaborole, tavaborole, was established to be an antifungal drug in 2006, and has been employed to treat onychomycosis (Figure 1.3).[29] Another benzoxaborole derivative, crisaborole, was approved by the

FDA for the treatment of atopic dermatitis (Figure 1.3).[30] The mechanisms of action of these benzoxaborole-based drugs demonstrates that the boron center interacts with the respective receptors to form a tetracoordinate sp[3] hybridized boron species.[29,31] This tetrahedral hybridization illustrates the importance of the Lewis acidic character of benzoxaborole, which makes it a versatile chemotype in drug discovery. Indeed, several other benzoxaborole derivatives have been reported to have anti-infective properties and are in different phases of clinical trials (Figure 1.4).[32,33]

AN2718
(antifungal)

AN2898
(PDE4 inhibitor)

SCYX-7158, acoziborole
(African trypanosomiasis)

GSK3036656
(tuberculosis)

AN3661
(antimalarial)

GSK2878175
(chronic hepatitis C)
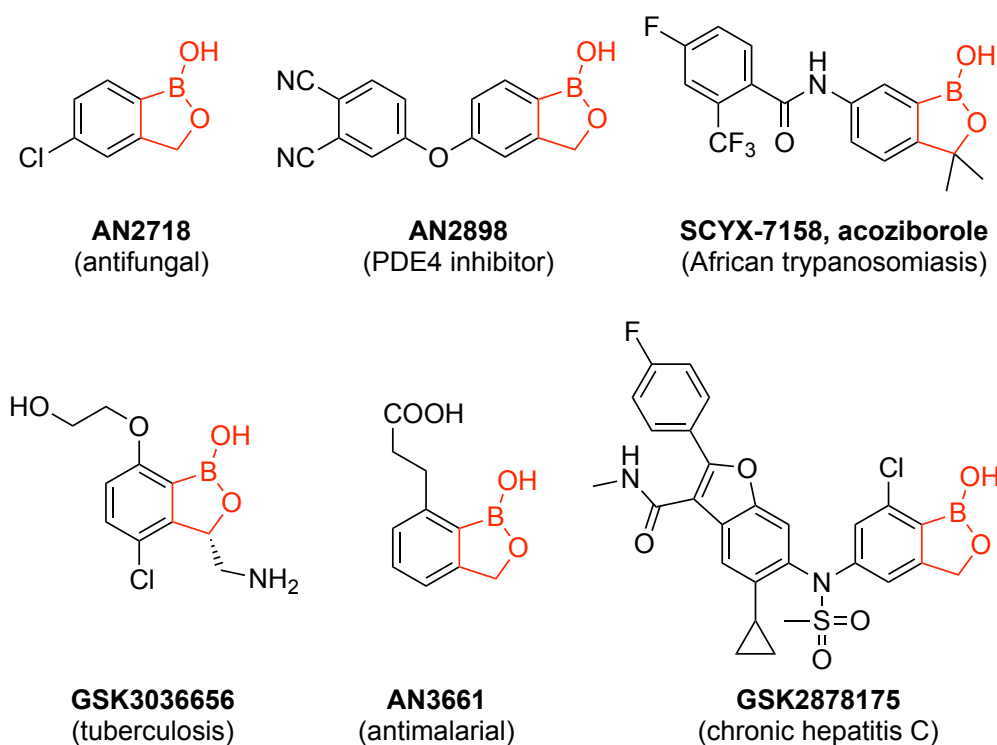
Figure 1.4. Examples of the benzoxaborole based compounds in clinical trials.

1.3 Bioisosteres and their Properties

In 1919, Langmuir proposed the concept of isosterism, which was based on the electronic configuration of a group of atoms.[34] For example, Langmuir suggested that the physical properties of nitrous oxide and carbon dioxide are quite similar since they possess the same number and arrangement of electrons. Such a pair of compounds was termed isosteric compounds or isosteres. In 1951, Friedman coined the term "bioisostere" for those isosteric compounds that exhibited similar biological activity.[35]

Later in 1991, Burger enounced a broader definition for bioisosteres, "compounds or groups that possess near-equal molecular shapes and volumes, approximately the same distribution of electrons, and which exhibit similar physical properties such as hydrophobicity. Bioisosteric compounds affect the same biochemically associated systems as agonist or antagonists and thereby produce biological properties that are related to each other".[36]

Identification of bioisosteres can lead to the development of new classes of bioactive compounds. These functional groups could influence the properties of the parent drug in terms of solubility, lipophilicity, pK_a, aromaticity, and covalent/non-covalent interactions, potentially improving drug efficacy. Classical bioisosteres are synthesized by the replacement of simple intuitive functional groups, such as the substitution of F for H in a biologically active molecule (Table 1.1).[37] On the other hand, non-classical bioisosteres are less intuitive and usually mimic the spatial arrangements or electronic properties of the functional group in the parent molecule, for example, a replacement of esters and amides with 1,2,4-oxadiazoles (Table 1.1).[37]

Table 1.1. Types of Bioisosteres

Bioisostere type	Functional group/atom	Replacement moiety
Classical	H	F
	OH	NH_2, SH
	C=C	C=N
Non-classical	OH	$MeSO_2NH$, pyrrole
	COOH	$CONHSO_2Ph$
	$COOR/CONH_2$	1,2,4-oxadiazole

Bioisosterism of rings is an increasingly popular strategy in drug discovery. For instance, the replacement of a fluoroaryl ring in **BMS-708,163** with a bicyclo[1.1.1]pentane (BCP) moiety resulted in molecule **1-1**, which displayed better aqueous solubility and passive permeability, in turn leading to better oral absorption characteristics (Figure 1.5a).[38] Similarly, Williams and co-workers demonstrated that

the replacement of a benzene motif with a cubane group resulted in molecules with increased or equal bioactivity.[39] For example, **1-3** exhibited improved pesticidal activity over the parent compound **1-2** (Figure 1.5b).
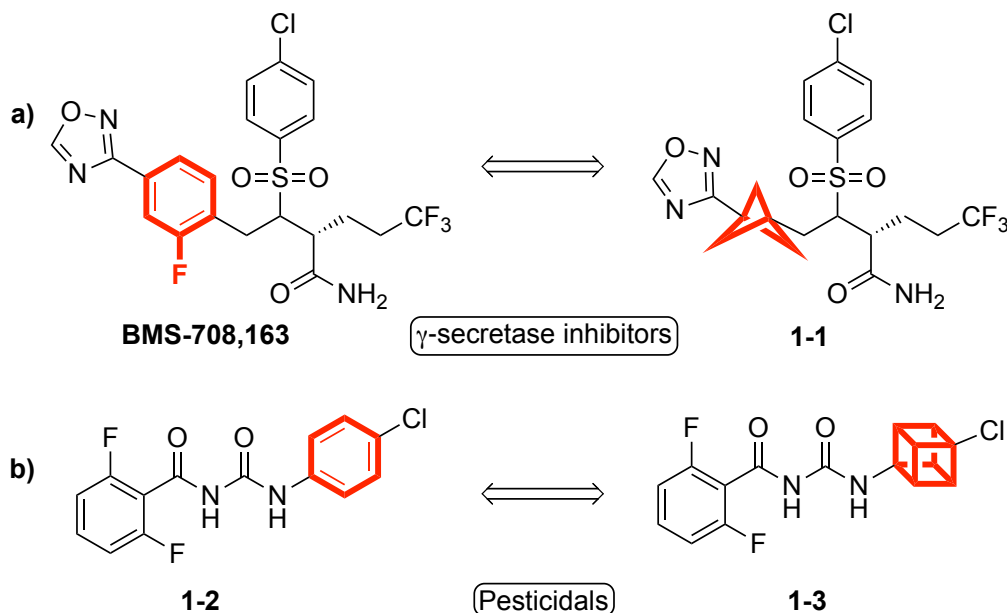
Figure 1.5. Isosteres obtained after replacement of an aryl group with **a)** BCP or **b)** cubane.

1.3.1 Azaborines as Bioisosteres

The isosteric substitution of a carbonaceous compound to generate a boron-containing compound can be viewed as the isosteric replacement of a C=C bond with a B—N/B—O bond, or a C=O bond to a B—OH bond. For example, azaborines are one of the most common isosteres of benzene, which are formed by the replacement of a C=C bond with a B—N bond. Azaborines are stable and pseudoaromatic compounds.[40] In a recent study, it was found that azaborine **1-5** is recognized by the aryl binding pocket of a T4 lysozyme in the same way as the all-carbon analog **1-4**, demonstrating the utility of azaborines as excellent arene mimics in a biological setting (Figure 1.6a).[41] In another publication, the authors showed that the additional nitrogen atom in 1,2-azaborine can provide additional interactions, such as H-bonding.[42] In a study with **propranolol** (a β-blocker drug), the bioisosteric replacement of a naphthalene ring with a benzazaborinine scaffold resulted in molecule **1-6**, which exhibited a similar inhibitory potency to the parent drug (Figure 1.6b).[43] Finally, Liu and co-workers presented a

comprehensive study on azaborines, where they explored the air and aqueous stability, aqueous solubility, and bioactivity of an azaborine isostere **1-8** and compared it with the carbonaceous analog **1-7** (Figure 1.6c).[44] The azaborine isostere **1-8** showed excellent air and water stability, even at 50 °C for 24 h. Due to the presence of polar functional groups (B and N), together with the ability of the N—H to undergo H-bonding, isostere **1-8** revealed better aqueous solubility, demonstrating the value of bioisosterism toward producing more soluble drugs.[45] The CDK2 inhibitor potency was also improved for isostere **1-8** (IC_{50} = 87 nM) compared to **1-7** (IC_{50} = 320 nM), which can be attributed to the additional H-bonding exhibited by the NH group (Figure 1.7).[44]
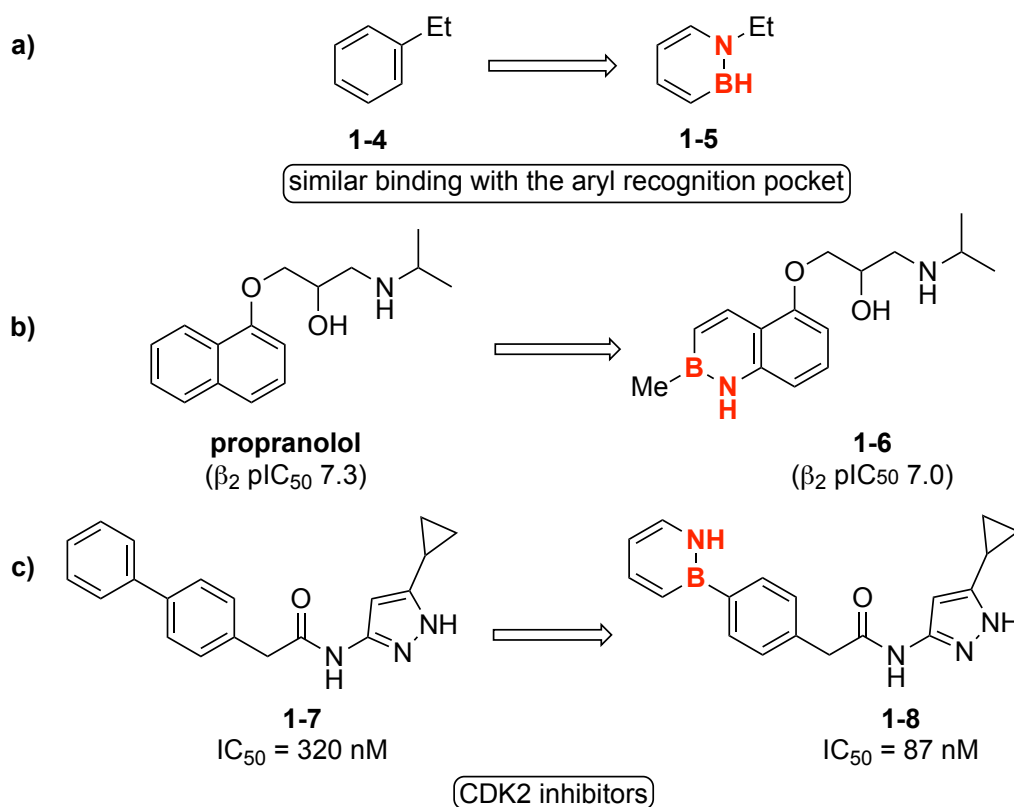
Figure 1.6. Azaborines as isosteres of arenes.
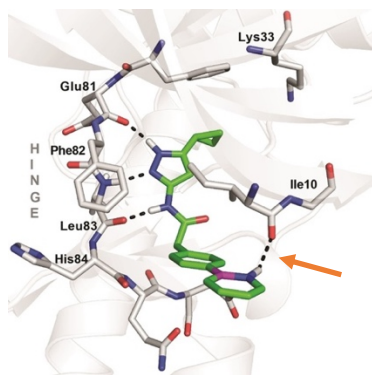
Figure 1.7. Binding mode of **1-8** in the ATP binding site of CDK2 featuring a new H-bonding interaction highlighted with the orange arrow (reused with permission from John Wiley and Sons).

1.3.2 Hemiboronic Acids as Isosteres

Benzoxazaborine (**1-9**) and benzodiazaborine derivatives (**1-10a–d**) are classes of hemiboronic acids (Figure 1.8). Just like azaborine, which is an isostere of benzene, benzoxazaborine and benzodiazaborine derivatives are isosteric and isoelectronic with 4-hydroxyisoquinoline and 1-hydroxynaphthalene. The boron heterocycle **1-9**, a cyclic oxime derivative, was discovered by Snyder and co-workers in 1958, while the B—N containing heterocycle class (**1-10a–d**) was prepared first by Dewar and Dougherty in 1962 and 1964.[46,47]
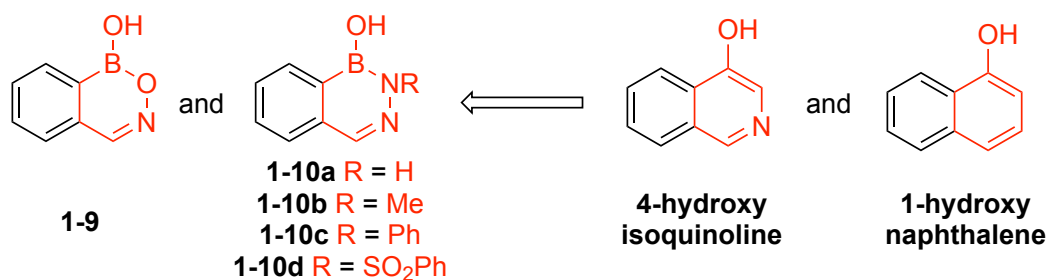
Figure 1.8. Isosteres of 4-hydroxyisoquinoline, benzoxazaborine **1-9** and benzodiazaborines **1-10**.

1.4 Properties and Applications of Benzoxazaborine (1-9) and Benzodiazaborine Derivatives (1-10a–d)

As discussed earlier, a wealth of knowledge exists regarding the aromaticity, stability, and biological properties for azaborines and benzoxaborole. However, there has yet to be a comprehensive study on benzoxazaborine (**1-9**) and benzodiazaborine derivatives

(**1-10a–d**). A thorough understanding of the aforementioned properties is crucial because some of these compounds and their derivatives have shown great potential in the field of drug discovery.[48] For example, Högenauer and Woisetschläger demonstrated that **1-11** is a potent inhibitor of *E. coli* and *S. typhimurium* (Figure 1.9a).[49] Subsequently, Grassberger and co-workers synthesized a library of derivatives of **1-11**, observing excellent antibacterial properties in some cases.[50] Westcott and co-workers synthesized several benzodiazaborine derivatives and tested them for antifungal activity.[51] For example, Heterocycle **1-12** exhibited antifungal activity against four different fungi species with zone of inhibition (ZOI) in the range of 7–9 mm (Figure 1.9b).

a)

1-11
MIC = 1.25 μg/mL (*E. coli)*
MIC = 2.5 μg/mL (*S. typhimurium*)

Antibacterial activity

b)

1-12
ZOI = 7 mm (*A. niger*) at a dose of 25 μg/disk
ZOI = 7 mm (*A. flavus*) at a dose of 25 μg/disk
ZOI = 9 mm (*C. albicans*) at a dose of 25 μg/disk
ZOI = 9 mm (*S. cerevisiae*) at a dose of 25 μg/disk
*no MIC/IC50 values were reported

Antifungal activity
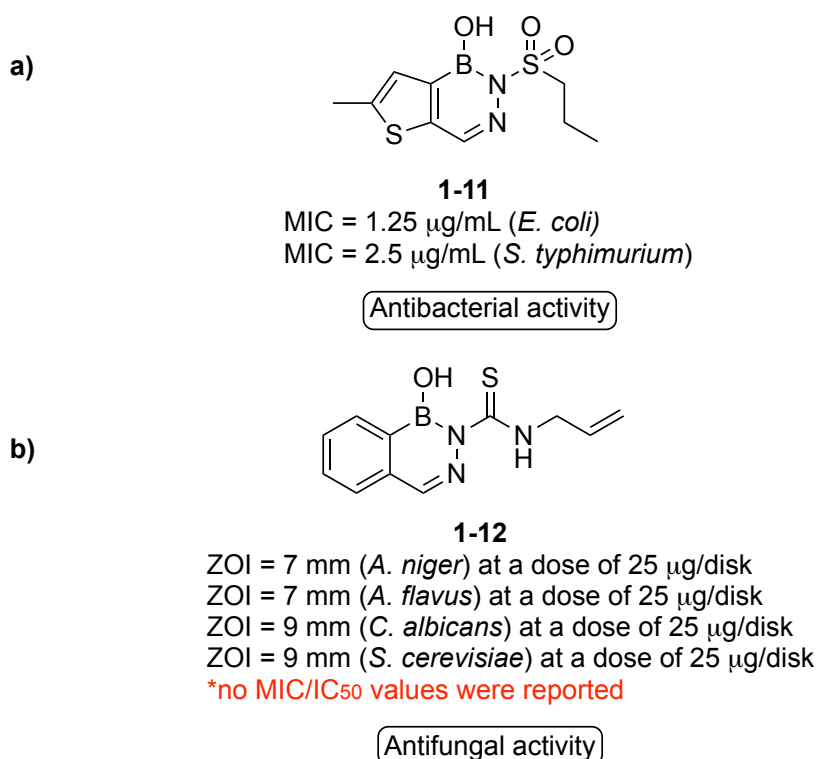
Figure 1.9. Benzo- and thiophene diazaborine derivatives as antimicrobial agents (**a** and **b**).

These benzo-/thiophene diazaborine derivatives inhibit the fatty acid synthesis by binding to the enoyl reductase enzyme through nicotinamide adenine dinucleotide (NAD$^+$).[52] For example, in the active site, the boron center of **1-11** binds covalently to the 2'-OH of the ribose in NAD$^+$, forming a tetrahedral species (sp^3) (Figure 1.10).
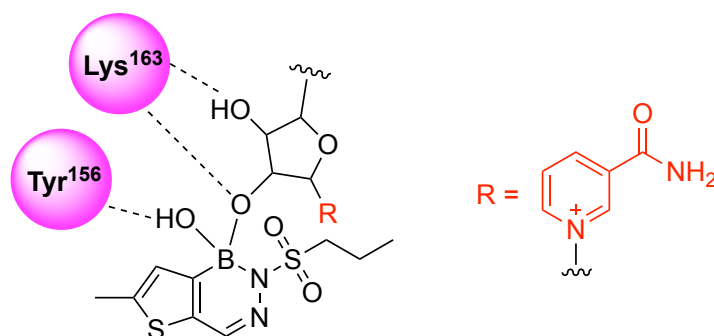
Figure 1.10. Mode of binding at the boron center for **1-11**.

Recently, Gois and co-workers showed that benzo- and thiophene diazaborine derivatives selectively inhibit human neutrophil elastase (HNE) serine proteases with IC$_{50}$ values in the low micromolar range (3.5 μM–12 μM).[53] For example, thiophene based *N*-sulphonyl diazaborine **1-13** exhibited the highest potency (Figure 1.11). Groziak and co-workers recently synthesized the first ever benzodiazaborine-based estrogen mimic **1-14** (Figure 1.11b).[54] Although the biological properties were not studied, compound **1-14** had similar physical properties to the mimicked compound equilenin, such as high planarity and a near identical O—O distance.
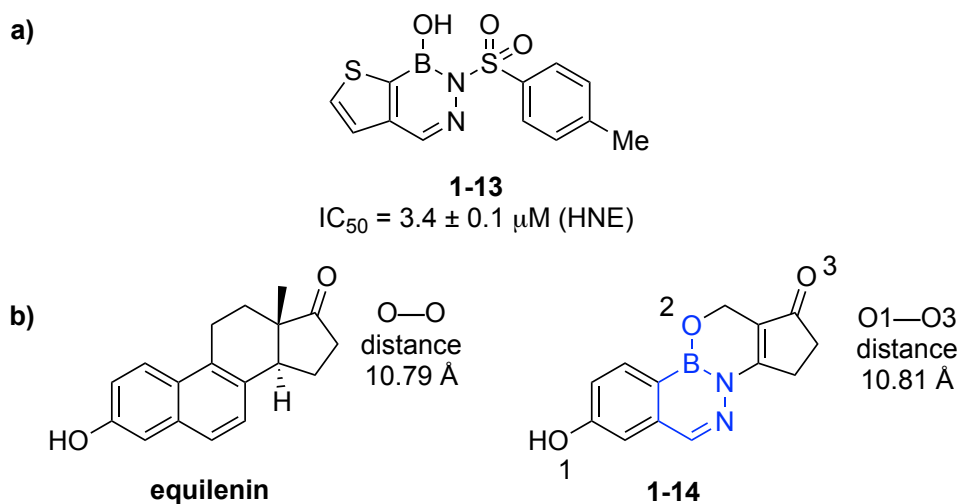
Figure 1.11. a) A thiophenediazaborine derivative **1-13** as an HNE inhibitor. **b)** A benzodiazaborine-based estrogen mimic.

The captivating applications of the above-mentioned heterocycles in the biological context warrants further examination of their properties, such as solubility,

stability, aromaticity, and acidity of the boron center. Although these molecules have been known for several decades (>50 years), their properties are the subject of some disagreement (see Section 3.2 of Chapter 3). A comprehensive study on the properties of the heterocycles **1-9** and **1-10a–d** is described in Chapter 3. This work addresses their acidic nature in solution-phase and solid-state systems. It also describes the aromatic character of these heterocycles, in comparison with their carbonaceous analog, 4-hydroxyisoquinoline, in an effort to reveal their isosteric and isoelectronic characteristics. Stability studies were also conducted, which are important to demonstrate the ability of these heterocycles to be applied in catalysis and medicinal chemistry.

1.5 Chemistry of Boron-Containing Heterocycles

1.5.1 Synthesis of Benzoxaboroles

The chemistry to synthesize benzoxaborole derivatives is well established, and yet is still growing due to their exceptional properties.[28,55] A plethora of benzoxaborole derivatives has been prepared, and can be categorized as utilizing either an early-stage or a late-stage synthetic approach (Figure 1.12).[56–59]
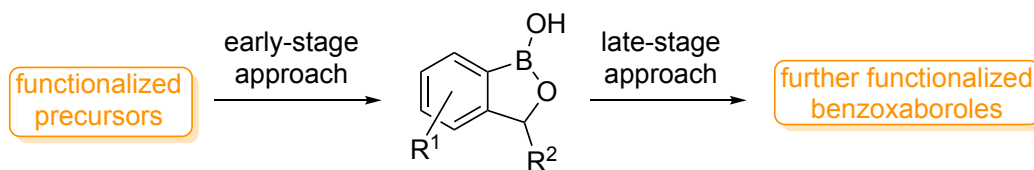
Figure 1.12. Synthetic approaches to obtain benzoxaborole derivatives.

Several derivatives of benzoxaborole have been synthesized from the *ortho*-substituted aryl bromides or from *ortho*-formyl arylboronic acids. For example, benzoxaborole derivatives **1-16** and **1-19** were synthesized from the corresponding *ortho*-carboxymethyl arylbromide (**1-15**) and *ortho*-methyl arylboronate (**1-18**), respectively (Scheme 1.1).[60,61] Similarly, a commercially available *ortho*-formyl arylboronic acid **1-20** underwent a Baylis-Hillman reaction to produce **1-21** (Scheme 1.2).[62]
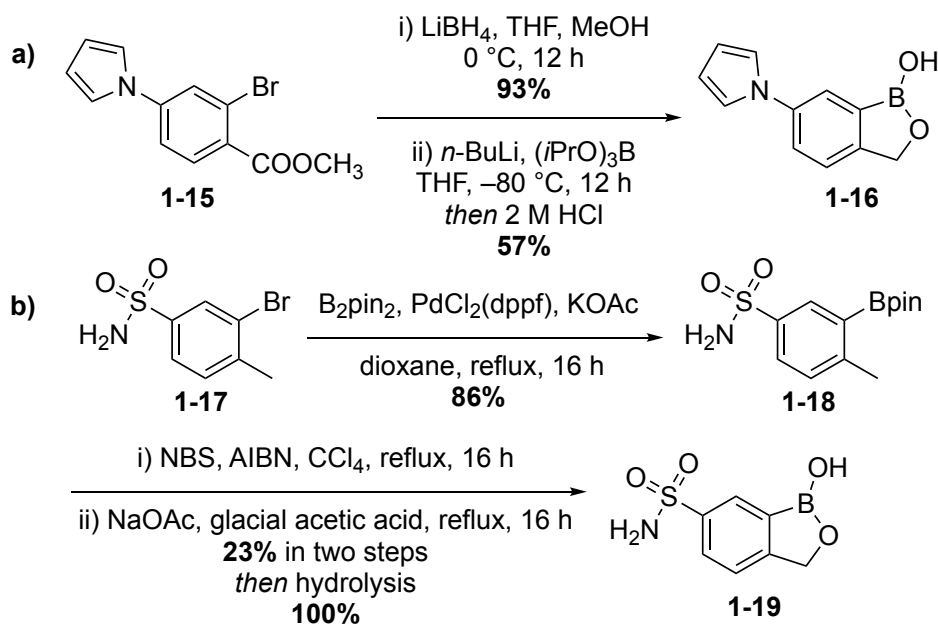
Scheme 1.1. Representative examples of syntheses of benzoxaborole derivatives using the early-stage approach.
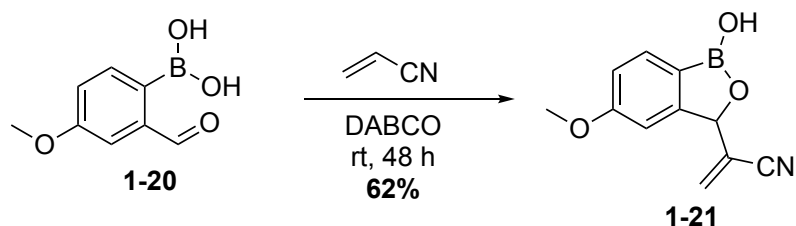
Scheme 1.2. Preparation of benzoxaborole derivative **1-21** from an *ortho*-formyl arylboronic acid.

Costa and co-workers synthesized the amino and hydroxymethyl derivatives of benzoxaborole by performing a diazotization reaction of an aniline precursor (**1-22**) followed by a borylation reaction.[63] The authors were able to achieve the late-stage reduction of the nitro group in **1-23** to afford the desired amine product **1-24** (Scheme 1.3), albeit with the formation of a C—B cleaved side product necessitating silica gel column chromatography for separation.
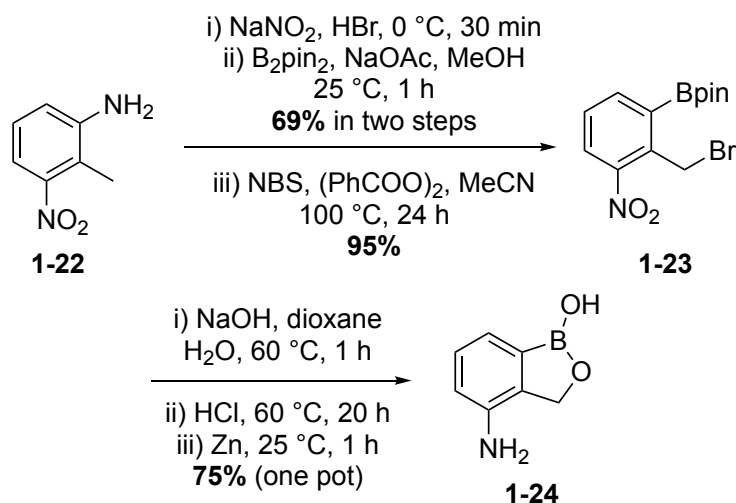
Scheme 1.3. Synthesis of a benzoxaborole derivative **1-22** using the early-stage approach featuring a late-stage nitro reduction.

The formyl substituted benzoxaborole **1-25** has been utilized in the synthesis of a variety of derivatives via the late-stage approach (e.g., Scheme 1.4a).[28,58] From a library of amide benzoxaborole derivatives, synthesized by late-stage amidation reactions, Anacor recently discovered a potential candidate for the treatment of Animal African Trypanosomiasis (AAT), **AN11736** (Scheme 1.4b).[64] The final amide products required a purification involving preparative TLC and preparative HPLC.
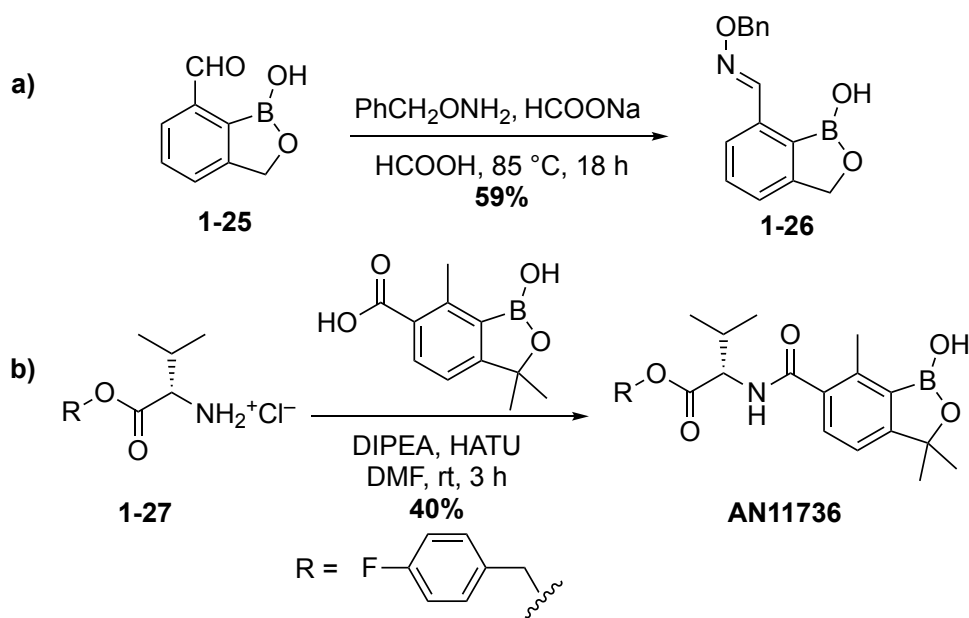
Scheme 1.4. Representative examples of syntheses of benzoxaborole derivatives, using the late-stage approach.

1.5.2 Synthesis of Azaborines

The chemistry associated with azaborines is well established. In 1959 and 1961, Dewar and co-workers reported their seminal work on the substitution of azaborines.[65,66] Pioneering work in this field was also reported by the Ashe Group, wherein ring-closing metathesis (RCM) was utilized to gain access to the azaborine **1-30** under mild reaction conditions (Scheme 1.5).[67] In addition to Ashe and co-workers, several other research groups have demonstrated the synthesis of azaborines and their derivatives.[68] Regioselective Negishi cross-coupling was applied to the late-stage synthesis of substituted azaborine (**1-32**) (Scheme 1.6a).[69] Similarly, the synthesis of the CDK2 inhibitor **1-8** (vide supra), was achieved using a late-stage amidation reaction between **1-33** and **1-34** (Scheme 1.6b).[44]
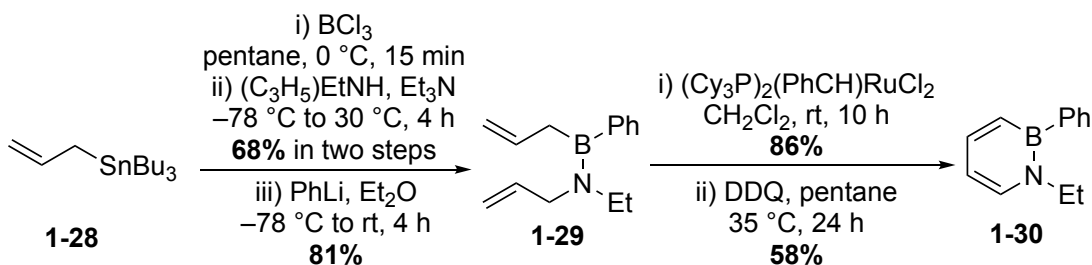
Scheme 1.5. Synthesis of azaborine derivative, **1-30**, using the early-stage approach.
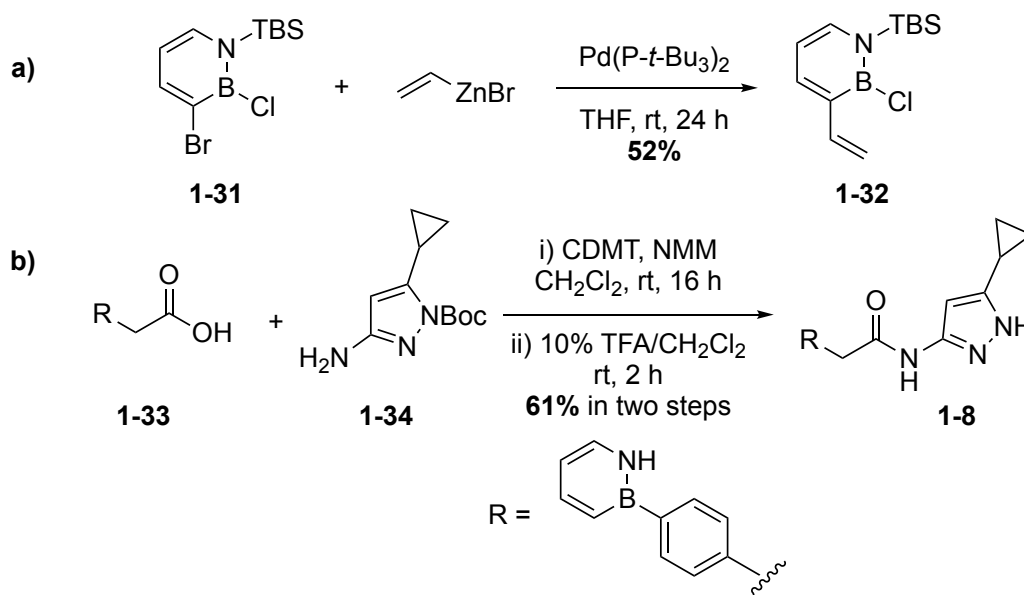
Scheme 1.6. Representative examples of synthesis of azaborine derivatives, using the late-stage approach.

1.5.3 Synthesis of Benzodiazaborine and Benzoxazaborine Derivatives

Contrary to benzoxaboroles and azaborines, the chemistry of benzodiazaborine derivatives (**1-10a**–**d**) is rather limited, with a general focus only on the *N*-sulphonyl heterocycles (cf. Figure 1.8 and 1.9).[53,70] After the discovery of benzoxazaborine (**1-9**) in the 1950s, there has been little effort to establish synthetic pathways to produce its derivatives. Their development, in terms of their properties and chemistry, offers the potential to explore new chemical space in drug discovery. Generally, the purification of boronic acids is challenging due to the relative instability of the C—B bond and requires extensive purifications, such as HPLC (vide supra). Therefore, to develop diverse libraries of these scaffolds (e.g., **1-9** and **1-10**), robust and straightforward synthesis and purification strategies are needed. The design and implementation of such an approach is described in Chapter 4, including the synthesis of several drug isosteres, and the screening of synthesized analogs for anti-fungal, anti-bacterial, and anti-cancer activity.

1.6 Thesis Objectives

The properties of boron trihalides have been well-studied and this has led to their utilization in several fields of chemistry. On the contrary, a thorough understanding of the properties of boron-containing heterocycles is underdeveloped. Studies regarding their properties, such as aromaticity, have only been focused on well-known heterocycles, like azaborines. Several boron-containing heterocycles have found use in catalysis, material science, and most recently in the field of medicinal chemistry. Gaining a thorough understanding of their properties and developing protocols for their synthesis is necessary to achieve the full potential of boron-containing heterocycles.

Due to their intrinsic Lewis acidity, boron trihalides are known to mediate ether cleavage reactions, and as such, are explored for the degradation of lignocellulose, as presented in Chapter 2. Lignocellulose is a biopolymer containing lignin and cellulose, defined by ether and acetal linkages. There is a need to obtain commodity chemicals from renewable resources to reduce the current reliance on non-renewables. Lignocellulose is an intriguing sustainable feedstock for this purpose. Generally, the current methods for separating lignin from lignocellulose result in unusual linkages in

the lignin, which impedes further depolymerization. The aim of Chapter 2 is to rectify this issue by using mild reaction conditions, which in turn results in relatively unmodified lignin.

Although, boron-containing heterocycles, such as benzoxazaborine and benzodiazaborine have been known for several decades, their properties are still unknown and disputed in the literature. Chapter 3 presents a detailed investigation of the properties of these boron-containing heterocycles, in a collective effort combining experimental and computational work. The key questions regarding their acidity, aromaticity, and stability are addressed satisfactorily.

In addition, the scaffolds exhibiting promising properties are further analyzed for their potential to serve as novel chemotypes in drug discovery. Also, there are no general methods described in the literature for the systematic derivatization of these boron-containing naphthoids. Moreover, boron-containing compounds generally suffer from purification challenges. For example, use of canonical purification methods, such as column chromatography are not feasible due to the instability of the C—B bond. In this regard, Chapter 4 describes new synthetic pathways and purification strategies to achieve an array of derivatives of these model compounds. Furthermore, the synthesized derivatives are tested for their biological activity.

1.7 References

(1)   Shriver, D. F.; Swanson, B. Nature of the Donor-Acceptor Interaction in Boron Trihalide Complexes. Vibrational Spectra and Vibrational Analysis of Acetonitrile-Boron Trichloride and Acetonitrile-Boron Tribromide. *Inorg. Chem.* **1971**, *10*, 1354–1365.

(2)   Brinck, T.; Murray, J. S.; Politzer, P. A Computational Analysis of the Bonding in Boron Trifluoride and Boron Trichloride and Their Complexes with Ammonia. *Inorg. Chem.* **1993**, *32*, 2622–2625.

(3)   Miller, J. M.; Onyszchuk, M. The Relative Acceptor Power of Boron Trihalides and Borane Toward Trimethylamine by proton N.M.R. Measurements. *Can. J. Chem.* **1964**, *42*, 1518–1523.

(4)   Bessac, F.; Frenking, G. Why is BCl$_3$ a Stronger Lewis Acid with Respect to Strong Bases than BF$_3$? *Inorg. Chem.* **2003**, *42*, 7990–7994.

(5)   Silva, D. R.; Santos, L. de A.; Freitas, M. P.; Guerra, C. F.; Hamlin, T. A. Nature and Strength of Lewis Acid/Base Interaction in Boron and Nitrogen Trihalides. *Chem. Asian J.* **2020**, *15*, 4043–4054.

(6)   Naganaboina, R. T.; Peddinti, R. K. BF$_3$·Etherate-Mediated Friedel–Crafts Arylation of 2-Hydroxy-1,4-Benzoxazines: Synthesis of 2-Aryl-1,4-Benzoxazine Derivatives. *J. Org. Chem.* **2013**, *78*, 12819–12824.

(7)   Ranu, B. C.; Bhar, S. Dealkylation of Ethers. A review. *Org. Prep. Proced. Int.* **1996**, *28*, 371–409.

(8)   Lappert, M. F.; Litzow, M. R.; Pedley, J. B.; Tweedale, A. Bonding Studies of Compounds of Boron and the Group IV Elements. Part V. Boron-11 Nuclear Magnetic Resonance Data for the Boron Trihalides and Mixed Trihalides. *J. Chem. Soc. A: Inorg., Phys., Theor.* **1971**, 2426–2428.

(9)   Boyd, P. D. W.; Taylor, M. J. Halogen Exchange in Boron Trihalides: The BCl$_3$-BI$_3$ Reaction. *Inorganica Chim Acta* **1992**, *193*, 1–3.

(10)   Atienza, B. J. P.; Truong, N.; Williams, F. J. Reliably Regioselective Dialkyl Ether Cleavage with Mixed Boron Trihalides. *Org. Lett.* **2018**, *20*, 6332–6335.

(11)   Mayer, U.; Gutmann, V.; Gerger, W. The Acceptor Number — A Quantitative Empirical Parameter for the Electrophilic Properties of Solvents. *Monatshefte für Chemie / Chemical Monthly* **1975**, *106*, 1235–1257.

(12)   Beckett, M. A.; Strickland, G. C.; Holland, J. R.; Sukumar Varma, K. A Convenient NMR Method for the Measurement of Lewis Acidity at Boron Centres: Correlation of Reaction Rates of Lewis Acid Initiated Epoxide Polymerizations with Lewis Acidity. *Polymer* **1996**, *37*, 4629–4631.

(13)   Childs, R. F.; Mulholland, D. L.; Nixon, A. The Lewis Acid Complexes of α,β-Unsaturated Carbonyl and Nitrile Compounds. A Nuclear Magnetic Resonance Study. *Can. J. Chem.* **1982**, *60*, 801–808.

(14)   Dowlut, M.; Hall, D. G. An Improved Class of Sugar-Binding Boronic Acids, Soluble and Capable of Complexing Glycosides in Neutral Water. *J. Am. Chem. Soc.* **2006**, *128*, 4226–4227.

(15)   Bérubé, M.; Dowlut, M.; Hall, D. G. Benzoboroxoles as Efficient Glycopyranoside-Binding Agents in Physiological Conditions: Structure and Selectivity of Complex Formation. *J. Org. Chem.* **2008**, *73*, 6471–6479.

(16)   Bhangu, J.; Whittal, R. M.; Hall, D. G. Design, Synthesis and Structure of a Frustrated Benzoxaborole and Its Applications in the Complexation of Amines, Amino Acids, and Protein Modification. *Org. Biomol. Chem.* **2020**, *18*, 3492–3500.

(17)   James, T. D.; Phillips, M. D.; Shinkai, S. The Molecular Recognition of Saccharides. Complexation of Boronic Acids with Saccharides. Fluorescent Sensors. Modular Fluorescent Sensors. Other Types of Sensor. Other Systems for Saccharide Recognition. RSC, **2006**, 3–176.

(18)   Kuivila, H. G.; Keough, A. H.; Soboczenski, E. J. Areneboronates from Diols and Polyols. *J. Org. Chem.* **1954**, *19*, 780–783.

(19)   Shin, S. B. Y.; Almeida, R. D.; Gerona-Navarro, G.; Bracken, C.; Jaffrey, S. R. Assembling Ligands in Situ Using Bioorthogonal Boronate Ester Synthesis. *Chem. Biol.* **2010**, *17*, 1171–1176.

(20)   Akgun, B.; Hall, D. G. Fast and Tight Boronate Formation for Click Bioorthogonal Conjugation. *Angew. Chem. Int. Ed.* **2016**, *55*, 3909–3913.

(21)   Sun, X.; Odyniec, M. L.; Sedgwick, A. C.; Lacina, K.; Xu, S.; Qiang, T.; Bull, S. D.; Marken, F.; James, T. D. Reaction-Based Indicator Displacement Assay (RIA) for the Colorimetric and Fluorometric Detection of Hydrogen Peroxide. *Org. Chem. Front.* **2017**, *4*, 1058–1062.

(22)   Kubo, Y.; Ishida, T.; Kobayashi, A.; James, T. D. Fluorescent Alizarin–Phenylboronic Acid Ensembles: Design of Self-Organized Molecular Sensors for Metal Ions and Anions. *J. Mater. Chem.* **2005**, *15*, 2889–2895.

(23) Duggan, P. J.; Offermann, D. A. The Preparation of Solid-Supported Peptide Boronic Acids Derived from 4-Borono-L-Phenylalanine and Their Affinity for Alizarin. *Aust. J. Chem.* **2007**, *60*, 829–834.

(24) Richardson, P. G.; Hideshima, T.; Anderson, K. C. Bortezomib (PS-341): A Novel, First-in-Class Proteasome Inhibitor for the Treatment of Multiple Myeloma and Other Cancers. *Cancer Control* **2003**, *10*, 361–369.

(25) Fernandes, G. F. S.; Denny, W. A.; Santos, J. L. D. Boron in Drug Design: Recent Advances in the Development of New Therapeutic Agents. *Eur. J. Med. Chem.* **2019**, *179*, 791–804.

(26) Richardson, P. G.; Zweegman, S.; O'Donnell, E. K.; Laubach, J. P.; Raje, N.; Voorhees, P.; Ferrari, R. H.; Skacel, T.; Kumar, S. K.; Lonial, S. Ixazomib for the Treatment of Multiple Myeloma. *Expert Opin. Pharmacother.* **2018**, *19*, 1949–1968.

(27) Vshyvenko, S.; Clapson, M. L.; Suzuki, I.; Hall, D. G. Characterization of the Dynamic Equilibrium between Closed and Open Forms of the Benzoxaborole Pharmacophore. *ACS Med. Chem. Lett.* **2016**, *7*, 1097–1101.

(28) Adamczyk-Woźniak, A.; Borys, K. M.; Sporzyński, A. Recent Developments in the Chemistry and Biological Applications of Benzoxaboroles. *Chem. Rev.* **2015**, *115*, 5224–5247.

(29) Rock, F. L.; Mao, W.; Yaremchuk, A.; Tukalo, M.; Crépin, T.; Zhou, H.; Zhang, Y.-K.; Hernandez, V.; Akama, T.; Baker, S. J.; Plattner, J. J.; Shapiro, L.; Martinis, S. A.; Benkovic, S. J.; Cusack, S.; Alley, M. R. K. An Antifungal Agent Inhibits an Aminoacyl-tRNA Synthetase by Trapping tRNA in the Editing Site. *Science* **2007**, *316*, 1759–1761.

(30) Akama, T.; Baker, S. J.; Zhang, Y.-K.; Hernandez, V.; Zhou, H.; Sanders, V.; Freund, Y.; Kimura, R.; Maples, K. R.; Plattner, J. J. Discovery and Structure–Activity Study of a Novel Benzoxaborole Anti-Inflammatory Agent (AN2728) for the Potential Topical Treatment of Psoriasis and Atopic Dermatitis. *Bioorg. Med. Chem. Lett.* **2009**, *19*, 2129–2132.

(31) Freund, Y. R.; Akama, T.; Alley, M. R. K.; Antunes, J.; Dong, C.; Jarnagin, K.; Kimura, R.; Nieman, J. A.; Maples, K. R.; Plattner, J. J.; Rock, F.; Sharma, R.; Singh, R.; Sanders, V.; Zhou, Y. Boron-Based Phosphodiesterase Inhibitors Show Novel Binding of Boron to PDE4 Bimetal Center. *FEBS Lett.* **2012**, *586*, 3410–3414.

(32) Nocentini, A.; Supuran, C. T.; Winum, J.-Y. Benzoxaborole Compounds for Therapeutic Uses: A Patent Review (2010- 2018). *Expert. Opin. Ther. Pat.* **2018**, *28*, 493–504.

(33) Gardner, S. D.; Kim, J.; Baptiste-Brown, S.; Lopez, V.; Hamatake, R.; Gan, J.; Edwards, S.; Elko-Simms, L.; Dumont, E. F.; Leivers, M.; Hong, Z.; Paff, M. T. GSK2878175, a Pan-Genotypic Non-Nucleoside NS5B Polymerase Inhibitor, in Healthy and Treatment-Naïve Chronic Hepatitis C Subjects. *J. Viral. Hepat.* **2018**, *25*, 19–27.

(34) Langmuir, I. Isomorphism, Isosterism and Covalence. *J. Am. Chem. Soc.* **1919**, *41*, 1543–1559.

(35) Friedman, H. L. *First Symposium on Chemical-Biological Correlation, May 26-27, 1950*; National Academies Press: Washington, D.C., 1951.

(36) Burger, A. Isosterism and Bioisosterism in Drug Design. In *Progress in Drug Research / Fortschritte der Arzneimittelforschung / Progrès des recherches pharmaceutiques*; Salmon, J. A., Garland, L. G., Hoyle, B. D., Costerton, J. W., Seiler, N., Raeburn, D., Karlsson, J.-A., Polak, A., Hartman, P. G., Rohmer, M., Bisseret, P., Sutter, B., Burger, A., Jucker, E., Eds.; Birkhäuser Basel: Basel, 1991; pp. 287–371.

(37) Patani, G. A.; LaVoie, E. J. Bioisosterism: A Rational Approach in Drug Design. *Chem. Rev.* **1996**, *96*, 3147–3176.

(38) Stepan, A. F.; Subramanyam, C.; Efremov, I. V.; Dutra, J. K.; O'Sullivan, T. J.; DiRico, K. J.; McDonald, W. S.; Won, A.; Dorff, P. H.; Nolan, C. E.; Becker, S. L.; Pustilnik, L. R.; Riddell, D. R.; Kauffman, G. W.; Kormos, B. L.; Zhang, L.; Lu, Y.; Capetta, S. H.; Green, M. E.; Karki, K.; Sibley, E.; Atchison, K. P.; Hallgren, A. J.; Oborski, C. E.; Robshaw, A. E.; Sneed, B.; O'Donnell, C. J. Application of the Bicyclo[1.1.1]Pentane Motif as a Nonclassical Phenyl Ring Bioisostere in the Design of a Potent and Orally Active γ-Secretase Inhibitor. *J. Med. Chem.* **2012**, *55*, 3414–3424.

(39) Chalmers, B. A.; Xing, H.; Houston, S.; Clark, C.; Ghassabian, S.; Kuo, A.; Cao, B.; Reitsma, A.; Murray, C.-E. P.; Stok, J. E.; Boyle, G. M.; Pierce, C. J.; Littler, S. W.; Winkler, D. A.; Bernhardt, P. v; Pasay, C.; De Voss, J. J.; McCarthy, J.; Parsons, P. G.; Walter, G. H.; Smith, M. T.; Cooper, H. M.; Nilsson, S. K.; Tsanaktsidis, J.; Savage, G. P.; Williams, C. M. Validating Eaton's Hypothesis: Cubane as a Benzene Bioisostere. *Angew. Chem. Int. Ed.* **2016**, *55*, 3580–3585.

(40) Baranac-Stojanović, M. Aromaticity and Stability of Azaborines. *Chem. Eur. J.* **2014**, *20*, 16558–16565.

(41) Liu, L.; Marwitz, A. J. V.; Matthews, B. W.; Liu, S.-Y. Boron Mimetics: 1,2-Dihydro-1,2-Azaborines Bind inside a Nonpolar Cavity of T4 Lysozyme. *Angew. Chem. Int. Ed.* **2009**, *48*, 6817–6819.

(42) Lee, H.; Fischer, M.; Shoichet, B. K.; Liu, S.-Y. Hydrogen Bonding of 1,2-Azaborines in the Binding Cavity of T4 Lysozyme Mutants: Structures and Thermodynamics. *J. Am. Chem. Soc.* **2016**, *138*, 12021–12024.

(43) Rombouts, F. J. R.; Tovar, F.; Austin, N.; Tresadern, G.; Trabanco, A. A. Benzazaborinines as Novel Bioisosteric Replacements of Naphthalene: Propranolol as an Example. *J. Med. Chem.* **2015**, *58*, 9287–9295.

(44) Zhao, P.; Nettleton, D. O.; Karki, R. G.; Zécri, F. J.; Liu, S.-Y. Medicinal Chemistry Profiling of Monocyclic 1,2-Azaborines. *ChemMedChem.* **2017**, *12*, 358–361.

(45) Stegemann, S.; Leveiller, F.; Franchi, D.; de Jong, H.; Lindén, H. When Poor Solubility Becomes an Issue: From Early Stage to Proof of Concept. *Eur. J. Pharm. Sci.* **2007**, *31*, 249–261.

(46) Snyder, H. R.; Reedy, A. J.; Lennarz, Wm. J. Synthesis of Aromatic Boronic Acids. Aldehydo Boronic Acids and a Boronic Acid Analog of Tyrosine. *J. Am. Chem. Soc.* **1958**, *80*, 835–838.

(47) Dewar, M. J. S.; Dougherty, R. C. Boron-Containing Analogs of Isoquinoline. *J. Am. Chem. Soc.* **1962**, *84*, 2648–2649.

(48) Das, B. C.; Adil Shareef, M.; Das, S.; Nandwana, N. K.; Das, Y.; Saito, M.; Weiss, L. M. Boron-Containing Heterocycles as Promising Pharmacological Agents. *Bioorg. Med. Chem.* **2022**, *63*, 116748.

(49) Högenauer, G.; Woisetschläger, M. A Diazaborine Derivative Inhibits Lipopolysaccharide Biosynthesis. *Nature* **1981**, *293*, 662–664.

(50) Grassberger, M. A.; Turnowsky, F.; Hildebrandt, J. Preparation and Antibacterial Activities of New 1,2,3-Diazaborine Derivatives and Analogs. *J. Med. Chem.* **1984**, *27*, 947–953.

(51) Hicks, J. W.; Kyle, C. B.; Vogels, C. M.; Wheaton, S. L.; Baerlocher, F. J.; Decken, A.; Westcott, S. A. Synthesis, Characterization, and Antifungal Activity of Boron-Containing Thiosemicarbazones. *Chem. Biodivers.* **2008**, *5*, 2415–2422.

(52) Baldock, C.; Rafferty, J. B.; Sedelnikova, S. E.; Baker, P. J.; Stuitje, A. R.; Slanas, A. R.; Hawkes, T. R.; Rice, D. W. A Mechanism of Drug Action Revealed by Structural Studies of Enoyl Reductase. *Science* **1996**, *274*, 2107–2110.

(53) António, J. P. M.; Gonçalves, L. M.; Guedes, R. C.; Moreira, R.; Gois, P. M. P. Diazaborines as New Inhibitors of Human Neutrophil Elastase. *ACS Omega* **2018**, *3*, 7418–7423.

(54) Dukes, A. O.; Carroll, X. B.; Groziak, M. P. Design, Development, Synthesis, and Crystal Structure of the Prototype of a New Class of Deep Blue-Fluorescing Boron Heterocycle Estrogen Mimics. *Bioorg. Med. Chem. Lett.* **2022**, *72*, 128864–128870.

(55) Adamczyk-Woźniak, A.; Cyrański, M. K.; Żubrowska, A.; Sporzyński, A. Benzoxaboroles – Old Compounds with New Applications. *J. Organomet. Chem.* **2009**, *694*, 3533–3541.

(56) Zhang, Y.-K.; Plattner, J. J.; Freund, Y. R.; Easom, E. E.; Zhou, Y.; Gut, J.; Rosenthal, P. J.; Waterson, D.; Gamo, F.-J.; Angulo-Barturen, I.; Ge, M.; Li, Z.; Li, L.; Jian, Y.; Cui, H.; Wang, H.; Yang, J. Synthesis and Structure–Activity Relationships of Novel Benzoxaboroles as a New Class of Antimalarial Agents. *Bioorg. Med. Chem. Lett.* **2011**, *21*, 644–651.

(57) Zhang, Y.-K.; Plattner, J. J.; Freund, Y. R.; Easom, E. E.; Zhou, Y.; Ye, L.; Zhou, H.; Waterson, D.; Gamo, F.-J.; Sanz, L. M.; Ge, M.; Li, Z.; Li, L.; Wang, H.; Cui, H. Benzoxaborole Antimalarial Agents. Part 2: Discovery of Fluoro-Substituted 7-(2-Carboxyethyl)-1,3-Dihydro-1-Hydroxy-2,1-Benzoxaboroles. *Bioorg. Med. Chem. Lett.* **2012**, *22*, 1299–1307.

(58) Ye, L.; Ding, D.; Feng, Y.; Xie, D.; Wu, P.; Guo, H.; Meng, Q.; Zhou, H. Convenient and Versatile Synthesis of Formyl-Substituted Benzoxaboroles. *Tetrahedron* **2009**, *65*, 8738–8744.

(59) Zhao, J.; Chen, J.; Xu, Q.; Li, H. Synthesis of Benzoxaboroles by Ortho-Oxalkylation of Arylboronic Acids with Aldehydes/Ketones in the Presence of Brønsted Acids. *Org. Lett.* **2021**, *23*, 1986–1990.

(60) Wu, P. H.; Meng, Q. Q.; Zhou, H. C. Synthesis of a Novel Pyrrolo-Benzoxaborole Scaffold and Its Derivatization via Friedel–Crafts Reaction Catalyzed by Anhydrous Stannic Chloride. *Chin. Chem. Lett.* **2011**, *22*, 1411–1414.

(61) Li, X.; Zhang, Y.-K.; Liu, Y.; Zhang, S.; Ding, C. Z.; Zhou, Y.; Plattner, J. J.; Baker, S. J.; Liu, L.; Bu, W.; Kazmierski, W. M.; Wright, L. L.; Smith, G. K.; Jarvest, R. L.; Duan, M.; Ji, J.-J.; Cooper, J. P.; Tallant, M. D.; Crosby, R. M.; Creech, K.; Ni, Z.-J.; Zou, W.; Wright, J. Synthesis of New Acylsulfamoyl Benzoxaboroles as Potent Inhibitors of HCV NS3 Protease. *Bioorg. Med. Chem. Lett.* **2010**, *20*, 7493–7497.

(62) Kumar, J. S.; Bashian, C. M.; Corsello, M. A.; Jonnalagadda, S. C.; Mereddy, V. R. Development of Practical Methodologies for the Synthesis of Functionalized Benzoboroxoles. *Tetrahedron Lett.* **2010**, *51*, 4482–4485.

(63) Fuscaldo, R. S.; Vontobel, P. H. V.; Boeira, E. O.; Moro, A. V.; Costa, J. S. da. Synthesis of Amino- and Hydroxymethyl Benzoxaboroles: Prominent Scaffolds for Further Functionalization. *Eur. J. Org. Chem.* **2019**, *2019*, 2050–2055.

(64) Akama, T.; Zhang, Y.-K.; Freund, Y. R.; Berry, P.; Lee, J.; Easom, E. E.; Jacobs, R. T.; Plattner, J. J.; Witty, M. J.; Peter, R.; Rowan, T. G.; Gillingwater, K.; Brun, R.; Nare, B.; Mercer, L.; Xu, M.; Wang, J.; Liang, H. Identification of a 4-Fluorobenzyl l-Valinate Amide Benzoxaborole (AN11736) as a Potential Development Candidate for the Treatment of Animal African Trypanosomiasis (AAT). *Bioorg. Med. Chem. Lett.* **2018**, *28*, 6–10.

(65) Dewar, M. J. S.; Kubba, V. P. New Heteroaromatic Compounds—IV: The Nitration and Chlorination of 10-Methyl-10:9- Borazarophenanthrene. *Tetrahedron* **1959**, *7*, 213–222.

(66) Dewar, M. J. S.; Dietz, R.; Kubba, V. P.; Lepley, A. R. New Heteroaromatic Compounds. Part X. Grignard Reactions and Hydride Reductions of B-Oxides Derived from 10,9-Borazarophenanthrene and 2,1-Borazaronaphthalene. *J. Am. Chem. Soc.* **1961**, *83*, 1754–1756.

(67) Ashe, A. J.; Fang. A Synthesis of Aromatic Five- and Six-Membered B−N Heterocycles via Ring Closing Metathesis. *Org. Lett.* **2000**, *2*, 2089–2091.

(68) Campbell, P. G.; Marwitz, A. J. V.; Liu, S.-Y. Recent Advances in Azaborine Chemistry. *Angew. Chem. Int. Ed.* **2012**, *51*, 6074–6092.

(69) Brown, A. N.; Li, B.; Liu, S.-Y. Negishi Cross-Coupling Is Compatible with a Reactive B–Cl Bond: Development of a Versatile Late-Stage Functionalization of 1,2-Azaborines and Its Application to the Synthesis of New BN Isosteres of Naphthalene and Indenyl. *J. Am. Chem. Soc.* **2015**, *137*, 8932–8935.

(70) Kanichar, D.; Roppiyakuda, L.; Kosmowska, E.; Faust, M. A.; Tran, K. P.; Chow, F.; Buglo, E.; Groziak, M. P.; Sarina, E. A.; Olmstead, M. M.; Silva, I.; Xu, H. H. Synthesis, Characterization, and Antibacterial Activity of Structurally Complex 2-Acylated 2,3,1-Benzodiazaborines and Related Compounds. *Chem. Biodivers.* **2014**, *11*, 1381–1397.

Chapter 2: Boron-Mediated Lignocellulose Degradation to Increase the Yield of Lignin Valorization[1]

2.1 Introduction

Lignocellulose is the structural component of plant cell walls. It consists of lignin, surrounding hemicellulose and encapsulating bundles of cellulose (Figure 2.1).[1] By mass, lignocellulose consists mainly of cellulose, followed by hemicellulose and lignin. Cellulose is the most abundant organic biopolymer on the planet and contains β-glycosidic linkages between D-glucose units connected by 1,4-linkages. Hemicellulose is an organic heteropolymer that consists of a variety of sugar residues, like glucose and xylose. Lignin is the most abundant aromatics containing biopolymer. It constitutes 30% of the organic carbon in the biosphere (Figure 2.2).[2,3]
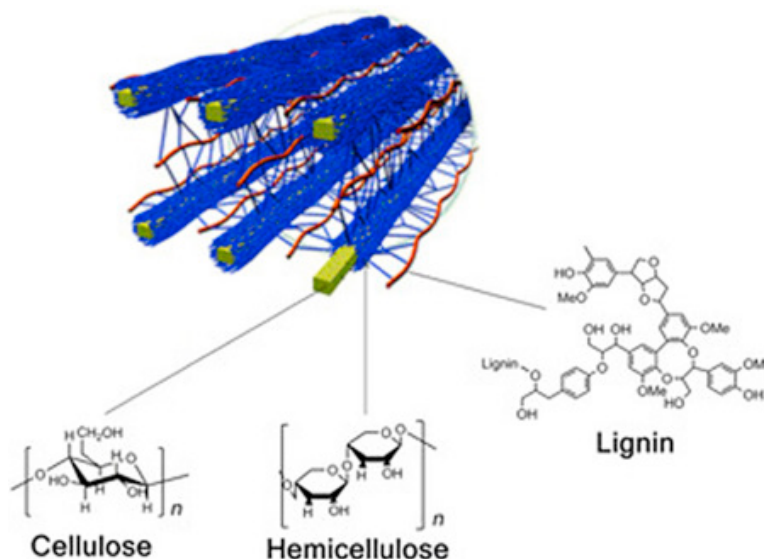
Figure 2.1. A model of lignocellulose. Reused with permission from Elsevier.

There is an environmental need to change the source for the chemicals produced by industries to have a secure future. Generally, benzene derivatives such as vanillin

---

[1] The contents of this chapter have been adapted from the following publication: Kazmi, M. Z. H.; Karmakar, A.; Michaelis, V. K.; Williams, F. J. Separation of Cellulose/Hemicellulose from Lignin in White Pine Sawdust Using Boron Trihalide Reagents. *Tetrahedron* **2019**, *75*, 1465–1470.

are produced from petrochemicals.[4] A defining approach to generate aromatic feedstocks would be to use renewable resources. Lignocellulose and lignin depolymerization can result in numerous potentially useful derivatives, such as vanillin, resulting from monomers, which are *para* coumaryl alcohol (**2-1**), coniferyl alcohol (**2-2**), and sinapyl alcohol (**2-3**) from this renewable natural resource (Figure 2.3).[5,6] Also, lignin is a sustainable chemical feedstock, and it could be an alternative source for these derivatives that currently are produced by the petrochemical industry.
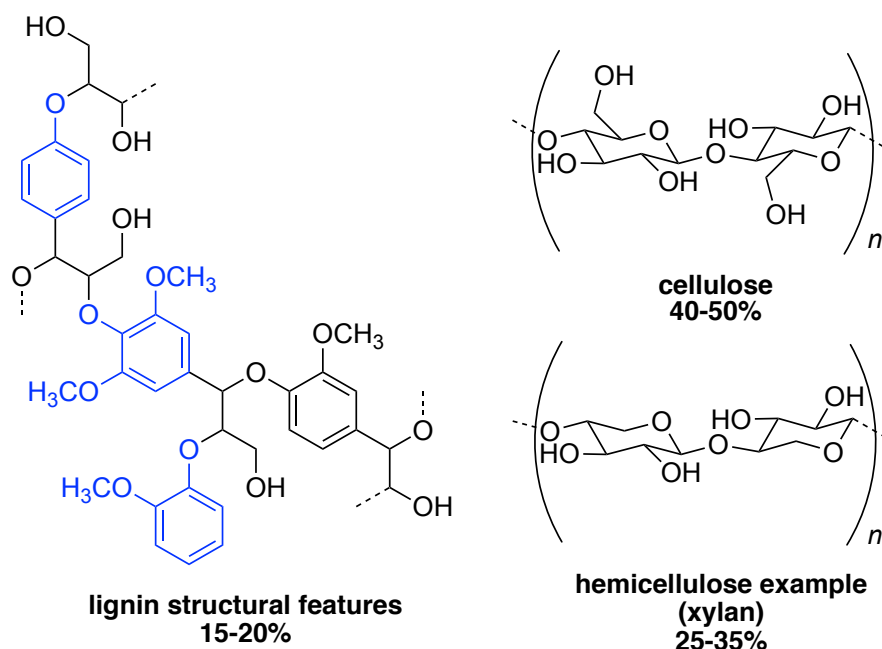
Figure 2.2. Lignocellulose composition.

Current methods to isolate lignin from lignocellulose generally use high temperature and Brønsted acids, which often results in modified and condensed lignin (vide infra) (Figure 2.3). Modifications include the introduction of sulphur groups and a high degree of polymerization by the introduction of new C—C bonds (Figure 2.3).[7,8] Because these modifications can preclude depolymerization, there is a need to isolate the lignin in such a way that it remains unmodified and uncondensed. Then, it could be used for further depolymerization to afford the desired monomers, which in turn can be utilized for biofuels, food, pharmaceuticals, and cosmetics. Therefore, a better way

to access the lignin in its native state would be to use milder conditions, such as using Lewis acids and in a low temperature environment.[9]
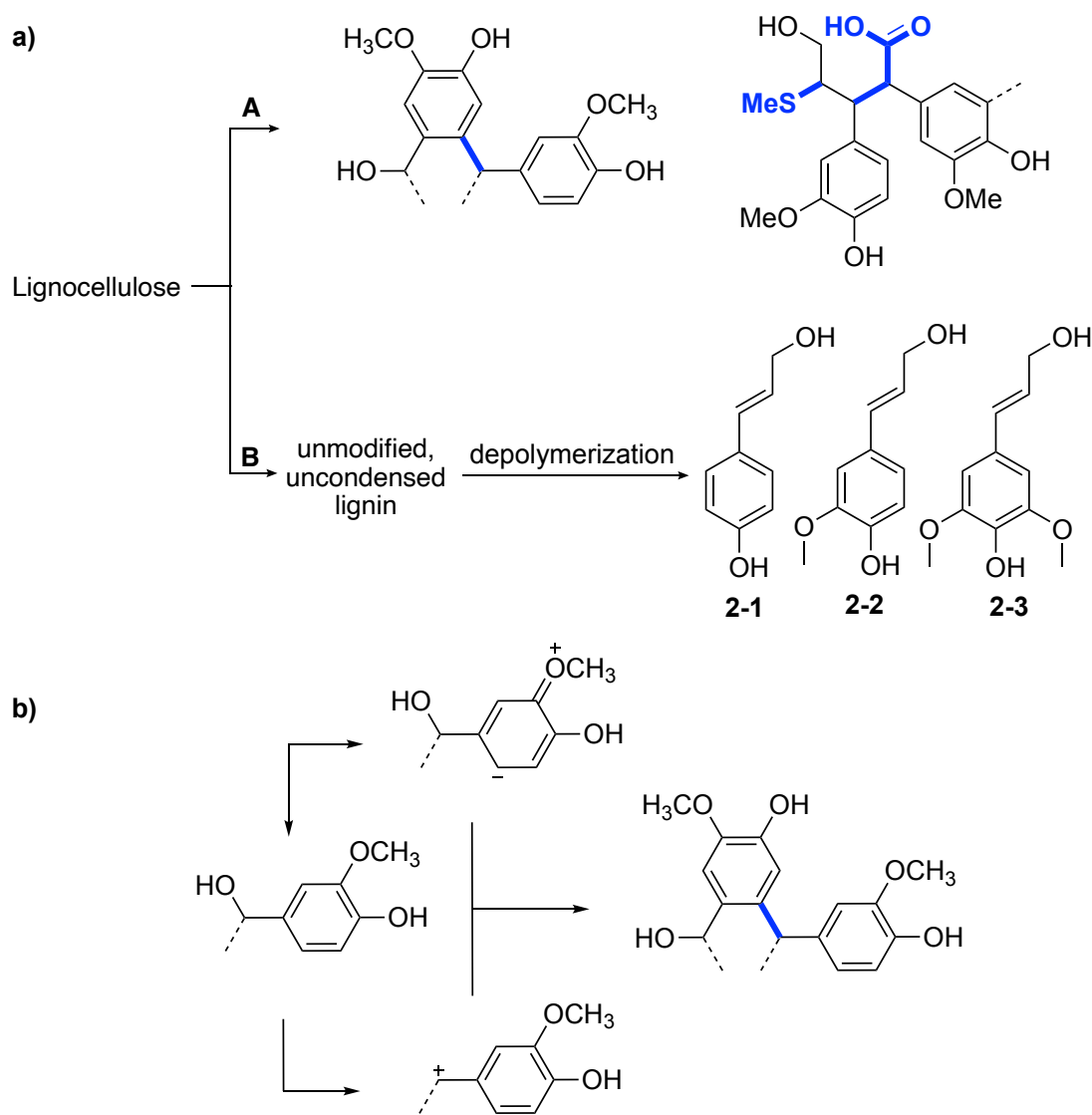
Figure 2.3. a) Lignocellulose degradation to achieve lignin and its fragments. **A** = methods, such as Kraft pulping and sulfite pulping.[10] **B** = desired method. **b)** One proposed mechanism for a lignin condensation process.[11] Blue bonds and blue functional groups show the new bonds formed, which were absent in the native lignin.

Boron Lewis acids are important reagents in the field of sustainable chemistry since the side product, boric acid, is non-toxic.[12] Differences in electronegativity between the carbon and oxygen centers in ether molecules make the C—O bond very polar and, therefore, a good target for cleavage reactions. Boron Lewis acids (especially

BBr$_3$) are used widely to cleave C—O bonds by increasing the polarity between carbon and oxygen through coordination at the oxygen atom (Scheme 2.1).[13,14] The coordination with oxygen occurs due to the inherent Lewis acidity of trivalent boron centers, arising from the vacant p orbital, which makes them strongly electrophilic. BBr$_3$ is used widely for C—O cleavage in aryl-alkyl ethers at room temperature but gives poor regioselectivity in the case of alkyl-alkyl ethers.[13,15] BCl$_3$, on the other hand, is known to make stable coordination complexes with ethers and, therefore, the cleavage is slow at room temperature.[16] The Lewis acidity of boron trihalides increases in the order BF$_3$ < BCl$_3$ < BBr$_3$ with respect to strong bases.[17] The reactivity of boron trihalides can be tamed by combining boron trihalides of different Lewis acidic strength. The Williams Group has shown that ether cleavage with reliable regioselectivity and better chemoselectivity can be achieved using a BBr$_3$ and BCl$_3$ combination as compared to BBr$_3$ alone (Scheme 2.1).[18]
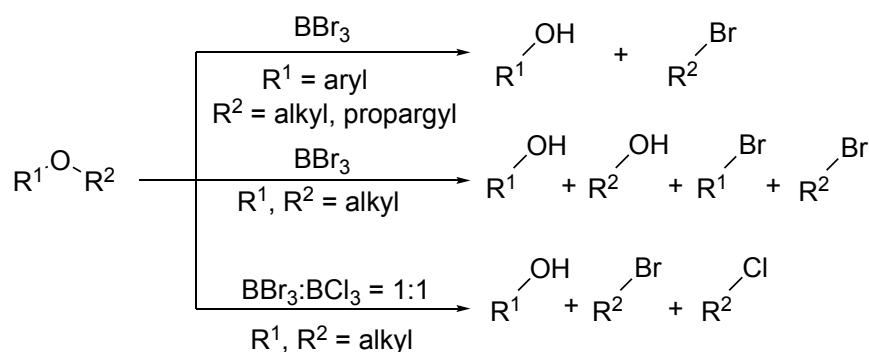
Scheme 2.1 Ether cleavage using boron trihalide reagents.

Therefore, we envisioned using the combination of the BBr$_3$ and BCl$_3$ reagent system to cleave lignin into lignin monomers directly from lignocellulose (lignin-first cleavage).[19] In this way, lignin monomers that are produced could be dissolved in organic solvents and separated from the cellulosic material. On the other hand, this reagent system could preferentially cleave the acetal linkages in cellulose, and the native lignin could be separated. Therefore, if there is any significant chemoselectivity for acetal or ether functional groups, a mixture of boron Lewis acids could help separate lignin and cellulose from lignocellulose under ambient reaction conditions.[20]

2.2 Initial Studies

The reaction with the BBr$_3$:BCl$_3$ (1:1) reagent system was performed on lignin model compounds **2-4** and **2-7**, and with nanocellulose to test chemoselectivity (Scheme 2.2a). The reaction with model compounds **2-4** and **2-7** gave the expected results, with catechol (**2-5**) as the main product and the corresponding side products **2-6** and **2-8**, respectively. The yield of **2-6** is presumed to have decreased due to the evaporation during workup.
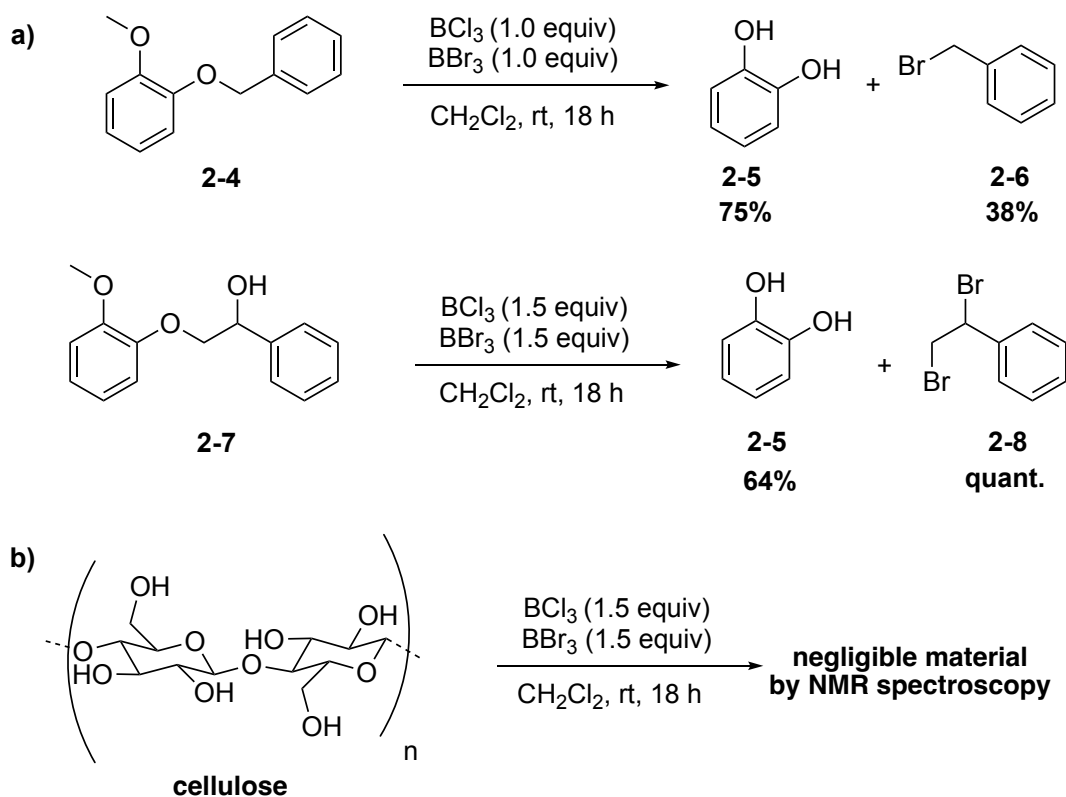
Scheme 2.2 a) Reaction with model lignin compounds. **b)** Reaction with nanocellulose.

Interestingly, no reaction was observed with commercial nanocellulose (Scheme 2.2b). Therefore, the reaction was performed with commercial lignin (dealkaline, TCI Chemicals) with varying amounts of BBr$_3$:BCl$_3$ in a 1:1 ratio. However, to our surprise the reaction did not result in the formation of monomers but showed only vanillin as the major compound. To confirm if vanillin was produced after the reaction or was an impurity in the commercial lignin, the lignin was dissolved in

CH$_2$Cl$_2$ and filtered. The filtrate was evaporated and showed vanillin, confirming the fact that the boron trihalides treatment does not result in the formation of monomers with this lignin source. Next, this boron trihalides reagent system was reacted with lignocellulose directly in a vision to achieve chemoselectivity between acetal and ether linkages (vide supra).

2.3 Lignin Separation

For the present study, white pine sawdust was used. Sawdust generally contains extractives such as, fats, waxes, and terpenes. Therefore, the TAPPI standard procedure was followed to remove them.[21] Then, this extractive-free sawdust was subjected to an equimolar ratio of the boron trihalides reagent system, BBr$_3$:BCl$_3$, for 18 h. Next, the reaction mixture was filtered through glass microfibre filter paper (Scheme 2.3).
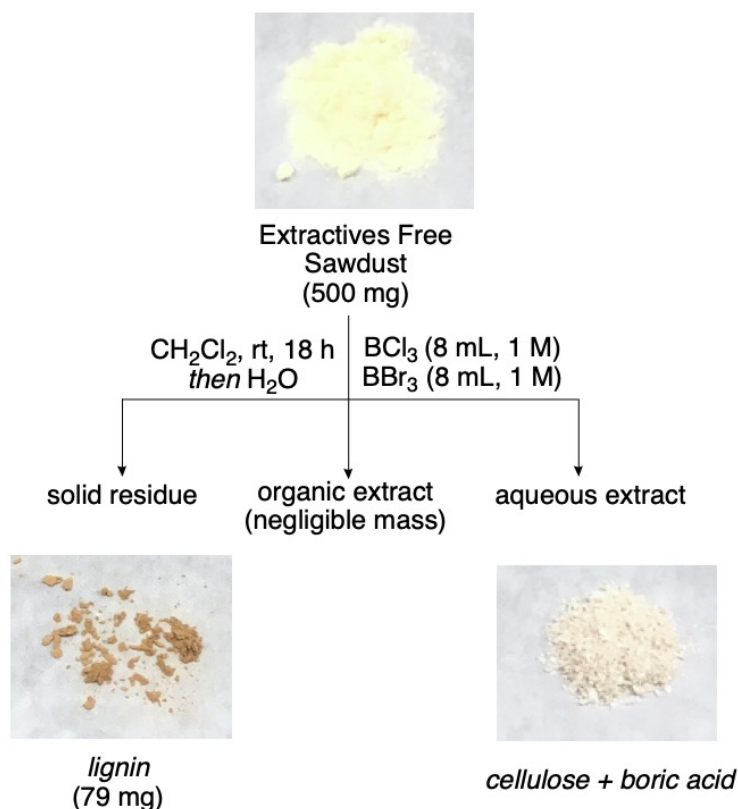
Scheme 2.3. Reaction with extractives free white pine sawdust.

Glass filter paper was used to avoid any leaching of cellulose from regular filter papers made from cellulose. The residue obtained was washed with water (which also quenches any remaining boron trihalides reagents to boric acid). The filtrate, now containing CH_2Cl_2 and water, was separated, and both layers were evaporated to dryness. Interestingly, the organic layer had negligible material (<10 mg), while the aqueous layer showed the presence of oligomeric or polymeric sugars with boric acid. The characterization of the aqueous layer was performed by ^{1}H NMR spectroscopy and showed the distinct peaks in the 3–5 ppm region, indicative of sugars, but did not show any aromatic signals (range 6.5–8.0 ppm), indicating that no lignin monomers were obtained after the reaction (vide infra). Matrix assisted laser desorption ionization (MALDI) mass spectrometry (MS) was also performed on the aqueous extract, along with a positive control, where nanocellulose was mixed with boric acid. The positive control (a) showed a similar pattern to the aqueous extract (c), indicating that the aqueous extract contains cellulose oligomers (Figure 2.4).
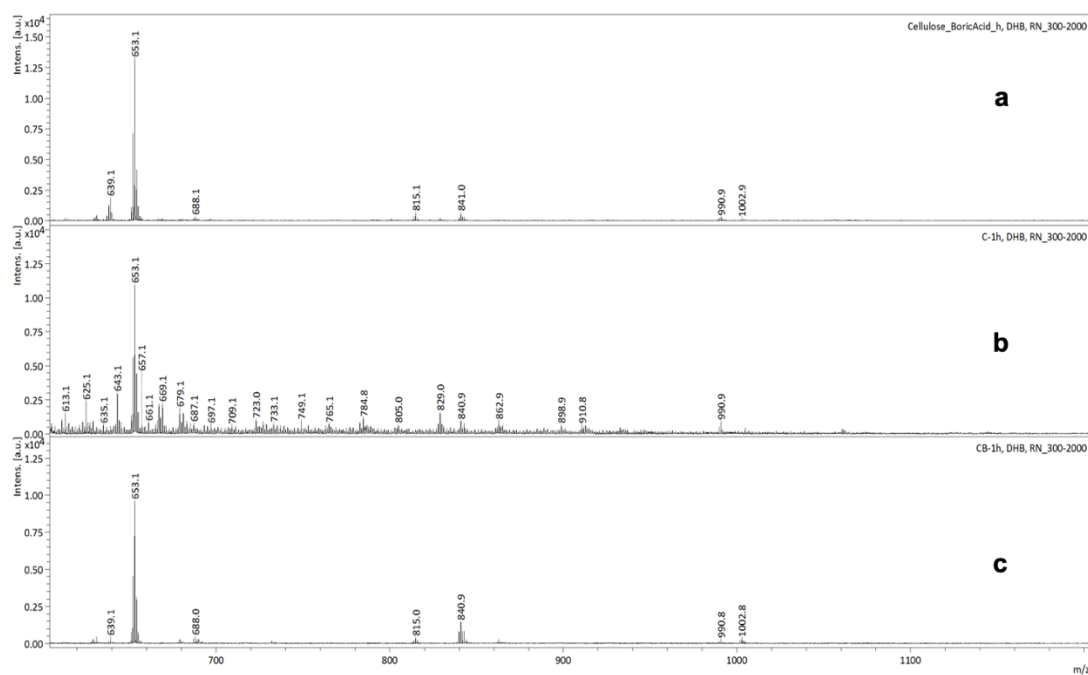
Figure 2.4. MALDI MS spectra of **a)** cellulose and boric acid **b)** cellulose **c)** aqueous extract.

These observations from MALDI MS spectra suggested that the boron trihalides reagent system actually is involved in depolymerizing and solubilizing

cellulose and/or hemicellulose exclusively instead of cleaving the ether linkages in lignin to produce lignin monomers (lignin-first cleavage). This indicates a possibility of selective hydrolysis of acetal linkages in polysaccharides, which results in water soluble oligomers, leaving the lignin mostly intact in its native form.

Having confirmed the release of cellulose and/or hemicellulose from the bulk solid, the solid residue from the first reaction was treated with the same sequence of reactions with boron trihalides, and another decrease in mass was observed for the solid material, with similar characteristics of the aqueous and organic layers (Table 2.1, entry 2). Four reaction cycles were performed, all resulting in the removal of polysaccharide only, leaving 16% mass of presumably lignin-rich solids. This value is under the known percentage of lignin (~29%) present in pine.[22]

Table 2.1. Exposure of Sawdust to Boron Trihalides for Degradation of the Polymer Structure

Extractives Free Sawdust (500 mg) $\xrightarrow[\begin{array}{c}CH_2Cl_2,\ rt,\ 18\ h\\ then\ H_2O\end{array}]{\begin{array}{c}BBr_3\ (8\ mL,\ 1\ M)\\ BCl_3\ (8\ mL,\ 1\ M)\end{array}}$ Solid Residue + Aqueous Extract

Entry	Source of SM	Starting Mass (mg)	Solid Residue (mg)	Mass Decrease (mg)	Aqueous Residue (mg)[a]
1	sawdust	500	320	180	870
2	entry 1	320	213	107	710
3	entry 2	213	116	97	765
4	entry 3	116	79	37	671
5[b]	sawdust	300	97	203	1600

Sawdust or solid residue from a previous reaction was treated with boron trihalide reagents in 30 mL CH_2Cl_2, After 18 h, the reaction mixture was filtered and the residue was washed with water. Finally the aqueous layer was separated from the organic layer
[a]Solids from aqueous extract after vacuo, which contains cellulosic material and boric acid as a by-product
[b]Performed using 20 mL CH_2Cl_2 and 19.2 mL of each boron trihalide reagent

The aqueous residue obtained after every reaction cycle was analyzed by ^{1}H NMR spectroscopy. A decrease in polymeric/oligomeric sugars extracted in each sequence (3–4 ppm peaks were assigned as polymeric/oligomeric sugars) and an

absence of aromatic signals (7–8 ppm) were observed, using imidazole as an internal standard (Figure 2.5).
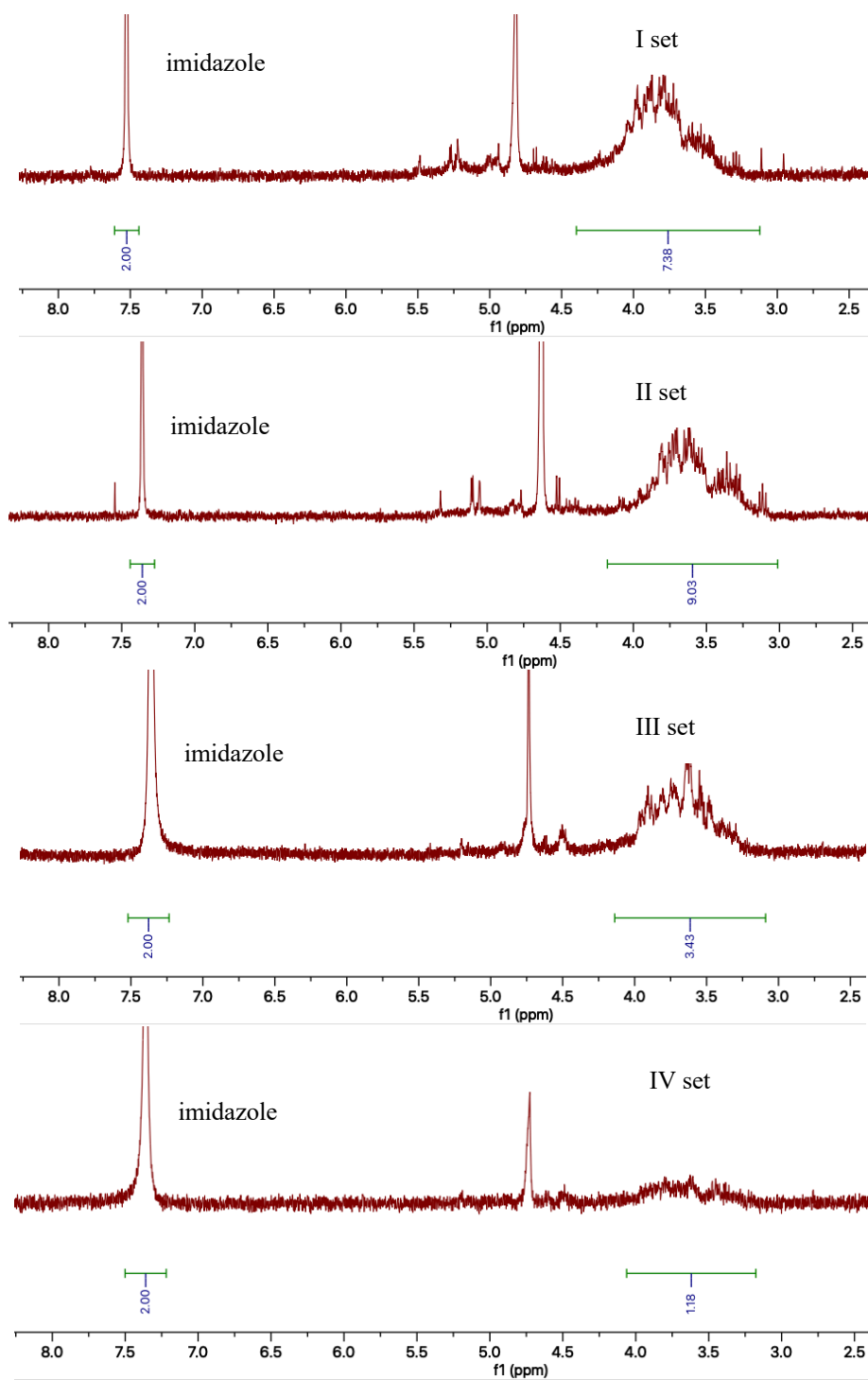
Figure 2.5. ^{1}H NMR (400 MHz, 500 MHz, and 600 MHz, D$_2$O) spectra of aqueous extracts from consecutive reactions (set I-IV, corresponding to Entries 1-4 in Table 2.1), using imidazole as an internal standard.

To assess the amount of cellulose-derived material present in the aqueous extract, dialysis (0.5–1 kDa membrane) was performed on a portion of aqueous extract. Based on the remaining cellulosic material following dialysis, it is estimated that a total of 0.30 g (60 %) of oligomeric cellulosic material was extracted over the four reaction cycles (see Section 2.6.7). This value is in line with the known percentage (~67%) of cellulosic material present in pine.[22]

To examine whether the sequential treatment with the boron trihalides was necessary, another reaction with extractive-free sawdust was set up, in which the amount of boron trihalide reagents used were equivalent to the total amount used over four reaction cycles (Table 2.1, entry 5). Though there was an increased degradation of lignocellulose, it was not to the same extent as with the batch-wise treatment, which shows that the batch-wise treatment was more efficient in removal of cellulose from lignocellulose as compared to the one-pot treatment.

Next, several experiments were performed to verify if the solid residue obtained after four reaction cycles was lignin without any hemicellulose or cellulose. A series of analytical assays were carried out. Solid state ^{13}C NMR spectroscopy was performed by Abhoy Karmakar from Dr. Vladimir Michaelis' lab, and the spectrum of the residue showed a decrease in aliphatic resonances (relative to the aromatic resonances) compared to the sawdust sample.[20] An analysis by FTIR spectroscopy also showed a decrease in alcohol signal, which was seen at 3300 cm^{-1}, indicative of polysaccharide removal from lignin (see section 2.6.5).[23]

Then, fluorescent staining analyses were performed. Calcofluor White stain generally is used for visualizing polysaccharides.[24,25] In the presence of polysaccharides, Calcofluor White fluoresces, and therefore the absence of fluorescence in a wood sample indicates a lack of polysaccharides. The extractive-free sawdust sample, the solid residue after the four reaction cycles (Table 2.1, entry 4), cellulose, and commercial lignin were treated with Calcofluor White. Fluorescence images were taken, along with differential interference contrast (DIC) images to confirm the presence of the sample particles, even when there was no fluorescence (Figure 2.6). The cellulose sample was used as a positive control, which shows strong

fluorescence (e/f). The extractive-free sawdust sample shows some fluorescence as well, due to the presence of cellulose/hemicellulose (a/b). Commercial lignin was used as a negative control, as it shows no fluorescence (g/h), similar to the solid residue (c/d). These results indicate the stripping of cellulose and hemicellulose from sawdust and, therefore, provide evidence that the solid residue consists primarily of lignin.
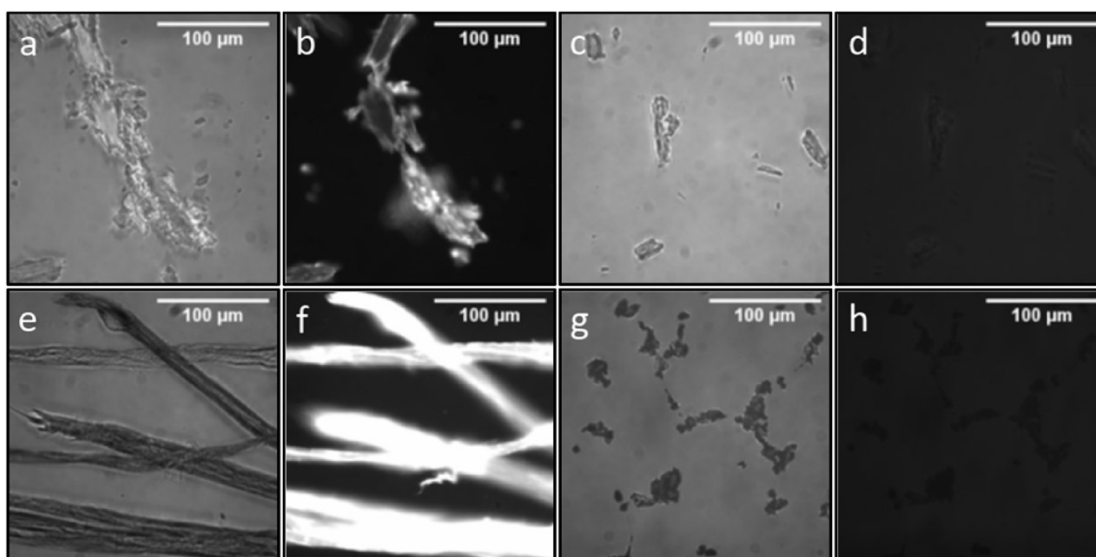
Figure 2.6. Epifluorescence imaging (150 ms) of **a/b)** sawdust, **c/d)** solid residue from Table 2.1, entry 4 **e/f),** cotton (cellulose), and **g/h)** commercial lignin.

To verify the identity of the solid residue further, Toluidine Blue O stain was employed. A colorimetric stain, Toluidine Blue O produces a blue-green color when interacting with lignin and shows a purple-pink color with cellulose.[25,26] The samples that contain lignin and cellulose, such as any wood sample, appear purple-blue with Toluidine Blue O. Therefore, sawdust, cellulose, commercial lignin, and the solid residue were stained with Toluidine Blue O stain (Figure 2.7).
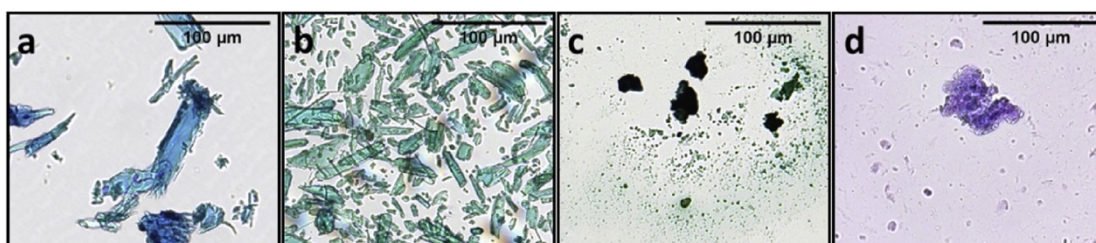
Figure 2.7. Bright field imaging of **a)** sawdust, **b)** solid residue, **c)** commercial lignin, and **d)** cellulose.

As expected, cellulose appears purple in color (d), and sawdust shows a purple-blue color (a). On the other hand, commercial lignin is a dark green color (c), and the solid residue looks green-blue in color (b). Again, these staining results offer confirmation that the solid residue was indeed lignin-rich and lacking cellulose and hemicellulose.

2.4. Lignin Hydrogenolysis

The solid residue that was determined to be lignin and that now will be referred to as "boron lignin", was further subjected to hydrogenolysis. For comparison, two more lignins of different kinds were synthesized, Klason lignin and formaldehyde (FA) lignin. Klason lignin was obtained by treating sawdust with concentrated acid, and FA lignin was synthesized following a modified procedure published by Luterbacher and co-workers.[27] FA lignin is currently the "state-of-the-art" to produce relatively uncondensed lignin, and the lignin produced is soluble in organic solvents.

Softwood, such as white pine, contains ~29% lignin by mass (vide supra), and the percentages of lignin, by mass, obtained after following different methods were calculated (Table 2.2).

Table 2.2. Lignin Extraction Using Three Different Approaches

S. No.	Method	Sawdust (mg)	Lignin obtained (mg)	Lignin (%)
1	Klason	500	165	33
2	FA	1000	632	63
3	boron	500	79	16

After separation, FA lignin shows more than double the amount of lignin than expected, which is likely due to the modification of lignin by the introduction of methylene groups (Table 2.2, entry 2) (Scheme 2.4).[27]
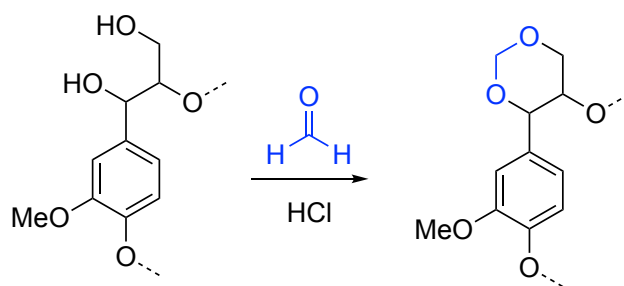
Scheme 2.4. Proposed reaction for the introduction of methylene group in the lignin fragment during FA lignin extraction.

Having both Klason and FA lignin in hand, all three lignins, including the boron lignin, were subjected to a high pressure (480 psi, actual pressure of the vessel at 250 °C = 1250 psi) hydrogenolysis reaction using Ru/C as a catalyst (Table 2.3).

Table 2.3. Hydrogenolysis of Lignin: Assessment of Condensation

$$\text{Lignin (150 mg)} \xrightarrow[\substack{250\ °C,\ \text{MeOH (15 mL)} \\ \text{time}}]{\text{Ru/C (40 mg), } H_2 \text{ (480 psi)}} \text{Monomers}$$

S. No.	Lignin	Time	Soluble material (%)	Insoluble material (%)
1	Klason	4 h	3	87
2	FA	4 h	50	N/A
3	boron	4 h	47	48
4	boron	2 days	21	7

After the hydrogenolysis reaction, the reaction mixture was filtered, the organic layer (soluble material) was evaporated, and weights of the insoluble material and the soluble material were obtained. Klason lignin contained mostly insoluble material and negligible soluble material, which is due to a high degree of condensation that is known to occur during the Klason lignin preparation (entry 1). Boron lignin and FA lignin, on the other hand, converted into mostly soluble material upon hydrogenolysis (entry 2 and 3). Performing the hydrogenolysis reaction for two days resulted in a decreased percentage of insoluble material for boron lignin, likely due to the extensive

hydrogenation of the boron lignin, resulting in volatile fragments (Table 2.3, entry 4). This hydrogenolysis data indicates that there is potentially lower condensation during the preparation of boron lignin compared to the Klason lignin, which is exemplified by the negligible amount of monomers obtained after the reaction with the Klason lignin (entry 1 vs entry 3).

To look into the identity of the monomers obtained after the hydrogenolysis reaction, the crude soluble material obtained was dissolved in CH_2Cl_2 with a known amount of *n*-decane as the internal standard and used for gas chromatography-mass spectrometry (GC-MS). The compounds were identified, using NIST libraries (and some of them, **M1**, **M2**, and **M3** were validated using the commercial compounds, see Section 2.6.12), and the percent yield of the monomers was calculated for all three lignins: Klason, FA, and boron lignins (Figure 2.8, also see Section 2.6.12). Even though GC-FID is more reliable than GC-MS for quantifications, a rough yield was calculated by using GC-MS analysis due to the limited number of available commercial monomers.[28] It should be noted that a calculated/predicted response factor (R_F) was used for many of these monomers,[29] and further, that there was not a concentration calibration curve for those monomers that were commercially available. As such, these rough yields should not be considered as representative of the true yields of this reaction. Rather, the GC-MS data can give a sense of the diversity of monomers obtained. The relative yield of monomers **M2**, **M4**, and **M7** for boron lignin was comparable to FA lignin, and hydrogenolysis of boron lignin also provided additional monomers (**M5** and **M6**) that were not detected with FA or Klason lignin. The soluble material from Klason lignin did not show any monomers by GC-MS, again corroborating that the Klason lignin is in a highly condensed state.
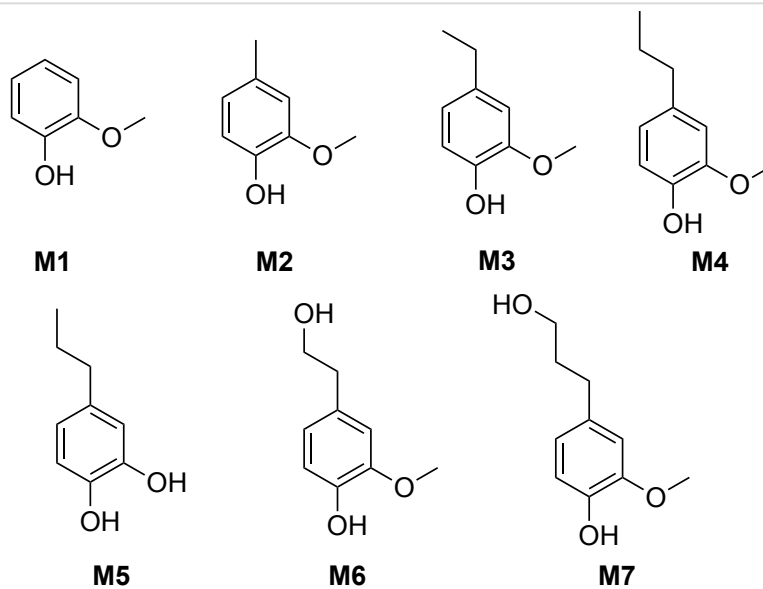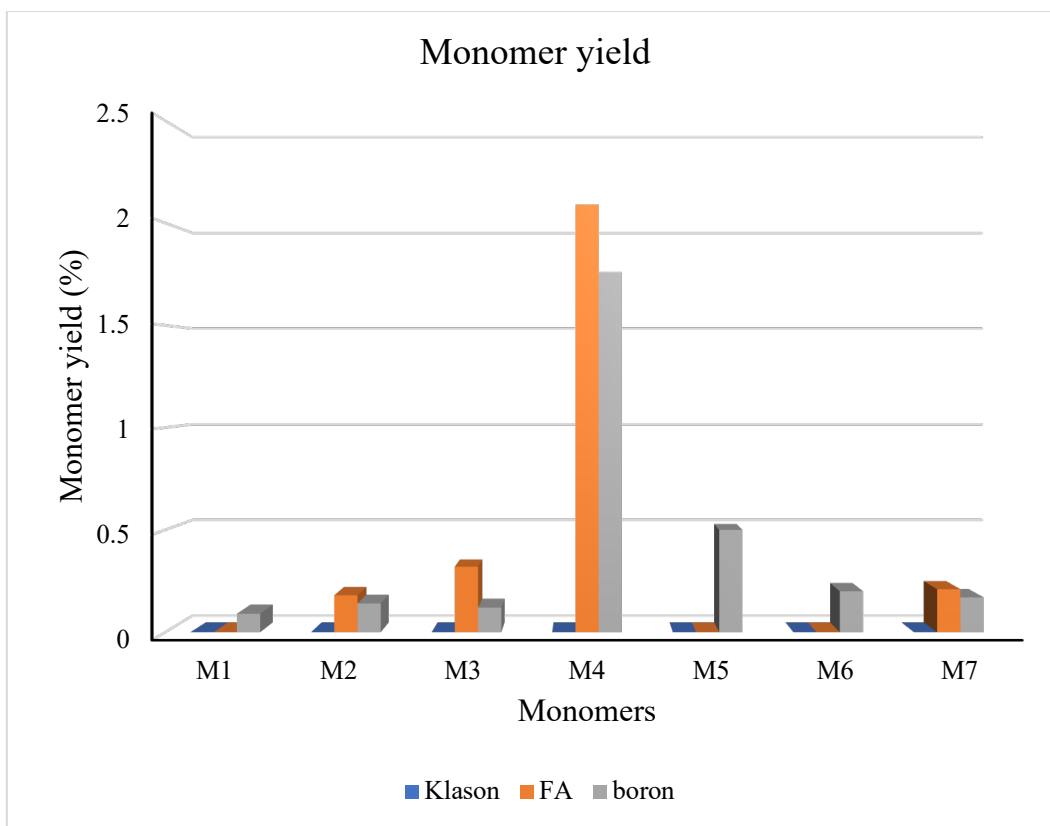
Figure 2.8. Above: Monomer yield after GC-MS analysis using *n*-decane as an internal standard. Below: Monomer structures.

2.5. Conclusion

Although the use of BBr₃ has been demonstrated to yield aromatic alkyl bromides from

lignin,[30] the use of boron trihalides for lignin removal from lignocellulose has not been

demonstrated before. Indeed, in this Chapter, it was demonstrated that by using a BB$_3$:BCl$_3$ combination at room temperature, cellulose/hemicellulose can be separated from the lignin present in a white pine sawdust.[20] Additionally, the lignin obtained has little to no condensation, which aids in a higher monomer yield.[8] It also was ascertained that the aqueous layer, obtained after quenching the reaction with water, contained cellulosic material and had no aromatic compounds. Another advantage of this method is that the side product is boric acid, which is environmentally benign.[12]

Though the reaction results were unexpected compared to model reactions, this work presents the first use of boron trihalides directly on sawdust to separate cellulose/hemicellulose from lignin. To the best of my knowledge, this work also establishes the very first application of Calcofluor and Toluidine Blue O stain for lignocellulose and its components, which in the past has been used only on whole plant slices, and not on the particulates.[25,26] The hydrogenolysis reactions performed on the lignin furthermore indicated that the boron lignin product can be utilized to produce high value chemical materials from renewable feedstock. Future work would be to explore other methods of hydrogenolysis, such as enzymatic cleavage reactions, which could result in higher monomer yields.[31]

2.6 Experimental

2.6.1 General Information

All reactions were carried out under air and water free conditions. Dichloromethane (CH$_2$Cl$_2$) was passed through a column of activated molecular sieves (4 Å, LC Technologies). Deuterated chloroform (CDCl$_3$) was treated with oven-dried molecular sieves (4 Å), whereas deuterated water (D$_2$O) was used without further treatment. Both boron reagents, BBr$_3$ (1 M in CH$_2$Cl$_2$) and BCl$_3$ (1 M in CH$_2$Cl$_2$), Toluidine Blue O stain and Calcofluor White stain were purchased from Sigma Aldrich. Commercial lignin (dealkaline lignin) was purchased from TCI Chemicals. Pine sawdust was obtained by sanding a sample of untreated white pine wood. NMR spectra (^{1}H NMR) were recorded at 400, 500 and 600 MHz. Fourier transform infrared (FT-IR) spectra were recorded by incorporating the analyte within a KBr pellet, and Matrix-Assisted

Laser Desorption/Ionization (MALDI) mass spectra were recorded using a dihydroxybenzoic acid (DHB) matrix. MALDI-MS analysis was performed on an ultraflexXtreme™ MALDI-TOF/TOF (Bruker Daltonics) mass spectrometer in negative MS mode. Dialysis was done using a micro float-a-lyzer (0.5–1 kDa, cellulose membrane) purchased from spectrum labs. Reverse phase HPLC was performed on an Agilent Technologies 1260 Infinity instrument (C18, 150 × 4.6 mm, 3 mL/min). The hydrogenation reaction was performed in the Stryker Lab at the Department of Chemistry, University of Alberta using a high-pressure reactor (Parr®) in a 100 mL stainless-steel vessel equipped with a rupture disk rated at 2000 psi. Bruker GCMS spectrometer (Scion 456-GC) equipped with a Phenomenex® Zebron capillary GC column (ZB-5MS) with the dimensions: 40 m length, 0.25 mm I.D., 0.25 μm film thickness, was used for GC-MS analysis.

2.6.2 Reaction of Lignin Model Compounds with BBr$_3$:BCl$_3$ Reagent System

Model lignin monomer **2-4** (25.0 mg, 0.117 mmol, 1.00 equiv) was dissolved in CH_2Cl_2 (2.00 mL) and added to a flame-dried 5 mL round bottom flask. The solution was cooled to 0 °C, and BCl$_3$ (120 mL, 1 M in CH_2Cl_2) was added, followed by BBr$_3$ (120 mL, 1 M in CH_2Cl_2). The reaction mixture was allowed to come to room temperature and was stirred for 18 h. Solvent was then removed in vacuo and the resulting residue was dissolved in CDCl$_3$ for NMR spectroscopic analysis (Figure 2.9).
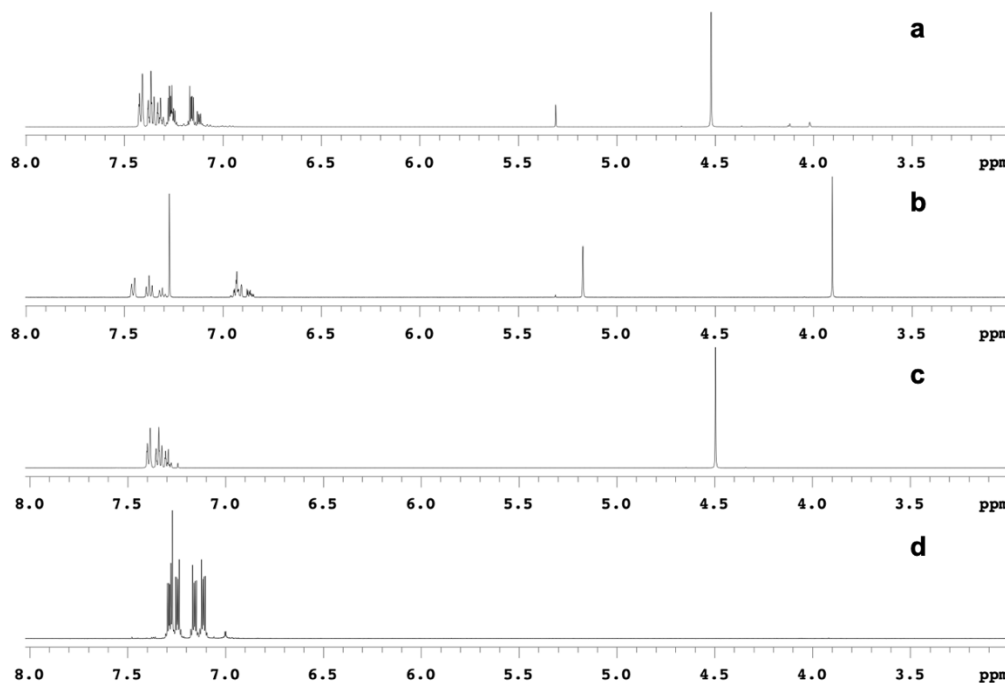
Figure 2.9. ^{1}H NMR (500 MHz, CDCl$_3$) spectrum of crude reaction material for model lignin compound **2-4** compared to ^{1}H NMR of starting material and expected reaction products. **a)** Model lignin compound **2-4** crude reaction. **b)** Model lignin compound **2-4**. **c)** benzyl bromide. **d)** a mixture of catecholboryl bromide and catecholboryl hydroxide.

The solution was concentrated in vacuo again and α,α,α-trifluorotoluene (0.100 mmol) was added as an internal standard for HPLC. The reaction mixture was then diluted in 3 mL acetonitrile and 2 mL water to produce a homogeneous solution. Reverse phase HPLC was used to provide yields of catechol **2-5** (75%) and benzyl bromide **2-6** (38%) (see Figure 2.11).

Model lignin monomer **2-7** (25.0 mg, 0.102 mmol, 1.00 equiv) was dissolved in CH$_2$Cl$_2$ (2 mL) and added to a flame-dried 5 mL round bottom flask. The solution was cooled to 0 °C, and BCl$_3$ (160 mL, 1 M in CH$_2$Cl$_2$) was added, followed by BBr$_3$ (160 mL, 1 M in CH$_2$Cl$_2$). The reaction mixture was allowed to come to room temperature and was stirred for 18 h. Solvent was then removed in vacuo and the resulting residue was dissolved in CDCl$_3$ for NMR spectroscopic analysis (Figure 2.10).
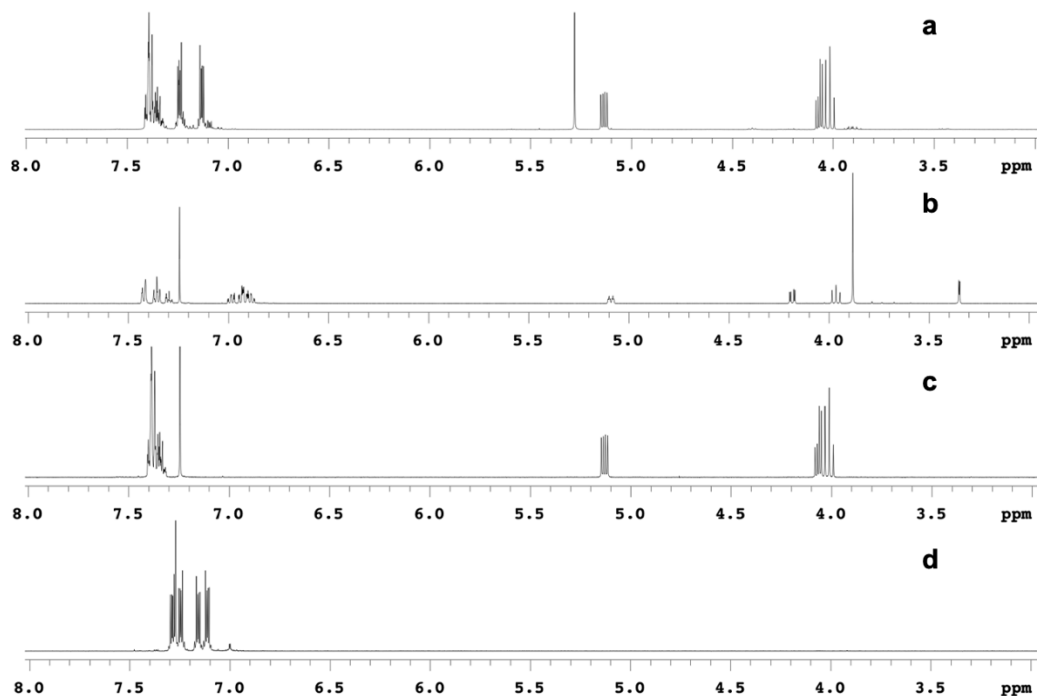
Figure 2.10. ^{1}H NMR (500 MHz, CDCl$_3$) spectrum of crude reaction material for model lignin compound **2-7** compared to ^{1}H NMR of starting material and expected reaction products. **a)** Model lignin compound **2-7** crude reaction. **b)** Model lignin compound **2-7**. **c)** 1,2-dibromoethylbenzene. **d)** a mixture of catecholboryl bromide and catecholboryl hydroxide.

The solution was concentrated in vacuo again and α,α,α-trifluorotoluene (0.100 mmol) was added as an internal standard for HPLC. The reaction mixture was then diluted in 3 mL acetonitrile and 2 mL water to produce a homogeneous solution. Reverse phase HPLC was used to provide yields of catechol **2-5** (80%) and brominated compound **2-8** (quant.) (Figure 2.11).
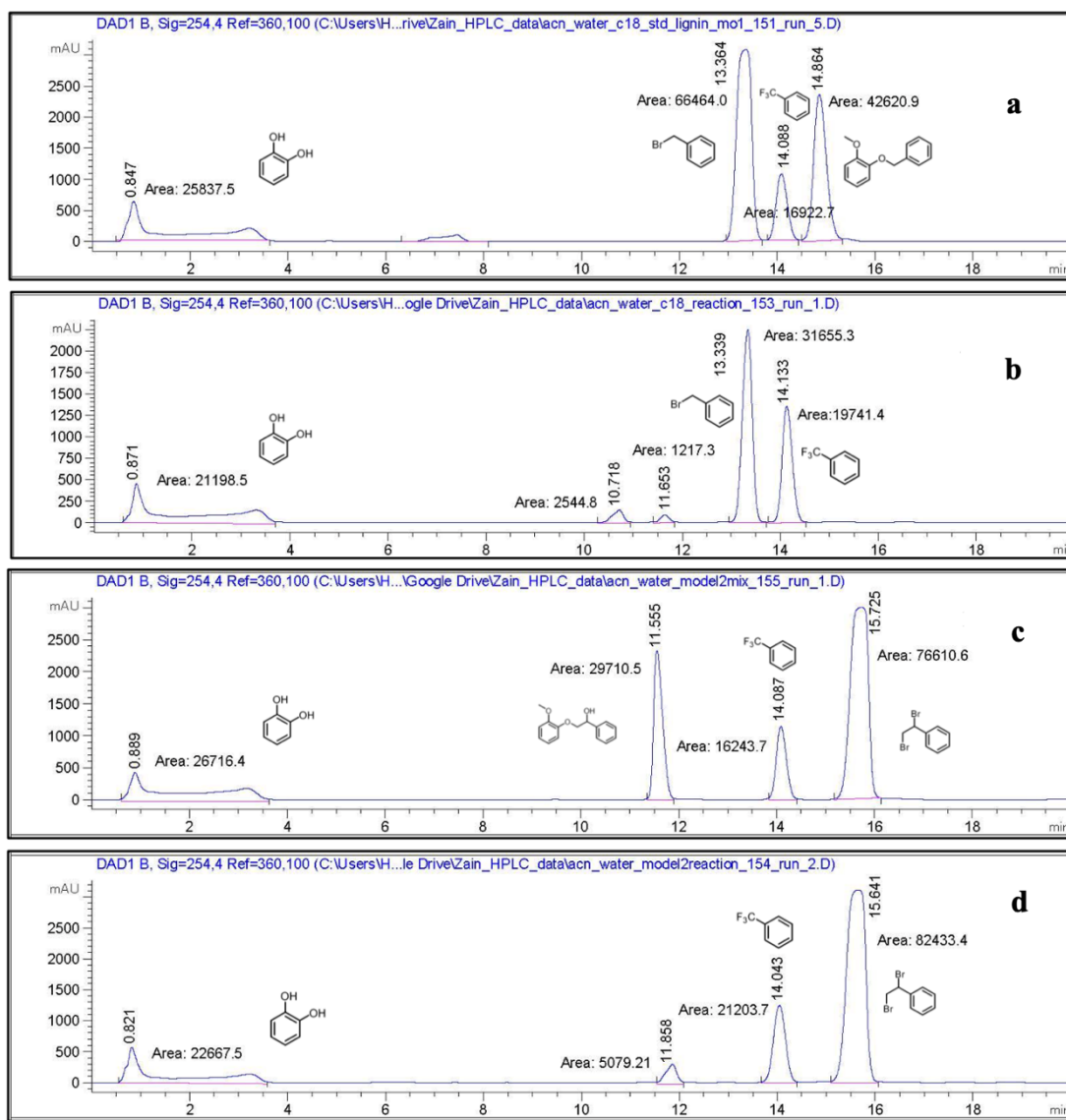
Figure 2.11. HPLC traces of **a) 2-4**:**2-5**:**2-6**:trifluorotoluene (1:1:1:1), **b)** BBr$_3$:BCl$_3$ (1:1) reaction with **2-4**, **c) 2-7**:**2-5**:**2-8**:trifluorotoluene (1:1:1:1), and **d)** BBr$_3$:BCl$_3$ (1:1) reaction with **2-7**.

HPLC conditions (C18, 3 mL/min; solvent A = acetonitrile, solvent B = water): 0–5 min: 10–30% A gradient; 5–10 min: 30–50% A gradient; 10–20 min: 50–60% A gradient. Two standard mixtures of starting materials, expected products, and α,α,α-trifluorotoluene (**2-4**:**2-5**:**2-6**:trifluorotoluene = 1:1:1:1; **2-7**:**2-5**:**2-8**:trifluorotoluene = 1:1:1:1) were analyzed to establish the UV absorption ratios of all components relative to α,α,α-trifluorotoluene. An aliquot (0.4 mL) of reaction solution with α,α,α-trifluorotoluene internal standard was then analyzed by HPLC, and UV absorption intensities at 254 nm were used to quantify yields. Catechol **2-5** R_t = 0.85–0.87 min;

benzyl bromide **2-6** R_t = 13.34–13.36 min; brominated compound **2-8**, R_t = 15.64–15.72 min. Benzyl bromide loss was presumed to have occurred during the removal of solvent in vacuo.

2.6.3 Reaction of Commercial Nanocellulose with BBr₃:BCl₃ Reagent System

To a sample of nanocellulose (0.05 g) in CH_2Cl_2 (3 mL) under vigorous stirring was added BCl_3 (0.8 mL, 1 M in CH_2Cl_2), followed by BBr_3 (0.8 mL, 1 M in CH_2Cl_2). The reaction mixture was stirred for 18 h, filtered through two glass microfibre filter papers, and then rinsed with 5 mL of hot distilled water. The aqueous and organic layers were separated. The organic layer was dried over Na_2SO_4 and filtered and both layers were then concentrated under reduced pressure. NMR spectroscopy was performed on materials extracted into the aqueous layer (Figure 2.12a and 2.12b).

Similarly, nanocellulose was subjected to the same reaction conditions using just BBr_3 (1.6 mL, 1 M in CH_2Cl_2). NMR spectroscopy was performed on materials extracted in the aqueous layer (Figure 2.12c).
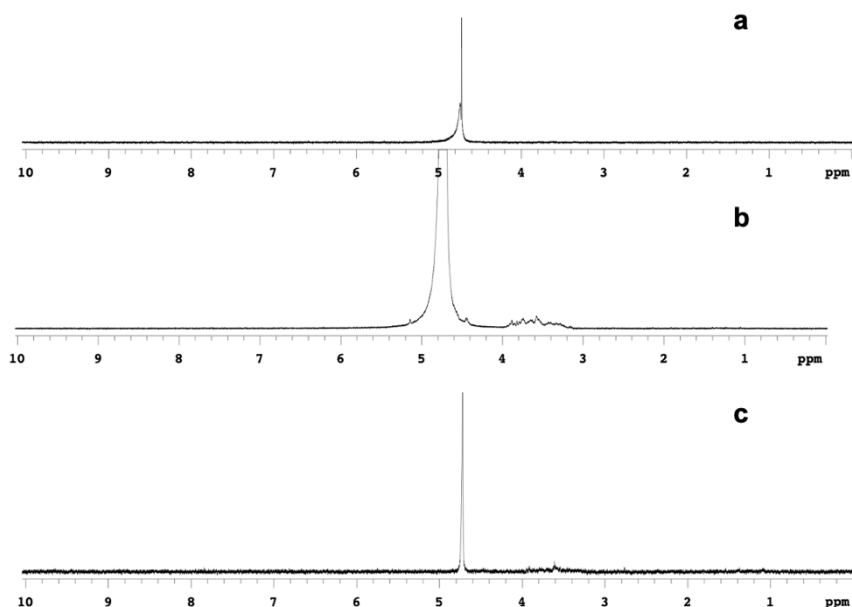
Figure 2.12. ^{1}H NMR (500 MHz, D_2O) spectrum of crude aqueous extract following treatment of commercial nanocellulose with either BCl_3:BBr_3 or BBr_3 alone. **a)** nanocellulose. **b)** Aqueous extract of nanocellulose treated with BCl_3:BBr_3. **c)** Aqueous extract of nanocellulose treated with BBr_3.

2.6.4 Removal of Extractives from White Pine Sawdust[21]

Pine sawdust (4.0 g) was heated at reflux in 50 mL of ethanol-benzene (1:2) for 6 h. The reaction mixture was filtered and washed with 20 mL ethanol. After drying in vacuo, the residual solid was added to 50 mL of ethanol and the mixture was heated at reflux for 4 h. The reaction mixture was filtered and washed with 50 mL water. After drying in vacuo, the residual solid was transferred to a beaker with 120 mL of distilled water, and the mixture was brought to a boil for 1 h. Finally, the mixture was filtered and washed with 150 mL distilled boiling water. The final solid residue obtained after the extract was dried under vacuum (0.10 torr) overnight to yield 3.3 g.

2.6.5 Removal of Polysaccharides from Extractives Free Sawdust

To a mixture of extractives-free pine sawdust (0.50 g) in CH_2Cl_2 (30 mL) under vigorous stirring was added BCl_3 (8.0 mL, 1 M in CH_2Cl_2), followed by BBr_3 (8.0 mL, 1 M in CH_2Cl_2). The reaction mixture was stirred for 18 h, filtered through two glass microfibre filter papers, and then rinsed with 50 mL of hot distilled water. The aqueous and organic layers were separated. The organic layer was dried over Na_2SO_4, filtered and both layers were then concentrated under reduced pressure. The solid material remaining after filtration (solid residue) was dried under high vacuum overnight to give 320 mg solid residue. The reaction sequence was then repeated using this solid residue an additional 3 times to ultimately provide 79 mg of residual solid material for analytical assays (cf. Table 2.1). NMR spectroscopy as well as MALDI mass spectrometry and FT-IR spectroscopy was performed on material extracted into the aqueous layers. FT-IR (Figure 2.13) and microscopic analysis with staining (vide infra) were performed on the residual solid.
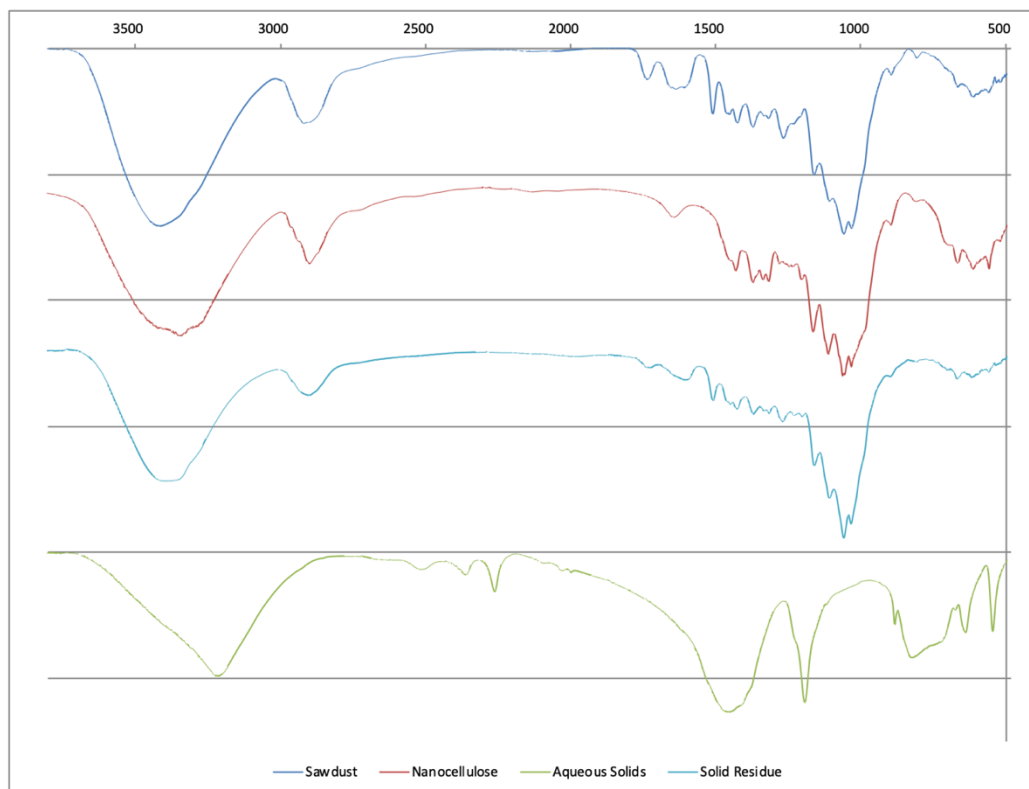
Figure 2.13. FT-IR spectra were acquired using KBr pellet.

2.6.6 One-Pot Boron Trihalide Treatment of Extractives Free Sawdust

To a mixture of extractives-free pine sawdust (0.30 g) in CH_2Cl_2 (20 mL) under vigorous stirring was added BCl_3 (19.2 mL, 1 M in CH_2Cl_2), followed by BBr_3 (19.2 mL, 1 M in CH_2Cl_2). The reaction mixture was stirred for 18 h, filtered through two glass microfibre filter papers, and then rinsed with 30 mL of hot distilled water. The aqueous and organic layers were separated. The organic layer was dried over Na_2SO_4, filtered and both layers were then concentrated under reduced pressure. The solid material remaining after filtration (solid residue) was dried under high vacuum overnight to provide 97 mg of residual solid material (cf. Table 2.1, entry 4).

2.6.7 Dialysis of Aqueous Residue Obtained After Boron Trihalide Treatment of Lignocellulose

Lyophilized aqueous extract from the reaction in Table 2.1, entry 1 (10.7 mg) was dissolved in water (0.5 mL) and dialysed in water (1.0 L, 12 h × 2), resulting in 1.40 mg of material remaining after drying in vacuo. Similarly, lyophilized aqueous extracts

from entries 2–4 (12.5 mg, 25.0 mg and 25.0 mg, respectively) were dialysed in the same manner to provide 2.00 mg, 1.60 mg, and 0.800 mg, respectively. By extrapolating these dialysis yields, the total mass of extracted cellulosic material from the lignocellulose sawdust sample is calculated to be 0.30 g dry weight. MALDI-MS analysis on dialyzed material remains consistent with polymeric and oligomeric cellulose (Figure 2.14).
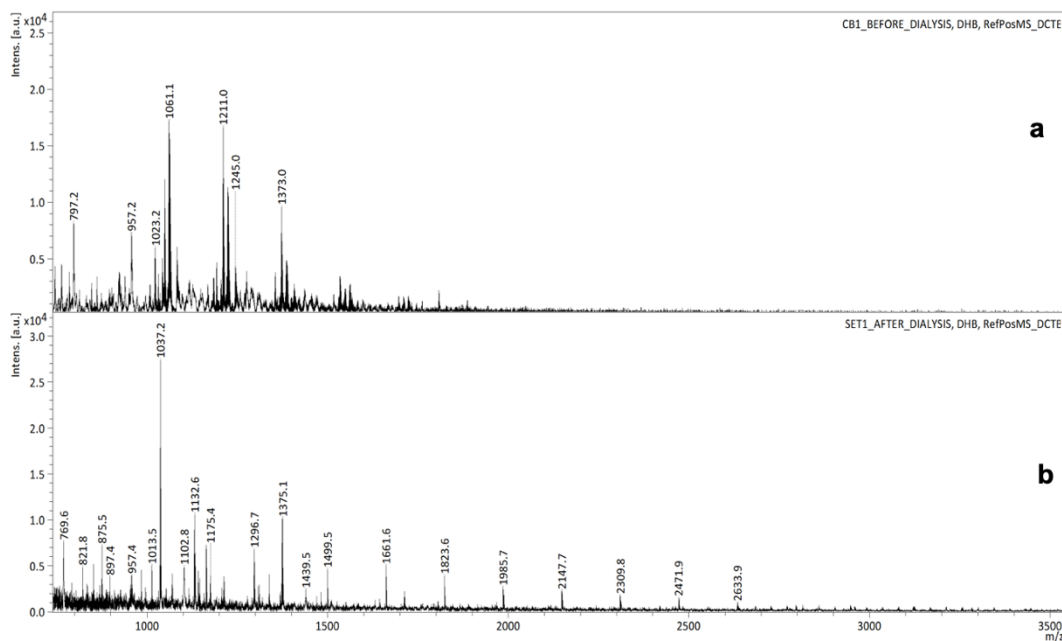
Figure 2.14. MALDI-MS analysis of aqueous extract **a)** before dialysis **b)** after dialysis.

2.6.8 Calcofluor White Staining[25]

Calcofluor White (2.00 mL, 0.1% solution) was dissolved in 98 mL Millipore water to make a stock staining solution (0.002%). Solid compounds (sawdust, residue, lignin, cotton) (2.00 mg each) were added microcentrifuge tubes (2.00 mL) separately followed by stain solution (500 mL). After ten minutes, the tubes were centrifuged. Excess stain was removed (480 mL) and water was added (480 mL) before centrifuging again. The remaining supernatant (480 mL) was removed. A portion (10.0 mL) of the suspension was placed on the glass slide, followed by the addition of 20.0 mL of water before addition of the coverslip, which was fixed to the glass slide. Stained solids were observed through a DAPI filter on an epifluorescence microscope (Nikon eclipse Ti) at 20X magnification (cf. Figure 2.6).

2.6.9 Toluidine Blue O Staining[25]

Toluidine Blue O (20.0 mg) was dissolved in 100 mL Millipore water to make a stock staining solution (0.0200%). Solid compounds (sawdust, solid residue, commercial lignin (TCI), nano-cellulose) (2.0 mg each) were added to microcentrifuge tubes followed by stain solution (500 mL). After five minutes, the tubes were centrifuged. Excess stain was removed (480 mL) and water was added (480mL) before centrifuging again. This process was repeated twice. The remaining supernatant (480 mL) was removed. A portion (10.0 mL) of the suspension was placed in a 6 well plate. Stained solids were observed using bright-field microscopy on a Cytation 5 microscope at 20X magnification (cf. Figure 2.7).

2.6.10 Klason Lignin Extraction[27]

A modified procedure was used. Extractives free sawdust (500 mg) was loaded in a 50 mL beaker with addition of 7.5 mL of a 72 wt. % H_2SO_4. The resulting mixture was left at room temperature for 2 h and stirred with glass rod every 10 min. After 2 h, water (290 mL) was added in the Erlenmeyer flask with the slurry and was boiled for 4 h. Insoluble materials (lignin) were filtered through a fritted glass funnel and rinsed with hot water (200 mL). The fritted glass funnel with lignin was dried in oven (100 °C) for 4 h, which resulted in 165 mg of Klason lignin.

2.6.11 FA Lignin Extraction[27]

Extractives free sawdust (1.00 g) was loaded in a 50.0 mL round bottom flask and was mixed with 9.00 mL dioxane, 420 mL HCl sol (37%) and 1.00 mL formaldehyde (FA) sol (37 wt. % in water). For the control experiment without FA, 690 mL of water was added instead of FA. The reaction vessel was heated to 80 °C (with condenser) and stirred at 300 rpm for 5 h. After the reaction was completed, the slurry was filtered and washed with dioxane until filtrate was colorless. Combined filtrate was then neutralized by addition of sodium bicarbonate (420 mg in 5 mL of water). Solvent was removed under vacuum at 60 °C. The dried residue was then dissolved in 25 mL THF to dissolve the lignin, leaving salts and carbohydrates as precipitates.

Without FA, 288 mg of lignin was obtained and with FA 632 mg of FA lignin was obtained.

2.6.12 Lignin Hydrogenolysis and Monomer Yield Calculations

Lignin (150 mg of B or FA or Klason) with 40 mg Ru/C along with methanol (15 mL) was added in the parr reactor (100 mL). The vessel was purged with H_2 (×3) and pressurized with 480 psi of H_2. The reactor was sealed and then heated to 250 °C using Dowtherm A oil (the oil evaporates so a layer of silicon oil was added at the top along with aluminium foil to minimize evaporation), and the pressure reached 1250 psi. After this temperature was reached, the reactor was heated for an additional 3 h. The reactor was cooled down to rt and the pressure was then released. Insoluble material was filtered (if there was any) and then rinsed with CH_2Cl_2 (10 mL). The filtrate was evaporated and weighed, and the residue obtained after evaporation was dissolved in 5 mL CH_2Cl_2. A portion of this solution (1 mL) was added to an autosample vial followed by the addition of 100 μL of internal standard (8 mg decane in 5 mL 1,4-dioxane). This solution was used for GC-MS analysis with an injection temperature of 250 °C. The set parameters were: 50 °C (1 min), 15 °C/min to 300 °C and then 300 °C (7 min). Split mode was used. The analyses were performed in a set of 3 repeated injections and the percentage yield was calculated by following a literature method as follows:[27]

$$n_{decane} = \frac{W_{decane}}{MW_{decane}}$$

$$n_{monomer} = \frac{A_{monomer\ in\ sample}}{A_{decane\ in\ sample}} \times n_{decane} \times \frac{ECN_{decane}}{ECN_{monomer}}$$

$$W_{monomer} = n_{monomer} \times MW_{monomer}$$

$$Y_{monomer} = \frac{W_{monomer} \times V}{W_{extracted\ lignin}} \times 100\%$$

In the equations,

W_{decane} (mg): the weight of decane in the sample;

MW_{decane} (mg mmol^{-1}): the molecular weight of decane;

n_{decane} (mmol): the moles of decane in the sample;

$n_{monomer}$ (mmol): the moles of monomer in the sample;

$A_{monomer\ in\ sample}$: the peak area of monomer in the GC-MS chromatogram;

$A_{decane\ in\ sample}$: the peak area of decane in the GC-MS chromatogram;

ECN_{decane}: the effective carbon number of decane;

$ECN_{monomer}$: the effective carbon number of the lignin monomer;

$MW_{monomer}$ (mg mmol^{-1}): the molecular weight of the lignin monomer;

$Y_{monomer}$: the yield of monomer based on the weight of extracted lignin;

$W_{extracted\ lignin}$ (mg): the weight of extracted lignin; and

V (mL): the total volume of sample, 1 mL of which was used for GC-MS analysis.

The effective carbon numbers (ECN) were validated by using the responses in the GC-FID by using a solution of commercial samples.[29] The solution was made by dissolving propyl benzene (48.1 mg), guaiacol (49.5 mg) (**M1**), 2,6-dimethoxyphenol (52.2 mg), 3-(4-methoxyphenyl)-1-propanol (54.3 mg), 2-methoxy-4-methyl phenol (52.9 mg) (**M2**), and 2-methoxy-4-ethyl phenol (52.9 mg) (**M3**) in CH_2Cl_2 (50 mL). A portion of this solution (1 mL) was doped with 100 μL of decane (81 mg in 50 mL dioxane).[27] $ECN_{monomer}$ was calculated as follows (Table 2.4):

$$ECN_{monomer}: \frac{A_{monomer}}{A_{decane}} \times \frac{n_{decane}}{n_{monomer}} \times ECN_{decane}$$

The theoretical ECN was calculated for all the commercial compounds as well as for the monomers observed after hydrogenolysis whose commercial samples were not available. The theoretical ECN ($ECN_{theoretical}$) is calculated as follows (Table 2.4):[27,29]

- Addition of 1 unit to the ECN for aliphatic or aromatic carbon atoms;
- Subtraction of 0.6 unit to the ECN for primary hydroxyl groups;
- Subtraction of 1 unit to the ECN for phenolic or ether oxygen.

Table 2.4. Theoretical and Experimental ECN values

Monomers	$ECN_{theoretical}$	$ECN_{monomer}$
propylbenzene	9.0	8.8
M1	5.0	5.5
2,6-dimethoxyphenol	5.0	5.3
3-(methoxyphenyl)-1-propanol	7.4	7.5
M2	6.0	6.0
M4	7.0	7.3

2.7 References

(1)   Nunes, C. S.; Kunamneni, A. Chapter 7 - Laccases—Properties and Applications. In *Enzymes in Human and Animal Nutrition*; Nunes, C. S., Kumar, V., Eds.; Academic Press, 2018; pp 133–161.

(2)   Klemm, D.; Heublein, B.; Fink, H.-P.; Bohn, A. Cellulose: Fascinating Biopolymer and Sustainable Raw Material. *Angew. Chem. Int. Ed.* **2005**, *44*, 3358–3393.

(3)   Boerjan, W.; Ralph, J.; Baucher, M. Lignin Biosynthesis. *Annu. Rev. Plant Biol.* **2003**, *54*, 519–546.

(4)   Ciriminna, R.; Fidalgo, A.; Meneguzzo, F.; Parrino, F.; Ilharco, L. M.; Pagliaro, M. Vanillin: The Case for Greener Production Driven by Sustainability Megatrend. *ChemistryOpen* **2019**, *8*, 660–667.

(5)   Arevalo-Gallegos, A.; Ahmad, Z.; Asgher, M.; Parra-Saldivar, R.; Iqbal, H. M. N. Lignocellulose: A Sustainable Material to Produce Value-Added Products with a Zero Waste Approach—A Review. *Int. J. Biol. Macromol.* **2017**, *99*, 308–318.

(6)   Adler, Erich. Structural Elements of Lignin. *Ind. Eng. Chem.* **1957**, *49*, 1377–1383.

(7)   Lange, H.; Decina, S.; Crestini, C. Oxidative Upgrade of Lignin – Recent Routes Reviewed. *Eur. Polym. J.* **2013**, *49*, 1151–1173.

(8)   Renders, T.; van den Bosch, S.; Koelewijn, S.-F.; Schutyser, W.; Sels, B. F. Lignin-First Biomass Fractionation: The Advent of Active Stabilisation Strategies. *Energy Environ. Sci.* **2017**, *10*, 1551–1557.

(9)   Sturgeon, M. R.; Kim, S.; Lawrence, K.; Paton, R. S.; Chmely, S. C.; Nimlos, M.; Foust, T. D.; Beckham, G. T. A Mechanistic Investigation of Acid-Catalyzed Cleavage of Aryl-Ether Linkages: Implications for Lignin Depolymerization in Acidic Environments. *ACS Sustain. Chem. Eng.* **2014**, *2*, 472–485.

(10)   Chung, H.; Washburn, N. R. 2 - Extraction and Types of Lignin. In *Lignin in Polymer Composites*; Faruk, O., Sain, M., Eds.; William Andrew Publishing, 2016; pp 13–25.

(11)   Gratzl, J. S.; Chen, C.-L. Chemistry of Pulping: Lignin Reactions. In *Lignin: Historical, Biological, and Materials Perspectives*; ACS Symposium Series; American Chemical Society, 1999; Vol. 742, pp 392–421.

(12)   See, A. S.; Salleh, A. B.; Bakar, F. A.; Yusof, N. A.; Abdulamir, A. S.; Heng, L. Y. Risk and Health Effect of Boric Acid. *Am. J. Appl. Sci.* **2010**, *7*, 620–627.

(13)   Ranu, B. C.; Bhar, S. Dealkylation of Ethers. A Review. *Org. Prep. Proced. Int.* **1996**, *28*, 371–409.

(14)   Kosak, T. M.; Conrad, H. A.; Korich, A. L.; Lord, R. L. Ether Cleavage Re-Investigated: Elucidating the Mechanism of BBr_3-Facilitated Demethylation of Aryl Methyl Ethers. *Eur. J. Org. Chem.* **2015**, *2015*, 7460–7467.

(15)   Benton, F. L.; Dillon, T. E. The Cleavage of Ethers with Boron Bromide. I. Some Common Ethers. *J. Am. Chem. Soc.* **1942**, *64*, 1128–1129.

(16)   Bhatt, M. V.; Kulkarni, S. U. Cleavage of Ethers. *Synthesis* **1983**, *1983*, 249–282.

(17)   Bessac, F.; Frenking, G. Why Is BCl_3 a Stronger Lewis Acid with Respect to Strong Bases than BF_3? *Inorg. Chem.* **2003**, *42*, 7990–7994.

(18)   Atienza, B. J. P.; Truong, N.; Williams, F. J. Reliably Regioselective Dialkyl Ether Cleavage with Mixed Boron Trihalides. *Org. Lett.* **2018**, *20*, 6332–6335.

(19)   Ding, T.; Wu, Y.; Zhu, X.; Lin, G.; Hu, X.; Sun, H.; Huang, Y.; Zhang, S.; Zhang, H. Promoted Production of Phenolic Monomers from Lignin-First Depolymerization of Lignocellulose over Ru Supported on Biochar by N,P-Co-Doping. *ACS Sustain. Chem. Eng.* **2022**, *10*, 2343–2354.

(20) Kazmi, M. Z. H.; Karmakar, A.; Michaelis, V. K.; Williams, F. J. Separation of Cellulose/Hemicellulose from Lignin in White Pine Sawdust Using Boron Trihalide Reagents. *Tetrahedron* **2019**, *75*, 1465–1470.

(21) Buchanan, M. Solvent Extractives of Wood and Pulp, Technical Association of the Pulp and Paper Industry, *T204cm-97*, **2007**, 1–6.

(22) Wiselogel, A.; Tyson, J.; Johnsson, D. Biomass Feedstock Resources and Composition. In *Handbook on Bioethanol: Production and Utilization*; Wyman, C. E., Ed.; Taylor & Francis: New York, 1996; pp 105–118.

(23) Risanto, L.; Hermiati, E.; Sudiyani, Y. Properties of Lignin from Oil Palm Empty Fruit Bunch and Its Application for Plywood Adhesive. *Makara J. Technol.* **2014**, *18*, 67.

(24) Wood, P. J. Specificity in the Interaction of Direct Dyes with Polysaccharides. *Carbohydr. Res.* **1980**, *85*, 271–287.

(25) Mitra, P. P.; Loqué, D. Histochemical Staining of Arabidopsis Thaliana Secondary Cell Wall Elements. *J. Vis. Exp.* **2014**, *87*, 51381.

(26) O'Brien, T. P.; Feder, N.; McCully, M. E. Polychromatic Staining of Plant Cell Walls by Toluidine Blue O. *Protoplasma* **1964**, *59*, 368–373.

(27) Li, S.; Talebi, A. M.; M, Q.-S. Y.; Florent, H.; Yanding, L.; Hoon, K.; Richard, M.; Clint, C.; John, R.; S, L. J. Formaldehyde Stabilization Facilitates Lignin Monomer Production during Biomass Depolymerization. *Science* **2016**, *354*, 329–333.

(28) Vékey, K. Mass Spectrometry and Mass-Selective Detection in Chromatography. *J. Chromatogr. A* **2001**, *921*, 227–236.

(29) Scanlon, J. T.; Willis, D. E. Calculation of Flame Ionization Detector Relative Response Factors Using the Effective Carbon Number Concept. *J. Chromatogr. Sci.* **1985**, *23*, 333–340.

(30) Li, X.; He, J.; Zhang, Y. BBr3-Assisted Preparation of Aromatic Alkyl Bromides from Lignin and Lignin Model Compounds. *J. Org. Chem.* **2018**, *83*, 11019–11027.

(31) Hämäläinen, V.; Grönroos, T.; Suonpää, A.; Heikkilä, M. W.; Romein, B.; Ihalainen, P.; Malandra, S.; Birikh, K. R. Enzymatic Processes to Unlock the Lignin Value. *Front. Bioeng. Biotechnol.* **2018**, *6*.

Chapter 3: Acidity, Aromaticity, and Stability Studies of Novel Boranol-Containing Naphthalene Analogs[1]

3.1 Introduction

Boron-containing heterocycles have immense importance in catalysis, materials science, and pharmaceutical chemistry (Figure 3.1).[1–4] For example, recently Hall and co-workers reported the applications of boron-containing heterocycles towards the enantioselective desymmetrization of diols as well as in biorthogonal conjugation.[5,6]
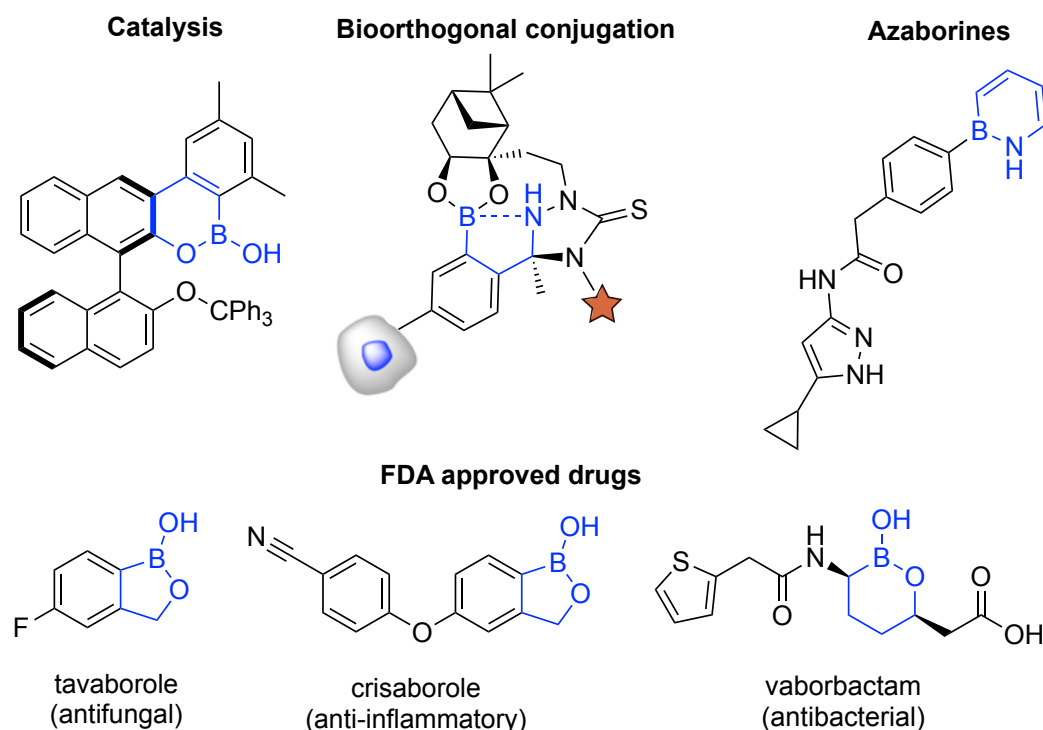
Figure 3.1. Applications of boron-containing heterocycles.

During the past decade, three drugs containing a boron heterocycle were approved by the FDA: tavaborole, crisaborole, and vaborbactam (Figure 3.1). There

---

are many other boron-containing heterocycles that are in various phases of clinical trials.[1] Generally, these boranol (B—OH) compounds possess a unique capability to exchange their hydroxy group with alcohols that are present on the target receptors. For example, looking more closely into the mechanism of action of tavaborole, it forms a tetravalent boron center with adenosine monophosphate (AMP) molecule, therefore, showing the importance of the B—OH moiety (Figure 3.2).[7]
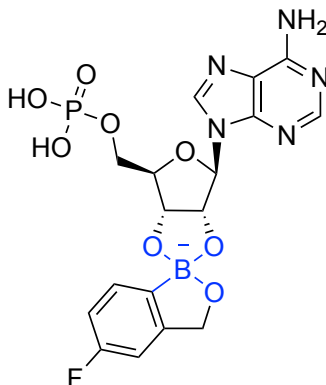
Figure 3.2. Tavaborole interaction with AMP exhibiting a tetrahedral boron center.

Isosteres possess functional groups that mimic the parent molecules but demonstrate different physicochemical properties. For instance, replacement of a C=C bond with a B—N/B—O bond leads to an isosteric molecule. A well-known boron-containing heterocycle, 1,2-azaborine, is one such example and is a pseudoaromatic compound. These azaborines have shown great potential in medicinal chemistry as an isostere of benzene.[8] For example, an analog of 1,2-azaborine displayed improved bioactivity, solubility, and bioavailability as compared to its carbon-based analog (Figure 3.1).[9] Two other examples of isosteres are hemiboronic acids, benzoxazaborine (**3-1**) and benzodiazaborines (**3-2** and **3-3**), which are isoelectronic to 4-hydroxyisoquinoline (**3-4**) or 1-hydroxynaphthalene (**3-5**) (Figure 3.3).
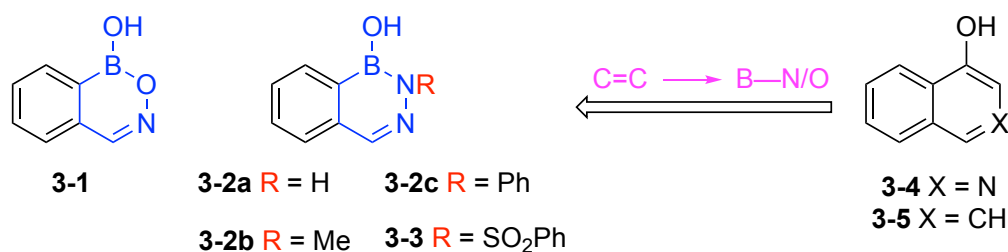
Figure 3.3. Isosterism shown for benzoxazaborine (**3-1**) and benzodiazaborines (**3-2** and **3-3**).

Hemiboronic acids are important, as they have shown great potential in catalysis and in drug discovery.[3,10] *N*-Sulphonyl containing benzodiazaborines, in particular, have shown antibacterial properties by inhibiting the enoyl reductase enzyme involved in the synthesis of fatty acids. The inhibition is caused by way of covalent bond formation between the 2′-hydroxyl group of the nicotinamide ribose and the boron atom of benzodiazaborine.[11]

The interesting applications of hemiboronic acids in drug discovery encourage further exploration of the properties of the aforementioned boron-containing naphthoid isosteres (Figure 3.3). Therefore, the results described in this chapter will help provide a more thorough understanding of aromatic character, acidity, and stability of heterocycles **3-1**–**3-3**, which can help optimize the scaffolds to tailor their use in medicinal chemistry, material science, and catalysis. In spite of the great potential of these hemiboronic heterocycles (**3-1**–**3-3**) in drug discovery, for several decades there has been confusion over these compounds' properties. Considering the lone pair donation of an O or N atom into the vacant *p* orbital of the boron atom in these benzoxazaborine and benzodiazaborine scaffolds, the boron-containing ring has six π electrons and, therefore, obeys Hückel's rule of aromaticity (Figure 3.4a). Still, there has been a long debate (vide infra) over their aromatic character, which also relates to their acidic character. If these molecules (**3-1**–**3-3**) are considered purely aromatic, then their conjugate bases would prefer to display an sp^2 hybridization of the boron atom and will exist in the oxide form **II** and not in their tetrahedral form (sp^3) **I** (Figure 3.4b). The reason is that in their oxide form **II**, these boron heterocycles (**3-1**–**3-3**) would retain their aromaticity, whereas in their tetrahedral form **I**, they would lose extended conjugation in the boron containing ring. If the conjugate base exists in form **II**, the

acid precursor would be considered a Brønsted acid, and if it exists in form **I**, it would behave as a Lewis acid. Moreover, there was no data to support the kinetic stability of these compounds (Figure 3.4c).
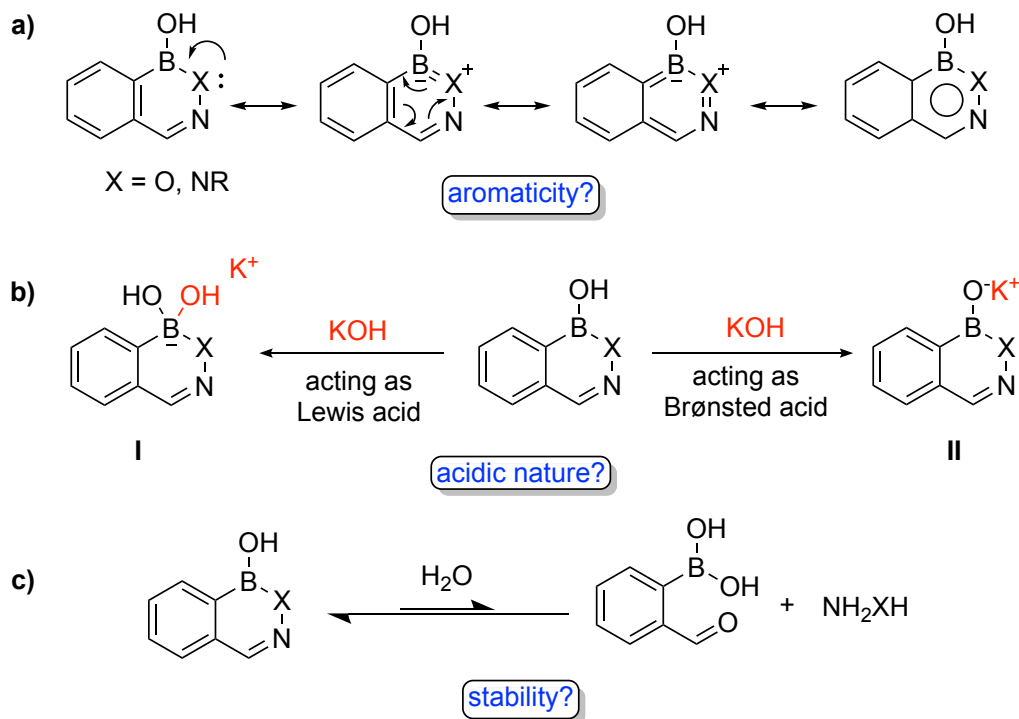
Figure 3.4. Questions raised for boron-containing rings over **a)** aromaticity **b)** acidity, and **c)** stability.

Indeed, there has been no comprehensive work on determining the aforementioned properties (aromaticity, acidity, and kinetic stability) of these boron-containing heterocycles (**3-1**–**3-3**). The X-ray crystal structure of the conjugate bases would help reveal whether these molecules exist in form **I** or **II** in the solid-state. In addition, the ^{11}B NMR spectra of the conjugate bases would assist in revealing their acidic nature (form **I** or **II**) in solution-phase (vide infra). Elucidating the aromatic character by density functional theory (DFT) calculations would offer insight towards the extent of aromaticity, and their behavior in aqueous conditions would give an indication of kinetic stability. A clear understanding of these properties will assist in utilizing the boron-containing heterocycles **3-1**–**3-3** to their full capability.

3.2 Debate Regarding Properties of Boron-Containing Heterocycles

Heterocycles **3-1**–**3-3** have been known for a long time, but there has been significant debate and confusion over their properties. In 1958, Snyder and co-workers found that the product obtained from the reaction of hydroxylamine with *ortho*-formyl phenylboronic acid had one less water molecule as compared to oxime formation.[12] This molecule was presumed to be the cyclic boronic acid **3-1**. In 1962 and 1964, Dewar and Dougherty synthesized the aza analogs **3-2a**, **3-2b**, and **3-2c** (cf. Figure 3.3).[13,14] When reacting **3-2a** and **3-2c** with concentrated hydrochloric acid or with potassium hydroxide, no cleavage (or hydrolysis) of the B—C bond of the heterocycles was observed, which is contrary to aliphatic hydrazones or aromatic boronic acids that normally decompose under these reaction conditions.[13] The reaction of benzodiazaborine **3-2a** with methylmagnesium bromide resulted in the formation of **3-6** (Figure 3.5a). In contrast, benzoxazaborine **3-1** did not furnish the methylated derivative **3-7** (Figure 3.5a).
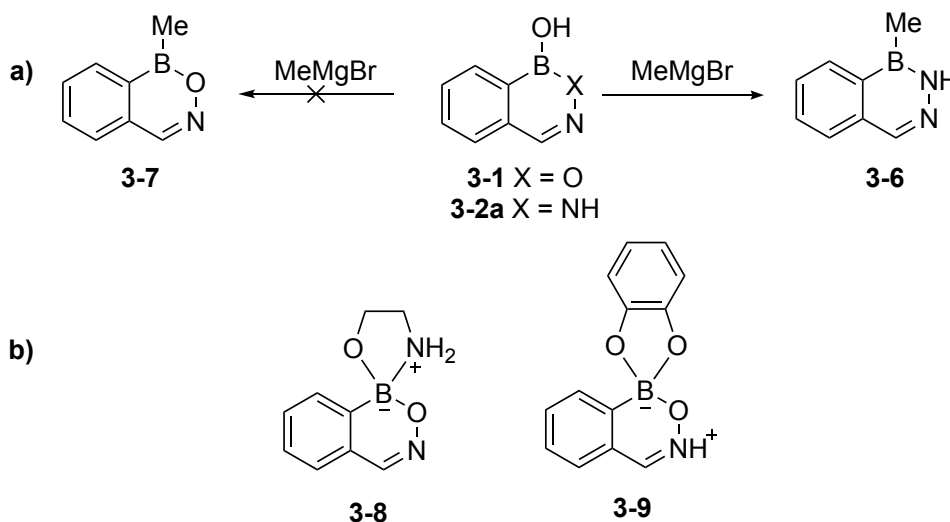
Figure 3.5. a) Reaction of MeMgBr with **3-1** or **3-2a**. **b)** Adducts reported in 1960s.

Based on all these observations, **3-2a** and **3-2c** were defined "very" aromatic and **3-1** "less" aromatic, with no definite explanation. In addition, the tetrahedral adduct of **3-1** (**3-8**) was synthesized, but the similar adduct of **3-2a** could not be achieved, to which authors again implied more aromatic character in **3-2a** as compared to **3-1**

(Figure 3.5b).[14] The ultraviolet (UV) spectrum of aromatic boronic acids, which are known to be Lewis acids, normally shows a hypsochromic shift under alkaline conditions.[13] The UV spectrum of **3-1** under the same conditions showed a bathochromic shift and, therefore, was considered a protic acid (Brønsted acid).[13] Similarly, **3-2a** in solution was declared a Brønsted acid.[14]

With the advent of NMR spectroscopy, Dewar and Jones in 1967 reported the ^{11}B NMR signal for these boron-containing heterocyclic compounds (**3-1** and **3-2a**).[15] The chemical shift of the boron peak by ^{11}B NMR spectroscopy reflects the hybridization and valency of the boron center in any boronic acid derivative. Generally, the resonance of neutral trivalent boronic acids, or hemiboronic acids, lies in the range of 28–30 ppm. On the other hand, boronic acids, which are Lewis acids, convert into their boronate form when reacting with Brønsted bases (salt formation), with a [11]B peak in the range of 0–5 ppm, which confirms that they exist in a tetracoordinate form. Therefore, knowing the chemical shifts of these heterocycles in neutral or basic conditions can provide evidence for the structure of the conjugate base and, consequently, can help determine their acidic nature (Lewis vs Brønsted) (Figure 3.6).
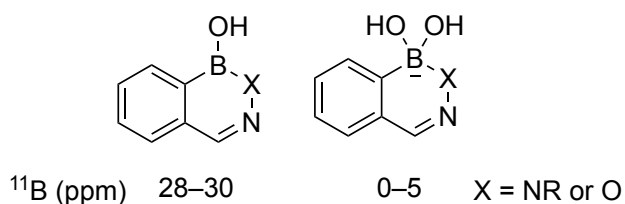
Figure 3.6. Expected [11]B chemical shifts for trivalent and tetracoordinate boron centers.

The authors analyzed compounds **3-1** and **3-2a** by ^{11}B NMR spectroscopy.[15] For the neutral form of **3-1**, the [11]B peak appeared at 30 ppm (in EtOH). Under basic conditions (20% KOH in EtOH), the [11]B peak appeared at 5 ppm. This result indicates that **3-1** is Lewis acidic and exists in the tetrahedral form **I** under basic conditions (Figure 3.4b). Even though this [11]B chemical shift data contradicted the results the authors obtained in 1962 by UV spectroscopy (vide supra) (which indicated **3-1** to be a Brønsted acid), Dewar and co-workers relied on unambiguous ^{11}B NMR spectroscopy results and concluded that **3-1** is indeed a Lewis acid. For **3-2a**, the authors did not

observe any significant change under basic conditions (20% KOH in EtOH) as compared to neutral conditions (EtOH) and, therefore, concluded that **3-2a** is a Brønsted acid and that its larger aromatic character inhibits the formation of a tetrahedral boron, which would otherwise disrupt the aromaticity in the boron-containing ring. Later in 1968, Snyder and co-workers reported the formation of diol adduct **3-9** by reaction between catechol and **3-1** (Figure 3.5b).[16] This adduct again confirmed the Lewis acidity of **3-1** and implied a lack of appreciable aromatic character, which would otherwise prohibit the formation of a tetravalent adduct.

Finally, in 1997, using new techniques, Groziak and co-workers explored the structural and chemical properties of **3-1** and **3-2a** using multinuclear NMR spectroscopy, X-ray crystallography of neutral compounds, and B—OH exchange using an $H_2^{18}O$ labelling experiment.[17] The authors also reinvestigated the acidic character of **3-1** and **3-2a**. First, the reaction between **3-1** and **3-2a** with MeOH was performed. The authors observed the formation of the B—OMe derivative of **3-1** (**3-10**) but not for **3-2a** (**3-11**) (Figure 3.7a). Even under forced conditions (65 °C, 24–30 h) **3-2a** resisted the formation of **3-11** on reaction with anhydrous MeOH. Later, the authors performed an $H_2^{18}O$ labelling experiment where **3-1** and **3-2a** were subjected to an excess of $H_2^{18}O$ in CH_3CN solution at 75 °C and observed the extent of labelling by acquisition under mass spectrometry.[17] The results obtained were contradictory to the MeOH exchange experiment. As compared to **3-1**, **3-2a** readily exchanged its B—OH bond to a B—^{18}OH bond (Figure 3.7b). Interestingly, the conflicting results between MeOH exchange and $H_2^{18}O$ exchange experiments led Groziak to claim that **3-2a** has a more pronounced Lewis acidic character as compared to **3-1**.[17] Following this claim, the authors executed NMR spectroscopy on these compounds. When changing solvent from CD_3CN to DMSO-d_6, the ^{1}H NMR spectra of compounds **3-1** and **3-2a** exhibited a downfield shift of the B—OH proton, which can be explained by the increased H-bond accepting ability of DMSO-d_6. The change in chemical shift was more pronounced in **3-1** as compared to **3-2a**. On account of these NMR experiments, without any further explanation, **3-1** was considered to be a Brønsted acid.[17]
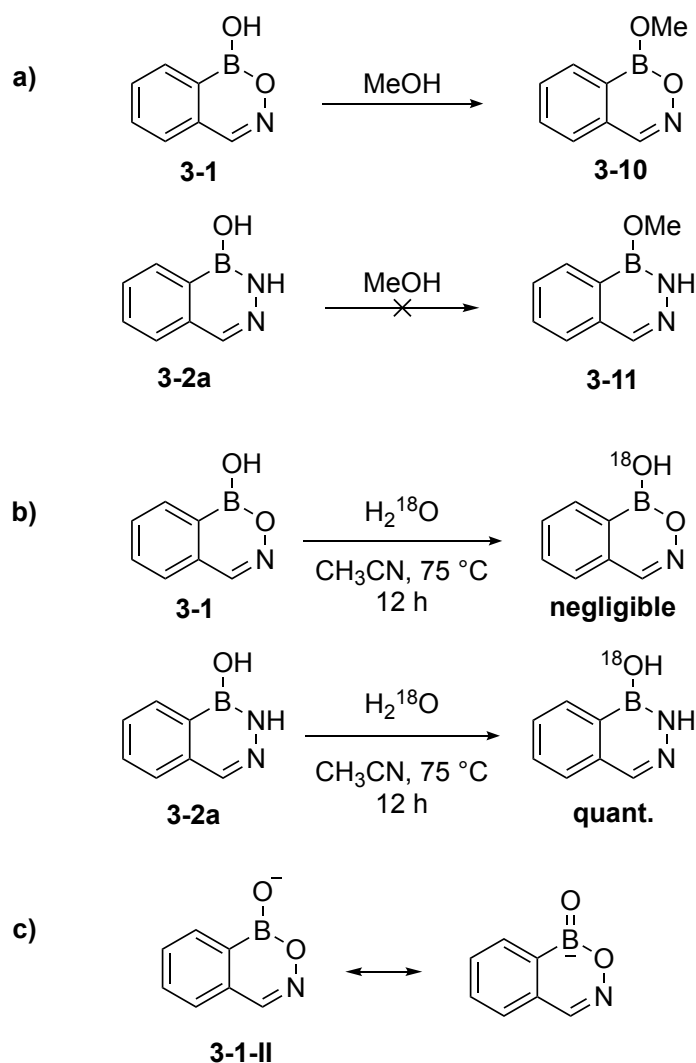
Figure 3.7. Exchange of B—OH with **a)** MeOH **b)** $H_2{}^{18}O$ and **c)** proposed conjugate base of **3-1**.[17]

Finally, the authors measured the compounds' [11]B chemical shift in alkaline conditions (aq. NaOH). Just like the observations made by Dewar,[15] Groziak also observed an upfield [11]B chemical shift for **3-1** but not for **3-2a**. Contrary to Dewar's conclusion, strangely, Groziak and co-workers claimed **3-1** to be a Brønsted acid. The upfield chemical shift in **3-1** was attributed to the trigonal planar form **3-1-II** (Figure 3.7c). Here, the authors suggested that the oxyanion can donate into the empty *p* orbital of boron atom, resulting in an upfield chemical shift, although there is no literature evidence of chemical shift for such a molecule in aqueous solution. The lack of change in the [11]B chemical shift in alkaline conditions for **3-2a** was attributed to its

designation as a Brønsted acid. In this case, the proposed explanation provided was that **3-2a** does indeed form the oxyanion structure, just like **3-1-II.** However, as claimed by the authors, the oxyanion does not donate to the empty *p* orbital of boron atom due to the electrostatic repulsion from *p* electrons from the adjacent nitrogen atom and, therefore, does not result in an upfield chemical shift.

Though, the pK_a of compounds **3-1** (4.8) and **3-2**–**3-3** (~8.0) were determined by Groziak and co-workers, they were measured potentiometrically.[17] The pK_a of boronic acids can be obtained with good reliability by ^{11}B NMR titration experiment.[18–20] Knowledge of pK_a is fundamental in drug discovery. For example, benzoxaborole, which is the pharmacophore of tavaborole and crisaborole (Figure 3.1), has a pK_a of 7.4. Therefore, at physiological pH, the molecule can exist in near-equal proportions in both the trivalent and tetravalent form and can undergo a variety of interactions with protein targets (Figure 3.8).
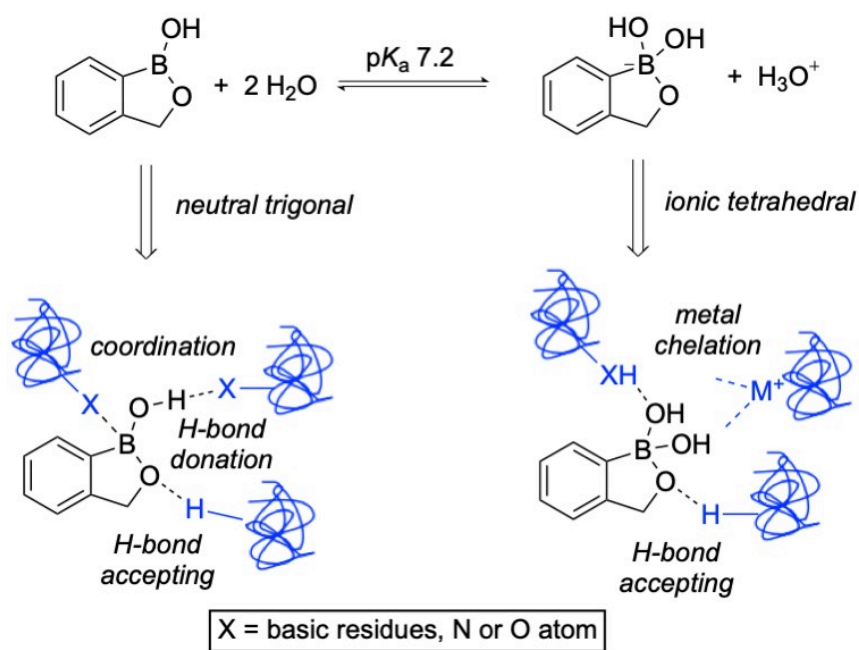
Figure 3.8. Equilibrium between trivalent and tetravalent forms of benzoxaborole.

The pK_a measurement by ^{11}B NMR titration can be performed by recording the [11]B chemical shift of a solution of a desired compound at varying pH levels (generally 2–13 pH range) (Figure 3.9, see Section 3.9.7 for details regarding calculations). [20]
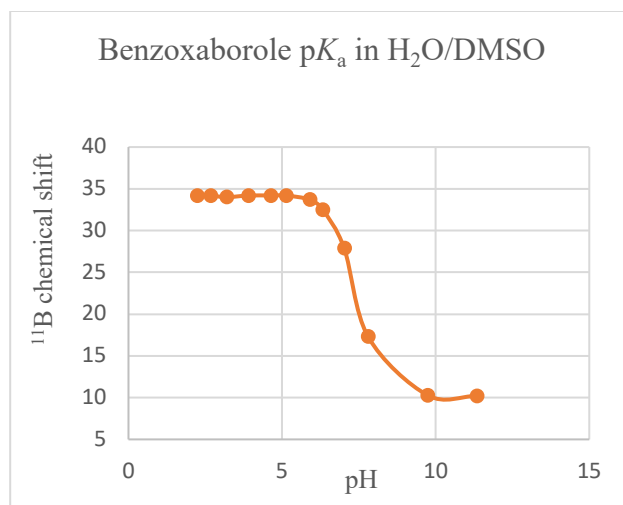
Figure 3.9. pK_a determination of benzoxaborole in aqueous solution with minimal DMSO.

Groziak and co-workers reported the X-ray crystal structures of **3-1** and **3-2a** but did not report a conjugate base crystal structure to prove the acidic nature of these boron-containing heterocycles, and so **3-1** and **3-2a** were concluded to be Brønsted acids.[17] Recently, Bane and Gillingham have studied the *N*-aryl/acyl derivatives of **3-2**, but their structures of conjugate base were still in question.[21–23]

3.3 Heterocycles Used in the Study

The heterocycles chosen for this study were **3-1**, **3-2a**, **3-2b**, **3-2c**, and **3-3** (Figure 3.10). They were synthesized by condensation of hydroxylamine or hydrazines with *ortho*-formyl phenylboronic acid. Some key ^{1}H and [11]B chemical shifts of these heterocycles as well as comparators were recorded in d_6-acetone (Figure 3.10).
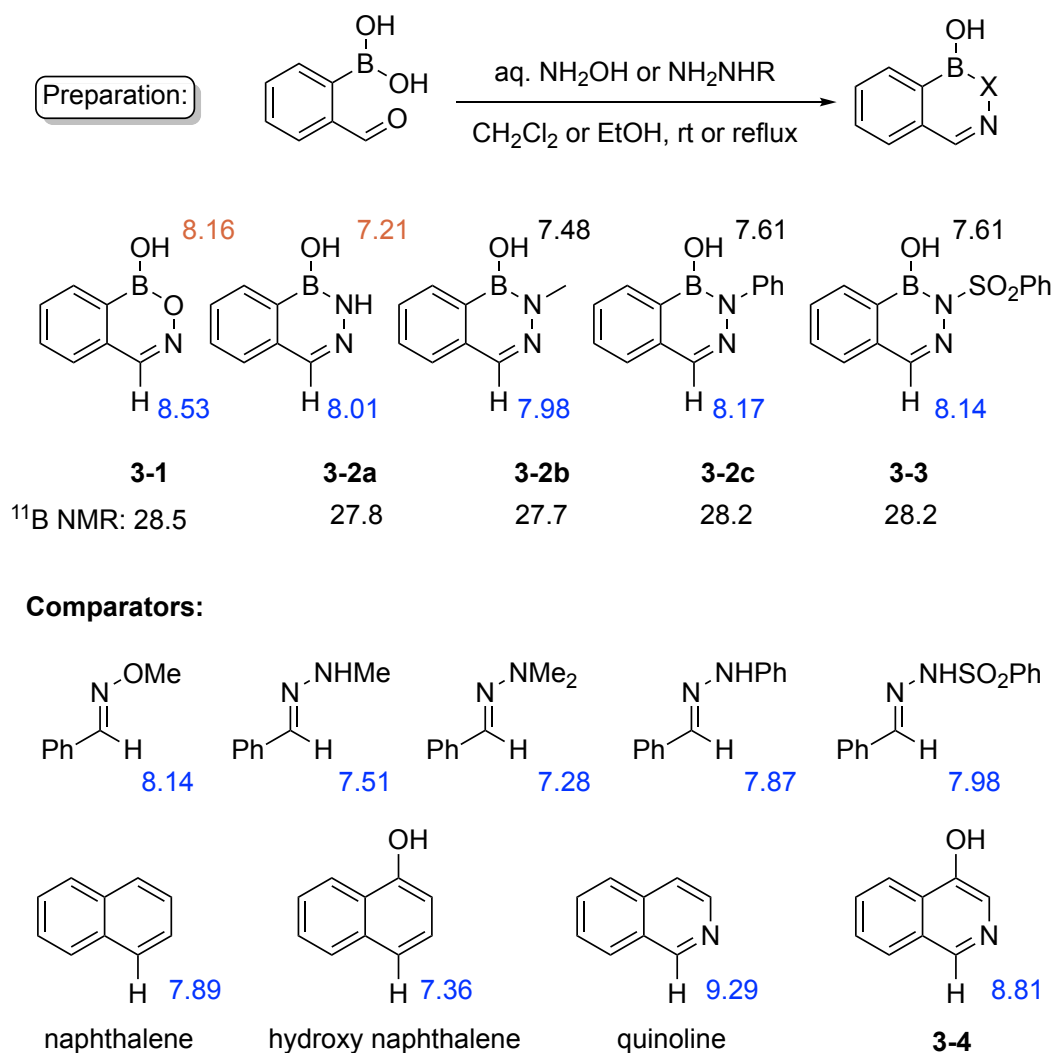
Figure 3.10. Key ^{1}H and [11]B chemical shifts of **3-1**, **3-2** and **3-3** with comparators (all shifts in ppm; solvent: d_6-acetone). (Some compounds were synthesized by Jason Rygus, Dr. Hwee Ting Ang, and Dr. Marco Paladino).
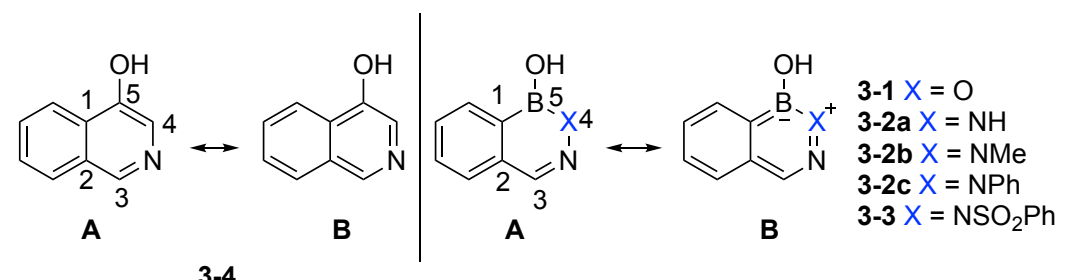
The [11]B chemical shifts are very similar for all compounds. In contrast, according to the ^{1}H NMR spectra of the model compounds, the B—OH proton of **3-1** is the most downfield, whereas for **3-2a**, it is the furthest upfield. The aldimine proton chemical shifts of all model compounds were found to be upfield as compared to their isostere 4-hydroxyisoquinoline **3-4**.[24] Upon comparing these chemical shifts with acyclic oximes or hydrazones, they are relatively downfield. The difference in chemical shifts, especially in **3-2a** and **3-2b**, hints at some aromaticity due to the anisotropy effect in these boron-containing heterocycles, but at the same time it could be due to other electronic factors, such as the electron withdrawing effect of boron.

To determine the aromaticity of the model compounds, DFT calculations were performed (see Section 3.4). A series of reactions and analyses were executed to establish their dynamic stability (solvent exchange methods and by cross-exchange between different heterocycles) (see Section 3.5). The pK_a of these naphthoid molecules (3-1–3-3) were measured by ^{11}B NMR titration experiments (see Section 3.6). Finally, the X-ray crystal structures of conjugate bases of 3-1, 3-2d (vide infra), and 3-3 were obtained to confirm their acidic nature (see Section 3.7).

3.4 Assessment of Aromatic Character

Density functional theory (DFT) calculations for ground-state equilibrium geometry and molecular orbitals of heterocycles 3-1, 3-2a, 3-2b, 3-2c, and 3-3 were performed by Dr. Dennis Hall using ωB97X-D/6-31G* level.[25] In addition, some key bond orders were compared with their C=C isostere, 4-hydroxyisoquinoline 3-4 (C=C isosterism with B—N/O)[9,26] (Table 3.1).

Table 3.1. Key Bond Orders for DFT (ωB97X-D/6-31G*) Optimized Structures

Bond order[a]	3-4	3-1	3-2a	3-2b	3-2c	3-3
B—OH	1.280 (C^5—OH)	1.512	1.456	1.452	1.472	1.551
C^1—B	1.231 (C^1—C^5)	1.041	1.056	1.062	1.057	1.043
B—X	1.528 (C^5=C^4)	1.357	1.325	1.276	1.232	1.172
X—N	1.461 (C^4—N)	1.217	1.319	1.293	1.263	1.251
N=C^3	1.765	2.004	1.931	1.914	1.929	1.951
C^2—C^3	1.273	1.127	1.153	1.158	1.150	1.138

[a]Lowdin bond order

Two resonance forms, **A** and **B** can be considered. Since **3-4** is an aromatic compound, all the bond orders in the *N*-containing ring are fractional, showing the contribution from both forms **3-4A** and **3-4B**. Therefore, **3-4** has very delocalized electron density in the *N*-containing ring. For the boron-containing heterocycles, the bond orders indicate less contribution from resonance form **B**, and therefore, more localized electron density. For example, comparing the bond orders of C^1—C^5/C^1—B, all boron-containing heterocycles have bond order values close to one indicating a single bond character as compared to **3-4**. Next, examining the B—X/C^5—C^4 bond orders, compounds **3-2a** and **3-2b** possess values of 1.325 and 1.276, respectively. This indicates double bond character, thus suggesting that they are fairly good isoelectronic mimics of the C=C bond of **3-4** (1.528). Particularly, **3-1** with a bond order of 1.357, proves to be the best mimic of the C=C bond of **3-4**. It is noteworthy that the bond orders of **3-1** are very different as compared to the aza analogs **3-2a**, **3-2b**, and **3-2c**. Heterocycle **3-1** has the lowest bond order for C^1—B (1.041) and the highest for N=C^3 (2.004), indicating minimal delocalization of its electron density in the boron-containing ring as compared to its aza analogs. Aza congeners show more delocalization in the boron-containing ring, which can be seen from their respective higher bond orders of C^1—B and lower bond orders of N=C^3. Another interesting parameter to note is the bond orders of B—OH for boron-containing heterocycles as compared to the bond order of C^5—OH of **3-4**. The boron atom has a vacant *p* orbital, allowing the oxygen atom to donate one of its lone pairs of electrons into the boron atom, generating more double bond character, which is indicated by the higher bond order of ~1.5 for B—OH in boron-containing heterocycles. On the other hand, the bond order of the C^5—OH bond in **3-4** is lower (1.28) since the oxygen atom can only donate into an antibonding π^* orbital.

Frontier molecular orbitals and electrostatic potential maps of the aforementioned compounds also were calculated. Remarkably, the HOMO orbitals of these heterocycles are very distinct from their isostere **3-4**, whose orbitals are extremely symmetrical (Figure 3.11). Amongst the boron-containing heterocycles, there is an overlap between the B—N and C^1—B bonds in the HOMO orbitals of **3-2a** and **3-2b**.

There is no such overlap in **3-1**, **3-2c**, and **3-3**, indicating that these species have less delocalization of the π electrons from the benzenoid ring into the boron-containing ring, as compared to **3-2a** and **3-2b**. This is expected due to the less basic nature of *O-* or *N-*aryl/sulfonyl atom/group. These results corroborate nicely with the electrostatic potential maps as well. An electrostatic potential map displays attractive and repulsive forces experienced by a positively charged species at various points near the surface of the molecule in question.[27] Therefore, the electrostatic potential map can be used to easily visualize the distribution of electron density in a molecule. Red colored regions correspond to an excess of electron density (attraction by the positively charged species), whereas a blue color corresponds to the regions with low electron density (repulsion by the positively charged species). Intermediate electron density is displayed by using green and orange colors. Based on the electrostatic potential maps of heterocycles **3-1**–**3-4**, contrary to **3-1** and **3-3**, boron heterocycles **3-2a**, **3-2b,** and to some extent **3-2c**, look similar to **3-4** (C=C isostere). Therefore, the electrostatic potential maps hints at a possibly similar aromatic character of **3-4** with **3-2a**, **3-2b**, and **3-2c**. Finally, calculated LUMO energies show that **3-1** and **3-3** have the lowest energies as compared to other model heterocycles, suggesting that there is a correlation between aromaticity and LUMO energy.
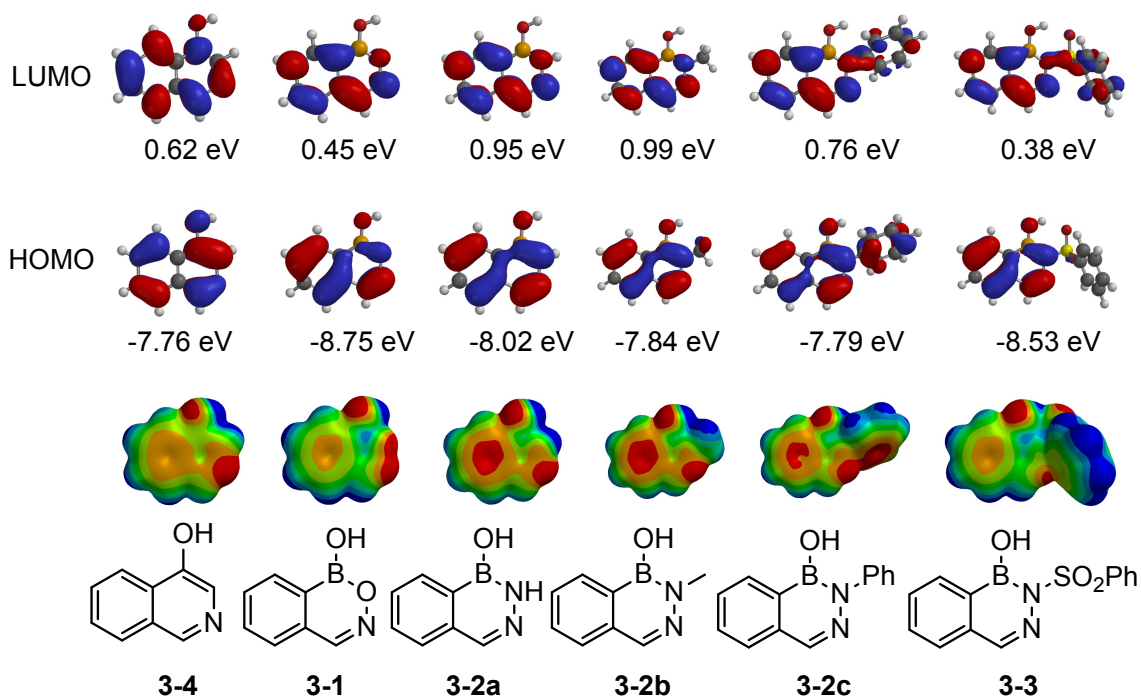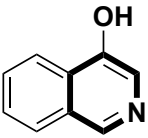
Figure 3.11. Frontier molecular orbitals, energies and electrostatic potential maps for boron heterocycles **3-1**, **3-2a**, **3-2b**, **3-2c**, **3-3**, and isostere **3-4** (ωB97X-D/6-31G*, gas phase). (Computations performed by Dr. Dennis Hall).[24]
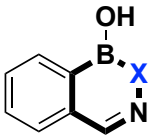
Another parameter that complements these relative aromaticity findings was the nucleus independent chemical shift (NICS) values, which were obtained by Matthew Johnson using GIAO-B3LYP function and 6-311+G(2d,p) basis set. NICS values provide a measure of aromaticity, and are acquired by placing a dummy atom (with no nucleus) at a location in a space around the molecule of interest.[28] It is evaluated by using the response of the aromatic system in the presence of an external magnetic field. NICS values are the negative of the absolute shielding. Generally, lower NICS values (more negative) indicates higher aromaticity, whereas the higher values (less negative) indicate lower aromaticity. It is to be noted that NICS values are relative values, so in this study NICS values for the C=C isostere (**3-4**) were also calculated. The NICS(0) index measures the magnetic shielding at the center of the ring caused by σ electron delocalization, whereas the NICS(1) index computes the average shielding 1 Å above the plane of the ring, where π contributions are dominant. The resulting NICS(0) and NICS(1) values showed that the boron-containing rings in all these heterocycles had

less negative values compared to the pyridine ring of **3-4** (Table 3.2).[24] As observed earlier from DFT calculations, NICS calculations also suggest that the oxazaborine ring of **3-1** possesses negligible aromatic character (e.g., NICS(0) = 0.79) compared to the heterocyclic ring of its C=C isostere (**3-4**).

Table 3.2. Nucleus-Independent Chemical Shift Calculations for Heterocycles **3-1**–**3-3** and **3-4** (GIAO-B3LYP/6-311+G(2d,p)) (Calculations performed by Matthew Johnson)

	3-1 X = O
	3-2a X = NH
	3-2b X = NMe
	3-2c X = NPh
	3-3 X = NSO$_2$Ph

Index	3-4	3-1	3-2a	3-2b	3-2c	3-3
NICS(0)	–7.87	0.79	–1.33	–1.91	–0.81	–1.34
NICS(1)	–9.95	–2.75	–4.35	–4.86	–3.75	–3.88

Overall, it can be concluded from DFT and NICS calculations that the model heterocycles **3-2a**, **3-2b**, and **3-2c** retain some degree of aromatic character in the boron-containing ring when compared to their C=C isostere **3-4**. Contrary to that, the boron-containing ring of **3-1** is not aromatic.

3.5 Assessment of Stability

The exchange of the hydroxy group from B—OH of heterocycles **3-1**, **3-2a**, **3-2b**, **3-2c**, and **3-3** could provide an indication about their acidity, stability, as well as aromaticity.

3.5.1 H$_2$^{18}O Exchange Experiments

Considering Scheme 3.1, if the B—OH exchange occurs, it could indicate Lewis acidity for the aforementioned heterocycles because it would likely have to go through a tetracoordinate boron. This exchange would also indicate the extent of stabilization provided through aromaticity since to form a Lewis acid adduct, any aromatic character would be temporarily halted by the formation of a tetrahedral boron atom.
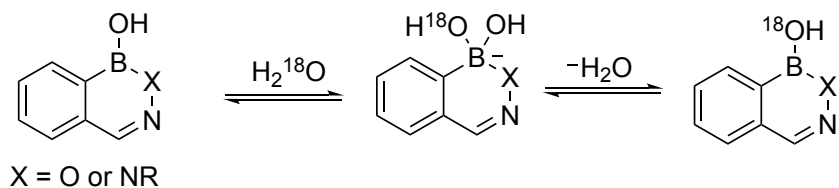
Scheme 3.1. $H_2{}^{18}O$ exchange experiments with the model heterocycles.

Groziak and co-workers performed $H_2{}^{18}O$ exchange experiments with **3-1**, **3-2a**, and **3-2b** in their previous investigation of benzoxazaborine and benzodiazaborines.[17] We set out to re-examine those exchange experiments, and used **3-1**, **3-2b**, and **3-3** as representative examples. Model boron heterocycles were dissolved in CH_3CN, and then excess of $H_2{}^{18}O$ was added in a sealed tube under argon atmosphere. The reaction was performed first at room temperature and then at 70 °C at different time intervals and further analyzed by mass spectrometry to obtain the percentage incorporation of ^{18}O labelled water. In the first trial, **3-1**, **3-2b**, and **3-3** heterocycles were used, and the reaction was executed at 70 °C. After 16 h, the reaction solutions were analyzed by Electrospray Ionization (ESI); no incorporation was observed with **3-1** or with **3-3**. Interestingly, with **3-2b**, only the ^{18}O incorporated product was detected. However, with more scans, the ^{18}O labelled product back exchanged with $H_2{}^{16}O$ and resulted in the formation of unlabelled starting material. Later, another set of reactions were carried out with **3-1** and **3-3** for 68 h, and the results showed >75% ^{18}O incorporation in both of them. By MS analysis, again it was observed that the labelling of **3-1** and **3-3** varies quickly in the presence of adventitious water in the spectrometer; therefore, getting exact percent labelling was deemed unfeasible. With these observations in hand, model heterocycles **3-1**, **3-2b**, and **3-3** were treated with $H_2{}^{18}O$ at room temperature and at 70 °C with varying time, and the products were analyzed by the initial scan on the mass spectrometer (Table 3.3).

Table 3.3. Percentage Incorporation of ^{18}O in Model Heterocycles **3-1**, **3-2b**, and **3-3**
($H_2{}^{18}O = 97\%$ ^{18}O)

X = O or NR
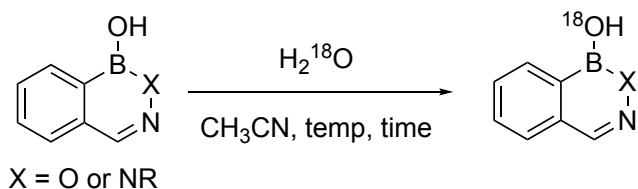
Heterocycle	% ^{18}O incorporation			
	16 h	40 h	68 h	Temp (°C)
3-1	>24	>62	>50	25
3-1	>30	>60	>75	70
3-2b	>95	>96	>96	25
3-2b	>95	>95	>95	70
3-3	>80	>96	>92	25
3-3	>80	>75	>75	70

The results were not dependent on the temperature but were unreliable due to reverse hydrolysis by the adventitious $H_2{}^{16}O$ in the chamber; consequently, they were disregarded. The visualization of labelled-oxygen incorporation also was attempted using ^1H NMR spectroscopy. Heterocycles **3-1** and **3-2a** were dissolved in DMSO-d_6, followed by the addition of 1 drop of $H_2{}^{18}O$. For control, instead of $H_2{}^{18}O$, regular deionized (DI) water ($H_2{}^{16}O$) was added and ^1H NMR spectra were compared; no change was observed in OH signals and no dual peaks of OH were visible.

Even though the reproducibility was difficult to achieve with the $H_2{}^{18}O$ labelling experiment, formation of ^{18}O labelled product suggest a Lewis acidic nature for these boron-containing heterocycles.

3.5.2 MeOH Exchange Experiments

MeOH exchange experiments for B—OH of model heterocycles **3-1**, **3-2a**, **3-2b**, **3-2c**, and **3-3** were performed by Jason Rygus. The heterocycles were treated with dry MeOH, and the reaction time was set at 30 min and 24 h. The exchange percentage of

model boron heterocycles (B—OH to B—OCH$_3$) was measured by ^{1}H NMR spectroscopy (Table 3.4).[24]

Table 3.4. MeOH Exchange with Model Boron Heterocycles (Performed by Jason Rygus)
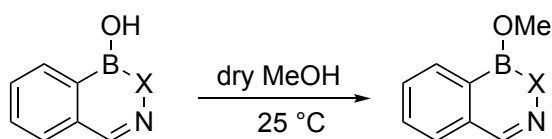
Compound	% Exchange	
	30 min	24 h
3-1 X = O	38	46
3-2a X = NH	50	54
3-2b X = NMe	<5	<5
3-2c X = NPh	<5 (42%conversion)[a]	<5 (40%conversion)[a]
3-3 X = NSO$_2$Ph	<5 (53%conversion)[a]	<5 (50%conversion)[a]

[a]Reaction with methanol for **3-2c** and **3-3** leads to B—N bond cleavage and opening of boron-containing ring

The ^{1}H NMR spectra revealed moderate B—OH to B—OCH$_3$ exchange for **3-1** and **3-2a** after 30 min of reaction. Even after 24 h, the increase in the exchange percentage was minimal. Heterocycle **3-2b** was inert to MeOH exchange. On the other hand, **3-2c** and **3-3** underwent B—C cleavage under these reaction conditions. Similar results were obtained when the reaction occurred in a polar aprotic solvent (CH$_3$CN) with five equivalents of MeOH.[24]

The unappreciable exchange of **3-2b** can be explained by the lack of H-bonding from the nitrogen atom when compared to **3-2a**, where this additional interaction could help the delivery of the OMe moiety (Figure 3.12). Overall, this experiment, just like the H$_2$[18]O labelling experiment, hints at a Lewis acidic character for these heterocycles.
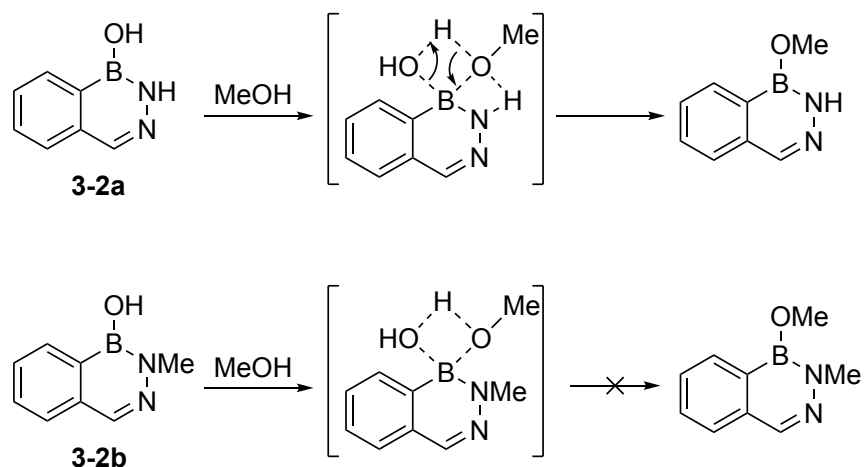
Figure 3.12. Proposed rationalization for MeOH exchange of **3-2a** vs **3-2b**.[24]

3.5.3 Crossover Experiments

The model boron heterocycles **3-1**–**3-3** are stable at room temperature, but this does not address the kinetic stability of these molecules. It could be envisioned that these molecules could undergo a dynamic, fast and reversible hydrolysis to give back the *ortho*-formyl phenylboronic acid (Figure 3.13a). Therefore, to determine the dynamic stability of these molecules, a series of crossover experiments were executed.

To initiate these studies, the exchange reaction was performed between fluorinated *ortho*-formyl phenylboronic acid **F-3-12** and all model boron-containing heterocycles **3-1**–**3-3** in both directions (Figure 3.13b). The reaction was performed for 24 h at room temperature, using CH_3CN/H_2O as the solvent system in the ratio of 3:1. The choice of solvent ratio was crucial to get a homogeneous reaction solution. After the reaction was completed, the reaction solution was observed first by Liquid Chromatography-Mass Spectrometry (LC-MS) analysis and then the crossover, if any, was measured quantitatively by ^{19}F NMR spectroscopy. In the event, no crossover was observed for heterocycles **3-1**, **3-2a**, **3-2b**, or **3-2c** under these reaction conditions. There was minimal crossover with **3-3** from both directions. The labile nature of **3-3** is similar to that of *N*-acyl derivatives, as was shown by Bane and co-workers.[23] Similar results were obtained when buffered CH_3CN/H_2O (pH = 6.9) was used as the solvent. Crossover experiments between fluorinated *ortho*-formyl phenylboronic and the model

heterocycles in MeOH were completed by Jason Rygus.[24] There was minimal crossover for all the heterocycles except **3-3**.
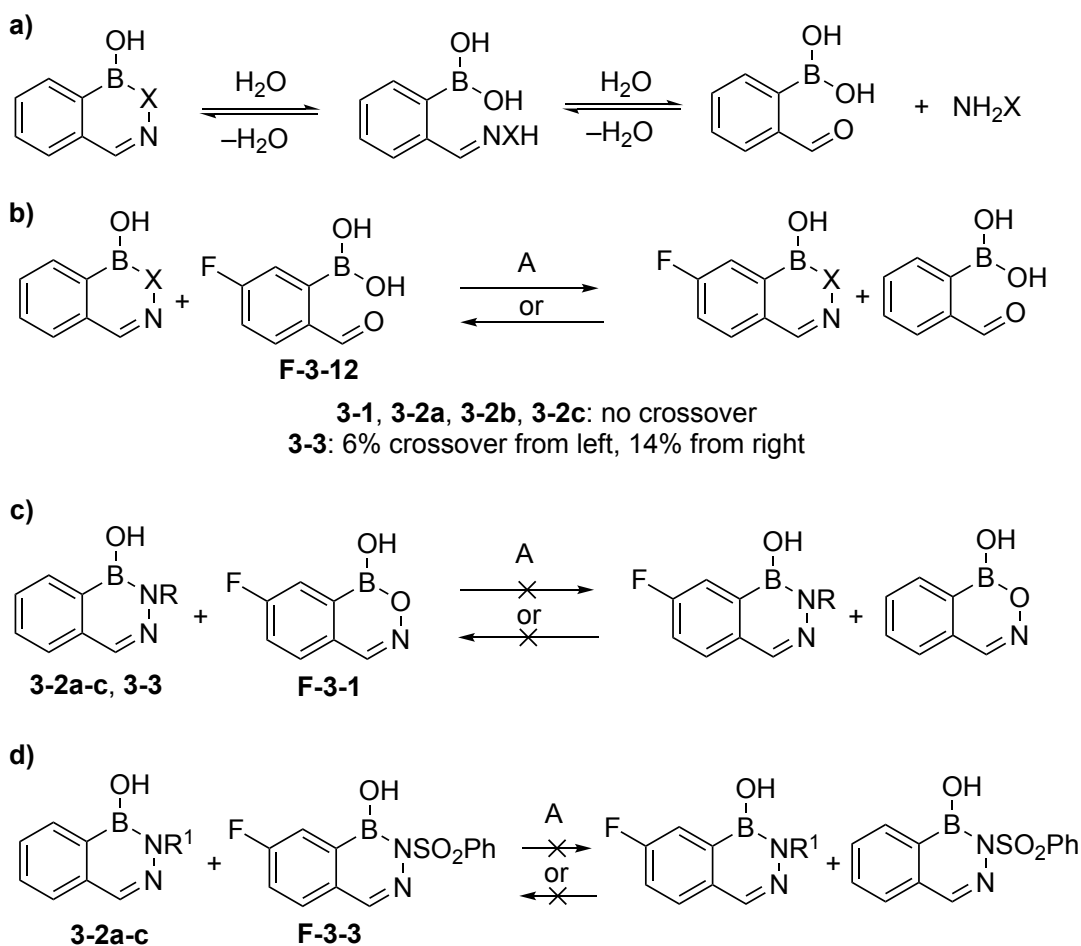
Figure 3.13. a) Possible hydrolytic instability of model heterocycles. **b-d)** Crossover experiments for model heterocycles using conditions A = 3:1 CH$_3$CN/H$_2$O at rt, 24 h.

In order to determine the exchange between different heterocycles, another set of crossover experiments were performed, where fluorinated **3-1** (**F-3-1**) was reacted with model heterocycles **3-2**–**3-3**, using CH$_3$CN/H$_2$O as the solvent system in a ratio of 3:1 for 24 h at room temperature. The reaction solution was then examined using LC-MS and quantitatively by ^{19}F NMR spectroscopy (Figure 3.13c). No crossover products were observed from either direction. Again, crossover was assessed in MeOH (by Jason Rygus) but resulted in the same outcome, i.e., no crossover from either direction.[24]

Finally, the crossover experiment was performed between fluorinated **3-3** (**F-3-3**) and other *N*-analogs, using CH$_3$CN/H$_2$O as the solvent system in the ratio of

3:1 for 24 h at room temperature and, yet again, there was no crossover in either direction (Figure 3.13d). As expected from the benzaldehyde exchange experiments (Figure 3.13b), when using MeOH as the solvent (performed by Jason Rygus), there was crossover between two distinct *N*-sulphonyl heterocycles.[24] Additional experiments were performed with **3-3**, and it was shown that the crossover only occurs in the presence of MeOH (see Section 3.9.6.2).

Overall, these crossover experiments ascertain the dynamic stability of boron-containing heterocycles **3-1**, **3-2a**, **3-2b**, **3-2c**, and to some extent **3-3** in aqueous conditions. Knowledge of this property is essential for these heterocycles to be used in medicinal chemistry and catalysis. In addition, since the solvent system of CH_3CN/H_2O is suitable for all of these model boron heterocycles, it was used for the pK_a measurements (vide infra).

3.6 Assessment of Acidic Character: pK_a Measurements

Next, we set out to measure the acidic character of all model boron heterocycles **3-1**, **3-2a**, **3-2b**, **3-2c**, and **3-3** by way of ^{11}B NMR titration experiments (for experimental details, see Section 3.9.7). Boronic acids have a tendency to undergo B—O—B dimerization in anhydrous solvents,[23] but in the presence of water, they exist as a monomer (see Section 3.9.4). All the model heterocycles, except **3-1**, display poor solubility in water. Solvent systems, such as ~10% DMSO, isopropanol, or acetonitrile in water, did not result in a clear stock solution for the heterocycles **3-2**–**3-3**. In order to achieve a homogeneous solution containing a select heterocycle, a buffered 1:1 CH_3CN/H_2O solvent system was used for obtaining [11]B chemical shifts. The pK_a of benzoxaborole in water has been measured in the past by using ^{11}B NMR titration and UV titration methods, therefore, it was used as a control.[18,19] The solubility of benzoxaborole and **3-1** is good in aqueous solutions with minimum organic solvent (~5%). Therefore, the pK_a of benzoxaborole and **3-1** were measured in both 1:1 CH_3CN/H_2O as well as in aqueous solution to assess the effect of organic co-solvent. The pK_a values obtained show an increase of 1.5–2.0 units in a 1:1 CH_3CN/H_2O solvent system as compared to water alone (Table 3.5). This increase of pK_a observed in the

medium containing an organic solvent is expected, with a reduced solution polarity resulting in a less favorable ionization.

Table 3.5. [11]B Chemical Shifts and pK_a's of Heterocycles in 1:1 CH$_3$CN/H$_2$O Solvent System

Heterocycle	δ acid (ppm)	δ conj. base (ppm)	pKa
benzoxaborole	32.8	8.5	9.2[a]
3-1	27.7	2.5	7.1[b]
3-2a	27.8	—[c]	>14
3-2b	27.5	—[c]	>14
3-2c	28.0	1.2	12.2
3-3	28.4	1.6	5.5

[a]7.4 in H$_2$O with ~4% DMSO. [b]5.5 in water with ~4% DMSO. [c]A negligible change in the chemical shift was observed upto a high pH: **3-2a**: 27.0 ppm at pH 13.4; **3-2b**: 27.1 ppm at pH 13.6

Model heterocycles **3-1** and **3-3** show a titration curve typical of a rapid equilibrium, i.e., on increasing the pH of the solution, the [11]B chemical shift gradually changes from downfield (~28 ppm) to upfield (~2 ppm) reflecting an averaging of resonances from the acid and the conjugate base (see Section 3.9.7). In other words, the equilibrium shifts to the right side and favours the formation of the tetrahedral form **I** (cf. Figure 3.4b) at high pH, thereby demonstrating Lewis acidity. The previous crossover experiments suggest that **3-3** is relatively unstable in an aqueous environment (cf. Figure 3.13b). Therefore, titration of the corresponding *ortho*-formyl phenylboronic acid was executed, and the [11]B chemical shift at high pH was found to be distinct from the titration curve for **3-3** (8.1 ppm vs 1.5 ppm at pH = 9.0); this ruled out the hydrolysis of **3-3** under titration conditions, proving that 5.5 is the genuine pK_a of **3-3** (see Section 3.9.7.5). The surprisingly low pK_a of **3-3** can be explained by the existence of internal H-bonding between sulfone O and B—O<u>H</u> (observed in the X-ray crystal structure of **3-3**), which makes boron more electrophilic (Figure 3.14).
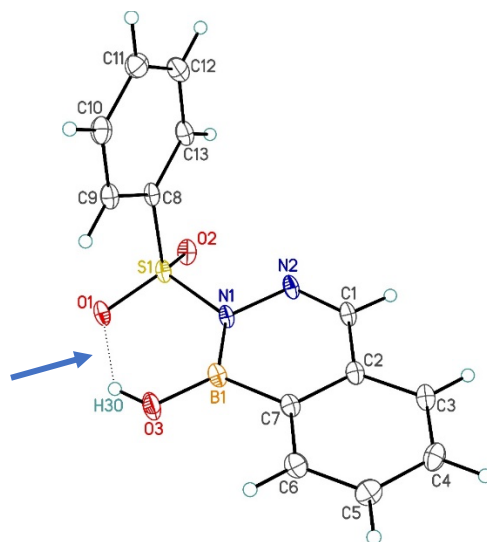
Figure 3.14. ORTEP representation of **3-3** showing internal H-bonding.

In the case of **3-2c**, with a change in pH from low to high, both forms of the equilibrium were observed on the NMR timescale instead of a weighted averaged chemical shift, indicative of a slower exchange process. However, at pH > 13, only one intense upfield resonance was visible at 1.2 ppm, indicating a shift of the equilibrium towards the conjugate base. To validate the formation of the conjugate base of heterocycle **3-2c**, a three-step approach was used. Firstly, **3-2c** was dissolved in a buffered 1:1 CD_3CN/H_2O, and two aliquots were taken. The aliquots were adjusted to pH 7.4 (Sample A) and 13.2 (Sample B). After acquiring ^{11}B and ^1H NMR spectra of both samples, the pH of Sample B was readjusted to 7.3 (Sample C), and again ^{11}B and ^1H NMR spectra were obtained (Figure 3.15). If the upfield peak in the ^{11}B NMR spectrum at pH 13.2 corresponds to the conjugate base, then decreasing the pH to 7.3 should result in its disappearance with virtually the same NMR spectra as was observed in the pH 7.4 sample (Sample C should be very similar to Sample A). The obtained spectra were consistent with this hypothesis. The ^1H NMR resonances were broadened at high pH (sample B), which may be attributed to intractable, reversible B—O—B anhydride formation.
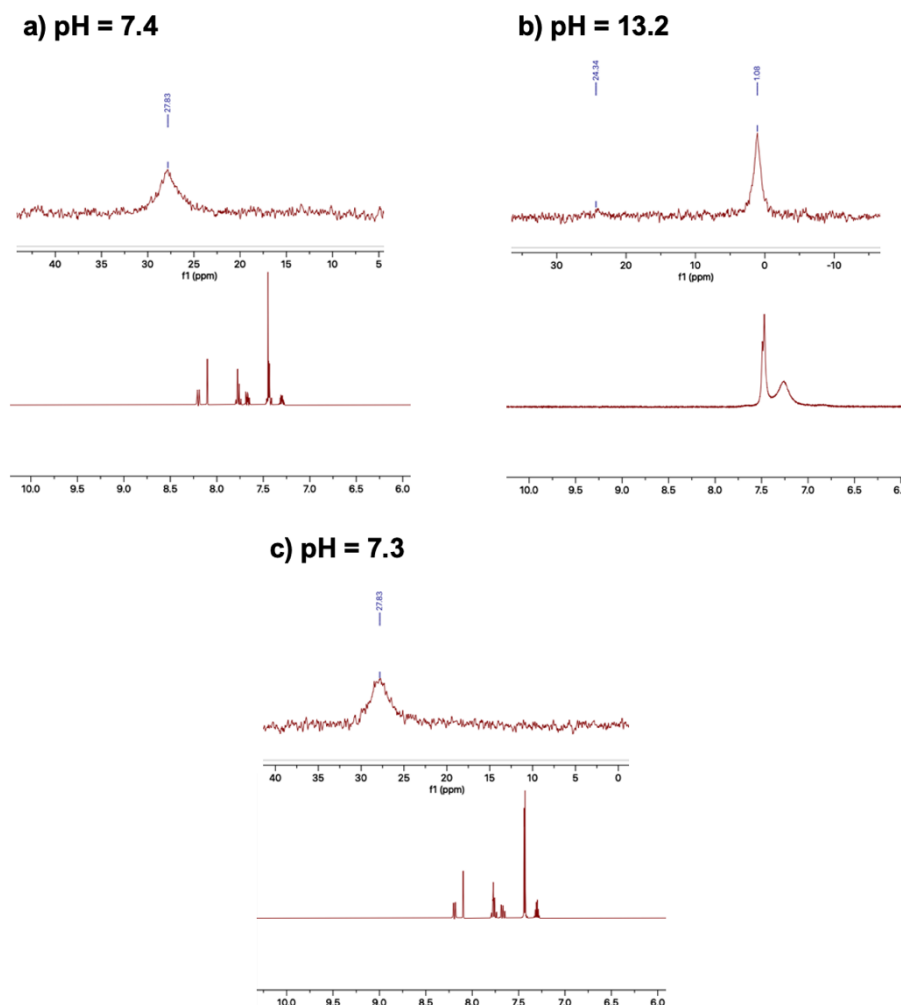
Figure 3.15. ^{11}B and ^{1}H NMR spectra in CD$_3$CN of heterocycle **3-2c** at **a)** pH 7.4 **b)** pH 13.2 **c)** pH 7.3 obtained by acidifying the pH 13.2 solution. Water suppression was used for obtaining ^{1}H NMR spectra.

Another validation was achieved by independently preparing the corresponding conjugate base. Heterocycle **3-2c** was dissolved in hot toluene, and 45% aqueous KOH (1 drop) was added. The resulting precipitate was analyzed by ^{11}B NMR spectroscopy in three separate conditions: a) in CD$_3$CN, b) in CD$_3$CN/H$_2$O (1:1), and c) in a 1:1 mixture of CD$_3$CN/phosphate buffer adjusted to pH 13.8 (Figure 3.16). In all cases, identical ^{11}B NMR spectra were obtained, except in CD$_3$CN/H$_2$O (1:1), where partial quenching was observed (Figure 3.16b). These results confirmed that the synthesized conjugate base is the same species that is formed during the pK_a titration.
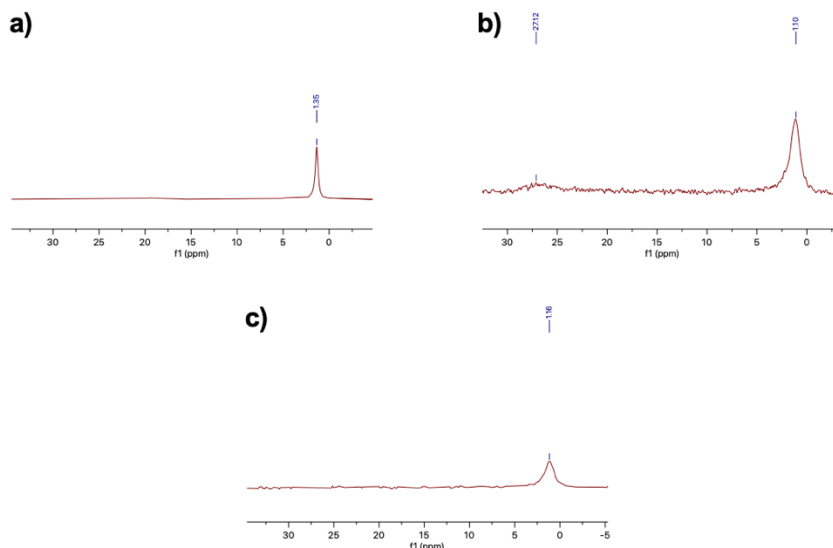
Figure 3.16. ^{11}B NMR spectra of the conjugate base of **3-2c** in **a)** CD$_3$CN **b)** CD$_3$CN/H$_2$O (1:1) and **c)** 1:1 mixture of CD$_3$CN and phosphate buffer adjusted to pH 13.8.

Since it is not practical to increase pH above ~13, the approximate pK_a of heterocycle **3-2c** was estimated by carefully adjusting the pH until the ^{11}B NMR signals corresponding to the acid and conjugate base forms showed equal integration, which occurred at approximately pH 12.2 (see Section 3.9.7.4).

Finally, to further validate the pK_a of **3-2c**, another derivative, **3-2d**, was synthesized with a strong electron withdrawing group attached at the *para* position of *N*-aryl moiety with an expectation to depress the pK_a (Figure 3.17).

3-2d
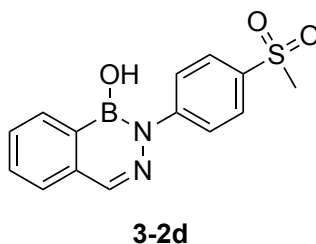
Figure 3.17. Model heterocycle **3-2d** as a variant of **3-2c**.

Remarkably, **3-2d** resulted in a typical titration curve with a single weighted average resonance at the transition point from acid to conjugate base with a pK_a of 9.4 (see Section 3.9.7).

Regarding **3-2a** and **3-2b**, no significant change in the ^{11}B NMR chemical shift was observed upon raising the pH in a buffered 1:1 CH$_3$CN/H$_2$O solvent system. Similar observations were noted by Groziak and co-workers.[17] Also, the stability of **3-2a** and **3-2b** in varying pH solutions was tested. Again, a three-step approach was used, which was accomplished in a manner similar to **3-2c**. Heterocycle **3-2a** or **3-2b** was dissolved in buffered 1:1 CD$_3$CN/H$_2$O, and two aliquots were taken. Then, the pH of the two separate aliquots was adjusted approximately to 7.0 (Sample A) and 13.0 (Sample B), and the ^{1}H and ^{11}B NMR spectra of each were recorded. Finally, after recording the ^{1}H and ^{11}B NMR spectra of Sample B, the pH of the solution was decreased to approximately 7.0, and ^{1}H and ^{11}B NMR spectra were recorded again (Sample C) (Figure 3.18 and 3.19).
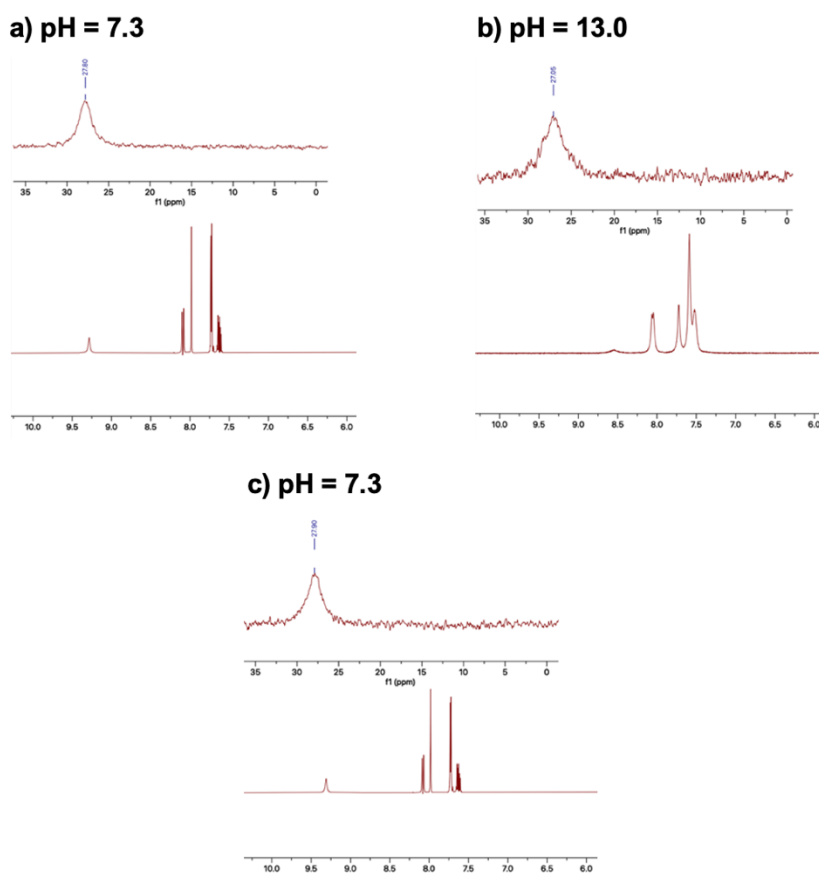
Figure 3.18. ^{11}B and ^{1}H NMR spectra in CD$_3$CN of heterocycle **3-2a** at **a)** pH 7.3 **b)** pH 13.0 **c)** pH 7.3 obtained by acidifying the pH 13.0 solution. Water suppression was used for obtaining ^{1}H NMR spectra.
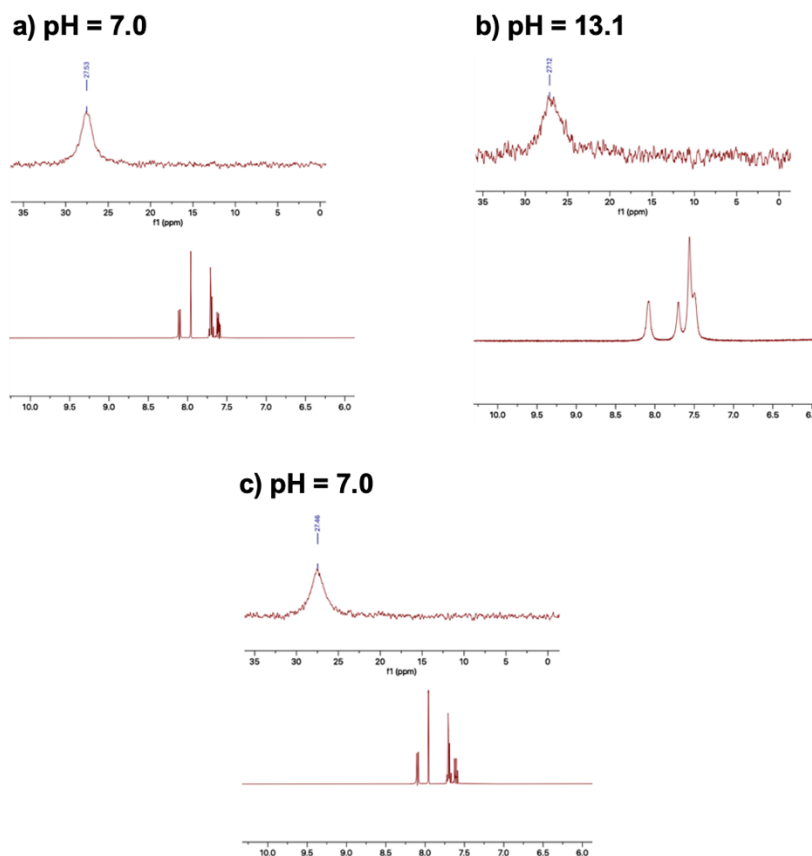
Figure 3.19. ^{11}B and ^{1}H NMR spectra in CD_3CN of heterocycle **3-2b** at **a)** pH 7.0 **b)** pH 13.1 **c)** pH 7.0 obtained by acidifying the pH 13.1 solution. Water suppression was used for obtaining ^{1}H NMR spectra.

For both heterocycles **3-2a** and **3-2b**, no upfield resonances in the ^{11}B NMR spectra were observed at high pH that could be assigned to the corresponding conjugate bases. Similar to **3-2c**, the ^{1}H NMR resonances for **3-2a** and **3-2b** were broadened at high pH, which may be attributed to intractable, reversible B—O—B anhydride formation. Decreasing the pH (Sample C) showed no sign of decomposition for either compound, and both heterocycles **3-2a** and **3-2b** were observed unchanged.

Consequently, the exact pK_a could not be determined for heterocycles **3-2a** and **3-2b** in a buffered 1:1 CH_3CN/H_2O solvent system and were assigned a value of >14. To our delight, the formation of the conjugate bases of **3-2a** and **3-2b** was achieved, using tetramethylammonium hydroxide (TMAH) in methanol/toluene (see Section 3.9.8.2).[29] To this end, **3-2a** or **3-2b** were dissolved in toluene, followed by the addition of TMAH in methanol. The solvents were evaporated, and the solid residue showed an

upfield resonance in ^{11}B NMR spectroscopy, observed in d-DMSO (from ampoule) for both **3-2a-I** and **3-2b-I**, confirming the formation of a conjugate base in organic solvents and, therefore, Lewis acidity (Scheme 3.2).

3-2a: R = NH
3-2b: R = NMe

3-2a-I: R = NH; [11]B δ(ppm) = 1.3
3-2b-I: R = NMe; [11]B δ(ppm) = 2.4
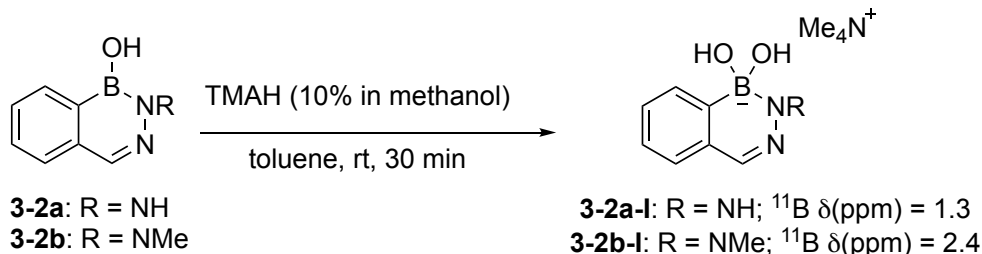
Scheme 3.2. Conjugate base formation of **3-2a** and **3-2b** with TMAH in methanol.

When CD$_3$CN was used as an NMR solvent, small amounts of quenching to regenerate heterocycle **3-2a** or **3-2b** was observed due to residual water in the solvent (also, see Section 3.9.8.3). This effect explains why it was difficult to observe the upfield [11]B chemical shift in the case of an aqueous environment (1:1 CH$_3$CN/H$_2$O). Since pH > 14 is not achievable under aqueous conditions, no upfield resonance could be observed because of the higher pK_a of **3-2a** and **3-2b**.

The pK_a's of **3-1**, **3-2c**, **3-2d**, and **3-3** also were validated by UV measurements and provided similar values (Table 3.6). Overall, all of the aforementioned experiments prove that model heterocycles **3-1**–**3-3** are Lewis acids.

Table 3.6. Summary of Experimental pK_a Values of Heterocycles **3-1**, **3-2c**, **3-2d**, and **3-3**

Heterocycle	pK_a by ^{11}B NMR	pK_a by UV spectroscopy
3-1	7.1	7.2
3-2c	12.2	12.3
3-2d	9.4	10.1
3-3	5.5	5.4

3.7 Assessment of Acidic and Aromatic Character: X-ray Crystallography

X-ray crystallographic analysis of the conjugate base is the most definitive method of proving the acidic nature of model heterocycles **3-1**–**3-3** in the solid-state. It also can

help assess the extent of aromaticity by comparing the bond orders and bond lengths of the solid-state parent molecules. Groziak and co-workers reported the X-ray crystal structures of **3-1** and **3-2a**.[17] Some of the key features are the bond lengths of C—B (1.533 and 1.530 Å), exocyclic B—O (1.350 and 1.351 Å), and endocyclic B—X (1.388 and 1.432 Å) bonds, respectively, for **3-1** and **3-2a**. From the C—B bond lengths, it can be inferred that they are intermediate between that of phenylboronic acid (C—B: 1.57 Å) and 1,2-dihydro-1,2-azaborine (C—B: 1.51 Å).[30,31] The lower bond length of the endocyclic B—O bond for **3-1**, as compared to the B—N bond for **3-2a**, suggests that the higher electrophilicity of the boron atom in **3-1** (indicated by a lower pK_a) is attributable to a larger inductive effect of a more electronegative oxygen atom. Both heterocycles display a trivalent boron atom, but there is a significant distortion of the sp^2 angles in **3-2a**. Specifically, there are meaningful differences in the bond angles of C—B—OH (122.5° for **3-1** vs 128.1° for **3-2a**), HO—B—X (118.1° for **3-1** vs 116.7 for **3-2a**), and C—B—X (119.4° for **3-1** vs 115.2° for **3-2a**).[17] Though intermolecular H-bonding exists in both the heterocycles (O<u>H</u>—imine N), there is one extra H-bond in **3-2a**, where the N<u>H</u> shows interaction with the <u>O</u>H.[17]

Prior to this work, there had never been a report on an X-ray crystal structure of conjugate bases of any of the model heterocycles mentioned in this chapter. The conjugate bases were obtained by the reaction of heterocycles in toluene with 45% aq. KOH (Scheme 3.3).

3-1 X = O
3-2d X = NC$_6$H$_4$-4-SO$_2$Me
3-3 X = NSO$_2$Ph

3-1-I X = O
3-2d-I X = NC$_6$H$_4$-4-SO$_2$M**e**
3-3-I X = NSO$_2$Ph
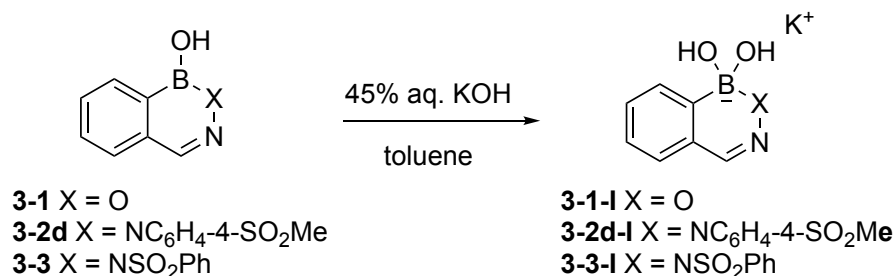
Scheme 3.3. Synthesis of conjugate bases of **3-1**, **3-2d** and **3-3** for X-ray crystallography.

The conjugate bases formed were subjected to various recrystallization techniques. Dr. Marco Paladino crystallized the conjugate base of **3-1** (**3-1-I**) (Figure 3.20). The X-ray crystal structure of **3-3-I** also was obtained successfully.

There was difficulty in obtaining the conjugate base crystal structure of **3-2c** due to its high pK_a (12.2). To our delight, the X-ray crystal structure of **3-2d-I**, the conjugate base of **3-2d** (pK_a = 9.4) (an analog of **3-2c**), was successfully acquired.
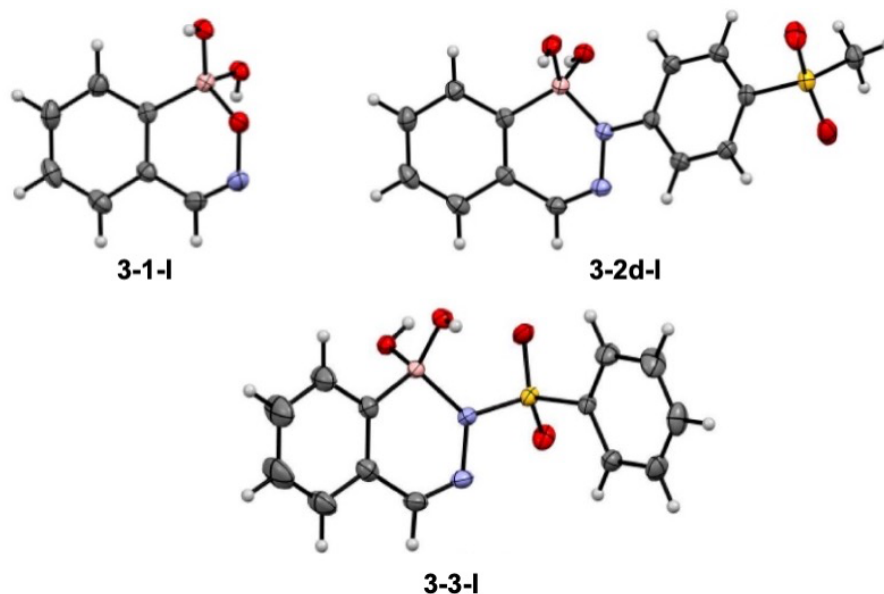
Figure 3.20. ORTEP representation of conjugate bases of **3-1**, **3-2d**, and **3-3**: **3-1-I**, **3-2d-I**, and **3-3-I**. Countercation and bound solvents have been removed for clarity.

With the X-ray crystallographic structures of conjugate bases in hand, clearly showing a tetracoordinate boron, it can be stated unambiguously that **3-1**, **3-2d** and **3-3** are Lewis acids. Moreover, because ^{11}B NMR chemical shift of these conjugate base crystals in CH_3CN/H_2O appears at ~2 ppm, it confirms that during the pK_a determination by ^{11}B NMR spectroscopy (vide supra), these heterocycles exist in form **I** (refer to Figure 3.4b) at high pH in the solution phase as well.

Key observations, such as the bond lengths and bond angles can be compared between crystal structures of the conjugate bases and the parent heterocycles (Table 3.7). In the conjugate bases, the C—B bond lengths are longer than in their respective parent heterocycle (for example, the C—B bond length of **3-1-I** = 1.613 Å vs the C—B bond length of **3-1** = 1.533 Å). The difference in endocyclic B—O/N bond lengths of conjugate bases as compared to their respective neutral heterocycles is even more pronounced. For instance, the endocyclic B—O bond of **3-1-I** (1.537 Å) is much

larger than the corresponding bond length in the parent heterocycle **3-1** (1.388 Å). Upon formation of the conjugate base, the hybridization of the boron center changes from sp^2 (trigonal planar) to sp^3 (tetrahedral). This phenomenon is reflected on the bond angles at the boron center. For example, the C—B—O bond angle changes from 119.4° for **3-1** to 107.8° for **3-1-I**. Similar observation can be noted for the *N*-analogs **3-2d** and **3-3**.

Table 3.7. Key Properties of Conjugate Bases **3-1-I**, **3-2d-I**, and **3-3-I** with Respect to Parent Heterocycles

Properties	3-1	3-1-I	3-2d	3-2d-I	3-3	3-3-I
Bond length C—B (Å)	1.533	1.613	1.554	1.619	1.540	1.608
Bond length B—O/N (Å)	1.388	1.537	1.442	1.602	1.461	1.622
Bond angle C—B—O/N	119.4°	107.8°	116.0°	106.9°	114.6	105.5°

Though, crystal structures of the conjugate bases of **3-2a**, **3-2b**, and **3-2c** could not be obtained due to their high pK_a or due to the moisture sensitivity of the conjugate bases, Dr. Hwee Ting Ang was able to obtain crystal structures of the diol adducts under anhydrous conditions.[24] These adducts provided evidence that heterocycles **3-2a**, **3-2b**, and **3-2c** can also display a tetrahedral boron which, in turn, demonstrates their Lewis acidic character. These adducts also revert back to their acid form when exposed to 1:1 CH_3CN/H_2O at pH 13.5, an observation that is supportive of a high (>14) pK_a.

3.8 Conclusion

This chapter documented the synthesis and characterization of various boron-containing heterocycles **3-1**–**3-3**. Utilizing these model compounds, a number of ambiguous results and conclusions regarding the acidic nature and aromatic character of these C=C/B—X isosteric naphthoid compounds were rectified. The properties were construed by the combination of experimental, computational, spectroscopic, and X-ray crystallographic analysis. All the model heterocycles **3-1**–**3-3** are confirmed to be Lewis acids in solution according to pK_a determination and ^{11}B NMR spectroscopy.

The most compelling results are achieved by single crystal X-ray structures of conjugate bases and diol adducts demonstrating a tetrahedral boron center in the solid-state. The Lewis acidity of the above-mentioned heterocycles are in the following order: **3-3** > **3-1** > **3-2d** > **3-2c** > **3-2a~3-2b**, with **3-3** being the most acidic and **3-2a/3-2b** the least. The Lewis acidic character is in agreement with the aromatic character, where **3-2a** and **3-2b** feature higher delocalization of electrons in the heterocyclic ring as compared to **3-1** or **3-3**, which have almost no aromatic character in the boron-containing ring. However, all these heterocycles show less aromatic stabilization as compared to the parent C=C isostere **3-4**. Furthermore, the stability of these heterocycles has been demonstrated by dynamic exchange and crossover experiments, where most of the heterocycles show good stability in the full pH range. This property would be useful in biological applications, as they can exist in both neutral (trivalent) and ionic (tetravalent) forms. Since many of these heterocycles were shown to undergo B—OH exchange with alcohols and water (methanol exchange experiment and $H_2{}^{18}O$ labelling), they are valuable for a variety of applications in drug discovery and catalysis.
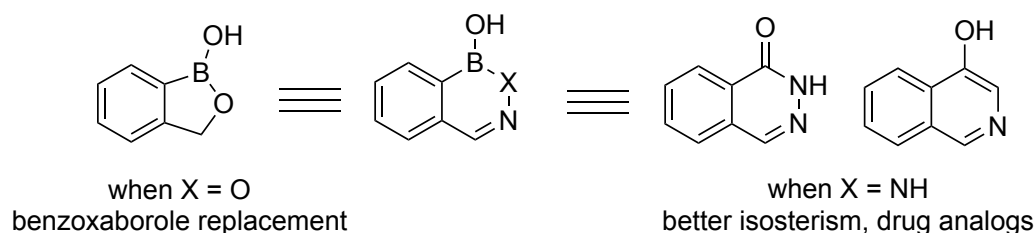
Figure 3.21. Applications of model boron heterocycles.

Heterocycle **3-1**, which shows enhanced Lewis acidic character in aqueous solutions, could be a good replacement for benzoxaboroles. On the other hand, **3-2a** with the most aromatic boron-containing ring could be a good isostere of naphthol like molecules (Figure 3.21).

In summary, this chapter resolves the inaccuracies in the literature reported over the past five decades. Additionally, it opens the door for the potential use of these heterocycles in the areas of catalysis and medicinal chemistry.

3.9 Experimental

3.9.1 General Information

All reactions were performed in regular glassware with no exclusion of air or moisture, unless otherwise noted. Anhydrous methanol (99.8%) was purchased from Sigma Aldrich and used as received. 2-Formylphenylboronic acid was purchased from Combi-Blocks and recrystallized from hot H_2O prior to use. $H_2^{18}O$ (97% ^{18}O, 1 mL ampoule) was purchased from Sigma Aldrich. Hydroxylamine (50 wt. % solution in water) was purchased from Sigma Aldrich and used as received. Acetonitrile (HPLC grade) was purchased from Sigma Aldrich and used as received. Dichloromethane (ACS reagent grade) and 95% ethanol (ACS reagent grade) for boron heterocycle synthesis were purchased from Sigma Aldrich and used as received. All other solvents were purchased as ACS reagent grade and used as received, and other chemicals were purchased from commercial suppliers and used as received. Thin layer chromatography was performed on Silicycle silica gel 60 F254 plates, which were visualized under UV light and with $KMnO_4$, phosphomolybdic acid (PMA) or curcumin stains. Column chromatographic separations were performed on silica gel 60 using ACS grade hexanes and ethyl acetate as eluents.

NMR spectra were recorded at ambient temperature using Varian DD2 MR two-channel 400 MHz, Varian INOVA two-channel 400 MHz, Varian INOVA four-channel 500 MHz, Varian VNMRS two-channel 500 MHz, Varian VNMRS four-channel 600 MHz and Agilent VNMRS four-channel, dual receiver 700 MHz spectrometers operating at the indicated frequency for ^1H NMR. All NMR chemical shifts are reported in ppm (δ) units with residual solvent peaks (d_6-acetone, CD_3CN or d_6-DMSO) as the internal reference. NMR data is reported using the following abbreviations: s, singlet; br s, broad singlet; d, doublet; t, triplet; q, quartet; h, hextet; dd, doublet of doublets; dt, doublet of triplets; td, triplet of doublets; ddd, doublet of doublet of doublets; dddd, doublet of doublet of doublet of doublets; app, apparent; m, multiplet. The error of coupling constants from ^1H NMR spectra is estimated to be approximately 0.3 Hz. The quaternary carbon bound to boron often is not observed due to the quadrupolar relaxation of boron,[32] which was the case for all boron-containing

compounds herein. A drop of D_2O usually was added to the NMR solution for compounds containing boranol (B—OH) units to prevent the formation of anhydrides (B—O—B dimers).

An OHAUS ST2100 pH meter with ST350 pH probe was used for pH measurements. High-resolution mass spectra were recorded by the University of Alberta Mass Spectrometry Services Laboratory using either electron impact (EI) or electrospray ionization (ESI) techniques. LC-MS was performed at the University of Alberta Mass Spectrometry Services Laboratory on an Agilent Technologies 6130 LC–MS using a Phenomenex Luna Omega Polar C18 1.6 μm column. A water/acetonitrile solvent system was used along with 0.1% formic acid, according to the following gradient: beginning from 99:1 water/acetonitrile, over 5.00 min the ratio was changed to 40:60 water/acetonitrile. Over the next 0.50 min, the ratio was changed to 5:95 water/acetonitrile, which was maintained for a further two min (total elution time of 7.50 min). Melting points were determined in a capillary tube using a melting point apparatus and are uncorrected. Fourier transform-infrared (FT-IR) spectra were obtained on a Nicolet Magna-IR instrument. For details on DFT and NICS calculations, see Appendix 5.

3.9.2 Preparation of Hemiboronic Acids

General Procedure for the Synthesis of O-Containing Hemiboronic Acids (GP1)
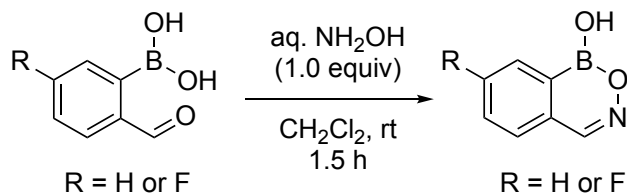
In a round bottom flask under air, the corresponding 2-formylarylboronic acid (1.0 equiv) was dissolved in CH_2Cl_2 (0.5 M) and stirred for five min, after which hydroxylamine (50 wt. % solution in water, 1.0 equiv) was added by syringe. The mixture was stirred at rt for 1.5 h, during which a precipitate was formed. Upon completion, the precipitate was collected by vacuum filtration and washed with H_2O

$(6 \times 50 \text{ mL})$ to remove excess hydroxylamine. After drying under high vacuum overnight, the desired compounds were obtained as solids.
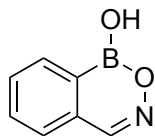
1H-Benzo[d][1,2,6]oxazaborinin-1-ol (3-1): Prepared according to **GP1** from 2-formylphenylboronic acid (609 mg, 4.06 mmol) and hydroxylamine (50 wt. % in H_2O, 248 μL, 4.06 mmol, 1.00 equiv). The title compound was isolated as a white solid (470 mg, 79%); **mp** = 145.5 – 147.9 °C; **^{1}H NMR** (400 MHz, d_6-acetone): δ 8.53 (s, 1 H), 8.16 (s, 1 H, exchanges with D_2O), 8.10 (d, J = 7.1 Hz, 1 H), 7.84 – 7.80 (m, 1 H), 7.75 (app t, J = 7.2 Hz, 2 H); **^{13}C NMR** (176 MHz, d_6-acetone): δ 150.8, 133.8, 133.7, 132.57, 132.56, 128.1; **^{11}B NMR** (128 MHz, d_6-acetone): δ 28.5; **FT-IR** (cast film, cm^{-1}): 3410 (br, w), 3061 (m), 3015 (m), 1710 (m), 1488 (m), 1402 (s), 1228 (s), 1057 (s), 912 (s), 722 (m); **HRMS** (EI) for $C_7H_6NO_2{}^{11}B$: Calculated: 147.0492; Found: 147.0493.
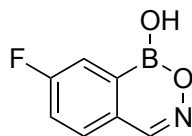
7-Fluoro-1*H*-benzo[*d*][1,2,6]oxazaborinin-1-ol (F-3-1): Prepared according to **GP1** from 5-fluoro-2-formylphenylboronic acid (2.00 g, 11.9 mmol) and hydroxylamine (50 wt. % in H_2O, 730 μL, 11.9 mmol, 1.00 equiv). The title compound was isolated as a white powder (1.63 g, 83%); **mp** > 300 °C (decomposition); **^{1}H NMR** (500 MHz, d_6-acetone + 1 drop D_2O): δ 8.52 (s, 1 H), 7.84 (dd, J = 8.5, 5.0 Hz, 1 H), 7.73 (dd, J = 8.5, 2.5 Hz, 1 H), 7.55 (app td, J = 9.0, 2.5 Hz, 1 H). In d_6-acetone alone without a drop of D_2O, the B–OH resonance is observed at 8.34 ppm (s, 1 H); **^{13}C NMR** (125 MHz, d_6-acetone + 1 drop D_2O): δ 165.2 (d, J = 251 Hz), 149.8, 131.6 (d, J = 8.5 Hz), 130.4 (d, J = 2.3 Hz), 121.6 (d, J = 23.1 Hz), 118.0 (d, J = 20.0 Hz); **^{11}B NMR** (128 MHz, d_6-acetone + 1 drop D_2O): δ 28.1; **^{19}F NMR** (376 MHz, d_6-acetone + 1 drop D_2O): δ – 107.7 (app td, J = 8.3, 4.5 Hz); **FT-IR** (KBr pellet, cm^{-1}): 3397 (br, w), 3074 (w), 1569

(s), 1493 (m), 1272 (s), 1055 (s); **HRMS** (EI) for $C_7H_5NO_2^{11}BF$: Calculated: 165.0397; Found: 165.0397.

General Procedure for the Synthesis of N-Containing Hemiboronic Acids (GP2)
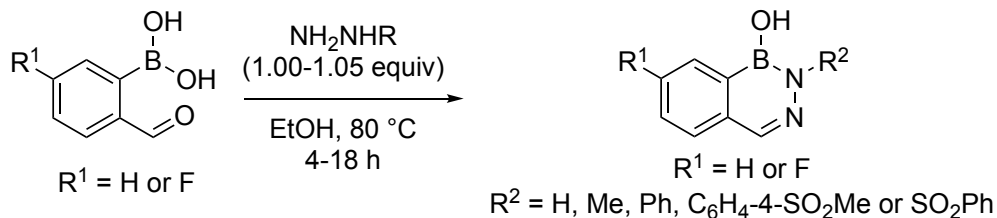
In a round bottom flask under air, the corresponding 2-formylarylboronic acid (1.0 equiv) was dissolved in 95% EtOH (0.5 M). The resulting homogeneous solution was then charged with the appropriate hydrazine derivative (1.00–1.05 equiv). The mixture was heated to reflux (80 °C) for 4–18 h. Upon completion, the reaction was allowed to cool to room temperature, where it was concentrated by rotary evaporation to remove ethanol. The resulting solid was suspended in cold H_2O, collected by vacuum filtration, and washed with cold H_2O (6 × 50 mL). After drying under high vacuum overnight, the desired compounds were obtained as solids.
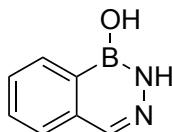
Benzo[*d*][1,2,3]diazaborinin-1(*2H*)-ol (3-2a): Prepared according to **GP2** from 2-formylphenylboronic acid (1.50 g, 10.0 mmol) and hydrazine monohydrate (509 µL, 10.5 mmol, 1.05 equiv) with a reaction time of 4 h. The title compound was isolated as a white solid (1.22 g, 83%); **mp** = 219 – 222 °C (turns yellow in color); **¹H NMR** (700 MHz, d_6-acetone): δ 9.37 (br s, 1 H), 8.19 (d, J = 7.6 Hz, 1 H), 7.98 (s, 1 H), 7.73 – 7.69 (m, 2 H), 7.58 (ddd, J = 7.6, 6.4, 2.0 Hz, 1 H), 7.18 (s, 1 H, exchanges with D_2O); **¹³C NMR** (176 MHz, d_6-acetone): δ 140.1, 137.2, 131.9, 131.5, 129.2, 127.6; **¹¹B NMR** (128 MHz, d_6-acetone): δ 28.0; **FT-IR** (cast film, cm⁻¹): 3331 (s), 3161 (m), 3066 (br, m), 1560 (m), 1459 (s), 1440 (s), 1345 (m), 1154 (m), 908 (m), 763 (m); **HRMS** (EI) for $C_7H_7N_2O^{11}B$: Calculated: 146.0651; Found: 146.0650.
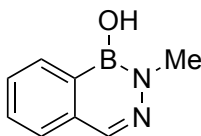
2-Methylbenzo[*d*][1,2,3]diazaborinin-1(*2H*)-ol (3-2b): Prepared according to **GP2** from 2-formylphenylboronic acid (1.50 g, 10.0 mmol) and monomethylhydrazine (553 μL, 10.5 mmol, 1.05 equiv) with a reaction time of 18 h. The title compound was isolated as a white solid (1.25 g, 78%); **mp** = 141.5 – 144.1 °C; **^{1}H NMR** (700 MHz, d_6-acetone + 1 drop D_2O): δ 8.24 (d, J = 7.7 Hz, 1 H), 7.96 (s, 1 H), 7.70 (d, J = 7.7 Hz, 1 H), 7.66 (app td, J = 7.4 Hz, 1.4 Hz, 1 H), 7.54 (app td, J = 7.4, 1.4 Hz, 1 H). In d_6-acetone alone without a drop of D_2O, approximately 9% suspected anhydride is observed, and the B–OH resonance is observed at 7.48 ppm (s, 1 H); **^{13}C NMR** (176 MHz, d_6-acetone + 1 drop D_2O): δ 138.5, 136.7, 131.52, 131.51, 129.2, 127.6, 39.1; **^{11}B NMR** (128 MHz, d_6-acetone + 1 drop D_2O): δ 27.6; **FT-IR** (cast film, cm^{-1}): 3181 (br, m), 3051 (m), 2955 (m), 2930 (m), 1611 (m), 1418 (m), 1380 (s), 1127 (m), 923 (m), 762 (m); **HRMS** (EI) for $C_8H_9N_2O^{11}B$: Calculated: 160.0808; Found: 160.0805.
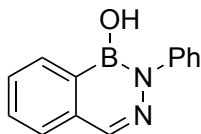
2-Phenylbenzo[*d*][1,2,3]diazaborinin-1(*2H*)-ol (3-2c): Prepared according to **GP2** from 2-formylphenylboronic acid (2.00 g, 13.3 mmol) and phenylhydrazine (1.38 mL, 14.0 mmol, 1.05 equiv) with a reaction time of 18 h. The title compound was obtained as an off-white solid (2.34 g, 79%); **mp** = 118.9 – 121.1 °C; **^{1}H NMR** (700 MHz, d_6-acetone + 1 drop D_2O): δ 8.35 (d, J = 7.6 Hz, 1 H), 8.17 (s, 1 H), 7.81 (d, J = 7.8 Hz, 1 H), 7.76 (app td, J = 7.5, 1.2 Hz, 1 H), 7.66 – 7.62 (m, 3 H), 7.41 – 7.38 (m, 2 H), 7.23 – 7.20 (m, 1 H). In d_6-acetone alone without a drop of D_2O, the B–OH resonance is observed at 7.61 ppm (s, 1 H); **^{13}C NMR** (176 MHz, d_6-acetone + 1 drop D_2O): δ 147.5, 140.2, 136.4, 132.3, 132.0, 129.8, 129.0, 127.8, 125.9, 125.7; **^{11}B NMR** (128 MHz, d_6-acetone + drop of D_2O): δ 28.3; **FT-IR** (cast film, cm^{-1}): 3255 (br, m), 3067 (m), 1598

(s), 1494 (s), 1387 (s), 1291 (m), 1104 (s), 899 (s), 762 (s), 698 (m); **HRMS** (ESI) for C$_{13}$H$_{12}$N$_2$O^{11}B [M+H]$^+$: Calculated: 223.1037; Found: 223.1034.
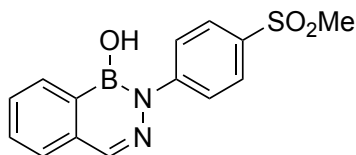
2-(4-(Methylsulfonyl)phenyl)benzo[*d*][1,2,3]diazaborinin-1(2*H*)-ol **(3-2d):** Prepared according to **GP2** from 2-formylphenylboronic acid (1.00 g, 6.67 mmol) and 4-(methylsulfonyl)phenyl hydrazine hydrochloride (1.56 g, 7.00 mmol, 1.05 equiv) with a reaction time of 18 h. The title compound was obtained as a white powder (1.75 g, 88%); **mp** = 164 – 166 °C; **^{1}H NMR** (500 MHz, d_6-acetone + 1 drop D$_2$O): δ 8.39 (d, *J* = 7.5 Hz, 1 H), 8.24 (s, 1 H), 8.00 (d, *J* = 9.0 Hz, 2 H), 7.96 (d, *J* = 9.0 Hz, 2 H), 7.84 (d, *J* = 7.5 Hz, 1 H), 7.84 (app td, *J* = 8.0, 1.0 Hz, 1 H), 7.67 (app td, *J* = 7.5, 1.0 Hz, 1 H), 3.14 (s, 3 H). In d_6-acetone alone without a drop of D$_2$O, the B–OH resonance is observed at 8.34 ppm (s, 1 H); **^{13}C NMR** (125 MHz, d_6-acetone + 1 drop D$_2$O): δ 152.1, 141.5, 137.9, 136.3, 132.8, 132.4, 130.4, 128.5, 128.2, 125.3, 44.6; **^{11}B NMR** (128 MHz, d_6-acetone + 1 drop D$_2$O): δ 28.5; **FT-IR** (KBr pellet, cm^{-1}): 3452 (m), 3047 (m), 2920 (m), 1589 (s), 1495 (s), 1333 (s), 1143 (s); **HRMS** m/z (ESI) for C$_{14}$H$_{13}$^{11}BN$_2$NaO$_3$S [M+Na]$^+$: Calculated: 323.0632; Found: 323.0629.
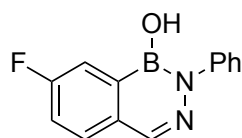
7-Fluoro-2-phenylbenzo[*d*][1,2,3]diazaborinin-1(2*H*)-ol **(F-3-2c):** Prepared according to **GP2** from 5-fluoro-2-formylphenylboronic acid (500 mg, 2.98 mmol) and phenylhydrazine (310 µL, 3.13 mmol, 1.05 equiv) with a reaction time of 18 h. The title compound was obtained as a white powder (556 mg, 78%); **mp** = 93 – 95 °C; **^{1}H NMR** (500 MHz, d_6-acetone + 1 drop D$_2$O): δ 8.17 (s, 1 H), 8.05 (dd, *J* = 9.5, 2.5 Hz, 1 H), 7.91 (dd, *J* = 8.5, 5.0 Hz, 1 H), 7.59 (d, *J* = 8.0 Hz, 2 H), 7.54 (app td, *J* = 9.0, 2.5 Hz, 1 H), 7.39 (app t, *J* = 8.0 Hz, 2 H), 7.21 (t, *J* = 7.5 Hz, 1 H). In d_6-acetone alone

without a drop of D_2O, the B–OH resonance is observed at 7.80 ppm (s, 1 H); **^{13}C NMR** (125 MHz, d_6-acetone + 1 drop D_2O): δ 163.8 (d, J = 248.0 Hz), 147.3, 139.3, 133.3, 131.2 (d, J = 8.3 Hz), 129.1, 126.1, 125.8, 120.5 (d, J = 23.6 Hz), 117.1 (d, J = 19.5 Hz); **^{11}B NMR** (128 MHz, d_6-acetone + 1 drop D_2O): δ 27.9; **^{19}F NMR** (376 MHz, d_6-acetone + 1 drop D_2O): δ –111.6 (app td, J = 9.0, 5.2 Hz); **FT-IR** (KBr pellet, cm[-1]): 3332 (br, m), 3067 (m), 1594 (s), 1493 (s), 1213 (s), 1110 (s); **HRMS** (EI) for $C_{13}H_{10}N_2O^{11}BF$: Calculated: 240.0870; Found: 240.0868.

Heterocycles **F-3-2a**, **F-3-2b**, **3-3**, **F-3-3** were synthesized by either Dr. Hwee Ting Ang or Jason Rygus.[24]

Crystallization of **3-3** was performed as follows: **3-3** (20 mg) was dissolved in hot acetonitrile (2 mL) with a drop of water in a 3-dram vial. The vial was sealed with a cap with a needle inserted through it to allow slow evaporation of the solvent. Plate shaped crystals were obtained and were used for X-ray crystallography (cf. Figure 3.14). See the supplementary information of the published article for full X-ray crystallography details.[24]

3.9.3 Preparation of Comparator Compounds (cf. Figure 3.10)
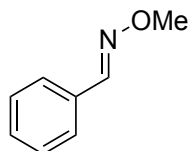
(**E**)-**Benzaldehyde *O*-Methyl Oxime (3-C1):** The title compound was synthesized according to a literature procedure[33] and the characterization data were in agreement with the literature. **^{1}H NMR** (400 MHz, d_6-acetone): δ 8.11 (s, 1 H), 7.63 – 7.60 (m, 2 H), 7.40 – 7.38 (m, 3 H).
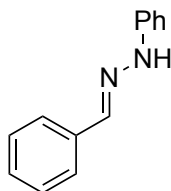
(***E***)-**1-Benzylidene-2-phenylhydrazine (3-C2):** The title compound was synthesized according to a literature procedure[34] and the characterization data were in agreement with the literature. **¹H NMR** (400 MHz, d_6-acetone + 1 drop D_2O): δ 7.86 (s, 1 H), 7.64 (dd, J = 8.4, 1.2 Hz, 2 H), 7.34 (app t, J = 7.6 Hz, 2 H), 7.25 (tt, J = 7.2, 1.2 Hz, 1 H), 7.19 (app td, J = 7.2, 2 Hz, 2 H), 7.11 (dd, J = 8.8, 1.2 Hz, 1 H), 6.73 (tt, J = 7.2, 1.2 Hz, 1 H).
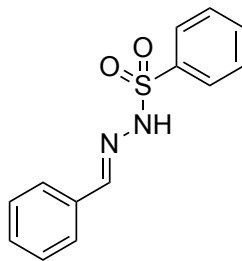
(***E***)-***N'***-**Benzylidenebenzenesulfonohydrazide** **(3-C3):** The compound was synthesized according to a literature procedure[35] with slight modifications. Benzaldehyde (100 mg, 0.940 mmol) was dissolved in ethanol (3 mL) followed by the addition of benzenesulfonyl hydrazide (162 mg, 0.94 mmol). The reaction mixture was stirred at room temperature for 16 h and then the solvent was evaporated. The characterization data were in agreement with the literature. **¹H NMR** (500 MHz, d_6-acetone + 1 drop D_2O): δ 7.98 (s, 1 H), 7.96 (dd, J = 6.4, 1.2 Hz, 2 H), 7.62 – 7.57 (m, 5 H), 7.36 (m, 3 H).
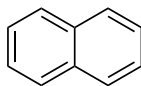
Naphthalene (3-C4): Purchased from Fisher Scientific and used as received. **¹H NMR** (400 MHz, d_6-acetone): δ 7.89 (dd, J = 6.2, 3.3 Hz, 4 H), 7.49 (dd, J = 6.3, 3.2 Hz, 4 H).
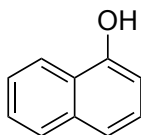
1-Hydroxynaphthalene (3-C5): Purchased from Sigma Aldrich and used as received. **¹H NMR** (400 MHz, d_6-acetone): δ 8.95 (s, 1 H), 8.23 (ddt, J = 7.1, 2.6, 0.9 Hz, 1 H), 7.81 (dd, J = 6.8, 2.3 Hz, 1 H), 7.51 – 7.40 (m, 2 H), 7.37 (d, J = 7.9 Hz, 1 H), 7.28 (t, J = 7.8 Hz, 1 H), 6.91 (dd, J = 7.4, 1.2 Hz, 1 H).
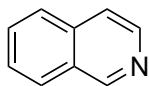
Isoquinoline (3-C6): Purchased from Sigma Aldrich and used as received. **¹H NMR** (400 MHz, d_6-acetone): δ 9.29 (d, J = 1.0 Hz, 1 H), 8.50 (d, J = 5.7 Hz, 1 H), 8.09 (d, J = 8.2 Hz, 1 H), 7.93 (d, J = 8.1 Hz, 1 H), 7.80 – 7.71 (m, 2 H), 7.67 (ddd, J = 8.2, 6.9, 1.2 Hz, 1 H).

Other comparators were synthesized by either Dr. Hwee Ting Ang or Dr. Marco Paladino.[24]

3.9.4 Crystallization and Hydrolysis of B—O—B-Dimer of 3-2c

The formation of **3-2c-BOB** was observed by X-Ray crystallographic analysis. Two samples of **3-2c** were recrystallized from different solvent systems. In the first, **3-2c** (10 mg) was dissolved in hot acetonitrile (2 mL), while in the second another sample of **3-2c** (10 mg) was dissolved in hot acetonitrile (2 mL) with a drop of water. Recrystallization was done in 3-dram vials. They were sealed with a cap with a needle inserted through it to allow slow evaporation of the solvent. Needle shaped crystals of **3-2c-BOB** were obtained when recrystallized from neat acetonitrile (Figure 3.22). Plate shaped crystals of **3-2c** were obtained from the acetonitrile/water sample (Figure 3.23). See supplementary information of the published article for full X-ray crystallography details.[24]
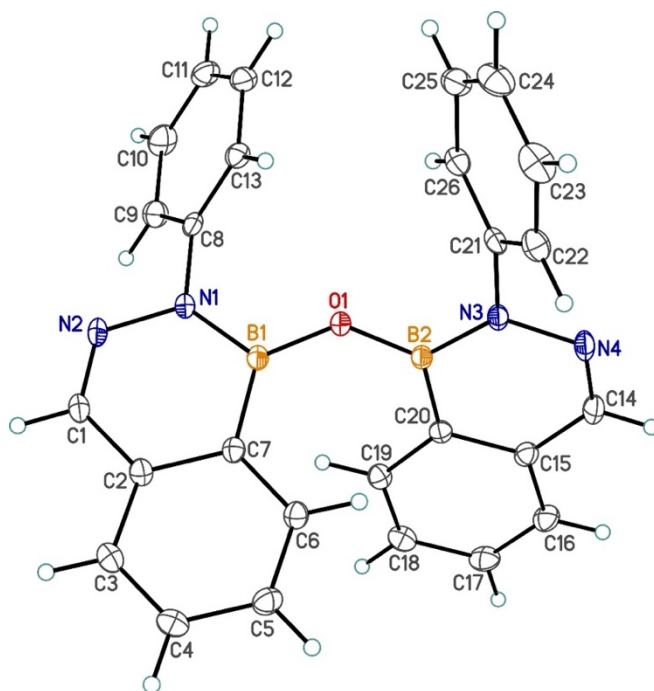
Figure 3.22. ORTEP representation of the BOB anhydride dimer of **3-2c** (**3-2c-BOB**) obtained from recrystallization in neat acetonitrile.
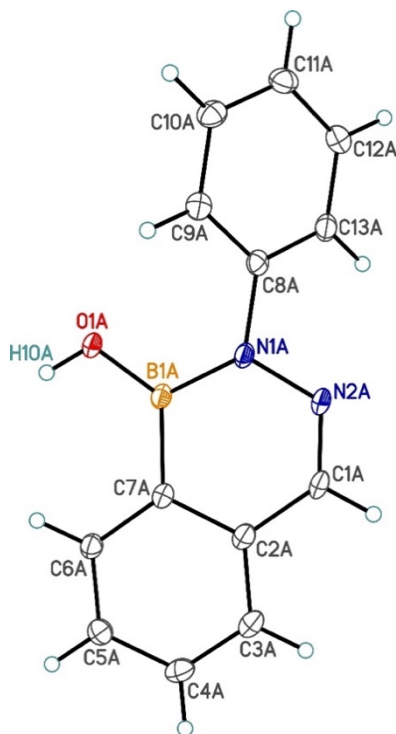
Figure 3.23. ORTEP representation of **3-2c** obtained from recrystallization in acetonitrile with a drop of water.

The ^{1}H NMR spectrum of heterocycle **3-2c** in CD$_3$CN showed small amounts of BOB anhydride dimer (Figure 3.24a). Addition of a drop of D$_2$O led to disappearance of the proposed BOB dimer peaks and full conversion to the corresponding B—OD hemiboronic acid (Figure 3.24b).

a) 3-2c in *d*-acetonitrile
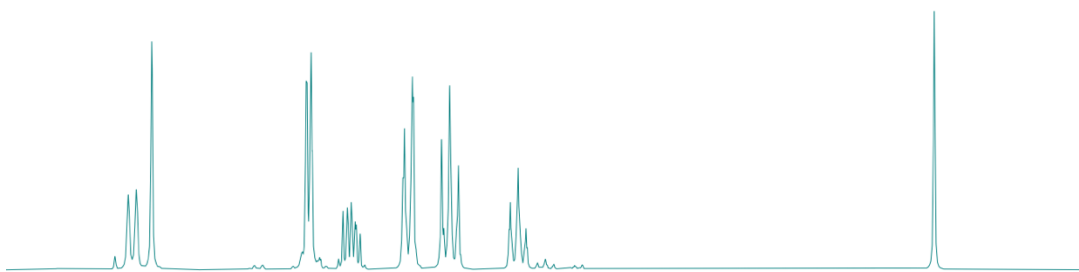
b) 3-2c in *d*-acetonitrile + 1 drop D$_2$O
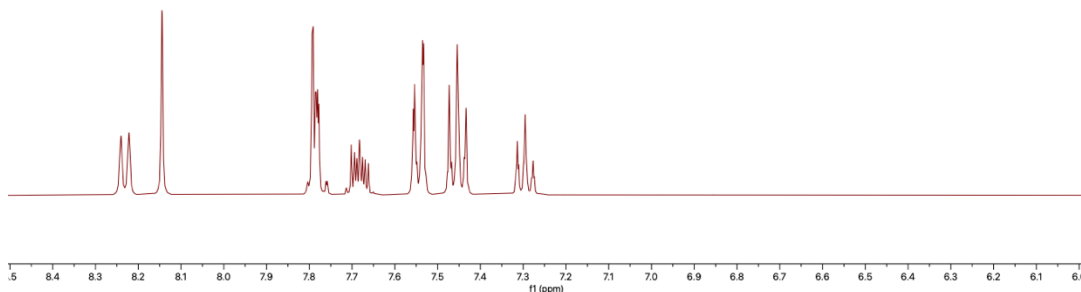
Figure 3.24. NMR spectra of heterocycle **3-2c** in CD$_3$CN before **a)** and after **b)** addition of a drop of D$_2$O.

3.9.5 H$_2$^{18}O Labelling Experiment

In a flame dried microwave vial, **3-1**, **3-2b** or **3-3** (2.50 mg) was charged and the vial was sealed with a septum. An argon balloon was inserted through the septum, and anhydrous acetonitrile (0.25 mL) was added, followed by H$_2$^{18}O (97% ^{18}O, 0.05 mL). The reaction solution was stirred at an indicated temperature for an indicated time (cf. Table 3.3). The reaction mixture was analyzed directly by flow injection analysis, and the ratio of ^{18}O labelled product and ^{16}O labelled product was recorded. High-resolution electrospray ionization (ESI) mass spectra were acquired by flow injection analysis using an Agilent 6220 oaTOF (Santa Clara, CA, USA), equipped with a dual sprayer electrospray ionization source with the second sprayer providing a

reference mass solution and an Agilent 1200 Series isocratic pump. Optima™ LC-MS grade acetonitrile was used as a carrier solvent at a flow rate of 0.2 mLmin^{-1}. Mass spectral conditions such as positive/negative ionization mode, VCap voltage and fragmentor voltage were varied based on the properties of each compound analysed. Drying gas was 10 Lmin^{-1}, nebulizer pressure was 25 psi. Data analysis was performed using the Agilent MassHunter Qualitative Analysis software package version B.03.01 SP3. For the reaction at rt and 68 h:

HRMS m/z (ESI) for $C_7H_6NO^{18}O^{11}B$ [M–H]$^-$ (^{18}O labelled **3-1**, 50%): Calculated: 148.0461; Found: 148.0443. **HRMS** m/z (ESI) for $C_7H_6NO_2^{11}B$ [M–H]$^-$ (**3-1**, 50%): Calculated: 146.0419; Found: 146.0401.
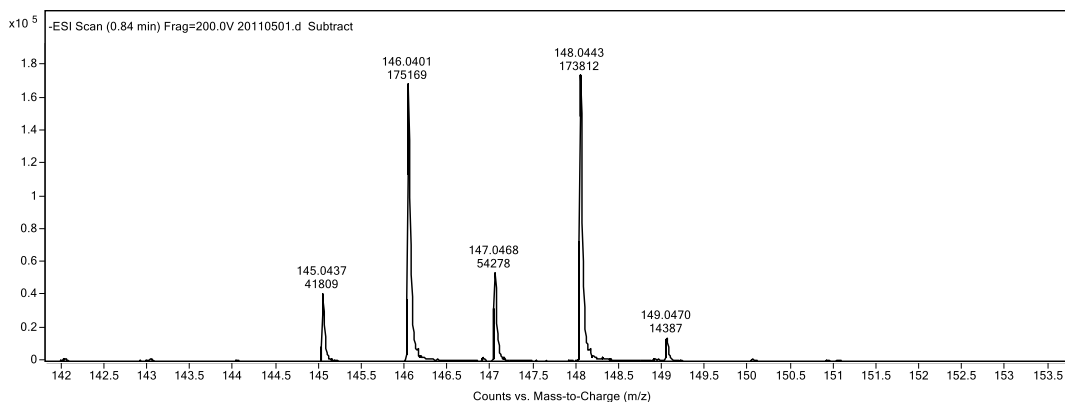
HRMS m/z (ESI) for $C_8H_{10}N_2^{18}O^{11}B$ [M+H]$^+$ (^{18}O labelled **3-2b**, >96%): Calculated: 163.0923; Found: 163.0923.
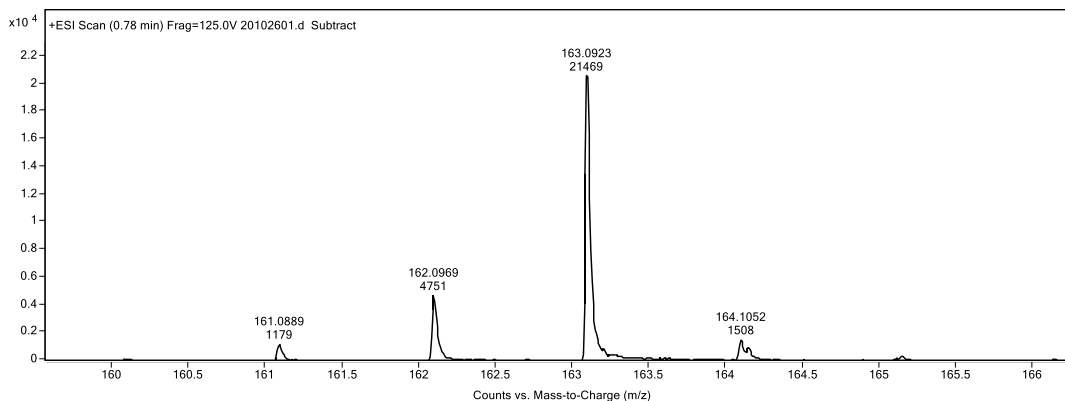
HRMS m/z (ESI) for $C_{13}H_{11}N_2NaO_2S^{18}O^{11}B$ [M+Na]$^+$ (^{18}O labelled **3-3**, >92%): Calculated: 311.0518; Found: 311.0537.
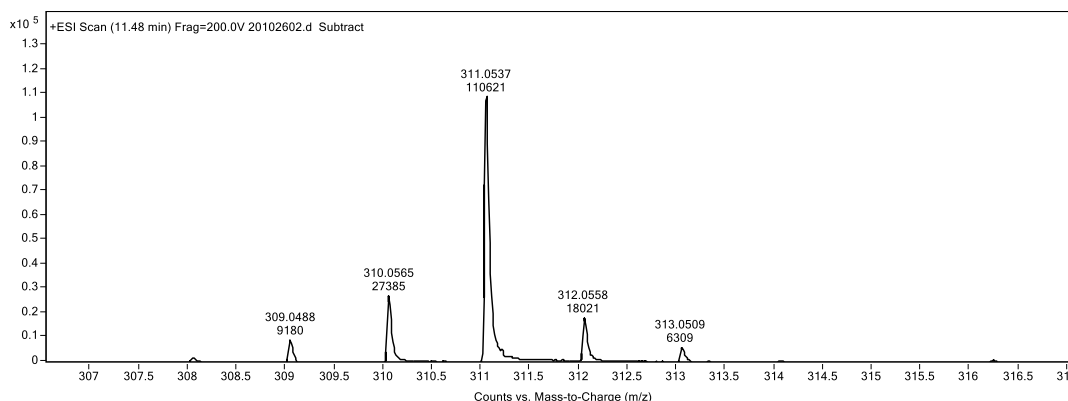
3.9.6 Crossover Experiments (cf. Figure 3.13)

3.9.6.1 Crossover Between Boron Heterocycles and 2-Formylarylboronic Acids

General Procedure for Crossover Reactions Between Hemiboronic Acids and 2-Formylarylboronic Acids in Acetonitrile/Water (GP3)
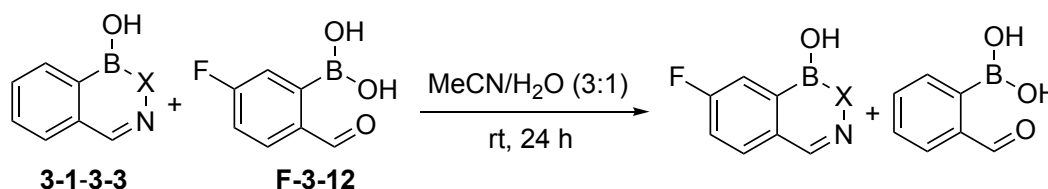
A round-bottom flask was charged with boron heterocycle **3-1**–**3-3** (0.05 mmol) and 2-formylarylboronic acid **F-3-12** (1.0 equiv). The solids were dissolved in MeCN (0.75 mL) and H_2O (0.25 mL) under air. The reaction mixture was stirred at rt for 24 h, after which it was concentrated by rotary evaporation, dried under vacuum, and analyzed by ^{19}F NMR spectroscopy in d_6-acetone with a drop of D_2O.
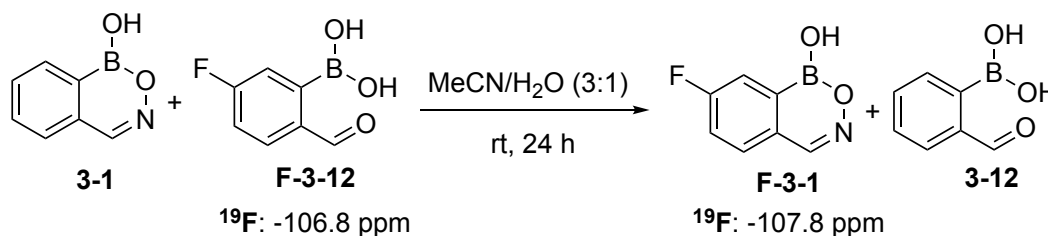
Following **GP3**, no crossover was observed in MeCN/H_2O (Figure 3.25).
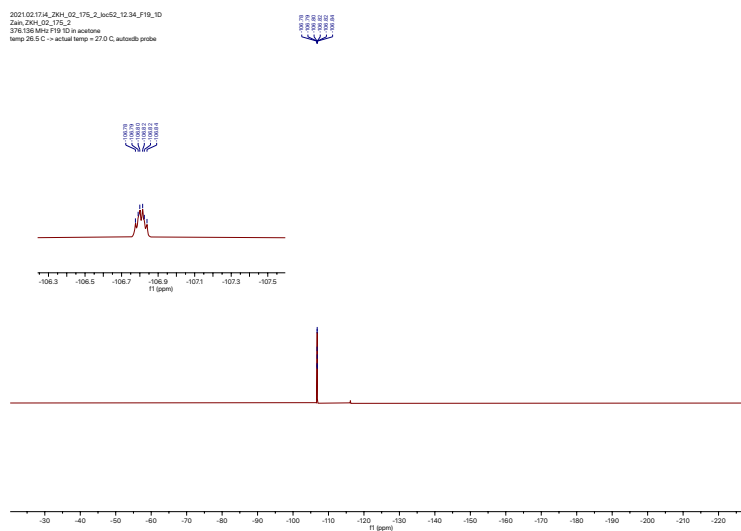
Figure 3.25. ^{19}F NMR spectrum in d_6-acetone of crossover reaction between **3-1** and **F-3-12** using MeCN/H$_2$O as the reaction solvent.
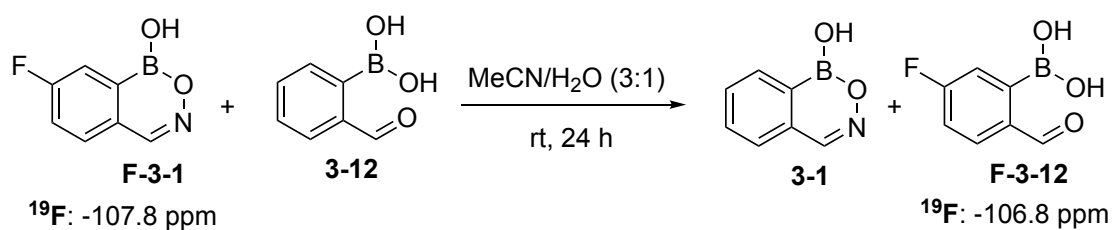
Following **GP3**, no crossover was observed in MeCN/H$_2$O (Figure 3.26).
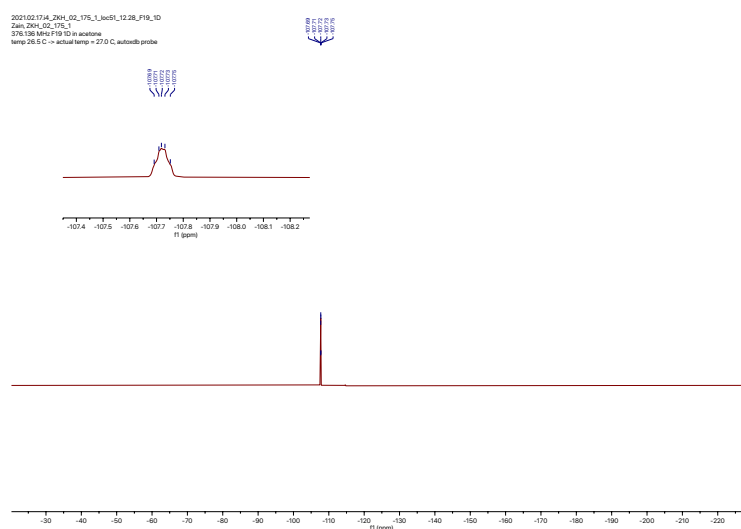
Figure 3.26. ^{19}F NMR spectrum in d_6-acetone of crossover reaction between **F-3-1** and **3-12** using MeCN/H$_2$O as the reaction solvent.

3-2a + **F-3-12** → **F-3-2a** + **3-12**

MeCN/H$_2$O (3:1), rt, 24 h

F-3-12 ^{19}**F**: -106.8 ppm

F-3-2a ^{19}**F**: -112.4 ppm
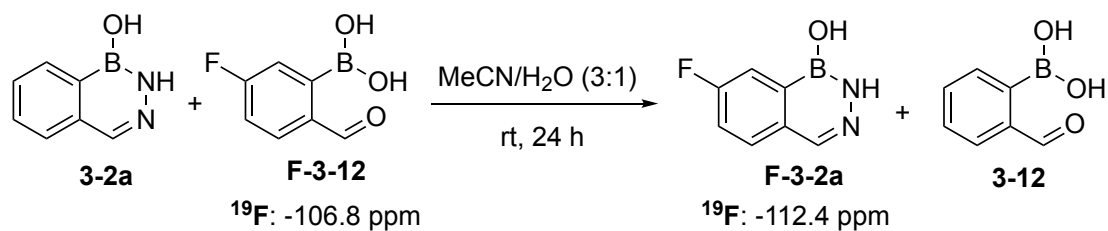
Following **GP3**, no crossover was observed in MeCN/H$_2$O (Figure 3.27).
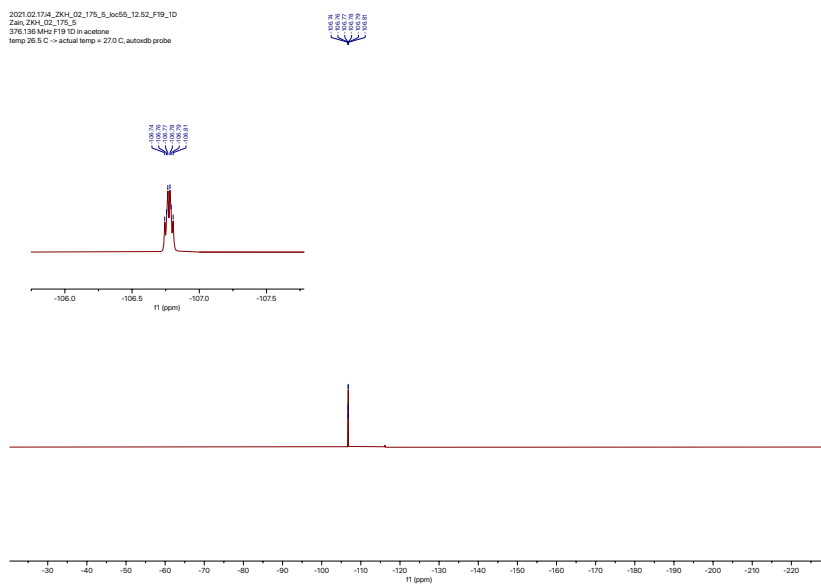
Figure 3.27. ^{19}F NMR spectrum in *d$_6$*-acetone of crossover reaction between **3-2a** and **F-3-12** using MeCN/H$_2$O as the reaction solvent.
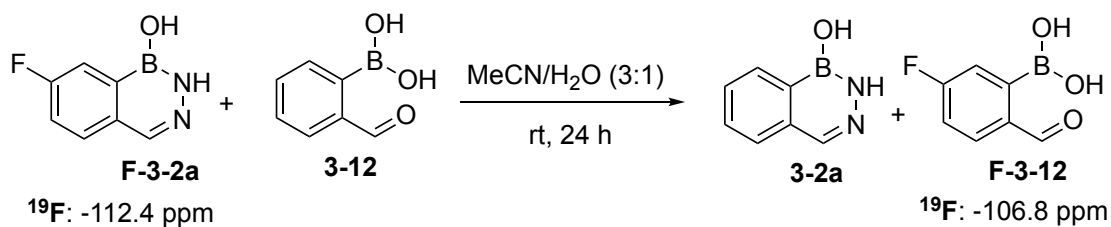
F-3-2a + **3-12** → **3-2a** + **F-3-12**

MeCN/H$_2$O (3:1), rt, 24 h

F-3-2a ^{19}**F**: -112.4 ppm

F-3-12 ^{19}**F**: -106.8 ppm

Following **GP3**, no crossover was observed in MeCN/H$_2$O (Figure 3.28).

Figure 3.28. ^{19}F NMR spectrum in d_6-acetone of crossover reaction between **F-3-2a** and **3-12** using MeCN/H$_2$O as the reaction solvent.

3-2b	**F-3-12**	
	^{19}**F**: -106.8 ppm	
	F-3-2b	**3-12**
	^{19}**F**: -112.4 ppm	

Following **GP3**, no crossover was observed in MeCN/H$_2$O (Figure 3.29).

Figure 3.29. ^{19}F NMR spectrum in d_6-acetone of crossover reaction between **3-2b** and **F-3-12** using MeCN/H$_2$O as the reaction solvent.

F-3-2b
^{19}**F**: -112.4 ppm

3-12

MeCN/H$_2$O (3:1)
rt, 24 h

3-2b

F-3-12
^{19}**F**: -106.8 ppm
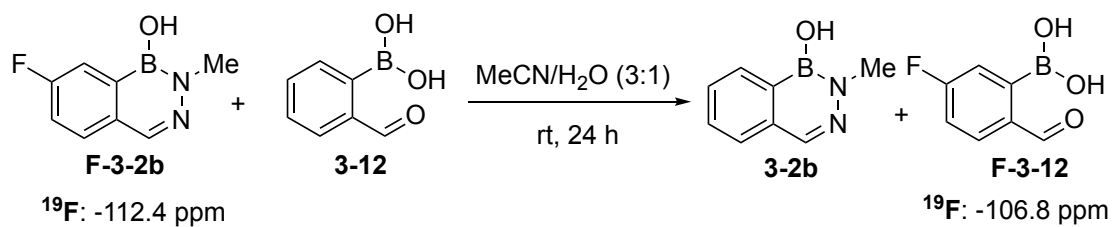
Following **GP3**, no crossover was observed in MeCN/H$_2$O (Figure 3.30).
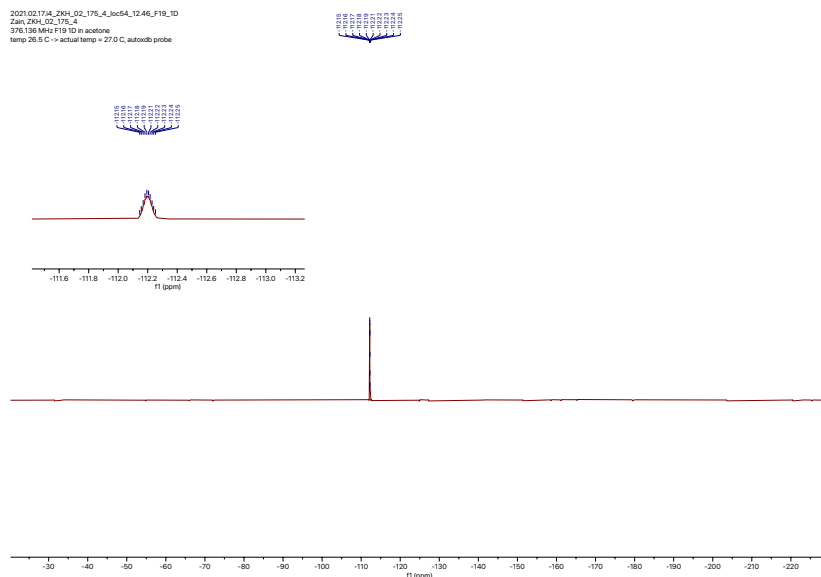
Figure 3.30. ^{19}F NMR spectrum in d_6-acetone of crossover reaction between **F-3-2b** and **3-12** using MeCN/H$_2$O as the reaction solvent.

3-2c

F-3-12
^{19}**F**: -106.8 ppm

MeCN/H$_2$O (3:1)
rt, 24 h

F-3-2c
^{19}**F**: -111.6 ppm

3-12
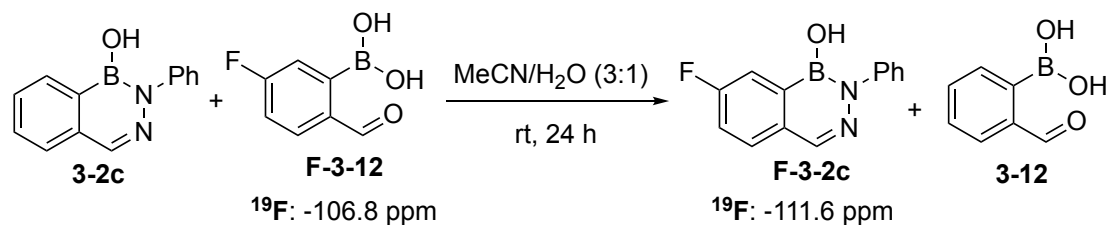
Following **GP3**, no crossover was observed in MeCN/H$_2$O (Figure 3.31).
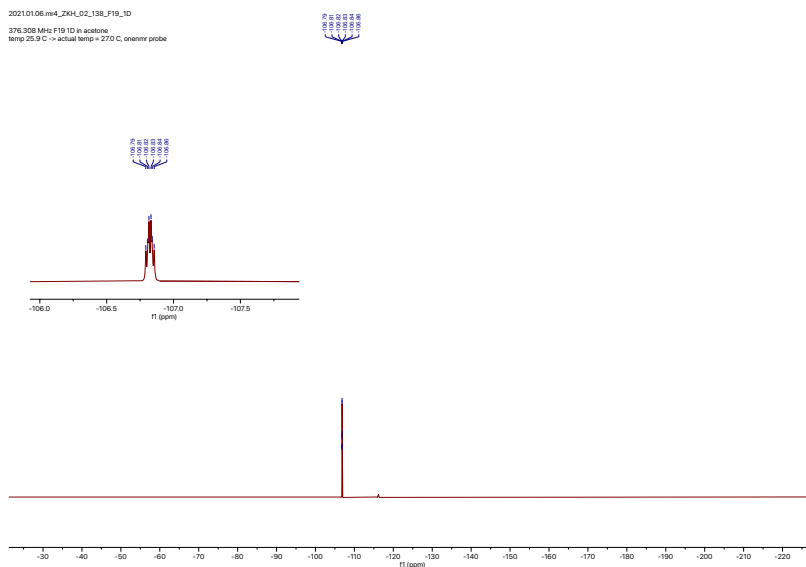
Figure 3.31. ^{19}F NMR spectrum in d_6-acetone of crossover reaction between **3-2c** and **F-3-12** using MeCN/H$_2$O as the reaction solvent.
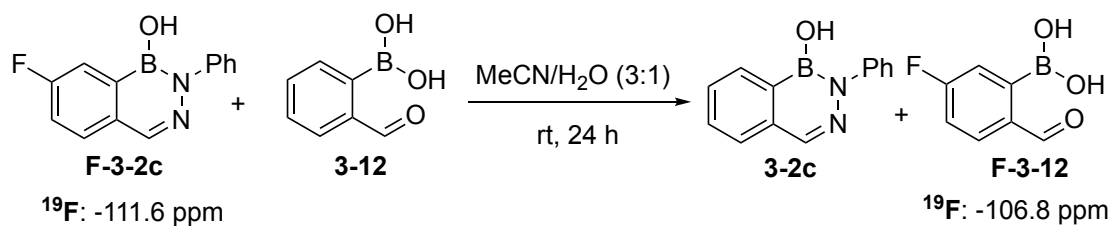
Following **GP3**, no crossover was observed in MeCN/H$_2$O (Figure 3.32).
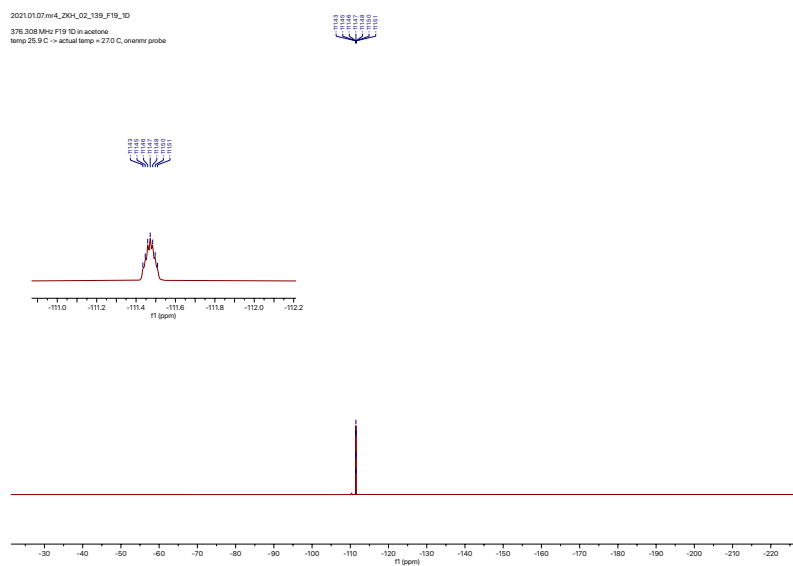
Figure 3.32. ^{19}F NMR spectrum in d_6-acetone of crossover reaction between **F-3-2c** and **3-12** using MeCN/H$_2$O as the reaction solvent.
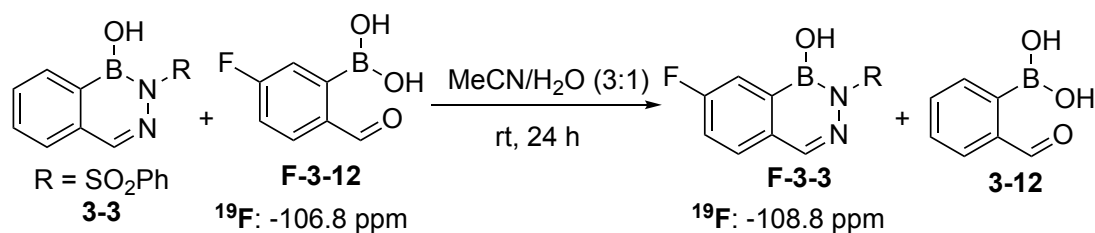
Following **GP3** in MeCN/H₂O, the ratio of **F-3-3** to **F-3-12** was 0.06:1.00, corresponding to 6% crossover (Figure 3.33).
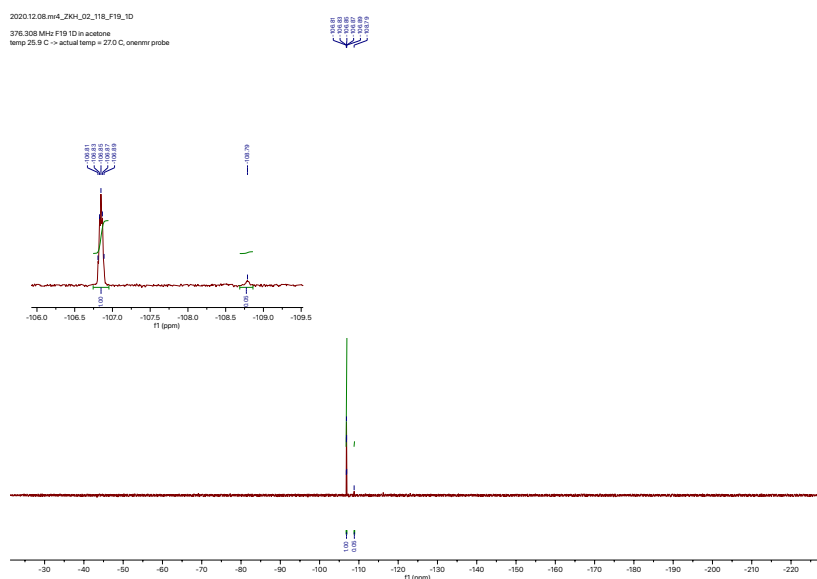
Figure 3.33. ^{19}F NMR spectrum in d_6-acetone of crossover reaction between **3-3** and **F-3-12** using MeCN/H₂O as the reaction solvent.
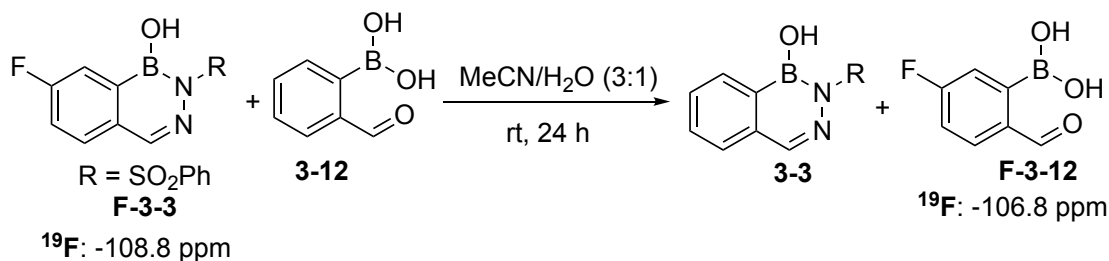
Following **GP3** in MeCN/H₂O, the ratio of **F-3-12** to **F-3-3** was 0.16:1.00, corresponding to 14% crossover (Figure 3.34).
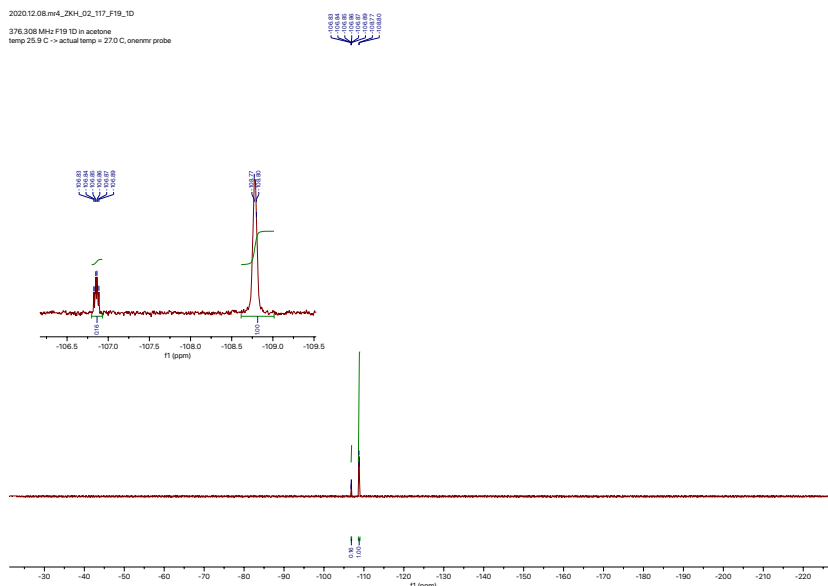
Figure 3.34. ^{19}F NMR spectrum in d_6-acetone of crossover reaction between **F-3-3** and **3-12** using MeCN/H$_2$O as the reaction solvent.

3.9.6.2 Crossover Between Two Boron Heterocycles

General Procedure for Crossover Reactions Between Two Hemiboronic Acids in Acetonitrile/Water (GP4)
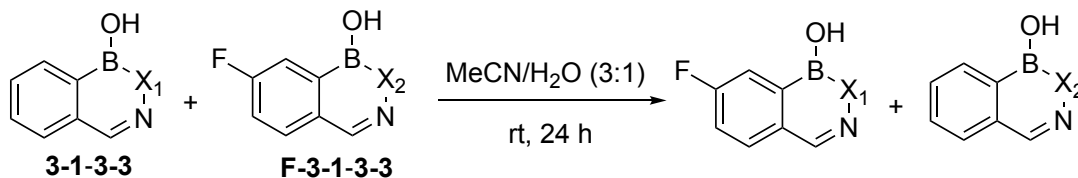
A round-bottom flask was charged with boron heterocycle **3-1**–**3-3** (0.05 mmol) and fluorinated boron heterocycle **F-3-1**–**3-3** (1.0 equiv). The solids were dissolved in MeCN (0.75 mL) and H$_2$O (0.25 mL) under air. The reaction mixture was stirred at rt for 24 h, after which it was concentrated by rotary evaporation, dried under vacuum, and analyzed by ^{19}F NMR spectroscopy in d_6-acetone with a drop of D$_2$O.

104
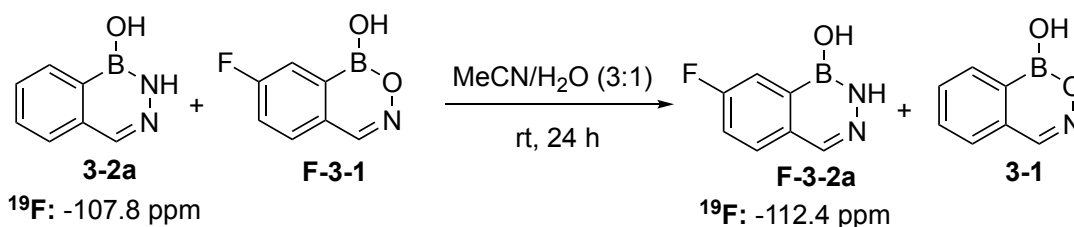
No crossover was detected following **GP4** in MeCN/H$_2$O (Figure 3.35).
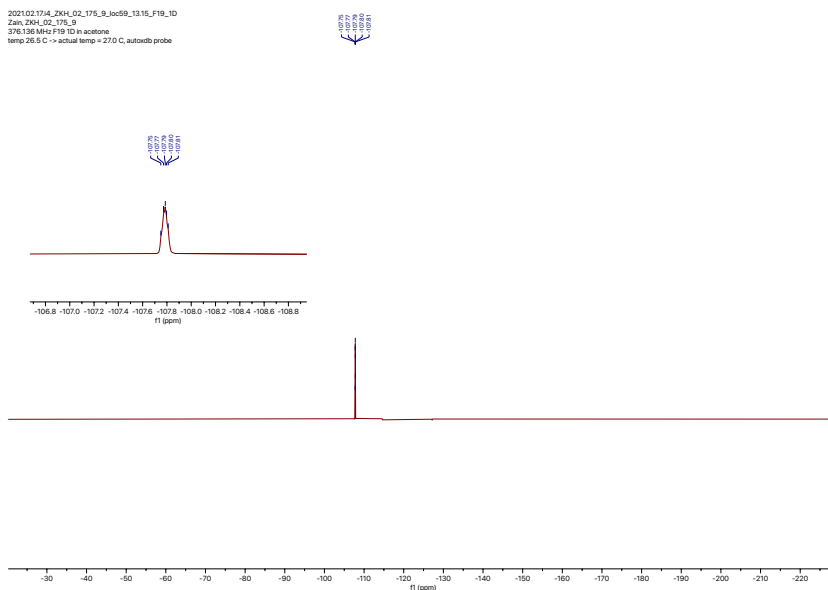
Figure 3.35. ^{19}F NMR spectrum in d_6-acetone of crossover reaction between **3-2a** and **F-3-1** using MeCN/H$_2$O as the reaction solvent.

3-1 + **F-3-2a** → **F-3-1** + **3-2a**

MeCN/H$_2$O (3:1)
rt, 24 h

F-3-2a
^{19}**F:** -112.4 ppm

F-3-1
^{19}**F:** -107.8 ppm
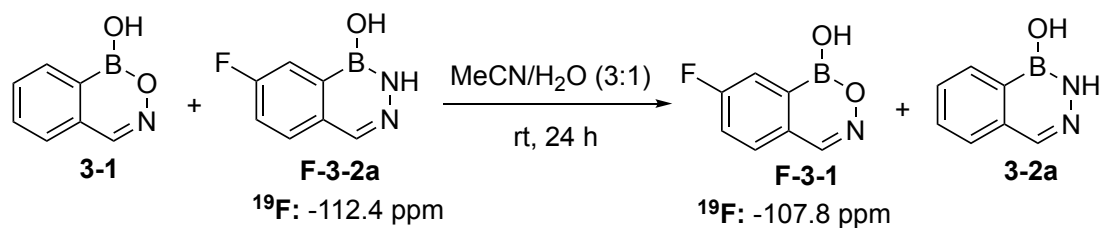
No crossover was detected following **GP4** in MeCN/H$_2$O (Figure 3.36).
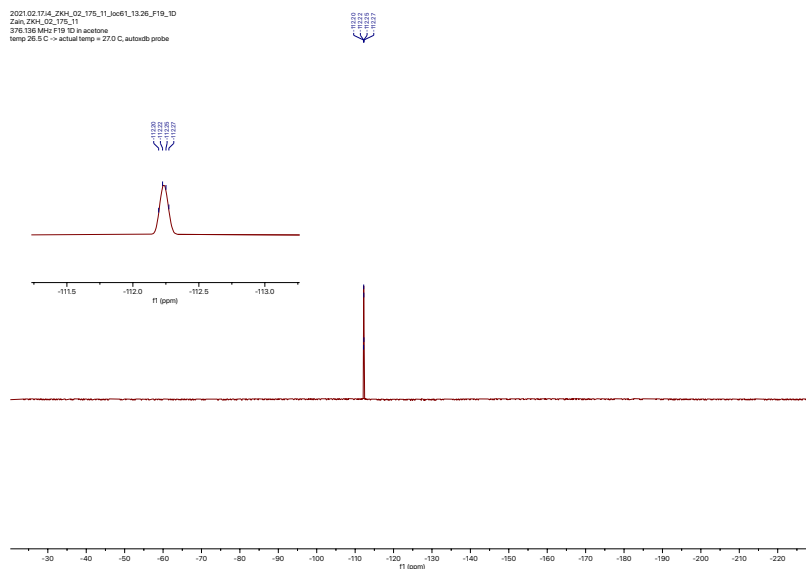
Figure 3.36. ^{19}F NMR spectrum in d_6-acetone of crossover reaction between **3-1** and **F-3-2a** using MeCN/H$_2$O as the reaction solvent.
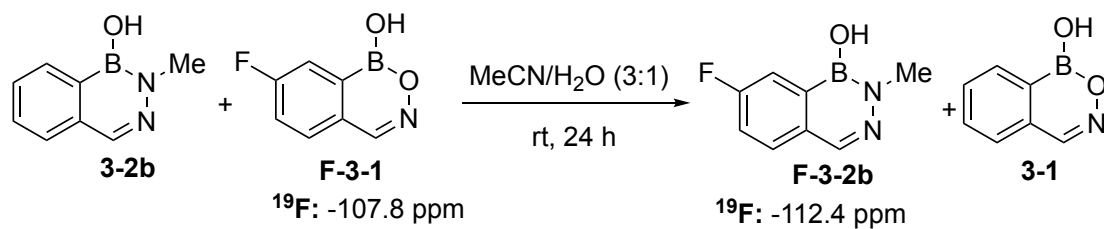
No crossover was detected following **GP4** in MeCN/H$_2$O (Figure 3.37).
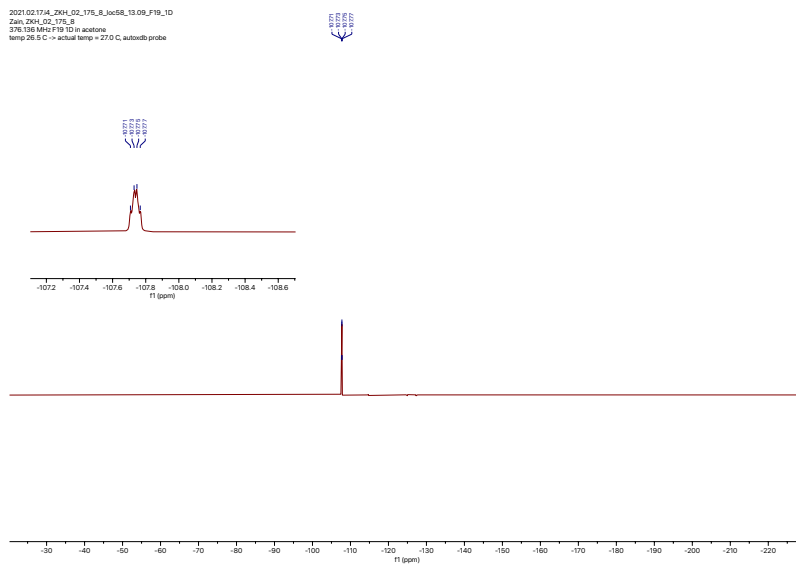
Figure 3.37. ^{19}F NMR spectrum in d_6-acetone of crossover reaction between **3-2b** and **F-3-1** using MeCN/H$_2$O as the reaction solvent.
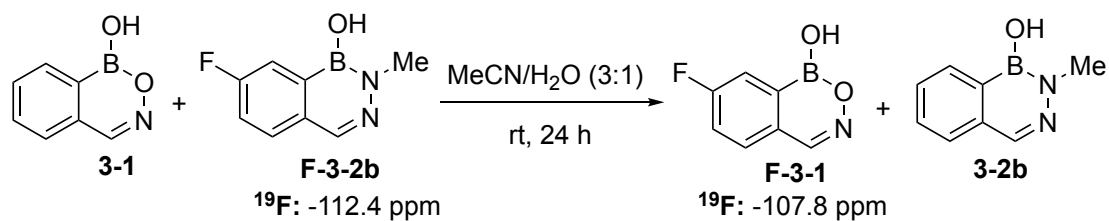
No crossover was detected following **GP4** in MeCN/H$_2$O (Figure 3.38).
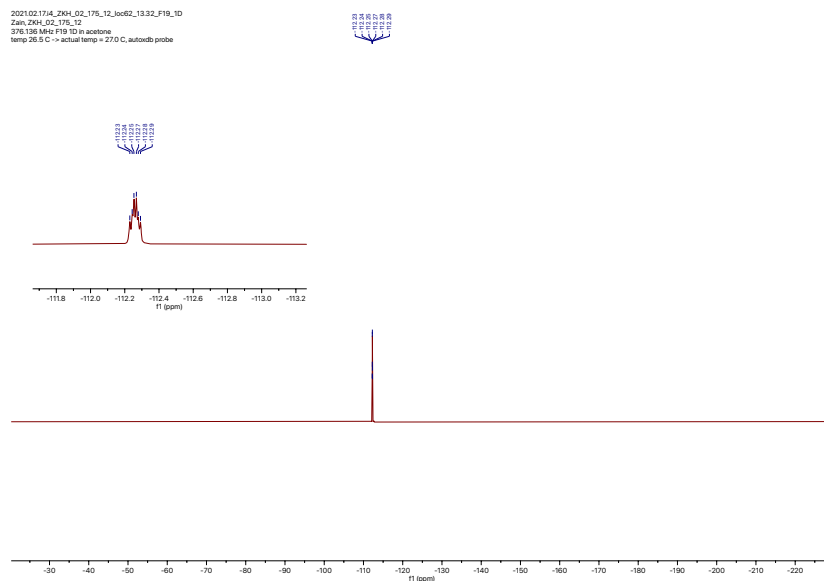
Figure 3.38. ^{19}F NMR spectrum in d_6-acetone of crossover reaction between **F-3-2b** and **3-1** using MeCN/H$_2$O as the reaction solvent.
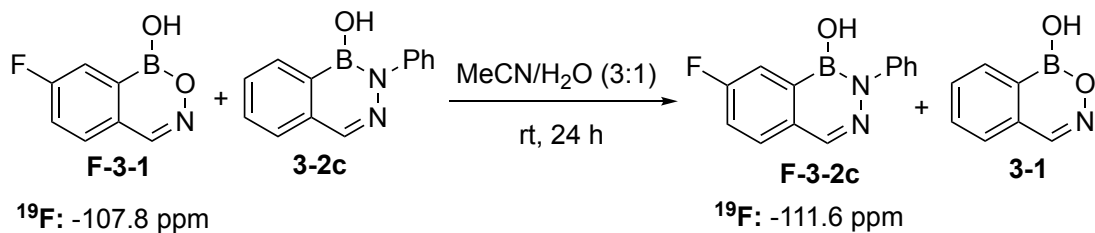
No crossover was detected following **GP4** in MeCN/H$_2$O (Figure 3.39).

Figure 3.39. ¹⁹F NMR spectrum in d_6-acetone of crossover reaction between **F-3-1** and **3-2c** using MeCN/H₂O as the reaction solvent.

No crossover was detected following **GP4** in MeCN/H₂O (Figure 3.40).

Figure 3.40. ¹⁹F NMR spectrum in d_6-acetone of crossover reaction between **F-3-2c** and **3-1** using MeCN/H₂O as the reaction solvent.
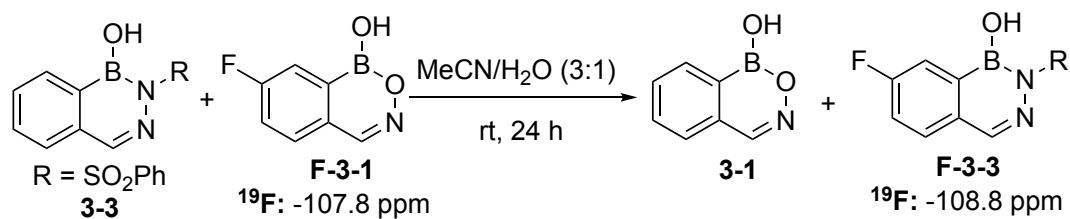
No crossover was detected following **GP4** in MeCN/H$_2$O (Figure 3.41).
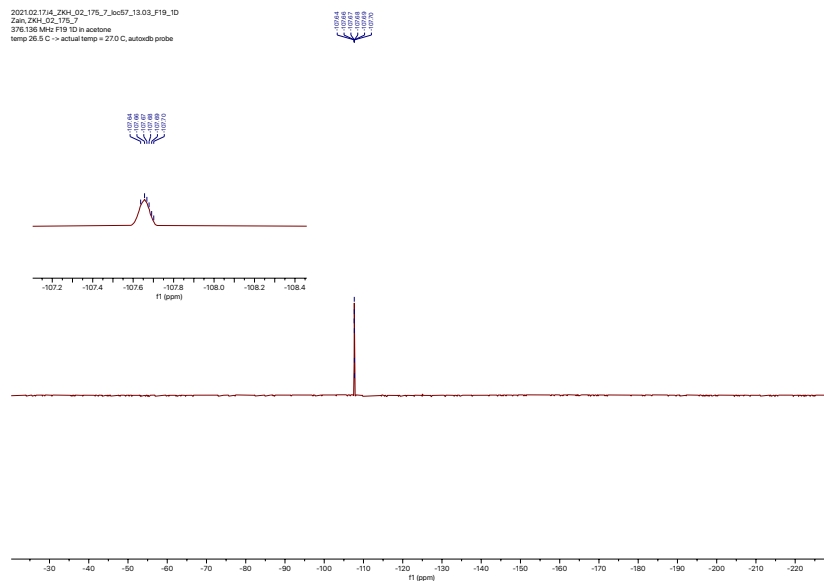
Figure 3.41. ^{19}F NMR spectrum in d_6-acetone of crossover reaction between **F-3-1** and **3-3** using MeCN/H$_2$O as the reaction solvent.
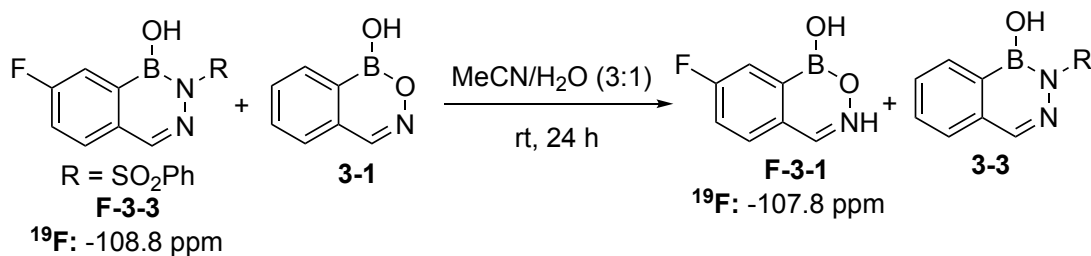
No crossover was detected following **GP4** in MeCN/H$_2$O (Figure 3.42).
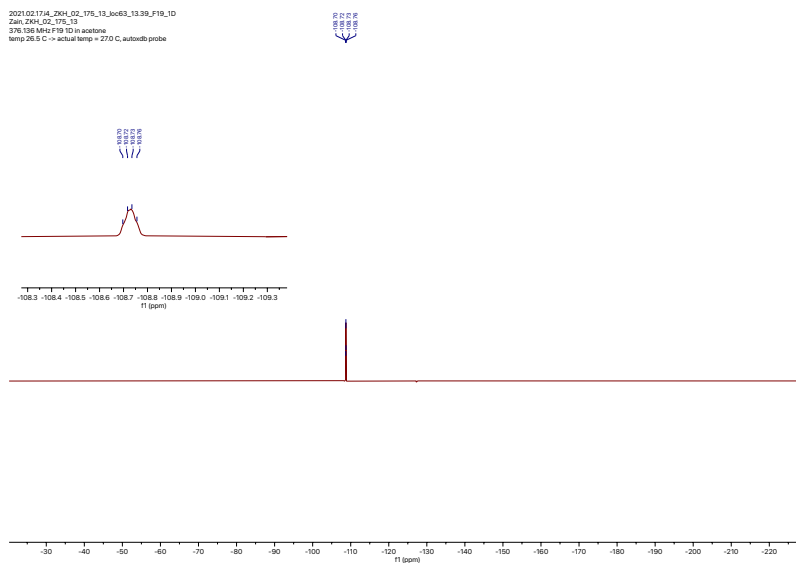
Figure 3.42. ^{19}F NMR spectrum in d_6-acetone of crossover reaction between **3-1** and **F-3-3** using MeCN/H$_2$O as the reaction solvent.
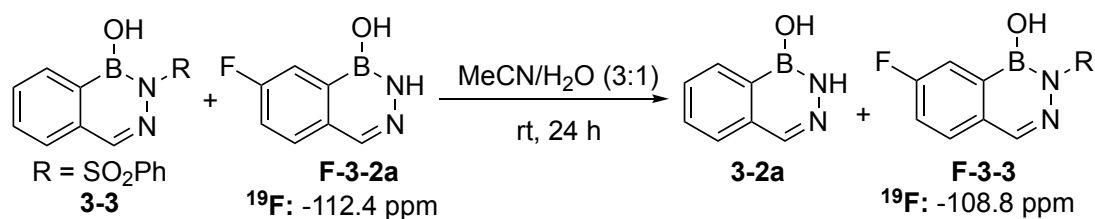
No crossover was detected following **GP4** in MeCN/H$_2$O (Figure 3.43).
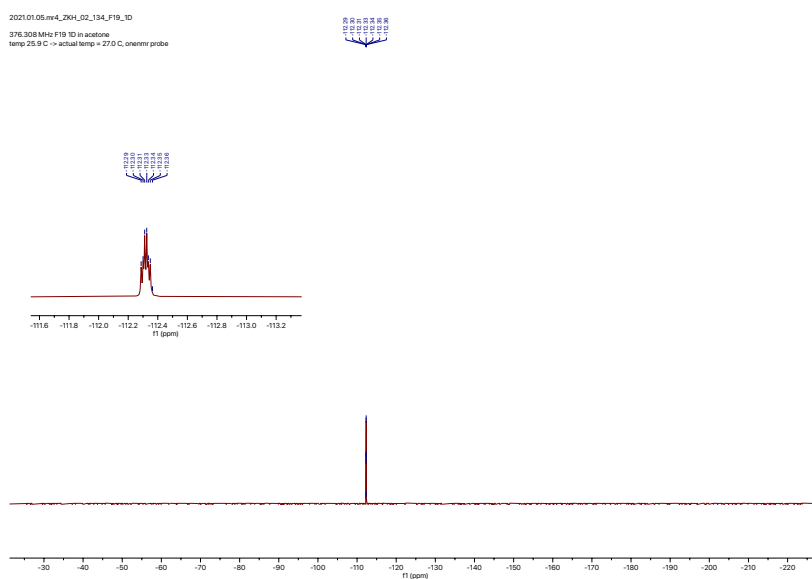
Figure 3.43. ^{19}F NMR spectrum in d_6-acetone of crossover reaction between **3-3** and **F-3-2a** using MeCN/H$_2$O as the reaction solvent.
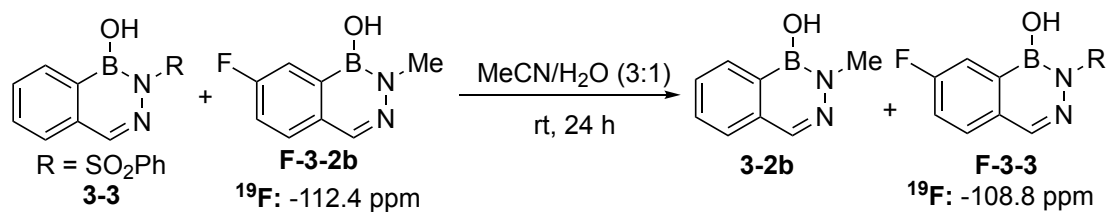
No crossover was detected following **GP4** in MeCN/H$_2$O (Figure 3.44).
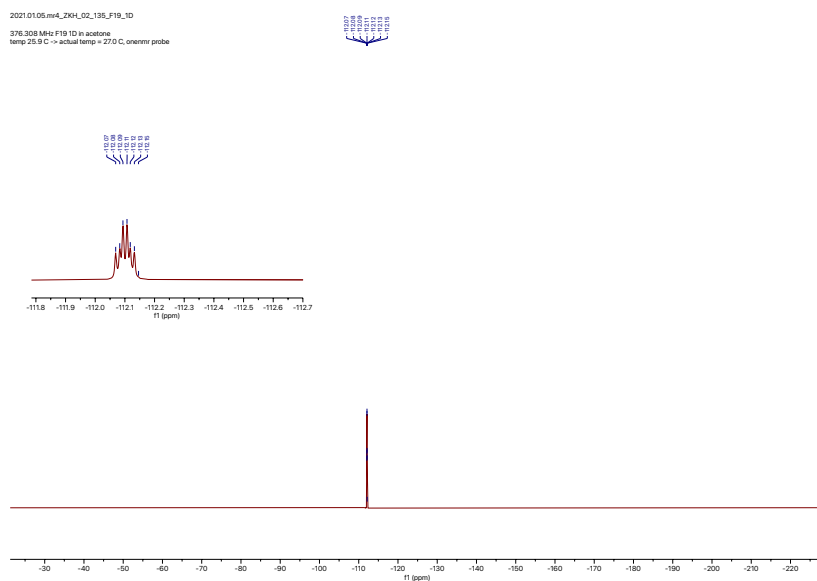
Figure 3.44. ^{19}F NMR spectrum in d_6-acetone of crossover reaction between **3-3** and **F-3-2b** using MeCN/H$_2$O as the reaction solvent.
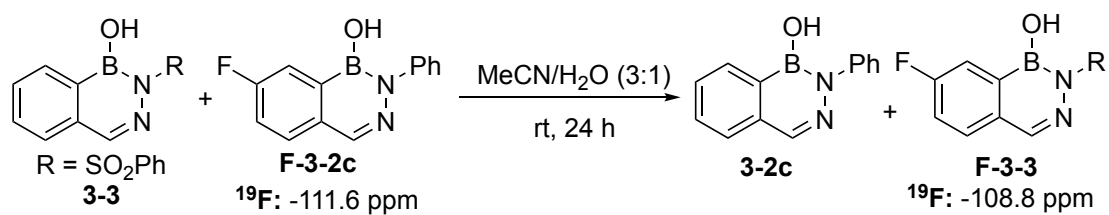
No crossover was detected following **GP4** in MeCN/H$_2$O (Figure 3.45).
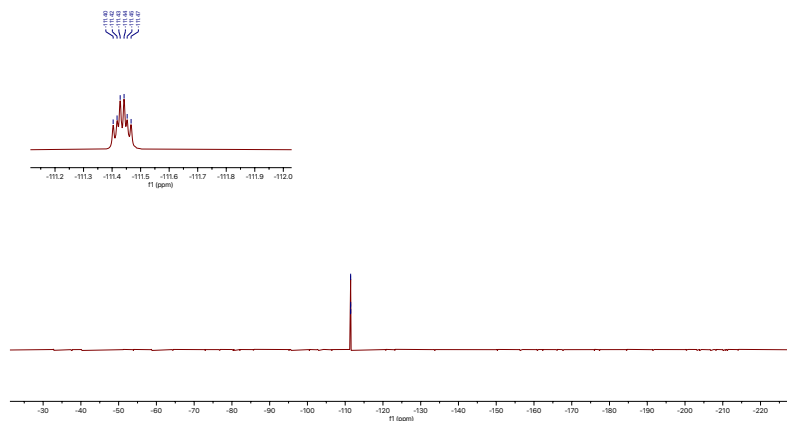
Figure 3.45. ^{19}F NMR spectrum in d_6-acetone of crossover reaction between **3-3** and **F-3-2c** using MeCN/H$_2$O as the reaction solvent.
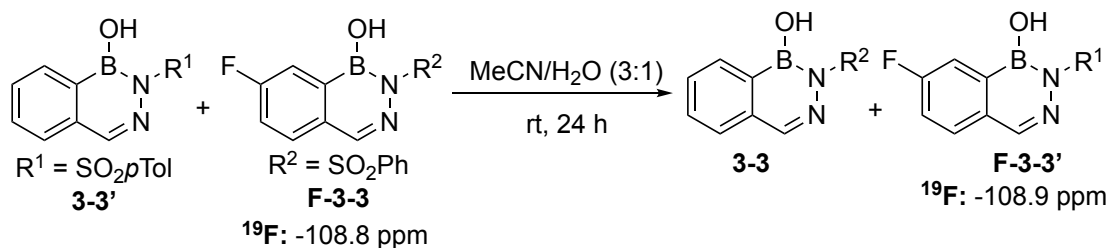
No crossover was detected following **GP4** in MeCN/H$_2$O (Figure 3.46).
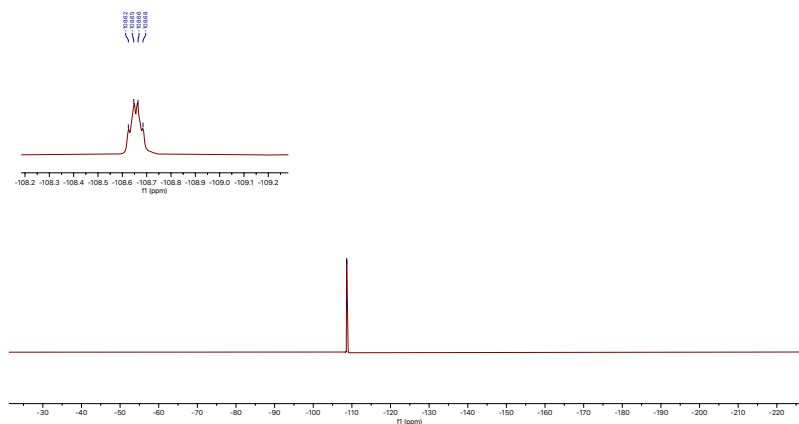
Figure 3.46. ^{19}F NMR spectrum in d_6-acetone of crossover reaction between **F-3-3** and **3-3'** using MeCN/H$_2$O as the reaction solvent.

Additional experiments with heterocycle **3-3** showed that crossover with fluorinated aldehyde **F-3-12** occurred only in the presence of methanol.

In MeCN alone following GP4, less than 2% crossover was observed (Figure 3.47).
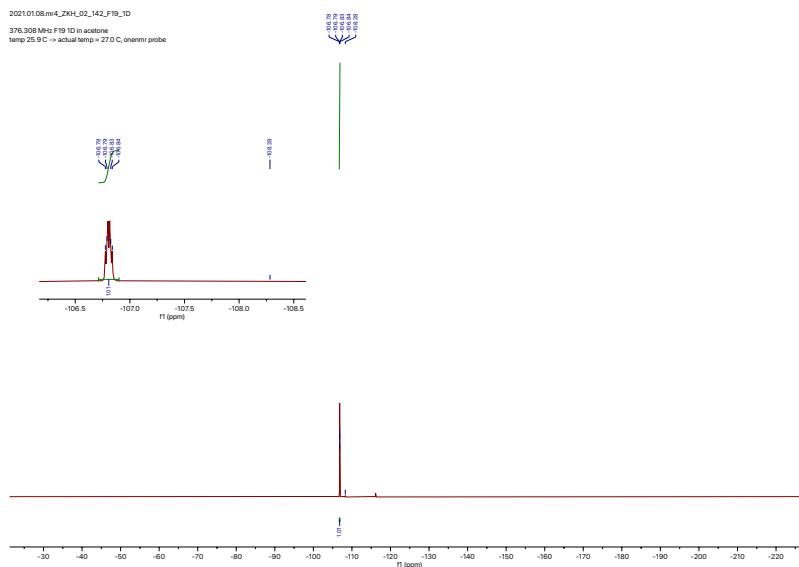
Figure 3.47. ^{19}F NMR spectrum in d_6-acetone of crossover reaction between **3-3** and **F-3-12** using MeCN as the reaction solvent.

In H$_2$O alone following **GP4**, less than 2% crossover was observed (Figure 3.48).
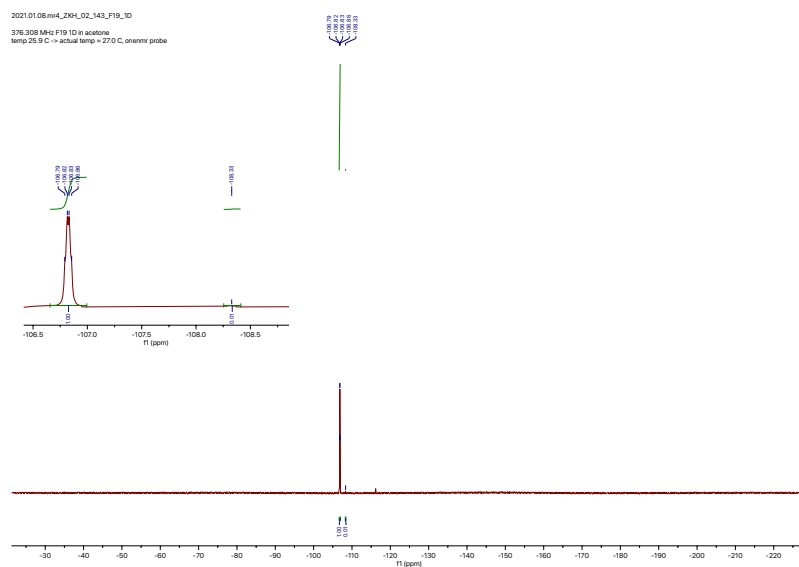
Figure 3.48. ^{19}F NMR spectrum in d_6-acetone of crossover reaction between **3-3** and **F-3-12** using H$_2$O as the reaction solvent.

Using a 1:1 mixture of MeCN and aqueous buffer (pH 6.9) following **GP4**, less than 2% crossover was observed (Figure 3.49).
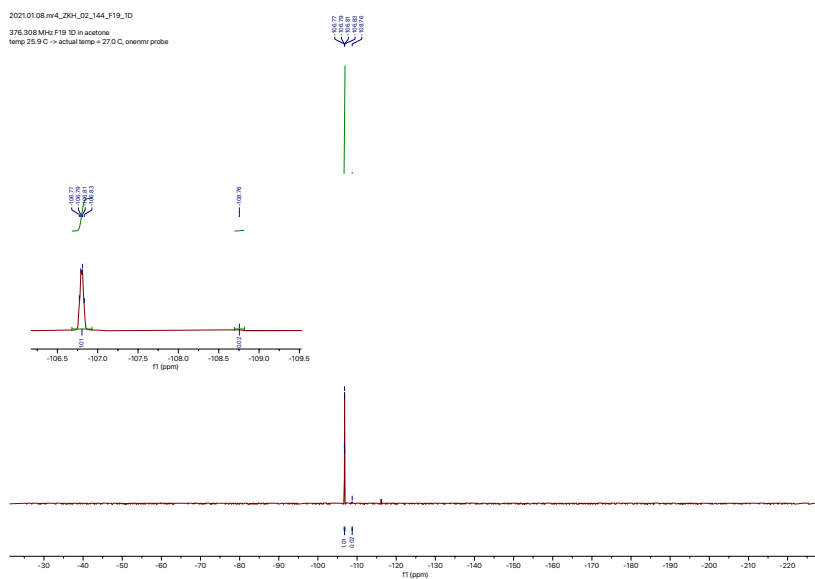
Figure 3.49. ^{19}F NMR spectrum in d_6-acetone of crossover reaction between **3-3** and **F-3-12** using a 1:1 mixture of MeCN and aqueous buffer (pH 6.92) as the reaction solvent.

In a MeCN/H$_2$O/MeOH (3:0.5:0.5) solvent mixture following **GP4**, 11% crossover was observed (Figure 3.50).
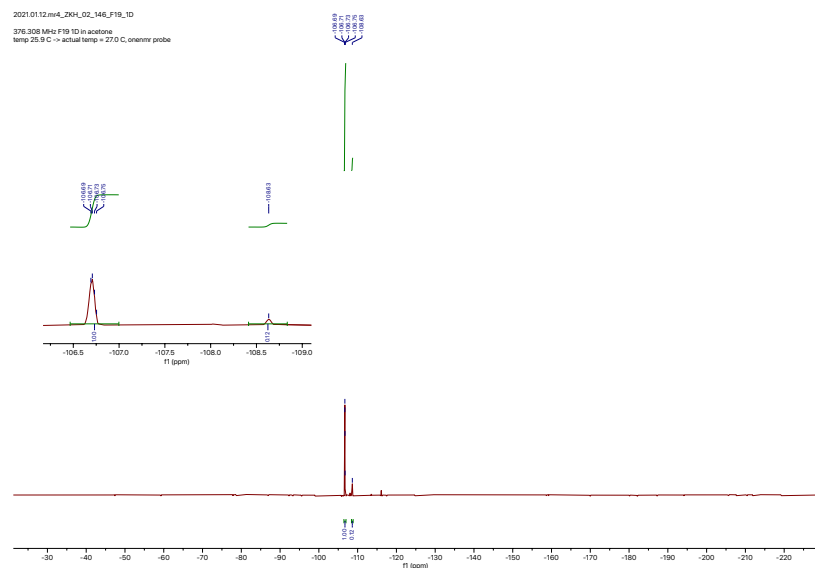
Figure 3.50. ^{19}F NMR spectrum in d_6-acetone of crossover reaction between **3-3** and **F-3-12** using MeCN/H$_2$O/MeOH (3:0.5:0.5) as the reaction solvent.

In a MeOH/H$_2$O (3:1) solvent mixture following **GP4**, 17% crossover was observed (Figure 3.51).

Figure 3.51. ^{19}F NMR spectrum in d_6-acetone of crossover reaction between **3-3** and **F-3-12** using MeOH/H$_2$O (3:1) as the reaction solvent.

3.9.7 pK_a Measurements for Boron Heterocycles (cf. Table 3.5)

General Procedure for the Determination of Boron Heterocycle pK_a in Acetonitrile/Water (1:1) by ^{11}B NMR (GP5)

Boron heterocycle (0.25 mmol) was dissolved in 2.0 mL CD$_3$CN and 10.5 mL MeCN (non-deuterated). The solution was further diluted with 12.5 mL of a phosphate buffer solution, which was prepared by dissolving 690 mg sodium phosphate monobasic monohydrate in 50.0 mL deionized water. From the resulting boron heterocycle stock solution, 2.0 mL aliquots were transferred to 3-dram vials. The pH of the solution of these aliquots was then adjusted using 1 M HCl, 0.1 M NaOH, 1 M NaOH or 2.5 M NaOH and measured using a pH meter. After the pH was adjusted, approximately 700 μL of each aliquot was transferred to an NMR tube and analyzed by ^{11}B NMR spectroscopy, using CD$_3$CN as the solvent for locking and shimming.

General Procedure for the Determination of Boron Heterocycle pK_a in Water with Minimal DMSO by ^{11}B NMR (GP6)

Boron heterocycle (0.25 mmol) was dissolved in minimal DMSO (0.7–1.0 mL) followed by addition of 5.0 mL D$_2$O. The solution was then diluted to a total volume of 25 mL using a phosphate buffer solution, which was prepared by dissolving 690 mg sodium phosphate monobasic monohydrate in 50.0 mL deionized water. From the resulting boron heterocycle stock solution, 2.0 mL aliquots were transferred to 3-dram vials. The pH of the solution of these aliquots was then adjusted using 1 M HCl, 0.1 M NaOH or 1 M NaOH and measured using a pH meter. After the pH was adjusted, approximately 700 µL of each aliquot was transferred to an NMR tube and analyzed by ^{11}B NMR spectroscopy, using D$_2$O as the solvent for locking and shimming.

General Procedure for the Determination of Boron Heterocycle pK_a in Acetonitrile/Water (1:1) by UV Spectrophotometry (GP7)

Boron heterocycle (0.10 mmol) was dissolved in 5.00 mL MeCN. The solution was further diluted with 5.00 mL of a phosphate buffer solution, which was prepared by dissolving 690 mg sodium phosphate monobasic monohydrate in 50.0 mL deionized water. From the resulting boron heterocycle stock solution, a 1.00 mL aliquot was taken and dissolved in 9.00 mL MeCN/buffer solution (10-fold dilution), from which 2.80 mL solution was taken and further dissolved in 25.2 mL MeCN/buffer solution (further 10-fold dilution). From the final solution, 2.0 mL aliquots were transferred to 3-dram vials. The pH of the solution of these aliquots was then adjusted using 0.1 M HCl, 1 M HCl, 0.1 M NaOH, 1 M NaOH or 2.5 M NaOH and measured using a pH meter. After the pH was adjusted, each aliquot was transferred to a quartz tube and analyzed by UV spectrophotometry in the wavelength region 230 nm to 500 nm, using MeCN/buffer (1:1) as the blank.

3.9.7.1 Calculations to Determine pK_a Values

The chemical shift observed by ^{11}B NMR was plotted as a function of the solution pH. To calculate the pK_a, a plot was constructed of pH as a function of $\log \frac{(\delta_{highest}) - (\delta_{pH})}{(\delta_{pH}) - (\delta_{lowest})}$, where $\delta_{highest}$ is the most downfield chemical shift observed by ^{11}B NMR spectroscopy during the titration (observed at the most acidic pH where the equilibrium is entirely

towards the free acid), δ_{lowest} is the most upfield chemical shift observed by ^{11}B NMR spectroscopy during the titration (observed at the most alkaline pH where the equilibrium is entirely towards the conjugate base), and δ_{pH} is the observed chemical shift by ^{11}B NMR spectroscopy at a particular pH. The pK_a is determined by the y-intercept of this plot.[20,36]

The absorbance observed by UV spectroscopy at the specific wavelength was plotted as a function of the solution pH. To calculate the pK_a, a plot was constructed of pH as a function of $\log\frac{(A_{highest})-(A_{pH})}{(A_{pH})-(A_{lowest})}$, where $A_{highest}$ is the maximum absorption observed by UV spectroscopy during the titration (observed at the most acidic pH for a specific wavelength where the equilibrium is entirely towards the free acid), A_{lowest} is the minimum absorption observed by UV spectroscopy during the titration (observed at the most alkaline pH where the equilibrium is entirely towards the conjugate base), and A_{pH} is the observed absorbance by UV spectroscopy at a particular pH. The pK_a is determined by the y-intercept of this plot.[20,36]

3.9.7.2 Experimental pK_a Values of Boron Heterocycles by ^{11}B NMR

Following **GP6**, the pK_a of benzoxaborole in aqueous solution with minimal DMSO was calculated to be 7.4.
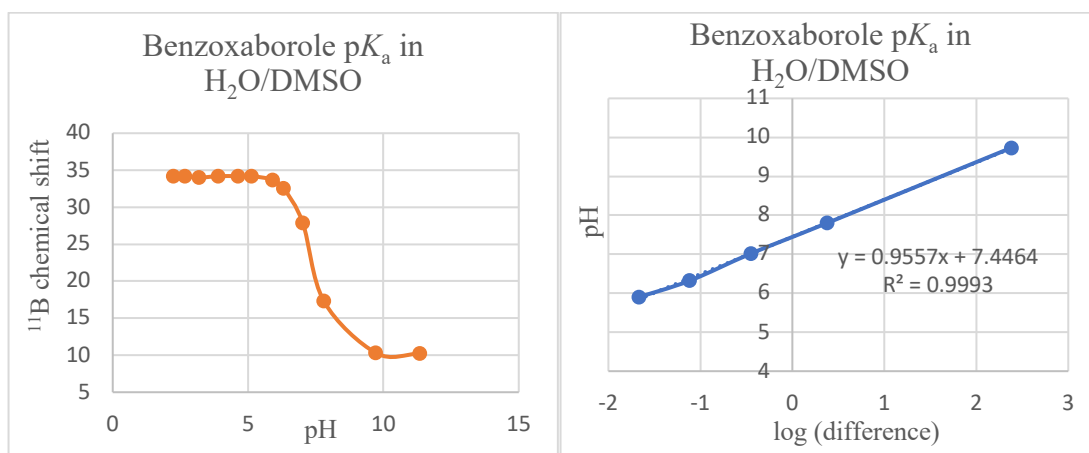
Figure 3.52. pK_a determination of benzoxaborole in aqueous solution with minimal DMSO.

Following **GP6**, the pK_a of heterocycle **3-1** in aqueous solution with minimal DMSO was calculated to be 5.5. This pK_a was also calculated separately by Dr. Marco Paladino.
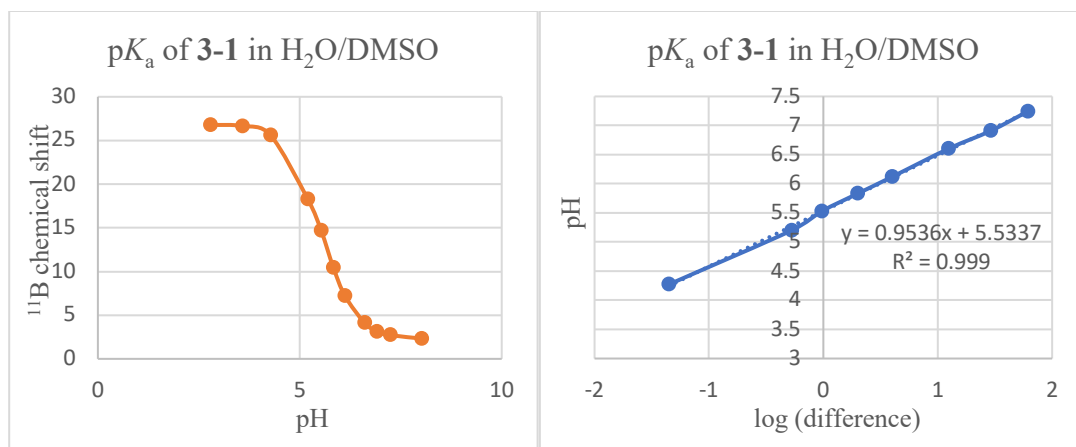
Figure 3.53. pK_a determination of **3-1** in aqueous solution with minimal DMSO.

Following **GP5**, the pK_a of benzoxaborole in 1:1 MeCN/H_2O was calculated to be 9.2.
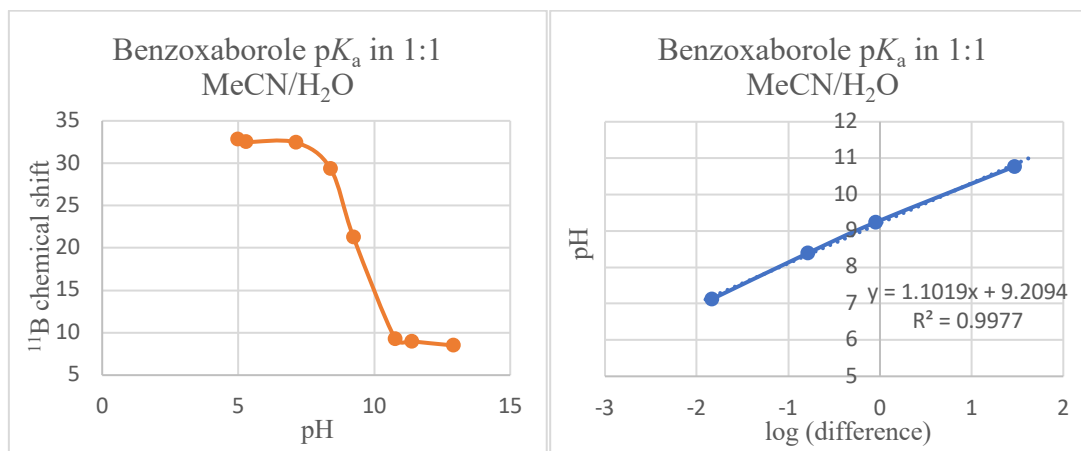
Figure 3.54. pK_a determination of benzoxaborole in 1:1 MeCN/H_2O.

Following **GP5**, the pK_a of heterocycle **3-1** in 1:1 MeCN/H_2O was calculated to be 7.1.
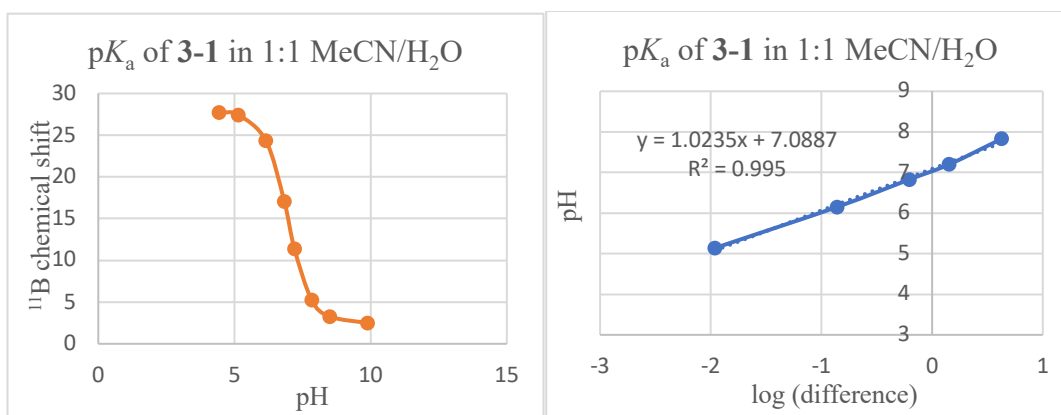
Figure 3.55. pK_a determination of **3-1** in 1:1 MeCN/H$_2$O.

Following **GP5**, the pK_a of heterocycle **3-2d** in 1:1 MeCN/H$_2$O was calculated to be 9.4.
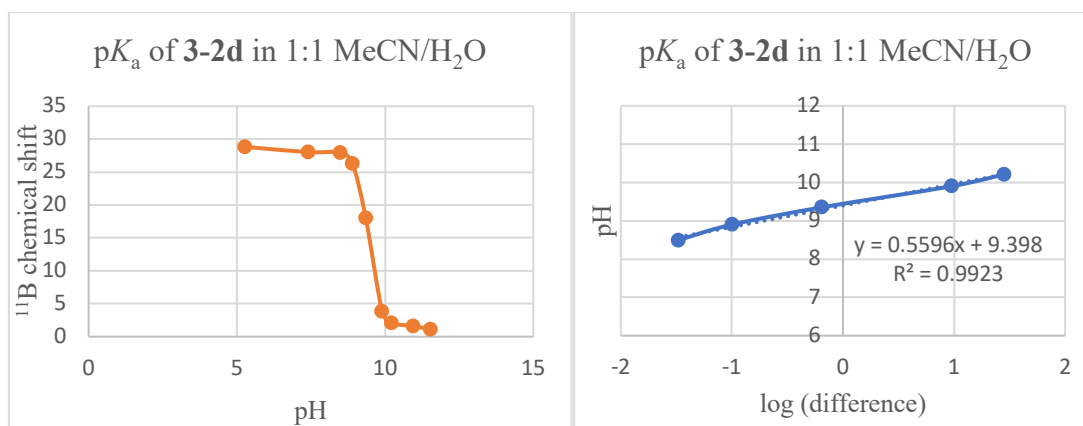
Figure 3.56. pK_a determination of **3-2d** in 1:1 MeCN/H$_2$O.

Following **GP5**, the pK_a of heterocycle **3-3** in 1:1 MeCN/H$_2$O was calculated to be 5.5.
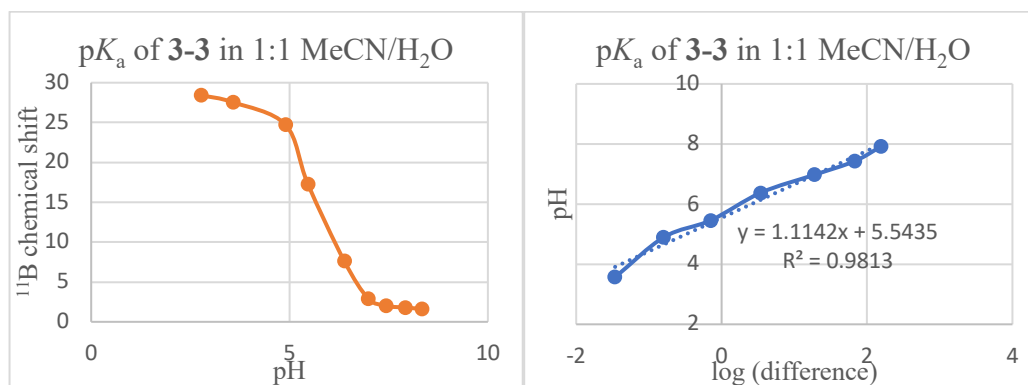
Figure 3.57. pK_a determination of **3-3** in 1:1 MeCN/H$_2$O.

3.9.7.3 Experimental pK_a Values of Boron Heterocycles by UV Spectrophotometry

Following **GP7**, the UV spectrum of heterocycle **3-1** in 1:1 MeCN/H$_2$O was obtained over a range of 230–500 nm.
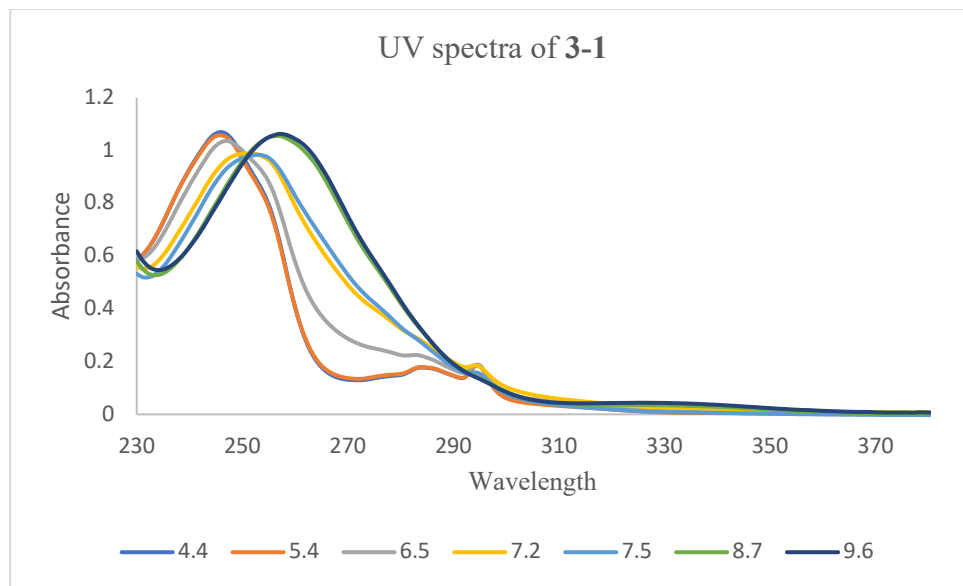
Figure 3.58. UV-Vis spectra of heterocycle **3-1** in 1:1 MeCN/H$_2$O. Legends indicate pH.

The pK_a of heterocycle **3-1** in 1:1 MeCN/H$_2$O was calculated to be 7.2.
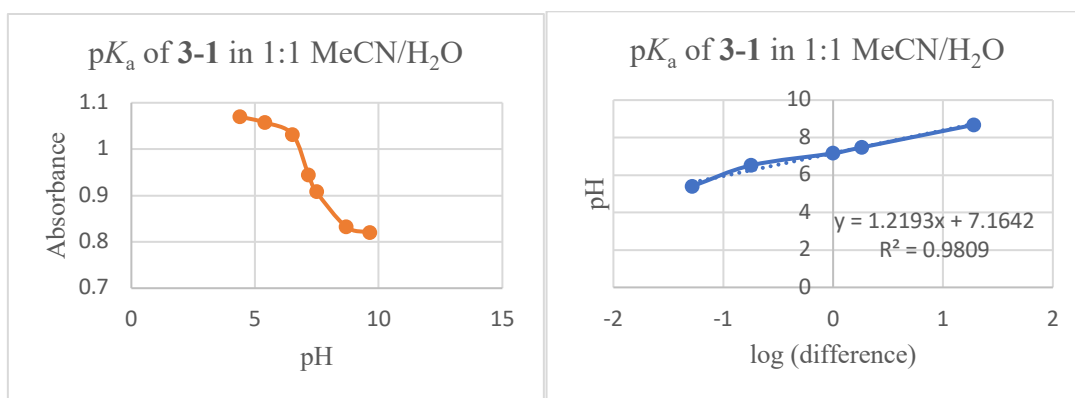
Figure 3.59. pK_a determination of heterocycle **3-1** in 1:1 MeCN/H$_2$O using λ = 246 nm.

Following **GP7**, the UV spectrum of heterocycle **3-2c** in 1:1 MeCN/H$_2$O was obtained over a range of 230–500 nm.
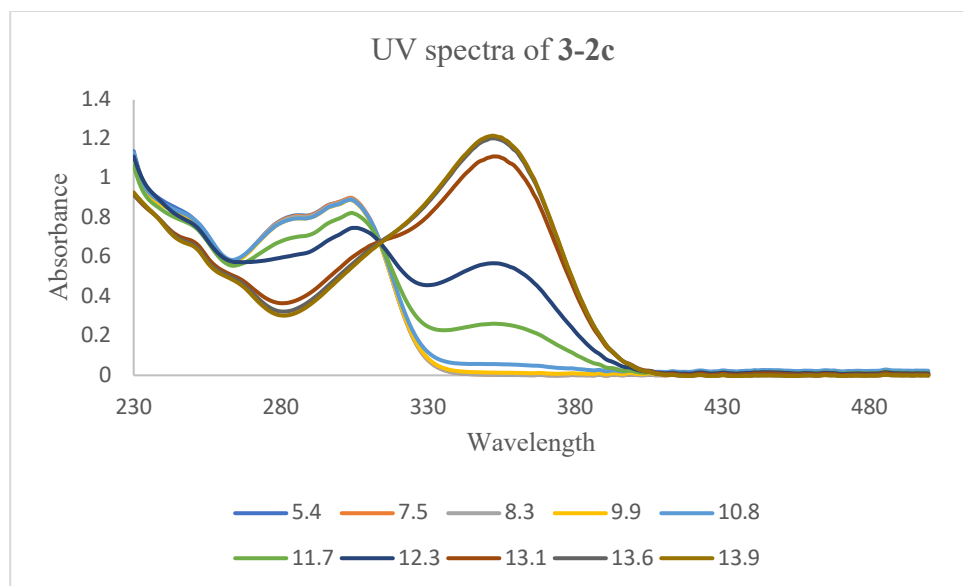
Figure 3.60. UV-Vis spectra of heterocycle **3-2c** in 1:1 MeCN/H$_2$O. Legends indicate pH.

The pK_a of heterocycle **3-2c** in 1:1 MeCN/H$_2$O was calculated to be 12.3.
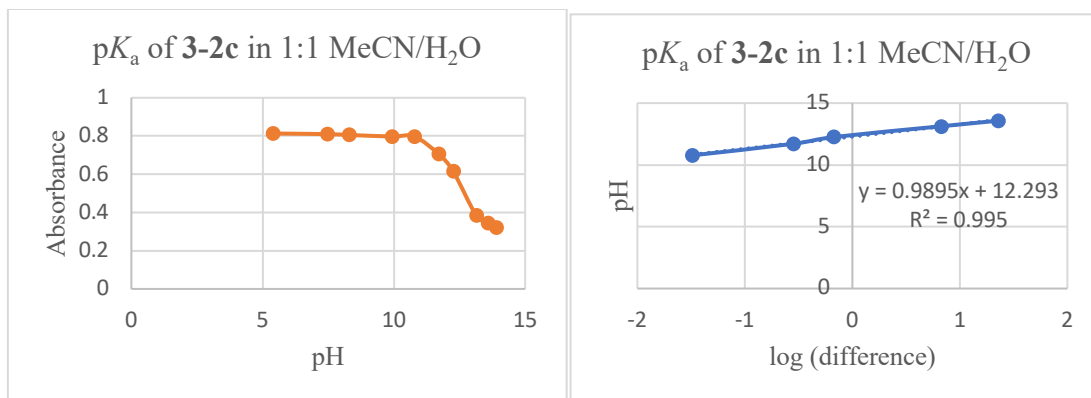
Figure 3.61. pK_a determination of heterocycle **3-2c** in 1:1 MeCN/H$_2$O using λ = 286 nm.

Following **GP7**, the UV spectrum of heterocycle **3-2d** in 1:1 MeCN/H$_2$O was obtained over a range of 230–500 nm.
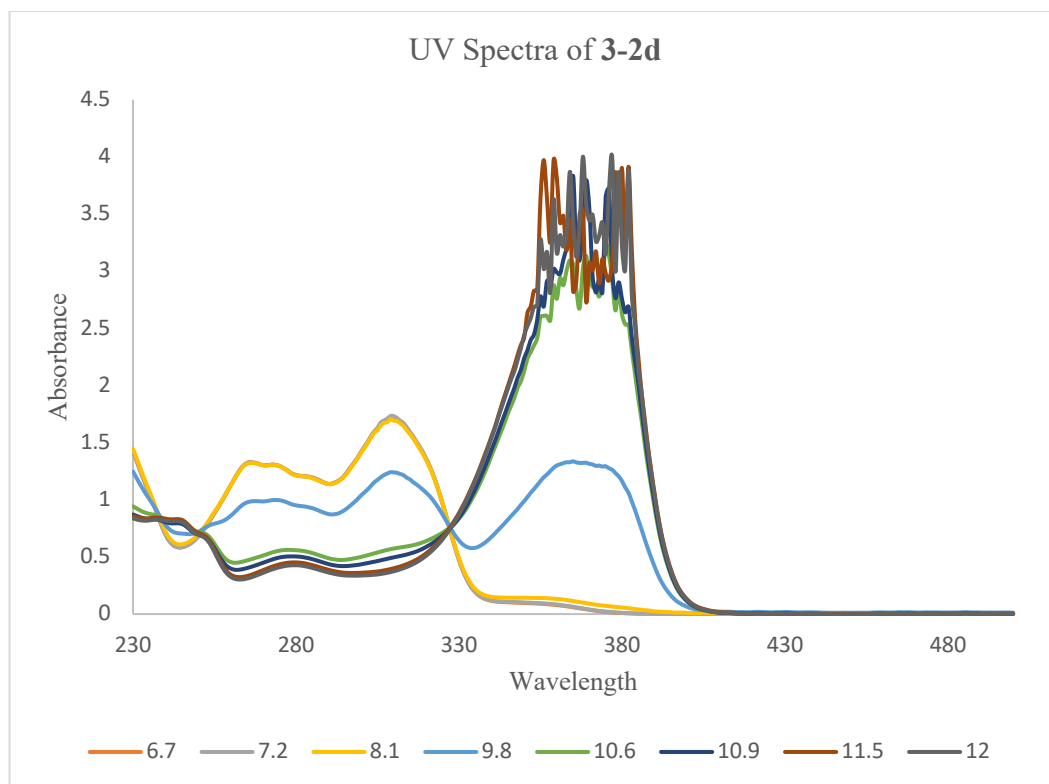
Figure 3.62. UV-Vis spectra of heterocycle **3-2d** in 1:1 MeCN/H$_2$O. Legends indicate pH. Detector saturation was observed above Absorbance = 2.5 for ~370 nm, which represents a possible conjugate base with high molar extinction coefficient.

Following **GP7**, the pK_a of heterocycle **3-2d** in 1:1 MeCN/H$_2$O was calculated to be 10.1.
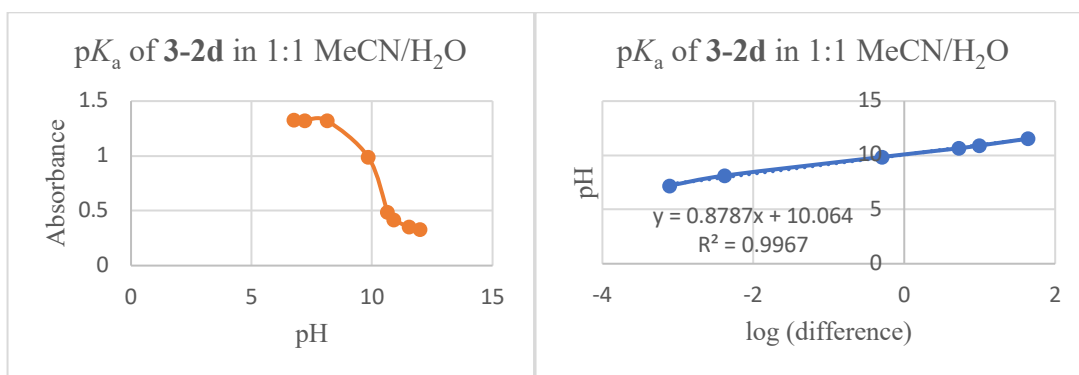
Figure 3.63. pK_a determination of heterocycle **3-2d** in 1:1 MeCN/H$_2$O using λ = 267 nm.

Following **GP7**, the UV spectrum of heterocycle **3-3** in 1:1 MeCN/H$_2$O was obtained over a range of 230–500 nm.
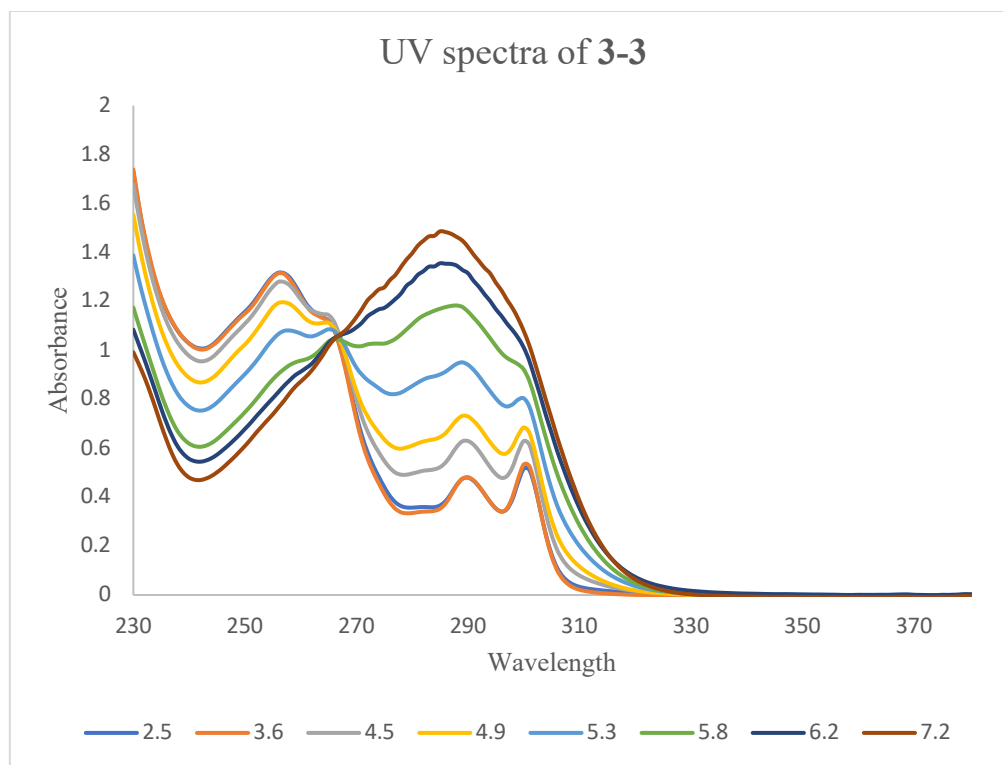
Figure 3.64. UV-Vis spectra of heterocycle **3-3** in 1:1 MeCN/H$_2$O. Legends indicate pH.

The pK_a of heterocycle **3-3** in 1:1 MeCN/H$_2$O was calculated to be 5.4.
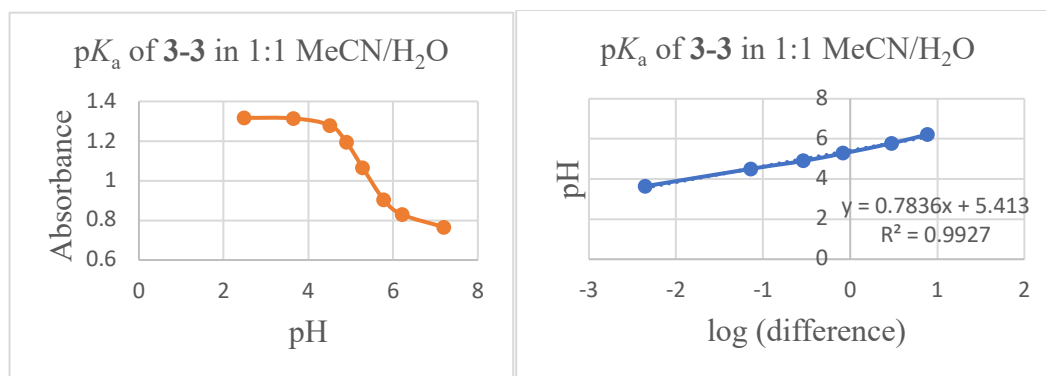
Figure 3.65. pK_a determination of heterocycle **3-3** in 1:1 MeCN/H$_2$O using λ = 256 nm.

3.9.7.4 Approximate pK_a for Heterocycle 3-2c by ^{11}B NMR

The approximate pK_a of heterocycle **3-2c** was estimated by carefully adjusting the pH until the ^{11}B NMR signals corresponding to the acid and conjugate base forms showed equal integration, which occurred at approximately pH 12.2 (Figure 3.66).

2020.12.11.mr4_ZKH_02_128_8_B11_1D
pH = 12.20
128.329 MHz B11{H1} 1D in cd3cn
temp 25.9 C -> actual temp = 27.0 C, onenmr probe
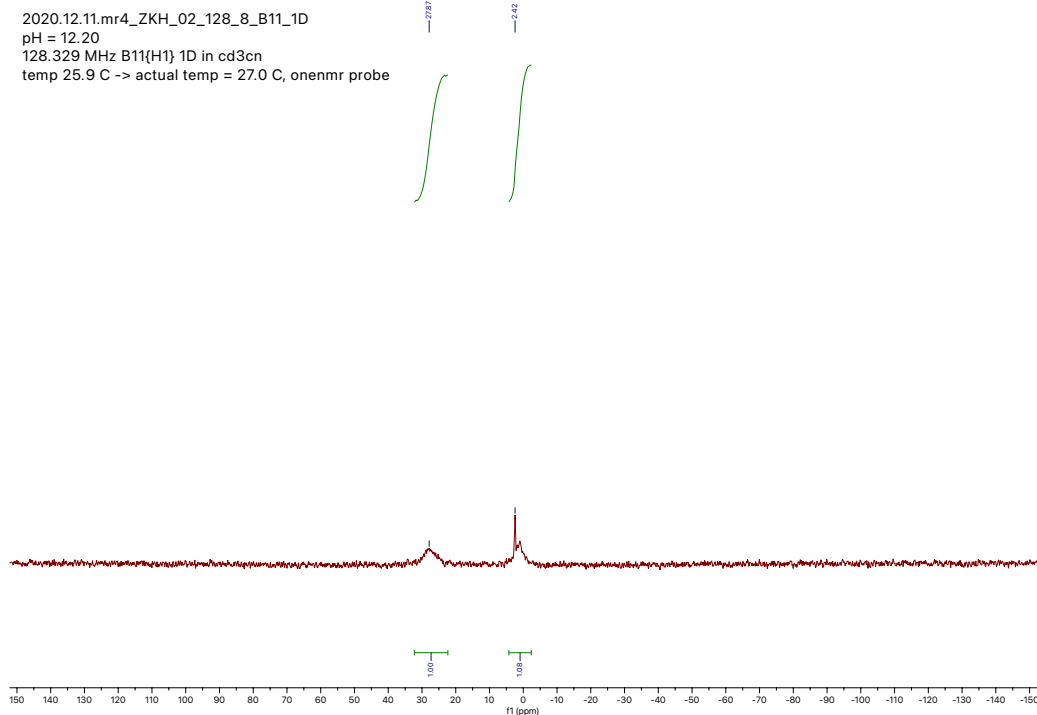
Figure 3.66. ^{11}B NMR spectrum of heterocycle **3-2c** at pH 12.2.

3.9.7.5 Validation of pK_a for Heterocycle 3-3

Heterocycle **3-3** was shown to be moderately labile in aqueous solvent in crossover experiments, which raised the possibility that B—N bond cleavage or hydrazone hydrolysis could occur at high pH to release 2-formylphenylboronic acid (**3-12**), which would give erroneous results in the pK_a titration. At pH 9.01, 2-formylphenylboronic acid displayed an ^{11}B NMR chemical shift of 8.1 ppm. In contrast, heterocycle **3-3** at the same pH had a distinct ^{11}B NMR chemical shift at 1.5 ppm, confirming that the measured pK_a indeed corresponds to heterocycle **3-3** rather than the parent 2-formylphenylboronic acid (Figure 3.67).

2021.01.13.mr4_ZKH_02_151_6_B11_1D
pH = 9.01
128.329 MHz B11{H1} 1D in cd3cn
temp 25.9 C -> actual temp = 27.0 C, onenmr probe
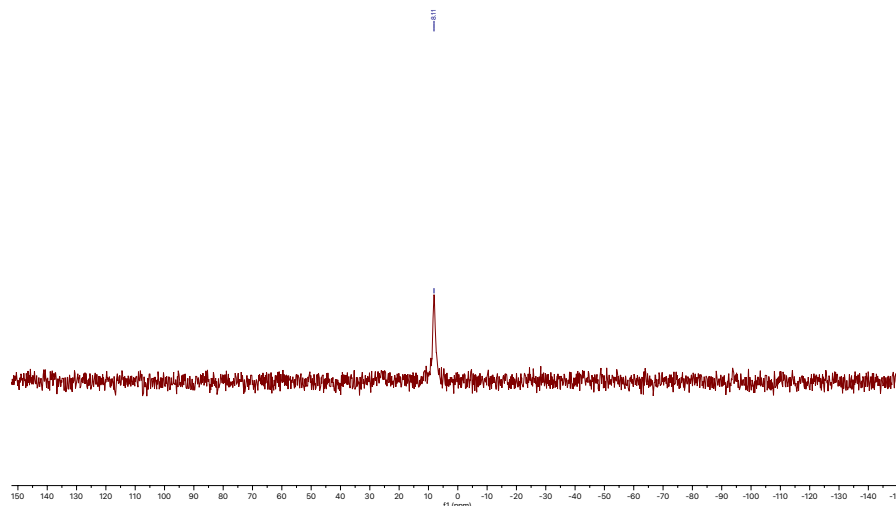
Figure 3.67. ^{11}B NMR spectrum in CD$_3$CN of 2-formylphenylboronic acid (**3-12**) at pH 9.01.

3.9.8 Synthesis and Characterization of Conjugate Bases

3.9.8.1 Synthesis of Conjugate Bases 3-1-I, 3-2d-I, and 3-3-I using Potassium Hydroxide

The conjugate bases of heterocycles **3-1**, **3-2d**, and **3-3** were synthesized by dissolving roughly 10 mg of the boron heterocycle in 3.0 mL hot toluene. Aqueous KOH (45%, 2 drops) was then added and the reaction mixture was stirred for 5 min. The precipitate was collected by vacuum filtration, washed with toluene (5 mL) and dried under high vacuum overnight.[37]
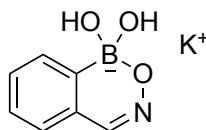
Potassium 1,1-Dihydroxy-1H-benzo[d][1,2,6]oxazaborinin-1-uide (3-1-I): mp >300 °C (decomposition, turned dark color); **^{1}H NMR** (500 MHz, d_6-DMSO + 1 drop D$_2$O): δ 7.63 (s, 1 H), 7.41 (d, J = 7.0 Hz, 1 H), 7.17 (app t, J = 7.0 Hz, 1 H), 7.08 (app t, J = 7.0 Hz, 1 H), 6.98 (d, J = 7.5 Hz, 1 H); **^{13}C NMR** (125 MHz, d_6-DMSO + 1 drop D$_2$O): δ 146.8, 130.1, 129.7, 128.6, 125.0, 123.2; **^{11}B NMR** (128 MHz, d_6-DMSO + 1 drop D$_2$O): δ 2.4.

Crystals suitable for X-ray analysis were synthesized by Dr. Marco Paladino.[24]
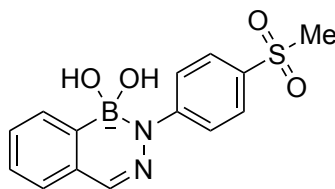
Potassium 1,1-Dihydroxy-2-(4-(methylsulfonyl)phenyl)-1,2-dihydrobenzo[*d*][1,2,3]diaza borinin-1-uide (3-2d-I): mp > 300 °C; **^{1}H NMR** (500 MHz, *d$_6$*-DMSO + 1 drop D$_2$O): δ 7.98 (d, *J* = 9.0 Hz, 2 H), 7.58 (d, *J* = 7.0 Hz, 1 H), 7.44 (d, *J* = 9.0 Hz, 2 H), 7.22 (s, 1 H), 7.11 – 7.06 (m, 2 H), 7.00 (d, *J* = 7.0 Hz, 1 H), 3.01 (s, 3 H); **^{13}C NMR** (125 MHz, *d$_6$*-DMSO + 1 drop D$_2$O): δ 156.3, 134.8, 131.6, 131.2, 126.7, 126.4, 125.3, 124.8, 123.0, 116.3, 44.7; **^{11}B NMR** (128 MHz, *d$_6$*-DMSO + 1 drop D$_2$O): δ 1.5.

To obtain crystals suitable for X-ray analysis, a small amount of **3-2d-I** was dissolved in hot MeCN (2.0 mL) with a drop of water in a 3-dram vial. The vial was sealed with a cap, and a needle was inserted through the cap to allow slow evaporation of the solvent. Needle shaped crystals were obtained. See supporting information of published article for full X-ray crystallography details.[24]
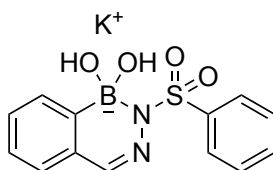
Potassium 1,1-Dihydroxy-2-(phenylsulfonyl)-1,2-dihydrobenzo[*d*][1,2,3]diazaborinin-1-uide (3-3-I): mp > 300 °C (decomposition, turned dark color); **^{1}H NMR** (500 MHz, *d$_6$*-acetone + 1 drop D$_2$O): δ 8.01 (dd, *J* = 8.0, 1.5 Hz, 2 H), 7.71 (d, *J* = 7.0 Hz, 1 H), 7.44 – 7.41 (m, 3 H), 7.20 – 7.17 (m, 2 H), 7.09 (app td, *J* = 7.5, 1.5 Hz, 1 H), 7.01 (d, *J* = 7.0 Hz, 1 H); **^{13}C NMR** (125 MHz, *d$_6$*-acetone + 1 drop D$_2$O): δ 143.8, 140.5, 132.1, 131.8, 131.7, 129.6, 129.1, 128.7, 126.6, 126.0; **^{11}B NMR** (128 MHz, *d$_6$*-acetone + 1 drop D$_2$O): δ 1.9.

To obtain crystals suitable for X-ray analysis, a small amount of **3-3-I** was dissolved in hot MeCN (2.0 mL) with a drop of water in a 3-dram vial. The vial was sealed with a cap, and a needle was inserted through the cap to allow slow evaporation of the solvent. Needle-shaped crystals were obtained. See supporting information of published article for full X-ray crystallography details.[24]

3.9.8.2 Synthesis of Conjugate Bases 3-2a-I and 3-2b-I using Tetramethylammonium Hydroxide

The conjugate bases of heterocycles **3-2a** and **3-2b** were synthesized by dissolving roughly 0.3 mmol of the boron heterocycle in 2.0 mL dry toluene. Tetramethylammonium hydroxide (TMAH, 10 wt. % in methanol, 0.5 mL, 1.5 equiv) was then added and the reaction mixture was stirred for 30 min at rt under argon. The volatiles were removed by rotary evaporation and the residue was dried under high vacuum overnight.[25]
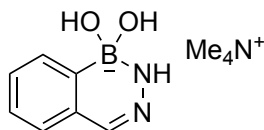
Tetramethylammonium 1,1-Dihydroxy-1,2-dihydrobenzo[*d*][1,2,3]diazaborinin-1-uide (3-2a-I): pale yellow hygroscopic solid; **^{1}H NMR** (700 MHz, d_6-DMSO): δ 7.30 (d, J = 7.0 Hz, 1 H), 6.97 (app td, J = 7.0, 1.4 Hz, 1 H), 6.92 (app td, J = 7.0, 1.4 Hz, 1 H), 6.82 (d, J = 7.7 Hz, 1 H), 6.63 (s, 1 H), 6.10 (br s, 1 H), 3.10 (s, tetramethylammonium peak overlapping with excess TMAH); **^{13}C NMR** (175 MHz, d_6-DMSO): δ 133.7, 130.9, 127.0, 124.1, 123.8, 121.4, 54.3; **^{11}B NMR** (128 MHz): δ 1.3.

*NOTE: Dry d_6-DMSO was used from an ampoule. When CD$_3$CN was used as an NMR solvent, small amounts of quenching to regenerate heterocycle **3-2a** was observed due to residual water in the solvent. The boranol B(OH)$_2$ resonances were not observed, potentially due to rapid exchange.
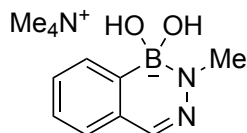
Tetramethylammonium 1,1-Dihydroxy-2-methyl-1,2-dihydrobenzo[*d*][1,2,3]diazaborinin-1-uide (3-2b-I): pale yellow hygroscopic solid; **^{1}H NMR** (700 MHz, d_6-DMSO): δ 7.25 (d, J = 7.0 Hz, 1 H), 6.94 (app td, J = 7.0, 1.4 Hz, 1 H), 6.88 (app td, J = 7.0, 1.4 Hz, 1 H), 6.77 (d, J = 7.7 Hz, 1 H), 6.53 (s, 1 H), 3.11 (s, tetramethylammonium peak overlapping with excess TMAH), 2.97 (s, 3 H); **^{13}C NMR** (175 MHz, d_6-DMSO): δ 136.5, 131.0, 124.1, 123.9, 123.3, 120.8, 54.3, 38.9; **^{11}B NMR** (128 MHz, d_6-DMSO): δ 2.4.

*NOTE: Dry d_6-DMSO was used from an ampoule. When CD_3CN was used as an NMR solvent, small amounts of quenching to regenerate heterocycle **3-2b** was observed due to residual water in the solvent. The boranol $B(OH)_2$ resonances were not observed, potentially due to rapid exchange.

3.9.8.3 NMR studies of Tetramethylammonium Conjugate Bases 3-2a-I and 3-2b-I in Mixed Acetonitrile/Aqueous Buffered Solutions

To further validate the high pK_a's of heterocycles **3-2a and 3-2b**, two different NMR spectra were taken for conjugate bases **3-2a-I** and **3-2b-I**. Two separate solutions containing 2.0 mL CD_3CN and 2.0 mL phosphate buffer solution (prepared as described in **GP5**) were made with pH = 7.1 and pH = 13.5. Conjugate base **3-2a-I** or **3-2b-I** was dissolved in one of the mixed CD_3CN/buffer solutions and ^{11}B and ^{1}H NMR were taken. In both cases, the conjugate bases reverted to their parent hemiboronic acid, confirming their high pK_a values under the titration conditions (Figure 3.68 and Figure 3.69).
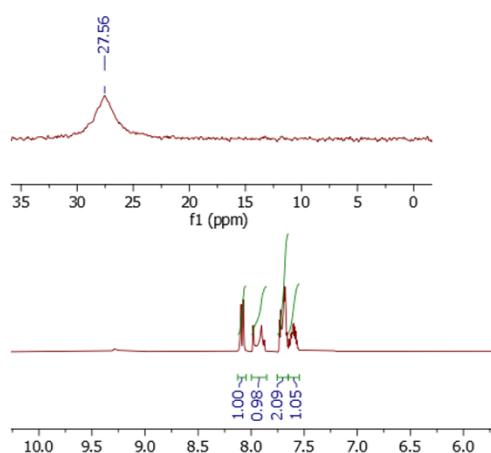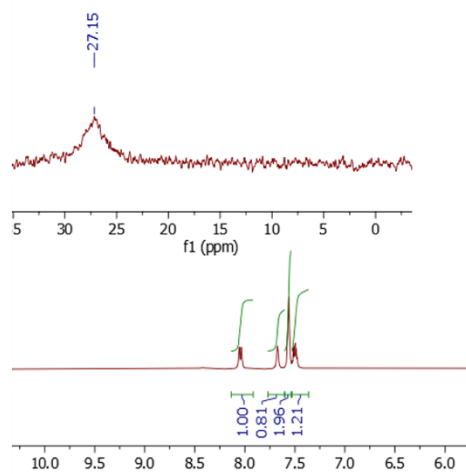
Figure 3.68. ^{11}B and ^{1}H NMR spectra in CD$_3$CN/phosphate buffer (1:1) of conjugate base **3-2a-I** at **a)** pH 7.1 **b)** pH 13.5. Some broadening and chemical shifts changes, particularly of the imine CH resonance, were observed at high pH relative to the NMR of **3-2a** in CD$_3$CN alone.
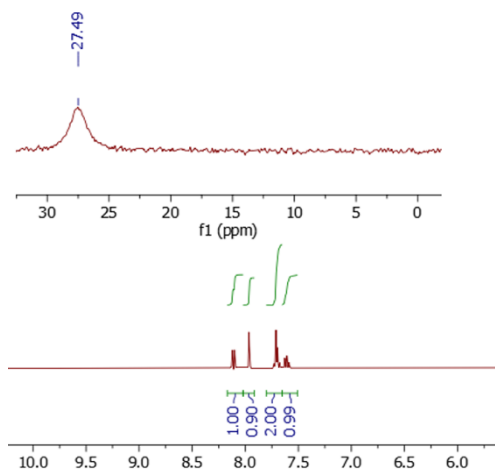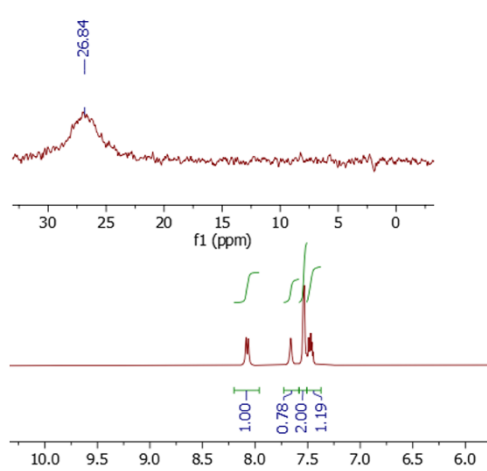
Figure 3.69. ^{11}B and ^{1}H NMR spectra in CD$_3$CN/phosphate buffer (1:1) of conjugate base **3-2b-I** at **a)** pH 7.1 **b)** pH 13.5. Some broadening and chemical shifts changes, particularly of the imine CH resonance, were observed at high pH relative to the NMR of **3-2b** in CD$_3$CN alone.

3.10 References

(1)   Das, B. C.; Adil Shareef, M.; Das, S.; Nandwana, N. K.; Das, Y.; Saito, M.; Weiss, L. M. Boron-Containing Heterocycles as Promising Pharmacological Agents. *Bioorg. Med. Chem.* **2022**, *63*, 116748.

(2)   Hackney, H. E.; Paladino, M.; Fu, H.; Hall, D. G. Diazaboryl-Naphthyl-Ketone: A New Scaffold with Bright Fluorescence, Aggregation-Induced Emission, and Application in the Quantitation of Trace Boronic Acids in Drug Intermediates. *Chem. Eur. J.* **2020**, *26*, 14324–14329.

(3)   Estrada, C. D.; Ang, H. T.; Vetter, K.-M.; Ponich, A. A.; Hall, D. G. Enantioselective Desymmetrization of 2-Aryl-1,3-Propanediols by Direct O-Alkylation with a Rationally Designed Chiral Hemiboronic Acid Catalyst That Mitigates Substrate Conformational Poisoning. *J. Am. Chem. Soc.* **2021**, *143*, 4162–4167.

(4)   Wang, B. J.; Groziak, M. P. Chapter Two - Recent Developments in the Chemistry of Boron Heterocycles. In *Advances in Heterocyclic Chemistry*; Scriven, E. F. V., Ramsden, C. A., Eds.; Academic Press, 2016; Vol. 118, pp 47–90.

(5)   Akgun, B.; Li, C.; Hao, Y.; Lambkin, G.; Derda, R.; Hall, D. G. Synergic "Click" Boronate/Thiosemicarbazone System for Fast and Irreversible Bioorthogonal Conjugation in Live Cells. *J. Am. Chem. Soc.* **2017**, *139*, 14285–14291.

(6)   Palvai, S.; Bhangu, J.; Akgun, B.; Moody, C. T.; Hall, D. G.; Brudno, Y. In Vivo Targeting Using Arylboronate/Nopoldiol Click Conjugation. *Bioconjug. Chem.* **2020**, *31*, 2288–2292.

(7)   Rock, F. L.; Mao, W.; Yaremchuk, A.; Tukalo, M.; Crépin, T.; Zhou, H.; Zhang, Y.-K.; Hernandez, V.; Akama, T.; Baker, S. J.; Plattner, J. J.; Shapiro, L.; Martinis, S. A.; Benkovic, S. J.; Cusack, S.; Alley, M. R. K. An Antifungal Agent Inhibits an Aminoacyl-TRNA Synthetase by Trapping TRNA in the Editing Site. *Science* **2007**, *316*, 1759–1761.

(8)   Rombouts, F. J. R.; Tovar, F.; Austin, N.; Tresadern, G.; Trabanco, A. A. Benzazaborinines as Novel Bioisosteric Replacements of Naphthalene: Propranolol as an Example. *J. Med. Chem.* **2015**, *58*, 9287–9295.

(9)   Zhao, P.; Nettleton, D. O.; Karki, R. G.; Zécri, F. J.; Liu, S.-Y. Medicinal Chemistry Profiling of Monocyclic 1,2-Azaborines. *ChemMedChem* **2017**, *12*, 358–361.

(10)   Baldock, C.; Rafferty, J. B.; Sedelnikova, S. E.; Baker, P. J.; Stuitje, A. R.; Slabas, A. R.; Hawkes, T. R.; Rice, D. W. A Mechanism of Drug Action Revealed by Structural Studies of Enoyl Reductase. *Science* **1996**, *274*, 2107–2110.

(11)   Baldock, C.; Boer, G-J. d.; Rafferty, J. B.; Stuitje, A. R.; Rice, D. W. Mechanism of Action of Diazaborines. *Biochem. Pharmacol.* **1998**, *55*, 1541–1550.

(12)   Snyder, H. R.; Reedy, A. J.; Lennarz, Wm. J. Synthesis of Aromatic Boronic Acids. Aldehydo Boronic Acids and a Boronic Acid Analog of Tyrosine. *J. Am. Chem. Soc.* **1958**, *80*, 835–838.

(13)   Dewar, M. J. S.; Dougherty, R. C. Boron-Containing Analogs of Isoquinoline. *J. Am. Chem. Soc.* **1962**, *84*, 2648–2649.

(14)   Dewar, M. J. S.; Dougherty, R. C. New Heteroaromatic Compounds. XX. Derivatives of 4,3-Borazaroisoquinoline. *J. Am. Chem. Soc.* **1964**, *86*, 433–436.

(15)   Dewar, M. J. S.; Jones, Richard. New Heteroaromatic Compounds. XXV. Studies of Salt Formation in Boron Oxyacids by Boron-11 Nuclear Magnetic Resonance. *J. Am. Chem. Soc.* **1967**, *89*, 2408–2410.

(16)   Dunn, H. E.; Catlin, J. C.; Snyder, H. R. Arylboronic Acids. Imino Derivatives from O-Formylbenzeneboronic Acid. *J. Org. Chem.* **1968**, *33*, 4483–4486.

(17)   Groziak, M. P.; Chen, L.; Yi, L.; Robinson, P. D. Planar Boron Heterocycles with Nucleic Acid-Like Hydrogen-Bonding Motifs. *J. Am. Chem. Soc.* **1997**, *119*, 7817–7826.

(18)   Bhangu, J.; Whittal, R. M.; Hall, D. G. Design, Synthesis and Structure of a Frustrated Benzoxaborole and Its Applications in the Complexation of Amines, Amino Acids, and Protein Modification. *Org. Biomol. Chem.* **2020**, *18*, 3492–3500.

(19)   Bérubé, M.; Dowlut, M.; Hall, D. G. Benzoboroxoles as Efficient Glycopyranoside-Binding Agents in Physiological Conditions: Structure and Selectivity of Complex Formation. *J. Org. Chem.* **2008**, *73*, 6471–6479.

(20)   Dowlut, M.; Hall, D. G. An Improved Class of Sugar-Binding Boronic Acids, Soluble and Capable of Complexing Glycosides in Neutral Water. *J. Am. Chem. Soc.* **2006**, *128*, 4226–4227.

(21)   Dilek, O.; Lei, Z.; Mukherjee, K.; Bane, S. Rapid Formation of a Stable Boron–Nitrogen Heterocycle in Dilute, Neutral Aqueous Solution for Bioorthogonal Coupling Reactions. *Chem. Comm.* **2015**, *51*, 16992–16995.

(22)   Stress, C. J.; Schmidt, P. J.; Gillingham, Dennis. G. Comparison of Boron-Assisted Oxime and Hydrazone Formations Leads to the Discovery of a Fluorogenic Variant. *Org. Biomol. Chem.* **2016**, *14*, 5529–5533.

(23)   Gu, H.; Chio, T. I.; Lei, Z.; Staples, R. J.; Hirschi, J. S.; Bane, S. Formation of Hydrazones and Stabilized Boron–Nitrogen Heterocycles in Aqueous Solution from Carbohydrazides and Ortho-Formylphenylboronic Acids. *Org. Biomol. Chem.* **2017**, *15*, 7543–7548.

(24)   Kazmi, M. Z. H.; Rygus, J. P. G.; Ang, H. T.; Paladino, M.; Johnson, M. A.; Ferguson, M. J.; Hall, D. G. Lewis or Brønsted? A Rectification of the Acidic and Aromatic Nature of Boranol-Containing Naphthoid Heterocycles. *J. Am. Chem. Soc.* **2021**, *143*, 10143–10156.

(25)   Shao, Y.; et al. Advances in molecular quantum chemistry contained in the Q-Chem 4 program package. *Mol. Phys.* **2015**, *113*, 184−215.

(26)   Ishibashi, J. S. A.; Dargelos, A.; Darrigan, C.; Chrostowska, A.; Liu, S.–Y. BN Tetracene: Extending the Reach of BN/CC Isosterism in Acenes *Organometallics* **2017**, *36*, 2494–2497.

(27)   Mottishaw, J. D.; Erck, A. R.; Kramer, J. H.; Sun, H.; Koppang, M. Electrostatic Potential Maps and Natural Bond Orbital Analysis: Visualization and Conceptualization of Reactivity in Sanger's Reagent. *J. Chem. Educ.* **2015**, *92*, 1846–1852.

(28)   Gershoni-Poranne, R.; Stanger, A. Chapter 4 - NICS—Nucleus-independent Chemical Shift. In *Aromaticity: Modern Computational Methods and Applications*; Fernandez, I., Ed.; Elsevier, 2021; pp 99–154.

(29)   Mikhailov, B. M.; Kuimova, M. E. Organoboron Compounds: CCCXVIII. On the Problem of the Aromatic Character of Boron Heterocyclic Compounds. *J. Organomet. Chem.* **1976**, *116*, 123–133.

(30)   Rettig, S. J.; Trotter, J. Crystal and Molecular Structure of Phenylboronic Acid, $C_6H_5B(OH)_2$. *Can. J. Chem.* **1977**, *55*, 3071–3075.

(31)   Tanjaroon, C.; Daly, A.; Marwitz, A. J. V.; Liu, S.-Y.; Kukolich, S. Microwave Measurements and Ab Initio Calculations of Structural and Electronic Properties of N-Et-1,2-Azaborine. *J. Chem. Phys.* **2009**, *131*, 224312.

(32)   Wrackmeyer, B. Carbon-13 NMR Spectroscopy of Boron Compounds. *Progress in NMR Spectroscopy* **1978**, *12*, 227–259.

(33)   Gantt, R. W.; Peltier-Pain, P.; Cournoyer, W. J.; Thorson, J. S. Using Simple Donors to Drive the Equilibria of Glycosyltransferase-Catalyzed Reactions. *Nat. Chem. Biol* **2011**, *7*, 685– 691.

(34)   Ribeiro, C. J. A.; Nunes, R. C.; Amaral, J. D.; Gonçalves, L. M.; Rodrigues, C. M. P.; Moreira, R.; Santos, M. M. M. Spirotriazoline Oxindoles: A Novel Chemical Scaffold With *In Vitro* Anticancer Properties. *Eur. J. Med. Chem.* **2017**, *140*, 494–509.

(35)   Martzel, T.; Lohier, J-F.; Gaumont, A-C.; Brière, J-F.; Perrio, S. Eur. Sulfinate-Organocatalyzed (3+2) Annulation Reaction of Propargyl or Allenyl Sulfones with Activated Imines. *J. Org. Chem.* **2018**, *36*, 5069–5073.

(36) Ricardo, C. L.; Mo, X.; McCubbin, J. A.; Hall, D. G. A Surprising Substituent Effect Provides a Superior Boronic Acid Catalyst for Mild and Metal-Free Direct Friedel–Crafts Alkylations and Prenylations of Neutral Arenes. *Chem. Eur. J.* **2015**, *21*, 4218–4223.

(37) Cammidge, A. N.; Goddard, V. H. M.; Gopee, H.; Harrison, N. L.; Hughes, D. L.; Schubert, C. J.; Sutton, B. M.; Watts, G. L.; Whitehead, A. J. Aryl Trihydroxyborates: Easily Isolated Discrete Species Convenient for Direct Application in Coupling Reactions. *Org. Lett.* **2006**, *8*, 4071–4074.

Chapter 4: Design, Synthesis and Applications of Boron-Containing Naphthoids

4.1 Introduction

There exists a constant need for the development of novel anti-infective drugs to fight ever-evolving bacterial and fungal resistance. For example, β-lactams are one of the largest classes of antibiotics, accounting for >65% of antibiotics marketed worldwide, although they suffer widely from resistance development.[1,2] Therefore, further exploration of non-toxic and druggable chemotypes in pharmaceutical chemistry is needed. Generally, small molecule drugs consist of carbon, hydrogen, nitrogen, and oxygen atoms, with over 85% of all bio-active compounds containing at least one heterocycle.[3] Among the small molecule drugs in the Essential Medicines List (EML), beyond carbon, hydrogen, nitrogen, and oxygen (CHNO), sulfur is the most represented element, with over 20% of the drugs in the list containing this element, while boron is one of the most underrepresented elements, appearing in less than 1% of the drugs.[4] This situation may have arisen from the concerns raised that boron could be toxic as a result of bacterial mutagenicity assays conducted for arylboronic acids.[5,6] However, several studies have shown that arylboronic acids are not in vivo mutagens[7] and boron is essentially non-toxic and thus can be used safely in drug discovery.[8,9]

Due to misconceptions and a lack of synthetic tools for preparing and handling boron-containing compounds, the advancement in the development of boron-based drugs is quite recent. The first ever FDA approved boron-containing drug, bortezomib (Velcade®), a peptidomimetic, came onto the market in 2003 and is used for the treatment of multiple myeloma (Figure 4.1A).[8,10] Subsequently, a boron-containing heterocycle, benzoxaborole, has been recognized as a versatile scaffold in the drug industry in the past decade. Examples of benzoxaborole derivatives are tavaborole (Kerydin®), an anti-fungal drug used for onychomycosis that is now owned by Pfizer, and crisaborole (Eucrisa®) prescribed for the treatment of atopic dermatitis (Figure 4.1C).[11,12] In 2017, another hemiboronic acid, vaborbactam (Vabomere®) was approved by FDA to be used as a β-lactamase inhibitor in combination with the

antibiotic meropenem (antibacterial and resistance inhibition) for adults with a complicated urinary tract infection (Figure 4.1B).[13]
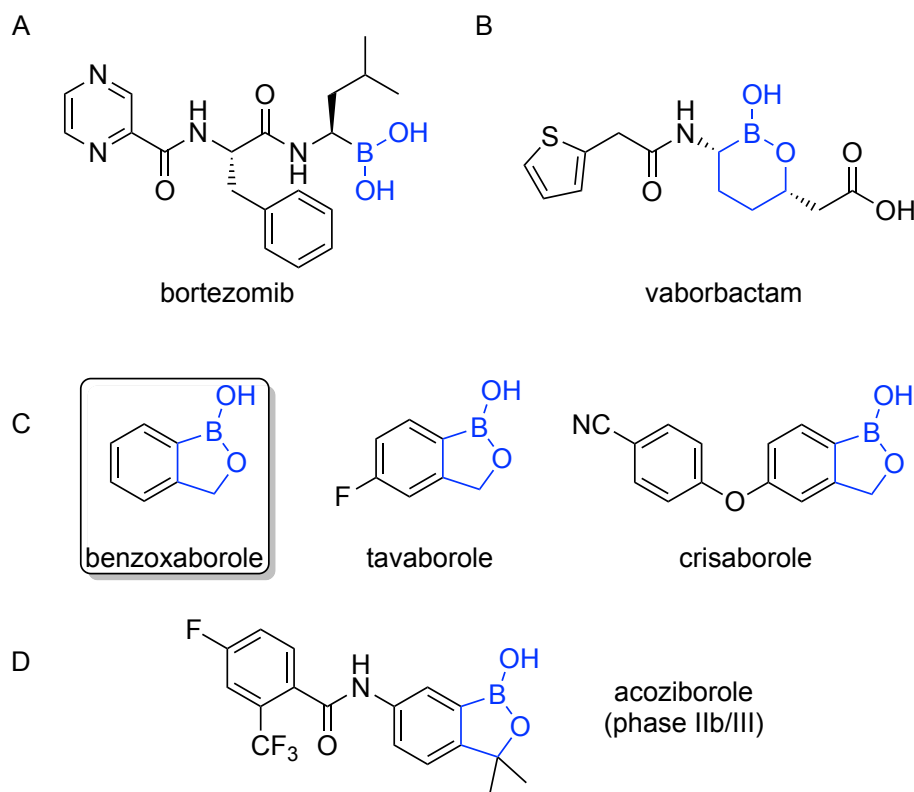
Figure 4.1. Boron-containing drugs approved by the FDA (A–C) and undergoing clinical trials (D).

There are several other benzoxaborole compounds that are in different phases of clinical trials.[14] Particularly, acoziborole is in phase IIb/III for the potential treatment of African trypanosomiasis (sleeping sickness) (Figure 4.1D).[15,16] Altogether, these discoveries paved the way for the use of boron heterocycles in pharmaceutical applications. Boron is an extraordinary element that is present in the same row as carbon and nitrogen and contains an empty *p* orbital. The mechanism of action of these drugs provides insight into the importance of the boron moiety in the structure. Crisaborole inhibits the phosphodiesterase 4B (PDE4B) enzyme, which is involved in the transformation of cyclic adenosine monophosphate (cAMP) to AMP as part of the inflammatory process. The boron center of crisaborole in the enzyme pocket exists in the sp^3 hybridized state at a physiological pH (hydrated boron), where it can mimic the

phosphate of cAMP.[17] Similarly, tavaborole also exists as a tetracoordinate adduct with AMP in the active site.[18] It is remarkable that the IC_{50} value of tavaborole is orders of magnitude better compared to the carbonaceous analog or the acyclic boronic acid counterpart (Figure 4.2).[18]

IC_{50} (µM)	2.1	>100	>100
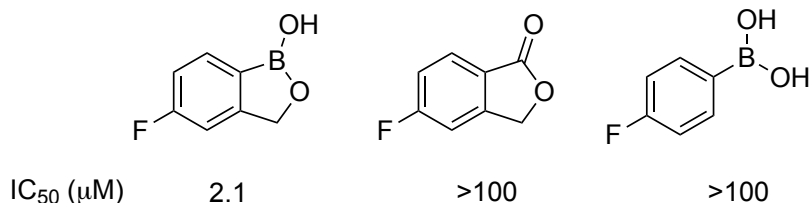
Figure 4.2. Comparison of IC_{50} values of tavaborole and other analogs.

The mechanism of action of these drugs and their outstanding activity are intriguing and warrant a closer look at the properties of benzoxaborole and its potential for bioisosterism. There exists a significant difference in properties of acyclic boronic acid (phenylboronic acid) compared to benzoxaborole, which consists of a phenyl ring attached to a 5-membered oxaborole ring. The exocyclic C—B—O bond angle is relatively larger than the endocyclic C—B—O bond angle (133.1° vs 108.6°) as compared to phenylboronic acid, where all such angles are equal.[19] Therefore, ring strain exists in benzoxaborole, which, in turn, decreases the pK_a as compared to phenylboronic acid (7.4 vs 8.8).[20] As described in Chapter 3, due to their pK_a being near the physiological pH, benzoxaboroles can form a variety of bonds with biological targets in either sp^2 or sp^3 hybridized state (cf. Figure 3.8). Stability is also an important characteristic of benzoxaboroles. Benzoxaboroles can be visualized as a lactone of *ortho*-hydroxymethyl phenylboronic acid. The internal B—O bond is resistant to hydrolysis compared to B—O bonds in phenylboronic esters.[21] Additionally, the B—C bond in benzoxaborole is more resistant to protodeboronation as compared to the B—C bond in phenylboronic acid, whereupon treatment with 10% HCl does not affect benzoxaborole, but readily protodeboronates phenylboronic acid.[22]

In Chapter 3, the properties of other boron heterocycles were studied, specifically boron-containing naphthoids.[20] It was shown that benzoxazaborine is related chemically to benzoxaborole, where a boron-containing ring has a negligible

aromatic character and is relatively acidic (pK_a 5.5 vs 7.4). On the other hand, the *N*-analog, NH-benzodiazaborine, displays more aromatic character and has a higher pK_a, making it more akin to naphthol-like molecules (cf. Figure 3.21). The development of this novel class of boron heterocycles could offer new scaffolds in drug discovery and expand upon the huge success of benzoxaboroles. However, there is a need to develop synthetic and purification tools for these boron-containing heterocycles to access an array of derivatives for pharmaceutical applications. To date, there is no chemistry known to systematically derivatize these scaffolds. Moreover, purification of boronic acids can be challenging due to their potential instability on silica and highly polar nature. As a result, there have been alternative approaches developed to mitigate these problems, such as pH-dependent phase-switch workup,[23] adduct formation, which reduces the polarity of boronic acid compounds,[24,25] or DEAM-PS-supported purification, where boronic acids are immobilized.[26]

In this Chapter, the chemistry on these scaffolds has been explored, such as chemoselective Suzuki-Miyaura, Chan-Lam, and amidation reactions, to develop a prototypic library of compounds (Figure 4.3). The compounds obtained are purified largely by phase-switch or crystallization or trituration techniques. In the process, several drug isosteres also are synthesized. Furthermore, select compounds are tested for antifungal, antibacterial, and anticancer activities.
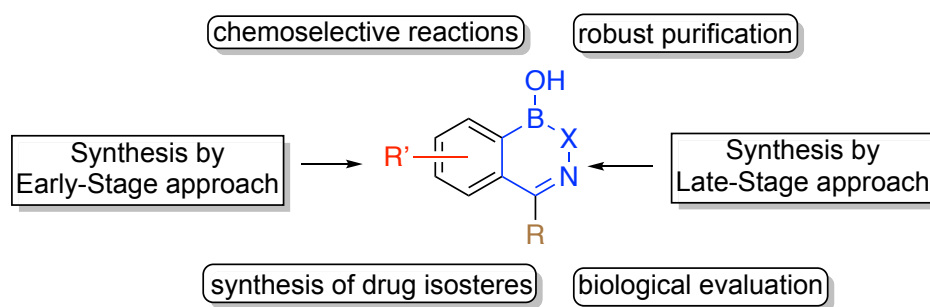
Figure 4.3. Design, synthesis, and applications of boron-containing naphthoids.

4.2 Properties of Boron Heterocycles

The properties of boron-containing naphthoids, such as aromaticity, stability, and acidity, were discussed extensively in Chapter 3.[20] In summary, the boron-containing

ring in **4-1** (benzoxazaborine) and **4-3** was found to possess negligible aromatic character, while **4-2a** (NH-benzodiazaborine), **4-2b**, and to some extent **4-2c** retained some aromaticity (Figure 4.4a). Based on the screening results shown in Section 4.6, the properties of a benzoxazaborine analog, **4-7a** (vide infra) were also evaluated. The pK_a of these model heterocycles were measured by a ^{11}B NMR titration experiment. Overall, benzoxazaborine exhibits a close analogy with benzoxaborole, while NH-benzodiazaborine displays potential to serve as a good isostere of isoquinoline. Finally, all the model heterocycles have acceptable lipophilicity for typical drug applications ($1 < \log P < 5$).

Property	4-1	4-7a	4-2a	4-2b	4-2c	4-3
pK_a	7.1 (5.5)	7.0	>14	>14	12.2	5.5
logP	1.23	2.60	1.94	2.33	3.18	2.05
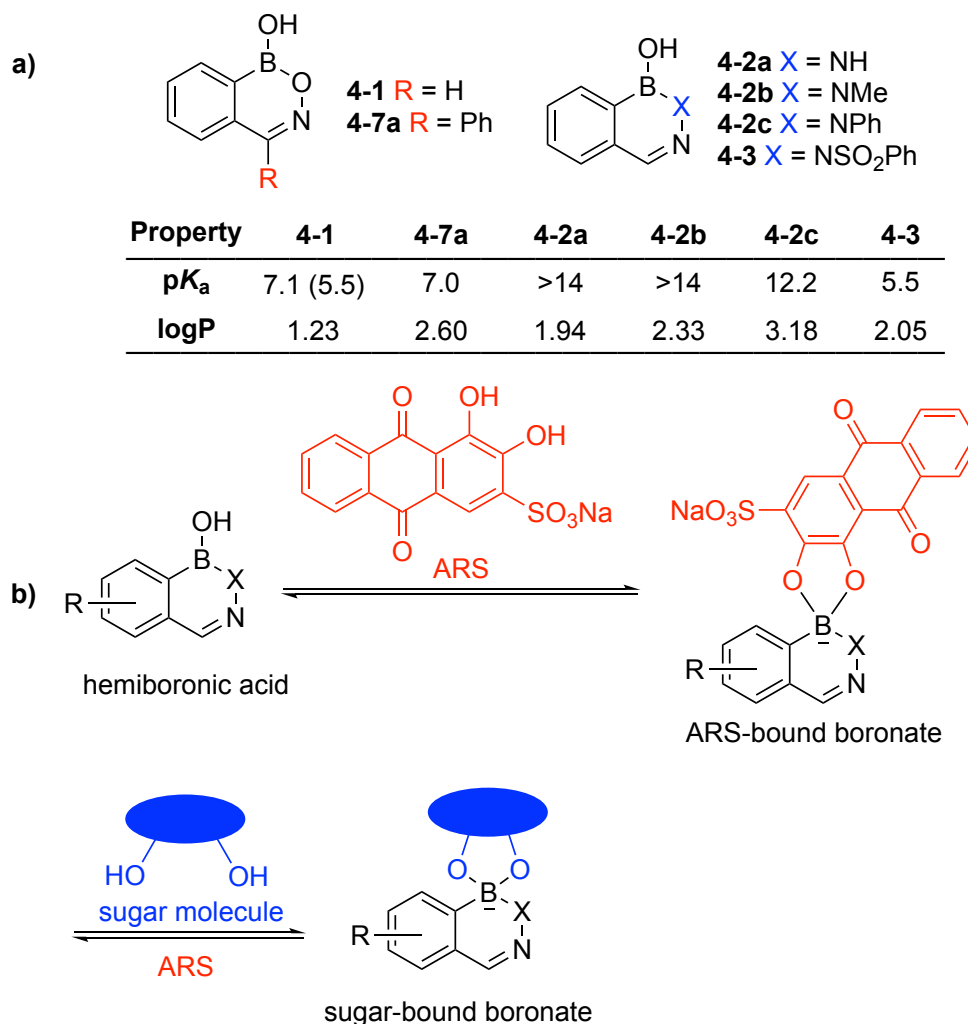
Figure 4.4. a) Chosen scaffolds with their respective pK_a's in 1:1 CH$_3$CN/H$_2$O or in water with 5% DMSO (in brackets) (refer to Chapter 3) and logP values (logP values were obtained by Ed Fu). **b)** Scheme showing competitive displacement of ARS by sugar from hemiboronic acid.

A colorimetric dye-displacement assay was performed on scaffolds **4-1**, **4-7a**, **4-2a**, **4-2b**, **4-2c**, and **4-3** to assess the suitability of molecules for binding with diol-containing saccharides (Figure 4.4b). This is a reliable procedure that has been used in the past by several laboratories, including the Hall Group.[27–30] This qualitative assay is dependent on the target compounds' binding to a diol moiety in either Alizarin Red S (ARS) or a monosaccharide compound (Figure 4.4b). ARS is a dye, which can bind to boronic acids at neutral pH (depending on the boronic acid pK_a), thereby causing a solution color change from red (free-ARS) to yellow (bound-ARS). The addition of a saccharide, such as glucose, fructose, or methyl α-galactopyranoside, establishes a second equilibrium between the ARS-bound boronate and the sugar-bound boronate. Thus, the competitive displacement of bound-ARS with the sugar liberates free ARS and causes a color shift from yellow back to red.

The assay for all model heterocycles was performed in buffered 2:3 THF/H_2O mixtures. The use of a mixed organic/aqueous solvent was necessary to ensure all the model heterocycles formed homogeneous solutions, even after the addition of sugar. The 1:1 CH_3CN/H_2O solvent system used for pK_a measurements (cf. Chapter 3), was not suitable for this dye-displacement assay, as it resulted in the formation of two layers after sugar addition. Benzoxaborole was used as a control for this dye-displacement assay. Since benzoxaborole and benzoxazaborine (**4-1**) are slightly soluble in water, the assay was also performed in water to account for the effect of an organic co-solvent on the solution pH. As expected from its pK_a, a yellow-to-red shift was observed for **4-1** upon addition of glucose or fructose, indicating that these sugars displace ARS (Figure 4.5). A similar color change was observed for benzoxaborole, **4-3**, and benzoxazaborine analog **4-7a**. On the other hand, due to the reluctance of boron to coordinate another ligand (i.e., high pK_a), **4-2a**, **4-2b**, and **4-2c** did not show binding even with ARS.

Figure 4.5. Dye-displacement assay for benzoxaborole and model scaffolds **4-1**, **4-7a**, **4-2a**, **4-2b**, **4-2c**, and **4-3** in a buffered 2:3 THF/water. Colors were determined directly from the corresponding vials using a Microsoft PowerPoint color picking tool (see Section 4.9.2). Red indicates the color of ARS, yellow/purple is the color of complex between heterocycle and ARS.

On the basis of the assessment of the properties and reactivity of these hemiboronic naphthoids, two scaffolds were selected for further study and chemistry. Scaffold **4-1** was chosen because of its similarity to benzoxaborole. From the class of *N*-analogs, **4-2a** was chosen for synthesizing libraries owing to its isosteric nature to 4-hydroxyisoquinoline and 1-naphthol.

4.3 Early-Stage Approach for the Synthesis of Analogs of 4-1 and 4-2a

At the outset, there was a particular focus on synthesizing **4-7a**, a ketoxime analog of benzoxazaborine (**4-1**) (Scheme 4.1). Initially, the synthesis commenced by the Miyaura borylation of 2-bromobenzophenone (**4-4a**) (step a). The second step, performed by Dr. Marco Paladino, involved a sodium periodate induced cleavage of the pinacol ester moiety of **4-5** to generate **4-6** (step b). A condensation reaction with aqueous hydroxylamine resulted in the formation of crude product **4-7a** (step c). Overall, this three-step procedure did result in the formation of crude **4-7a**, but it suffered from the following disadvantages: 1) The step involving sodium periodate

reagent for the ester cleavage (step b) was not ideal, as the sodium periodate addition was conducted through several consecutive additions of this reagent, on the basis of color change from yellow to orange. If the reaction was incomplete, more sodium periodate was required. 2) The final product after step c always contained undetermined quantities of iodine (originating from $NaIO_4$ in step b). A charcoal workup to remove iodine was not effective, as the desired product also got removed by the charcoal. A trituration by diethyl ether also did not result in pure compound.
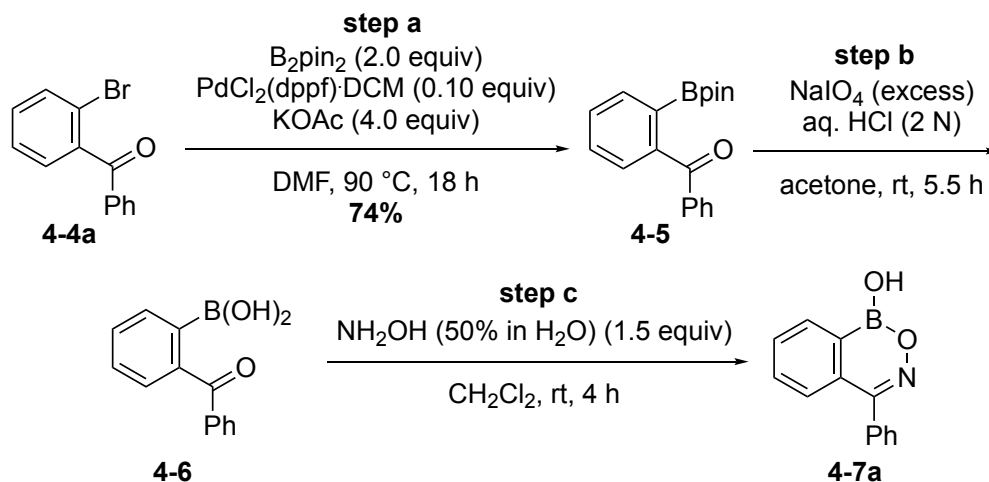
Scheme 4.1 Initial sequence of reactions for the synthesis of the **4-1** analog, **4-7a**.

A modification was therefore needed to develop a robust procedure for synthesizing these analogs (Scheme 4.2). In the first step of the sequence (step a), dioxane was used as a solvent instead of DMF, for ease of removal. After workup, the crude boronate product was passed through a silica gel column to elute product **4-5**, along with a protodeboronation side-product (benzophenone, ~20% by NMR analysis) and B_2pin_2. The crude boronate product **4-5** was carried through to the next step, where it was converted to **4-6** via a transesterification reaction with $MeB(OH)_2$ (transfer of the pinacol group) (step b).[31] This reaction resulted in the formation of the unprotected arylboronic acid **4-6**, and the side products ($MeB(OH)_2$ and MeBpin) were removed under vacuum due to their volatility. Finally, condensation with aqueous hydroxylamine resulted in the formation of the crude product (**4-7a**) (step c). This crude product was triturated with diethyl ether (to remove the protodeboronated side-product)

and then washed with water (to remove borates and excess NH$_2$OH), which resulted in the pure desired product **4-7a** in good overall yield (Figure 4.6).
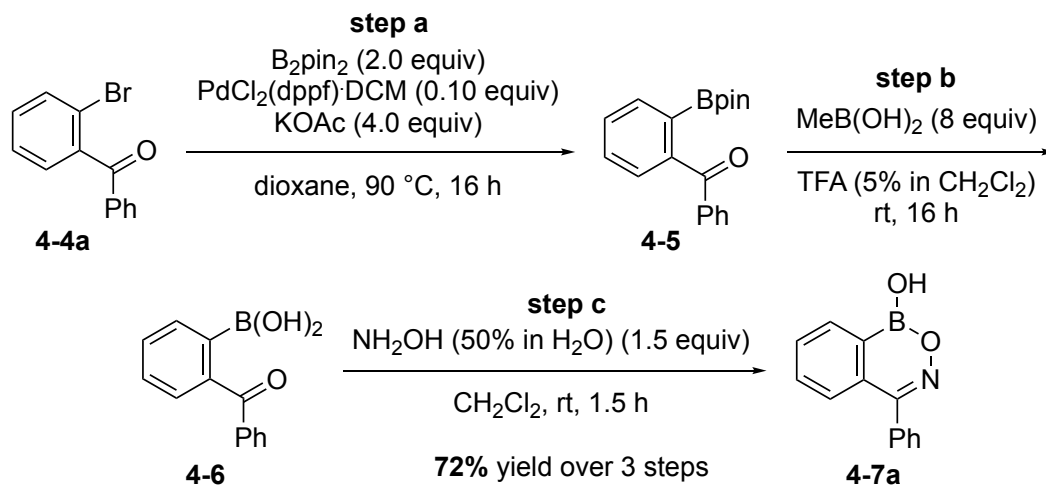
Scheme 4.2. Modified reaction sequence for the synthesis of the benzoxazaborine analog, **4-7a**.
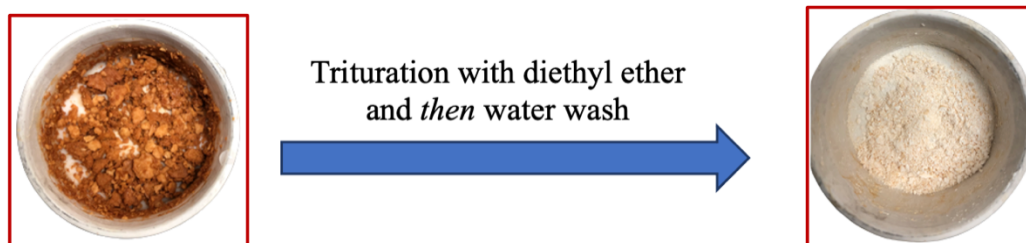
Figure 4.6. Purification of crude **4-7a** by Et$_2$O/water wash obtained after three steps of the reaction.

The starting materials for the synthesis of ketoxime analogs of benzoxazaborine and NH-benzodiazaborine, substituted 2-bromobenzophenones (**4-4**), were synthesized by transformation of substituted 2-bromobenzoic acid into the corresponding acyl chloride, followed by a Friedel-Craft acylation reaction (Scheme 4.3).
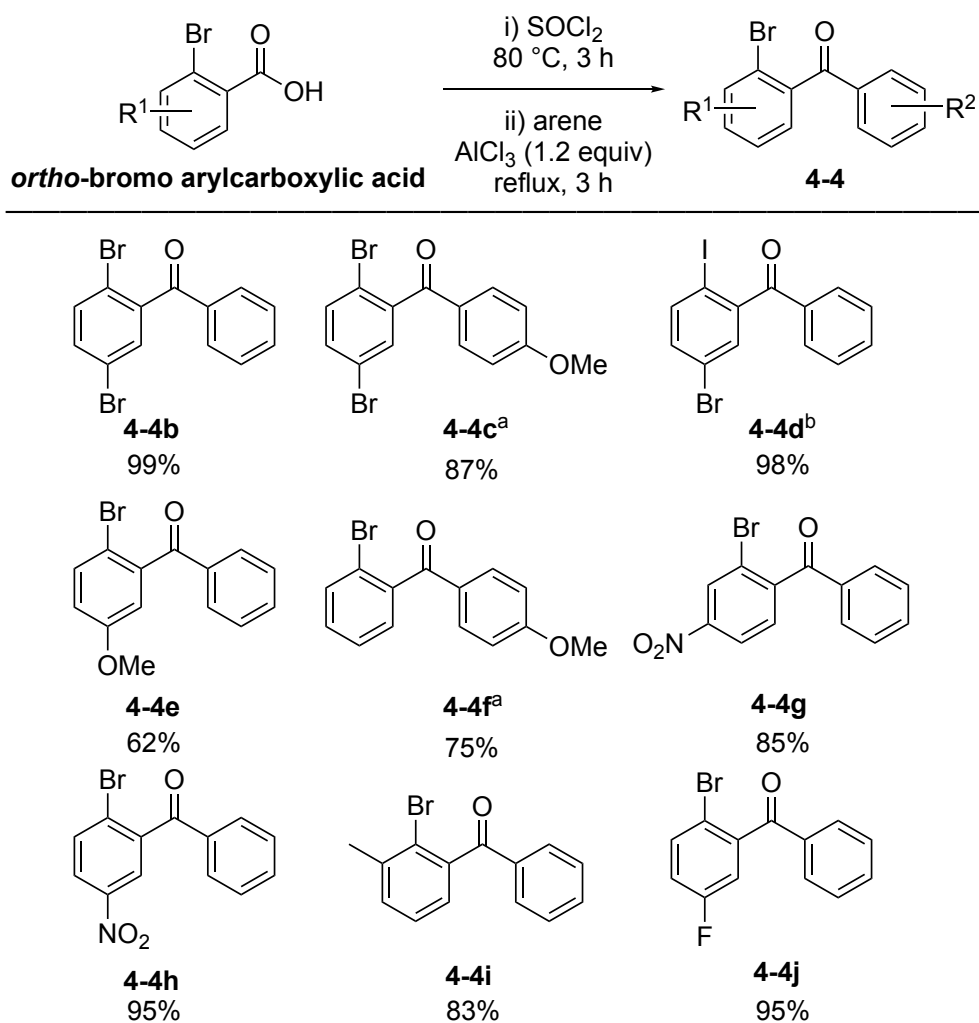
Scheme 4.3. Synthesis of the precursors for the preparation of ketoxime analogs of benzoxazaborine and NH-benzodiazaborine.

The modified three-step procedure was employed to synthesize a variety of analogs of benzoxazaborine and NH-benzodiazaborine, where in the latter case $NH_2NH_2 \cdot H_2O$ was used instead of aq. NH_2OH for step c (cf. Scheme 4.2). The ketoxime analogs were synthesized from the substituted 2-bromobenzophenones (**4-4**), while the aldehyde precursors (substituted 2-bromobenzaldehyde or substituted *ortho*-formyl phenylboronic acid) were utilized for the synthesis of aldoxime analogs (Scheme 4.4 and 4.5).

Scheme 4.4. Synthesis of analogs of benzoxazaborine by the early-stage approach. Yields reported over three steps, unless stated otherwise.

The reaction scheme shows starting material **4-4** (ortho-bromo aryl ketone with R¹ substituent, R² = H, Me or Ar) converting to product **4-7** via:

i) B_2pin_2 (2.0 equiv), $PdCl_2(dppf) \cdot DCM$ (0.10 equiv), KOAc (4.0 equiv), dioxane, 90 °C, 16 h

ii) $MeB(OH)_2$ (8 equiv), TFA (5% in CH_2Cl_2), rt, 16 h

iii) NH_2OH (50% in H_2O) (1.5 equiv), CH_2Cl_2, rt, 1.5 h

Products:

- **4-7a** 72% (Ph)
- **4-7b**[a] 95% (Me)
- **4-7c** 76% (HO, H)
- **4-7d**[a] 83% (F, H)
- **4-7e**[a] 94% (MeO, H)
- **4-7f** 63% (O-C₆H₄-CN, H)
- **4-7g** 70% (C₆H₄-OMe)
- **4-7h**[b] 63% ((HO)₂B, C₆H₄-OMe)
- **4-7i**[b] 34% ((HO)₂B, Ph)
- **4-7j** 59% (MeO, Ph)
- **4-7k** 54% (Me, Ph)
- **4-7l** 40% (F, Ph)
- **4-7m** 38% (O₂N, Ph)
- **4-7n** (33%)[c] (H₂N, Ph)

[a]Synthesized from the commercially available substituted *ortho*-carbonyl phenylboronic acid using step iii, yield reported for one step

[b]B_2pin_2 (4.0 equiv), $PdCl_2(dppf) \cdot DCM$ (0.20 equiv), KOAc (8.0 equiv)

[c]Yield measured using internal standard

Scheme 4.5. Synthesis of analogs of NH-benzodiazaborine by the early-stage approach. Yields reported over three steps, unless stated otherwise.

The reaction sequence worked for a variety of substrates containing electron-withdrawing or electron-donating groups with substituents ortho, meta, or para to the C—B bond. Some analogs were synthesized directly from the commercially available corresponding *ortho*-carbonyl phenylboronic acids, using only the last step of condensation (**4-7b**, **4-7d**, **4-7e**, and **4-8d**). Hydroxy substituted aldoxime analogs (**4-7c** and **4-8b**) were obtained from the corresponding, commercially available aldehyde precursor (5-hydroxy-2-bromobenzaldehyde). The starting material for the synthesis of nitro substituted aldoxime analog **4-8c**, 2-bromo-4-nitrobenzaldehyde, was obtained from 2-bromo-4-nitrobenzoic acid after undergoing a full reduction to the alcohol, and partial oxidation to the aldehyde (Scheme 4.6).[32]
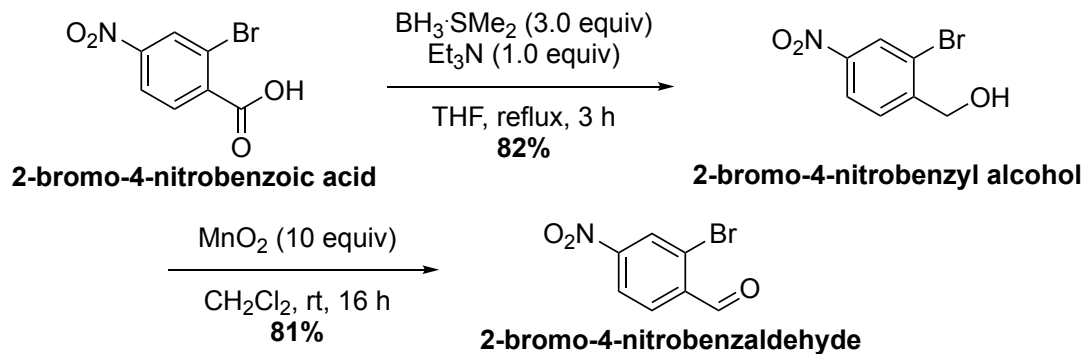
Scheme 4.6. Preparation of the precursor for the synthesis of **4-8c**.

For analogs of benzoxazaborine (**4-7**), the purification of the desired product was performed as follows: 1) After the final step, the solvent was removed under vacuum, followed by the addition of water in the reaction flask. 2) The resulting precipitate was filtered and then washed with diethyl ether to furnish the desired pure analog (**4-7**). The precursors for the synthesis of **4-7n**, **4-8f** or **4-8g** were obtained after the reduction of the nitro group of the corresponding nitro-substituted 2-bromobenzophenone, **4-4h** or **4-4g** (Scheme 4.7).[33] Purification of **4-7n** was challenging due to the similar pK_a of the aryl amine (~4.6) and the hemiboronic acid (5.5). Therefore, column chromatography was performed after the final reaction, using MeOH/CH$_2$Cl$_2$ with 0.5% AcOH as the eluent, which eluted the product as the acetic acid salt. The yield was calculated using an internal standard, 1,3,5-trimethoxybenzene, and the product was used as such for further late-stage reactions (vide infra).
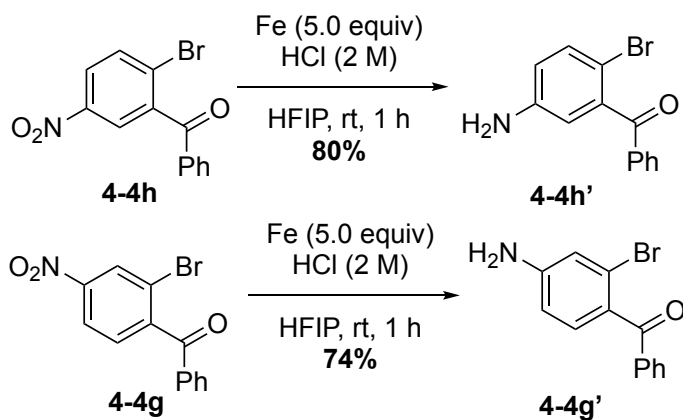
Scheme 4.7. Preparation of the precursors for the synthesis of **4-7n**, **4-8f** or **4-8g**.

In the case of NH-benzodiazaborine derivatives (**4-8**) with pK_a > 14, washing with saturated aq. sodium bicarbonate and diethyl ether was sufficient to obtain the pure product (for example, **4-8f**). To this end, using the early-stage approach, several drug analogs were synthesized, such as tavaborole analogs (**4-7d** and **4-8d**) and the crisaborole analog (**4-7f**). The precursor for the synthesis of **4-7f** was obtained by a series of aldehyde protection, S$_n$Ar, and deprotection reactions (Scheme 4.8).[12] The aldehyde functionality in 2-bromo-5-hydroxybenzaldehyde was protected using trimethyl orthoformate, followed by a S$_n$Ar reaction with 4-fluorobenzonitrile, and finally deprotected with aq. HCl, affording the desired precursor **4-7f'**.
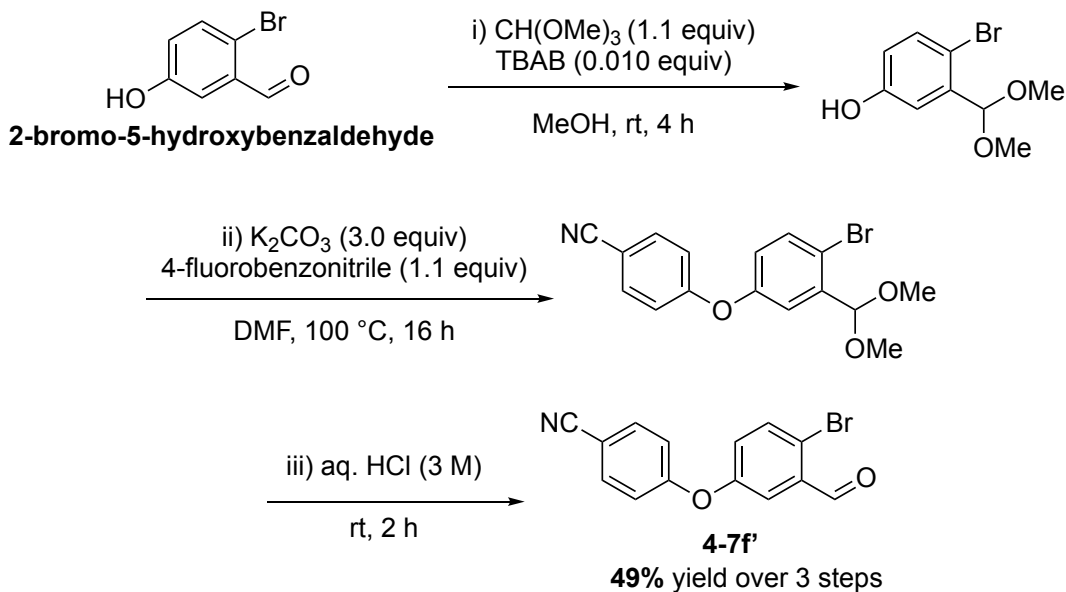
Scheme 4.8. Preparation of the precursor **4-7f'** for the synthesis of **4-7f**.

4.4 Precursors Used for the Late-Stage Synthesis of Analogs of 4-1 and 4-2a

Some analogs synthesized with an early-stage approach (vide supra), also were subjected to late-stage modifications (Figure 4.7).
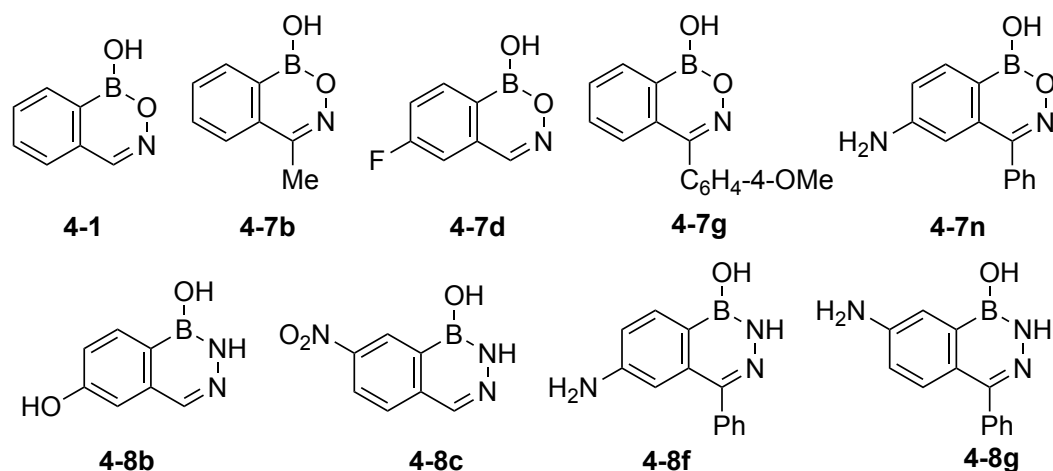
Figure 4.7. Precursors used for the synthesis of analogs of **4-1** and **4-2a** utilizing a late-stage approach.

The triflate analogs of benzoxazaborine and NH-benzodiazaborine (**4-9** and **4-10**, respectively) were synthesized and also used for late-stage modifications (Scheme 4.9). See Section 4.5.4 for details regarding phase-switch workup.
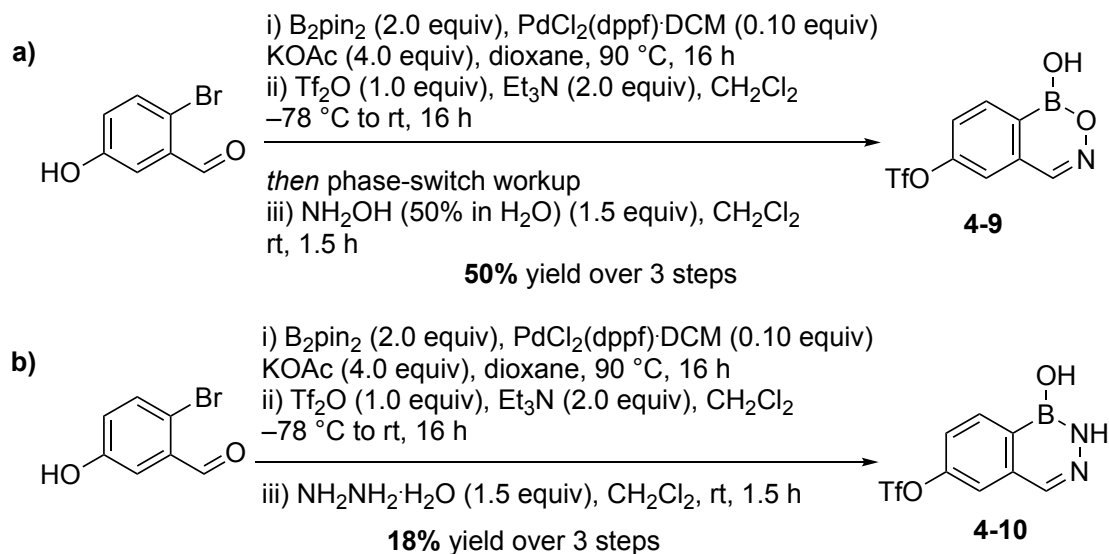
Scheme 4.9. Synthesis of the triflate analogs of **4-1** and **4-2a** for the late-stage modifications.

4.5 Late-Stage Approach for the Synthesis of Analogs of 4-1 and 4-2a

To date, there is virtually no literature describing the systematic derivatization of these scaffolds via late-stage transformation reactions. Late-stage diversification is important

in drug discovery, as several derivatives can be synthesized from the same scaffold. At the outset, a focus was placed towards oxime reduction, amide formation, and chemoselective reactions, such as Chan-Lam coupling and the Suzuki-Miyaura reaction. Halogenation reactions also were performed.

4.5.1 Oxime Reduction

Hydrogenation of the oxime in benzoxazaborine could assist in obtaining a variety of reduced derivatives that could be further derivatized via electrophilic functionalization of the resulting secondary hydroxylamine. Moreover, this oxime reduction could also provide new scaffolds. Various reagents and catalysts were employed to affect the reduction of the oxime group in **4-1** and **4-7b** (see Section 4.4) (Table 4.1).

Table 4.1. Attempted Hydrogenation of **4-1** and **4-7b**

4-1 R = H
4-7b R = CH$_3$

Entry	Reagents	Solvent	Result
1	NaBH$_4$, CeCl$_3\cdot$7H$_2$O	ethanol	>96% conversion
2	H$_2$, Pd/C	ethanol	N—O cleaved
3	*S*-CBS, BH$_3\cdot$SMe$_2$	THF	N—O cleaved
4	NaBH$_4$	ethanol	no reaction
5	NaBH$_4$, NiCl$_2\cdot$6H$_2$O	methanol	N—O cleaved
6	NaBH$_4$, NiCl$_2$	methanol	no reaction
7	(*t*BuO)$_3$AlHLi	THF	no reaction
8	NaEt$_3$BH	THF	N—O cleaved
9	NaBH$_4$, CuCl	THF	no reaction
10	NaBH$_4$, ZrCl$_4$, Al$_2$O$_3$	neat	no reaction
11	PhMe$_2$SiH	1:1 TFA/CH$_2$Cl$_2$	no reaction
12	Ph$_2$SiH, Wilkinson's catalyst	CH$_2$Cl$_2$	no desired product

Most of the reagents resulted either in no reaction or furnished N—O cleaved products (entry 2–12). Interestingly, the Luche reduction, first performed by Shang Li in the Hall Group, indicated the formation of the hydrochloride salt of the product, which was obtained after quenching the reaction with dilute HCl solution (entry 1). Further optimization of the Luche reduction conditions, led to the conclusion that a portion-wise addition of NaBH$_4$ is necessary to achieve a better yield of the product. This procedure resulted in the addition of excess reagents (20 equivalent of NaBH$_4$ and 12 equivalent of CeCl$_3$·7H$_2$O). Both product and side-products, such as an excess of boric acid and cerium salts, were soluble in water and, as a result, were difficult to separate. To confirm the formation of the desired reduced product **4-7b'** (i.e., to exclude the possibility of the N—O cleaved product), an amidation reaction was performed on the reduced product (**4-7b'**) (Figure 4.8a). A portion of the crude amide product (**4-11**) obtained was recrystallized and then subjected to X-ray crystallographic analysis, which confirmed that **4-7b'** was indeed the desired product (Figure 4.8b).
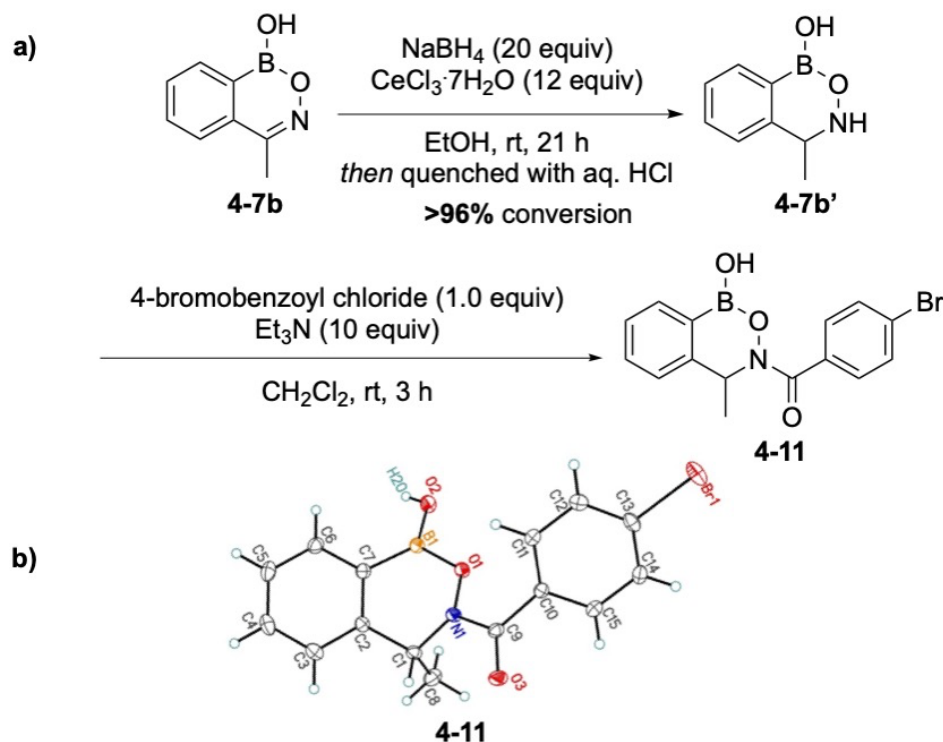
Figure 4.8. a) Luche reduction of **4-7b** followed by an amidation reaction of **4-7b'**. **b)** ORTEP representation of the amide product, **4-11**.

Although, this amidation product (**4-11**) was found to be unstable in MeOH, where it resulted in the formation of 4-bromobenzoic acid and **4-7b'** (Figure 4.9, also observed by LC-MS). This phenomenon could be explained by invoking the electron-withdrawing (inductive) property of the endocyclic oxygen atom, which would result in decreased electron density on the nitrogen atom, therefore, resulting in increased electrophilicity of the carbonyl group. This increased electrophilic character would make the C=O bond more susceptible to the nucleophilic attack by MeOH.
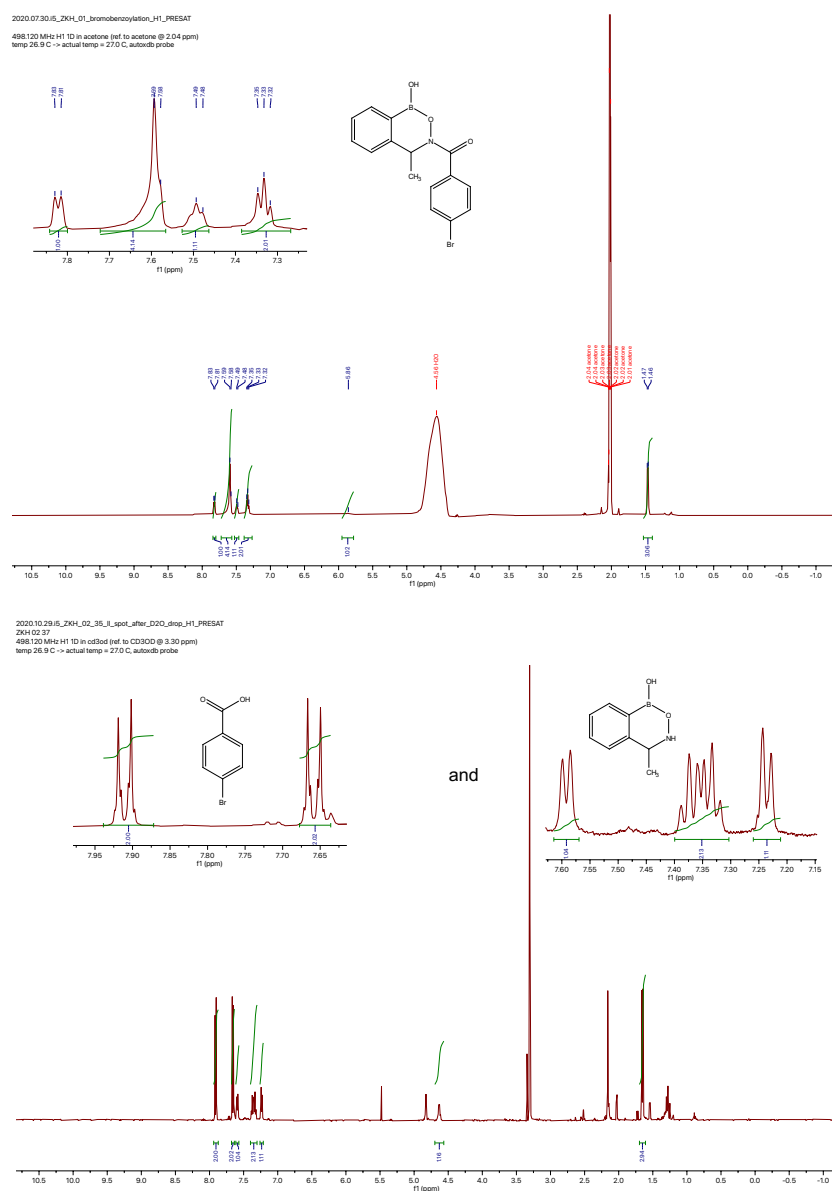
Figure 4.9. Amidation product, **4-11**, in d_6-acetone (top) and in d_4-MeOH (bottom, showing two individual molecules).

Alternative approaches were explored for achieving a clean reduction of the oxime functionality. In this regard, Cramer and co-workers have demonstrated the use of an Ir-catalyzed acid-assisted hydrogenation reaction for the transformation of oximes to hydroxylamines.[34] Since benzoxazaborines contain an oxime moiety, it was envisioned that they could also be hydrogenated using the same catalytic system. Thus, catalyst **4-12** was synthesized and employed for the reduction of benzoxazaborine **4-1** (Scheme 4.10).[34] Remarkably, the reaction resulted in the formation of the desired product **4-13** with high conversion (>99%). The same reaction conditions also resulted in the reduction of **4-7b** to **4-14**, and **4-7d** (tavaborole analog) to **4-15**.
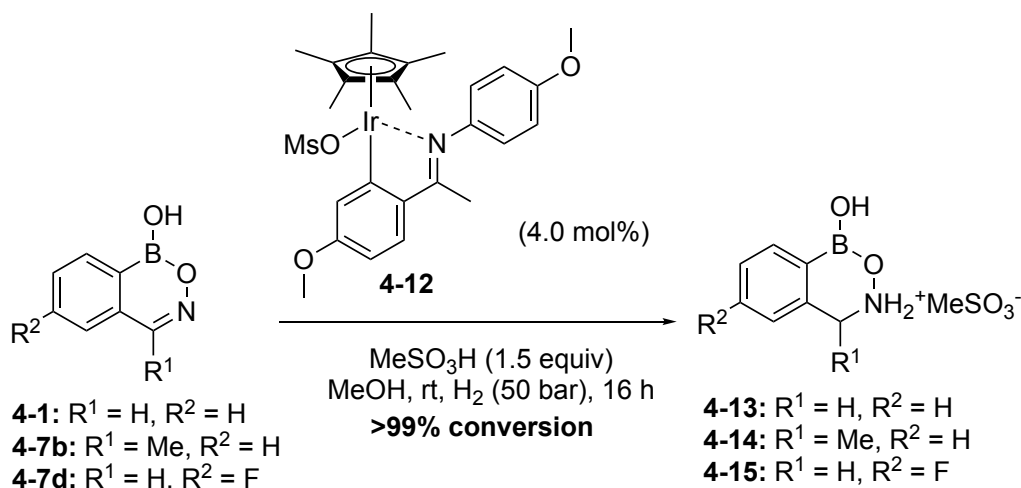
Scheme 4.10. Oxime hydrogenation of **4-1**, **4-7b**, and **4-7d** using an Ir catalyst **4-12**.

The ^{11}B chemical shift of **4-13**–**4-15** in D$_2$O (due to the polar/zwitterionic nature of these compounds, they were found to be soluble in water and insoluble in organic solvents, such as acetone) appears between 7–10 ppm. This relatively upfield chemical shift indicates the possibility that the acid/conjugate base equilibrium for these compounds (**4-13**–**4-15**) weighs towards the preference for the boron atom exhibiting a tetracoordinate center. Such an upfield chemical shift in neutral conditions suggests a low pK_a (<4) for these reduced analogs (**4-13**–**4-15**). Still, the ^{11}B NMR titration was performed using **4-13** as an example but no inflection point was observed upon changing the pH of the solution from low to high (1–10) (see Section 4.9.2.1).

On the other hand, when the Ir-catalyzed reduction, or a Luche reduction were applied to **4-7a** (where R^1 = Ph and R^2 = H), these conditions did not afford the corresponding reduction product (**4-16**) likely due to the extended electron conjugation of the ketoxime group with the additional phenyl ring (Figure 4.10).
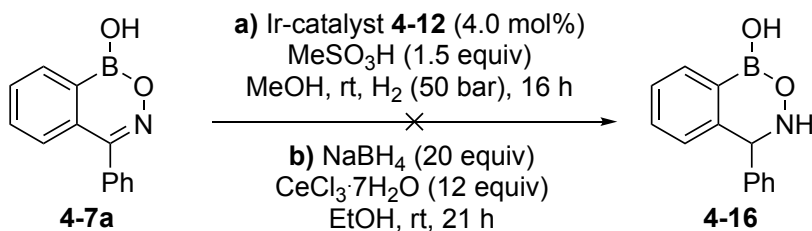
Figure 4.10. Attempted oxime hydrogenation of **4-7a**.

4.5.2 Protection of Benzoxazaborine

Since the reduced analog of **4-7a** (**4-16**) could not be obtained by either hydrogenation conditions (vide supra), it was reasoned that by first protecting the boranol unit of benzoxazaborine **4-1**, the same products maybe formed via the reaction at the oxime group with arylated nucleophiles, such as phenylmagnesium bromide, to afford the desired phenyl-substituted analog **4-16**. Different protecting groups were considered to assess their compatibility with benzoxazaborines. Raines and co-workers have shown that the bifunctional nucleophiles, salicimine and 3-dimethylaminopropanol can be used for the protection of benzoxaboroles.[24] These protecting groups were found to be suitable with benzoxazaborines, allowing for the synthesis of protected **4-1** (**4-17** and **4-19**) and **4-7b** (**4-18**) (Scheme 4.11).
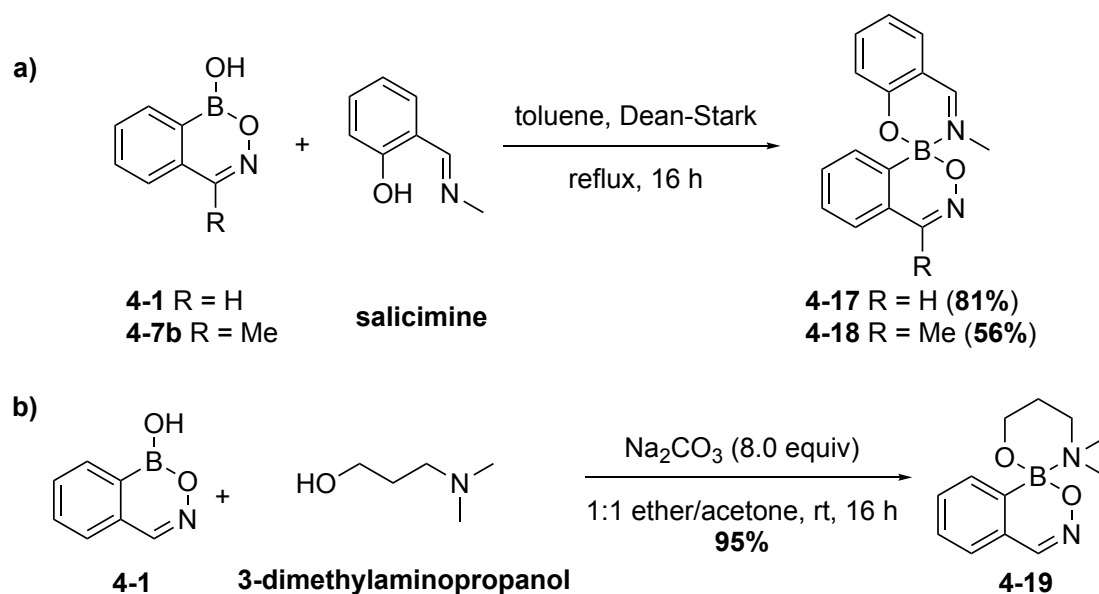
Scheme 4.11. Protection of **4-1** and **4-7b** with salicimine and/or 3-dimethylaminopropanol.

Formation of the phenyl-substituted reduced benzoxazaborine **4-16** was then attempted through addition of phenylmagnesium bromide to the protected benzoxazaborines **4-17** or **4-19**. Unfortunately, neither reaction produced the desired product **4-16** (Figure 4.11a, b). LC-MS analysis of the crude mixtures obtained after each reaction (**a** or **b**) indicated the presence of undesired **4-20**, formed via the addition of the aryl group to the boron center (Figure 4.11c).
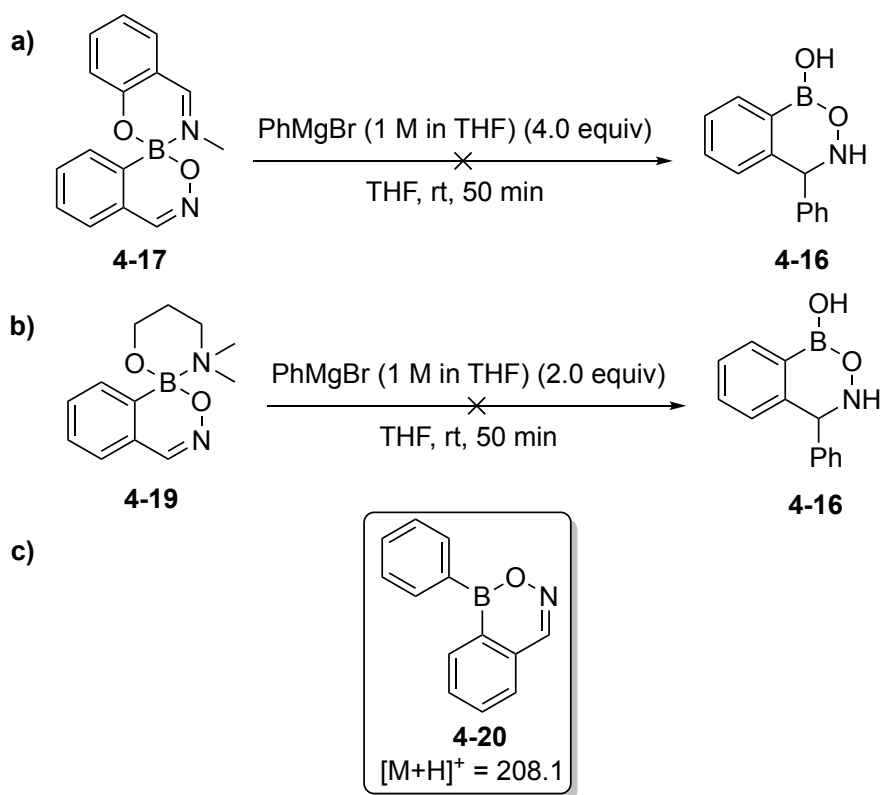
Figure 4.11. Reaction of phenylmagnesium bromide with protected benzoxazaborine (**4-17** or **4-19**) (**a** and **b**). **c)** Product **4-20** observed from the reactions **a** and **b**.

4.5.3 Bromination of a Ketoxime Analog of 4-1

Bromination of benzoxazaborine analogs can give rise to another versatile handle for further late-stage modifications. To this end, **4-7g** (see Section 4.4) was subjected to bromination with *N*-bromosuccinimide (NBS), resulting in clean conversion to *ortho*-brominated product **4-21** (Scheme 4.12).
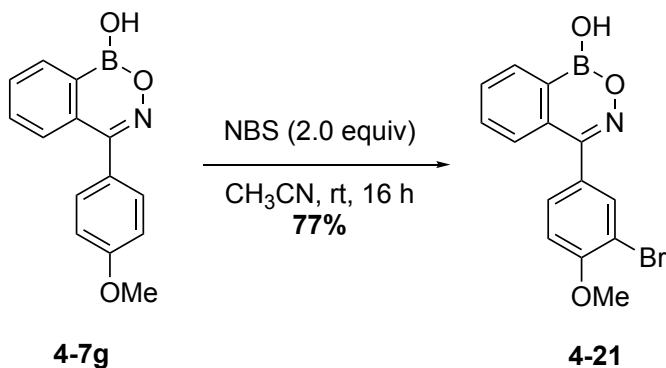
Scheme 4.12. Monobromination of **4-7g**.

Interestingly, this reaction produced only the monobrominated product, even in the presence of excess NBS. The brominated product **4-21** can potentially be further modified by reactions, such as the Suzuki-Miyaura cross-coupling.

4.5.4 Amide Formation Reactions from Aniline Derivatives of 4-1

The amide group is one of the most important functional groups in chemistry. It is found in several bioactive molecules.[35–37] Several reaction conditions were exploited for the formation of amide **4-22a** from the aniline derivative **4-7n** (an analog of benzoxazaborine (**4-1**), see Section 4.4) (Scheme 4.13). Initially, an amidation reaction between **4-7n** and benzoyl chloride was attempted using Et₃N base and CH₂Cl₂ as the solvent (conditions a). The reaction resulted in the formation of product **4-22a**, along with undetermined impurities. Trituration with Et₂O, or subjection to an acid/base workup did not result in the pure product. Silica gel column chromatography was avoided due to the high polarity of **4-22a** (see Section 4.1).
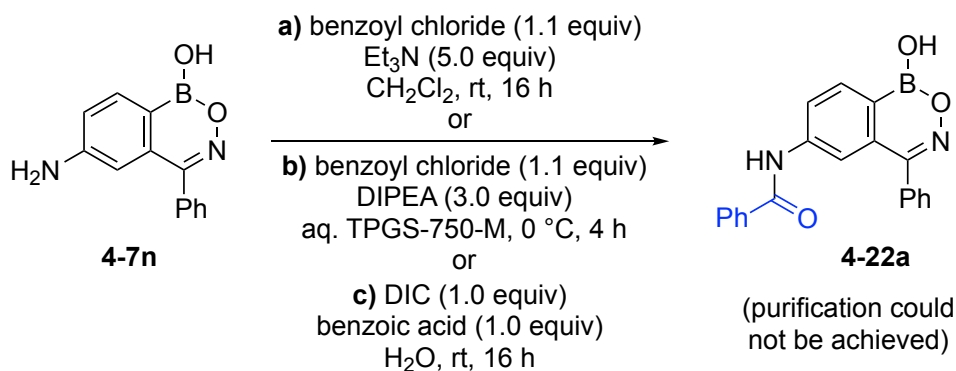
Scheme 4.13. Attempted amidation reactions for the synthesis of **4-20a** from **4-7n**.

A protocol developed by Novartis™ Pharmaceuticals for a "chromatography-free" amidation reaction between an amine and acyl chloride, employing Hünig's base (DIPEA) and aqueous TPGS-750-M (a surfactant) was next considered.[38] The reaction resulted in the desired product, but also suffered from a difficult purification due to the presence of unreacted starting material (conditions b). Subsequently, a classic diimide induced coupling with a carboxylic acid partner was attempted. This reaction also resulted in the desired product **4-22a**, but similarly caused purification challenges (conditions c). Likewise, a phase-switch workup or a trituration

with EtOAc/hexanes did not afford a pure product. The phase-switch workup was performed by dissolving the crude compound in a basic (pH ~10) aqueous sorbitol solution, trapping the boronic acid in the aqueous phase as a diol adduct.[23] The neutral or basic impurities were then removed by washing the aqueous phase with organic solvent (e.g., EtOAc). The aqueous phase was then acidified to a pH of ~2, followed by extracting the neutral boronic acid with the organic solvent, leaving the water-soluble impurities in the aqueous phase.

Thus, in an effort to minimize any side reactivity and achieve an atom-economical pathway (which would also help in purification), *N*-methyl-2-pyrrolidone (NMP) was utilized in the dual role of a mild base and solvent for the amidation between benzoyl chloride and **4-7n** (Scheme 4.14).[39] The reaction resulted in the clear conversion to the desired product **4-22a**. Purification was achieved in two stages: 1) A phase-switch workup, which gave **4-22a**, along with benzoic acid; 2) Recrystallization with EtOAc/hexanes, affording **4-22a** as a crystalline product, which was found suitable for X-ray crystallographic analysis (Figure 4.12).
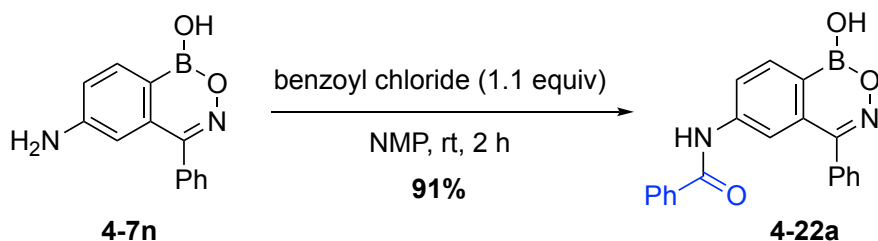
Scheme 4.14. Optimized amidation reaction for the synthesis of **4-20a** from **4-7n**.
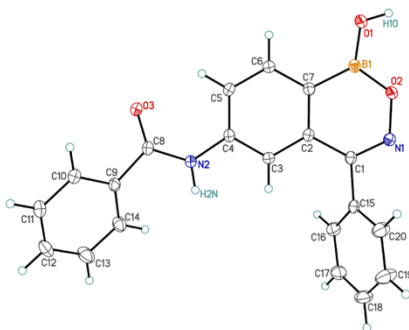
Figure 4.12. ORTEP representation of **4-22a**.

156

With these optimized conditions in hand, a range of amide products were synthesized from the amine precursor **4-7n**, generally using the same 2-stage purification procedure mentioned above (Scheme 4.15). A diverse selection of acyl chloride derivatives were chosen, containing various electron-donating groups, electron-withdrawing groups, and heterocycles. Acyl chlorides containing fluorine were also selected, as fluorine is known to often positively influence drug metabolism and is recognized as an important element in drug discovery.[40]
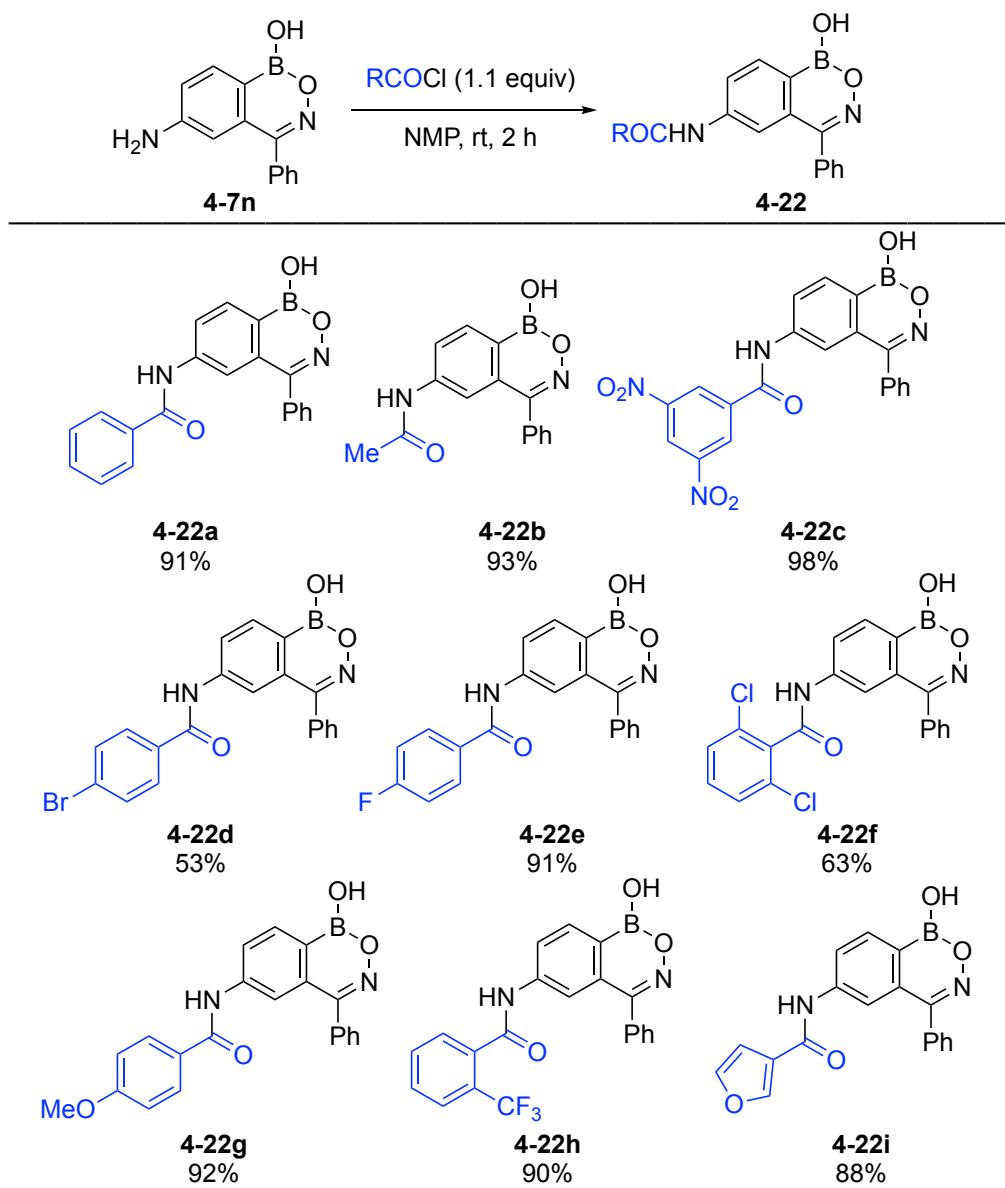
Scheme 4.15. Amidation of a benzoxazaborine aniline precursor, **4-7n**.

Altogether, halogenated derivatives (**4-22d**–**4-22f**), derivatives containing electron-donating groups (**4-22g** and **4-22i**), and electron-withdrawing groups (**4-22c** and **4-22h**), were synthesized. A reaction with an aliphatic acyl chloride (acetyl chloride) also resulted in the desired amide product (**4-22b**) in high yield.

Another amide derivative, **4-22j**, was prepared through a series of reactions, starting from an aniline precursor **4-4g'** (cf. Scheme 4.7) (Scheme 4.16). The product obtained shows a close resemblance to acoziborole (cf. Figure 4.1).
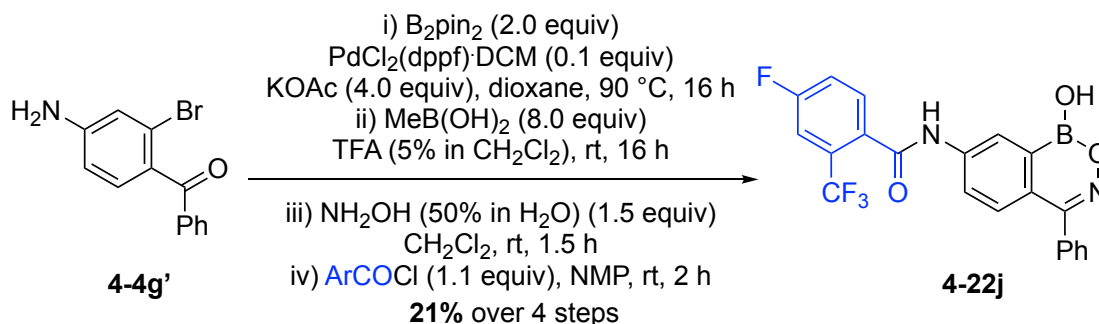
Scheme 4.16. Amidation of **4-4g'** to afford acoziborole mimetic **4-22j**.

Other amide derivatives, such as, **4-22k** and **4-22l**, were synthesized from multistep reactions featuring a late-stage reduction of the nitro group, followed by the amidation reaction (Scheme 4.17). The reduction of the nitro group was accomplished through a Fe/HCl reduction reaction, and no N—O cleavage was observed in the late-stage reduction, whereas using H_2/Pd-C led to the N—O cleaved product. Generally, it was observed that the nitro group at the *meta* position of 2-bromobenzaldehyde resulted in the formation of boronic acid instead of the Bpin product after a Miyaura borylation (hydrolysis in the work-up), which made the purification challenging (Scheme 4.17b). Therefore, in most of the cases where nitro group was at a *meta* position, HPLC purification was required, which also resulted in lower yield (e.g., **4-22l**). To this end, acoziborole analogs, such as, **4-22l**, along with other chemically similar analogs (**4-22j** and **4-22k**) were synthesized.
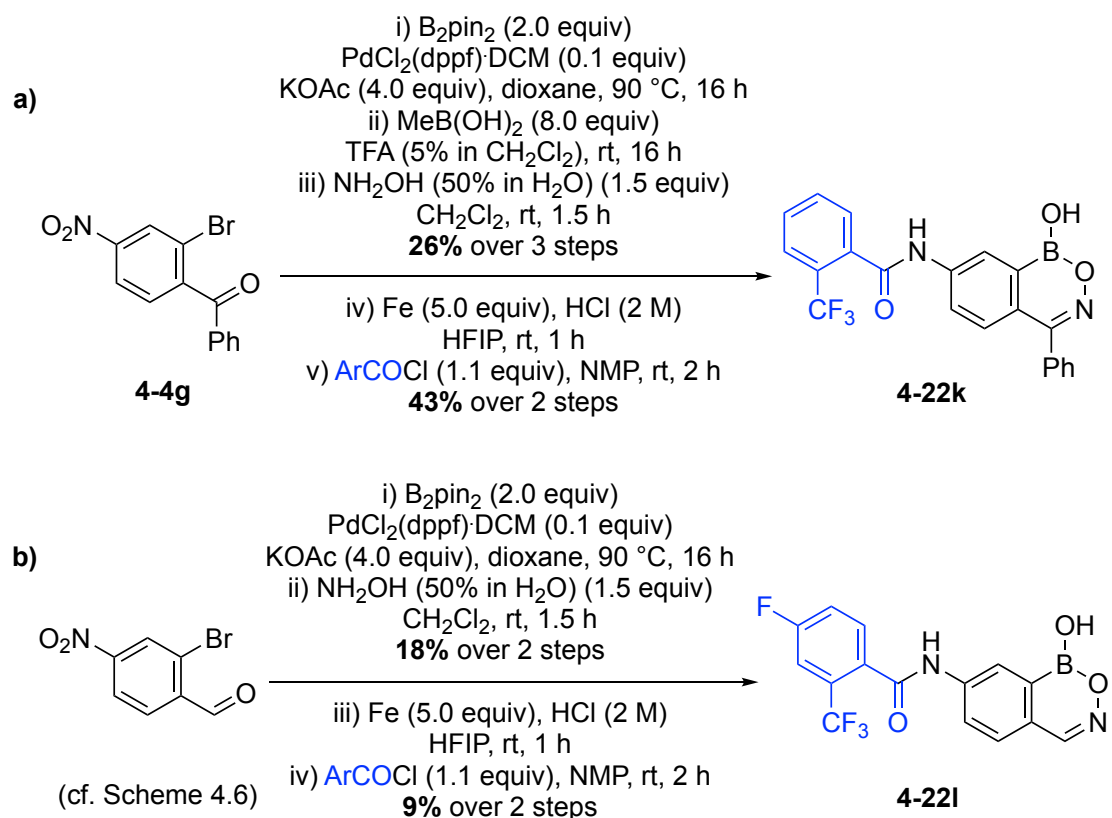
Scheme 4.17. Synthesis of **4-22k** and acoziborole mimetic **4-22l** featuring a late-stage nitro reduction.

4.5.5 Amide Formation Reactions from Analogs of 4-2a

The amidation of NH-benzodiazaborine (**4-2a**) analogs was achieved by using the same conditions employed with the benzoxazaborine (**4-1**) analog. A series of acyl chlorides similar to those used previously (for the benzoxazaborine analogs) were chosen, with an emphasis on fluorine/trifluoromethyl (acoziborole type) derivatives. A variety of amide products were synthesized from NH-benzodiazaborine analogs **4-8f** and **4-8g** (see Section 4.4) as shown in Scheme 4.18. Since the pK_a of NH-benzodiazaborine (**4-2a**) is greater than 14, a wash with saturated aq. sodium bicarbonate was performed on the crude amide products to remove the excess of acid chlorides (in the form of their corresponding carboxylic acids), followed by recrystallization from CH$_2$Cl$_2$/hexanes to achieve the pure product.
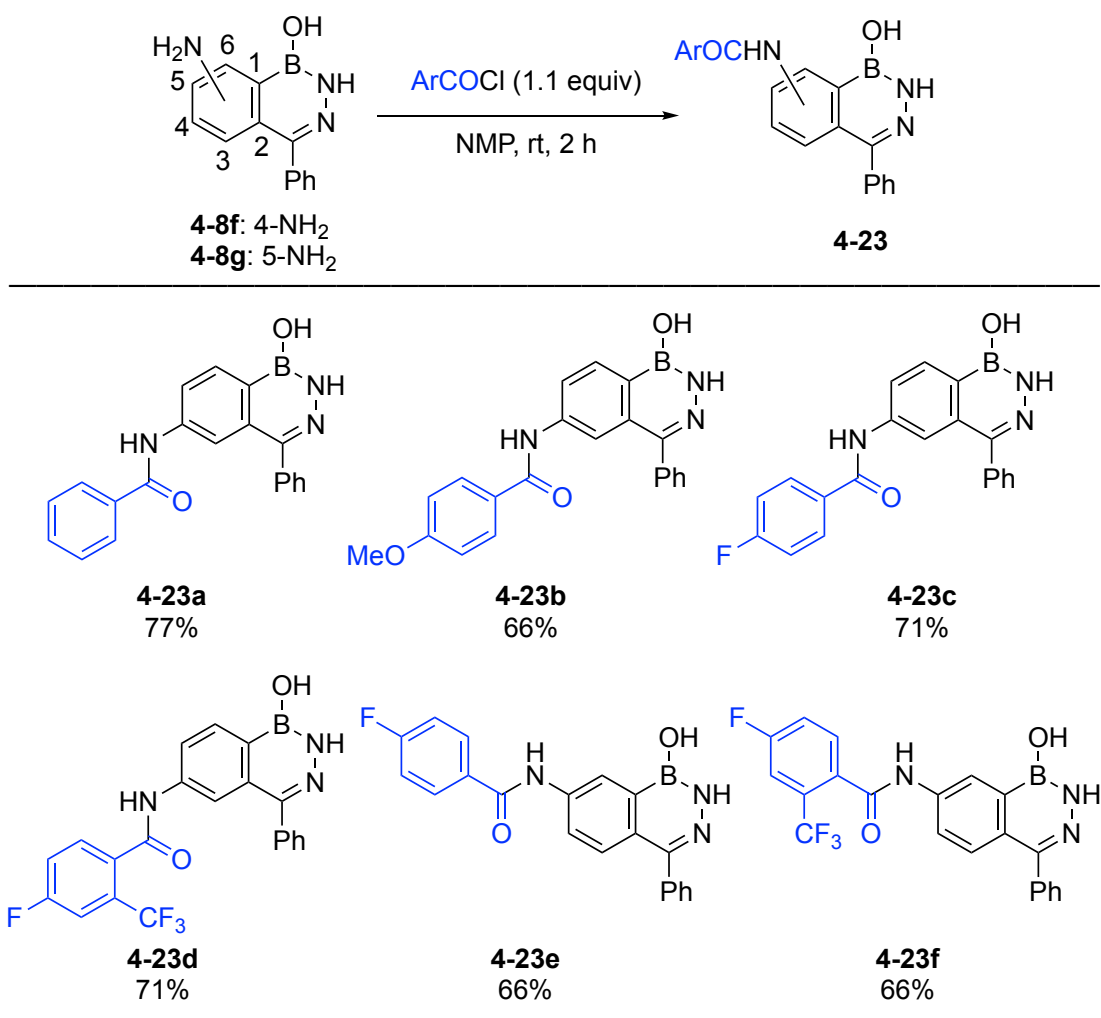
Scheme 4.18. Amidation of NH-benzodiazaborine analogs, **4-8f** and **4-8g**.

Products **4-23a**–**4-23d** were prepared from **4-8f**, while analogs **4-23e** and **4-23f** were synthesized from **4-8g**. Compounds **4-23g**–**4-23i** were prepared after reduction of the nitro group in **4-8c** (see Section 4.4) to produce **4-8c'**, which was converted further to amide products (Scheme 4.19). In the case of nitro analogs of NH-benzodiazaborines, reduction with H_2/Pd-C led to a clean conversion to the amine product, with no sign of N—N cleavage (contrary to benzoxazaborine analogs, vide supra).
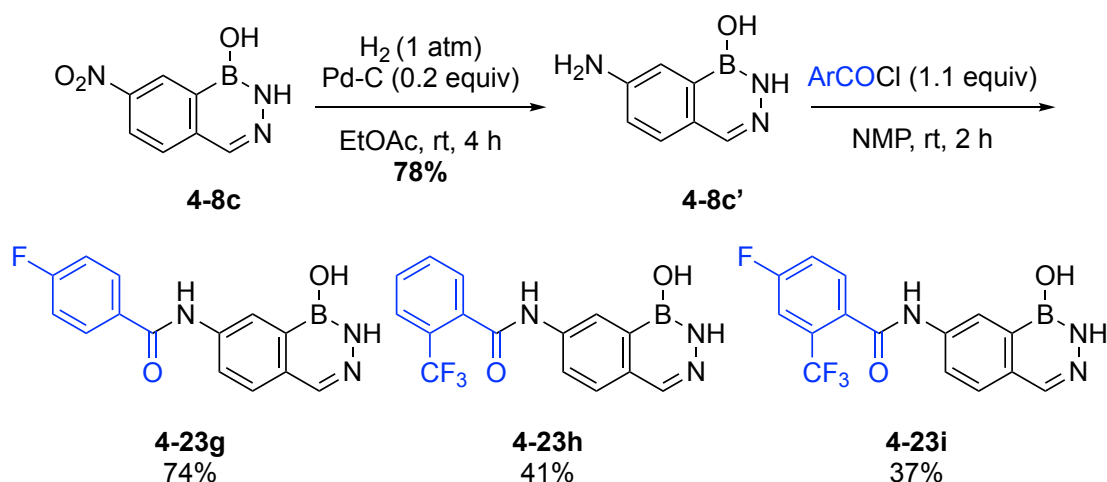
Scheme 4.19. Synthesis of **4-23g**–**4-23i** featuring a late-stage nitro reduction.

Overall, derivatives containing electron-donating groups (**4-23b**) and electron-withdrawing groups (**4-23c**–**4-23i**) were synthesized. To this end, acoziborole analogs, such as **4-23i** were synthesized along with positional isomers and other chemically similar analogs (**4-23e**–**4-23h**).

4.5.6 Chemoselective Chan-Lam Reaction and Ether Cleavage

To obtain ether analogs of benzoxazaborine (**4-1**), a phenolic derivative **4-7c** (see Scheme 4.4) was employed. The mechanism of the Chan-Lam reaction reveals that the boron center needs to become ionized for the transmetalation step to occur (transfer of the boronic acid aryl group to the copper species).[41,42] Since benzoxazaborine has a pK_a of 5.5, a chemoselectivity challenge was expected. Initially, classical Chan-Lam reaction conditions were attempted (Scheme 4.20). Since the Chan-Lam reaction can also produce the protodeboronated side-product and the oxidative deboronated by-product (phenol), an excess of arylboronic acid coupling partner was used.[42,43] The reaction resulted in the formation of the desired product **4-7f**, along with the unreacted **4-7c** (~1:1), 4-cyanophenylboronic acid, and other undetermined impurities (observed by LC-MS analysis and ^{1}H NMR spectroscopy). Neither trituration with Et$_2$O, phase-switch workup, nor silica chromatography furnished the desired pure product. The lack of appreciable selectivity was probably due to the associated low pK_a of **4-1**, which would result in the undesired coupling with the endocyclic B—C bond of **4-7c**.
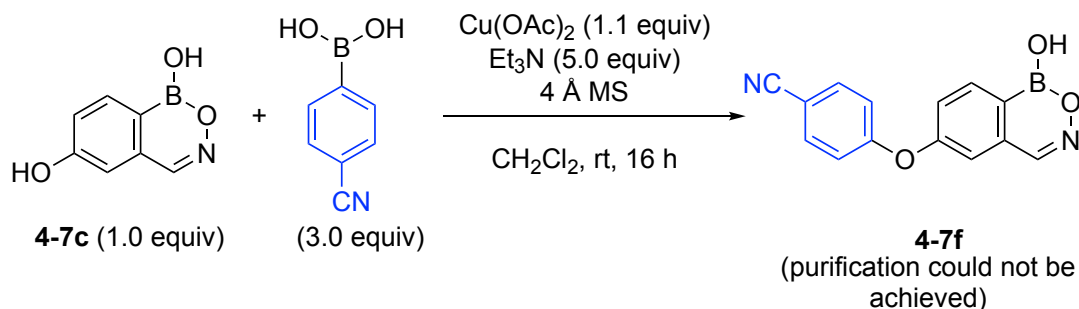
Scheme 4.20. Attempted Chan-Lam reaction with benzoxazaborine analog, **4-7c**.

Alternative approaches using trifluoroborate or diaryliodonium salt coupling partners were then evaluated (Scheme 4.21a, b).[44,45] Unfortunately, neither reaction furnished the desired ether product. Similarly, there was no evidence of product formation (**4-7f**) using conditions reported by the Buchwald Group (Scheme 4.21c).[46]
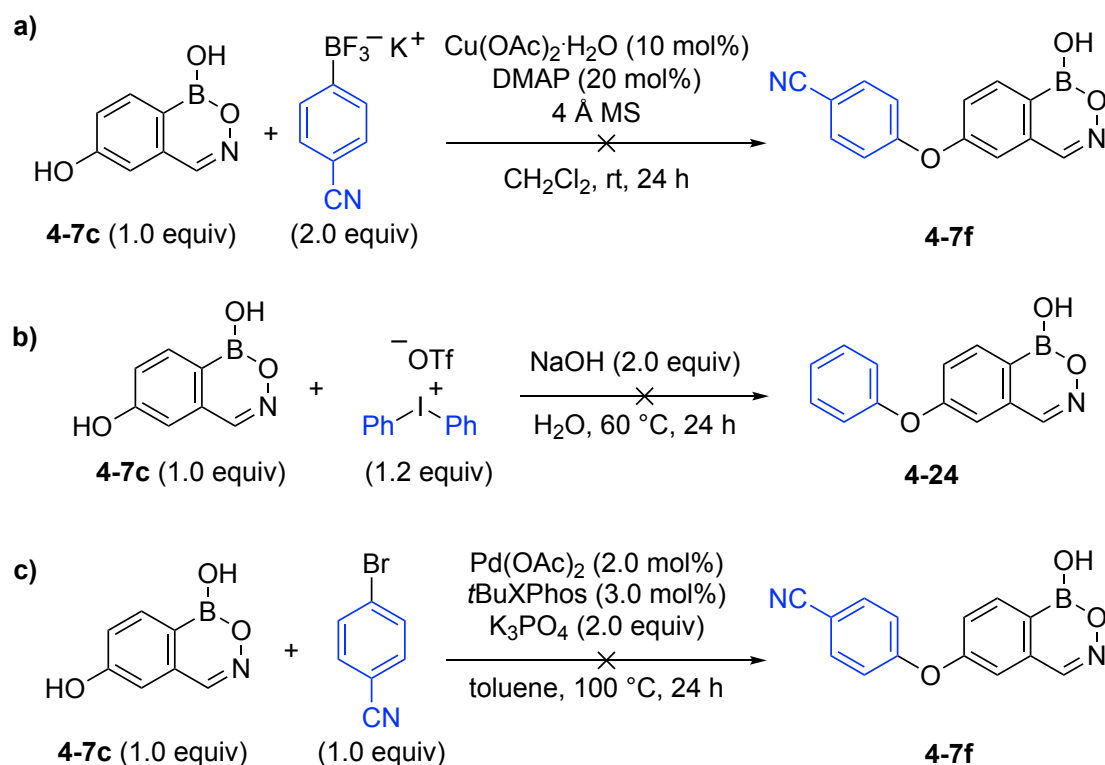
Scheme 4.21. Attempted formation of ether products from benzoxazaborine analog, **4-7c**.

Since the pK_a of NH-benzodiazaborine (**4-2a**) is greater than 14, it was envisioned that a phenolic analog of NH-benzodiazaborine (**4-8b**) (see Section 4.4) could undergo a chemoselective Chan-Lam reaction with arylboronic acids. Hence,

employing the reaction conditions shown in Scheme 4.20, ether derivatives of **4-8b** were synthesized (Scheme 4.22). Arylboronic acid coupling partners were chosen to mimic crisaborole (cf. Figure 4.1).

Arylboronic acids containing electron-withdrawing groups, as well as electron-donating groups, were tolerated for the coupling reaction (**4-25b**–**4-25e**). The purification was achieved in four stages: 1) Filtration through Celite® to remove most of the metallic impurities and molecular sieves; 2) Concentration of the filtrate under reduced pressure and subjection of the residue to column chromatography (3% MeOH/CH$_2$Cl$_2$ with 0.5% AcOH), resulting in the desired product, along with arylboronic acid and minor impurities; 3) Washing of the crude materials from the previous step with a basic sorbitol solution to remove the arylboronic acid; 4) Recrystallization with MeOH/water to afford the anticipated ether analogs. The reaction generally exhibited quantitative conversion by LC-MS analysis, but the yields were impacted due to the multistep purification procedure. No competitive reaction at the endocyclic B—C bond or at the NH functional group of **4-8b** was observed. Using this approach, a crisaborole analog of NH-benzodiazaborine (**4-25e**) was also synthesized (cf. Figure 4.1).
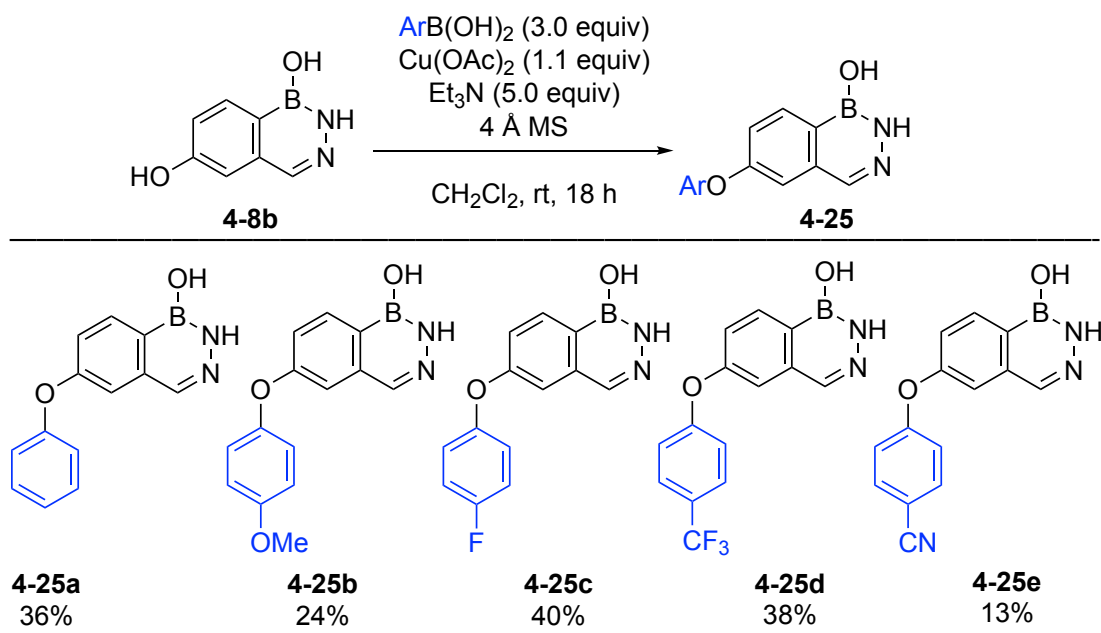
Scheme 4.22. Chemoselective Chan–Lam reaction of **4-8b** with a panel of arylboronic acids.

Ether cleavage of a benzoxazaborine analog (**4-7j**, see Section 4.4) was found to be feasible with a strong Lewis acid, BBr$_3$ (Scheme 4.23). Performing the Chan-Lam reaction between **4-26** and 4-cyanophenylboronic acid resulted in the formation of the desired ether product **4-27**, albeit in a lower yield (vide supra), and a purification by HPLC was required.
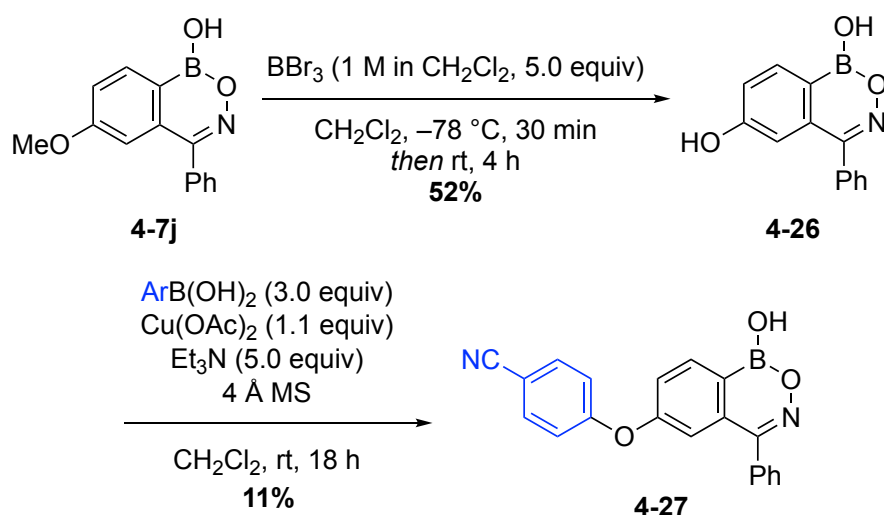
Scheme 4.23. Ether cleavage of **4-7j** with BBr$_3$ followed by a Chan-Lam reaction.

4.5.7 Chemoselective Suzuki-Miyaura Cross-Coupling with Analogs of 4-1 and 4-2a

A chemoselectivity challenge was expected due to the possibility of the undesired Suzuki-Miyaura cross-coupling at the endocyclic B—C bond of benzoxazaborine (and NH-benzodiazaborine), resulting in oligomeric product competing with the desired reaction with the arylboronic acids (Scheme 4.24).
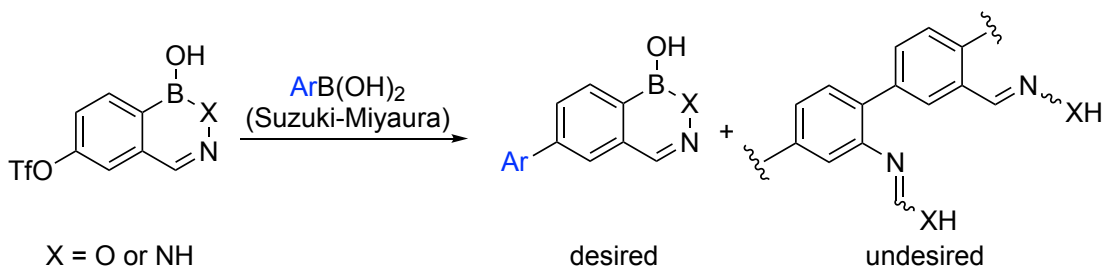
Scheme 4.24. A chemoselectivity challenge expected in the Suzuki-Miyaura cross-coupling.

Therefore, test reactions were performed with benzoxazaborine and NH-benzodiazaborine. An aryltriflate, **4-28**, was synthesized as the electrophilic coupling partner for the Suzuki-Miyaura cross-coupling (Scheme 4.25).

OH → OTf

Tf$_2$O (1.1 equiv), Et$_3$N (2.0 equiv)

CH$_2$Cl$_2$, 0 °C to rt, 16 h

93%

***para*-cresol**

4-28
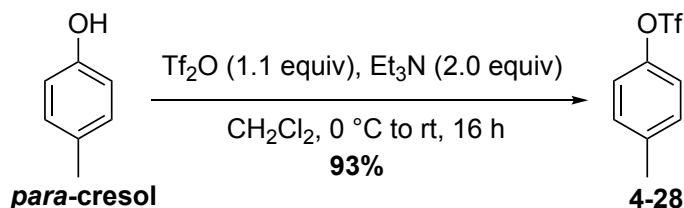
Scheme 4.25. Synthesis of **4-28** for a test Suzuki-Miyaura cross-coupling with benzoxazaborine and NH-benzodiazaborine.

With the triflate derivative **4-28** in hand, the classical Suzuki-Miyaura cross-coupling conditions were employed with both **4-1** and **4-2a** (Figure 4.13a). Interestingly, the LC-MS analysis of the crude reaction did not indicate the formation of the anticipated reaction product **4-29**. However, the reaction with benzoxazaborine (**4-1**) showed a minor oxidative deboronated side-product (transformation of C—B to C—OH) at 2.9 min and an undetermined side product at 3.6 min (Figure 4.13b). This side reactivity could be caused by the relatively low pK_a of benzoxazaborine. In both reactions, the majority of peak area was accounted for by the unreacted boron heterocycle precursor (Figure 4.13b). Notably, a mass corresponding to a tetraarylphosphonium salt **4-30** was observed, which suggests that reductive elimination was faster than transmetalation for these boron heterocycles (Figure 4.13c). There is literature precedence for such a reaction.[47]
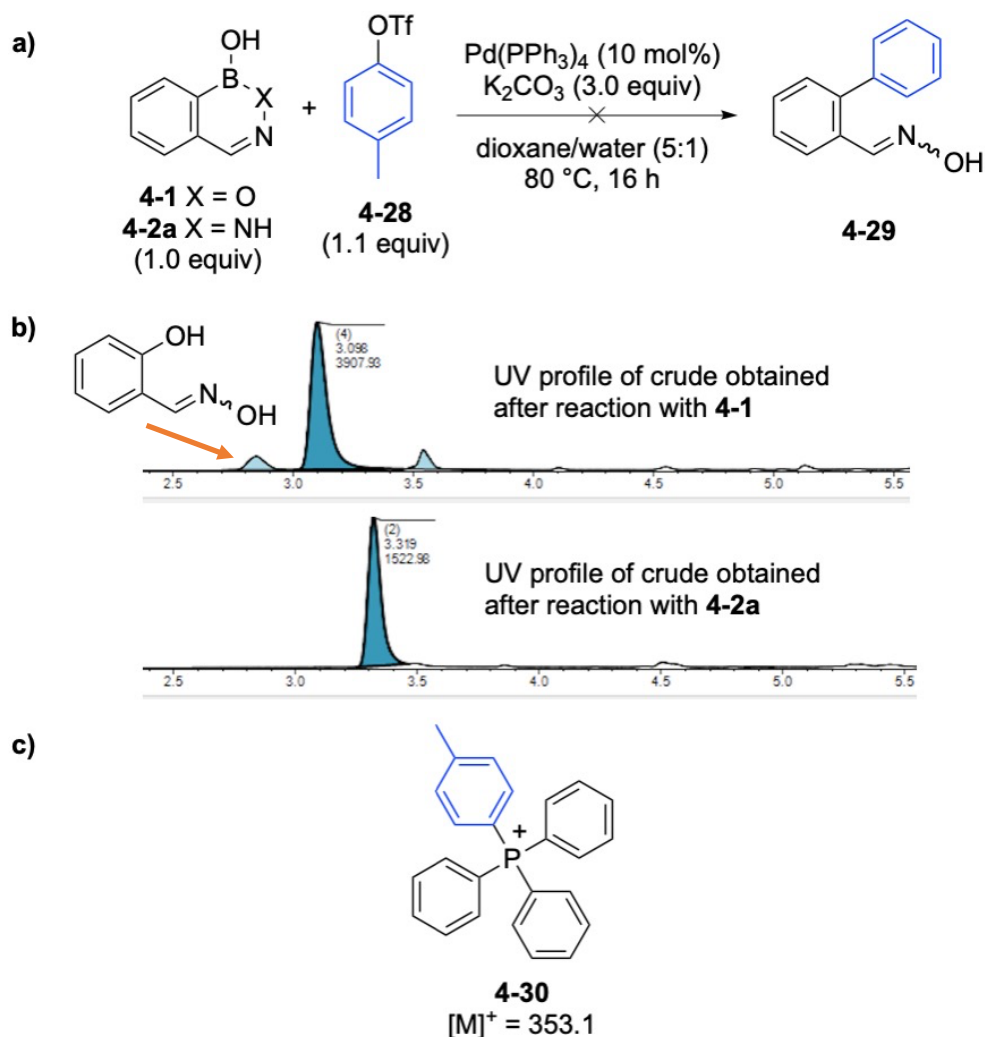
Figure 4.13. a) Suzuki-Miyaura control reactions with **4-1** and **4-2a**. **b)** UV profiles for reactions either with **4-1** or **4-2a**. **c)** Observed side product with both the reactions.

Since in both cases, the unreacted boron heterocycle was observed as the main material, these Suzuki-Miyaura conditions could be used for the synthesis of arylated benzoxazaborine and NH-benzodiazaborine derivatives (vide infra).

4.5.7.1 Chemoselective Suzuki-Miyaura Cross-Coupling with a Triflate Analog of 4-1

The triflate analog of benzoxazaborine (**4-9**, see Section 4.4) was employed for chemoselective Suzuki-Miyaura cross-coupling with arylboronic acids (Scheme 4.26). Arylboronic acids were chosen that contained functional groups, such as ether, fluoro, and chloro, that are most frequently found in bioactive molecules.[48] In addition, heterocyclic boronic acids were also used. The Suzuki-Miyaura cross-coupling of **4-9**

with arylboronic acids tolerated electron-withdrawing groups as well as electron-donating groups (**4-31b**–**4-31j**). Synthesis of halogenated derivatives (**4-31e**–**4-31h**) was successfully accomplished. Using the same approach, thiophene and furan containing products were also synthesized (**4-31i** and **4-31j**, respectively). Due to the low pK_a of the benzoxazaborine analogs, the Suzuki-Miyaura cross-coupling led to a complex mixture of products (vide supra). Also, there was difficulty in separating the desired product from the arylboronic acid coupling partner. Therefore, a phase-switch workup, followed by HPLC purification was required for this library of compounds. Ultimately, lower chemoselectivity and sequential purification steps resulted in somewhat low yields for these products. Moreover, the purification of the product obtained from reaction between **4-9** and quinoline-3-boronic (similar to **4-32j**, vide infra) was further aggravated due to the basic nitrogen atom, which resulted in the amphoteric product being trapped in the aqueous layer during the phase-switch workup.
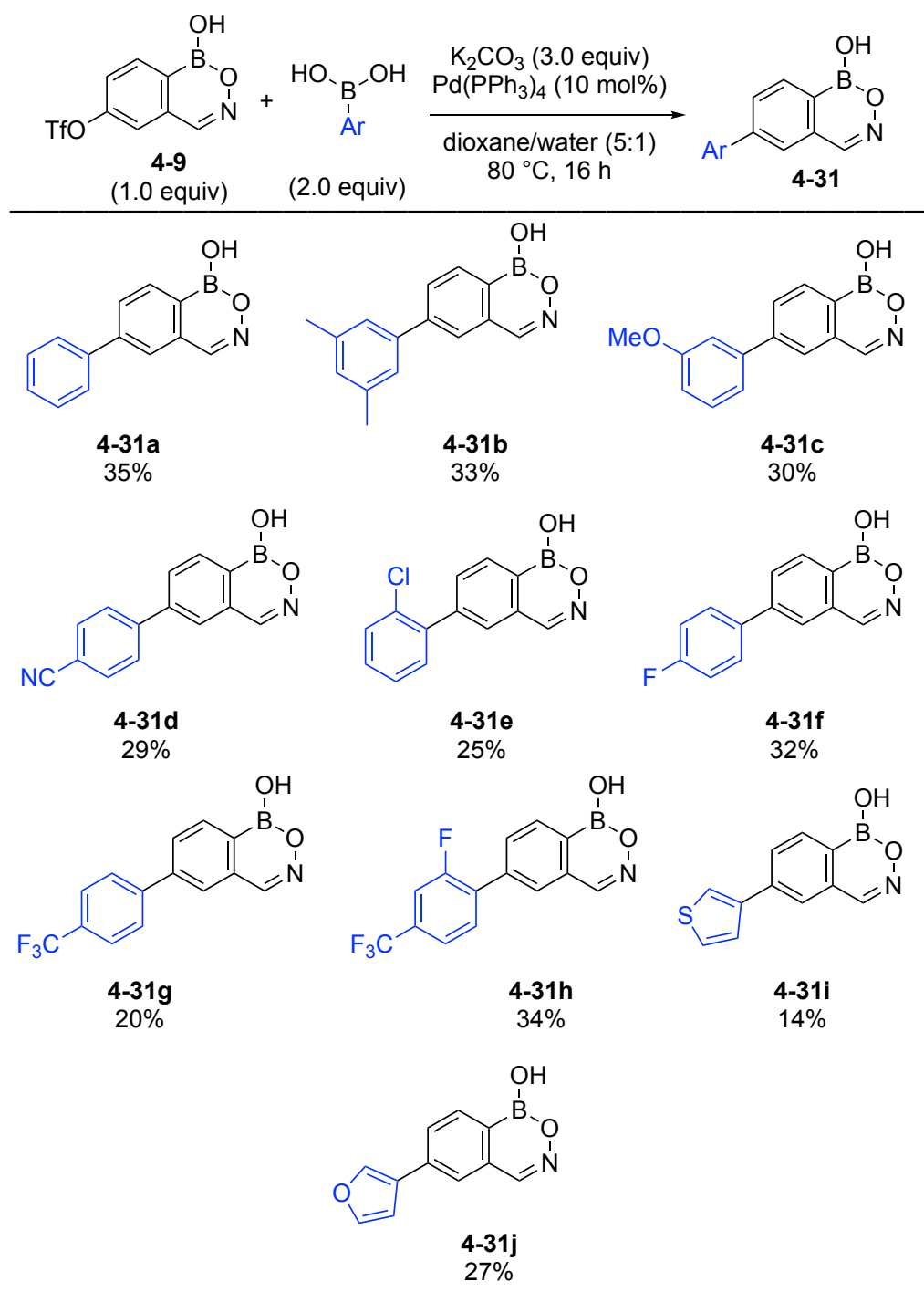
Scheme 4.26. Suzuki-Miyaura cross-coupling products derived from a triflate analog of benzoxazaborine, **4-9**.

4.5.7.2 Chemoselective Suzuki-Miyaura Cross-Coupling with a Triflate Analog of 4-2a

A triflate analog of NH-benzodiazaborine (**4-10**, see Section 4.4) was employed for a series of chemoselective Suzuki-Miyaura cross-couplings (Scheme 4.27). The choice

of arylboronic acid coupling partners was based on the same criteria that was used for the synthesis of benzoxazaborine analogs (vide supra).
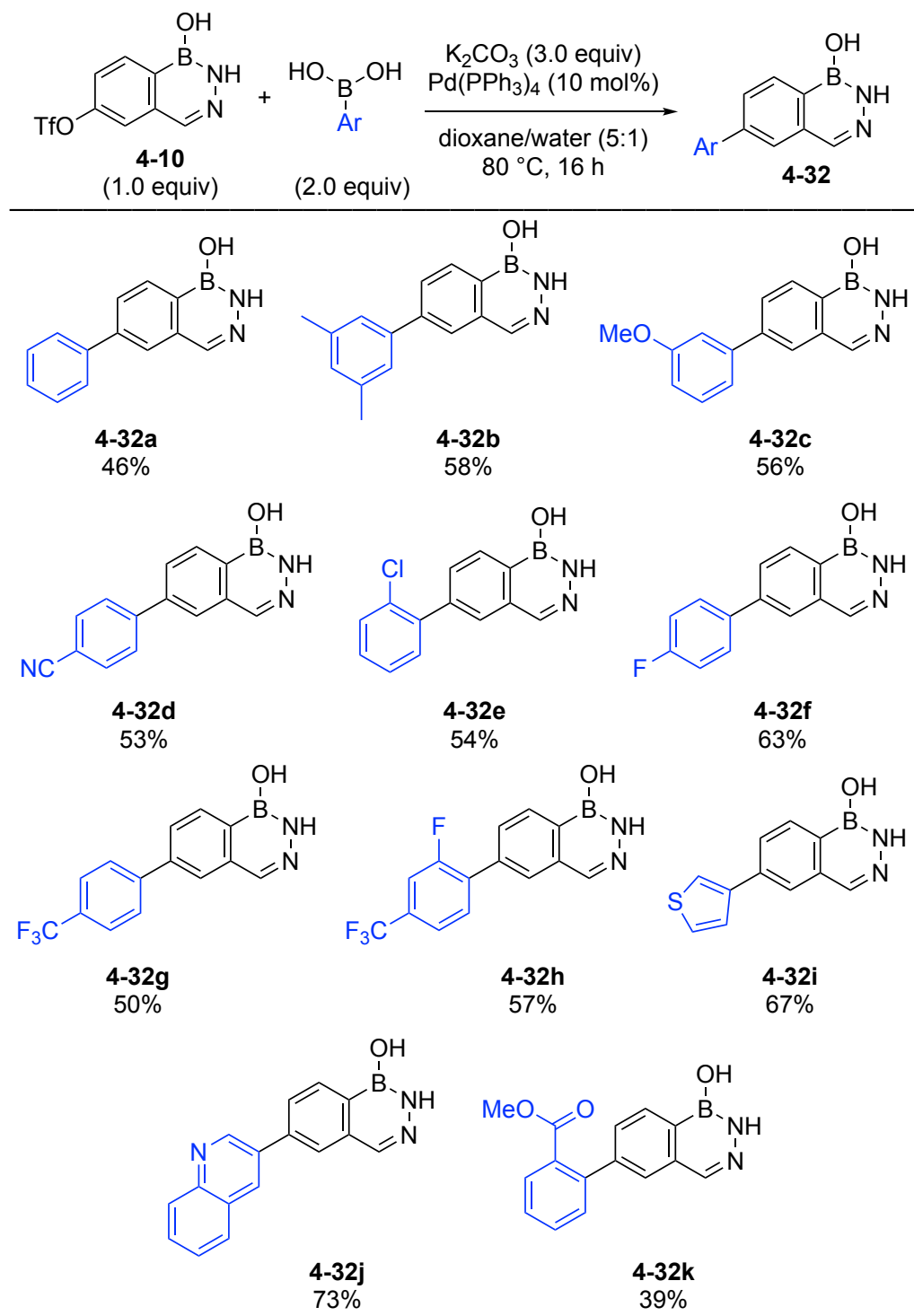
Scheme 4.27. Suzuki-Miyaura cross-coupling products derived from a triflate analog of NH-benzodiazaborine, **4-10**.

Similar to the Suzuki-Miyaura cross-coupling substrate scope for the benzoxazaborine scaffold, an array of NH-benzodiazaborine derivatives (**4-32a**–**4-32k**) was synthesized by coupling arylboronic acids with **4-10**. Generally, all the reactions displayed full conversion to the corresponding product by LC-MS analysis. The purification of the final products was achieved by filtration of the crude materials through Celite®, followed by a basic sorbitol wash, which removed the catalyst and the excess of boronic acid coupling partner. Finally, recrystallization from CH_2Cl_2/hexanes resulted in a pure crystalline product. The yields are impacted during the purification steps.

All substituents at the *ortho* position (**4-32e**, **4-32h**, and **4-32k**), *meta* position (**4-32b** and **4-32c**), and *para* position (**4-32d**, **4-32f**–**4-32h**) were tolerated well. Boronic acid coupling partners containing a heterocycle, such as thiophene-3-boronic acid and quinoline-3-boronic acid (**4-32i** and **4-32j**, respectively), also resulted in a good yield of the coupled product. During the synthesis of **4-32k**, some hydrolysis of the product was observed (ester conversion into the carboxylic acid), which likely accounts for its lower yield.
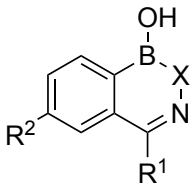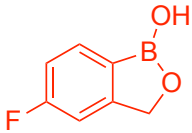
4.6 Biological Evaluation of Model Libraries

A selection of molecules from the libraries described above (cf. Scheme 4.4 and Scheme 4.5) were tested for antibacterial and antifungal activity (performed by labmate Olivia Schneider). Tavaborole (antifungal), vancomycin (antibacterial, Gram positive), colistin (antibacterial, Gram negative), and fluconazole (antifungal) were used as positive controls. For antifungal assay, *C. albicans* was used, while for the antibacterial assays, methicillin-resistant *S. aureus* (MRSA) (ATC 4330) and *E. coli* (ATCC 25922) were used. Microbes were selected to cover a broad spectrum of potential activity, and for their relevance. *C. albicans* was chosen for screening because it is known to be susceptible to tavaborole. MRSA and *E. coli* were selected, respectively as Gram positive and Gram negative representatives of the globally prevalent ESKAPE pathogens.[49]

The initial one-point screening was performed at 100 μM against the above-mentioned microbes. The assessment of the compounds' activity was based on

the percentage inhibition, where "*active*" corresponds to greater than 80% inhibition, "*partially active*" corresponds to 50–80% inhibition, and "*inactive*" corresponds to less than 50% inhibition. Compounds with modified Z-score values above 2.5 were also classified as active. None of the screened compounds displayed any activity against *E. coli*, and consequently those results will not be included here. Results for *C. albicans* and *S. aureus* are displayed in Table 4.2 below.

Table 4.2. Preliminary Antimicrobial Testing of Selected Compounds Using Tavaborole, Vancomycin, and Fluconazole as Positive Controls. (Assays Performed by Olivia Schneider)

Entry	Compound	Structure	Activity (100 μM) C. albicans	S. aureus
1	**4-1**	X = O; R^1, R^2 = H	Active	Inactive
2	**4-2a**	X = NH; R^1, R^2 = H	Partial	Inactive
3	**4-7d**	X = O; R^1 = H; R^2 = F	Active	Inactive
4	**4-8d**	X = NH; R^1 = H; R^2 = F	Partial	Inactive
5	**4-7b**	X = O; R^1 = Me; R^2 = H	Active	Inactive
6	**4-7a**	X = O; R^1 = Ph; R^2 = H	Active	Partial
7	**4-8a**	X = NH; R^1 = Ph; R^2 = H	Partial	Inactive
8	**4-7g**	X = O; R^1 = C_6H_4-4-OMe; R^2 = H	Active	Active
9	**4-7j**	X = O; R^1 = Ph; R^2 = OMe	Active	Active
10	**4-7h**	X = O; R^1 = C_6H_4-4-OMe; R^2 = $B(OH)_2$	Inactive	Active
11	**4-7i**	X = O; R^1 = Ph; R^2 = $B(OH)_2$	Inactive	Active
12	tavaborole		Active	Partial
13	vancomycin		N/A	Active
14	fluconazole		Active	N/A

The preliminary testing showed that, just like tavaborole (entry 12), all the benzoxazaborine (**4-1**) analogs were active against the fungi *C. albicans* (entries 1, 3, 5, 6, 8, 9, and entry 12), with the exception of **4-7h** and **4-7i** (entry 10 and 11). This result is in accordance with the similarity of benzoxazaborine with the benzoxaborole scaffold, such as lower pK_a and a non-aromatic boron-containing ring (vide supra). Tavaborole exhibits diol binding with AMP (see Section 4.1 and Section 3.1). Moreover, Chapter 3 also described the boranol (B—OH) exchange ability of NH-benzodiazaborine scaffold with alcohols, which is exemplified here by its analogs' partial activity towards *C. albicans* (entry 2, 4, and 7).

Gratifyingly, some of the aryl ketoxime analogs of benzoxazaborine that were tested demonstrated suitable activity against *S. aureus* (entry 8-11). With these preliminary antifungal and antibacterial results in hand, minimum inhibitory concentration (MIC) values were obtained by Olivia Schneider for the compounds that showed activity against *C. albicans* or activity/partial activity against *S. aureus* (Table 4.3).

Benzoxazaborine (**4-1**) and its tavaborole analog (**4-7d**) showed apparent activity against *C. albicans*, however slightly lower in comparison to tavaborole (entries 1 and 2 vs entry 9). On the other hand, an aryl ketoxime analog, **4-7j**, exhibited excellent activity against *S. aureus* (entry 6). Notably, microbial activity appears sensitive to substitution differences between compounds. For example, addition of the methoxy group or introduction of a boronic acid functional group on the phenyl ring attached to the boron heterocycle demonstrate enhanced activity (MIC of **4-7a** = 128 μM vs MIC of **4-7j** = 8 μM or MIC of **4-7i** = 32 μM, entry 4, 6, and 8). Ultimately, a full screening of all the compound libraries will provide a more complete understanding of the structure-activity relationship (SAR).

Though the benzoxazaborine analogs displayed appreciable activity against *C. albicans* and *S. aureus*, high throughput screening of the rest of the heterocycles is required for elucidating the most effective derivative. These antimicrobial results are promising and could lead to the introduction of a novel chemotype in drug discovery.

Table 4.3. MIC Values of Selected Compounds Using Tavaborole, Vancomycin, and Fluconazole as Positive Controls. (Assays Performed by Olivia Schneider)

Entry	Compound	Structure	MIC (μM) C. albicans	MIC (μM) S. aureus
1	**4-1**	X = O; R^1, R^2 = H	16	>128
2	**4-7d**	X = O; R^1 = H; R^2 = F	8	>128
3	**4-7b**	X = O; R^1 = Me; R^2 = H	128	>128
4	**4-7a**	X = O; R^1 = Ph; R^2 = H	32	128
5	**4-7g**	X = O; R^1 = C_6H_4-4-OMe; R^2 = H	128	64
6	**4-7j**	X = O; R^1 = Ph; R^2 = OMe	128	8
7	**4-7h**	X = O; R^1 = C_6H_4-4-OMe; R^2 = B(OH)$_2$	>128	>128
8	**4-7i**	X = O; R^1 = Ph; R^2 = B(OH)$_2$	>128	32
9	tavaborole		1	128
10	vancomycin		N/A	4
11	fluconazole		4	N/A

4.7 Bioisosterism of Established Drugs

In drug development, isosteric replacement is often employed to fine-tune the activity and/or properties of drug molecules, and in some cases leads to the development of new drug classes.[50] One example of an isosteric pair is 1,2-azaborine and benzene. The B—N bond is isosteric to the C=C bond, due to the lone pair donation from the nitrogen atom to an empty *p* orbital of the boron atom. Monocyclic 1,2-azaborines are an established pharmacophore (bioisosteres) that often display better bioactivity, bioavailability, and aqueous solubility as compared to their carbon-based analogs.[51] Therefore, while designing bioisosteres, structural changes are made in the molecule

of interest, such as replacing functional groups, which are capable of retaining similar interactions with the target, resulting in improved biological properties (refer to Chapter 1). Hence, the aim of this approach was to determine if the boranol unit (B—OH) could act as an effective drug isostere for the replacement of a C=O bond of a drug with a B—OH unit, with potentially better physicochemical properties. The B—O bond is a good mimic of the C=O bond, because B—O also exhibits double bond character, resulting from lone pair donation by the oxygen into the vacant boron p orbital (bond order ~1.5, see Section 3.4). Thus, to illustrate the viability of hemiboronic naphthoids as drug scaffolds, isosteres of commercially available drugs were designed and synthesized. To test this approach, olaparib (Lynparza®) was used as an example.

Olaparib is a highly potent PARP (poly ADP-ribose polymerase) inhibitor (IC$_{50}$ < 0.1 μM, vide infra) and is prescribed for the treatment of ovarian cancer. PARP1 and PARP2 are members of the PARP family that play an important role in DNA repair, a process by which certain tumors rely on for their survival.[52] Even though both PARP1 and PARP2 have similar catalytic domain, it has been suggested, on the basis of structural studies, that each may have different protein targets.[53] The receptor-ligand interactions map shows some key interactions with the diaza-carbonyl ring of the olaparib structure (Figure 4.14a).[54]

In designing a bioisostere of olaparib, the NH-benzodiazaborine analog would seem to be the most promising (Figure 4.14b). The C=O bond is well mimicked by the B—O bond due to its significant double bond character (vide supra). Hypothetically, replacement of the olaparib C=O bond with a B—OH bond (as in a NH-benzodiazaborine) could still allow for H-bonding with Ser470 or Gly429, with potentially additional covalent or dative interactions with boron (B—OH to B—OSer). This interaction can be envisioned based on the precedent that the boranol (B—OH) in benzodiazaborines can exchange with alcohols (see Section 3.5.2). Since the boron-containing ring in benzodiazaborines is partially aromatic,[20] π-π interactions with His428 and Tyr473 may be maintained. The NH functional group of olaparib acts as a H-bond donor by interacting with Gly429, and this is expected to be maintained

by the analog of NH-benzodiazaborine. On the other hand, although the benzoxazaborine analog could maintain H-bonding with Ser470 or Gly429, it would lose the π-π interactions, due to the non-aromatic character in the boron-containing ring.[20]
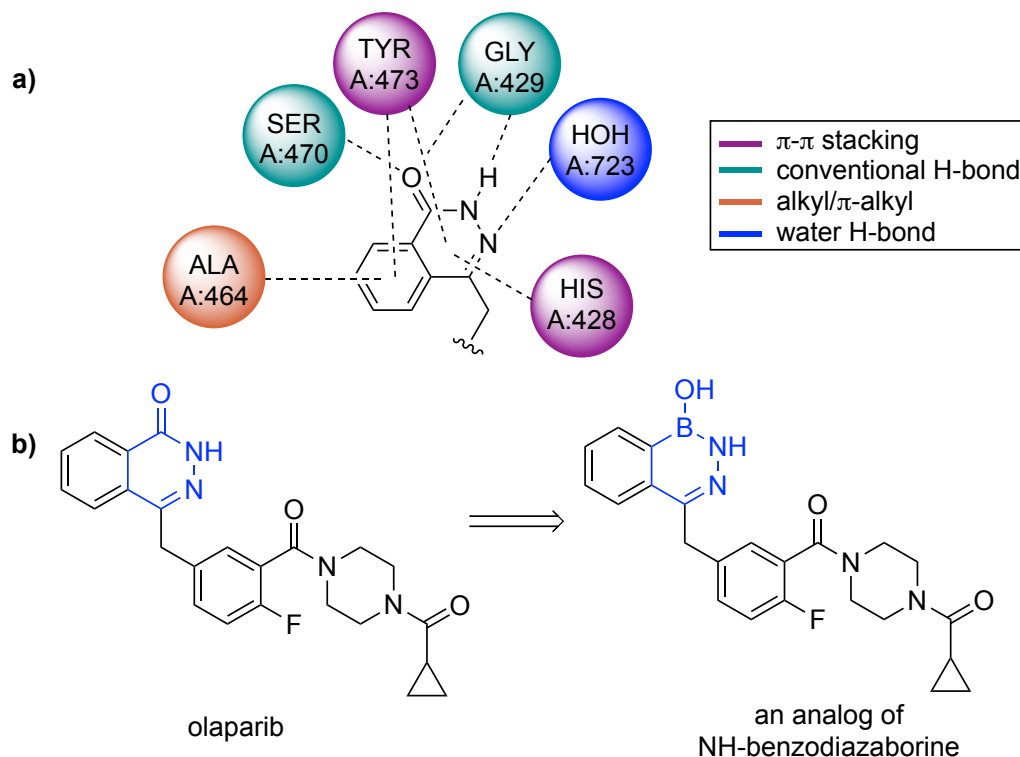
Figure 4.14. a) Partial receptor-ligand interactions map for olaparib.[54] **b)** Isosteric resemblance of olaparib and an analog of NH-benzodiazaborine.

With these hypotheses in mind, the synthesis of olaparib isosteres commenced (Scheme 4.28). The commercially available 2-fluoro-5-iodobenzoic acid was converted into an ester, **4-33**, followed by an α-arylation reaction to obtain **4-34**.[55] An amidation reaction of **4-34** with a Boc protected piperazine occurred quantitatively using HATU as the coupling agent to produce **4-35**, which after deprotection, resulted in the hydrolyzed product **4-36** in 84% yield. The secondary amine of **4-36** underwent an amide formation reaction with cyclopropane carbonyl chloride, followed by a Molander borylation. Finally, a condensation reaction with NH_2NH_2 resulted in the formation of the desired olaparib analog **4-37** (a NH-benzodiazaborine derivative). An olaparib analog of benzoxazaborine (**4-38**) also was synthesized by changing NH_2NH_2

to NH_2OH in the last step of the reaction sequence. The Molander borylation reaction also resulted in the undesired reduction of the *ortho*-carbonyl group (observed by LC-MS),[56] which caused a lower yield of the final olaparib analogs, **4-37** and **4-38**. The final products required HPLC purification and were characterized by ^{1}H NMR, ^{11}B NMR, and ^{13}C NMR spectrometry, and HRMS analyses.
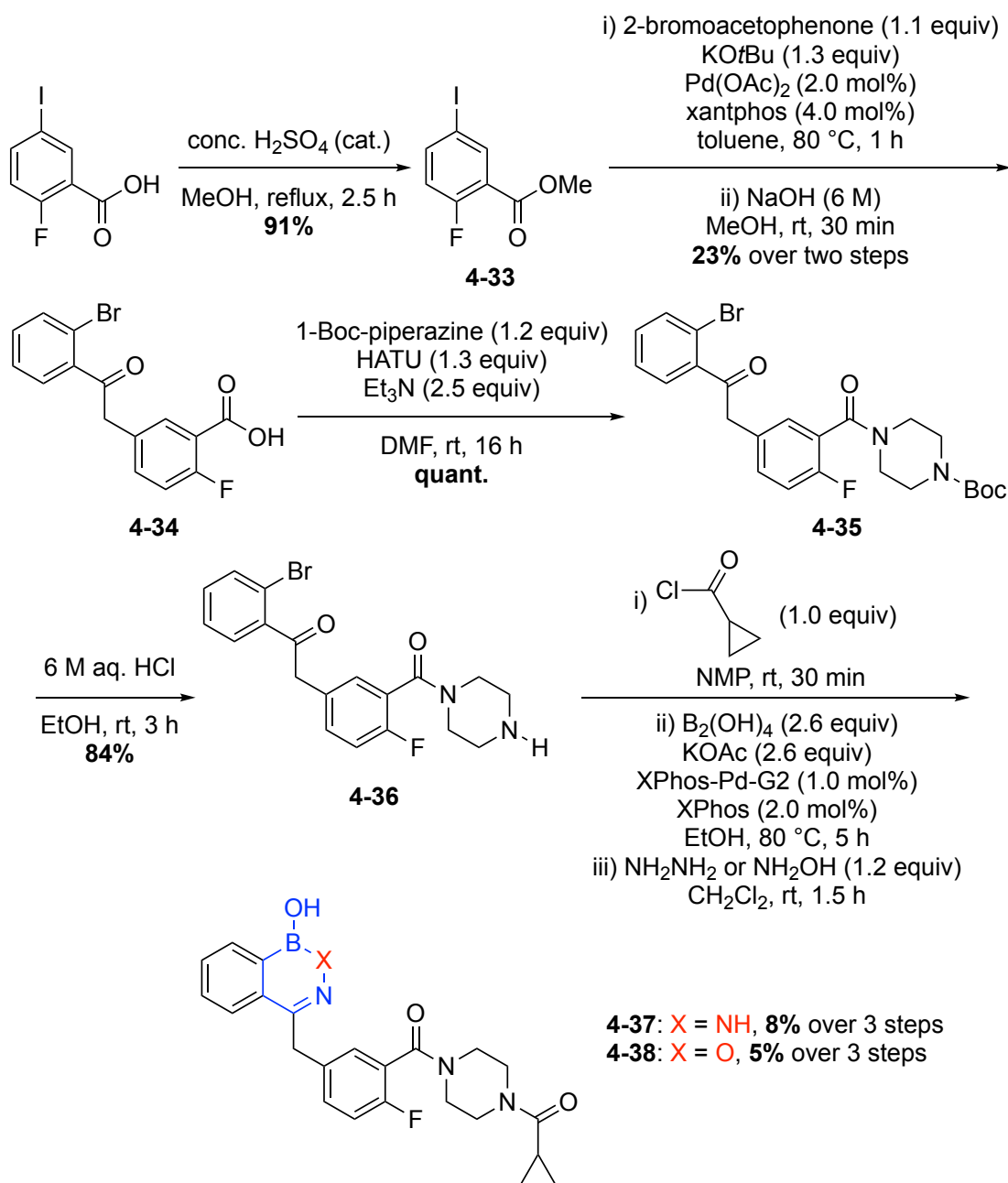
Scheme 4.28. Reaction sequence for the synthesis of olaparib isosteres, **4-37** and **4-38**.

The resulting analogs were tested for PARPs inhibition (performed by BPS Bioscience), wherein olaparib was used as a positive control. The results are summarized in Table 4.4.

Table 4.4. Inhibitory Effect of Olaparib and Olaparib Analogs on PARP Activities

Compound	IC_{50}	
	PARP1	PARP2
4-37	~0.54 μM	0.12 μM
4-38	>1000 nM no inhibition at 1000 nM	>1000 nM 18% inhibition at 1000 nM
olaparib	0.51 nM	0.13 nM

As expected from the molecular interactions map (cf. Figure 4.14a), the olaparib isostere of NH-benzodiazaborine **4-37** showed superior activity compared to the benzoxazaborine analog (**4-38**). Contrary to NH-benzodiazaborine, the boron-containing ring in benzoxazaborine is not aromatic (vide supra), therefore, the analog of benzoxazaborine (**4-38**) likely loses the π-π interactions with His428 and Tyr473. Furthermore, due to the absence of the NH functional group, **4-38** loses one of the H-bonds with Gly429. Compared to the olaparib molecule, both analogs, **4-37** and **4-38**, displayed inferior activity. The lower IC_{50} for both analogs probably results from loss of one of the H-bonds (which means the loss of two H-bonds for **4-38**, vide supra) from either Ser470 or Gly429. Presumably, this loss is not compensated by the formation of new interactions described above.

Even though the PARP inhibition activity of the boron analogs was lower than the olaparib drug molecule, these analogs served as a proof of concept, i.e., changing C=O to B—OH could result in a novel class of potential bioisosteric drugs. There is more exploration needed in the design of the bioisosteres, where, with the right targets, instead of loss of activity, a gain of activity could be realized, probably by covalent or coordinative interactions with the boron center or where B—<u>OH</u> acts as a H-bond donor. This example of bioisosterism reveals a new area of chemical space and a new

approach to modulate the activity and physical properties using boron-containing heterocycles.

4.8 Conclusion

In the present study, benzoxazaborine (**4-1**) and NH-benzodiazaborine (**4-2a**) scaffolds were chosen for elaboration as new drug discovery motifs, based on the comparable acidity of benzoxazaborine with benzoxaborole, and the isosteric and isoelectronic relationship of NH-benzodiazaborine with 4-hydroxyisoquinoline and 1-naphthol. The ARS-based dye-displacement assays of benzoxazaborine and NH-benzodiazaborine were consistent with their Lewis acidic character. Whereas the ARS bound to benzoxazaborine undergoes exchange with sugars, NH-benzodiazaborine does not even bind with the reporter dye, ARS. Several analogs of benzoxazaborine and NH-benzodiazaborine were synthesized using both the early- and late-stage approach. The late-stage approach resulted in a library of compounds synthesized by various reactions found to be orthogonal, such as amidation, Chan-Lam reaction, and Suzuki-Miyaura cross-coupling. Moreover, the oxime bond of benzoxazaborine can be hydrogenated with Ir-catalyzed hydrogenation reaction, resulting in another scaffold.

In the process, several drug isosteres were synthesized, such as tavaborole analogs (**4-7d** and **4-8d**), crisaborole analogs (**4-7f** and **4-25e**), and acoziborole analogs (**4-22l** and **4-23i**) (Figure 4.15).

4-7d X = O
4-8d X = NH
tavaborole analogs

4-7f X = O
4-25e X = NH
crisaborole analogs

4-22l X = O
423i X = NH
acoziborole analogs
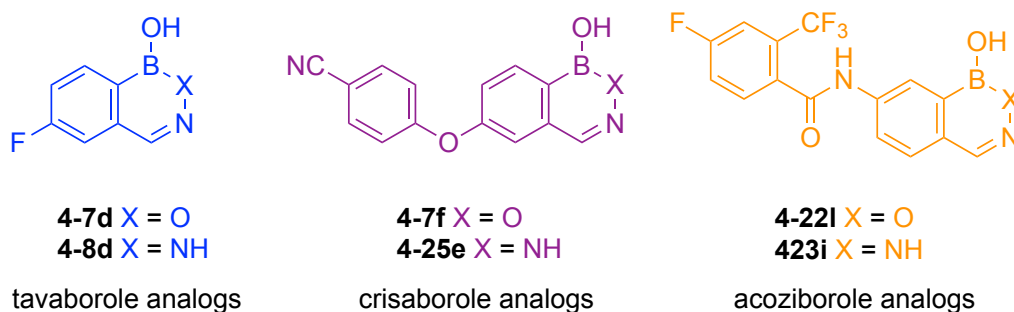
Figure 4.15. Drug isosteres derived from benzoxazaborine and NH-benzodiazaborine.

A selection of compounds was tested for antifungal and antibacterial activity and the results showed that benzoxazaborine is a potent isostere of the benzoxaborole

scaffold, displaying substantial antifungal activity (MIC = 8 μM). Other benzoxazaborine analogs exhibited considerable activity, leading to the discovery of an effective antibacterial compound **4-7j** (MIC = 8 μM), which provides a valuable lead for future SAR series (Figure 4.16). Further future testing of the entire library of compounds is required to find the most potent derivative.
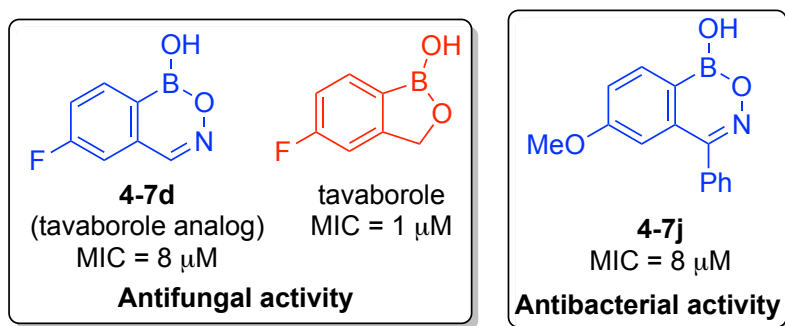
Figure 4.16. Antifungal and antibacterial activity exhibited by analogs of benzoxazaborine.

Bioisosterism of an anticancer drug, olaparib, was demonstrated by an isosteric and isoelectronic NH-benzodiazaborine analog. To this end, **4-37** was synthesized, which acted as a PARP2 inhibitor but displayed lower activity than olaparib (IC_{50} = 0.12 μM for **4-37** vs IC_{50} = 0.13 nM for olaparib). Nonetheless, these inhibition results partially validate the hypothesis that B—OH can serve as a functional isostere of a carbonyl and demonstrate the potential of this approach in the field of drug discovery. Moving forward, further investigation into the application of B—OH as an isostere of C=O is required to fully realize the potential of these structures.

This chapter demonstrated the importance of the Lewis acidity and aromatic character of the studied boron heterocycles, and subsequently highlighted their ability to mimic other boron- or carbon-based drugs. It is envisioned that a bioisostere will be utilized in the future, where a gain of activity is realized by invoking H-bond donation from a B—OH, and/or by productive additional interactions with the boron center. Moreover, further screening of the synthesized analogs is required to identify improved anti-infective agents, and this could also reveal an understanding of structure-activity relationships.

4.9 Experimental

4.9.1 General Information

All reactions were performed in regular glassware with no exclusion of air or moisture unless otherwise noted. Alizarin Red S (ARS) (97%) was purchased from Sigma Aldrich and used as received. $Cu(OAc)_2$ (95%), $MeB(OH)_2$ (98%), 2-formylphenylboronic acid (97%), and B_2pin_2 (98%) were purchased from Combi-Blocks. Hydroxylamine (50 wt. % solution in water) was purchased from Sigma Aldrich and used as received. $NH_2NH_2 \cdot H_2O$ (99%) was purchased from Alfa Aesar and used as received. $Pd(PPh_3)_4$ (99%), $[Cp^*IrCl_2]_2$ (98%), and $PdCl_2(dppf) \cdot CH_2Cl_2$ (99%) were purchased from Strem Chemicals. Acetonitrile (HPLC grade) was purchased from Sigma Aldrich and used as received. Dioxane was distilled with sodium and benzophenone before use for Miyaura borylation reactions. Dichloromethane (ACS reagent grade) and methanol (ACS reagent grade) were purchased from Sigma Aldrich and used as received. All other solvents were purchased as ACS reagent grade and used as received, and other chemicals were purchased from commercial suppliers and used as received. Thin layer chromatography was performed on Silicycle silica gel 60 F254 plates, which were visualized under UV light and with $KMnO_4$, phosphomolybdic acid (PMA) or curcumin stains. Column chromatographic separations were performed on silica gel 60 using hexanes, ethyl acetate, methanol, dichloromethane as eluents. In some cases, acetic acid was also added to the solvent system.

NMR spectra were recorded at ambient temperature using Varian DD2 MR two-channel 400 MHz, Varian INOVA two-channel 400MHz, Varian INOVA four-channel 500 MHz, Varian VNMRS two-channel 500 MHz, Varian VNMRS four-channel 600 MHz and Agilent VNMRS four-channel, dual receiver 700 MHz spectrometers operating at the indicated frequency for ^1H NMR. All NMR chemical shifts are reported in ppm (δ) units with residual solvent peaks (d_6-acetone, $CDCl_3$ or D_2O) as the internal reference. In case of the ^{13}C NMR analysis of samples run in D_2O, acetone is used as the internal reference. NMR data is reported using the following abbreviations: s, singlet; br s, broad singlet; d, doublet; t, triplet; q, quartet; h, hextet; dd, doublet of doublets; dt, doublet of triplets; td, triplet of doublets; ddd, doublet of

doublet of doublets; dddd, doublet of doublet of doublet of doublets; app, apparent; m, multiplet. The error of coupling constants from ^{1}H NMR spectra is estimated to be approximately 0.3 Hz. The quaternary carbon bound to boron is often not observed due to the quadrupolar relaxation of boron. A drop of D_2O was commonly added to the NMR solution for compounds containing boranol (B—OH) units to prevent the formation of anhydrides (B—O—B dimers) in the NMR tube, which would otherwise complicate the analysis.

The hydrogenation reactions for **4-1**, **4-7b**, and **4-7d** were performed in the Stryker Lab at the Department of Chemistry, University of Alberta using a sealed 8 mL microwave vial pierced with a 18G needle, placed in a high-pressure reactor (Parr®) with a stainless-steel vessel equipped with a rupture disk rated at 2000 psi. Some compounds required purification by HPLC, which was performed by Dr. Ed Fu. High-resolution mass spectra were recorded by the University of Alberta Mass Spectrometry Services Laboratory using electrospray ionization (ESI) techniques. LC-MS was performed at the University of Alberta Mass Spectrometry Services Laboratory on an Agilent Technologies 6130 LC-MS using a Phenomenex Luna Omega Polar C18 1.6 μm column. A water/acetonitrile solvent system was used along with 0.1% formic acid according to the following gradient: beginning from 99:1 water/acetonitrile, over 5 minutes the ratio was changed to 40:60 water/acetonitrile. Over the next 0.5 minutes, the ratio was changed to 5:95 water/acetonitrile, which was maintained for a further two minutes (total elution time of 7.5 minutes). For more details on the assays discussed in Section 4.6, see the thesis of Olivia Schneider.

4.9.2 Properties of Boron Heterocycles

4.9.2.1 pK_a Measurements for Boron Heterocycles (cf. Figure 4.4)

The pK_a values of compounds **4-1**, **4-2a**, **4-2b**, **4-2c**, and **4-3** were determined previously in Chapter 3 (Section 3.9.7). Using the same procedure, the pK_a of **4-7a** was measured by an ^{11}B NMR titration experiment. For details regarding solution preparation and calculations, please see Section 3.9.7.

The pK_a of **4-7a** in 1:1 CH_3CN/H_2O was calculated to be 7.0.
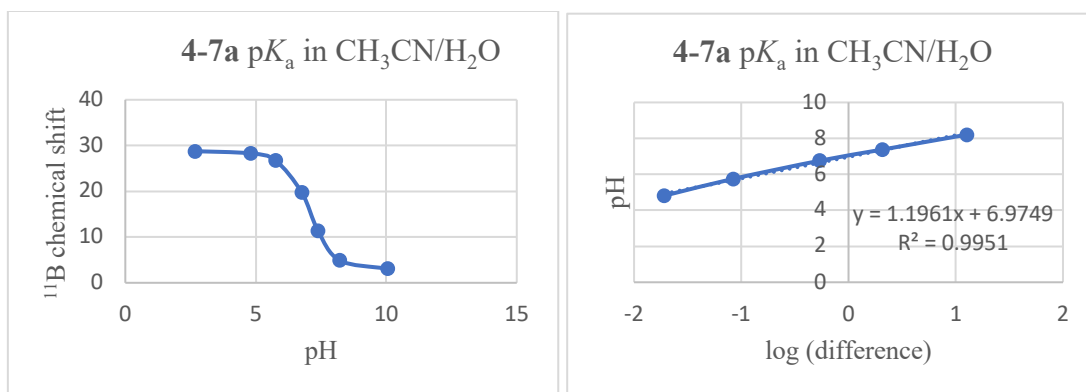
Figure 4.17. pK_a determination of **4-7a** in 1:1 CH$_3$CN/H$_2$O.

The pK_a determination of **4-13** was attempted using a slight modification to the procedure described in Section 3.9.7. Due to the high solubility of **4-13** in water, no organic solvent was required. The graph obtained for ^{11}B chemical shift vs pH for **4-13** is shown below.
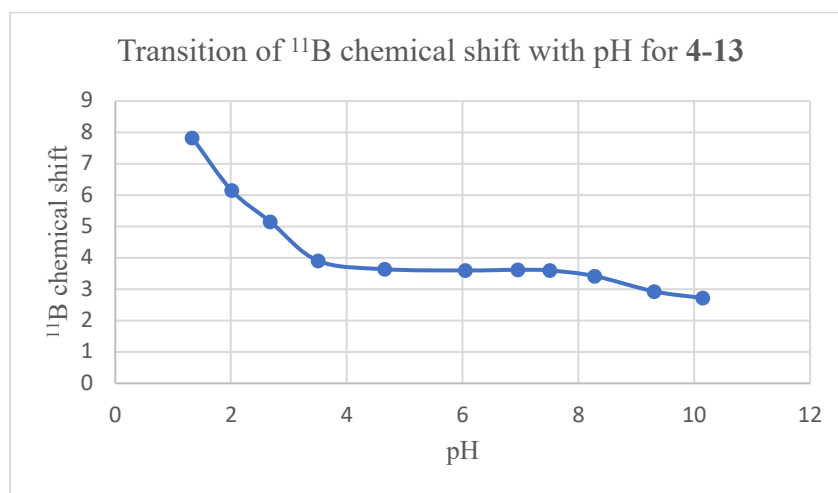
Figure 4.18. Transition of ^{11}B chemical shift with pH variation for **4-13**.

The heterocycle **4-13** exhibits an upfield chemical shift even at pH ~1, suggesting a low pK_a (<4).

4.9.2.2 Qualitative ARS Test (cf. Figure 4.5)[57]

ARS stock solution (10^{-3} M) was made by dissolving 18.0 mg of ARS in 50.0 mL (0.1 M) sodium phosphate monobasic buffer solution. This solution was further diluted 10-

fold by addition of 450 mL (0.1 M) sodium phosphate monobasic buffer solution. pH of the solution was adjusted to 7.4 using aqueous sodium hydroxide (4 M). The resultant 10^{-4} M ARS solution was used as a stock solution (solution A).

The controls (solution B) were prepared by dissolving the boronic acid (0.100 mmol) in 5% DMSO or 40% THF, followed by the addition of solution A in a 5 mL volumetric flask to give 0.02 M solution with respect to the boronic acid. The pH of the solution B of benzoxaborole in 5% DMSO and solution A was measured as 7.4. The pH of the solution B of benzoxazaborine (**4-1**) in 5% DMSO and solution A readjustment to 7.4 was needed using aqueous sodium hydroxide (1 M). The pH of the solution B of benzoxaborole in 40% THF and solution A was measured as 8.2 accounting for an increase of 0.8 pH on addition of THF. Therefore, the pH of the solution B of other boron heterocycles (**4-1**, **4-7a**, **4-2a**, **4-2b**, **4-2c**, and **4-3**) in 40% THF and solution A were adjusted to a pH of 8.2 using aqueous sodium hydroxide (1.00 or 2.00 M).

Finally, sugar (0.500 mmol) was added to 1 mL of solution B in a 2 mL flask and change in color was observed. Solution A showed red color. Solution B either showed a yellow color when the heterocycle underwent complexation with ARS or showed a purple color when there was no complexation with ARS. When sugar was added to the solution B: if there was complexation, a red/pink color was regenerated, therefore, demonstrating the release of ARS and competitive binding by the sugar. If there was no complexation with the sugar analyte, no change in color was observed.
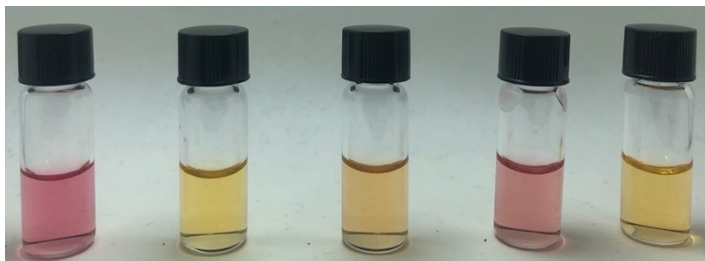
Figure 4.19. ARS dye-displacement assay for benzoxaborole (with 5% DMSO and solution A). From left to right: ARS solution, benzoxaborole in ARS solution, with glucose, with fructose, and with methyl α-D-galactopyranoside.
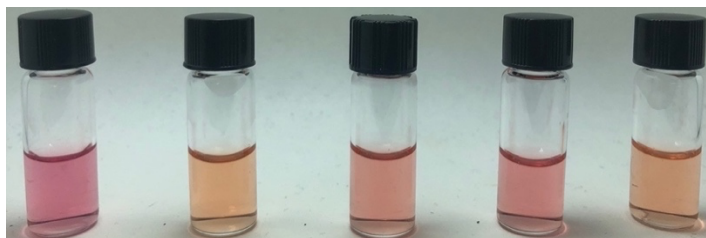
Figure 4.20. ARS dye-displacement assay for **4-1** (with 5% DMSO and solution A). From left to right: ARS solution, **4-1** in ARS solution, with glucose, with fructose, and with methyl α-D-galactopyranoside.
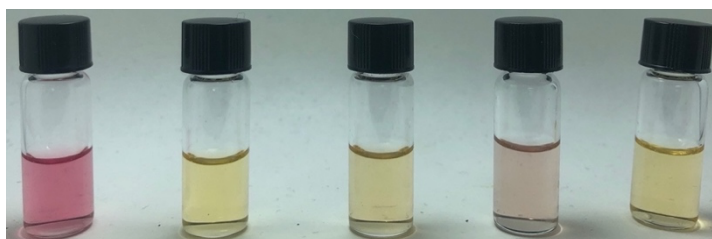
Figure 4.21. ARS dye-displacement assay for benzoxaborole (with 40% THF and solution A). From left to right: ARS solution, benzoxaborole in ARS solution, with glucose, with fructose, and with methyl α-D-galactopyranoside.
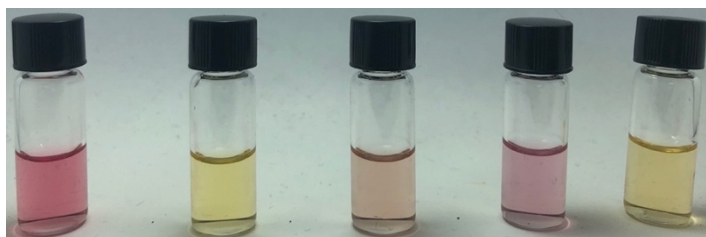
Figure 4.22. ARS dye-displacement assay for **4-1** (with 40% THF and solution A). From left to right: ARS solution, **4-1** in ARS solution, with glucose, with fructose, and with methyl α-D-galactopyranoside.
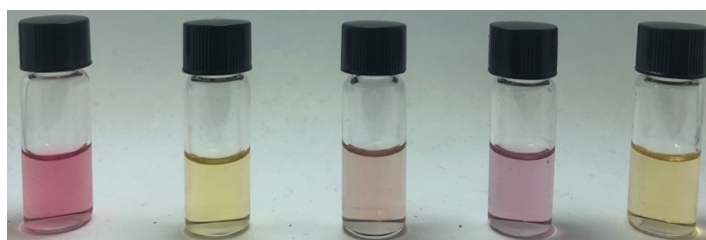
Figure 4.23. ARS dye-displacement assay for **4-7a** (with 40% THF and solution A). From left to right: ARS solution, **4-7a** in ARS solution, with glucose, with fructose, and with methyl α-D-galactopyranoside.
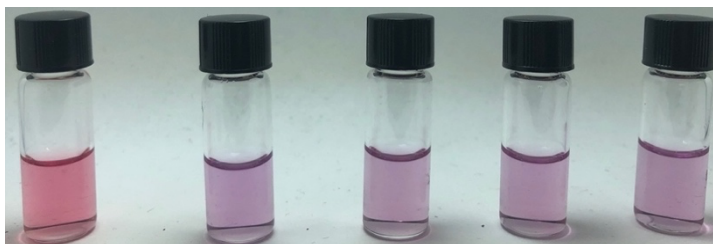
Figure 4.24. ARS dye-displacement assay for **4-2a** (with 40% THF and solution A). From left to right: ARS solution, **4-2a** in ARS solution, with glucose, with fructose, and with methyl α-D-galactopyranoside.
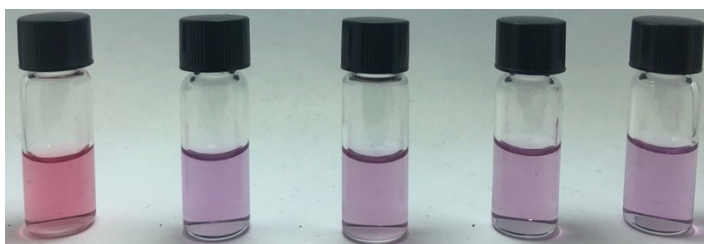
Figure 4.25. ARS dye-displacement assay for **4-2b** (with 40% THF and solution A). From left to right: ARS solution, **4-2b** in ARS solution, with glucose, with fructose, and with methyl α-D-galactopyranoside.
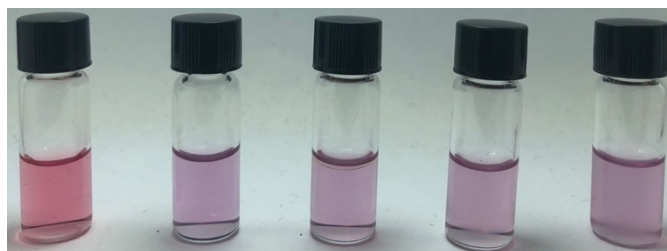
Figure 4.26. ARS dye-displacement assay for **4-2c** (with 40% THF and solution A). From left to right: ARS solution, **4-2c** in ARS solution, with glucose, with fructose, and with methyl α-D-galactopyranoside.
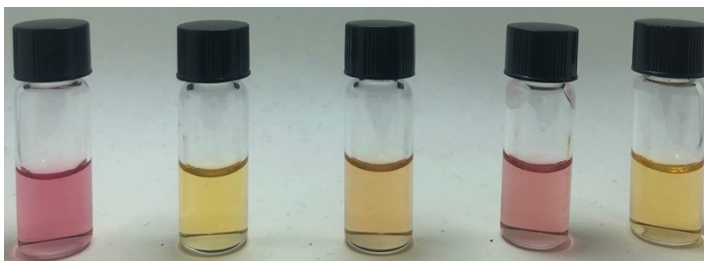
Figure 4.27. ARS dye-displacement assay for **4-3** (with 40% THF and solution A). From left to right: ARS solution, **4-3** in ARS solution, with glucose, with fructose, and with methyl α-D-galactopyranoside.

4.9.3 Preparation of 2-Bromobenzophenones

General Procedure for Friedel-Crafts Acylation using Benzene (GP1)[58]

The corresponding 2-bromobenzoic acid (1.0 equiv) was charged in a 2-neck round bottom flask, followed by the addition of thionyl chloride (0.4 M) by a syringe under nitrogen. The reaction mixture was stirred at 80 °C for 1.5 h, during which a homogeneous solution was formed. The volatiles were distilled and then benzene (0.4 M) was added, followed by the addition of aluminium trichloride (1.2 equiv) to initiate the Friedel-Crafts acylation. The reaction mixture was stirred for 3 h at 80 °C. Upon completion, the reaction contents were poured into 100 mL ice cold 2 M HCl and then extracted with ethyl acetate (3 × 50 mL). The combined organic layers were washed with water (50 mL) and dried over Na_2SO_4, filtered, and evaporated under reduced pressure. The residue obtained was used as such for further reactions. In some cases, the crude product was purified by flash column chromatography or by recrystallization techniques.

General Procedure for Friedel-Crafts Acylation using Anisole (GP2)[59]

The corresponding 2-bromobenzoic acid (1.0 equiv) was charged in a 2-neck round bottom flask, followed by the addition of thionyl chloride (0.4 M) by a syringe under nitrogen. The mixture was stirred at 80 °C for 1.5 h, during which a homogeneous solution was formed. The volatiles were distilled and then the residue was dissolved in CH_2Cl_2 (0.4 M) and the reaction was brought to 0 °C. Anisole (1.5 equiv) was added, followed by the addition of aluminium trichloride (1.2 equiv) to initiate the Friedel-Crafts acylation. The reaction mixture was brought to rt and stirred for 6 h. Upon completion, the reaction contents were poured into 100 mL ice cold 2 M HCl and then extracted with ethyl acetate (3 × 50 mL). The combined organic layers were washed with water (50 mL) and dried over Na_2SO_4, filtered, and evaporated. The residue was purified by flash column chromatography or by recrystallization techniques.
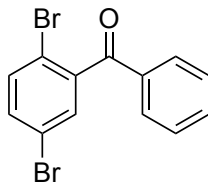
(2,5-Dibromophenyl)(phenyl)methanone (4-4b): Prepared according to **GP1** from 2,5-dibromobenzoic acid (3.00 g, 10.7 mmol), SOCl$_2$ (26.8 mL, 0.400 M), AlCl$_3$ (1.71 g, 12.8 mmol), and benzene (26.8 mL). The title compound was isolated as a brown solid (3.60 g, 99%). Characterization data were in agreement with that found in the literature.[58] **^{1}H NMR** (500 MHz, CDCl$_3$): δ 7.80 – 7.78 (m, 2 H), 7.63 – 7.60 (m, 1 H), 7.51 – 7.45 (m, 5 H).
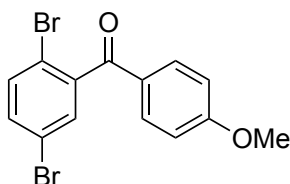
(2,5-Dibromophenyl)(4-methoxyphenyl)methanone (4-4c): Prepared according to **GP2** from 2,5-dibromobenzoic acid (3.00 g, 10.7 mmol), SOCl$_2$ (26.8 mL, 0.400 M), AlCl$_3$ (1.71 g, 12.8 mmol), and anisole (1.20 g, 11.0 mmol). The crude product was purified by flash chromatography using 5-10% EtOAc/hexanes as the solvent system and the title compound was isolated as a white solid (3.40 g, 87%). Characterization data were in agreement with that found in the literature.[59] **^{1}H NMR** (500 MHz, CDCl$_3$): δ 7.76 (d, J = 8.9 Hz, 2 H), 7.50 – 7.46 (m, 1 H), 7.46 – 7.42 (m, 2 H), 6.94 (d, J = 8.9 Hz, 2 H), 3.87 (s, 3 H).
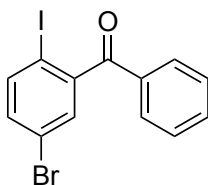
(5-Bromo-2-iodophenyl)(phenyl)methanone (4-4d): Prepared according to **GP1** from 5-bromo-2-iodobenzoic acid (3.00 g, 9.18 mmol), SOCl$_2$ (23.0 mL, 0.400 M), AlCl$_3$ (1.47 g, 13.2 mmol), and benzene (23.0 mL). The title compound was isolated

as a brown solid (3.51 g, 98%). Characterization data were in agreement with that found in the literature.[60] **¹H NMR** (500 MHz, CDCl$_3$): δ 7.76 (dd, J = 8.4, 1.3 Hz, 2 H), 7.73 (d, J = 8.4 Hz, 1 H), 7.61 – 7.57 (m, 1 H), 7.46 (d, J = 7.4 Hz, 1 H), 7.40 (d, J = 7.2 Hz, 1 H), 7.38 (d, J = 2.4 Hz, 1 H), 7.28 (dd, J = 8.4, 2.4 Hz, 1 H).
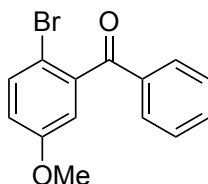
(2-Bromo-5-methoxyphenyl)(phenyl)methanone (4-4e): Prepared according to **GP1** from 2-bromo-5-methoxybenzoic acid (3.00 g, 13.0 mmol), SOCl$_2$ (32.5 mL, 0.400 M), AlCl$_3$ (2.08 g, 15.6 mmol), and benzene (32.5 mL). The crude product was purified by flash column chromatography using 10% EtOAc/hexanes as the solvent system and the title compound was isolated as a yellow liquid (2.30 g, 62%). Characterization data were in agreement with that found in the literature.[55] **¹H NMR** (600 MHz, CDCl$_3$): δ 7.85 (dd, J = 8.4, 1.3 Hz, 2 H), 7.65 – 7.60 (m, 1 H), 7.54 (d, J = 8.8 Hz, 1 H), 7.52 – 7.47 (m, 2 H), 6.93 (dd, J = 8.8, 3.1 Hz, 1 H), 6.90 (d, J = 3.1 Hz, 1 H), 3.83 (s, 3 H).
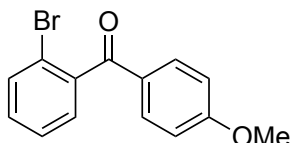
(2-Bromophenyl)(4-methoxyphenyl)methanone (4-4f): Prepared according to **GP2** from 2-bromobenzoic acid (3.00 g, 14.9 mmol), SOCl$_2$ (25.0 mL, 0.400 M), AlCl$_3$ (2.39 g, 17.9 mmol), and anisole (2.42 g, 22.4 mmol). The crude product was purified by crystallization as follows: the crude material was dissolved in a minimum amount of hot ethyl acetate in a round bottom flask and then ~1 mL of hexanes was added. The flask was kept at rt, which resulted in light brown shiny crystals. The crystals were filtered and washed with cold hexanes to afford the title compound as a light brown solid (2.43 g, 75%). Characterization data were in agreement with that found in the literature.[59] **¹H NMR** (600 MHz, CDCl$_3$): δ 7.79 (d, J = 8.9 Hz, 2 H), 7.64 (d, J = 8.1

Hz, 1 H), 7.41 (app t, J = 6.9 Hz, 1 H), 7.38 – 7.30 (m, 2 H), 6.94 (d, J = 8.9 Hz, 2 H), 3.88 (s, 3 H).
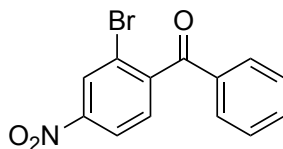
(2-Bromo-4-nitrophenyl)(phenyl)methanone (4-4g): Prepared according to **GP1** from 2-bromo-4-nitrobenzoic acid (500 mg, 2.00 mmol), $SOCl_2$ (5.00 mL, 0.400 M), $AlCl_3$ (320 mg, 2.40 mmol), and benzene (5.00 mL). The crude product was purified by flash column chromatography using 10% EtOAc/hexanes as the solvent system and the title compound was isolated as an off-white solid (518 mg, 85%). Characterization data were in agreement with that found in the literature.[61] **^{1}H NMR** (400 MHz, CDCl$_3$): δ 8.51 (d, J = 2.1 Hz, 1 H), 8.27 (dd, J = 8.4, 2.1 Hz, 1 H), 7.76 (dd, J = 8.4, 1.3 Hz, 2 H), 7.68 – 7.60 (m, 1 H), 7.52 – 7.44 (m, 3 H).
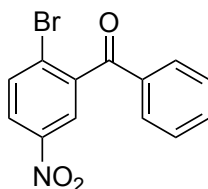
(2-Bromo-5-nitrophenyl)(phenyl)methanone (4-4h): Prepared according to **GP1** from 2-bromo-5-nitrobenzoic acid (10.0 g, 40.6 mmol), $SOCl_2$ (100 mL, 0.400 M), $AlCl_3$ (6.50 g, 48.8 mmol), and benzene (100 mL). The crude product was purified by flash column chromatography using 5% EtOAc/hexanes as the solvent system and the title compound was isolated as a beige colored solid (11.8 g, 95%); **^{1}H NMR** (600 MHz, CDCl$_3$): δ 8.22 (m, 2 H), 7.90 – 7.85 (m, 1 H), 7.81 (d, J = 7.2 Hz, 2 H), 7.67 (app t, J = 8.0 Hz, 1 H), 7.52 (app t, J = 7.9 Hz, 2 H); **^{13}C NMR** (126 MHz, CDCl$_3$): 193.4, 147.0, 142.0, 135.1, 134.6, 134.5, 130.2, 129.1, 127.0, 125.5, 123.8.
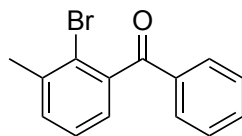
(2-Bromo-3-methylphenyl)(phenyl)methanone (4-4i): Prepared according to **GP1** from 2-bromo-3-methylbenzoic acid (3.96 g, 18.4 mmol), $SOCl_2$ (46.0 mL, 0.400 M), $AlCl_3$ (2.94 g, 22.1 mmol), and benzene (20.0 mL). The crude product was purified by flash column chromatography using 10% EtOAc/hexanes as the solvent system and the title compound was isolated as an off-white solid (4.18 g, 83%). Characterization data were in agreement with that found in the literature.[59] **¹H NMR** (400 MHz, CDCl₃): δ 7.79 (dd, J = 8.5, 1.4 Hz, 2 H), 7.60 – 7.53 (m, 1 H), 7.43 (app t, J = 7.7 Hz, 2 H), 7.33 (dd, J = 7.9, 1.5 Hz, 1 H), 7.28 (app t, J = 7.5 Hz, 1 H), 7.10 (dd, J = 7.3, 1.2 Hz, 1 H), 2.45 (s, 3 H).
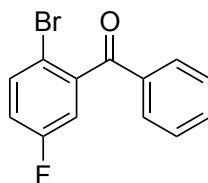
(2-Bromo-5-fluorophenyl)(phenyl)methanone (4-4j): Prepared according to **GP1** from 2-bromo-5-fluorobenzoic acid (1.00 g, 4.57 mmol), $SOCl_2$ (11.0 mL, 0.400 M), $AlCl_3$ (731 mg, 22.1 mmol), and benzene (11.0 mL). The crude product was purified by flash column chromatography using 3% EtOAc/hexanes as the solvent system and the title compound was isolated as a yellow liquid (1.21 g, 95%); **¹H NMR** (400 MHz, CDCl₃): δ 7.79 (dd, J = 8.4, 1.3 Hz, 2 H), 7.64 – 7.58 (m, 1 H), 7.47 (app t, J = 8.1 Hz, 2 H), 7.40 (dd, J = 8.3, 2.4 Hz, 1 H), 7.36 (dd, J = 8.5, 5.9 Hz, 1 H), 7.14 (td, J = 8.3, 2.5 Hz, 1 H); **¹³C NMR** (126 MHz, CDCl₃): δ 195.0, 163.0 (d, J = 254 Hz), 136.8 (d, J = 3.78 Hz), 136.2, 133.9, 130.7 (d, J = 8.82 Hz), 130.2, 128.7, 120.8 (d, J = 23.94 Hz), 114.6 (d, J = 21.42 Hz); **¹⁹F NMR** (376 MHz, CDCl₃): δ –108.12 (q, J = 8.0 Hz).

4.9.4 Attempted Synthesis of 4-7a
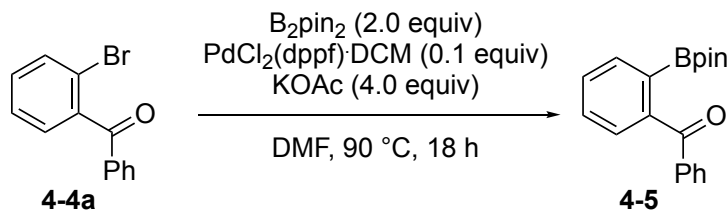
Miyaura Borylation of 2-Bromobenzophenone[63]

A flame dried round bottom flask was charged with 2-bromobenzophenone (500 mg, 1.91 mmol), B_2pin_2 (965 mg, 3.82 mmol), KOAc (746 mg, 7.64 mmol), and $PdCl_2(dppf)\cdot CH_2Cl_2$ (155 mg, 0.190 mmol) under a nitrogen atmosphere. DMF (7.6 mL) was added in the reaction flask and the reaction solution was stirred at 90 °C for 16 h. Upon completion, the reaction contents were transferred to a separatory funnel and diluted with water (20 mL). The crude compound was extracted using Et_2O (10 mL × 3) and the combined organic layer was dried over Na_2SO_4, filtered, and concentrated under reduced pressure. The crude material obtained was subjected to a flash column chromatography using 15% EtOAc/hexanes and the material obtained was used as such for next step.
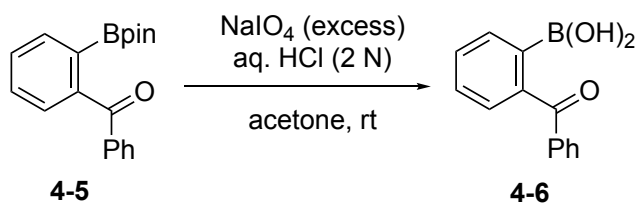
Sodium Periodate Cleavage of Boronic Ester

The crude material obtained after Miyaura borylation was dissolved in acetone (14 mL) in a round bottom flask. Aqueous HCl (2.9 mL, 2 M) was added to the reaction flask followed by the addition of $NaIO_4$ (1.6 g, 7.6 mmol). The reaction solution was stirred at rt for 3 h where the reaction color turned from yellow to orange and TLC (20% EtOAc/hexanes) did not indicate the formation of the desired product. Therefore, additional $NaIO_4$ (1.6 g) and aqueous HCl (2.9 mL) was added, which turned the solution colour to yellow and after 1.5 h TLC indicated the formation of product along with the left-over starting material (boronic ester). After leaving the reaction for

additional 1 h, the volatiles were removed under vacuum. The residue obtained was dissolved in EtOAc (20 mL) followed by addition of water (20 mL). The organic layer was separated and the aqueous layer was extracted again with EtOAc (10 mL × 3). The combined organic layer was dried over Na_2SO_4, filtered, and concentrated under reduced pressure. The crude product obtained was used as such for the next step.
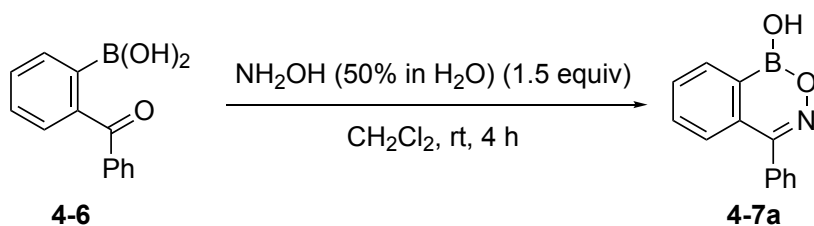
Condensation with Aqueous Hydroxylamine

The crude material obtained (boronic acid) from the previous step was dissolved in CH_2Cl_2 (7.6 mL), followed by the addition of NH_2OH (50 wt. % solution in water, 189 μL, 1.50 equiv) and the reaction solution was stirred at rt for 4 h. Upon completion, the solvent was removed under reduced pressure. The residue obtained was washed with Et_2O (3 mL × 3) and dried in air resulting in 50% crude yield over 3 steps. The product obtained contained unknown quantities of iodine and B_2pin_2. Addition of charcoal reduced the quantity of the desired product (**4-7a**). **^{1}H NMR** (400 MHz, d_6-acetone + 1 drop D_2O): δ 8.15 – 8.17 (m, 1 H), 7.69 – 7.74 (m, 2 H), 7.51 (app s, 5 H), 7.37 – 7.40 (m, 1 H). **^{11}B NMR** (160 MHz, d_6-acetone + 1 drop D_2O): δ 28.4. Full characterization of this compound is shown in Section 4.9.5.

4.9.5 Modified Procedure for the Synthesis of Analogs of 4-1 and 4-2a
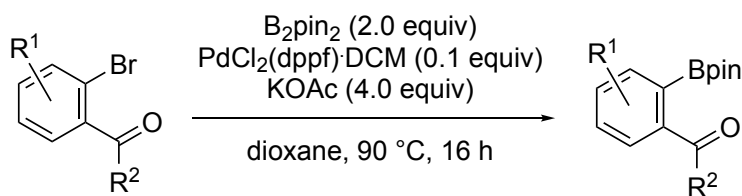
General Procedure for Miyaura Borylation (GP3)[63]

A flame dried round bottom flask was charged with the corresponding 2-bromobenzophenone (1.0 equiv), B_2pin_2 (2.0 equiv), KOAc (4.0 equiv), and $PdCl_2(dppf) \cdot CH_2Cl_2$ (0.1 equiv) under a nitrogen environment. Dioxane (0.4 M) was

added in the reaction flask and the reaction solution was stirred at 90 °C for 16 h. Upon completion (can be checked using LC-MS), the contents of the reaction flask was transferred to a separatory funnel and diluted with water (20 mL). The crude compound was extracted using Et_2O (50 mL × 3) and the combined organic layer was dried over Na_2SO_4, filtered, and concentrated under reduced pressure. The crude material obtained was passed through a silica plug or flash column chromatography was performed, and the material obtained was used as such for the next step.
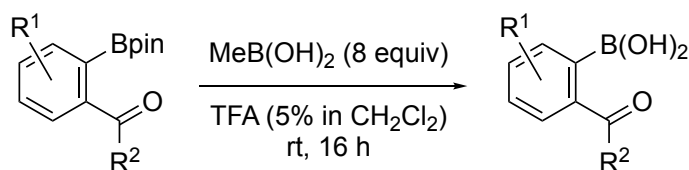
General Procedure for Transesterification (GP4)[31]

The product from the Miyaura borylation was charged in a round bottom flask followed by the addition of $MeB(OH)_2$ (8.0 equiv) and the solvent, consisting of 5% TFA in CH_2Cl_2 (0.1 M). The reaction mixture was stirred at rt for 16 h. Upon completion, the solvent, along with volatiles, such as $MeB(OH)_2$ and MeBpin were removed under reduced pressure. The residue obtained was used as such for the next step.
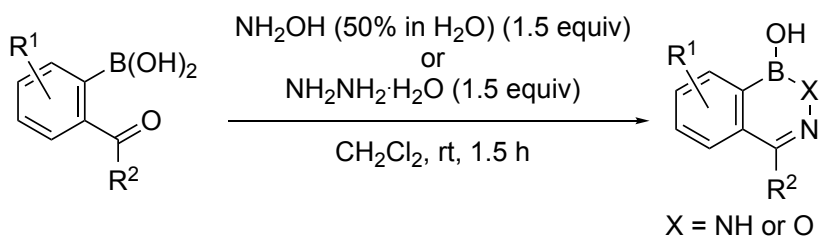
General Procedure for Condensation with Hydroxylamine or Hydrazine (GP5)

The crude material obtained (boronic acid) from the previous step was dissolved in CH_2Cl_2 (0.1 M), followed by the addition of NH_2OH (50 wt. % solution in water, 1.5 equiv) or $NH_2NH_2 \cdot H_2O$ (1.5 equiv), and the reaction solution was stirred at rt for 1.5 h. Upon completion, the solvent was removed under reduced pressure. The residue obtained was washed with minimum amount of Et_2O (to remove undesired protodeboronated side product) and then with water (to remove any excess of hydrazine or hydroxylamine). In some cases, recrystallization resulted in a pure product.
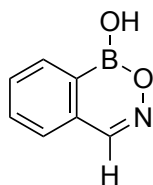
1*H*-benzo[*d*][1,2,6]oxazaborinin-1-ol (4-1): Prepared according to **GP5** from 2-formylphenylboronic acid (2.00 g, 13.3 mmol) and NH_2OH (50 wt. % in water, 1.23 mL, 20.1 mmol). The crude product was washed with water (10 mL × 3) and then air-dried to furnish the title compound as a white solid (1.62 g, 90%); **^{1}H NMR** (500 MHz, d_6-acetone + 1 drop D_2O): δ 8.53 (s, 1 H), 8.11 (d, J = 8.1 Hz, 1 H), 7.84 – 7.78 (m, 1 H), 7.77 – 7.71 (m, 2 H); **^{13}C NMR** (176 MHz, d_6-acetone + 1 drop D_2O): δ 151.0, 133.9, 133.8, 132.6, 132.7, 128.2; **^{11}B NMR** (128 MHz, d_6-acetone + 1 drop D_2O): δ 28.4; **HRMS** (ESI) for $C_7H_5NO_2{}^{11}B$ (M – H)$^-$: Calculated: 146.0419; Found: 146.0418.
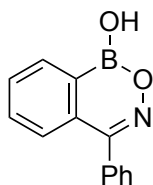
4-Phenyl-1*H*-benzo[*d*][1,2,6]oxazaborinin-1-ol (4-7a): Prepared according to **GP3** from **4-4a** (3.00 g, 11.5 mmol), B$_2$pin$_2$ (5.84 g, 23.0 mmol), KOAc (4.51 g, 46.0 mmol), PdCl$_2$(dppf)·CH$_2$Cl$_2$ (938 mg, 1.15 mmol), and dioxane (50 mL). The crude material was subjected to flash column chromatography (10% EtOAc/hexanes), and then used as such for the transesterification reaction (**GP4**: MeB(OH)$_2$ (6.88 g, 115 mmol)) followed by the condensation reaction (**GP5**: NH$_2$OH (50 wt. % solution in water, 860 μL, 13.8 mmol). Final crude material was washed with Et$_2$O (5 mL) and water (10 mL × 3). The residue obtained was then air-dried to furnish the title compound as a pale yellow solid (1.84 g, 72 %); **^{1}H NMR** (400 MHz, d_6-acetone + 1 drop D_2O): δ 8.23 – 8.19 (m, 1 H), 7.81 – 7.74 (m, 2 H), 7.56 (app s, 5 H), 7.47 – 7.41 (m, 1 H); **^{13}C NMR** (126 MHz, d_6-acetone + 1 drop D_2O): δ 160.3, 135.5, 134.1, 133.7, 133.0, 132.2, 130.5, 130.0, 129.3, 128.2; **^{11}B NMR** (128 MHz, d_6-acetone + 1 drop D_2O): δ 28.4; **HRMS** (ESI) for $C_{13}H_9NO_2{}^{11}B$ (M – H)$^-$: Calculated: 222.0732; Found: 222.0740.
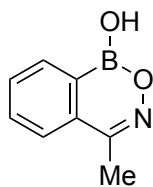
4-Methyl-1*H*-benzo[*d*][1,2,6]oxazaborinin-1-ol (4-7b): Prepared according to **GP5** from 2-acetylphenylboronic acid (2.00 g, 12.2 mmol) and NH_2OH (50 wt. % in water, 1.12 mL, 18.3 mmol). The crude product was washed with water (10 mL × 3) and then air-dried to furnish the title compound as a white solid (1.86 g, 95%); **¹H NMR** (400 MHz, d_6-acetone + 1 drop D_2O): δ 8.12 (d, *J* = 7.4 Hz, 1 H), 7.83 (d, *J* = 3.7 Hz, 2 H), 7.77 – 7.70 (m, 1 H), 2.50 (s, 3 H); **¹³C NMR** (126 MHz, d_6-acetone + 1 drop D_2O): δ 155.4, 134.4, 133.8, 132.8, 132.1, 126.3, 29.91, 29.75, 17.8; **¹¹B NMR** (128 MHz, d_6-acetone + 1 drop D_2O): δ 28.6; **HRMS** (ESI) for $C_8H_9NO_2{}^{11}B$ (M + H)$^+$: Calculated: 162.0721; Found: 162.0721.
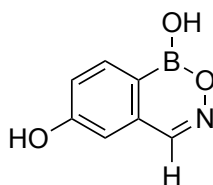
1*H*-benzo[*d*][1,2,6]oxazaborinine-1,6-diol (4-7c): Prepared according to **GP3** from 2-bromo-5-hydroxybenzaldehyde (1.38 g, 6.85 mmol), B_2pin_2 (3.48 g, 13.7 mmol), KOAc (2.69 g, 27.4 mmol), $PdCl_2$(dppf)·CH_2Cl_2 (559 mg, 0.680 mmol), and dioxane (20 mL). The crude material was subjected to flash column chromatography (10% EtOAc/hexanes), and then used as such for the transesterification reaction (**GP4**: $MeB(OH)_2$ (2.46 g, 41.1 mmol, 6.00 equiv)) followed by the condensation reaction (**GP5**: NH_2OH (50 wt. % solution in water, 630 μL, 10.3 mmol). The final crude material was washed with Et_2O (5 mL) and water (10 mL × 3). The residue obtained was then air-dried to furnish the title compound as an off-white solid (849 mg, 76%); **¹H NMR** (400 MHz, d_6-acetone + 1 drop D_2O): δ 8.41 (s, 1 H), 7.98 (d, *J* = 8.2 Hz, 1 H), 7.24 (dd, *J* = 8.2, 2.3 Hz, 1 H), 7.14 (d, *J* = 2.3 Hz, 1 H); **¹³C NMR** (126 MHz, d_6-acetone + 1 drop D_2O): δ 162.4, 150.9, 135.9, 134.7, 120.9, 113.2; **¹¹B NMR** (128

MHz, d_6-acetone + 1 drop D_2O): δ 28.4; **HRMS** (ESI) for $C_7H_5NO_3{}^{11}B$ (M − H)$^-$: Calculated: 162.0368; Found: 162.0367.
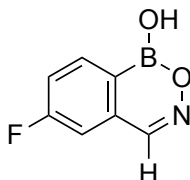
6-Fluoro-1*H*-benzo[*d*][1,2,6]oxazaborinin-1-ol (4-7d): Prepared according to **GP5** from 4-fluoro-2-formylphenylboronic acid (500 mg, 2.98 mmol) and NH_2OH (50 wt. % in water, 220 μL, 3.58 mmol). The crude product was washed with water (10 mL × 3) and then air-dried to furnish the title compound as a white solid (410 mg, 83%); **¹H NMR** (400 MHz, d_6-acetone + 1 drop D_2O): δ 8.57 (s, 1 H), 8.21 (app td, J = 6.1, 2.1 Hz, 1 H), 7.53 (m, 2 H); **¹³C NMR** (126 MHz, d_6-acetone + 1 drop D_2O): δ 166.5 (d, J = 248 Hz), 150.2, 136.1 (d, J = 8.54 Hz), 136.0 (d, J = 8.78 Hz), 120.5 (d, J = 21.7 Hz), 114.0 (d, J = 21.4 Hz); **¹¹B NMR** (128 MHz, d_6-acetone + 1 drop D_2O): δ 27.9; **¹⁹F NMR** (376 MHz, d_6-acetone + 1 drop D_2O): δ −107.2 (app q, J = 8.4 Hz); **HRMS** (ESI) for $C_7H_6FNO_2{}^{11}B$ (M + H)$^+$: Calculated: 166.0470; Found: 166.0470.
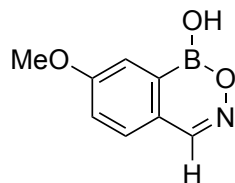
7-Methoxy-1*H*-benzo[*d*][1,2,6]oxazaborinin-1-ol (4-7e): Prepared according to **GP5** from 5-methoxy-2-formylphenylboronic acid (1.00 g, 5.56 mmol) and NH_2OH (50 wt. % in water, 410 μL, 6.66 mmol). The crude product was washed with water (10 mL × 3) and then air-dried to furnish the title compound as a white solid (921 mg, 94%); **¹H NMR** (400 MHz, d_6-acetone + 1 drop D_2O): δ 8.43 (s, 1 H), 7.71 (d, J = 8.6 Hz, 1 H), 7.59 (d, J = 2.7 Hz, 1 H), 7.36 (dd, J = 8.6, 2.7 Hz, 1 H), 3.95 (s, 3 H); **¹³C NMR** (126 MHz, d_6-acetone + 1 drop D_2O): δ 163.2, 150.2, 130.4, 127.4, 121.5, 114.9, 56.1; **¹¹B NMR** (128 MHz, d_6-acetone + 1 drop D_2O): δ 28.5; **HRMS** (ESI) for $C_8H_7NO_3{}^{11}B$ (M − H)$^-$: Calculated: 176.0524; Found: 176.0525.
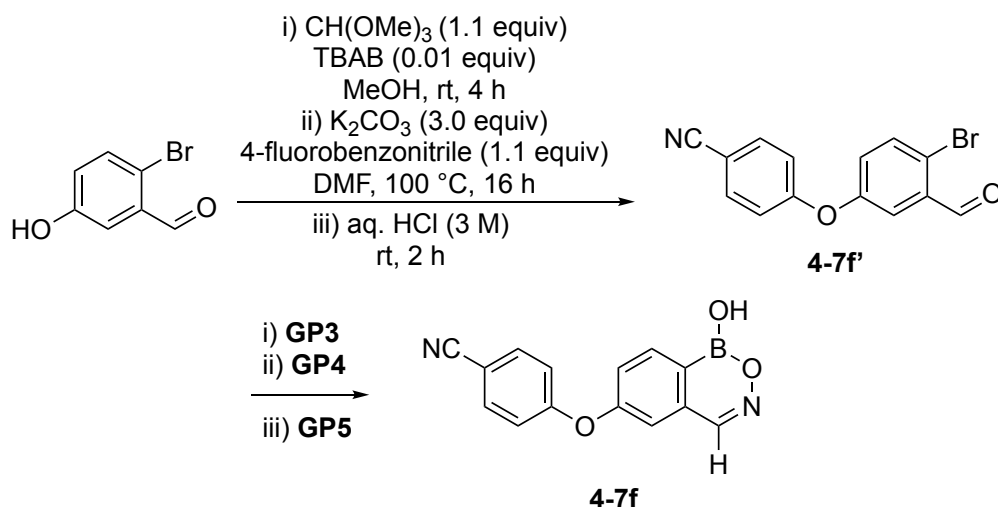
4-((1-Hydroxy-1*H*-benzo[*d*][1,2,6]oxazaborinin-6-yl)oxy)benzonitrile (4-7f): The starting material **4-7f'** for the synthesis of the title compound was prepared using a slight modification of a literature procedure.[12] A round bottom flask was charged with 2-bromo-5-hydroxybenzaldehyde (500 mg, 2.49 mmol) and trimethylorthoformate (264 mg, 2.49 mmol), followed by the addition of MeOH (5 mL). A drop of conc. H_2SO_4 was added to the reaction flask. The reaction solution was heated at reflux for 2.5 h. Upon completion, the reaction mixture was cooled down and a saturated solution of NaOMe in MeOH was added dropwise until a desired pH (~10) was obtained. The solvent was evaporated and the residue obtained was dissolved in DMF (2 mL). K_2CO_3 (1.00 g, 7.47 mmol) was added to the reaction solution, followed by 4-fluorobenzonitrile (332 mg, 2.74 mmol). The reaction mixture was heated at 100 °C for 16 h. Upon completion, the reaction solution was brought down to rt and water (10 mL) was added. The crude product was extracted with Et_2O (10 mL × 3). The combined organic layer was dried over Na_2SO_4, filtered, and concentrated in vacuo to afford the crude product as a pale yellow solid (684 mg, 79% yield over 2 steps); **¹H NMR** (400 MHz, CDCl₃): δ 7.58 (d, *J* = 9.0 Hz, 2 H), 7.56 (d, *J* = 8.6 Hz, 1 H), 7.31 (d, *J* = 3.0 Hz, 1 H), 6.98 (d, *J* = 8.9 Hz, 2 H), 6.90 (dd, *J* = 8.6, 3.0 Hz, 1 H), 5.49 (s, 1 H), 3.36 (s, 6 H). The crude material was dissolved in MeOH (5.0 mL) and then aq. HCl (10 mL, 3.0 M) was added. The reaction solution was stirred at rt for 2 h. Upon completion, the MeOH was evaporated in vacuo and the crude compound was extracted with EtOAc (10 mL × 3). The combined organic layer was evaporated to afford the desired

compound (**4-7f'**) as a white solid (370 mg, 63%); **¹H NMR** (400 MHz, CDCl₃): δ 10.30 (s, 1 H), 7.66 (d, J = 8.7 Hz, 1 H), 7.62 (d, J = 8.9 Hz, 2 H), 7.55 (d, J = 3.0 Hz, 1 H), 7.17 (dd, J = 8.7, 3.0 Hz, 1 H), 7.01 (d, J = 8.9 Hz, 2 H).

The title compound was prepared according to **GP3** from **4-7f'** (270 mg, 0.890 mmol), B₂pin₂ (454 mg, 1.79 mmol), KOAc (351 mg, 3.58 mmol), PdCl₂(dppf)·CH₂Cl₂ (73.0 mg, 90.0 μmol), and dioxane (5 mL). The crude material was subjected to flash column chromatography (10% EtOAc/hexanes), and then used as such for the transesterification reaction (**GP4**: MeB(OH)₂ (321 mg, 5.36 mmol, 6.00 equiv)) followed by the condensation reaction (**GP5**: NH₂OH (50 wt. % solution in water, 80.0 μL, 1.33 mmol). The final crude material was washed with Et₂O (5 mL) and water (10 mL × 3). The residue obtained was left in water (5 mL) overnight and then filtered, air-dried to furnish the title compound as a pale yellow solid (149 mg, 63%); **¹H NMR** (400 MHz, d_6-acetone + 1 drop D₂O): δ 8.53 (s, 1 H), 8.18 (d, J = 8.1 Hz, 1 H), 7.84 (d, J = 9.0 Hz, 2 H), 7.49 (d, J = 8.1 Hz, 1 H), 7.46 (s, 1 H), 7.27 (d, J = 9.0 Hz, 2 H); **¹³C NMR** (126 MHz, d_6-acetone + 1 drop D₂O): δ 161.1, 160.4, 150.4, 136.0, 135.5, 135.5, 124.3, 120.5, 119.1, 117.8, 108.2; **¹¹B NMR** (128 MHz, d_6-acetone + 1 drop D₂O): δ 28.0; **HRMS** (ESI) for $C_{14}H_8N_2O_3{}^{11}B$ (M − H)⁻: Calculated: 263.0633; Found: 263.0629.
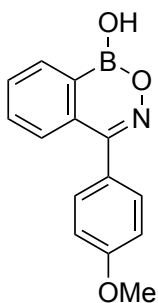
4-(4-Methoxyphenyl)-1*H*-benzo[*d*][1,2,6]oxazaborinin-1-ol **(4-7g):** Prepared according to **GP3** from **4-4f** (2.00 g, 6.87 mmol), B₂pin₂ (3.49 g, 13.7 mmol), KOAc (2.70 g, 27.5 mmol), PdCl₂(dppf)·CH₂Cl₂ (561 mg, 0.690 mmol), and dioxane (20 mL). The crude material was passed through a silica plug (20% EtOAc/hexanes), and then used as such for the transesterification reaction (**GP4**: MeB(OH)₂ (4.11 g, 68.7 mmol, 10.0 equiv)), followed by the condensation reaction (**GP5**: NH₂OH (50 wt. % solution

in water, 630 μL, 10.3 mmol). The final crude material was washed with water (10 mL × 3) and then with Et$_2$O (5 mL). The residue obtained was then air-dried to furnish the title compound as an off white solid (1.21 g, 70%); **^{1}H NMR** (400 MHz, d_6-acetone + 1 drop D$_2$O): δ 8.22 – 8.14 (m, 1 H), 7.83 – 7.70 (m, 2 H), 7.47 (d, J = 8.8 Hz, 3 H), 7.09 (d, J = 8.8 Hz, 2 H), 3.88 (s, 3 H); **^{13}C NMR** (126 MHz, d_6-acetone + 1 drop D$_2$O): δ 161.4, 160.0, 134.2, 133.6, 133.1, 132.2, 131.8, 128.2, 127.5, 114.8, 55.8; **^{11}B NMR** (128 MHz, d_6-acetone + 1 drop D$_2$O): δ 28.5; **HRMS** (ESI) for C$_{14}$H$_{11}$NO$_3$^{11}B (M – H)$^-$: Calculated: 252.0837; Found: 252.0836.
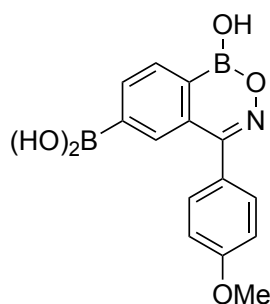
(1-Hydroxy-4-(4-methoxyphenyl)-1*H*-benzo[*d*][1,2,6]oxazaborinin-6-yl)boronic acid (4-7h): Prepared according to **GP3** from **4-4c** (2.00 g, 5.41 mmol), B$_2$pin$_2$ (5.50 g, 21.6 mmol, 4.00 equiv), KOAc (4.24 g, 43.2 mmol, 8.00 equiv), PdCl$_2$(dppf)·CH$_2$Cl$_2$ (883 mg, 1.08 mmol, 0.200 equiv), and dioxane (15 mL). The crude material was subjected to flash column chromatography (20% EtOAc/hexanes), and then used as such for the transesterification reaction (**GP4**: MeB(OH)$_2$ (3.24 g, 54.1 mmol, 10.0 equiv)), followed by the condensation reaction (**GP5**: NH$_2$OH (50 wt. % solution in water, 500 μL, 8.10 mmol). The final crude material was washed with Et$_2$O (5 mL) and water (10 mL × 3). The residue obtained was then air-dried to furnish the title compound as an off white solid (1.02 g, 63%); **^{1}H NMR** (400 MHz, d_6-acetone + 1 drop D$_2$O): δ 8.20 (d, J = 8.4 Hz, 1 H), 8.17 (d, J = 6.6 Hz, 1 H), 8.04 (s, 1 H), 7.50 (d, J = 8.8 Hz, 2 H), 7.11 (d, J = 8.8 Hz, 2 H), 3.90 (s, 3 H); **^{13}C NMR** (126 MHz, d_6-acetone + 1 drop D$_2$O): δ 161.3, 160.4, 137.3, 134.1, 133.5, 131.9, 131.9, 127.8, 114.7, 55.8; **^{11}B NMR** (128 MHz, d_6-acetone + 1 drop D$_2$O): δ 28.3; **HRMS** (ESI) for C$_{16}$H$_{13}$F$_3$NO$_7$^{11}B$_2$ (M + CF$_3$COO$^-$)$^+$: Calculated: 410.0836; Found: 410.0836.
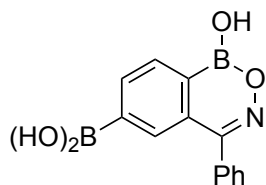
(1-Hydroxy-4-phenyl-1*H*-benzo[*d*][1,2,6]oxazaborinin-6-yl)boronic acid (4-7i): Prepared according to **GP3** from **4-4b** (500 mg, 1.47 mmol), B$_2$pin$_2$ (1.50 g, 5.90 mmol, 4.00 equiv), KOAc (1.15 g, 11.76 mmol, 8.00 equiv), PdCl$_2$(dppf)·CH$_2$Cl$_2$ (240 mg, 0.290 mmol, 0.200 equiv), and dioxane (5 mL). The crude material was subjected to flash column chromatography (10% EtOAc/hexanes), and then used as such for the transesterification reaction (**GP4**: MeB(OH)$_2$ (704 mg, 11.8 mmol)), followed by the condensation reaction (**GP5**: NH$_2$OH (50 wt. % solution in water, 140 μL, 2.20 mmol). The final crude material was washed with Et$_2$O (5 mL) and water (10 mL × 3). The residue obtained was left in water (5 mL) overnight and then filtered, air-dried to furnish the title compound as a white solid (134 mg, 34%); **^{1}H NMR** (600 MHz, *d$_6$*-acetone + 1 drop D$_2$O): δ 8.18 (d, *J* = 8.4 Hz, 1 H), 8.15 (d, *J* = 8.2 Hz, 1 H), 7.95 (s, 1 H), 7.54 (app s, 5 H); **^{13}C NMR** (126 MHz, *d$_6$*-acetone + 1 drop D$_2$O): δ 160.7, 137.5, 135.6, 134.1, 133.3, 132.0, 130.6, 130.0, 129.4; **^{11}B NMR** (128 MHz, *d$_6$*-acetone + 1 drop D$_2$O): δ 28.0; **HRMS** (ESI) for C$_{13}$H$_{10}$NO$_4$^{11}B$_2$ (M − H)$^−$: Calculated: 266.0801; Found: 266.0809.
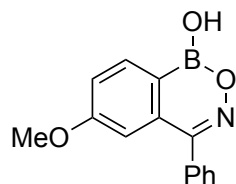
6-Methoxy-4-phenyl-1*H*-benzo[*d*][1,2,6]oxazaborinin-1-ol (4-7j): Prepared according to **GP3** from **4-4e** (1.67 g, 5.75 mmol), B$_2$pin$_2$ (2.92 g, 11.5 mmol), KOAc (2.30 g, 23.0 mmol), PdCl$_2$(dppf)·CH$_2$Cl$_2$ (470 mg, 0.580 mmol), and dioxane (15 mL). The crude material was subjected to flash column chromatography (10% EtOAc/hexanes) and then used as such for the transesterification reaction (**GP4**: MeB(OH)$_2$ (2.75 g, 46.0 mmol)), followed by the condensation reaction (**GP5**: NH$_2$OH (50 wt. % solution in water, 530 μL, 8.63 mmol). The final crude material was washed

with Et$_2$O (15 mL) and then with water (10 mL × 3). The residue obtained was then air-dried to furnish the title compound (460 mg). Precipitation was observed in the filtrate, therefore, precipitate was filtered and then again washed with water and Et$_2$O (5 mL). This second crop of compound was then air-dried to furnish the title compound as an off-white solid (total mass of 862 mg, 59%); **^{1}H NMR** (400 MHz, d_6-acetone + 1 drop D$_2$O): δ 8.14 (d, J = 8.3 Hz, 1 H), 7.55 (app s, 5 H), 7.35 (dd, J = 8.3, 2.4 Hz, 1 H), 6.88 (d, J = 2.4 Hz, 1 H), 3.80 (s, 3 H); **^{13}C NMR** (126 MHz, d_6-acetone + 1 drop D$_2$O): δ 164.0, 160.2, 136.0, 135.5, 135.1, 130.4, 130.0, 129.4, 119.2, 112.2, 55.8; **^{11}B NMR** (128 MHz, d_6-acetone + 1 drop D$_2$O): δ 28.4; **HRMS** (ESI) for C$_{14}$H$_{13}$NO$_3$^{11}B (M + H)$^+$: Calculated: 254.0983; Found: 254.0983.
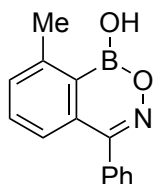
8-Methyl-4-phenyl-1H-benzo[d][1,2,6]oxazaborinin-1-ol **(4-7k):** Prepared according to **GP3** from **4-4i** (1.00 g, 3.65 mmol), B$_2$pin$_2$ (1.85 g, 7.30 mmol), KOAc (1.43 g, 14.6 mmol), PdCl$_2$(dppf)·CH$_2$Cl$_2$ (298 mg, 0.370 mmol), and dioxane (10 mL). The crude material was subjected to flash column chromatography (10% EtOAc/hexanes), and then used as such for the transesterification reaction (**GP4**: MeB(OH)$_2$ (1.72 g, 28.8 mmol)), followed by the condensation reaction (**GP5**: NH$_2$OH (50 wt. % solution in water, 330 μL, 5.47 mmol). The final crude material was washed with Et$_2$O (5 mL) and water (10 mL × 3). The compound was soluble in ether; therefore the ether layer was evaporated and the residue was taken in a vial, dissolved in hot EtOAc (3 mL) followed by the addition of hexanes (0.5 mL). The vial was left in the fridge, which resulted in the precipitation of the desired compound, which was then filtered and air-dried to furnish the title compound as a pale yellow solid (470 mg, 54%); **^{1}H NMR** (400 MHz, d_6-acetone + 1 drop D$_2$O): δ 7.61 (t, J = 7.7 Hz, 1 H), 7.57 – 7.55 (m, 2 H), 7.55 – 7.48 (m, 4 H), 7.20 (d, J = 7.8 Hz, 1 H), 2.79 (s, 3 H); **^{13}C NMR** (126 MHz, d_6-acetone + 1 drop D$_2$O): δ 160.8, 146.3, 135.9, 135.1, 134.2, 133.3, 130.5,

130.0, 129.4, 126.1, 22.6; **^{11}B NMR** (128 MHz, d_6-acetone + 1 drop D$_2$O): δ 28.4; **HRMS** (ESI) for C$_{14}$H$_{11}$NO$_2$^{11}B (M − H)$^-$: Calculated: 236.0888; Found: 236.0890.
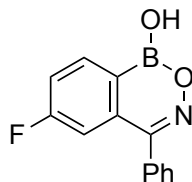
6-Fluoro-4-phenyl-1H-benzo[d][1,2,6]oxazaborinin-1-ol (4-7l): Prepared according to **GP3** from **4-4j** (299 mg, 1.07 mmol), B$_2$pin$_2$ (543 mg, 2.14 mmol), KOAc (420 mg, 4.28 mmol), PdCl$_2$(dppf)·CH$_2$Cl$_2$ (87.4 mg, 0.107 mmol), and dioxane (4 mL). The crude material was passed through a silica plug (20% EtOAc/hexanes), and then used as such for the transesterification reaction (**GP4**: MeB(OH)$_2$ (513 mg, 8.56 mmol)), followed by the condensation reaction (**GP5**: NH$_2$OH (50 wt. % solution in water, 100 μL, 1.60 mmol). The final crude material was washed with Et$_2$O (5 mL) and water (10 mL × 3). The residue obtained was air-dried to furnish the title compound as a yellow oil (104 mg, 40%); **^{1}H NMR** (600 MHz, d_6-acetone + 1 drop D$_2$O): δ 7.81 (d, J = 8.0 Hz, 1 H), 7.53 (app s, 5 H), 7.48 (d, J = 6.8 Hz, 2 H); **^{13}C NMR** (126 MHz, d_6-acetone + 1 drop D$_2$O): δ 165.0 (d, J = 253 Hz), 159.4, 135.4, 131.7 (d, J = 8.52 Hz), 130.8, 130.2, 129.5, 121.2 (d, J = 22.1 Hz), 118.4 (d, J = 19.9 Hz); **^{11}B NMR** (128 MHz, d_6-acetone + 1 drop D$_2$O): δ 27.7; **^{19}F NMR** (376 MHz, d_6-acetone + 1 drop D$_2$O) δ − 108.38 (app q, J = 7.7 Hz); **HRMS** (ESI) for C$_{13}$H$_{10}$FNO$_2$^{11}B (M + H)$^+$: Calculated: 241.0943; Found: 241.0946.
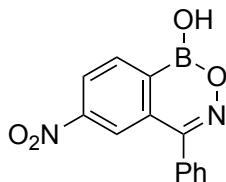
6-Nitro-4-phenyl-1H-benzo[d][1,2,6]oxazaborinin-1-ol (4-7m): Prepared according to **GP3** from **4-4h** (2.00 g, 6.54 mmol), B$_2$pin$_2$ (3.32 g, 13.1 mmol), KOAc (2.57 g, 26.2 mmol), PdCl$_2$(dppf)·CH$_2$Cl$_2$ (534 mg, 650 μmol), and dioxane (20 mL). The crude material was subjected to flash column chromatography (10% EtOAc/hexanes), and

then used as such for the transesterification reaction (**GP4**: MeB(OH)$_2$ (3.13 g, 52.3 mmol))**,** followed by the condensation reaction (**GP5**: NH$_2$OH (50 wt. % solution in water, 600 μL, 9.81 mmol). The final crude material was washed by dropwise addition of Et$_2$O (5 mL) (product partially soluble in ether, along with the protodeboronated side product) and then with water (10 mL × 3). The residue obtained was air-dried to furnish the title compound as a white solid (669 mg, 38%); **^{1}H NMR** (500 MHz, d_6-acetone + 1 drop D$_2$O): δ 8.65 (dd, J = 8.2, 2.1 Hz, 1 H), 8.55 (d, J = 8.2 Hz, 1 H), 8.31 (d, J = 2.1 Hz, 1 H), 7.77 – 7.68 (m, 5 H); **^{13}C NMR** (126 MHz, d_6-acetone + 1 drop D$_2$O): δ 159.4, 151.8, 135.1, 135.1, 134.4, 130.6, 130.5, 129.7, 126.1, 122.7; **^{11}B NMR** (128 MHz, d_6-acetone + 1 drop D$_2$O): δ 27.8; **HRMS** (ESI) for C$_{13}$H$_8$N$_2$O$_4$^{11}B (M − H)$^-$: Calculated: 267.0583; Found: 267.0587.
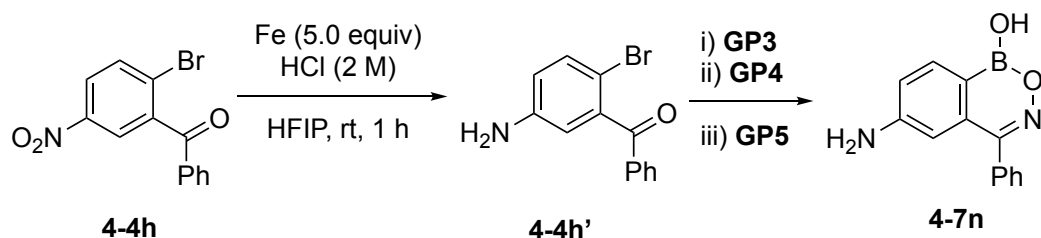
6-Amino-4-phenyl-1H-benzo[d][1,2,6]oxazaborinin-1-ol (4-7n): The starting material (**4-4h'**) for the synthesis of the title compound was prepared by reduction of the nitro group of **4-4h**.[33] A round bottom flask was charged with **4-4h** (5.00 g, 16.3 mmol) and HFIP (17.2 mL), followed by the addition of aq. HCl (163 mL, 2 M) and Fe powder (4.60 g, 81.7 mmol). The reaction mixture was stirred at rt for 1 h. Upon completion, saturated aq. NaHCO$_3$ (20 mL) was added and the compound was extracted with EtOAc (10 mL × 3). The combined organic layer was evaporated and the crude material was subjected to flash column chromatography (10-20% EtOAc/hexanes) to afford the desired product **4-4h'** as a pale yellow solid (3.62 g, 80%); **^{1}H NMR** (600 MHz, CDCl$_3$): δ 7.84 (d, J = 6.9 Hz, 2 H), 7.60 (t, J = 7.5 Hz, 1 H), 7.47 (t, J = 7.8 Hz, 2 H), 7.36 (d, J = 8.5 Hz, 1 H), 6.67 (dd, J = 8.4, 2.9 Hz, 1 H), 6.65 (d, J = 2.9 Hz, 1 H), 3.87 (s, 2 H).

The title compound was prepared according to **GP3** from **4-4h'** (2.20 g, 7.97 mmol), B$_2$pin$_2$ (4.05 g, 15.9 mmol), KOAc (3.13 g, 31.9 mmol), PdCl$_2$(dppf)·CH$_2$Cl$_2$

(651 mg, 800 µmol), and dioxane (30 mL). The crude material was subjected to flash column chromatography (10% EtOAc/hexanes), and then used as such for the transesterification reaction (**GP4**: MeB(OH)$_2$ (2.86 g, 47.8 mmol, 6.00 equiv)), followed by the condensation reaction (**GP5**: NH$_2$OH (50 wt. % solution in water, 730 µL, 11.9 mmol)). Due to the zwitterionic nature of the product, the Et$_2$O and water wash was not sufficient to get the pure product. The final crude material was subjected to flash column chromatography (3-5% MeOH/CH$_2$Cl$_2$ with 0.5% AcOH), to yield the desired product as an acetic acid salt. The residue obtained was air-dried to furnish the crude title compound as a brown solid (1.52 g, 33%). The yield was calculated by ^{1}H NMR spectroscopy with an internal standard of 1,3,5-trimethoxybenzene in d$_6$-acetone. Based on the ^{1}H NMR spectrum, the actual mass of the title compound was 622 mg, which was used without further purification for the late-stage modifications. **^{1}H NMR** (500 MHz, d$_6$-acetone + 1 drop D$_2$O): δ 7.84 (d, J = 8.1 Hz, 1 H), 7.50 – 7.38 (m, 5 H), 6.98 (dd, J = 8.1, 2.1 Hz, 1 H), 6.55 (d, J = 2.1 Hz, 1 H); **^{13}C NMR** (176 MHz, d$_6$-acetone + 1 drop D$_2$O): δ 173.4, 160.5, 153.0, 135.7, 134.5, 130.3, 129.8, 129.2, 119.3, 111.9; **^{11}B NMR** (160 MHz, d$_6$-acetone + 1 drop D$_2$O): δ 28.6; **HRMS** (ESI) for C$_{13}$H$_{12}$N$_2$O$_2$^{11}B (M + H)$^+$: Calculated: 239.0986; Found: 239.0986.
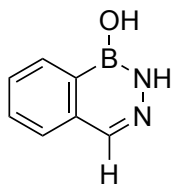
Benzo[d][1,2,3]diazaborinin-1(2H)-ol (4-2a): Prepared according to **GP5** from 2-formylphenylboronic acid (100 mg, 670 µmol) and NH$_2$NH$_2$·H$_2$O (50.0 µL, 1.00 mmol). The crude material was washed with water (2 mL × 3) and then air-dried to furnish the title compound as a white solid (84.1 mg, 86%); **^{1}H NMR** (500 MHz, d$_6$-acetone + 1 drop D$_2$O): δ 8.20 (d, J = 7.6 Hz, 1 H), 7.99 (s, 1 H), 7.75 – 7.67 (m, 2 H), 7.62 – 7.52 (m, 1 H); **^{13}C NMR** (126 MHz, d$_6$-acetone + 1 drop D$_2$O): δ 140.2, 140.1, 137.2, 132.0, 131.7, 129.4, 127.8; **^{11}B NMR** (128 MHz, d$_6$-acetone + 1 drop D$_2$O): δ 27.9; **HRMS** (ESI) for C$_7$H$_6$N$_2$O^{11}B (M – H)$^-$: Calculated: 145.0579; Found: 145.0579.
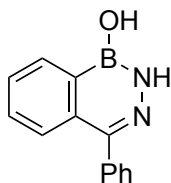
4-Phenylbenzo[*d*][1,2,3]diazaborinin-1(2*H*)-ol (4-8a): Prepared according to **GP3** from **4-4a** (1.50 g, 5.70 mmol), B_2pin_2 (2.92 g, 11.5 mmol), KOAc (2.24 g, 22.8 mmol), $PdCl_2(dppf)\cdot CH_2Cl_2$ (466 mg, 0.570 mmol), and dioxane (15 mL). The crude material was subjected to flash column chromatography (10% EtOAc/hexanes), and then used as such for the transesterification reaction (**GP4**: $MeB(OH)_2$ (2.73 g, 45.6 mmol)), followed by the condensation reaction (**GP5**: $NH_2NH_2\cdot H_2O$ (420 μL, 8.55 mmol). The crude material was dissolved in hot methanol (5 mL) and then a drop of water was added to afford a crystalline compound. The precipitate was filtered and washed with water, then air-dried to furnish the title compound as a white crystalline solid (648 mg, 58%); **^{1}H NMR** (400 MHz, d_6-acetone + 1 drop D_2O): δ 8.27 (dd, J = 7.8, 1.7 Hz, 1 H), 7.67 – 7.55 (m, 3 H), 7.53 – 7.38 (m, 5 H); **^{13}C NMR** (126 MHz, d_6-acetone + 1 drop D_2O): δ 148.4, 139.7, 136.2, 132.0, 131.7, 130.6, 129.1, 129.0, 128.6, 127.6; **^{11}B NMR** (128 MHz, d_6-acetone + 1 drop D_2O): δ 27.8; **HRMS** (ESI) for $C_{13}H_{12}N_2O^{11}B$ $(M + H)^+$: Calculated: 223.1037; Found: 223.0964.
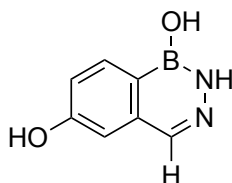
Benzo[*d*][1,2,3]diazaborinine-1,6(2*H*)-diol (4-8b): Prepared according to **GP3** from 2-bromo-5-hydroxybenzaldehyde (2.00 g, 9.95 mmol), B_2pin_2 (5.05 g, 19.9 mmol), KOAc (3.91 g, 39.8 mmol), $PdCl_2(dppf)\cdot CH_2Cl_2$ (813 mg, 1.00 mmol), and dioxane (25 mL). The crude material was subjected to flash column chromatography (10% EtOAc/hexanes), and then used as such for the transesterification reaction (**GP4**: $MeB(OH)_2$ (4.74 g, 79.2 mmol)), followed by the condensation reaction (**GP5**: $NH_2NH_2\cdot H_2O$ (730 μL, 14.9 mmol)). The crude material was added to a solution of saturated aq. $NaHCO_3$ (20 mL), filtered and the residue was washed with water (10 mL

× 3) and then air-dried to furnish the title compound as a white solid (709 mg, 44%); **¹H NMR** (500 MHz, d_6-acetone + 1 drop D$_2$O): δ 8.12 (d, J = 8.0 Hz, 1 H), 7.91 (s, 1 H), 7.21 – 7.15 (m, 2 H); **¹³C NMR** (126 MHz, d_6-acetone + 1 drop D$_2$O): δ 160.9, 140.0, 139.7, 139.2, 133.6, 118.7, 111.8; **¹¹B NMR** (128 MHz, d_6-acetone + 1 drop D$_2$O): δ 27.8; **HRMS** (ESI) for C$_7$H$_8$N$_2$O$_2$^{11}B (M + H)$^+$: Calculated: 163.0673; Found: 163.0674.
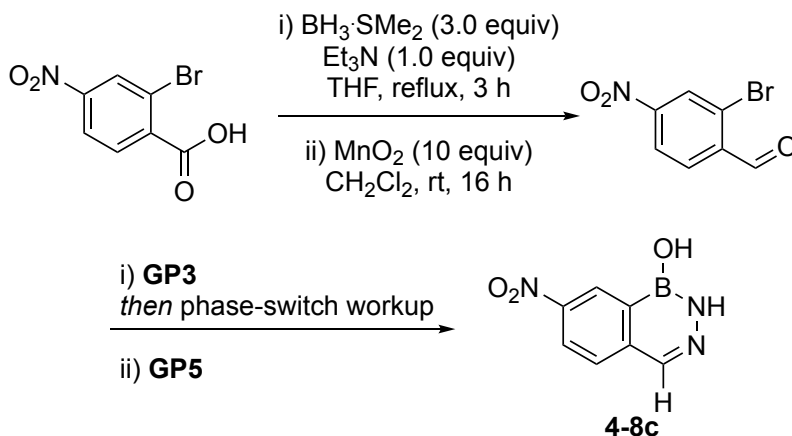
7-Nitrobenzo[*d*][1,2,3]diazaborinin-1(2*H*)-ol (4-8c): The starting material (2-bromo-4-nitrobenzaldehyde) for the synthesis of the title compound was prepared using a slight modification of a literature procedure.[32] A flame dried round bottom flask was charged with 2-bromo-5-nitrobenzoic acid (5.00 g, 20.3 mmol), BH$_3$·SMe$_2$ (6.20 mL, 61.0 mmol), and Et$_3$N (2.83 mL, 20.3 mmol), followed by the addition of THF (5 mL) under nitrogen. The reaction solution was heated at reflux for 3 h. Upon completion, the temperature of the reaction solution was brought down to rt, and the reaction was slowly quenched with water (2.5 mL). The reaction solution was brought to a pH of ~1 with aq. HCl (6 M). Finally, the reaction mixture was diluted with water (20 mL) and then extracted with CH$_2$Cl$_2$ (20 mL × 3). The organic layer was combined, dried over Na$_2$SO$_4$, filtered, and then concentrated in vacuo. The residue obtained was dissolved in a minimum amount of hot CH$_2$Cl$_2$ in a vial, and then hexanes (0.5 mL) was added. Leaving the vial in the refrigerator for 3 h resulted in the formation of crystals. The crystals were filtered, washed with hexanes, and then air-dried to afford the reduction product (alcohol) as a white crystalline solid (3.88 g, 82%); **¹H NMR** (400 MHz,

CDCl$_3$): δ 8.43 (d, J = 2.3 Hz, 1 H), 8.24 (dd, J = 8.5, 2.3 Hz, 1 H), 7.79 (d, J = 8.5 Hz, 1 H), 4.86 (d, J = 5.7 Hz, 2 H), 2.13 (t, J = 5.8 Hz, 1 H). This alcohol product (3.88 g, 16.7 mmol) was charged in the round bottom flask and dissolved in CH$_2$Cl$_2$ (30 mL), followed by the addition of activated MnO$_2$ (14.5 g, 167 mmol). The reaction mixture was stirred at rt for 16 h. Upon completion, the reaction solution was filtered through Celite® and washed with CH$_2$Cl$_2$ (10 mL). The organic layer was concentrated in vacuo to yield the aldehyde product as a pale-yellow solid (3.10 g, 81%).

The title compound was prepared according to **GP3** from aldehyde product (2.00 g, 8.69 mmol), B$_2$pin$_2$ (4.42 g, 17.4 mmol), KOAc (3.41 g, 34.8 mmol), PdCl$_2$(dppf)·CH$_2$Cl$_2$ (710 mg, 0.870 mmol), and dioxane (25 mL). The crude material obtained showed the direct formation of the B(OH)$_2$ containing product instead of the Bpin containing product according to the LC-MS (hydrolysis during workup), therefore, it was filtered through Celite® and then the solvent was evaporated under reduced pressure. The residue was subjected to a phase-switch workup. Sorbitol solution (1 M) was prepared by dissolving Na$_2$CO$_3$ (53.0 g, 500 mmol) and sorbitol (91.0 g, 1.11 mol) in water (500 mL).[23] The residue was dissolved in EtOAc (10 mL) followed by the addition of sorbitol solution (10 mL) and was transferred to a separatory funnel. After vigorous shaking for 5 min, the aqueous layer was separated. The aqueous layer was adjusted to a pH of 3 with aq. HCl (6 M) and then the compound was extracted with EtOAc (10 mL × 3). The combined organic layer was washed with water (10 mL) and brine (10 mL), and then dried over Na$_2$SO$_4$, filtered, and concentrated in vacuo. The crude boronic acid obtained was used as such for the condensation reaction (**GP5**: NH$_2$NH$_2$·H$_2$O (0.64 mL, 13.0 mmol)). The crude material was added to a solution of saturated aq. NaHCO$_3$ (20 mL), filtered, and the residue was washed with water (10 mL × 3) and Et$_2$O (5 mL), and then air-dried to furnish the title compound as a yellow solid (815 mg, 49%); **^{1}H NMR** (500 MHz, d_6-acetone + 1 drop D$_2$O): δ 8.98 (d, J = 2.4 Hz, 1 H), 8.45 (dd, J = 8.7, 2.4 Hz, 1 H), 8.14 (s, 1 H), 7.97 (d, J = 8.7 Hz, 1 H); **^{13}C NMR** (126 MHz, d_6-acetone + 1 drop D$_2$O): δ 148.1, 140.6, 138.9, 138.8, 129.5, 127.3, 126.3; **^{11}B NMR** (128 MHz, d_6-acetone + 1 drop D$_2$O): δ 27.6; **HRMS** (ESI) for C$_7$H$_5$N$_3$O$_3$^{11}B (M − H)$^-$: Calculated: 190.0429; Found: 190.0428.
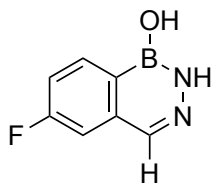
6-Fluorobenzo[*d*][1,2,3]diazaborinin-1(2*H*)-ol (4-8d): Prepared according to **GP5** from 4-fluoro-2-formylphenylboronic acid (200 mg, 1.19 mmol) and $NH_2NH_2 \cdot H_2O$ (60.0 μL, 1.25 mmol). The crude material was washed with water (5 mL × 3), and then air-dried to furnish the title compound as a white solid (193 mg, 99%); **^{1}H NMR** (400 MHz, d_6-acetone + 1 drop D_2O): δ 8.26 (dd, J = 8.4, 6.1 Hz, 1 H), 8.01 (s, 1 H), 7.49 (dd, J = 9.9, 2.5 Hz, 1 H), 7.39 (ddd, J = 9.4, 8.4, 2.5 Hz, 1 H); **^{13}C NMR** (126 MHz, d_6-acetone + 1 drop D_2O): δ 165.4 (d, J = 256 Hz), 139.3 (d, J = 8.09 Hz), 139.2 (d, J = 2.85 Hz), 134.8 (d, J = 8.61 Hz), 117.5 (d, J = 22.0 Hz), 112.5 (d, J = 20.2 Hz); **^{11}B NMR** (128 MHz, d_6-acetone + 1 drop D_2O): δ 27.6; **^{19}F NMR** (376 MHz, d_6-acetone + 1 drop D_2O) δ −110.23 (td, J = 9.6, 6.0 Hz); **HRMS** (ESI) for $C_7H_5N_2O^{11}B$ (M − H)$^-$: Calculated: 163.0484; Found: 163.0483.
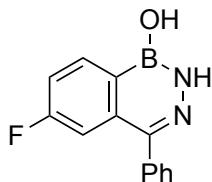
6-Fluoro-4-phenylbenzo[*d*][1,2,3]diazaborinin-1(2*H*)-ol (4-8e): Prepared according to **GP3** from **4-4j** (699 mg, 2.51 mmol), B_2pin_2 (1.27 g, 5.02 mmol), KOAc (985 mg, 10.0 mmol), $PdCl_2$(dppf)·CH_2Cl_2 (205 mg, 0.251 mmol), and dioxane (10 mL). The crude material was subjected to flash column chromatography (20% EtOAc/hexanes), and then used as such for the transesterification reaction (**GP4**: $MeB(OH)_2$ (1.20 g, 20.1 mmol)), followed by the condensation reaction (**GP5**: $NH_2NH_2 \cdot H_2O$ (0.184 mL, 3.77 mmol)). The crude material was added in water (10 mL), filtered, washed with water (10 mL × 3), and then air-dried to furnish the title compound as a white solid (391 mg, 65%); **^{1}H NMR** (400 MHz, d_6-acetone + 1 drop D_2O): δ 7.93 (dd, J = 8.9, 2.8 Hz, 1 H), 7.69 (dd, J = 8.9, 5.1 Hz, 1 H), 7.52 − 7.47 (m, 4 H), 7.47 − 7.40 (m, 2 H); **^{13}C NMR** (126 MHz, d_6-acetone + 1 drop D_2O): δ 163.2 (d, J = 250 Hz), 147.8, 139.6,

133.2 (d, J = 2.37 Hz), 131.1 (d, J = 8.01 Hz), 130.7, 129.2, 128.9, 119.8 (d, J = 23.2 Hz), 116.8 (d, J = 18.9 Hz); ^{11}**B NMR** (128 MHz, d_6-acetone + 1 drop D_2O): δ 27.4; ^{19}**F NMR** (376 MHz, d_6-acetone + 1 drop D_2O) δ –112.96; **HRMS** (ESI) for $C_7H_5N_2O^{11}B$ (M – H)$^-$: Calculated: 241.0943; Found: 241.0946.
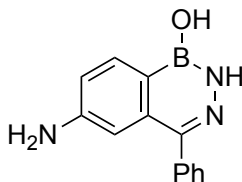
6-Amino-4-phenylbenzo[*d*][1,2,3]diazaborinin-1(2*H*)-ol (4-8f): Prepared according to **GP3** from **4-4h'** (1.00 g, 3.62 mmol), B$_2$pin$_2$ (1.84 g, 7.25 mmol), KOAc (1.42 g, 14.5 mmol), PdCl$_2$(dppf)·CH$_2$Cl$_2$ (296 mg, 0.362 mmol), and dioxane (16 mL). The crude material was subjected to flash column chromatography (20% EtOAc/hexanes), and then used as such for the transesterification reaction (**GP4**: MeB(OH)$_2$ (1.30 g, 21.7 mmol, 6.00 equiv)), followed by the condensation reaction (**GP5**: NH$_2$NH$_2$·H$_2$O (210 μL, 4.34 mmol)). The crude material was added to a solution of saturated aq. NaHCO$_3$ (20 mL), filtered, and the residue was washed with water (10 mL × 3) and Et$_2$O (5 mL), and then air-dried to furnish the title compound as a pale-yellow solid (432 mg, 50%); ^{1}**H NMR** (500 MHz, d_6-acetone + 1 drop D_2O): δ 7.97 (d, J = 8.2 Hz, 1 H), 7.46 – 7.38 (m, 5 H), 6.95 (dd, J = 8.2, 2.1 Hz, 1 H), 6.78 (d, J = 2.2 Hz, 1 H); ^{13}**C NMR** (126 MHz, d_6-acetone + 1 drop D_2O): δ 151.8, 148.2, 140.3, 138.2, 133.3, 130.6, 128.9, 128.4, 117.5, 110.6; ^{11}**B NMR** (128 MHz, d_6-acetone + 1 drop D_2O): δ 27.6; **HRMS** (ESI) for $C_{13}H_{11}N_3O^{11}B$ (M – H)$^-$: Calculated: 236.1001; Found: 236.1001.
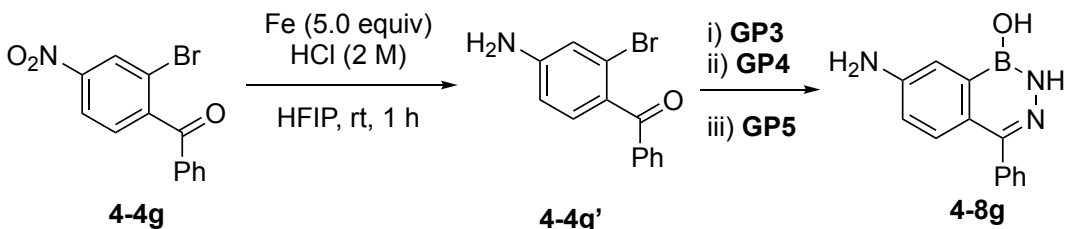
7-Amino-4-phenylbenzo[*d*][1,2,3]diazaborinin-1(2*H*)-ol (4-8g): The starting material (**4-4g'**) for the synthesis of the title compound was prepared by reduction of

the nitro group of **4-4g**.[33] A round bottom flask was charged with **4-4g** (4.33 g, 14.2 mmol) and HFIP (15 mL), followed by the addition of aq. HCl (142 mL, 2 M) and Fe powder (3.96 g, 71.0 mmol). The reaction mixture was stirred at rt for 1 h. Upon completion, saturated aq. NaHCO$_3$ (20 mL) was added and the compound was extracted with EtOAc (10 mL × 3). The combined organic layer was evaporated to afford **4-4g'** as a crude yellow solid (2.91 g, 74%). The title compound was prepared according to **GP3** from the crude **4-4g'** (1.24 g, 4.49 mmol), B$_2$pin$_2$ (2.28 g, 8.98 mmol), KOAc (1.76 g, 18.0 mmol), PdCl$_2$(dppf)·CH$_2$Cl$_2$ (367 mg, 0.449 mmol), and dioxane (20.0 mL). The crude material was passed through Celite® and rinsed with EtOAc (20 mL). The filtrate obtained was evaporated under reduced pressure and the residue was used as such for the transesterification step (**GP4**: MeB(OH)$_2$ (2.15 g, 35.9 mmol)), followed by the condensation reaction (**GP5**: NH$_2$NH$_2$·H$_2$O (330 μL, 6.74 mmol)). The crude material was subjected to preparative HPLC (Agilent C18, 100 × 50 mm, 5 μm using isocratic 70% acetonitrile/water over 11 min with a flow rate of 30 mL/min, R_t = 7.3 min) to afford the title compound as a yellow solid (540 mg, 51%); **^{1}H NMR** (500 MHz, d_6-acetone + 1 drop D$_2$O): δ 7.48 – 7.37 (m, 6 H), 7.34 (d, J = 8.7 Hz, 1 H), 6.95 (dd, J = 8.7, 2.6 Hz, 1 H); **^{13}C NMR** (126 MHz, d_6-acetone + 1 drop D$_2$O): δ 149.6, 148.8, 140.4, 130.7, 130.6, 129.4, 128.4, 127.2, 119.1, 114.47; **^{11}B NMR** (128 MHz, d_6-acetone + 1 drop D$_2$O): δ 27.7; **HRMS** (ESI) for C$_{13}$H$_{11}$N$_3$O^{11}B (M − H)$^-$: Calculated: 236.1001; Found: 236.1001.
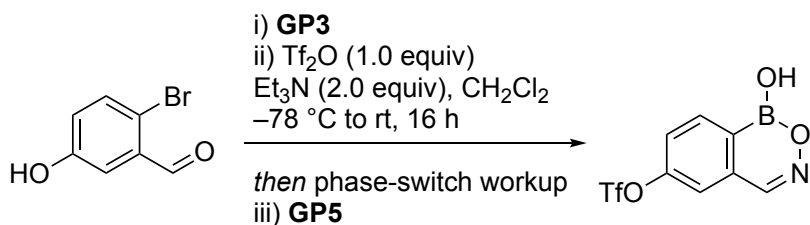
1-Hydroxy-1H-benzo[d][1,2,6]oxazaborinin-6-yl trifluoromethanesulfonate (4-9): Prepared according to **GP3** from 2-bromo-5-hydroxybenzaldehyde (5.00 g, 24.9 mmol), B$_2$pin$_2$ (12.6 g, 49.7 mmol), KOAc (9.76 g, 99.5 mmol), PdCl$_2$(dppf)·CH$_2$Cl$_2$ (1.20 g, 1.49 mmol), and dioxane (60 mL). The crude material was subjected to silica plug (30% EtOAc/hexanes), and the filtrate obtained was evaporated under reduced

pressure to afford a solid residue, which was then dissolved in CH_2Cl_2 (100 mL) in a round bottom flask. The reaction flask was brought down to –78 °C and then Et_3N (6.94 mL, 49.8 mmol) was added. The reaction solution was stirred for 5 min and then Tf_2O (4.18 mL, 24.9 mmol) was added dropwise. The reaction solution was stirred for 16 h under an argon balloon. Upon completion, water (100 mL) was added to the reaction flask and the organic layer was separated. The aqueous layer was again extracted with CH_2Cl_2 (50 mL). The combined organic layer was washed with brine (10 mL) and dried over Na_2SO_4, filtered, and evaporated to dryness. The residue obtained was dissolved in EtOAc (20 mL) followed by the addition of a basic sorbitol solution (30 mL). Sorbitol solution (1 M) was prepared by dissolving Na_2CO_3 (53.0 g, 500 mmol) and sorbitol (91.0 g, 1.11 mol) in water (500 mL).[23] The organic layer was discarded and the pH of the aqueous layer was brought to ~3 with aq. HCl (6 M). The aqueous layer was extracted with EtOAc (20 mL × 3). The combined organic layer was washed with water (10 mL) and brine (10 mL). The organic layer was then dried over Na_2SO_4, filtered, and evaporated under reduced pressure. The solid residue obtained was subjected to the condensation reaction (**GP5**: NH_2OH (50 wt% in water, 3.00 mL, 49.7 mmol)). The crude material obtained was mixed with water (20 mL), and the resulting precipitate was filtered, washed with water (10 mL × 3), and then air-dried to afford the title compound as a white powder (3.66 g, 50% over 3 steps). Note: When the procedure similar to the synthesis of **4-10** (vide infra) was used (i.e., no phase-switch workup after the hydroxy protection reaction) only 18% yield was obtained; **^{1}H NMR** (500 MHz, d_6-acetone + 1 drop D_2O): δ 8.68 (s, 1 H), 8.30 (d, J = 8.3 Hz, 1 H), 7.89 (s, 1 H), 7.80 (d, J = 8.3 Hz, 1 H); **^{13}C NMR** (126 MHz, d_6-acetone + 1 drop D_2O): δ 153.9, 153.4, 149.7, 136.0, 135.7, 125.7, 120.7, 119.7 (q, J = 321 Hz); **^{11}B NMR** (128 MHz, d_6-acetone + 1 drop D_2O) δ 27.5; **^{19}F NMR** (376 MHz, d_6-acetone + 1 drop D_2O) δ –74.04; **HRMS** (ESI) for $C_8H_4SF_3NO_5{}^{11}B$ (M – H)$^-$: Calculated: 293.9861; Found: 293.9861.
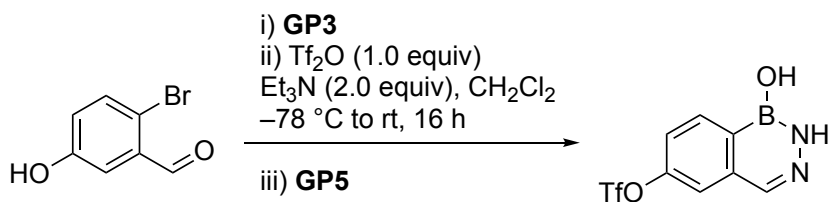
1-Hydroxy-1,2-dihydrobenzo[*d*][1,2,3]diazaborinin-6-yl

trifluoromethanesulfonate (4-10): Prepared according to **GP3** from 2-bromo-5-hydroxybenzaldehyde (5.00 g, 24.9 mmol), B$_2$pin$_2$ (12.6 g, 49.7 mmol), KOAc (9.76 g, 99.5 mmol), PdCl$_2$(dppf)·CH$_2$Cl$_2$ (1.20 g, 1.49 mmol), and dioxane (60 mL). The crude material was subjected to silica plug (30% EtOAc/hexanes), and the filtrate obtained was evaporated under reduced pressure to afford a solid residue, which was then dissolved in CH$_2$Cl$_2$ (100 mL) in a round bottom flask. The reaction flask was brought down to –78 °C and then Et$_3$N (6.94 mL, 49.8 mmol) was added. The reaction solution was stirred for 5 min and then Tf$_2$O (4.18 mL, 24.9 mmol) was added dropwise. The reaction solution was stirred for 16 h under argon. Upon completion, water (100 mL) was added to the reaction flask and the organic layer was separated. The aqueous layer was again extracted with CH$_2$Cl$_2$ (50 mL). The combined organic layer was partially evaporated until ~50 mL of CH$_2$Cl$_2$ was remaining, and then subjected to the condensation reaction (**GP5**: NH$_2$NH$_2$·H$_2$O (2.30 mL, 49.8 mmol)). The crude material obtained was dissolved in EtOAc (50 mL) and washed with a basic sorbitol solution (10 mL × 2), water (10 mL), followed by brine (10 mL). Sorbitol solution (1 M) was prepared by dissolving Na$_2$CO$_3$ (53.0 g, 500 mmol) and sorbitol (91.0 g, 1.11 mol) in water (500 mL).[23] The organic layer was evaporated under reduced pressure and the residue obtained was dissolved in minimum amount of hot CH$_2$Cl$_2$ (5 mL) in a vial followed by the addition of hexanes until the cloudiness persisted. The vial was left in the refrigerator for 30 min and the precipitate formed was filtered, washed with 10% CH$_2$Cl$_2$/hexanes (10 mL), and then air-dried to afford the title compound as a white solid (1.28 g, 18% over 3 steps); **^{1}H NMR** (400 MHz, d_6-acetone + 1 drop D$_2$O): δ 8.39 (d, J = 8.4 Hz, 1 H), 8.13 (s, 1 H), 7.87 (d, J = 2.4 Hz, 1 H), 7.64 (dt, J = 8.6, 2.7 Hz, 1 H); **^{13}C NMR** (126 MHz, d_6-acetone + 1 drop D$_2$O): δ 152.4, 138.9, 138.8, 135.2, 122.4, 119.8 (q, J = 321 Hz), 119.8; **^{11}B NMR** (128 MHz,

d_6-acetone + 1 drop D_2O): δ 27.4; **^{19}F NMR** (376 MHz, d_6-acetone + 1 drop D_2O) δ – 74.15 – –74.19 (m); **HRMS** (ESI) for $C_8H_5F_3SN_3O_4$[11]B (M – H)⁻: Calculated: 3293.0021; Found: 293.0021.

4.9.6 Oxime Reduction

4.9.6.1 Attempted Oxime Reduction

H₂/Pd-C Reduction: To a flame dried round bottom flask, Pd-C (10% loading of Pd on C, 33 mg, 30 μmol, 0.20 equiv) was added and the reaction flask was sealed with a septum. The reaction flask was placed under vacuum and then refilled with nitrogen. Heterocycle **4-7b** (25 mg, 0.55 mmol, 1.0 equiv) dissolved in EtOAc (4 mL) was charged into the reaction flask and then the vacuum was applied for a brief moment to remove the gases from the headspace and quickly the H_2 balloon was inserted. The reaction mixture was stirred at rt for 3 h. The reaction resulted in a N—O cleaved product as was observed by LC-MS analysis.

S-CBS/BH₃·THF Reduction:[63] In a flame dried round bottom flask under argon environment, *S*-2-methyl-CBS-oxazaborolidine (34 mg, 0.12 mmol) dissolved in THF (1 mL) was charged, and the reaction solution was cooled down to 0 °C. BH_3 (1 M in THF, 28 mg, 0.37 mmol) was added, along with **4-7b** (20 mg, 0.12 mmol), and the reaction mixture was stirred at rt for 16 h. No desired product was observed by ^{1}H NMR spectroscopy.

NaBH₄ Reduction: In a round bottom flask, **4-7b** (20 mg, 0.12 mmol) dissolved in EtOH (2 mL) was charged, followed by the addition of $NaBH_4$ (47 mg, 1.2 mmol). The reaction was stirred at rt for 3 h. No reaction was observed by LC-MS analysis or by ^{1}H NMR spectroscopy.

NaBH₄/NiCl₂·6H₂O Reduction:[64] To a solution of **4-7b** (10 mg, 0.060 mmol) in MeOH (3 mL), added $NiCl_2·6H_2O$ (30 mg, 0.12 mmol) followed by the addition of $NaBH_4$ (12 mg, 0.31 mmol). Reaction mixture was stirred at rt for 2.5 h. Upon completion, the crude material showed the presence of exclusively N—O cleaved product by ^{1}H NMR spectroscopy and LC-MS; **^{1}H NMR** (400 MHz, d_6-acetone + 1

drop D_2O): δ 7.69 (d, J = 7.4 Hz, 1 H), 7.51 (d, J = 7.9 Hz, 1 H), 7.43 (td, J = 7.6, 1.6 Hz, 1 H), 7.32 (tt, J = 7.4, 2.1 Hz, 1 H), 4.95 (q, J = 6.9 Hz, 1 H), 1.63 (dd, J = 6.9, 1.5 Hz, 3 H); **^{11}B NMR** (128 MHz, d_6-acetone + 1 drop D_2O): δ 29.1.

NaBH$_4$/NiCl$_2$ Reduction: To a solution of **4-7b** (10 mg, 0.060 mmol), added NiCl$_2$ (16 mg, 0.12 mmol) and MeOH (3 mL), followed by the addition of NaBH$_4$ (12 mg, 0.31 mmol). Reaction mixture was stirred at rt for 2.5 h. The crude material showed the presence of unreacted **4-7b** by LC-MS analysis.

NaEt$_3$BH Reduction: To a solution of **4-7b** (10 mg, 0.060 mmol) in THF (3 mL), added NaEt$_3$BH (1 M in toluene, 0.13 mL, 0.12 mmol). The reaction mixture was stirred at rt for 16 h. No reaction was observed by LC-MS analysis.

(*t*BuO)$_3$AlHLi Reduction: To a solution of **4-7b** (10 mg, 0.060 mmol) in THF (3 mL), added (*t*BuO)$_3$AlHLi (32 mg, 0.12 mmol). The reaction mixture was stirred at rt for 2.5 h. No reaction was observed by LC-MS analysis.

CuCl/NaBH$_4$ Reduction: To a solution of **4-7b** (10 mg, 0.060 mmol) in THF (2 mL), added CuCl (13 mg, 0.12 mmol) followed by the addition of NaBH$_4$ (12 mg, 0.31 mmol). The reaction mixture was stirred at rt for 2.5 h. No reaction was observed by LC-MS analysis.

NaBH$_4$/ZrCl$_4$/Al$_2$O$_3$ Reduction:[65] ZrCl$_4$ (14.5 mg, 0.0620 mmol) and Al$_2$O$_3$ (6.30 mg, 0.0620 mmol) were grounded using mortar and pestle. Heterocycle **4-7b** (10.0 mg, 0.0620 mmol) was added followed by the addition of NaBH$_4$ (12.0 mg, 0.310 mmol). All the contents in the mortar were grounded for 5 min. No desired product was observed by ^{1}H NMR spectroscopy.

PhMe$_2$SiH Reduction:[66] To a solution of **4-1** (20 mg, 0.14 mmol) in TFA/CH$_2$Cl$_2$ (2 mL, 1:1), added PhMe$_2$SiH (22 mg, 0.16 mmol). The reaction mixture was stirred at rt for 16 h. No reaction was observed by LC-MS analysis.

Ph$_2$SiH$_2$/Wilkinson's Catalyst Reduction: To a solution of **4-1** (20 mg, 0.14 mmol) in CH$_2$Cl$_2$ (2 mL), added Ph$_2$SiH$_2$ (38 mg, 0.20 mmol) and Wilkinson's catalyst (13 mg, 0.010 mmol). The reaction mixture was stirred at rt for 16 h. No desired product was observed by LC-MS analysis.

Luche Reduction of 4-1: To a solution of **4-1** (200 mg, 1.36 mmol) in EtOH (10 mL), added CeCl$_3$·7H$_2$O (3.00 g, 8.16 mmol), followed by the portion-wise addition of NaBH$_4$ (517 mg, 13.6 mmol) (~50 mg every two min). The reaction mixture was stirred at rt for 16 h. Again, CeCl$_3$·7H$_2$O (3.00 g, 8.16 mmol) was added, followed by the portion-wise addition of NaBH$_4$ (517 mg, 13.6 mmol) (~50 mg every two min). The reaction mixture was stirred at rt for 5 h. Upon completion, the reaction was quenched by the addition of aq. HCl (50 mL, 2 M). The solvent was evaporated, which resulted in a white solid containing the reduced product and excess of borates and Ce salts (>96% conversion); **^{1}H NMR** (500 MHz, D$_2$O): δ 7.58 (d, J = 3.6 Hz, 1 H), 7.40 – 7.32 (m, 2 H), 7.26 – 7.22 (m, 1 H), 4.45 (s, 2 H). ^{11}B NMR spectroscopy showed only the intense peak of boric acid by product (~19 ppm). Full characterization of the reduced product shown in Section 4.9.6.2

Luche Reduction of 4-7b: To a solution of **4-7b** (200 mg, 1.24 mmol) in EtOH (10 mL), added CeCl$_3$·7H$_2$O (2.80g, 7.45 mmol), followed by the portion-wise addition of NaBH$_4$ (471 mg, 12.4 mmol) (~50 mg every two min). The reaction mixture was stirred at rt for 16 h. Again, CeCl$_3$·7H$_2$O (2.80g, 7.45 mmol) was added, followed by the portion-wise addition of NaBH$_4$ (471 mg, 12.4 mmol) (~50 mg every two min). The reaction mixture was stirred at rt for 5 h. Upon completion, the reaction was quenched by the addition of aq. HCl (50 mL, 2 M). The solvent was evaporated, which resulted in a white solid containing the reduced product and excess of borates and Ce salts (>96% conversion); **^{1}H NMR** (400 MHz, D$_2$O): δ 7.74 (t, J = 4.0 Hz, 1 H), 7.47 (dd, J = 5.6, 3.3 Hz, 2 H), 7.33 (dd, J = 5.5, 3.6 Hz, 1 H), 4.75 (q, J = 7.0 Hz, 1 H), 1.71 (d, J = 6.9 Hz, 3 H). ^{11}B NMR spectroscopy showed only the intense peak of boric acid by product (~19 ppm). Full characterization of the reduced product shown in Section 4.8.6.2.
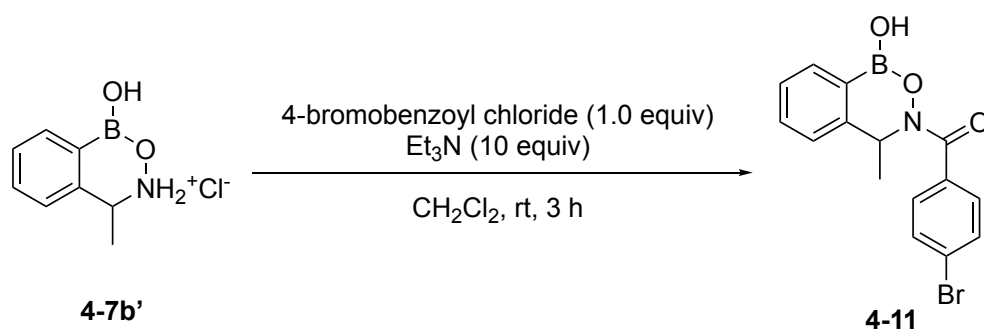
The crude product (**4-7b'**) obtained after the reduction reaction of **4-7b** was charged in a round bottom flask and CH_2Cl_2 (28 mL) was added, followed by the addition of Et_3N (1.70 mL, 124 mmol). The reaction contents were stirred for 10 min. To initiate the amidation reaction, 4-bromobenzoyl chloride (272 mg, 1.24 mmol) was added and the reaction mixture was stirred at rt for 3 h. Upon completion, aq. HCl (50 mL, 1 M) was added, followed by the extraction with EtOAc (10 mL × 3). The organic layer was combined and then evaporated under reduced pressure. ^{1}H NMR spectroscopy of the crude material revealed the formation of the amide product **4-11**, along with 2-bromobenzoic acid. A portion of the crude material (20 mg) was dissolved in hot acetonitrile in a 2-dram vial and 1 drop of water was added, which resulted in the needle shaped colorless crystals. X-ray crystallographic analysis confirmed the formation of the desired product, which confirmed that **4-7b'** was indeed the desired product (cf. Figure 4.8). **^{1}H NMR** (498 MHz, d_6-acetone + 1 drop D$_2$O): δ 7.82 (d, J = 7.4 Hz, 1 H), 7.58 – 7.65 (m, 4 H), 7.48 – 7.52 (m, 1 H), 7.33 (t, J = 7.4 Hz, 2 H), 5.86 (br s, 1 H), 1.47 (d, J = 6.9 Hz, 3 H).

Attempted Luche Reduction of 4-7a: To a solution of **4-7a** (10.0 mg, 0.0450 mmol) in EtOH (3 mL), added $CeCl_3 \cdot 7H_2O$ (100 mg, 0.270 mmol), followed by the portion-wise addition of NaBH$_4$ (17.1 mg, 0.450 mmol) (~5 mg every two min). The reaction mixture was stirred at rt for 16 h. Again, $CeCl_3 \cdot 7H_2O$ (100 mg, 0.270 mmol) was added, followed by the portion-wise addition of NaBH$_4$ (17.1 mg, 0.450 mmol) (~5 mg every two min). The reaction mixture was stirred at rt for 5 h. No reaction was observed.

4.9.6.2 Ir-Catalyzed Oxime Hydrogenation

Synthesis of Ir Catalyst 4-12 for the Oxime Hydrogenation
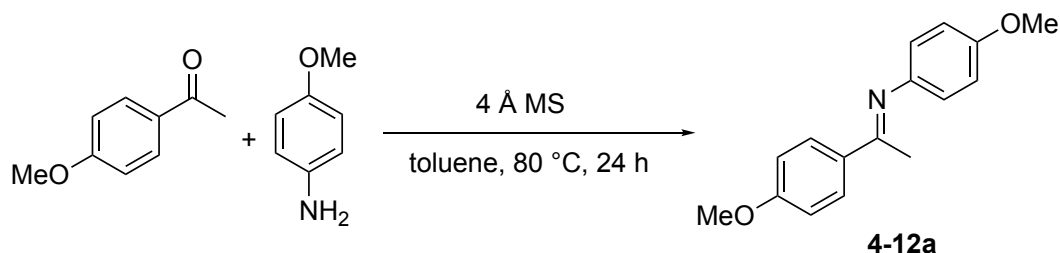
4-12a

The precursor (**4-12a**) for the synthesis of Ir catalyst was prepared by following a literature procedure.[67] In a flame dried round bottom flask, a mixture of aniline (410 mg, 3.33 mmol), ketone (500 mg, 3.33 mmol), and MS (4 Å, 100 mg) was added, followed by the addition of anhydrous toluene (6 mL). The reaction mixture was heated at 80 °C under N_2 for 24 h. Upon completion, the resulting suspension was filtered through Celite® and the filtrate was evaporated under reduced pressure to afford **4-7a** as a pale yellow solid, which was used as such for the next step (519 mg, 61%); **^{1}H NMR** (400 MHz, $CDCl_3$): δ 7.90 (d, J = 9.0 Hz, 2 H), 6.92 (d, J = 9.1 Hz, 2 H), 6.87 (d, J = 8.9 Hz, 2 H), 6.71 (d, J = 8.9 Hz, 2 H), 3.84 (s, 3 H), 3.79 (s, 3 H), 2.19 (s, 3 H).
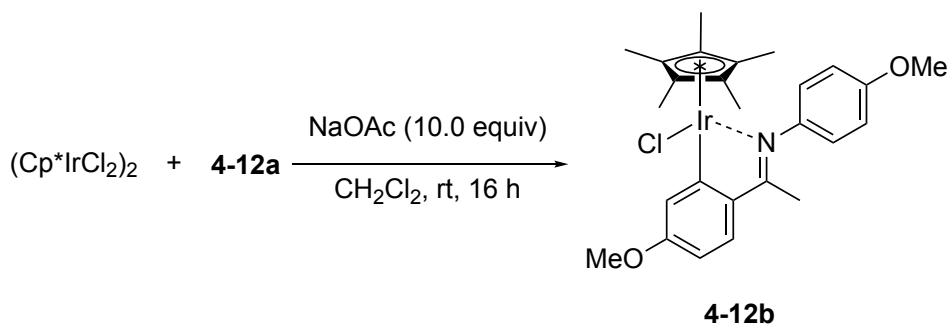
4-12b

The precursor (**4-12b**) for the synthesis of Ir catalyst was prepared by following a literature procedure.[68] A flame dried Schlenk tube was charged with **4-12a** (70.4 mg, 0.276 mmol), iridium chloride dimeric complex (Cp*IrCl$_2$)$_2$ (100 mg, 0.125 mmol), and NaOAc (103 mg, 1.25 mmol), followed by the addition of anhydrous CH_2Cl_2 (10 mL) under N_2. The Schlenk tube was degassed and recharged with N_2 (× 3). The resulting mixture was stirred at rt for 16 h. Upon completion, the reaction contents were filtered through Celite® and rinsed with CH_2Cl_2 (10 mL). The filtrate obtained was

dried over MgSO₄, filtered, and evaporated under reduced pressure. The crude material obtained was dissolved in Et$_2$O (3 mL), followed by the addition of hexanes (1 mL), which resulted in the precipitation of **4-12b**, which was filtered and air-dried to afford an orange-colored solid (149 mg, 96%); **¹H NMR** (600 MHz, CDCl$_3$): δ 7.45 (d, *J* = 8.5 Hz, 1 H), 7.34 (d, *J* = 2.5 Hz, 1 H), 6.93 (br s, 4 H), 6.58 (dd, *J* = 8.5, 2.5 Hz, 1 H), 3.91 (s, 3 H), 3.85 (s, 3 H), 2.38 (s, 3 H), 1.44 (s, 15 H).

4-12b → MsOAg (1.0 equiv), CHCl$_3$, rt, 18 h, **95%** → **4-12**
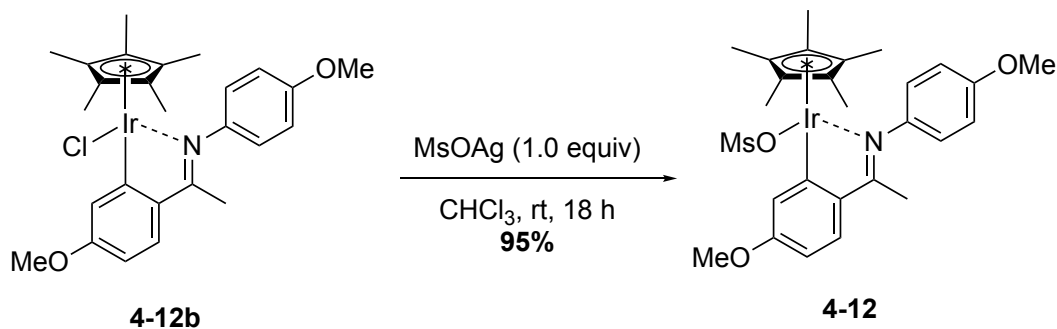
A modification of the literature procedure was employed for the synthesis of Ir catalyst **4-12**.[34] In a flame dried microwave vial, MsOAg (49.0 mg, 0.241 mmol) and **4-12b** (149 mg, 0.241 mmol) was added, followed by the addition of CHCl$_3$ (4 mL) under N$_2$. The reaction mixture was stirred at rt for 18 h. Upon completion, the reaction contents were filtered through Celite® and rinsed with CHCl$_3$ (10 mL). The filtrate obtained was dried over MgSO₄, filtered, and evaporated under reduced pressure to furnish **4-12** as an orange solid (158 mg, 95%); **¹H NMR** (600 MHz, CDCl$_3$): δ 7.69 (d, *J* = 2.5 Hz, 1 H), 7.44 (d, *J* = 8.5 Hz, 1 H), 6.97 (br s, 4 H), 6.62 (dd, *J* = 8.5, 2.5 Hz, 1 H), 3.93 (s, 3 H), 3.85 (s, 3 H), 2.32 (s, 3 H), 1.77 (s, 3 H), 1.41 (s, 15 H).

Oxime Hydrogenation of Benzoxazaborines using 4-12 as a Catalyst[34]
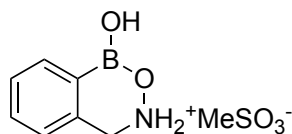
Synthesis of Reduced 4-1 (4-13): A microwave vial equipped with a magnetic stir bar was charged with **4-1** (50 mg, 0.34 mmol) and **4-12** (2.3 mg, 1.0 mol%). The vial was sealed with a septum and then MeSO$_3$H (33 μL, 0.35 mmol) in MeOH (1 mL) was

added. The septum was pierced with a needle and the reaction vessel (with the needle) was placed in a high-pressure hydrogenation reactor. The hydrogenation reactor was purged with H_2 ($\times$ 3) and then pressurized to 725 psi. The reaction solution was stirred at rt for 16 h. Upon completion, the reactor was depressurized and water (5 mL) was added in the reaction flask. The catalyst impurities were extracted with CH_2Cl_2 (5 mL) and the aqueous layer was evaporated under reduced pressure to furnish the desired product **4-13** as a yellow oil (quant. conversion); **^{1}H NMR** (400 MHz, D_2O): δ 7.56 (t, J = 4.4 Hz, 1 H), 7.40 – 7.31 (m, 2 H), 7.26 – 7.18 (m, 1 H), 4.41 (s, 2 H), 2.71 (s, 3 H, overlaps with $MeSO_3H$); **^{13}C NMR** (126 MHz, D_2O): δ 133.1, 131.9, 129.2, 128.3, 126.6, 50.3, 38.4; **^{11}B NMR** (128 MHz, D_2O): δ 10.3; **HRMS** (ESI) for $C_7H_9NO_2^{11}B$ (M + H)$^+$: Calculated: 150.0721; Found: 150.0721.
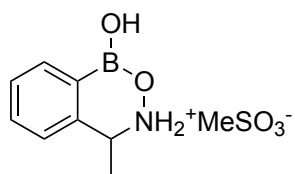
Synthesis of Reduced 4-7b (4-14): A microwave vial equipped with a magnetic stir bar was charged with **4-7b** (200 mg, 1.24 mmol) and **4-12** (9.00 mg, 1.00 mol %). The vial was sealed with a septum and then $MeSO_3H$ (120 μL, 0.310 mmol) in MeOH (4 mL) was added. The septum was pierced with a needle and the reaction vessel (with the needle) was placed in a high-pressure hydrogenation reactor. The hydrogenation reactor was purged with H_2 ($\times$ 3) and then pressurized to 725 psi. The reaction solution was stirred at rt for 16 h. Upon completion, the reactor was depressurized and water (5 mL) was added in the reaction flask. The catalyst impurities were extracted with CH_2Cl_2 (5 mL) and the aqueous layer was evaporated under reduced pressure to furnish the desired product **4-14** as a yellow oil (quant. conversion); **^{1}H NMR** (400 MHz, D_2O): δ 7.55 (dd, J = 5.7, 2.8 Hz, 1 H), 7.41 – 7.34 (m, 2 H), 7.25 – 7.21 (m, 1 H), 4.65 (q, J = 6.9 Hz, 1 H), 2.76 (s, 3 H, overlaps with $MeSO_3H$), 1.59 (d, J = 6.9 Hz, 3 H); **^{13}C NMR** (176 MHz, D_2O): δ 139.8, 132.3, 129.7, 128.8, 125.5, 56.7, 39.3, 17.5; **^{11}B NMR** (128 MHz, D_2O): δ 6.7.

The image depicts a chemical structure showing a benzoxaborole derivative with fluorine substituent, an OH group on boron, and NH₂⁺MeSO₃⁻.
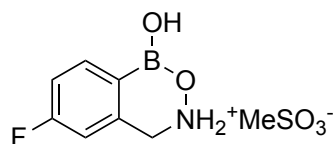
Synthesis of Reduced 4-7d (4-15): A microwave vial equipped with a magnetic stir bar was charged with **4-7d** (50 mg, 0.30 mmol) and **4-12** (2.0 mg, 1.0 mol %). The vial was sealed with a septum and then $MeSO_3H$ (19 μL, 0.31 mmol) in MeOH (1 mL) was added. The septum was pierced with a needle and the reaction vessel (with the needle) was placed in a high-pressure hydrogenation reactor. The hydrogenation reactor was purged with H_2 (× 3) and then pressurized to 725 psi. The reaction solution was stirred at rt for 16 h. Upon completion, the reactor was depressurized and water (5 mL) was added in the reaction flask. The catalyst impurities were extracted with CH_2Cl_2 (5 mL) and the aqueous layer was evaporated under reduced pressure to furnish the desired product **4-15** as a yellow oil (quant. conversion); **¹H NMR** (400 MHz, D_2O): δ 7.53 (s, 1 H), 7.15 – 7.06 (m, 1 H), 6.98 (dd, J = 10.1, 2.5 Hz, 1 H), 4.42 (s, 2 H), 2.79 (s, 3 H, overlaps with $MeSO_3H$); **¹³C NMR** (126 MHz, D_2O): δ 162.5 (d, J = 244 Hz), 135.6, 133.8, 115.0 (d, J = 19.9 Hz), 112.5, 49.6, 38.5; **¹¹B NMR** (128 MHz, D_2O): δ 6.4; **¹⁹F NMR** (376 MHz, D_2O): δ –113.90; **HRMS** (ESI) for $C_7H_8FNO_2{}^{11}B$ $(M + H)^+$: Calculated: 168.0627; Found: 168.0628.

Attempted Synthesis of Reduced 4-7a (4-16): A microwave vial equipped with a magnetic stir bar was charged with **4-7a** (10 mg, 0.045 mmol) and **4-12** (0.30 mg, 1.0 mol %). The vial was sealed with a septum and then $MeSO_3H$ (5.0 μL, 0.067 mmol) in MeOH (0.3 mL) was added. The septum was pierced with a needle and the reaction vessel (with the needle) was placed in a high-pressure hydrogenation reactor. The hydrogenation reactor was purged with H_2 (× 3) and then pressurized to 725 psi. The reaction solution was stirred at rt for 16 h. No reaction was observed.

4.9.7 Protection of Benzoxazaborine
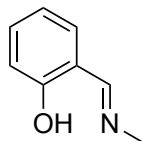
(*E*)-2-((methylimino)methyl)phenol: Protecting group for the benzoxazaborine protection was synthesized following a literature procedure.[25] In a round bottom flask, salicylaldehyde (6.90 g, 56.6 mmol) in EtOH (150 mL) was charged, followed by the addition of MeNH$_2$ (40 wt % in water, 3.51 g, 113 mmol). The reaction solution was stirred at rt for 6 h, and the solvent was removed under reduced pressure to afford a yellow oil, which was used without further purification (6.36 g, 83%); **^{1}H NMR** (400 MHz, d_6-acetone): δ 8.50 (s, 1 H), 7.37 (dd, *J* = 8.4, 1.7 Hz, 1 H), 7.31 (td, *J* = 8.1, 1.7 Hz, 1 H), 6.88 (dd, *J* = 8.0, 6.4 Hz, 2 H), 3.48 (s, 3 H).
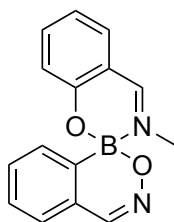
Protection of 4-1 with salicimine (4-17): Prepared by following a literature procedure.[25] Salicimine (239 mg, 1.77 mmol) and **4-1** (200 mg, 1.36 mmol) were charged in a round bottom flask, followed by the addition of toluene (12 mL). The reaction vessel was fitted with a Dean-Stark apparatus and was heated at reflux for 16 h. Upon completion, the solvent was removed under reduced pressure and the crude product obtained was subjected to flash column chromatography (EtOAc containing 0.5% Et$_3$N) to afford the title compound as a pale-yellow solid (291 mg, 81%); **^{1}H NMR** (400 MHz, d_6-acetone): δ 8.72 (s, 1 H), 7.94 (s, 1 H), 7.60 – 7.56 (m, 2 H), 7.48 – 7.37 (m, 3 H), 7.37 – 7.28 (m, 1 H), 6.97 (td, *J* = 7.5, 1.0 Hz, 1 H), 6.90 – 6.83 (m, 1 H), 3.18 (s, 3 H); **^{11}B NMR** (128 MHz, d_6-acetone): δ 3.5.
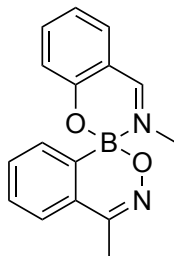
Protection of 4-7b with salicimine (4-18): Prepared by following a literature procedure.[25] Salicimine (21.8 mg, 0.160 mmol) and **4-7b** (20.0 mg, 0.124 mmol) were charged in a round bottom flask, followed by the addition of toluene (3 mL). The reaction vessel was fitted with a Dean-Stark apparatus and was heated at reflux for 16 h. Upon completion, the solvent was removed under reduced pressure and the crude product obtained was subjected to flash column chromatography (EtOAc containing 0.5% Et₃N) to afford the title compound as a white solid (19 mg, 56%); **¹H NMR** (400 MHz, d_6-acetone): δ 8.71 (s, 1 H), 7.61 – 7.52 (m, 2 H), 7.51 – 7.47 (m, 1 H), 7.44 – 7.38 (m, 3 H), 6.94 (td, J = 7.4, 1.1 Hz, 1 H), 6.88 – 6.81 (m, 1 H), 3.17 (s, 3 H), 2.32 (s, 3 H); **¹¹B NMR** (128 MHz, d_6-acetone): δ 3.6.
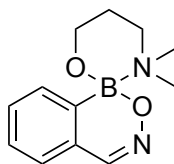
Protection of 4-1 with 3-dimethylaminopropanol (4-19): Prepared by following a literature procedure.[25] To a flame dried round bottom flask, 3-dimethylaminopropanol (70.8 mg, 0.690 mmol), **4-1** (100 mg, 0.680 mmol), and Na₂CO₃ (773 mg, 5.44 mmol) were added, followed by the addition of ether/acetone (1:1, 4 mL) under N₂. The reaction mixture was stirred at rt for 16 h. Upon completion, the reaction contents were filtered and the filtrate was evaporated under reduced pressure to afford the title compound as a hygroscopic solid (150 mg, 95%); **¹H NMR** (400 MHz, CDCl₃): δ 7.94 (s, 1 H), 7.65 (d, J = 7.2 Hz, 1 H), 7.46 (td, J = 7.3, 1.3 Hz, 1 H), 7.39 (td, J = 7.5, 1.5 Hz, 1 H), 7.21 (d, J = 7.5 Hz, 1 H), 4.13 (q, J = 7.1 Hz, 2 H), 3.22 (br s, 2 H), 2.32 (s, 6 H), 1.94 (br s, 2 H); **¹¹B NMR** (128 MHz, CDCl₃): δ 4.9.
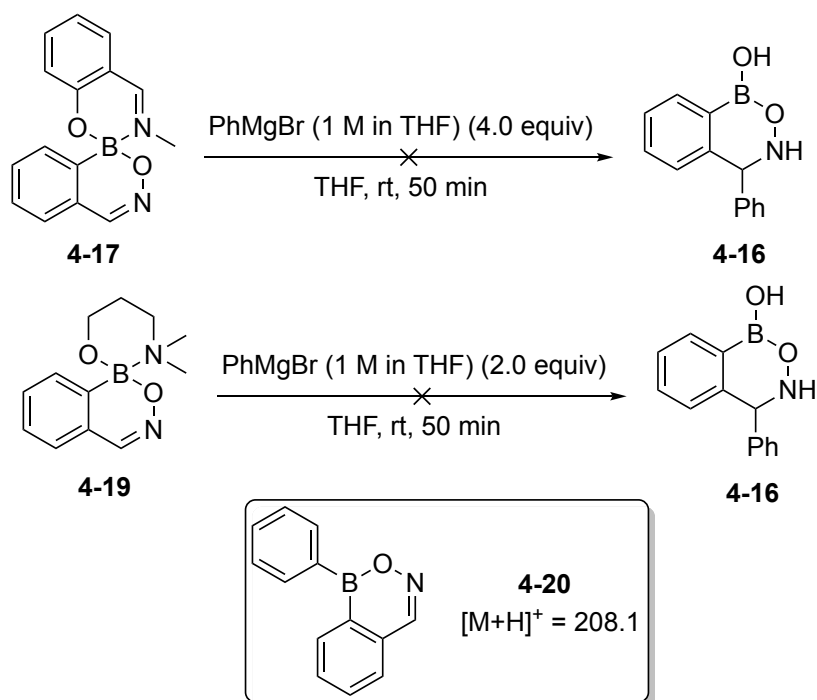
Attempted synthesis of 4-16: To a flame dried round bottom flask, **4-17** (20 mg, 0.076 mmol) was added, followed by the addition of anhydrous THF (3 mL) under N$_2$. PhMgBr (0.30 mL, 1 M in THF) was added dropwise to the reaction flask at rt. The reaction solution was stirred at that temperature for 50 min. The LC-MS spectrum of the crude reaction mixture showed the presence of **4-20**, indicating the desired product **4-16** was not formed. Another attempt was made by using **4-19** as the precursor. To a flame dried round bottom flask, **4-19** (70 mg, 0.030 mmol) was added, followed by the addition of anhydrous THF (4 mL) under N$_2$. PhMgBr (0.61 mL, 1 M in THF) was added dropwise to the reaction flask at rt. The reaction solution was stirred at that temperature for 50 min. The LC-MS spectrum of the crude reaction mixture just showed the presence of **4-20**, indicating the desired product **4-16** was not formed.

4.9.8 Bromination of 4-7g
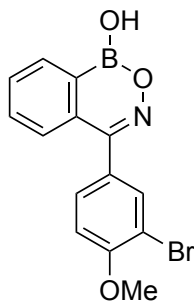
4-(3-bromo-4-methoxyphenyl)-1*H*-benzo[*d*][1,2,6]oxazaborinin-1-ol (4-21): NBS (35.2 mg, 0.198 mmol) and **4-7g** (25.0 mg, 99.0 µmol) were charged in a round bottom flask followed by the addition of CH$_3$CN (1 mL). The reaction solution was stirred at rt for 16. Upon completion, the solvent was removed under reduced pressure and then water (5 mL) was added. The suspension obtained was filtered, washed with water (10 mL), and then air-dried to afford the title compounds as a pale-yellow solid (25 mg, 77%). Instead of CH$_3$CN, DMF as a solvent can be employed as well; **^{1}H NMR** (400 MHz, *d$_6$*-acetone + 1 drop D$_2$O): δ 8.23 – 8.10 (m, 1 H), 7.80 – 7.71 (m, 3 H), 7.53 (dd, *J* = 8.5, 2.1 Hz, 1 H), 7.49 – 7.44 (m, 1 H), 7.25 (d, *J* = 8.5 Hz, 1 H), 3.98 (s, 3 H); **^{13}C NMR** (126 MHz, *d$_6$*-acetone + 1 drop D$_2$O): δ 159.0, 157.7, 135.0, 134.0, 133.8, 133.2, 132.5, 131.3, 129.0, 128.1, 113.2, 111.9, 57.0; **^{11}B NMR** (128 MHz, *d$_6$*-acetone + 1 drop D$_2$O): δ 28.6; **HRMS** (ESI) for C$_{14}$H$_{12}$NBrO$_3$^{11}B (M + H)$^+$: Calculated: 332.0088; Found: 332.0080.

4.9.9 Amidation Reactions
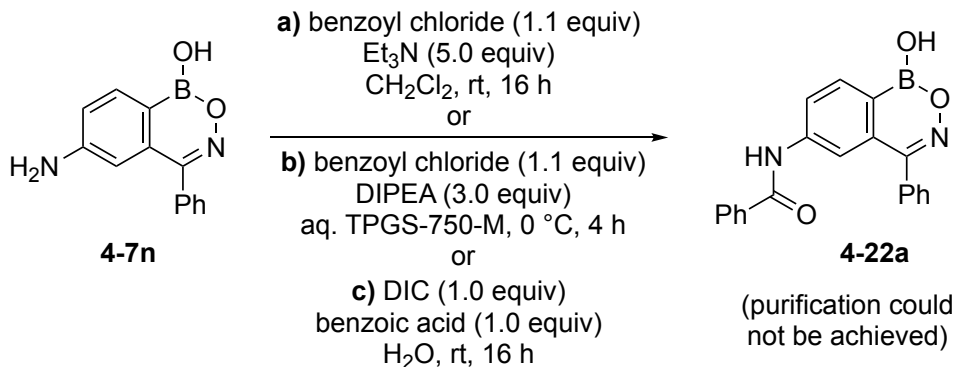
Attempted Synthesis and Purification of 4-22a: a) To a round bottom flask, **4-7n** (25.0 mg, 0.105 mmol) was charged, followed by the addition of CH_2Cl_2 (2 mL). Et_3N (73.0 μL, 0.525 mmol) was added to the reaction flask, followed by the addition of benzoyl chloride (17.7 mg, 0.126 mmol). The reaction solution was stirred at rt for 16 h. LC-MS analysis of the crude material showed the presence of **4-22a**, along with undetermined impurities. The crude material was dissolved in EtOAc (5 mL) and water (5 mL) with a pH of 2.3 was added. The organic layer was separated, dried over Na_2SO_4, filtered, and then evaporated under reduced pressure. LC-MS analysis of the residue showed the presence of benzoic acid, desired product **4-22a**, and other undetermined impurities. Trituration with Et_2O also did not afford the pure desired product. **b)**[38] To a round bottom flask, **4-7n** (25.0 mg, 0.105 mmol) was charged, followed by the addition of DIPEA (5.00 μL, 0.315 mmol). The reaction flask was placed in the ice bath and aq. 2 wt% TPGS-750-M (1 mL) was added, followed by the addition of benzoyl chloride (17.7 mg, 0.126 mmol). The reaction solution was stirred at that temperature for 4 h. LC-MS of the crude material showed the presence of **4-22a**, along with the precursor **4-7n**, and undetermined impurities. The purification was attempted by addition of aq. HCl (5 mL), and the suspension was filtered, which did not result in the pure desired product. Trituration with Et_2O also did not afford the pure product. **c)** To a round bottom flask, benzoic acid (12.8 mg, 0.105 mmol) was added in H_2O (2 mL), followed by the addition of DIC (13.3 mg, 0.105 mmol), and the reaction mixture was stirred for 1 h. After this period, **4-7n** (25.0 mg, 0.105 mmol) was added and the reaction mixture was stirred at rt for 16 h. LC-MS of the crude material showed the presence of **4-22a**, along with the precursor **4-7n**, and other undetermined impurities. The purification was attempted by addition of aq. HCl (5 mL, 2 M), and the suspension was filtered, which did not result in the pure desired product. A phase-switch workup was also attempted by using basic sorbitol solution, but did not result in the pure product. Finally, recrystallization attempt with EtOAc/hexanes also did not afford the pure desired product.

General Procedure for the Amide Formation Reaction (GP6)[39]

Aniline analog of the boron heterocycle (1.0 equiv) was charged in a round bottom flask, followed by the addition of NMP (0.5 mL) and the corresponding acyl chloride (1.1 equiv). The reaction solution was stirred at rt for 2 h.

In the case of **4-1** derivatives, after the completion of the reaction, a phase-switch workup was required, where basic sorbitol solution (10 mL) was added to the reaction flask, followed by the extraction with EtOAc (10 mL). Sorbitol solution (1 M) was prepared by dissolving Na_2CO_3 (53.0 g, 0.500 mol) and sorbitol (91.0 g, 1.11 mol) in water (500 mL).[23] The organic layer was discarded and the pH of the aqueous layer was brought to ~3 with aq. HCl (6 M). The aqueous layer was extracted with EtOAc (10 mL × 3). The combined organic layer was washed with water (5 mL) and then with brine (5 mL). The organic layer was then dried over Na_2SO_4, filtered, and evaporated under reduced pressure to afford the desired product, along with alkane or arene carboxylic acid and some residual NMP.

In the case of **4-2a** derivatives, after the completion of the reaction, saturated aq. $NaHCO_3$ (10 mL) was added followed by the extraction with EtOAc (10 mL × 3). The combined organic layer was then dried over Na_2SO_4, filtered, and evaporated under reduced pressure to afford the desired product, along with some residual NMP.

Generally, the final organic residue obtained after the workup was dissolved in minimum amount of hot EtOAc or hot CH_2Cl_2 (~2 mL) in a vial, followed by the addition of hexanes (~0.5 mL). The precipitate was formed overnight after leaving the vial in the refrigerator, which was filtered, washed with hexanes (5 mL), and then air-dried to afford the desired product.
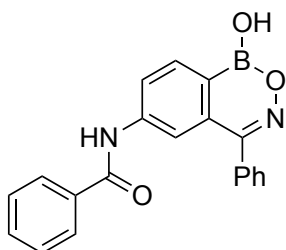
***N*-(1-hydroxy-4-phenyl-1*H*-benzo[*d*][1,2,6]oxazaborinin-6-yl)benzamide (4-22a):**
Prepared according to **GP6** from **4-7n** (60.0 mg, 0.235 mmol), NMP (0.5 mL), and

benzoyl chloride (36.4 mg, 0.259 mmol). Purification was achieved by a phase-switch workup followed by recrystallization with EtOAc/hexanes to afford the title compound as a pale-yellow crystalline solid (73 mg, 91%); **^{1}H NMR** (500 MHz, d_6-acetone + 1 drop D$_2$O): δ 8.23 (dd, J = 8.2, 2.0 Hz, 1 H), 8.15 (d, J = 8.2 Hz, 1 H), 7.95 (d, J = 2.0 Hz, 1 H), 7.93 – 7.87 (m, 2 H), 7.58 – 7.47 (m, 6 H), 7.47 – 7.40 (m, 2 H); **^{13}C NMR** (126 MHz, d_6-acetone + 1 drop D$_2$O): δ 166.9, 160.3, 144.3, 135.7, 135.5, 135.1, 134.0, 132.8, 130.6, 130.0, 129.4, 129.4, 128.5, 124.1, 118.7; **^{11}B NMR** (128 MHz, d_6-acetone + 1 drop D$_2$O): δ 28.7; **HRMS** (ESI) for C$_{20}$H$_{14}$N$_2$O$_3$^{11}B (M − H)$^−$: Calculated: 341.1103; Found: 341.1103.

The crystals obtained after EtOAc/hexanes recrystallization were also suitable for X-ray crystallographic analysis (cf. Figure 4.12).
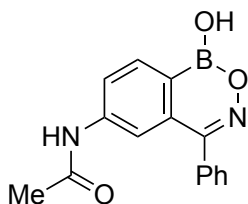
***N*-(1-hydroxy-4-phenyl-1*H*-benzo[*d*][1,2,6]oxazaborinin-6-yl)acetamide (4-22b):** Prepared according to **GP6** from **4-7n** (60.0 mg, 0.235 mmol), NMP (0.5 mL), and acetyl chloride (20.3 mg, 0.259 mmol). Purification was achieved by a phase-switch workup followed by recrystallization with EtOAc/hexanes to afford the title compound as a pale-yellow solid (61 mg, 93%); **^{1}H NMR** (500 MHz, d_6-acetone + 1 drop D$_2$O): δ 8.21 (d, J = 8.2 Hz, 1 H), 8.12 – 8.04 (m, 1 H), 7.88 (br d, J = 2.1 Hz, 1 H), 7.61 (app s, 5 H), 2.15 (s, 3 H, overlaps with acetone signal); **^{13}C NMR** (126 MHz, d_6-acetone + 1 drop D$_2$O): δ 170.1, 160.3, 144.2, 135.4, 135.0, 134.1, 130.5, 130.0, 129.4, 123.1, 117.7, 24.3; **^{11}B NMR** (160 MHz, d_6-acetone + 1 drop D$_2$O): δ 28.4; **HRMS** (ESI) for C$_{15}$H$_{12}$N$_2$O$_3$^{11}B (M − H)$^−$: Calculated: 279.0946; Found: 279.0944.

N-(1-hydroxy-4-phenyl-1H-benzo[d][1,2,6]oxazaborinin-6-yl)-3,5-dinitrobenzamide (4-22c): Prepared according to **GP6** from **4-7n** (21.0 mg, 0.0880 mmol), NMP (0.5 mL), and acyl chloride (10.1 mg, 0.130 mmol). Purification was achieved by a phase-switch workup followed by recrystallization with EtOAc/hexanes to afford the title compounds as a pale-yellow solid (37 mg, 98%); **^{1}H NMR** (500MHz, d_6-acetone + 1 drop D_2O): δ 9.11 (d, J = 2.1 Hz, 2 H), 9.05 (t, J = 2.1 Hz, 1 H), 8.26 (dd, J = 8.2, 2.0 Hz, 1 H), 8.19 (d, J = 8.2 Hz, 1 H), 7.90 (d, J = 1.9 Hz, 1 H), 7.58 – 7.48 (m, 5 H); **^{13}C NMR** (126 MHz, d_6-acetone + 1 drop D_2O): δ 162.8, 160.2, 149.6, 143.4, 138.8, 135.4, 135.1, 134.2, 130.6, 130.1, 129.4, 128.8, 124.2, 122.1, 119.1; **^{11}B NMR** (128 MHz, d_6-acetone + 1 drop D_2O): δ 28.0; **HRMS** (ESI) for $C_{20}H_{12}N_4O_7{}^{11}B$ (M – H)$^{-}$: Calculated: 431.0805; Found: 431.0807.
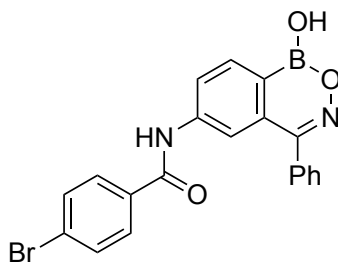
4-Bromo-N-(1-hydroxy-4-phenyl-1H-benzo[d][1,2,6]oxazaborinin-6-yl)benzamide (4-22d): Prepared according to **GP6** from **4-7n** (42.0 mg, 0.175 mmol), NMP (0.5 mL), and 4-bromobenzoyl chloride (42.2 mg, 0.192 mmol). Purification was achieved by a phase-switch workup, followed by recrystallization with EtOAc/hexanes. The solid obtained was left in Et_2O (2 mL) overnight to afford the title compounds as a white solid (39 mg, 53%); **^{1}H NMR** (500 MHz, d_6-acetone + 1 drop D_2O): δ 8.27 (d, J = 1.2 Hz, 2 H), 8.09 (m, 1 H), 7.97 (d, J = 8.6 Hz, 2 H), 7.76 (d, J = 8.5 Hz, 2 H),

7.69 – 7.60 (m, 5 H); **¹³C NMR** (126 MHz, d_6-acetone + 1 drop D_2O): δ 166.1, 160.3, 144.0, 135.4, 135.0, 134.8, 134.1, 132.6, 130.6, 130.5, 130.1, 129.4, 126.9, 124.2, 119.0; **¹¹B NMR** (128 MHz, d_6-acetone + 1 drop D_2O): δ 27.9; **HRMS** (ESI) for $C_{20}H_{13}BrN_2O_3{}^{11}B$ $(M - H)^-$: Calculated: 419.0208; Found: 419.0217.
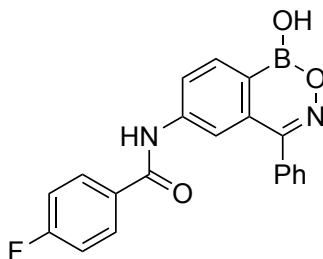
4-Fluoro-*N*-(1-hydroxy-4-phenyl-1*H*-benzo[*d*][1,2,6]oxazaborinin-6-yl)benzamide (4-22e): Prepared according to **GP6** from **4-7n** (42.0 mg, 0.175 mmol), NMP (0.5 mL), and 4-fluorobenzoyl chloride (30.5 mg, 0.192 mmol). Purification was achieved by a phase-switch workup followed by recrystallization with EtOAc/hexanes to afford the title compound as a pale-yellow crystalline solid (57 mg, 91%); **¹H NMR** (400 MHz, d_6-acetone + 1 drop D_2O): δ 8.26 (d, $J = 8.1$ Hz, 1 H), 8.20 (d, $J = 8.2$ Hz, 1 H), 8.07 – 8.01 (m, 2 H), 7.99 (s, 1 H), 7.63 – 7.52 (m, 5 H), 7.31 – 7.21 (m, 2 H); **¹³C NMR** (126 MHz, d_6-acetone + 1 drop D_2O): δ 165.8 (d, $J = 251$ Hz), 165.8, 160.3, 144.2, 135.5, 135.0, 134.0, 132.1 (d, $J = 3.10$ Hz), 131.3 (d, $J = 9.30$ Hz), 130.6, 130.0, 129.4, 124.1, 118.8, 116.2 (d, $J = 22.2$ Hz); **¹¹B NMR** (128 MHz, d_6-acetone + 1 drop D_2O): δ 28.2; **¹⁹F NMR** (376 MHz, d_6-acetone + 1 drop D_2O): δ –109.75 (tt, $J = 9.3$, 5.6 Hz); **HRMS** (ESI) for $C_{20}H_{13}FN_2O_3{}^{11}B$ $(M - H)^-$: Calculated: 359.1009; Found: 359.1005.

2,6-Dichloro-*N*-(1-hydroxy-4-phenyl-1*H*-benzo[*d*][1,2,6]oxazaborinin-6-yl)benzamide (4-22f): Prepared according to **GP6** from **4-7n** (42.0 mg, 0.175 mmol), NMP (0.5 mL), and 2,6-dichlorobenzoyl chloride (40.2 mg, 0.192 mmol). Purification was performed by preparative HPLC (C18, 100 × 50 mm, 5 μm using the gradient: 0.0 min, 50% acetonitrile/water; 5.0 min, 95% acetonitrile/water; 8.0 min, 95% acetonitrile/water; 8.1 min, 50% acetonitrile/water for a total of 12 min with a flow rate of 30 mL/min, and the fractions were collected between 5–7 min) to afford the title compound as a white solid (45 mg, 63%); **¹H NMR** (500 MHz, d_6-acetone + 1 drop D$_2$O): δ 8.34 – 8.26 (m, 2 H), 7.99 – 7.97 (m, 1 H), 7.69 – 7.59 (m, 5 H), 7.56 – 7.55 (m, 3 H); **¹³C NMR** (126 MHz, d_6-acetone + 1 drop D$_2$O): δ 163.6, 160.2, 143.5, 137.0, 135.4, 135.2, 134.4, 132.6, 132.4, 130.5, 130.1, 129.4, 129.1, 123.4, 118.2; **¹¹B NMR** (128 MHz, d_6-acetone + 1 drop D$_2$O): δ 28.5; **HRMS** (ESI) for C$_{20}$H$_{12}$Cl$_2$N$_2$O$_3$^{11}B (M – H)⁻: Calculated: 409.0324; Found: 409.0334.
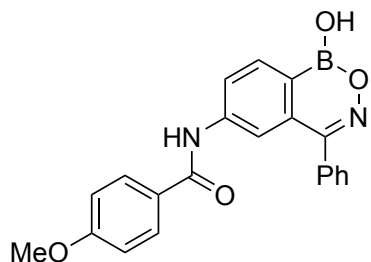
***N*-(1-hydroxy-4-phenyl-1*H*-benzo[*d*][1,2,6]oxazaborinin-6-yl)-4-methoxybenzamide (4-22g):** Prepared according to **GP6** from **4-7n** (42.0 mg, 0.175 mmol), NMP (0.5 mL), and 4-methoxybenzoyl chloride (30.5 mg, 0.192 mmol). Purification was achieved by a phase-switch workup, followed by recrystallization with EtOAc/hexanes to afford the title compound as an orange colored solid (60 mg, 92%); **¹H NMR** (400 MHz, d_6-acetone + 1 drop D$_2$O): δ 8.28 – 8.21 (m, 1 H), 8.18 (d, *J* = 8.1

Hz, 1 H), 8.00 (s, 1 H), 7.94 (d, J = 9.1 Hz, 2 H), 7.62 – 7.52 (m, 5 H), 7.01 (d, J = 9.1 Hz, 2 H), 3.86 (s, 3 H); ^{13}C NMR (126 MHz, d_6-acetone + 1 drop D$_2$O): δ 166.4, 163.6, 160.3, 144.5, 135.5, 135.0, 134.0, 130.6, 130.5, 130.0, 129.4, 127.7, 124.1, 118.7, 114.6, 56.0; ^{11}B NMR (128 MHz, d_6-acetone + 1 drop D$_2$O): δ 28.3; HRMS (ESI) for C$_{21}$H$_{16}$N$_2$O$_4$^{11}B (M – H)$^-$: Calculated: 371.1209; Found: 371.1218.
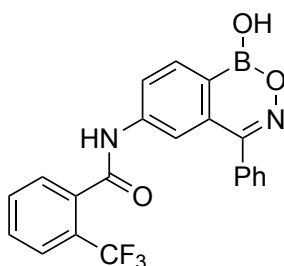
N-(1-hydroxy-4-phenyl-1H-benzo[d][1,2,6]oxazaborinin-6-yl)-2-(trifluoromethyl)benzamide (4-22h): Prepared according to **GP6** from **4-7n** (42.0 mg, 0.175 mmol), NMP (0.5 mL), and 2-trifluoromethylbenzoyl chloride (40.2 mg, 0.192 mmol). Purification was performed by preparative HPLC (Agilent C18, 100 × 50 mm, 5 μm using a gradient: 0.0 min, 50% acetonitrile/water; 5.0 min, 95% acetonitrile/water; 8.0 min, 95% acetonitrile/water; 8.1 min, 50% acetonitrile/water for a total of 12 min with a flow rate of 30 mL/min, and the fractions were collected between 5–7 min) to afford the title compound as a white solid (64 mg, 90%); ^{1}H NMR (500 MHz, d_6-acetone + 1 drop D$_2$O): δ 8.37 (dd, J = 8.3, 1.8 Hz, 1 H), 8.32 (d, J = 8.2 Hz, 1 H), 7.95 (s, 1 H), 7.88 (d, J = 7.6 Hz, 1 H), 7.86 – 7.73 (m, 3 H), 7.66 (dd, J = 6.6, 3.3 Hz, 2 H), 7.63 – 7.56 (m, 3 H); ^{13}C NMR (126 MHz, d_6-acetone + 1 drop D$_2$O): δ 167.0, 160.2, 143.9, 136.9, 135.4, 135.2, 134.3, 133.3, 131.2, 130.5, 130.0, 129.4, 127.7 (q, J = 32.0 Hz), 127.3 (q, J = 4.94 Hz), 125.9, 123.8, 123.5, 118.2; ^{11}B NMR (128 MHz, d_6-acetone + 1 drop D$_2$O): δ 28.2; ^{19}F NMR (376 MHz, d_6-acetone + 1 drop D$_2$O): δ –59.53; HRMS (ESI) for C$_{21}$H$_{15}$F$_3$N$_2$O$_3$^{11}B (M + H)$^+$: Calculated: 411.1122; Found: 411.1126.
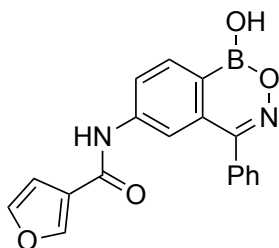
N-(1-hydroxy-4-phenyl-1H-benzo[d][1,2,6]oxazaborinin-6-yl)furan-3-carboxamide (4-22i): Prepared according to **GP6** from **4-7n** (42.0 mg, 0.175 mmol), NMP (0.5 mL), and 3-furoyl chloride (25.1 mg, 0.192 mmol). Purification was achieved by a phase-switch workup followed by recrystallization with CH_2Cl_2/hexanes to afford the title compound as a pale-yellow solid (51 mg, 88%); **^{1}H NMR** (400 MHz, d_6-acetone + 1 drop D_2O): δ 8.23 (s, 1 H), 8.21 – 8.14 (m, 2 H), 7.90 (br s, 1 H), 7.64 (t, J = 1.7 Hz, 1 H), 7.61 – 7.51 (m, 5 H), 6.90 (s, 1 H); **^{13}C NMR** (126 MHz, d_6-acetone + 1 drop D_2O): δ 161.7, 160.3, 146.8, 145.1, 144.0, 135.6, 135.1, 134.0, 130.6, 130.0, 129.4, 124.0, 123.8, 118.4, 109.9; **^{11}B NMR** (128 MHz, d_6-acetone + 1 drop D_2O): δ 28.4; **HRMS** (ESI) for $C_{18}H_{14}N_2O_4{}^{11}B$ (M + H)$^+$: Calculated: 333.1041; Found: 333.1041.

4-4g'

4-22j

4-fluoro-N-(1-hydroxy-4-phenyl-1H-benzo[d][1,2,6]oxazaborinin-7-yl)-2-(trifluoromethyl)benzamide (4-22j): The amine derivative of the boron heterocycle was prepared according to **GP3** from **4-4g'** (300 mg, 1.09 mmol), B_2pin_2 (552 mg, 2.17 mmol), KOAc (428 mg, 4.36 mmol), $PdCl_2$(dppf)·CH_2Cl_2 (89.0 mg, 0.109 mmol), and dioxane (4 mL). The crude material was filtered through Celite® and used without further purification for the transesterification reaction (**GP4**: MeB(OH)$_2$ (522 mg, 8.72 mmol)), followed by the condensation reaction (**GP5**: NH_2OH (50 wt. % solution in water, 0.100 mL, 1.63 mmol)). The crude material obtained was subjected to **GP6** (NMP (0.500 mL), and 4-fluoro-2-trifluoromethylbenzoyl chloride (247 mg, 1.09

mmol). Purification was performed by semi-preparative HPLC (C18, 250 × 4.6 mm, 5 μm using 0.1% formic acid in water and acetonitrile as a solvent system with the gradient as follows: 0.0 min, 50% acetonitrile; 9.0 min, 95% acetonitrile; 10.6 min, 50% acetonitrile for a total of 15 min with a flow rate of 3.0 mL/min, and the fractions were collected between 8.0–9.2 min) to afford the title compound as a white solid (98 mg, 21% over 4 steps); ^{1}**H NMR** (500 MHz, d_6-acetone + 1 drop D_2O): δ 8.58 (s, 1 H), 8.10 (dd, J = 8.7, 2.3 Hz, 1 H), 7.88 (dd, J = 8.6, 5.4 Hz, 1 H), 7.62 (dd, J = 9.2, 2.6 Hz, 1 H), 7.58 − 7.53 (m, 6 H), 7.44 (d, J = 8.7 Hz, 1 H); ^{13}**C NMR** (126 MHz, d_6-acetone + 1 drop D_2O): δ 166.3, 163.6 (d, J = 250 Hz), 159.8, 142.4, 135.5, 133.5, 132.4 (d, J = 8.67 Hz), 130.5, 130.1, 130.0, 129.5, 129.4, 125.1, 124.8, 122.9 (d, J = 10.6 Hz), 122.8, 120.2 (d, J = 21.5 Hz), 115.1 (dq, J = 25.8, 5.20 Hz); ^{11}**B NMR** (128 MHz, d_6-acetone + 1 drop D_2O): δ 28.1; ^{19}**F NMR** (376 MHz, d_6-acetone + 1 drop D_2O): δ −59.90, −110.11; **HRMS** (ESI) for $C_{21}H_{14}F_4N_2O_3{}^{11}B$ (M +H)$^+$: Calculated: 429.1028; Found: 429.1029.
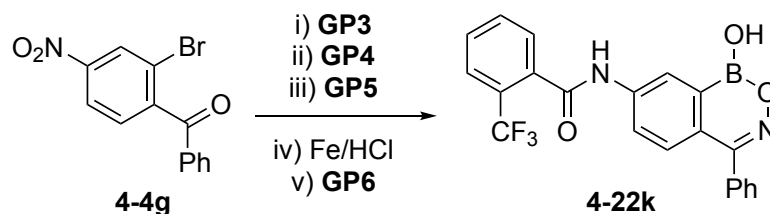
N-(1-hydroxy-4-phenyl-1H-benzo[d][1,2,6]oxazaborinin-7-yl)-2-(trifluoromethyl)benzamide (4-22k): Prepared in five consecutive steps. The nitro derivative of the boron heterocycle was prepared according to **GP3** from **4-4g** (500 mg, 1.64 mmol), B_2pin_2 (833 mg, 3.28 mmol), KOAc (644 mg, 6.56 mmol), $PdCl_2(dppf)\cdot CH_2Cl_2$ (134 mg, 0.164 mmol), and dioxane (8 mL). The crude material was subjected to flash column chromatography (10% EtOAc/hexanes), and then used as such for the transesterification reaction (**GP4**: $MeB(OH)_2$ (766 mg, 12.8 mmol)), followed by the condensation reaction (**GP5**: NH_2OH (50 wt. % solution in water, 0.121 mL, 1.97 mmol)). The final crude material obtained was washed with water, transferred to a vial, and then dissolved in hot EtOAc (3 mL). Precipitation occurred in the vial after addition of hexanes (1 mL). The vial was kept in the refrigerator overnight

and then the precipitate was filtered, and air-dried to afford the nitro derivative of the boron heterocycle (115 mg, 26%); **¹H NMR** (400 MHz, d_6-acetone + 1 drop D_2O): δ 8.96 (d, J = 2.5 Hz, 1 H), 8.57 (dd, J = 8.8, 2.5 Hz, 1 H), 7.73 (d, J = 8.7 Hz, 1 H), 7.61 (app s, 5 H); **¹¹B NMR** (128 MHz, d_6-acetone + 1 drop D_2O): δ 28.1. This nitro derivative (36.0 mg, 0.134 mmol), dissolved in HFIP (1 mL) was charged in a round bottom flask, followed by the addition of Fe powder (37.4 mg, 0.670 mmol) and aq. HCl (1 mL, 2 M).[33] The reaction mixture was stirred at rt for 1 h and then the contents of the reaction flask were filtered through Celite® and rinsed with EtOAc (10 mL). The filtrate was evaporated under reduced pressure and used without further purification for the next step. The residue obtained was charged in a round bottom flask and was subjected to **G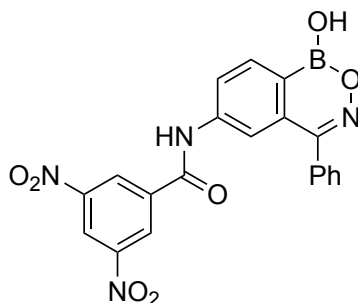P6** (NMP (0.500 mL), and 2-trifluoromethylbenzoyl chloride (30.7 mg, 0.147 mmol)). Purification was achieved by a phase-switch workup followed by recrystallization with CH_2Cl_2/hexanes to afford the title compound as a pale-yellow solid (23 mg, 43% over two steps); **¹H NMR** (400 MHz, d_6-acetone + 1 drop D_2O): δ 8.61 (t, J = 2.5 Hz, 1 H), 8.10 (dd, J = 8.7, 2.4 Hz, 1 H), 7.84 (d, J = 7.7 Hz, 1 H), 7.80 – 7.69 (m, 3 H), 7.56 (m, 5 H), 7.45 (d, J = 8.7 Hz, 1 H); **¹³C NMR** (126 MHz, d_6-acetone + 1 drop D_2O): δ 167.0, 159.8, 142.5, 137.0, 135.5, 133.4, 131.2, 130.5, 130.0, 129.9, 129.4, 129.4, 127.8 (q, J = 31.8 Hz), 127.4 (q, J = 4.90 Hz), 126.0, 124.7, 123.8, 122.6; **¹¹B NMR** (128 MHz, d_6-acetone + 1 drop D_2O): δ 28.4; **¹⁹F NMR** (376 MHz, d_6-acetone + 1 drop D_2O): δ –59.52 – –59.60 (m); **HRMS** (ESI) for $C_{21}H_{13}F_3N_2O_3{}^{11}B$ (M – H)⁻: Calculated: 409.0977; Found: 409.0988.

2-bromo-4-nitrobenzaldehyde

4-22l
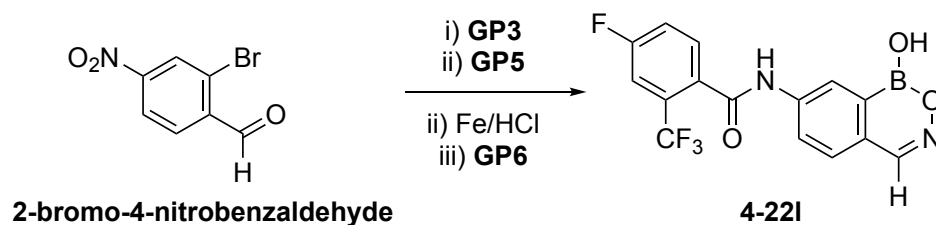
4-Fluoro-*N*-(1-hydroxy-1*H*-benzo[*d*][1,2,6]oxazaborinin-7-yl)-2-(trifluoromethyl)benzamide (4-22l): The starting material (2-bromo-4-nitrobenzaldehyde) was prepared following a literature procedure (see preparation of 4-8c).[32] The amine derivative of the boron heterocycle was prepared according to **GP3**

from 2-bromo-4-nitrobenzaldehyde (2.00 g, 8.69 mmol), B_2pin_2 (4.42 g, 17.4 mmol), KOAc (3.41 g, 34.8 mmol), $PdCl_2(dppf) \cdot CH_2Cl_2$ (709 mg, 0.869 mmol), and dioxane (40 mL). The crude material was filtered through Celite® and used after phase-switch workup with basic sorbitol for the condensation reaction (**GP5**: NH_2OH (50 wt. % solution in water, 0.799 mL, 13.03 mmol)), which resulted in a crude yellow solid (901 mg, 18%, calculated using internal standard). A portion of this crude nitro derivative (145 mg, 0.260 mmol), dissolved in HFIP (0.5 mL) was charged in a round bottom flask followed by the addition of Fe powder (157 mg, 1.30 mmol) and aq. HCl (2.50 mL, 2.00 M).[33] The reaction mixture was stirred at rt for 1 h. Upon completion, the contents of the reaction flask were filtered through Celite® and the crude material obtained was used without any further purification for amidation reaction according to **GP6** (NMP (0.500 mL), and 4-fluoro-2-trifluoromethylbenzoyl chloride (69.3 mg, 0.260 mmol)). Purification was performed by semi-preparative HPLC (C8, 250 × 4.6 mm, 5 μm using 0.1% formic acid in water and acetonitrile as a solvent system with a gradient: 0.0 min, 20% acetonitrile; 14.0 min, 95% acetonitrile; 15.0 min, 95% acetonitrile; 15.1 min, 20% acetonitrile for a total of 19 min with a flow rate of 3.0 mL/min, and the fractions were collected between 11–14 min) to afford the title compound as a pale-yellow solid (8 mg, 9% over 2 steps); **^{1}H NMR** (500 MHz, d_6-acetone + 1 drop D_2O): δ 8.60-8.57 (m, 2 H), 8.27 (dd, J = 8.4, 2.2 Hz, 1 H), 8.03 – 7.95 (m, 1 H), 7.87 (d, J = 8.4 Hz, 1 H), 7.72 (dd, J = 9.2, 2.6 Hz, 1 H), 7.70 – 7.64 (m, 1 H); **^{13}C NMR** (126 MHz, d_6-acetone + 1 drop D_2O): δ 166.1, 166.0, 163.6 (d, J = 250 Hz), 150.3, 142.8, 133.5, 132.4 (d, J = 8.45 Hz), 129.9, 129.4, 125.1, 122.4, 120.2 (d, J = 2.68 Hz), 115.0 (dq, J = 25.2, 5.38 Hz), CF_3 quartet is not visible due to low signal to noise ratio; **^{11}B NMR** (128 MHz, d_6-acetone + 1 drop D_2O): δ 28.1; **^{19}F NMR** (376 MHz, d_6-acetone + 1 drop D_2O): δ –59.97 (s, 3 F), –110.21 (q, J = 8.6 Hz); **HRMS** (ESI) for $C_{15}H_{10}F_4N_2O_3{}^{11}B$ (M +H)$^+$: Calculated: 353.0715; Found: 353.0719.
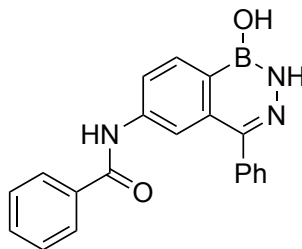
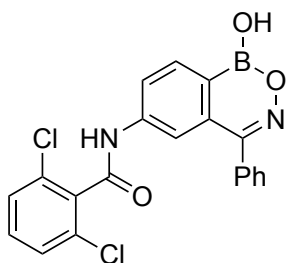**N-(1-hydroxy-4-phenyl-1,2-dihydrobenzo[*d*][1,2,3]diazaborinin-6-yl)benzamide (4-23a):** Prepared according to **GP6** from **4-8f** (50.0 mg, 0.210 mmol), NMP (1 mL), and benzoyl chloride (32.5 mg, 0.230 mmol). Purification was performed by saturated aq. NaHCO$_3$/EtOAc extraction, followed by recrystallization with CH$_2$Cl$_2$/hexanes to afford the title compound as a pale-yellow solid (55 mg, 77%); **^{1}H NMR** (500 MHz, *d$_6$*-acetone + 1 drop D$_2$O): δ 8.36 (d, *J* = 8.3 Hz, 1 H), 8.27 – 8.24 (m, 1 H), 8.21 (s, 1 H), 8.05 (d, *J* = 6.6 Hz, 2 H), 7.67 – 7.62 (m, 3 H), 7.59 – 7.50 (m, 5 H); **^{13}C NMR** (126 MHz, *d$_6$*-acetone + 1 drop D$_2$O): δ 166.7, 148.3, 142.5, 139.8, 137.1, 136.0, 132.9, 132.6, 130.7, 129.3, 129.0, 128.6, 128.5, 121.8, 118.1; **^{11}B NMR** (128 MHz, *d$_6$*-acetone + 1 drop D$_2$O): δ 27.5; **HRMS** (ESI) for C$_{20}$H$_{17}$N$_3$O$_2$^{11}B (M + H)$^+$: Calculated: 342.1408; Found: 342.1398.
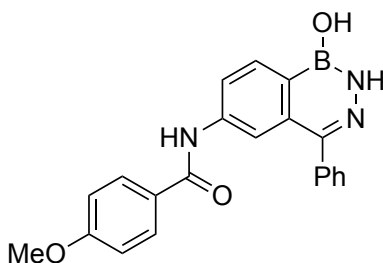
N-(1-hydroxy-4-phenyl-1,2-dihydrobenzo[*d*][1,2,3]diazaborinin-6-yl)-4-methoxybenzamide (4-23b): Prepared according to **GP6** from **4-8f** (50.0 mg, 0.210 mmol), NMP (1 mL), and 4-methoxybenzoyl chloride (39.2 mg, 0.230 mmol). Purification was performed by saturated aq. NaHCO$_3$/EtOAc extraction, followed by recrystallization with EtOAc/hexanes to afford the title compound as a pale-yellow solid (50 mg, 66%); **^{1}H NMR** (600 MHz, *d$_6$*-acetone + 1 drop D$_2$O): δ 8.24 (d, *J* = 8.3 Hz, 1 H), 8.14 (dd, *J* = 8.3, 2.0 Hz, 1 H), 8.08 (d, *J* = 2.0 Hz, 1 H), 7.95 – 7.91 (m, 2 H), 7.55 – 7.50 (m, 2 H), 7.50 – 7.44 (m, 2 H), 7.44 – 7.39 (m, 1 H), 7.02 – 6.96 (m, 2

H), 3.84 (s, 3 H); ^{13}**C NMR** (126 MHz, d_6-acetone + 1 drop D$_2$O): δ 166.1, 163.5, 148.3, 142.7, 139.8, 137.1, 132.8, 130.7, 130.4, 129.0, 128.6, 128.1, 121.8, 118.0, 114.5, 55.9; ^{11}**B NMR** (160 MHz, d_6-acetone + 1 drop D$_2$O): δ 27.5; **HRMS** (ESI) for C$_{21}$H$_{19}$N$_3$O$_3$^{11}B (M + H)$^+$: Calculated: 372.1514; Found: 372.1514.
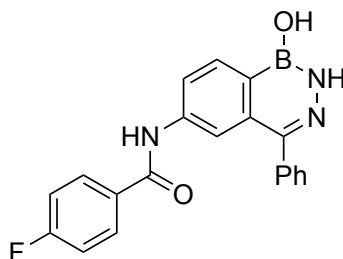
**4-Fluoro-*N*-(1-hydroxy-4-phenyl-1,2-dihydrobenzo[*d*][1,2,3]diazaborinin-6-yl)benzamide (4-23c):** Prepared according to **GP6** from **4-8f** (50.0 mg, 0.210 mmol), NMP (1 mL), and 4-fluorobenzoyl chloride (36.5 mg, 0.230 mmol). Purification was performed by saturated aq. NaHCO$_3$/EtOAc extraction, followed by recrystallization with CH$_2$Cl$_2$/hexanes to afford the title compound as a pale-yellow solid (53 mg, 71%); ^{1}**H NMR** (500 MHz, d_6-acetone + 1 drop D$_2$O): δ 8.23 (d, *J* = 8.3 Hz, 1 H), 8.15 – 8.11 (m, 1 H), 8.03 (s, 1 H), 7.99 (dd, *J* = 9.0, 5.4 Hz, 2 H), 7.50 (d, *J* = 8.0 Hz, 2 H), 7.46 – 7.37 (m, 3 H), 7.20 (app t, *J* = 8.8 Hz, 2 H); ^{13}**C NMR** (126 MHz, d_6-acetone + 1 drop D$_2$O): δ 165.7 (d, *J* = 250 Hz), 165.6, 165.6, 148.3, 142.6, 139.8, 137.1 (d, *J* = 2.00 Hz), 132.8, 131.2 (d, *J* = 9.10 Hz), 130.7, 129.0, 128.6, 121.9, 118.1, 116.2 (d, *J* = 22.2 Hz); ^{11}**B NMR** (128 MHz, d_6-acetone + 1 drop D$_2$O): δ 27.2; ^{19}**F NMR** (376 MHz, d_6-acetone + 1 drop D$_2$O): δ –110.0 – –110.1 (m); **HRMS** (ESI) for C$_{20}$H$_{16}$FN$_3$O$_2$^{11}B (M + H)$^+$: Calculated: 360.1314; Found: 360.1314.
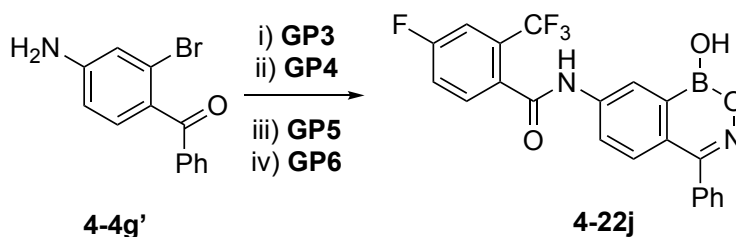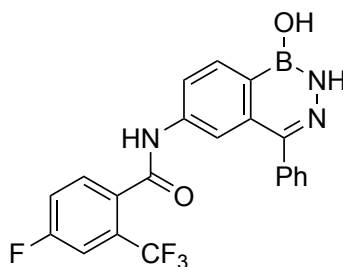
4-Fluoro-*N*-(1-hydroxy-4-phenyl-1,2-dihydrobenzo[*d*][1,2,3]diazaborinin-6-yl)-2-(trifluoromethyl)benzamide (4-23d): Prepared according to **GP6** from **4-8f** (50.0 mg, 0.210 mmol), NMP (1 mL), and 4-fluoro-2-trifluoromethylbenzoyl chloride (52.1 mg, 0.230 mmol). Purification was performed by saturated aq. NaHCO$_3$/EtOAc extraction, followed by recrystallization with CH$_2$Cl$_2$/hexanes to afford the title compound as a pale-yellow solid (53 mg, 71%); **^{1}H NMR** (500 MHz, d_6-acetone + 1 drop D$_2$O): δ 8.25 (d, J = 8.3 Hz, 1 H), 8.10 – 8.08 (m, 1 H), 7.92 (s, 1 H), 7.76 (dd, J = 8.6, 5.4 Hz, 1 H), 7.55 (dd, J = 9.2, 2.7 Hz, 1 H), 7.52 – 7.45 (m, 3 H), 7.43 – 7.34 (m, 3 H); **^{13}C NMR** (126 MHz, d_6-acetone + 1 drop D$_2$O): δ 165.8, 163.5 (d, J = 250 Hz), 148.1 (d, J = 9.89 Hz), 142.1, 139.7, 137.2 (d, J = 2.04 Hz), 133.8, 133.1, 132.2 (d, J = 8.63 Hz), 130.6, 130.1 (dq, J = 32.9, 7.75 Hz), 129.0, 128.6, 121.2, 120.1 (d, J = 21.4 Hz), 117.5, 114.9 (dq, J = 25.6, 5.01 Hz); **^{11}B NMR** (128 MHz, d_6-acetone + 1 drop D$_2$O): δ 27.6; **^{19}F NMR** (376 MHz, d_6-acetone + 1 drop D$_2$O): δ –60.01 (s, 3 F), –110.49 – –110.5 (m, 1 F); **HRMS** (ESI) for C$_{21}$H$_{15}$F$_4$N$_3$O$_2$^{11}B (M + H)$^+$: Calculated: 428.1192; Found: 428.1190.
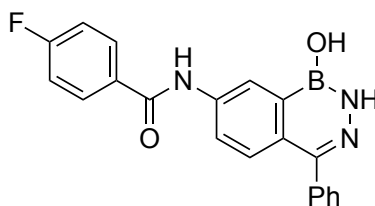
4-Fluoro-*N*-(1-hydroxy-4-phenyl-1,2-dihydrobenzo[*d*][1,2,3]diazaborinin-7-yl)benzamide (4-23e): Prepared according to **GP6** from **4-8g** (50.0 mg, 0.210 mmol), NMP (1 mL), and 4-fluoromethylbenzoyl chloride (36.5 mg, 0.230 mmol). Purification was performed by saturated aq. NaHCO$_3$/EtOAc extraction, followed by recrystallization with CH$_2$Cl$_2$/hexanes to afford the title compound as a pale-yellow

solid (50 mg, 66%); **¹H NMR** (500 MHz, d_6-acetone + 1 drop D_2O): δ 8.76 (d, J = 2.3 Hz, 1 H), 8.27 – 8.19 (m, 2 H), 8.16 (dd, J = 8.8, 2.4 Hz, 1 H), 7.70 (d, J = 8.8 Hz, 1 H), 7.62 – 7.51 (m, 5 H), 7.38 (app t, J = 8.8 Hz, 2 H); **¹³C NMR** (126 MHz, d_6-acetone + 1 drop D_2O): δ 165.7 (d, J = 250 Hz), 165.7, 148.1, 140.0, 139.7, 132.4 (d, J = 3.07 Hz), 132.4, 131.3 (d, J = 9.2 Hz), 130.6, 129.0, 128.6, 128.5, 124.1, 122.1, 116.2 (d, J = 22.1 Hz); **¹¹B NMR** (128 MHz, d_6-acetone + 1 drop D_2O): δ 27.7; **¹⁹F NMR** (376 MHz, d_6-acetone + 1 drop D_2O): δ –110.10 (ddd, J = 14.0, 8.9, 5.3 Hz); **HRMS** (ESI) for $C_{20}H_{16}FN_3O_2{}^{11}B$ (M + H)⁺: Calculated: 360.1314; Found: 360.1313.
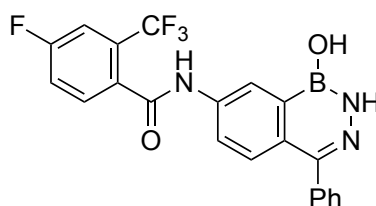
4-Fluoro-*N*-(1-hydroxy-4-phenyl-1,2-dihydrobenzo[*d*][1,2,3]diazaborinin-7-yl)-2-(trifluoromethyl)benzamide (4-23f): Prepared according to **GP6** from **4-8g** (50.0 mg, 0.210 mmol), NMP (1 mL), and 4-fluoro-2-trifluoromethylbenzoyl chloride (52.1 mg, 0.230 mmol). Purification was performed by saturated aq. $NaHCO_3$/EtOAc extraction followed by recrystallization with CH_2Cl_2/hexanes to afford the title compound as a pale-yellow solid (60 mg, 66%); **¹H NMR** (400 MHz, d_6-acetone + 1 drop D_2O): δ 8.65 (d, J = 2.3 Hz, 1 H), 7.96 (dd, J = 8.8, 2.4 Hz, 1 H), 7.88 (dd, J = 8.5, 5.4 Hz, 1 H), 7.65 – 7.61 (m, 2 H), 7.58 (td, J = 8.4, 2.7 Hz, 1 H), 7.54 – 7.43 (m, 5 H); **¹³C NMR** (126 MHz, d_6-acetone + 1 drop D_2O): δ 165.9, 163.5 (d, J = 250 Hz), 148.1, 139.6, 133.8, 132.3 (d, J = 8.62 Hz), 130.6, 130.4 (d, J = 8.06 Hz), 130.1 (d, J = 8.01 Hz); 129.0, 128.7, 128.6, 123.6, 121.6, 120.2, 120.1, 115.0 (dq, J = 25.7, 3.91 Hz); **¹¹B NMR** (128 MHz, d_6-acetone + 1 drop D_2O): δ 27.8; **¹⁹F NMR** (376 MHz, d_6-acetone + 1 drop D_2O): δ -59.93 (s, 3 F), -110.4 – 110.5 (m, 1 F); **HRMS** (ESI) for $C_{21}H_{15}F_4N_3O_2{}^{11}B$ (M + H)⁺: Calculated: 428.1188; Found: 428.1193.
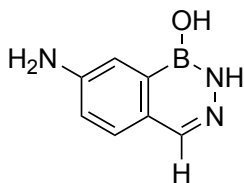
7-Aminobenzo[*d*][1,2,3]diazaborinin-1(2*H*)-ol (4-8c'): A round bottom flask was charged with Pd (10% loading on carbon, 223 mg, 0.200 mmol) and the flask was sealed with a septum. The vacuum was applied to remove any air from the headspace and then the flask was back filled with nitrogen. Analog **4-8c** (200 mg, 1.05 mmol), dissolved in EtOAc (24 mL) was added to the reaction flask. Afterwards, the reaction flask was again put under vacuum to remove any residual air or nitrogen, followed by the quick insertion of the H_2 balloon. The reaction mixture was stirred at rt for 4 h. Upon completion, the contents of the reaction flask were filtered through Celite® and then rinsed with EtOAc (5 mL). The filtrate obtained was evaporated under reduced pressure to afford the title compound as a pale-yellow solid (132 mg, 78%); **^{1}H NMR** (500 MHz, d_6-acetone + 1 drop D_2O): δ 7.81 (s, 1 H), 7.52 (d, *J* = 8.4 Hz, 1 H), 7.40 (d, *J* = 2.4 Hz, 1 H), 7.12 (dd, *J* = 8.4, 2.4 Hz, 1 H); **^{13}C NMR** (126 MHz, d_6-acetone + 1 drop D_2O): δ 149.9, 140.2, 129.3, 128.3, 119.6, 113.9; **^{11}B NMR** (128 MHz, d_6-acetone + 1 drop D_2O): δ 27.8; **HRMS** (ESI) for $C_7H_8N_3O^{11}B$ (M + H)$^+$: Calculated: 162.0833; Found: 162.0832.
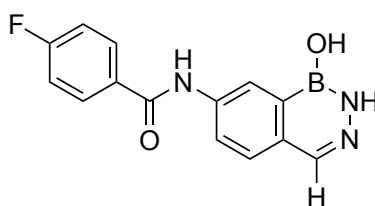
4-Fluoro-*N*-(1-hydroxy-1,2-dihydrobenzo[*d*][1,2,3]diazaborinin-7-yl)benzamide (4-23g): Prepared according to **GP6** from **4-8c'** (50.0 mg, 0.310 mmol), NMP (1 mL), and 4-fluorobenzoyl chloride (54.1 mg, 0.340 mmol). Purification was performed by saturated aq. NaHCO₃/EtOAc extraction, followed by recrystallization with MeOH/water to afford the title compound as a pale-yellow solid (65 mg, 74%); **^{1}H NMR** (500 MHz, d_6-acetone + 1 drop D_2O): δ 8.64 (d, *J* = 2.2 Hz, 1 H), 8.26 – 8.20

(m, 3 H), 8.04 (br s, 1 H), 7.82 (d, J = 8.5 Hz, 1 H), 7.37 (app t, J = 8.8 Hz, 2 H); **^{13}C NMR** (126 MHz, d_6-acetone + 1 drop D_2O): δ 165.8, 165.7 (d, J = 250 Hz), 140.2, 139.8, 132.5 (d, J = 3.05 Hz), 131.3 (d, J = 9.19 Hz), 128.6, 124.6, 121.9, 116.2 (d, J = 22.0 Hz), a carbon between the C—B and C—NHCO bonds is missing, which is correlated to the broad C—H in ^{1}H NMR (8.04 ppm); **^{11}B NMR** (128 MHz, d_6-acetone + 1 drop D_2O): δ 27.8; **^{19}F NMR** (376 MHz, d_6-acetone + 1 drop D_2O): δ –110.07 (tt, J = 9.1, 5.3 Hz); **HRMS** (ESI) for $C_{14}H_{12}FN_3O_2{}^{11}B$ (M + H)$^+$: Calculated: 284.1001; Found: 284.1005.
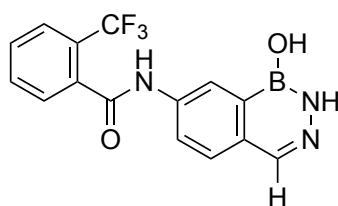
N-(1-hydroxy-1,2-dihydrobenzo[d][1,2,3]diazaborinin-7-yl)-2-(trifluoromethyl)benzamide (4-23h): Prepared according to **GP6** from **4-8c'** (25.0 mg, 0.160 mmol), NMP (0.5 mL), and 2-trifluoromethylbenzoyl chloride (35.6 mg, 0.170 mmol). Purification was performed by saturated aq. NaHCO$_3$/EtOAc extraction, followed by recrystallization with MeOH/water to afford the title compound as a pale-yellow solid (21 mg, 41%); **^{1}H NMR** (500 MHz, d_6-acetone + 1 drop D_2O): δ 8.67 (s, 1 H), 8.19 – 8.12 (m, 1 H), 8.04 (s, 1 H), 7.92 (d, J = 7.7 Hz, 1 H), 7.89 – 7.83 (m, 3 H), 7.80 (app td, J = 7.0, 2.7 Hz, 1 H); **^{13}C NMR** (126 MHz, d_6-acetone + 1 drop D_2O): δ 166.8, 140.0, 139.6, 137.3, 133.6, 133.3, 131.0, 129.4, 128.7, 127.7 (q, J = 31.8 Hz), 127.3 (q, J = 4.96 Hz), 126.0, 124.0, 121.3; **^{11}B NMR** (128 MHz, d_6-acetone + 1 drop D_2O): δ 27.8; **^{19}F NMR** (376 MHz, d_6-acetone + 1 drop D_2O): δ –59.55; **HRMS** (ESI) for $C_{15}H_{12}F_3N_3O_2{}^{11}B$ (M + H)$^+$: Calculated: 334.0969; Found: 334.0972.
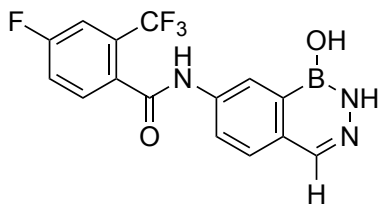
4-fluoro-*N*-(1-hydroxy-1,2-dihydrobenzo[*d*][1,2,3]diazaborinin-7-yl)-2-(trifluoromethyl)benzamide (4-23i): Prepared according to **GP6** from **4-8c'** (50.0 mg, 0.310 mmol), NMP (1 mL), and 4-fluoro-2-trifluoromethylbenzoyl chloride (77.3 mg, 0.340 mmol). Purification was performed by saturated aq. NaHCO$_3$/EtOAc extraction, followed by recrystallization with MeOH/water to afford the title compound as a pale-yellow solid (40 mg, 37%); **^{1}H NMR** (500 MHz, d_6-acetone + 1 drop D$_2$O): δ 8.62 (d, J = 6.1 Hz, 1 H), 8.15 – 8.12 (m, 1 H), 8.04 (br s, 1 H), 8.00 – 7.93 (m, 1 H), 7.84 (d, J = 8.5 Hz, 1 H), 7.72 (d, J = 9.1 Hz, 1 H), 7.66 (app t, J = 8.4 Hz, 1 H); **^{13}C NMR** (126 MHz, d_6-acetone + 1 drop D$_2$O): δ 165.9, 163.5 (d, J = 250 Hz), 139.9, 139.7, 133.8, 132.3 (d, J = 8.66 Hz), 128.7, 125.1, 124.1, 121.3, 120.2, 120.1, 115.0 (dq, J = 25.7, 4.98 Hz), a quartet of CF$_3$ is missing due to a low signal to noise ratio; **^{11}B NMR** (128 MHz, d_6-acetone + 1 drop D$_2$O): δ 27.8; **^{19}F NMR** (376 MHz, d_6-acetone + 1 drop D$_2$O): δ –59.96 (s, 3 F), –110.48 – –110.55 (m, 1 F); **HRMS** (ESI) for C$_{15}$H$_{11}$F$_4$N$_3$O$_2$^{11}B (M + H)$^+$: Calculated: 352.0875; Found: 352.0876.

4.9.10 Chan-Lam Reaction

4-7c (1.0 equiv)   (3.0 equiv)

4-7f
(purification could not be achieved)
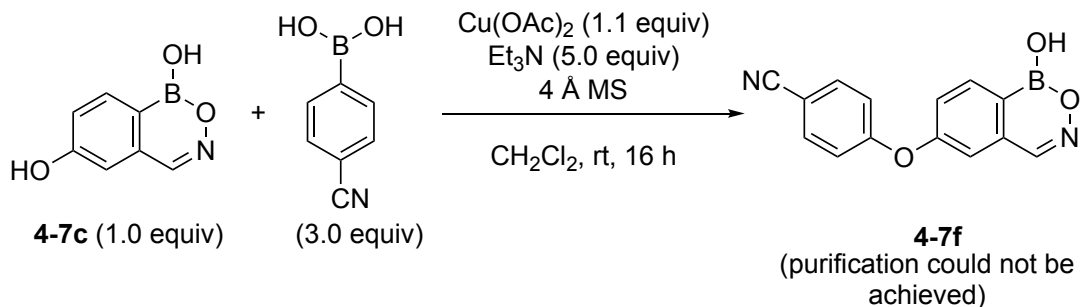
Attempted Chan-Lam Reaction Between 4-7c and 4-Cyanophenylboronic Acid: Hydroxy analog of **4-1**, **4-7c** (25 mg, 0.15 mmol) was charged in a round bottom flask followed by the addition of Cu(OAc)$_2$ (30 mg, 0.17 mmol), 4-cyanophenylboronic acid (67 mg, 0.46 mmol), Et$_3$N (77 mg, 0.76 mmol), and MS (125 mg, 4 Å).[69] CH$_2$Cl$_2$ (1 mL) was added to the reaction flask and the reaction mixture was stirred at rt under the O$_2$ balloon for 18 h. The contents of the reaction flask were filtered through Celite® and the filtrate was evaporated under reduced pressure. The residue obtained was subjected to a phase-switch workup using basic sorbitol solution. Sorbitol solution (1

M) was prepared by dissolving Na_2CO_3 (53.0 g, 0.50 mol) and sorbitol (91.0 g, 1.11 mol) in water (500 mL).[23] The organic layer was then evaporated and the crude material obtained showed the presence of **4-7f** and unreacted **4-7c** in the ratio of ~1:1, along with 4-cyanophenyl boronic acid, and other undetermined impurities (Figure 4.26). The crude material was subjected to silica gel column chromatography but did not afford the pure desired product. Similarly, trituration with Et_2O also did not result in the pure product.
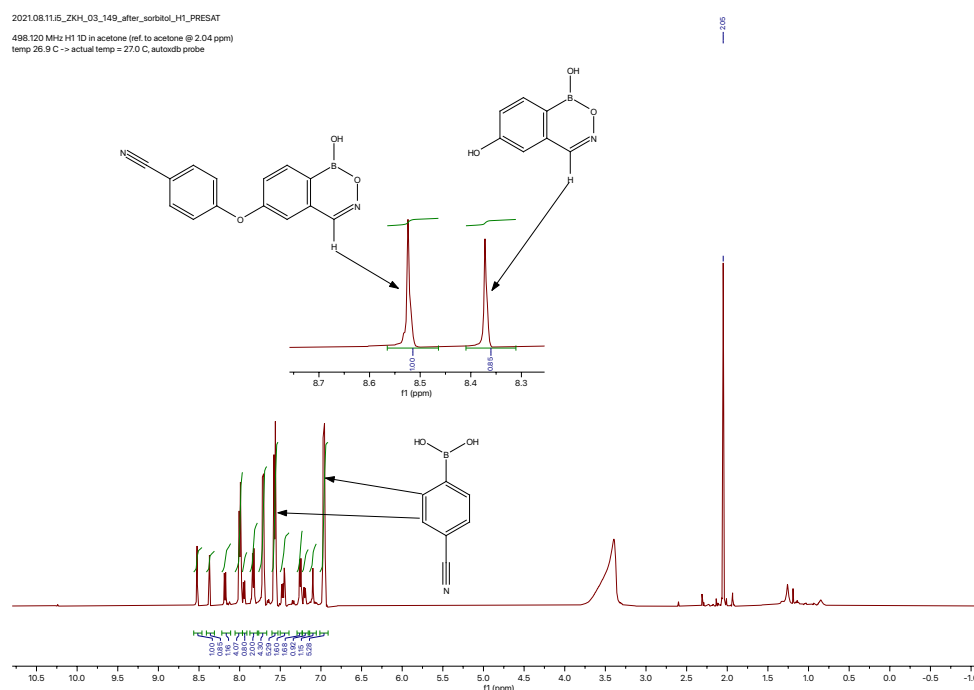
Figure 4.28. The ^1H NMR spectrum of the crude material obtained after a phase-switch workup of the Chan-Lam reaction between **4-7c** and 4-cyanophenylboronic acid.

a)

4-7c (1.0 equiv)   (2.0 equiv)   **4-7f**

b)

4-7c (1.0 equiv)   (1.2 equiv)   **4-24**

c)

4-7c (1.0 equiv)   (1.0 equiv)   **4-7f**
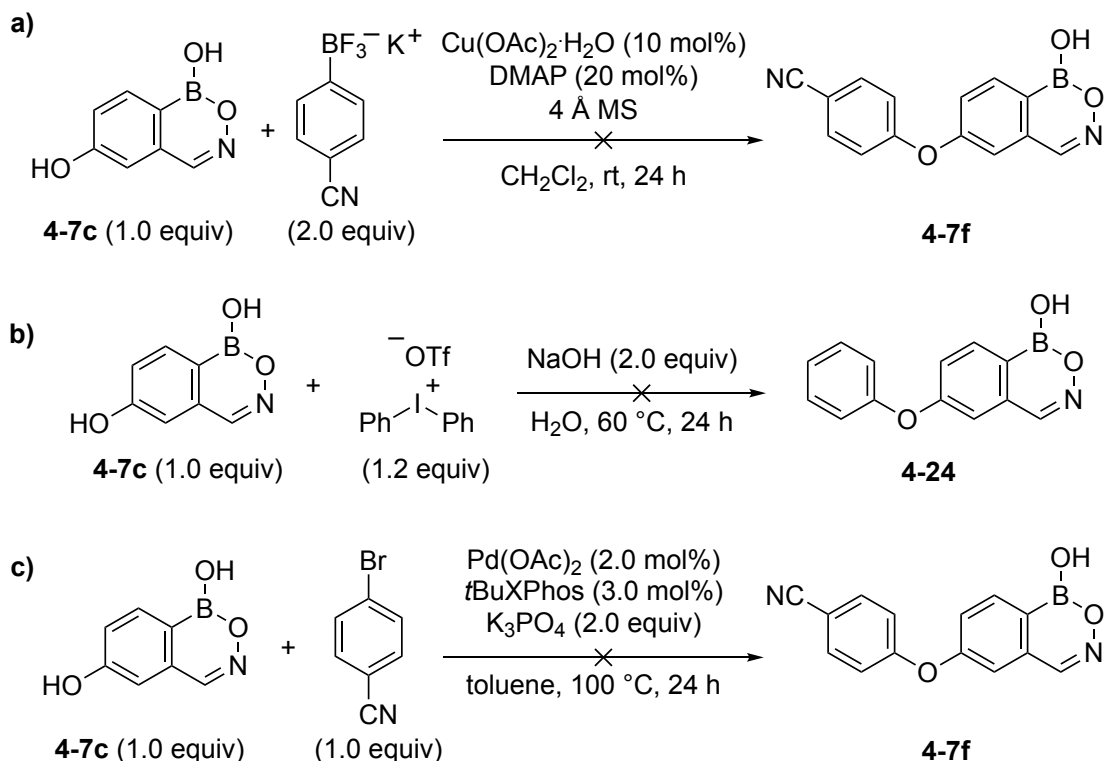
Attempted Ether Formation Reaction with 4-7c: Alternative approaches for obtaining the ether products were attempted. **a)**[45] Aryl trifluoroborate (65.4 mg, 0.305 mmol), Cu(OAc)$_2$·H$_2$O (3.00 mg, 10 mol%), DMAP (3.70 mg, 20 mol%), and powdered 4 Å MS (57.0 mg) were charged in a round bottom flask, followed by the addition of CH$_2$Cl$_2$ (1 mL). The suspension was stirred at rt for 5 min. Heterocycle **4-7c** (25.0 mg, 0.153 mmol) was added to the reaction flask, and the reaction mixture was stirred for 24 h. The LC-MS of the crude reaction material did not show the formation of the anticipated ether product **4-7f**. **b)**[44] NaOH (12.3 mg, 0.307 mmol) dissolved in water (1 mL) was charged in a round bottom flask, followed by the addition of **4-7c** (25.0 mg, 0.153 mmol). The reaction mixture was stirred at rt for 5 min and then the iodonium salt (79.2 mg, 0.184 mmol) was added. The reaction mixture was stirred at 60 °C for 24 h. The LC-MS of the crude reaction material did not show the formation of the anticipated ether product **4-24**. **c)**[46] A flame dried round bottom flask was charged with *t*BuXPhos (1.9 mg, 3.0 mol%), Pd(OAc)$_2$ (0.70 mg, 2.0 mol%), K$_3$PO$_4$ (65 mg, 0.31 mmol), **4-7c** (25 mg, 0.15 mmol), followed by the addition of 4-bromobenzonitrile (28 mg, 0.15 mmol) under argon. The reaction flask was put under

vacuum and then refilled with argon. Anhydrous toluene (1 mL) was added and then the reaction mixture was heated at 100 °C for 24 h. The LC-MS of the crude reaction material did not show the formation of the anticipated ether product **4-7f**.

General Procedure for the Chan-Lam Reaction for Analogs of 4-2a (GP7)

Hydroxy analog of **4-2a**, **4-8b** (50.0 mg, 0.310 mmol, 1.00 equiv) was charged in a round bottom flask followed by the addition of Cu(OAc)$_2$ (136 mg, 0.340 mmol, 1.10 equiv), arylboronic acid (0.920 mmol, 3.00 equiv), Et$_3$N (157 mg, 1.55 mmol, 5.00 equiv), and MS (150 mg, 4 Å).[69] CH$_2$Cl$_2$ (2 mL) was added to the reaction flask and the reaction mixture was stirred at rt under the O$_2$ balloon for 18 h. Upon completion, the suspension was filtered through Celite® and rinsed with EtOAc (10 mL). The filtrate was concentrated under reduced pressure and the residue obtained was subjected to a silica gel column chromatography (3% MeOH/CH$_2$Cl$_2$ with 0.5% AcOH), which resulted in a desired ether product, along with arylboronic acid and minor impurities. The crude material obtained was dissolved in EtOAc (10 mL) and then washed with a basic sorbitol solution (5 mL × 2) to remove the excess arylboronic acid. Sorbitol solution (1 M) was prepared by dissolving Na$_2$CO$_3$ (53.0 g, 0.500 mol) and sorbitol (91.0 g, 1.11 mol) in water (500 mL).[23] The organic layer was then evaporated under reduced pressure and the crude material obtained was subjected to recrystallization with MeOH/water to afford the anticipated ether analog.
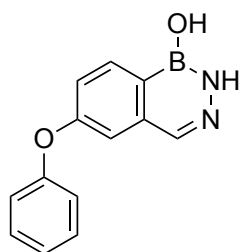
6-Phenoxybenzo[*d*][1,2,3]diazaborinin-1(2*H*)-ol (4-25a): Prepared according to **GP7** using phenylboronic acid (112 mg, 0.920 mmol). Final purification was achieved by recrystallization with MeOH/water to afford the title compound as a pale-yellow crystalline solid (26 mg, 36%); **^{1}H NMR** (400 MHz, *d$_6$*-acetone + 1 drop D$_2$O): δ 8.20 (d, *J* = 8.1 Hz, 1 H), 7.92 (s, 1 H), 7.45 (dd, *J* = 8.6, 7.5 Hz, 2 H), 7.28 – 7.19 (m, 3 H),

7.12 (dd, J = 8.7, 1.1 Hz, 2 H); **^{13}C NMR** (126 MHz, d_6-acetone + 1 drop D$_2$O): δ 161.0, 157.4, 139.6, 139.1, 134.0, 131.0, 125.0, 120.6, 120.5, 115.0; **^{11}B NMR** (128 MHz, d_6-acetone + 1 drop D$_2$O): δ 27.8; **HRMS** (ESI) for C$_{13}$H$_{10}$N$_2$O$_2$^{11}B (M − H)$^-$: Calculated: 237.0841; Found: 237.0844.
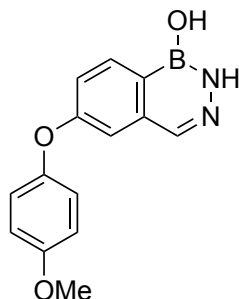
6-(4-Methoxyphenoxy)benzo[*d*][1,2,3]diazaborinin-1(2*H*)-ol **(4-25b):** Prepared according to **GP7** using 4-methoxyphenylboronic acid (140 mg, 0.920 mmol). Final purification was achieved by recrystallization with MeOH/water to afford the title compound as a pale-yellow solid (20 mg, 24%); **^{1}H NMR** (400 MHz, d_6-acetone + 1 drop D$_2$O): δ 8.16 (d, J = 8.4 Hz, 1 H), 7.88 (br s, 1 H), 7.19 (dd, J = 8.4, 2.3 Hz, 1 H), 7.15 – 6.96 (m, 5 H), 3.82 (s, 3 H); **^{13}C NMR** (126 MHz, d_6-acetone + 1 drop D$_2$O): δ 162.2, 157.7, 150.2, 139.6, 139.2, 134.1, 122.4, 119.8, 116.1, 113.7, 56.1; **^{11}B NMR** (128 MHz, d_6-acetone + 1 drop D$_2$O): δ 27.7; **HRMS** (ESI) for C$_{14}$H$_{14}$N$_2$O$_3$^{11}B (M + H)$^+$: Calculated: 269.1092; Found: 269.1095.
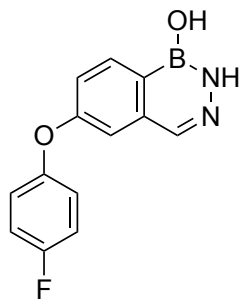
6-(4-Fluorophenoxy)benzo[*d*][1,2,3]diazaborinin-1(2*H*)-ol **(4-25c):** Prepared according to **GP7** using 4-fluorophenylboronic acid (129 mg, 0.920 mmol). Final purification was achieved by recrystallization with MeOH/water to afford the title compound as a pale-yellow solid (32 mg, 40%); **^{1}H NMR** (500 MHz, d_6-acetone + 1

drop D$_2$O): δ 8.27 (d, J = 8.3 Hz, 1 H), 7.99 (s, 1 H), 7.33 – 7.27 (m, 4 H), 7.26 – 7.21 (m, 2 H); ^{13}**C NMR** (126 MHz, d_6-acetone + 1 drop D$_2$O): δ 161.2, 160.2 (d, J = 241 Hz), 153.2 (d, J = 2.58 Hz), 139.6, 139.0, 134.2, 122.5 (d, J = 8.55 Hz), 120.2, 117.5 (d, J = 23.7 Hz), 114.5; ^{11}**B NMR** (128 MHz, d_6-acetone + 1 drop D$_2$O): δ 27.7; ^{19}F NMR (376 MHz, d_6-acetone + 1 drop D$_2$O): δ –120.52 – –120.63 (m); **HRMS** (ESI) for C$_{13}$H$_{11}$FN$_2$O$_2$^{11}B (M + H)$^+$: Calculated: 257.0892; Found: 257.0896.
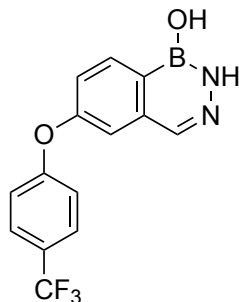
6-(4-(Trifluoromethyl)phenoxy)benzo[*d*][1,2,3]diazaborinin-1(2*H*)-ol **(4-25d):** Prepared according to **GP7** using 4-trifluoromethylphenylboronic acid (177 mg, 0.920 mmol). Final purification was achieved by recrystallization with MeOH/water to afford the title compound as a pale-yellow solid (36 mg, 38%); ^{1}**H NMR** (500 MHz, d_6-acetone + 1 drop D$_2$O): δ 8.23 (d, J = 8.3 Hz, 1 H), 7.95 (br s, 1 H), 7.73 (d, J = 8.8 Hz, 2 H), 7.38 (d, J = 2.3 Hz, 1 H), 7.31 (dd, J = 8.3, 2.3 Hz, 1 H), 7.22 (d, J = 7.0 Hz, 2 H); ^{13}**C NMR** (126 MHz, d_6-acetone + 1 drop D$_2$O): δ 161.2, 159.2, 139.5, 134.4, 128.4 (q, J = 3.88 Hz), 126.5, 125.8 (app d, J = 32.6 Hz), 124.3, 121.5, 119.8, 116.8; ^{11}**B NMR** (160 MHz, d_6-acetone + 1 drop D$_2$O): δ 27.8; ^{19}F NMR (469 MHz, d_6-acetone + 1 drop D$_2$O): δ –62.25; **HRMS** (ESI) for C$_{14}$H$_{11}$F$_3$N$_2$O$_2$^{11}B (M + H)$^+$: Calculated: 307.0860; Found: 307.0863.
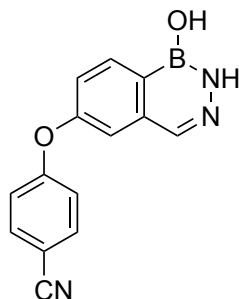
4-((1-Hydroxy-1,2-dihydrobenzo[*d*][1,2,3]diazaborinin-6-yl)oxy)benzonitrile (4-25e): Prepared according to **GP7** using 4-cyanophenylboronic acid (136 mg, 0.920 mmol). Final purification was achieved by recrystallization with MeOH/water to afford the title compound as a yellow solid (10 mg, 13%); **^{1}H NMR** (500 MHz, d_6-acetone + 1 drop D$_2$O): δ 8.37 (d, J = 8.3 Hz, 1 H), 8.07 (br s, 1 H), 7.91 (d, J = 9.0 Hz, 2 H), 7.53 (app t, J = 2.1 Hz, 1 H), 7.44 (dt, J = 8.3, 2.2 Hz, 1 H), 7.31 (dd, J = 8.9, 1.7 Hz, 2 H); **^{13}C NMR** (126 MHz, d_6-acetone + 1 drop D$_2$O): δ 161.9, 158.6, 139.4, 139.3, 135.4, 134.6, 121.8, 119.9, 119.3, 117.3, 107.5, a low signal intensity observed at 139.4 due to the associated broad ^{1}H signal; **^{11}B NMR** (128 MHz, d_6-acetone + 1 drop D$_2$O): δ 27.9; **HRMS** (ESI) for C$_{14}$H$_{11}$N$_3$O$_2$^{11}B (M + H)$^+$: Calculated: 264.0939; Found: 264.0940.
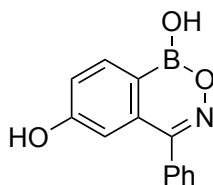
4-Phenyl-1*H*-benzo[*d*][1,2,6]oxazaborinine-1,6-diol (4-26): A flame dried round bottom flask was charged with **4-7j** (500 mg, 1.98 mmol), followed by the addition of CH$_2$Cl$_2$ (15 mL) under argon. The reaction solution was brought down to –78 °C and then BBr$_3$ (9.88 mL, 1 M in CH$_2$Cl$_2$) was added dropwise. The reaction solution was stirred at that temperature for 30 min and then the reaction solution was brought to rt and stirred for 4 h. Upon completion, the reaction was slowly quenched with water (4 mL). The reaction solution was further diluted with water (50 mL) and then extracted with EtOAc (25 mL × 2). The combined organic layer was washed with brine (10 mL), dried over Na$_2$SO$_4$, filtered, and then evaporated under reduced pressure. The yellow

crystalline solid obtained was then dissolved in a minimum quantity of hot methanol (~2 mL), followed by the addition of hexanes (~0.2 mL). The precipitate formed was filtered, and then washed with cold methanol (5 mL) and water (5 mL) to afford the title compound as a white crystalline solid (263 mg, 52%); ^{1}**H NMR** (500 MHz, d_6-acetone + 1 drop D_2O): δ 8.14 (d, J = 8.2 Hz, 1 H), 7.65 – 7.60 (m, 5 H), 7.32 (dd, J = 8.2, 2.3 Hz, 1 H), 6.91 (d, J = 2.3 Hz, 1 H); ^{13}**C NMR** (126 MHz, d_6-acetone + 1 drop D_2O): δ 162.3, 160.2, 136.2, 135.7, 135.2, 130.4, 129.9, 129.3, 120.5, 113.7; ^{11}**B NMR** (128 MHz, d_6-acetone + 1 drop D_2O): δ 28.5; **HRMS** (ESI) for $C_{13}H_{11}NO_3^{11}B$ (M + H)$^+$: Calculated: 240.0827; Found: 240.0826.
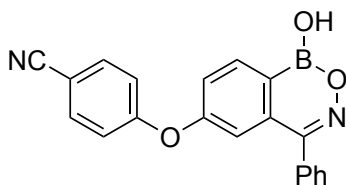
4-((1-Hydroxy-4-phenyl-1H-benzo[d][1,2,6]oxazaborinin-6-yl)oxy)benzonitrile (4-27): Hydroxy analog of **4-1**, **4-26** (50.0 mg, 0.210 mmol) was charged in a round bottom flask followed by the addition of Cu(OAc)$_2$ (42.0 mg, 0.230 mmol), 4-cyanophenylboronic acid (92.0 mg, 0.630 mmol), Et$_3$N (0.150 mL, 1.10 mmol), and MS (150 mg, 4 Å). CH$_2$Cl$_2$ (2 mL) was added to the reaction flask and the reaction mixture was stirred at rt under the O$_2$ balloon for 18 h. Upon completion, the suspension was filtered through Celite® and rinsed with EtOAc (10 mL) and water (5 mL). The combined filtrate was concentrated under reduced pressure and the residue obtained was subjected to phase-switch workup with basic sorbitol solution. Sorbitol solution (5 mL) was added to the residue followed by the extraction with EtOAc (5 mL). Sorbitol solution (1 M) was prepared by dissolving Na$_2$CO$_3$ (53.0 g, 0.500 mol) and sorbitol (91.0 g, 1.11 mol) in water (500 mL).[23] The organic layer was discarded and the pH of the aqueous layer was brought to ~3 with aq. HCl (6 M). The aqueous layer was extracted with EtOAc (5 mL × 3). The combined organic layer was washed with water (5 mL) and then with brine (5 mL). The organic layer was then dried over Na$_2$SO$_4$, filtered, and evaporated under reduced pressure. The residue obtained was subjected to semi-preparative HPLC purification using 0.1% formic acid in water and acetonitrile

as the solvent system (Agilent C18, 250 × 4.6 mm, 5 μm using a gradient: 0.0 min, 40% acetonitrile; 2.0 min, 40% acetonitrile; 10 min, 95% acetonitrile; 12 min, 95% acetonitrile; 12.1 min, 60% acetonitrile for a total of 16 min with a flow rate of 3.0 mL/min, and the fractions were collected between 10–12 min) to afford the title compound as a white solid (8.0 mg, 11%); **¹H NMR** (400 MHz, d_6-acetone + 1 drop D₂O): δ 8.28 (dd, J = 8.2, 3.1 Hz, 1 H), 7.82 – 7.77 (m, 2 H), 7.60 – 7.45 (m, 6 H), 7.25 – 7.16 (m, 2 H), 7.09 – 7.04 (m, 1 H); **¹³C NMR** (126 MHz, d_6-acetone + 1 drop D₂O): δ 161.1, 159.9, 159.7, 136.3, 136.0, 135.5, 135.0, 130.4, 130.2, 129.5, 123.9, 120.2, 119.1, 118.2, 108.0; **¹¹B NMR** (128 MHz, d_6-acetone + 1 drop D₂O): δ 28.3; **HRMS** (ESI) for $C_{20}H_{14}N_2O_3{}^{11}B$ (M + H)⁺: Calculated: 341.1092; Found: 341.1095.

4.9.11 Suzuki-Miyaura Cross-Coupling
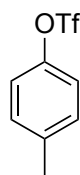
***p*-Tolyl trifluoromethanesulfonate (4-28):** Prepared by following a literature procedure.[70] To a solution of *para*-cresol (1.00 g, 9.25 mmol) in CH₂Cl₂ (9 mL), added Et₃N (2.58 mL, 8.50 mmol) at 0 °C. The reaction solution was stirred for 5 min and then Tf₂O (1.87 mL, 11.1 mmol) was added. The reaction solution was allowed to warm to rt and stirred at that temperature for 16 h. The reaction was quenched with water (10 mL) and then extracted with CH₂Cl₂ (10 mL x 2). The combined organic layer was dried over Na₂SO₄, filtered, and then evaporated under reduced pressure. The residue obtained was subjected to flash column chromatography (100% pentane) to afford the title compound as a colorless liquid (2.06 g, 93%); **¹H NMR** (400 MHz, CDCl₃): δ 7.28 – 7.20 (m, 2 H), 7.20 – 7.12 (m, 2 H), 2.38 (s, 3 H); **¹³C NMR** (126 MHz, CDCl₃): δ 147.6, 138.5, 130.7, 121.0, 118.8 (q, J = 321.5 Hz), 20.9; **¹⁹F NMR** (376 MHz, CDCl₃): δ –72.94.
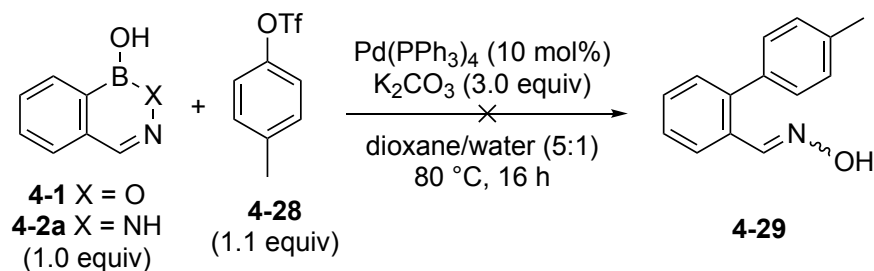
Suzuki-Miyaura Cross-Coupling of 4-28 with Either 4-1 or 4-2a: Heterocycle **4-1** (50.0 mg, 0.340 mmol) or **4-2a** (50.0 mg, 0.340 mmol) was charged in a round bottom flask, followed by the addition of K$_2$CO$_3$ (141 mg, 1.02 mmol), Pd(PPh$_3$)$_4$ (23.9 mg, 10 mol%), and **4-28** (89.8 mg, 0.370 mmol) under an argon balloon.[62] Degassed dioxane/water (4 mL, 4:1) was added to the reaction flask and the reaction solution was stirred at 80 °C for 16 h. The LC-MS of the crude material obtained showed the presence of mostly the unreacted respective precursors (**4-1** or **4-2a**) (cf. Figure 4.13b). In the case of reaction with **4-1**, oxidative product, along with some undetermined impurities were also observed (cf. Figure 4.13b).

General Procedure for Suzuki-Miyaura Cross-Coupling of 4-9 (GP8)[62]

A triflate analog of **4-1**, **4-9** (50 mg, 0.17 mmol, 1.0 equiv) was charged in a flame dried round bottom flask under an argon balloon, followed by the addition of arylboronic acid (0.34 mmol, 2.0 equiv), K$_2$CO$_3$ (71 mg, 0.51 mmol, 3.0 equiv), and Pd(PPh$_3$)$_4$ (12 mg, 0.020 mmol, 10 mol%). Degassed dioxane/water (5:1, 4 mL) was added to the reaction flask and the reaction mixture was stirred at 80 °C for 16 h. Upon completion, the solvent was evaporated under reduced pressure and the residue obtained was dissolved in EtOAc (10 mL), followed by the addition of a basic sorbitol solution (10 mL). Sorbitol solution (1 M) was prepared by dissolving Na$_2$CO$_3$ (53.0 g, 0.500 mol) and sorbitol (91.0 g, 1.11 mol) in water (500 mL).[23] The organic layer was discarded and the pH of the aqueous layer was brought to ~3 with aq. HCl (6 M). The aqueous layer was extracted with EtOAc (5 mL × 3). The combined organic layer was washed with water (5 mL) and then with brine (5 mL). The organic layer was then dried over Na$_2$SO$_4$, filtered, and evaporated under reduced pressure. The residue obtained was subjected to HPLC purification to obtain the anticipated cross-coupled product.

General Procedure for Suzuki-Miyaura Cross-Coupling of 4-10 (GP9)[62]

A triflate analog of **4-2a**, **4-10** (50 mg, 0.17 mmol, 1.0 equiv) was charged in a flame dried round bottom flask under an argon balloon, followed by the addition of arylboronic acid (0.34 mmol, 2.0 equiv), K_2CO_3 (71 mg, 0.51 mmol, 3.0 equiv), and $Pd(PPh_3)_4$ (12 mg, 0.020 mmol, 10 mol%). Degassed dioxane/water (5:1, 4 mL) was added to the reaction flask and the reaction mixture was stirred at 80 °C for 16 h. Upon completion, the suspension was filtered through Celite® and rinsed with EtOAc (10 mL). The filtrate was concentrated under reduced pressure and the residue obtained was dissolved in EtOAc (10 mL) and then washed with a basic sorbitol solution (5 mL × 2), water (5 mL), followed by brine (5 mL) to remove the arylboronic acid. Sorbitol solution (1 M) was prepared by dissolving Na_2CO_3 (53.0 g, 0.500 mol) and sorbitol (91.0 g, 1.11 mol) in water (500 mL).[23] The organic layer was then dried over Na_2SO_4, filtered, and then evaporated under reduced pressure. The residue obtained was subjected to recrystallization with CH_2Cl_2/hexanes to give the anticipated cross-coupled product.
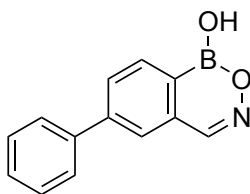

6-Phenyl-1*H*-benzo[*d*][1,2,6]oxazaborinin-1-ol (4-31a): Prepared according to **GP8** using phenylboronic acid (41.4 mg, 0.340 mmol). Final purification was performed by preparative HPLC (Agilent C18, 100 × 50 mm, 5 μm using acetonitrile/water with gradient: 0.0 min, 50% acetonitrile/water; 1.0 min, 60% acetonitrile/water; 10.0 min, 95% acetonitrile/water; 12.0 min, 95% acetonitrile/water; 12.1 min, 50% acetonitrile/water for a total of 14 min with a flow rate of 30 mL/min and the fractions were collected between 7 – 10 min) to afford the title compound as a white solid (13.2 mg, 35%); **¹H NMR** (500 MHz, d_6-acetone + 1 drop D_2O): δ 8.63 (s, 1 H), 8.20 (d, J = 8.5 Hz, 1 H), 8.06 – 8.05 (m, 2 H), 7.82 – 7.76 (m, 2 H), 7.54 (dd, J = 8.3, 6.9 Hz, 2 H), 7.49 – 7.42 (m, 1 H); **¹³C NMR** (126 MHz, d_6-acetone + 1 drop D_2O): δ 151.2, 146.5, 140.7, 134.7, 133.5, 131.3, 130.2, 129.4, 128.3, 126.4; **¹¹B NMR** (128 MHz,

d_6-acetone + 1 drop D$_2$O): δ 28.5; **HRMS** (ESI) for C$_{13}$H$_{11}$NO$_2$^{11}B (M + H)$^+$: Calculated: 224.0877; Found: 224.0876.
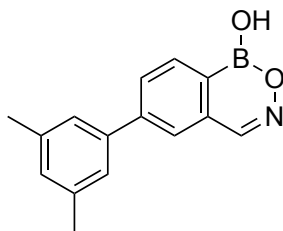
6-(3,5-Dimethylphenyl)-1H-benzo[d][1,2,6]oxazaborinin-1-ol **(4-31b):** Prepared according to **GP8** using 3,5-dimethylphenylboronic acid (51.0 mg, 0.340 mmol). Final purification was performed by semi-preparative HPLC (Agilent C18, 250 × 4.6 mm, 5 μm using acetonitrile/water with gradient: 0.0 min, 60% acetonitrile/water; 2.0 min, 60% acetonitrile/water; 9.0 min, 95% acetonitrile/water; 11.0 min, 95% acetonitrile/water; 11.1 min, 60% acetonitrile/water for a total of 15 min with a flow rate of 2.0 mL/min and the fractions were collected between 11.8 – 13.0 min) to afford the title compound as a white solid (14.2 mg, 33%); ^{1}**H NMR** (500 MHz, d_6-acetone + 1 drop D$_2$O): δ 8.59 (s, 1 H), 8.16 (d, J = 7.7 Hz, 1 H), 8.01 – 7.96 (m, 2 H), 7.36 (s, 2 H), 7.06 (s, 1 H), 2.36 (s, 6 H); ^{13}**C NMR** (126 MHz, d_6-acetone + 1 drop D$_2$O): δ 151.2, 146.5, 140.5, 139.5, 134.4, 133.4, 131.2, 130.8, 126.3, 125.9, 21.4; ^{11}**B NMR** (128 MHz, d_6-acetone + 1 drop D$_2$O): δ 28.0; **HRMS** (ESI) for C$_{15}$H$_{13}$NO$_2$^{11}B (M – H)$^-$: Calculated: 250.1045; Found: 250.1043.

6-(3-Methoxyphenyl)-1H-benzo[d][1,2,6]oxazaborinin-1-ol **(4-31c):** Prepared according to **GP8** using 3-methoxyphenylboronic acid (51.7 mg, 0.340 mmol). Final purification was performed by semi-preparative HPLC (Agilent C18, 250 × 4.6 mm, 5 μm using acetonitrile/water with gradient: 0.0 min, 60% acetonitrile/water; 2.0 min, 60% acetonitrile/water; 9.0 min, 95% acetonitrile/water; 11.0 min, 95%

acetonitrile/water; 11.1 min, 60% acetonitrile/water for a total of 15 min with a flow rate of 2.0 mL/min and the fractions were collected between 8.0 – 9.5 min) to afford the title compound as a white solid (13.1 mg, 30%); **¹H NMR** (500 MHz, d_6-acetone + 1 drop D$_2$O): δ 8.61 (s, 1 H), 8.19 (d, J = 8.2 Hz, 1 H), 8.05 – 8.03 (m, 2 H), 7.44 (app t, J = 7.9 Hz, 1 H), 7.37 – 7.29 (m, 2 H), 7.02 (dd, J = 8.3, 2.5 Hz, 1 H), 3.89 (s, 3 H); **¹³C NMR** (126 MHz, d_6-acetone + 1 drop D$_2$O): δ 161.4, 151.2, 146.3, 142.1, 134.6, 133.5, 131.4, 131.2, 126.5, 120.5, 114.9, 113.7, 55.9; **¹¹B NMR** (160 MHz, d_6-acetone + 1 drop D$_2$O): δ 28.5; **HRMS** (ESI) for C$_{14}$H$_{11}$NO$_3$¹¹B (M – H)⁻: Calculated: 252.0837; Found: 252.0839.
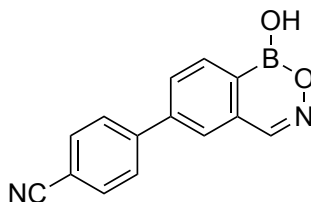
4-(1-Hydroxy-1*H*-benzo[*d*][1,2,6]oxazaborinin-6-yl)benzonitrile (4-31d): Prepared according to **GP8** using 4-cyanophenylboronic acid (50.0 mg, 0.340 mmol). Final purification was performed by preparative HPLC (Agilent C18, 100 × 50 mm, 5 µm using acetonitrile/water with gradient: 0.0 min, 50% acetonitrile/water; 1.0 min, 60% acetonitrile/water; 10.0 min, 95% acetonitrile/water; 12.0 min, 95% acetonitrile/water; 12.1 min, 50% acetonitrile/water for a total of 14 min with a flow rate of 30 mL/min and the fractions were collected between 7 – 10 min) to afford the title compound as a pale-yellow solid (12.4 mg, 29%); **¹H NMR** (700 MHz, d_6-acetone + 1 drop D$_2$O): δ 8.62 (s, 1 H), 8.22 (d, J = 7.4 Hz, 1 H), 8.13 – 8.07 (m, 2 H), 8.00 (d, J = 7.6 Hz, 2 H), 7.92 (d, J = 8.3 Hz, 2 H); **¹³C NMR** (176 MHz, d_6-acetone + 1 drop D$_2$O): δ 151.0, 145.1, 144.3, 134.6, 133.9, 133.8, 131.4, 129.2, 126.9, 119.4, 112.8, two artifacts ~200 and ~250 ppm; **¹¹B NMR** (160 MHz, d_6-acetone + 1 drop D$_2$O): δ 28.2; **HRMS** (ESI) for C$_{14}$H$_{18}$N$_2$O$_2$¹¹B (M – H)⁻: Calculated: 247.0684; Found: 247.0682.
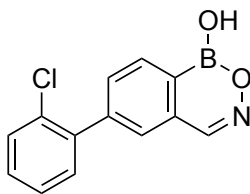
6-(2-Chlorophenyl)-1*H*-benzo[*d*][1,2,6]oxazaborinin-1-ol **(4-31e):** Prepared according to **GP8** using 2-chlorophenylboronic acid (53.2 mg, 0.340 mmol). Final purification was performed by semi-preparative HPLC (Agilent C18, 250 × 4.6 mm, 5 µm using acetonitrile/water with gradient: 0.0 min, 60% acetonitrile/water; 2.0 min, 60% acetonitrile/water; 9.0 min, 95% acetonitrile/water; 11.0 min, 95% acetonitrile/water; 11.1 min, 60% acetonitrile/water for a total of 15 min with a flow rate of 2.0 mL/min and the fractions were collected between 10.0 – 11.8 min) to afford the title compound as a white solid (10.8 mg, 25%); **¹H NMR** (700 MHz, d_6-acetone + 1 drop D_2O): δ 8.60 (s, 1 H), 8.19 (d, J = 7.6 Hz, 1 H), 7.82 (s, 1 H), 7.80 (s, 1 H), 7.57 (d, J = 7.4 Hz, 1 H), 7.49 – 7.44 (m, 3 H); **¹³C NMR** (176 MHz, d_6-acetone + 1 drop D_2O): δ 150.9, 144.8, 140.3, 133.9, 133.8, 132.8, 132.7, 132.5, 131.0, 130.8, 128.9, 128.6, two artifacts ~200 and ~250 ppm; **¹¹B NMR** (160 MHz, d_6-acetone + 1 drop D_2O): δ 28.3; **HRMS** (ESI) for $C_{13}H_{10}ClNO_2{}^{11}B$ (M + H)⁺: Calculated: 258.0491; Found: 258.0491.
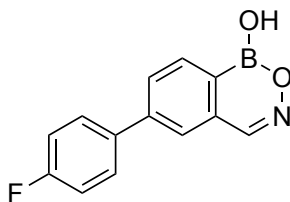
6-(4-Fluorophenyl)-1*H*-benzo[*d*][1,2,6]oxazaborinin-1-ol **(4-31f):** Prepared according to **GP8** using 4-fluorophenylboronic acid (47.6 mg, 0.340 mmol). Final purification was performed by preparative HPLC (Agilent C18, 100 × 50 mm, 5 µm using acetonitrile/water with gradient: 0.0 min, 50% acetonitrile/water; 1.0 min, 60% acetonitrile/water; 10.0 min, 95% acetonitrile/water; 12.0 min, 95% acetonitrile/water; 12.1 min, 50% acetonitrile/water for a total of 14 min with a flow rate of 30 mL/min and the fractions were collected between 7 – 10 min) to afford the title compound as a

white solid (13.2 mg, 32%); **¹H NMR** (500 MHz, d_6-acetone + 1 drop D_2O): δ 8.61 (s, 1 H), 8.19 (d, J = 8.3 Hz, 1 H), 8.05 – 8.00 (m, 2 H), 7.83 (dd, J = 8.9, 5.3 Hz, 2 H), 7.34 – 7.25 (m, 2 H); **¹³C NMR** (176 MHz, d_6-acetone + 1 drop D_2O): δ 164.0 (d, J = 247 Hz), 151.1, 145.2, 137.0 (d, J = 3.35 Hz), 134.6, 133.6, 131.2, 130.2 (d, J = 8.34 Hz), 126.3, 116.9 (d, J = 21.8 Hz); **¹¹B NMR** (160 MHz, d_6-acetone + 1 drop D_2O): δ 28.4; **¹⁹F NMR** (376 MHz, d_6-acetone + 1 drop D_2O): δ –115.61 – –115.84 (m); **HRMS** (ESI) for $C_{13}H_{10}FNO_2{}^{11}B$ (M + H)⁺: Calculated: 242.0783; Found: 242.0782.
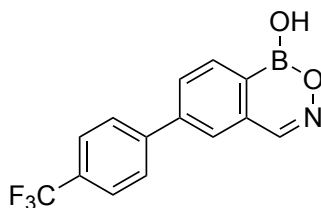
6-(4-(Trifluoromethyl)phenyl)-1*H*-benzo[*d*][1,2,6]oxazaborinin-1-ol **(4-31g):** Prepared according to **GP8** using 4-trifluoromethylphenylboronic acid (64.6 mg, 0.340 mmol). Final purification was performed by semi-preparative HPLC (Agilent C18, 250 × 4.6 mm, 5 μm using acetonitrile/water with gradient: 0.0 min, 50% acetonitrile/water; 2.0 min, 50% acetonitrile/water; 9.0 min, 95% acetonitrile/water; 11.0 min, 95% acetonitrile/water; 11.1 min, 50% acetonitrile/water for a total of 15 min with a flow rate of 2.0 mL/min and the fractions were collected between 11.6 – 12.6 min) to afford the title compound as a white solid (10.0 mg, 20%); **¹H NMR** (500 MHz, d_6-acetone + 1 drop D_2O): δ 8.64 (s, 1 H), 8.24 (d, J = 7.7 Hz, 1 H), 8.15 – 8.08 (m, 2 H), 8.02 (d, J = 8.2 Hz, 2 H), 7.87 (d, J = 8.2 Hz, 2 H);); **¹³C NMR** (176 MHz, d_6-acetone + 1 drop D_2O): δ 151.0, 144.7, 144.6, 134.6, 133.7, 131.4, 130.6 (q, J = 32.4 Hz), 129.0, 127.0 (q, J = 3.89 Hz), 126.8, 125.5 (q, J = 272 Hz); **¹¹B NMR** (128 MHz, d_6-acetone + 1 drop D_2O): δ 28.2; **¹⁹F NMR** (376 MHz, d_6-acetone + 1 drop D_2O) δ -63.01; **HRMS** (ESI) for $C_{14}H_8F_3NO_2{}^{11}B$ (M – H)⁻: Calculated: 290.0606; Found: 290.0603.
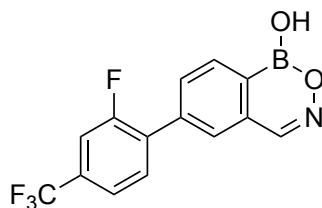
6-(2-Fluoro-4-(trifluoromethyl)phenyl)-1*H*-benzo[*d*][1,2,6]oxazaborinin-1-ol (4-31h): Prepared according to **GP8** using 2-fluoro-4-trifluoromethylphenylboronic acid (70.7 mg, 0.340 mmol). Final purification was performed by semi-preparative HPLC (Agilent C18, 250 × 4.6 mm, 5 μm using acetonitrile/water with gradient: 0.0 min, 60% acetonitrile/water; 2.0 min, 60% acetonitrile/water; 9.0 min, 95% acetonitrile/water; 11.0 min, 95% acetonitrile/water; 11.1 min, 60% acetonitrile/water for a total of 15 min with a flow rate of 2.0 mL/min and the fractions were collected between 10.8 – 12.0 min) to afford the title compound as a white solid (18.1 mg, 34%); **^{1}H NMR** (500 MHz, d_6-acetone + 1 drop D_2O): δ 8.64 (s, 1 H), 8.25 (d, J = 7.5 Hz, 1 H), 8.00 (d, J = 10.6 Hz, 2 H), 7.90 (app t, J = 7.8 Hz, 1 H), 7.76 – 7.68 (m, 2 H); **^{13}C NMR** (176 MHz, d_6-acetone + 1 drop D_2O): δ 160.4 (d, J = 250 Hz), 150.8, 139.6, 134.3, 133.3, 133.3, 133.2, 132.9 (d, J = 13.2 Hz), 132.6 (dq, J = 33.1, 8.45 Hz), 128.7, 125.6, 123.5, 122.9 – 122.8 (m), 114.7 (dq, J = 26.4, 4.09 Hz); **^{11}B NMR** (128 MHz, d_6-acetone + 1 drop D_2O): δ 27.9; **^{19}F NMR** (376 MHz, d_6-acetone + 1 drop D_2O): δ – 63.24 (3 F), –116.55 (t, J = 9.1 Hz, 1 F); **HRMS** (ESI) for $C_{14}H_7F_4NO_2{}^{11}B$ (M − H)⁻: Calculated: 308.0511; Found: 308.0507.
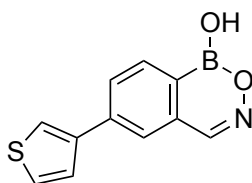
6-(Thiophen-3-yl)-1*H*-benzo[*d*][1,2,6]oxazaborinin-1-ol (4-31i): Prepared according to **GP8** using thiophene-3-boronic acid (43.5 mg, 0.340 mmol). Final purification was performed by semi-preparative HPLC (Agilent C18, 250 × 4.6 mm, 5 μm using acetonitrile/water with gradient: 0.0 min, 50% acetonitrile/water; 1.0 min, 50% acetonitrile/water; 8.0 min, 95% acetonitrile/water; 10.0 min, 95%

acetonitrile/water; 10.1 min, 50% acetonitrile/water for a total of 14 min with a flow rate of 2.0 mL/min and the fractions were collected between 8.0 – 9.2 min) to afford the title compound as a white solid (5.6 mg, 14%); **^{1}H NMR** (500 MHz, d_6-acetone + 1 drop D_2O): δ 8.57 (s, 1 H), 8.15 (d, $J = 8.3$ Hz, 1 H), 8.13 – 8.08 (m, 2 H), 7.98 (dd, $J = 2.8$, 1.4 Hz, 1 H), 7.67 (dd, $J = 5.1$, 1.5 Hz, 1 H), 7.64 (dd, $J = 5.0$, 2.8 Hz, 1 H); **^{13}C NMR** (126 MHz, d_6-acetone + 1 drop D_2O): δ 151.1, 141.9, 141.0, 134.7, 133.5, 130.6, 128.2, 127.1, 125.5, 123.5; **^{11}B NMR** (128 MHz, d_6-acetone + 1 drop D_2O): δ 28.3; **HRMS** (ESI) for $C_{11}H_7SNO_2{}^{11}B$ (M − H)$^-$: Calculated: 228.0296; Found: 228.0299.
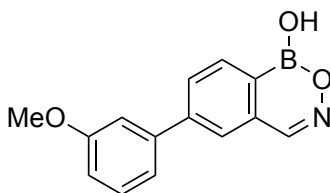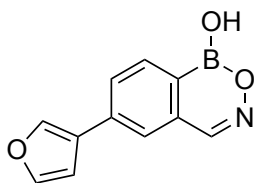

6-(Furan-3-yl)-1*H*-benzo[*d*][1,2,6]oxazaborinin-1-ol (4-31j): Prepared according to **GP8** using furan-3-boronic acid (38.0 mg, 0.340 mmol). Final purification was performed by semi-preparative HPLC (Agilent C18, 250 × 4.6 mm, 5 μm using acetonitrile/water with gradient: 0.0 min, 60% acetonitrile/water; 2.0 min, 60% acetonitrile/water; 9.0 min, 95% acetonitrile/water; 11.0 min, 95% acetonitrile/water; 11.1 min, 60% acetonitrile/water for a total of 15 min with a flow rate of 2.0 mL/min and the fractions were collected between 6.5 – 8.0 min) to afford the title compound as a white solid (9.9 mg, 27%); **^{1}H NMR** (500 MHz, d_6-acetone + 1 drop D_2O): δ 8.53 (s, 1 H), 8.21 (s, 1 H), 8.11 (d, $J = 8.2$ Hz, 1 H), 7.99 (dd, $J = 4.9$, 1.7 Hz, 2 H), 7.69 (app t, $J = 1.7$ Hz, 1 H), 7.02 (s, 1 H); **^{13}C NMR** (126 MHz, d_6-acetone + 1 drop D_2O): δ 151.0, 145.6, 141.4, 138.0, 134.5, 133.5, 130.0, 126.5, 124.8, 109.5; **^{11}B NMR** (160 MHz, d_6-acetone + 1 drop D_2O): δ 28.4; **HRMS** (ESI) for $C_{11}H_7NO_3{}^{11}B$ (M − H)$^-$: Calculated: 212.0524; Found: 212.0526.

6-Phenylbenzo[*d*][1,2,3]diazaborinin-1(2*H*)-ol (4-32a): Prepared according to **GP9** using phenylboronic acid (41.4 mg, 0.340 mmol). Final purification was achieved by recrystallization with CH_2Cl_2/hexanes to afford the title compound as a pale-yellow solid (17.3 mg, 46%); **^{1}H NMR** (400 MHz, d_6-acetone + 1 drop D_2O): δ 8.28 (d, J = 7.9 Hz, 1 H), 8.08 (s, 1 H), 8.01 (d, J = 1.2 Hz, 1 H), 7.89 (dd, J = 7.9, 1.8 Hz, 1 H), 7.82 – 7.75 (m, 2 H), 7.56 – 7.47 (m, 2 H), 7.46 – 7.38 (m, 1 H); **^{13}C NMR** (126 MHz, d_6-acetone + 1 drop D_2O): δ 144.5, 141.5, 140.4, 140.3, 137.9, 132.5, 130.0, 128.9, 128.2, 125.9; **^{11}B NMR** (128 MHz, d_6-acetone + 1 drop D_2O): δ 27.9; **HRMS** (ESI) for $C_{13}H_{12}N_2O^{11}B$ (M + H)$^+$: Calculated: 223.1037; Found: 223.1036.
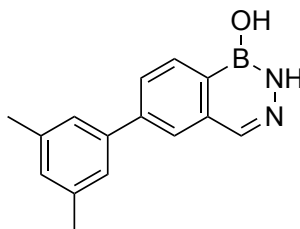

6-(3,5-Dimethylphenyl)benzo[*d*][1,2,3]diazaborinin-1(2*H*)-ol (4-32b): Prepared according to **GP9** using 3,5-dimethylyphenylboronic acid (51.0 mg, 0.340 mmol). Final purification was achieved by recrystallization with CH_2Cl_2/hexanes to afford the title compound as a pale-yellow solid (24.6 mg, 58%); **^{1}H NMR** (500 MHz, d_6-acetone + 1 drop D_2O): δ 8.25 (d, J = 7.9 Hz, 1 H), 8.06 (s, 1 H), 7.97 (d, J = 1.7 Hz, 1 H), 7.85 (dd, J = 7.9, 1.7 Hz, 1 H), 7.38 (s, 2 H), 7.05 (s, 1 H), 2.37 (s, 6 H); **^{13}C NMR** (126 MHz, d_6-acetone + 1 drop D_2O): δ 144.7, 141.3, 140.4, 139.4, 137.8, 132.4, 130.4, 128.3, 126.0, 125.8, 21.49; **^{11}B NMR** (128 MHz, d_6-acetone + 1 drop D_2O): δ 27.7; **HRMS** (ESI) for $C_{15}H_{16}N_2O^{11}B$ (M + H)$^+$: Calculated: 251.1350; Found: 251.1352.
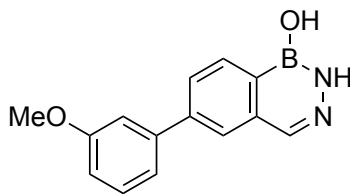
6-(3-Methoxyphenyl)benzo[*d*][1,2,3]diazaborinin-1(2*H*)-ol **(4-32c):** Prepared according to **GP9** using 3-methoxyphenylboronic acid (51.7 mg, 0.340 mmol). Final purification was achieved by recrystallization with CH_2Cl_2/hexanes to afford the title compound as an off-white solid (23.8 mg, 56%); **¹H NMR** (400 MHz, d_6-acetone + 1 drop D_2O): δ 8.27 (d, *J* = 7.9 Hz, 1 H), 8.07 (s, 1 H), 8.01 (d, *J* = 1.7 Hz, 1 H), 7.88 (dd, *J* = 7.9, 1.8 Hz, 1 H), 7.43 (t, *J* = 7.9 Hz, 1 H), 7.38 – 7.28 (m, 2 H), 6.99 (ddd, *J* = 8.2, 2.6, 1.1 Hz, 1 H), 3.89 (s, 3 H); **¹³C NMR** (126 MHz, d_6-acetone + 1 drop D_2O): δ 161.3, 144.4, 142.9, 140.4, 140.3, 137.8, 132.5, 131.1, 128.3, 125.9, 120.5, 114.5, 113.7, 55.8; **¹¹B NMR** (128 MHz, d_6-acetone + 1 drop D_2O): δ 27.9; **HRMS** (ESI) for $C_{14}H_{14}N_2O_2{}^{11}B$ (M + H)⁺: Calculated: 253.1143; Found: 253.1143.
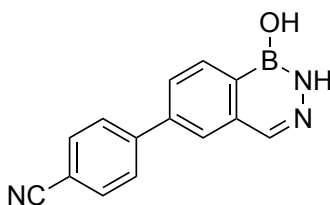
4-(1-Hydroxy-1,2-dihydrobenzo[*d*][1,2,3]diazaborinin-6-yl)benzonitrile **(4-32d):** Prepared according to **GP9** using 4-cyanophenylboronic acid (50.0 mg, 0.340 mmol). Final purification was achieved by recrystallization with CH_2Cl_2/hexanes to afford the title compound as a light brown solid (22.2 mg, 53%); **¹H NMR** (400 MHz, d_6-acetone + 1 drop D_2O): δ 8.31 (d, *J* = 7.9 Hz, 1 H), 8.11 – 8.10 (m, 2 H), 8.01 (d, *J* = 8.2 Hz, 2 H), 7.95 (dd, *J* = 7.9, 1.8 Hz, 1 H), 7.92 (d, *J* = 8.4 Hz, 2 H); **¹³C NMR** (126 MHz, d_6-acetone + 1 drop D_2O): δ 145.8, 142.4, 140.1, 137.8, 133.8, 132.9, 129.1, 128.2, 126.4, 119.5, 112.2; **¹¹B NMR** (128 MHz, d_6-acetone + 1 drop D_2O): δ 27.5; **HRMS** (ESI) for $C_{14}H_{11}N_3O{}^{11}B$ (M + H)⁺: Calculated: 248.0990; Found: 248.0990.
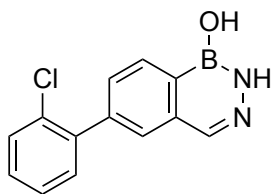
6-(2-Chlorophenyl)benzo[*d*][1,2,3]diazaborinin-1(2*H*)-ol **(4-32e):** Prepared according to **GP9** using 2-chlorophenylboronic acid (53.2 mg, 0.340 mmol). Final purification was achieved by recrystallization with CH_2Cl_2/hexanes to afford the title compound as a pale-yellow solid (23.7 mg, 54%); **^{1}H NMR** (400 MHz, d_6-acetone + 1 drop D_2O): δ 8.28 (d, J = 7.8 Hz, 1 H), 8.06 (s, 1 H), 7.78 (d, J = 1.3 Hz, 1 H), 7.66 (dd, J = 7.8, 1.7 Hz, 1 H), 7.59 – 7.55 (m, 1 H), 7.51 – 7.42 (m, 3 H); **^{13}C NMR** (126 MHz, d_6-acetone + 1 drop D_2O): δ 143.0, 141.0, 140.1, 140.1, 137.2, 132.9, 132.6, 131.7, 131.0, 130.5, 130.4, 128.4, 128.4; **^{11}B NMR** (128 MHz, d_6-acetone + 1 drop D_2O): δ 27.8; **HRMS** (ESI) for $C_{13}H_{11}ClN_2O^{11}B$ (M + H)$^+$: Calculated: 257.0647; Found: 257.0645.
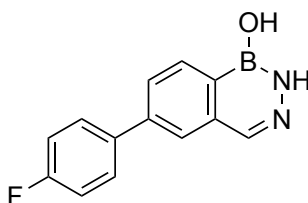

6-(4-Fluorophenyl)benzo[*d*][1,2,3]diazaborinin-1(2*H*)-ol **(4-32f):** Prepared according to **GP9** using 4-fluorophenylboronic acid (47.6 mg, 0.340 mmol). Final purification was achieved by recrystallization with CH_2Cl_2/hexanes to afford the title compound as a light brown solid (25.6 mg, 63%); **^{1}H NMR** (500 MHz, d_6-acetone + 1 drop D_2O): δ 8.26 (d, J = 7.9 Hz, 1 H), 8.06 (s, 1 H), 7.99 (d, J = 1.2 Hz, 1 H), 7.86 (dd, J = 7.9, 1.8 Hz, 1 H), 7.84 – 7.80 (m, 2 H), 7.32 – 7.23 (m, 2 H); **^{13}C NMR** (126 MHz, d_6-acetone + 1 drop D_2O): δ 163.7 (d, J = 246 Hz), 143.3, 140.2, 137.8, 137.7 (d, J = 3.19 Hz), 132.6, 130.1 (d, J = 8.08 Hz), 128.1, 125.8, 116.7 (d, J = 21.8 Hz); **^{11}B NMR** (128 MHz, d_6-acetone + 1 drop D_2O): δ 27.8; **^{19}F NMR** (376 MHz, d_6-acetone + 1 drop D_2O): δ –116.45; **HRMS** (ESI) for $C_{13}H_{11}FN_2O^{11}B$ (M + H)$^+$: Calculated: 241.0943; Found: 241.0944.
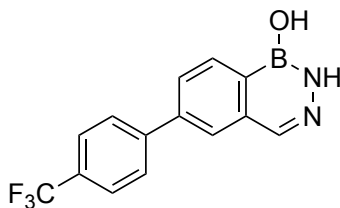
6-(4-(Trifluoromethyl)phenyl)benzo[*d*][1,2,3]diazaborinin-1(2*H*)-ol **(4-32g):** Prepared according to **GP9** using 4-trifluoromethylphenylboronic acid (64.6 mg, 0.340 mmol). Final purification was achieved by recrystallization with CH_2Cl_2/hexanes to afford the title compound as a light brown solid (24.7 mg, 50%); **^{1}H NMR** (400 MHz, d_6-acetone + 1 drop D_2O): δ 8.31 (d, *J* = 7.9 Hz, 1 H), 8.09 (app s, 2 H), 8.01 (d, *J* = 8.3 Hz, 2 H), 7.94 (dd, *J* = 7.9, 1.7 Hz, 1 H), 7.85 (d, *J* = 8.2 Hz, 2 H); **^{13}C NMR** (126 MHz, d_6-acetone + 1 drop D_2O): δ 145.4, 142.8, 140.2, 140.2, 137.9, 132.8, 130.2 (q, *J* = 32.3 Hz), 129.0, 128.2, 126.9 (q, *J* = 3.88 Hz), 126.4, 125.6 (q, *J* = 272 Hz); **^{11}B NMR** (128 MHz, d_6-acetone + 1 drop D_2O): δ 27.8; **^{19}F NMR** (376 MHz, d_6-acetone + 1 drop D_2O): δ –62.97; **HRMS** (ESI) for $C_{14}H_9F_3N_2O^{11}B$ $(M - H)^-$: Calculated: 289.0766; Found: 289.0757.
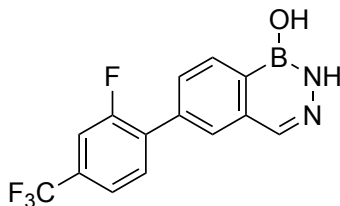
6-(2-Fluoro-4-(trifluoromethyl)phenyl)benzo[*d*][1,2,3]diazaborinin-1(2*H*)-ol **(4-32h):** Prepared according to **GP9** using 2-fluoro-4-trifluoromethylphenylboronic acid (70.7 mg, 0.340 mmol). Final purification was achieved by recrystallization with CH_2Cl_2/hexanes to afford the title compound as an off-white solid (29.6 mg, 57%); **^{1}H NMR** (400 MHz, d_6-acetone + 1 drop D_2O): δ 8.32 (d, *J* = 7.8 Hz, 1 H), 8.09 (s, 1 H), 7.98 (s, 1 H), 7.88 (t, *J* = 7.8 Hz, 1 H), 7.82 (dt, *J* = 7.9, 1.7 Hz, 1 H), 7.74 – 7.63 (m, 2 H); **^{13}C NMR** (126 MHz, d_6-acetone + 1 drop D_2O): δ 160.3 (d, *J* = 250 Hz), 140.0, 137.7, 133.5 (d, *J* = 12.8 Hz), 133.3 (d, *J* = 3.59 Hz), 132.4, 132.1 (dq, *J* = 33.1, 8.01 Hz), 129.9, 128.2 (d, *J* = 2.95 Hz), 123.4, 122.7, 122.7 (d, *J* = 7.85 Hz), 114.5 (dq, *J* = 26.6, 3.96 Hz); **^{11}B NMR** (128 MHz, d_6-acetone + 1 drop D_2O): δ 27.5; **^{19}F NMR** (376

MHz, d_6-acetone + 1 drop D_2O): δ –63.11 (3 F), –116.57 – –116.69 (m, 1 F); **HRMS** (ESI) for $C_{14}H_8F_4N_2O^{11}B$ (M – H)⁻: Calculated: 307.0671; Found: 307.0664.
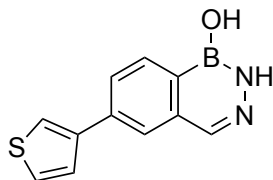
6-(Thiophen-3-yl)benzo[*d*][1,2,3]diazaborinin-1(2*H*)-ol (4-32i): Prepared according to **GP9** using thiophene-3-boronic acid (43.5 mg, 0.340 mmol). Final purification was achieved by recrystallization with CH_2Cl_2/hexanes to afford the title compound as a light brown solid (26.0 mg, 67%); **¹H NMR** (500 MHz, d_6-acetone + 1 drop D_2O): δ 8.17 (d, *J* = 7.9 Hz, 1 H), 8.02 (d, *J* = 1.7 Hz, 1 H), 7.98 (s, 1 H), 7.89 (dd, *J* = 7.9, 1.7 Hz, 1 H), 7.88 – 7.86 (m, 1 H), 7.61 (dt, *J* = 5.1, 1.4 Hz, 1 H), 7.56 (ddd, *J* = 5.0, 2.9, 1.1 Hz, 1 H); **¹³C NMR** (126 MHz, d_6-acetone + 1 drop D_2O): δ 142.6, 140.2, 139.2, 137.9, 132.5, 127.9, 127.6, 127.2, 125.0, 122.7; **¹¹B NMR** (160 MHz, d_6-acetone + 1 drop D_2O): δ 27.6; **HRMS** (ESI) for $C_{11}H_{10}SN_2O^{11}B$ (M + H)⁺: Calculated: 229.0601; Found: 229.0601.
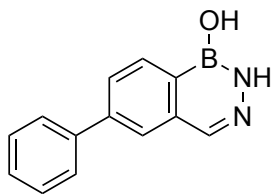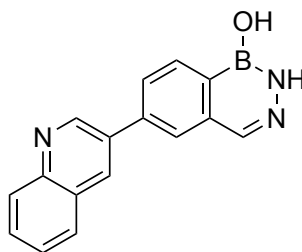

6-(Quinolin-3-yl)benzo[*d*][1,2,3]diazaborinin-1(2*H*)-ol (4-32j): Prepared according to **GP8** using quinoline-3-boronic acid (58.8 mg, 0.340 mmol). Final purification was achieved by recrystallization with CH_2Cl_2/hexanes to afford the title compound as a yellow solid (33.9 mg, 73%); **¹H NMR** (400 MHz, d_6-acetone + 1 drop D_2O): δ 9.34 (d, *J* = 2.3 Hz, 1 H), 8.73 (d, *J* = 2.4 Hz, 1 H), 8.37 (d, *J* = 7.9 Hz, 1 H), 8.25 (d, *J* = 1.7 Hz, 1 H), 8.18 – 8.07 (m, 4 H), 7.81 (ddd, *J* = 8.4, 6.9, 1.5 Hz, 1 H), 7.67 (ddd, *J* = 8.1, 6.8, 1.2 Hz, 1 H); **¹³C NMR** (126 MHz, d_6-acetone + 1 drop D_2O): δ 150.6, 148.5, 141.2, 140.3, 137.9, 134.8, 134.1, 132.9, 130.8, 129.9, 129.5, 129.1, 128.4, 128.2,

126.4; **^{11}B NMR** (128 MHz, d_6-acetone + 1 drop D$_2$O): δ 27.8; **HRMS** (ESI) for C$_{16}$H$_{13}$N$_3$O^{11}B (M + H)$^+$: Calculated: 274.1146; Found: 274.1150.
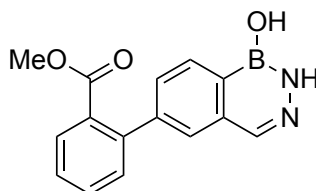
Methyl 2-(1-hydroxy-1,2-dihydrobenzo[d][1,2,3]diazaborinin-6-yl)benzoate (4-32k): Prepared according to **GP9** using 2-methoxycarbonylphenylboronic acid (61.2 mg, 0.340 mmol). Final purification was achieved by recrystallization with CH$_2$Cl$_2$/hexanes to afford the title compound as a yellow solid (18.7 mg, 39%); **^{1}H NMR** (500 MHz, d_6-acetone + 1 drop D$_2$O): δ 8.22 (d, J = 7.8 Hz, 1 H), 8.03 (s, 1 H), 7.84 (dd, J = 7.7, 1.4 Hz, 1 H), 7.69 – 7.64 (m, 2 H), 7.56 – 7.50 (m, 3 H), 3.57 (s, 3 H); **^{13}C NMR** (126 MHz, d_6-acetone + 1 drop D$_2$O): δ 169.5, 145.0, 142.7, 140.2, 140.1, 137.2, 132.5, 132.2, 131.8, 131.6, 130.7, 129.8, 128.7, 127.2, 52.4; **^{11}B NMR** (128 MHz, d_6-acetone + 1 drop D$_2$O): δ 27.8; **HRMS** (ESI) for C$_{15}$H$_{14}$N$_2$O$_3$^{11}B (M + H)$^+$: Calculated: 281.1093; Found: 181.1092.

4.9.12 Synthesis of Olaparib Isosteres
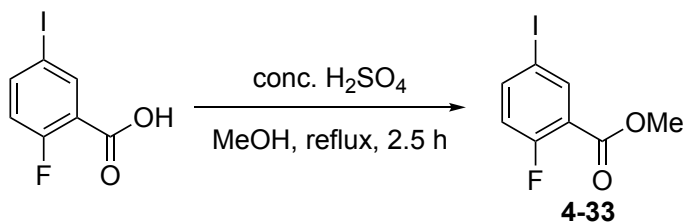
Methyl 2-fluoro-5-iodobenzoate (4-33): In a round bottom flask, 2-fluoro-5-iodobenzoic acid (3.00 g, 11.3 mmol) was charged, followed by the addition of MeOH (75 mL) and conc. H$_2$SO$_4$ (3 mL). The reaction solution was heated at reflux for 2.5 h. Upon completion, Et$_2$O (100 mL) was added and the organic and aqueous layer were separated. The organic layer was washed with water (50 mL × 2), saturated aq. NaHCO$_3$ (50 mL), and brine (50 mL). The organic layer was then dried over Na$_2$SO$_4$, filtered, and evaporated under reduced pressure to afford the title compound as a yellow

liquid (2.87 g, 91%); **^{1}H NMR** (600 MHz, CDCl$_3$): δ 8.23 (dd, J = 6.7, 2.4 Hz, 1 H),

7.80 (ddd, J = 8.6, 4.4, 2.4 Hz, 1 H), 6.91 (dd, J = 10.3, 8.7 Hz, 1 H), 3.93 (s, 3 H); **^{13}C**

NMR (151 MHz, CDCl$_3$): δ 162.7, 162.2 (d, J = 313 Hz); 143.2 (d, J = 7.40 Hz), 140.7,

120.7 (d, J = 8.91 Hz), 119.2 (d, J = 19.6 Hz), 86.5 (d, J = 3.30 Hz), 52.6; **^{19}F NMR**

(376 MHz, CDCl$_3$): δ –110.77 (ddd, J = 10.7, 6.7, 4.4 Hz).
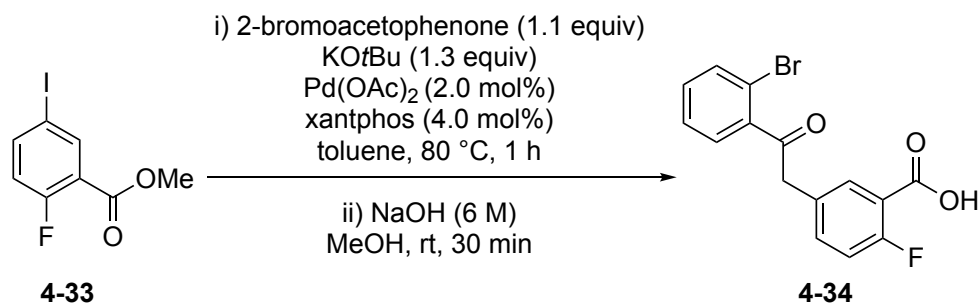
5-(2-(2-Bromophenyl)-2-oxoethyl)-2-fluorobenzoic acid (4-34): Prepared according

to a literature procedure with modifications.[55] In a flame dried round bottom flask under

N$_2$, **4-33** (1.00 g, 3.57 mmol) was charged, followed by the addition of

2-bromoacetophenone (782 mg, 0.530 mL, 3.92 mmol), Pd(OAc)$_2$ (16.0 mg, 2.00

mol%), xantphos (82.6 mg, 4.00 mol%), and KOtBu (521 mg, 4.64 mmol). Anhydrous

toluene (28 mL) was added to the reaction flask and the reaction mixture was stirred at

80 °C for 1 h. Upon completion, the temperature of the reaction flask was brought down

to rt and MeOH (15 mL) was added followed by the addition of 6 M aq. NaOH (15

mL). The reaction mixture was stirred at that temperature for 30 min. Upon completion,

the contents of the reaction flask were transferred to a separatory funnel and EtOAc (50

mL) was added. The organic and aqueous layer were separated and the organic layer

was again extracted with water (50 mL). The pH of the combined aqueous layer was

brought down to ~2 using 6 M aq. HCl. The resulting acidic aqueous layer was

extracted with EtOAc (20 mL × 3). The combined organic layer was dried over

Na$_2$SO$_4$, filtered, and evaporated under reduced pressure. The residue obtained was

subjected to silica gel column chromatography (10–20% EtOAc/hexanes containing

0.5% AcOH). The product obtained was triturated with Et$_2$O (5 mL) to obtain the title

compound as a white solid (279 mg, 23%); **^{1}H NMR** (400 MHz, CDCl$_3$): δ 7.90 (dd, J

= 6.8, 2.4 Hz, 1 H), 7.50 (ddd, J = 8.5, 4.5, 2.4 Hz, 1 H), 7.41 – 7.28 (m, 3 H), 7.15 (dd,

$J = 10.5$, 8.5 Hz, 1 H), 4.27 (s, 2 H); ^{13}C NMR (126 MHz, CDCl$_3$): δ 200.7, 168.6, 161.8 (d, $J = 263$ Hz), 141.2, 137.0 (d, $J = 9.20$ Hz), 133.9, 133.7, 131.9, 129.7 (d, $J = 3.93$ Hz), 128.6, 127.6, 118.7, 117.5 (d, $J = 2.87$ Hz), 48.0; ^{19}F NMR (376 MHz, CDCl$_3$): δ −110.43 (dt, $J = 11.2$, 5.4 Hz); HRMS (ESI) for C$_{15}$H$_{11}$FO$_3$Br (M − H)$^-$: Calculated: 334.9725; Found: 334.9726.
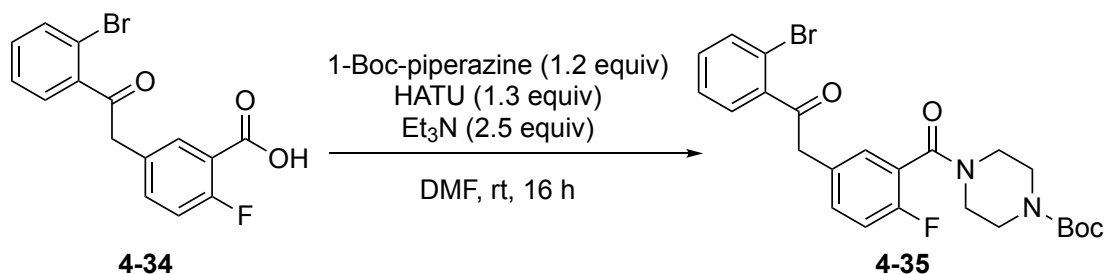
***tert*-Butyl 4-(5-(2-(2-bromophenyl)-2-oxoethyl)-2-fluorobenzoyl)piperazine-1-carboxylate (4-35):** In a round bottom flask, **4-34** (200 mg, 0.590 mmol) in DMF (3 mL) was charged, followed by the addition of HATU (292 mg, 0.770 mmol) and 1-Boc-piperazine (132 mg, 0.710 mmol). Et$_3$N (149 mg, 1.48 mmol) was added to the reaction flask and the reaction solution was stirred at rt for 16 h. Upon completion, saturated aq. NaHCO$_3$ (10 mL) was added and then extracted with EtOAc (10 mL × 2). The combined organic layer was dried over Na$_2$SO$_4$, filtered, and evaporated under reduced pressure. The residue obtained was subjected to silica gel column chromatography (35–40% EtOAc/hexanes) to afford the title compound as a colorless liquid (297 mg, quant.); ^{1}H NMR (400 MHz, CDCl$_3$): δ 7.76 (d, $J = 7.8$ Hz, 1 H), 7.55 – 7.44 (m, 4 H), 7.42 (dd, $J = 6.3$, 2.3 Hz, 1 H), 7.22 (app t, $J = 8.8$ Hz, 1 H), 4.38 (s, 2 H), 3.92 (app s, 2 H), 3.68 (app t, $J = 5.3$ Hz, 2 H), 3.57 (app t, $J = 5.1$ Hz, 2H), 3.45 (app s, 2 H), 1.64 (s, 9 H); ^{13}C NMR (126 MHz, CDCl$_3$): δ 200.7, 165.0, 157.2 (d, $J = 248$ Hz), 154.5, 141.1, 133.7, 132.9 (d, $J = 8.04$ Hz), 131.8, 130.4 (d, $J = 3.74$ Hz), 130.2 (d, $J = 3.57$ Hz), 128.5, 127.5, 123.8 (d, $J = 18.2$ Hz), 118.6, 116.0 (d, $J = 22.0$ Hz), 80.3, 48.0, 46.9, 41.9, 28.4; ^{19}F NMR (376 MHz, CDCl$_3$): δ −117.44 – −117.50 (m); HRMS (ESI) for C$_{24}$H$_{26}$FN$_2$O$_4$BrNa (M + Na)$^+$: Calculated: 527.0952; Found: 527.0952.
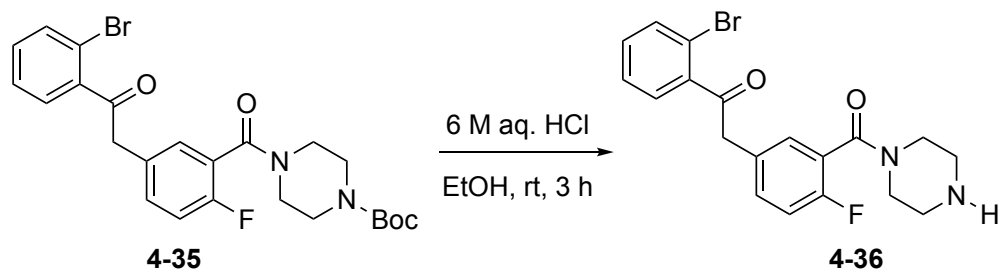
1-(2-Bromophenyl)-2-(4-fluoro-3-(piperazine-1-carbonyl)phenyl)ethan-1-one (4-36): In a round bottom flask, **4-35** (48 mg, 0.10 mmol) in EtOH (1 mL) was charged, followed by the addition of 6 M aq. HCl (3.0 mL). The reaction solution was stirred at rt for 3 h. Upon completion, the reaction solution was adjusted to a pH of 10 with 5 M aq. NH₄OH solution and then extracted with EtOAc (10 mL × 3). The combined organic layer was washed with water (10 mL) and then dried over Na₂SO₄, filtered, and evaporated under reduced pressure to afford the title compound as a pale-yellow liquid (41 mg, 84%); ^{1}**H NMR** (500 MHz, CDCl₃): δ 7.62 (d, J = 7.9 Hz, 1 H), 7.39 – 7.28 (m, 4 H), 7.26 (dd, J = 6.3, 2.3 Hz, 1 H), 7.06 (app t, J = 8.8 Hz, 1 H), 4.23 (s, 2 H), 3.78 (app t, J = 5.2 Hz, 2 H), 3.30 (app s, 2 H), 2.95 (app t, J = 5.1 Hz, 2 H), 2.82 (app s, 2 H); ^{13}**C NMR** (126 MHz, CDCl₃): δ 200.9, 164.9, 157.3 (d, J = 249 Hz), 141.2, 133.7, 132.6 (d, J = 8.00 Hz), 131.8, 130.4 (d, J = 3.96 Hz), 130.1 (d, J = 3.58 Hz), 128.5, 127.5, 124.2 (d, J = 18.3 Hz), 118.7, 116.0 (d, J = 22.0 Hz), 48.3, 48.2, 46.4, 45.8, 43.1; ^{19}**F NMR** (376 MHz, CDCl₃): δ –117.46 (dt, J = 10.2, 5.8 Hz); **HRMS** (ESI) for C₁₉H₁₉FN₂O₂Br (M + H)$^+$: Calculated: 405.0608; Found: 405.0605.
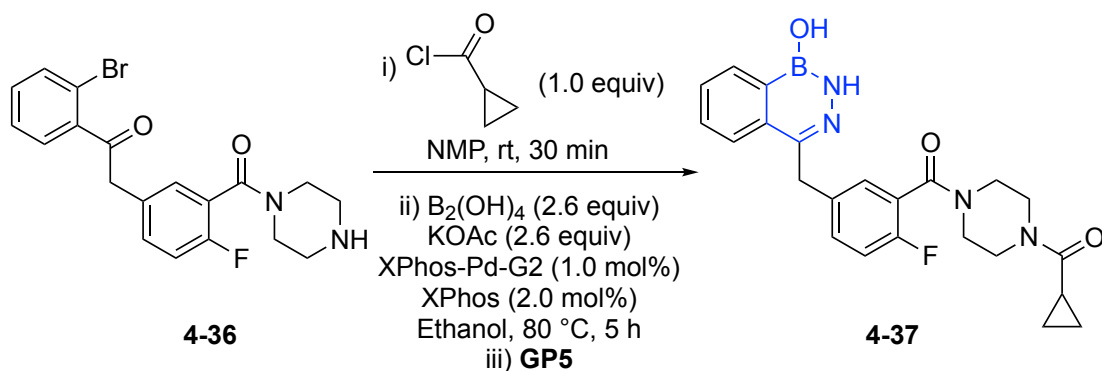
(4-(Cyclopropanecarbonyl)piperazin-1-yl)(2-fluoro-5-((1-hydroxy-1,2-dihydrobenzo[*d*][1,2,3]diazaborinin-4-yl)methyl)phenyl)methanone (4-37): The

piperazine derivative **4-36** (97.0 mg, 0.220 mmol) was charged in a round bottom flask, followed by the addition of NMP (0.5 mL) and cyclopropanecarbonyl chloride (27.6 mg, 0.264 mmol). The reaction solution was stirred at rt for 30 min.[39] Upon completion, saturated aq. $NaHCO_3$ (5 mL) was added and then extracted with EtOAc (10 mL). The organic layer was washed with brine (5 mL) and dried over Na_2SO_4, filtered, and evaporated under reduced pressure to afford the crude "amido cyclopropane" derivative as a pale-yellow solid, which was used without further purification for the Molander borylation reaction.[56] The crude compound, dissolved in degassed EtOH (4 mL) was charged into a flame dried round bottom flask, followed by the addition of $B_2(OH)_4$ (57.0 mg, 0.634 mmol), KOAc (62.2 mg, 0.634 mmol), XPhos-Pd-G2 (1.70 mg, 1.00 mol%), and XPhos (2.0 0mg, 2.00 mol%). The reaction mixture was stirred at 80 °C for 5 h. Upon completion, water (10 mL) was added to the reaction flask and then extracted with EtOAc (10 mL × 2). The combined organic layer was dried over Na_2SO_4, filtered, and evaporated under reduced pressure to afford the crude boronic acid product, which was then subjected to a condensation reaction (**GP5**: $NH_2NH_2 \cdot H_2O$ (10.0 μL, 0.260 mmol)). The final purification was performed by semi-preparative HPLC (Agilent C18, 250 × 4.6 mm, 5 mm using 0.1% formic acid in water and acetonitrile as the solvent system with gradient: 0.0 min, 10% acetonitrile; 3.0 min, 10% acetonitrile; 10.0 min, 50% acetonitrile; 15.0 min, 95% acetonitrile; 16.0 min, 95% acetonitrile; 16.1 min, 10% acetonitrile for a total of 20 min with a flow rate of 3.0 mL/min and the fractions were collected between 11.0 – 12.0 min) to afford the title compound as a white solid (7.2 mg, 8% over 3 steps); **¹H NMR** (400 MHz, d_6-acetone + 1 drop D_2O): δ 8.22 (d, J = 8.4 Hz, 1 H), 7.84 (d, J = 8.1 Hz, 1 H), 7.64 (td, J = 7.7, 1.5 Hz, 1 H), 7.55 (td, J = 7.4, 1.1 Hz, 1 H), 7.43 (ddd, J = 8.0, 5.0, 2.3 Hz, 1H), 7.34 (dd, J = 6.5, 2.3 Hz, 1 H), 7.12 (app t, J = 9.0 Hz, 1H), 4.31 (s, 2 H), 3.80 – 3.64 (m, 5 H), 3.49 (app s, 1 H), 3.27 (app s, 2 H), 2.00 – 1.90 (m, 1 H), 0.84 – 0.80 (m, 2 H), 0.78 – 0.69 (m, 2 H); **¹³C NMR** (176 MHz, d_6-acetone + 1 drop D_2O): δ 172.3, 165.4, 157.7 (d, J = 244 Hz), 145.3, 137.7 (d, J = 3.34 Hz), 136.0, 132.1 (d, J = 7.90 Hz), 132.0, 131.7, 129.7 (d, J = 3.91 Hz), 129.0, 126.3, 125.0 (d, J = 18.6 Hz), 116.4 (d, J = 21.8 Hz), 47.4, 45.7, 42.7, 42.3, 11.2, 7.4, artifacts at 1.1, 201.5, and

248.5; **^{19}F NMR** (376 MHz, d_6-acetone + 1 drop D$_2$O): δ –121.45 – –121.50 (m); **HRMS** (ESI) for C$_{23}$H$_{25}$FN$_4$O$_3$N^{11}B (M + H)$^+$: Calculated: 435.1998; Found: 435.1998.
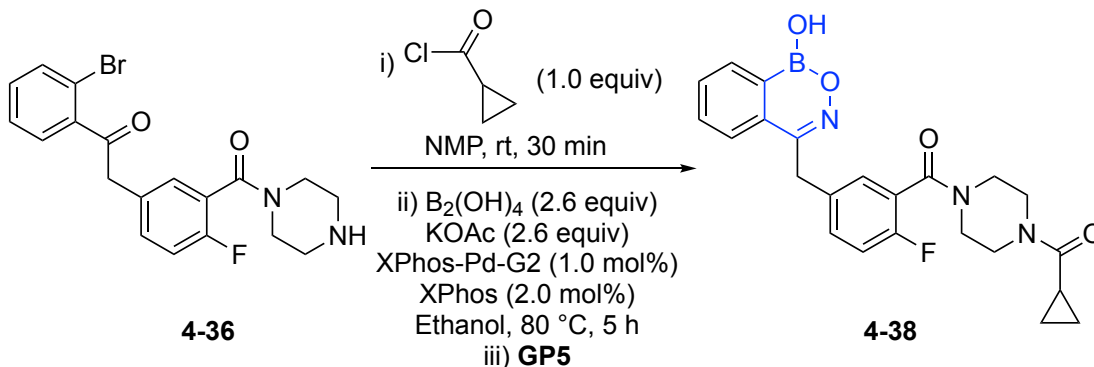
(4-(Cyclopropanecarbonyl)piperazin-1-yl)(2-fluoro-5-((1-hydroxy-1*H*-benzo[*d*][1,2,6]oxazaborinin-4-yl)methyl)phenyl)methanone (4-38): The piperazine derivative **4-36** (194 mg, 0.480 mmol) was charged in a round bottom flask, followed by the addition of NMP (0.5 mL) and cyclopropanecarbonyl chloride (55.2 mg, 0.528 mmol). The reaction solution was stirred at rt for 30 min.[39] Upon completion, saturated aq. NaHCO$_3$ (10 mL) was added and then extracted with EtOAc (20 mL). The organic layer was washed with brine (10 mL) and dried over Na$_2$SO$_4$, filtered, and evaporated under reduced pressure to afford the crude "amido cyclopropane" derivative as a pale-yellow solid, which was used without further purification for the Molander borylation reaction.[56] The crude compound, dissolved in degassed EtOH (8.00 mL) was charged into a flame dried round bottom flask followed by the addition of B$_2$(OH)$_4$ (114 mg, 1.27 mmol), KOAc (125 mg, 1.27 mmol), XPhos-Pd-G2 (3.80 mg, 1.00 mol%), and XPhos (4.60 mg, 2.00 mol%). The reaction mixture was stirred at 80 °C for 5 h. Upon completion, water (10 mL) was added to the reaction flask and then extracted with EtOAc (10 mL × 2). The combined organic layer was dried over Na$_2$SO$_4$, filtered, and evaporated under reduced pressure to afford the crude boronic acid product, which was subjected to a condensation reaction (**GP5**: NH$_2$OH (50 wt. % solution in water, 40.0 μL, 0.580 mmol). Final purification was performed by semi-preparative HPLC (Agilent C8, 250 × 4.6 mm, 5 μm using 0.1% formic acid in water

and acetonitrile as the solvent system with gradient: 0.0 min, 10% acetonitrile; 3.0 min, 10% acetonitrile; 10.0 min, 50% acetonitrile; 15.0 min, 95% acetonitrile; 16.0 min, 95% acetonitrile; 16.1 min, 10% acetonitrile for a total of 20 min with a flow rate of 3.0 mL/min and the fractions were collected between 11.0 – 12.5 min) to afford the title compound as a white solid (9.8 mg, 5% over 3 steps); **^{1}H NMR** (400 MHz, d_6-acetone + 1 drop D_2O): δ 8.13 (d, J = 7.3 Hz, 1 H), 7.83 (d, J = 7.0 Hz, 1 H), 7.72 (dtd, J = 17.0, 7.3, 1.4 Hz, 2 H), 7.52 (ddd, J = 8.0, 5.0, 2.3 Hz, 1 H), 7.44 (dd, J = 6.4, 2.4 Hz, 1 H), 7.16 (app t, J = 9.0 Hz, 1 H), 4.35 (s, 2 H), 3.59 – 3.50 (m, 6 H), 3.28 (app s, 2H), 2.01 – 1.87 (m, 1 H), 0.86 – 0.80 (m, 2 H), 0.74 – 0.72 (m, 2 H); **^{13}C NMR** (126 MHz, d_6-acetone + 1 drop D_2O): δ 172.3, 165.1, 162.4, 157.9 (d, J = 246 Hz), 157.1, 135.7 (d, J = 3.36 Hz), 133.6, 133.3, 133.0, 132.2 (d, J = 8.05 Hz), 132.1, 129.8 (d, J = 4.13 Hz), 126.7, 125.3 (d, J = 18.5 Hz), 116.7 (d, J = 22.1 Hz), 47.4, 46.2, 42.8, 42.2, 11.2, 7.4; **^{11}B NMR** (128 MHz, d_6-acetone + 1 drop D_2O): δ 28.6; **^{19}F NMR** (376 MHz, d_6-acetone + 1 drop D_2O): δ –120.66 (dt, J = 10.1, 5.5 Hz); **HRMS** (ESI) for $C_{23}H_{23}FN_3O_4Na^{11}B$ (M + Na)$^+$: Calculated: 458.1658; Found: 458.1659.

4.10 References

(1)   Poole, K. Resistance to β-Lactam Antibiotics. *Cell. Mol. Life Sci.* **2004**, *61*, 2200–2223.

(2)   Worthington, R. J.; Melander, C. Overcoming Resistance to β-Lactam Antibiotics. *J. Org. Chem.* **2013**, *78*, 4207–4213.

(3)   Heravi, M. M.; Zadsirjan, V. Prescribed Drugs Containing Nitrogen Heterocycles: An Overview. *RSC Adv.* **2020**, *10*, 44247–44311.

(4)   Serafini, M.; Cargnin, S.; Massarotti, A.; Pirali, T.; Genazzani, A. A. Essential Medicinal Chemistry of Essential Medicines. *J. Med. Chem.* **2020**, *63*, 10170–10187.

(5)   O'Donovan, M. R.; Mee, C. D.; Fenner, S.; Teasdale, A.; Phillips, D. H. Boronic Acids—A Novel Class of Bacterial Mutagen. *Mutat. Res. Genet. Toxicol. Environ. Mutagen* **2011**, *724*, 1–6.

(6)   Hansen, M. M.; Jolly, R. A.; Linder, R. J. Boronic Acids and Derivatives—Probing the Structure–Activity Relationships for Mutagenicity. *Org. Process Res. Dev.* **2015**, *19*, 1507–1516.

(7)   Masuda-Herrera, M. J.; et al. In Vivo Mutagenicity Testing of Arylboronic Acids and Esters. *Environ. Mol. Mutagen.* **2019**, *60*, 766–777.

(8)   Baker, S. J.; Ding, C. Z.; Akama, T.; Zhang, Y.-K.; Hernandez, V.; Xia, Y. Therapeutic Potential of Boron-Containing Compounds. *Future Med. Chem.* **2009**, *1*, 1275–1288.

(9)   Das, B. C.; Thapa, P.; Karki, R.; Schinke, C.; Das, S.; Kambhampati, S.; Banerjee, S. K.; Van Veldhuizen, P.; Verma, A.; Weiss, L. M.; Evans, T. Boron Chemicals in Diagnosis and Therapeutics. *Future Med. Chem.* **2013**, *5*, 653–676.

(10) Trippier, P. C.; McGuigan, C. Boronic Acids in Medicinal Chemistry: Anticancer, Antibacterial and Antiviral Applications. *MedChemComm.* **2010**, *1*, 183–198.

(11) Baker, S. J.; Zhang, Y.-K.; Akama, T.; Lau, A.; Zhou, H.; Hernandez, V.; Mao, W.; Alley, M. R. K.; Sanders, V.; Plattner, J. J. Discovery of a New Boron-Containing Antifungal Agent, 5-Fluoro-1,3-Dihydro-1-Hydroxy-2,1- Benzoxaborole (AN2690), for the Potential Treatment of Onychomycosis. *J. Med. Chem.* **2006**, *49*, 4447–4450.

(12) Akama, T.; Baker, S. J.; Zhang, Y.-K.; Hernandez, V.; Zhou, H.; Sanders, V.; Freund, Y.; Kimura, R.; Maples, K. R.; Plattner, J. J. Discovery and Structure–Activity Study of a Novel Benzoxaborole Anti-Inflammatory Agent (AN2728) for the Potential Topical Treatment of Psoriasis and Atopic Dermatitis. *Bioorg. Med. Chem. Lett.* **2009**, *19*, 2129–2132.

(13) Novelli, A.; del Giacomo, P.; Rossolini, G. M.; Tumbarello, M. Meropenem/Vaborbactam: A next Generation β-Lactam β-Lactamase Inhibitor Combination. *Expert Rev Anti Infect Ther* **2020**, *18*, 643–655.

(14) Nocentini, A.; Supuran, C. T.; Winum, J.-Y. Benzoxaborole Compounds for Therapeutic Uses: A Patent Review (2010- 2018). *Expert Opin. Ther. Pat.* **2018**, *28*, 493–504.

(15) Lutje, V.; Probyn, K.; Seixas, J.; Bergman, H.; Villanueva, G. Chemotherapy for Second-Stage Human African Trypanosomiasis: Drugs in Use. *Cochrane Database Syst. Rev.* **2021**, *2021*.

(16) Trial Number: NCT03087955.

(17) Freund, Y. R.; Akama, T.; Alley, M. R. K.; Antunes, J.; Dong, C.; Jarnagin, K.; Kimura, R.; Nieman, J. A.; Maples, K. R.; Plattner, J. J.; Rock, F.; Sharma, R.; Singh, R.; Sanders, V.; Zhou, Y. Boron-Based Phosphodiesterase Inhibitors Show Novel Binding of Boron to PDE4 Bimetal Center. *FEBS Lett.* **2012**, *586*, 3410–3414.

(18) Rock, F. L.; Mao, W.; Yaremchuk, A.; Tukalo, M.; Crépin, T.; Zhou, H.; Zhang, Y.-K.; Hernandez, V.; Akama, T.; Baker, S. J.; Plattner, J. J.; Shapiro, L.; Martinis, S. A.; Benkovic, S. J.; Cusack, S.; Alley, M. R. K. An Antifungal Agent Inhibits an Aminoacyl-TRNA Synthetase by Trapping TRNA in the Editing Site. *Science* **2007**, *316*, 1759–1761.

(19) Adamczyk-Woźniak, A.; Cyrański, M. K.; Żubrowska, A.; Sporzyński, A. Benzoxaboroles – Old Compounds with New Applications. *J. Organomet. Chem.* **2009**, *694*, 3533–3541.

(20) Kazmi, M. Z. H.; Rygus, J. P. G.; Ang, H. T.; Paladino, M.; Johnson, M. A.; Ferguson, M. J.; Hall, D. G. Lewis or Brønsted? A Rectification of the Acidic and Aromatic Nature of Boranol-Containing Naphthoid Heterocycles. *J. Am. Chem. Soc.* **2021**, *143*, 10143–10156.

(21) Cummings, W. M.; Cox, C. H.; Snyder, H. R. Arylboronic Acids. Medium-Size Ring-Containing Boronic Ester Groups. *J. Org. Chem.* **1969**, *34*, 1669–1674.

(22) Snyder, H. R.; Reedy, A. J.; Lennarz, Wm. J. Synthesis of Aromatic Boronic Acids. Aldehydo Boronic Acids and a Boronic Acid Analog of Tyrosine. *J. Am. Chem. Soc.* **1958**, *80*, 835–838.

(23) Mothana, S.; Grassot, J.-M.; Hall, D. G. Multistep Phase-Switch Synthesis by Using Liquid–Liquid Partitioning of Boronic Acids: Productive Tags with an Expanded Repertoire of Compatible Reactions. *Angew. Chem. Int. Ed.* **2010**, *49*, 2883–2887.

(24) VanVeller, B.; Aronoff, M. R.; Raines, R. T. A Divalent Protecting Group for Benzoxaboroles. *RSC Adv.* **2013**, *3*, 21331–21334.

(25) Gamrat, J. M.; Mancini, G.; Burke, S. J.; Colandrea, R. C.; Sadowski, N. R.; Figula, B. C.; Tomsho, J. W. Protection of the Benzoxaborole Moiety: Synthesis and Functionalization of Zwitterionic Benzoxaborole Complexes. *J. Org. Chem.* **2018**, *83*, 6193–6201.

(26) Gravel, M.; Thompson, K. A.; Zak, M.; Bérubé, C.; Hall, D. G. Universal Solid-Phase Approach for the Immobilization, Derivatization, and Resin-to-Resin Transfer Reactions of Boronic Acids. *J. Org. Chem.* **2002**, *67*, 3–15.

(27) Bérubé, M.; Dowlut, M.; Hall, D. G. Benzoboroxoles as Efficient Glycopyranoside-Binding Agents in Physiological Conditions: Structure and Selectivity of Complex Formation. *J. Org. Chem.* **2008**, *73*, 6471–6479.

(28) Sun, X.; Odyniec, M. L.; Sedgwick, A. C.; Lacina, K.; Xu, S.; Qiang, T.; Bull, S. D.; Marken, F.; James, T. D. Reaction-Based Indicator Displacement Assay (RIA) for the Colorimetric and Fluorometric Detection of Hydrogen Peroxide. *Org. Chem. Front.* **2017**, *4*, 1058–1062.

(29) Kubo, Y.; Ishida, T.; Kobayashi, A.; James, T. D. Fluorescent Alizarin–Phenylboronic Acid Ensembles: Design of Self-Organized Molecular Sensors for Metal Ions and Anions. *J. Mater. Chem.* **2005**, *15*, 2889–2895.

(30) Duggan, P. J.; Offermann, D. A. The Preparation of Solid-Supported Peptide Boronic Acids Derived from 4-Borono-L-Phenylalanine and Their Affinity for Alizarin. *Aust. J. Chem.* **2007**, *60*, 829–834.

(31) Hinkes, S. P. A.; Klein, C. D. P. Virtues of Volatility: A Facile Transesterification Approach to Boronic Acids. *Org. Lett.* **2019**, *21*, 3048–3052.

(32) Wurst, J. M.; Liu, G.; Tan, D. S. Hydrogen-Bonding Catalysis and Inhibition by Simple Solvents in the Stereoselective Kinetic Epoxide-Opening Spirocyclization of Glycal Epoxides to Form Spiroketals. *J. Am. Chem. Soc.* **2011**, *133*, 7916–7925.

(33) Chen, X.-L.; Ai, B.-R.; Dong, Y.; Zhang, X.-M.; Wang, J.-Y. Hexafluoro-2-Propanol-Assisted Quick and Chemoselective Nitro Reduction Using Iron Powder as Catalyst under Mild Conditions. *Tetrahedron Lett.* **2017**, *58*, 3646–3649.

(34) Mas-Roselló, J.; Smejkal, T.; Cramer, N. Iridium-Catalyzed Acid-Assisted Asymmetric Hydrogenation of Oximes to Hydroxylamines. *Science* **2020**, *368*, 1098–1102.

(35) Brown, D. G.; Boström, J. Analysis of Past and Present Synthetic Methodologies on Medicinal Chemistry: Where Have All the New Reactions Gone? *J. Med. Chem.* **2016**, *59*, 4443–4458.

(36) Pattabiraman, V. R.; Bode, J. W. Rethinking Amide Bond Synthesis. *Nature* **2011**, *480*, 471–479.

(37) Kaspar, A. A.; Reichert, J. M. Future Directions for Peptide Therapeutics Development. *Drug Discov. Today* **2013**, *18*, 807–817.

(38) Shi, M.; Ye, N.; Chen, W.; Wang, H.; Cheung, C.; Parmentier, M.; Gallou, F.; Wu, B. Simple Synthesis of Amides via Their Acid Chlorides in Aqueous TPGS-750-M. *Org. Process Res. Dev.* **2020**, *24*, 1543–1548.

(39) Liu, M. G. H. Preparation Method of 4-Aminophenylboronic Acid Derivative from 4-Nitrophenylboronic Acid via Hydrogenation Reduction and Acylation. CN 106946920 A, July 14, 2017.

(40) Gillis, E. P.; Eastman, K. J.; Hill, M. D.; Donnelly, D. J.; Meanwell, N. A. Applications of Fluorine in Medicinal Chemistry. *J. Med. Chem.* **2015**, *58*, 8315–8359.

(41) King, A. E.; Brunold, T. C.; Stahl, S. S. Mechanistic Study of Copper-Catalyzed Aerobic Oxidative Coupling of Arylboronic Esters and Methanol: Insights into an Organometallic Oxidase Reaction. *J. Am. Chem. Soc.* **2009**, *131*, 5044–5045.

(42) King, A. E.; Ryland, B. L.; Brunold, T. C.; Stahl, S. S. Kinetic and Spectroscopic Studies of Aerobic Copper(II)-Catalyzed Methoxylation of Arylboronic Esters and Insights into Aryl Transmetalation to Copper(II). *Organometallics* **2012**, *31*, 7948–7957.

(43) Lam, P. Y. S.; Bonne, D.; Vincent, G.; Clark, C. G.; Combs, A. P. N-Arylation of α-Aminoesters with p-Tolylboronic Acid Promoted by Copper(II) Acetate. *Tetrahedron Lett.* **2003**, *44*, 1691–1694.

(44)   Jalalian, N.; Petersen, T. B.; Olofsson, B. Metal-Free Arylation of Oxygen Nucleophiles with Diaryliodonium Salts. *Chem. Eur. J.* **2012**, *18*, 14140–14149.

(45)   Quach, T. D.; Batey, R. A. Copper(II)-Catalyzed Ether Synthesis from Aliphatic Alcohols and Potassium Organotrifluoroborate Salts. *Org. Lett.* **2003**, *5*, 1381–1384.

(46)   Burgos, C. H.; Barder, T. E.; Huang, X.; Buchwald, S. L. Significantly Improved Method for the Pd-Catalyzed Coupling of Phenols with Aryl Halides: Understanding Ligand Effects. *Angew. Chem. Int. Ed.* **2006**, *45*, 4321–4326.

(47)   Marcoux, D.; Charette, A. B. Palladium-Catalyzed Synthesis of Functionalized Tetraarylphosphonium Salts. *J. Org. Chem.* **2008**, *73*, 590–593.

(48)   Ertl, P.; Altmann, E.; McKenna, J. M. The Most Common Functional Groups in Bioactive Molecules and How Their Popularity Has Evolved over Time. *J. Med. Chem.* **2020**, *63*, 8408–8418.

(49)   Zhen, X.; Lundborg, C. S.; Sun, X.; Hu, X.; Dong, H. Economic Burden of Antibiotic Resistance in ESKAPE Organisms: A Systematic Review. *Antimicrob. Resist. Infect. Control* **2019**, *8*, 137.

(50)   Hamada, Y.; Kiso, Y. The Application of Bioisosteres in Drug Design for Novel Drug Discovery: Focusing on Acid Protease Inhibitors. *Expert Opin. Drug Discov.* **2012**, *7*, 903–922.

(51)   Zhao, P.; Nettleton, D. O.; Karki, R. G.; Zécri, F. J.; Liu, S.-Y. Medicinal Chemistry Profiling of Monocyclic 1,2-Azaborines. *ChemMedChem* **2017**, *12*, 358–361.

(52)   Morales, J.; Li, L.; Fattah, F. J.; Dong, Y.; Bey, E. A.; Patel, M.; Gao, J.; Boothman, D. A. Review of Poly (ADP-Ribose) Polymerase (PARP) Mechanisms of Action and Rationale for Targeting in Cancer and Other Diseases. *Crit. Rev. Eukaryot. Gene Expr.* **2014**, *24*, 15–28.

(53)   Yelamos, J.; Farres, J.; Llacuna, L.; Ampurdanes, C.; Martin-Caballero, J. PARP-1 and PARP-2: New Players in Tumour Development. *Am. J. Cancer Res*. **2011**, *1*, 328–346.

(54)   Thorsell, A.-G.; Ekblad, T.; Karlberg, T.; Löw, M.; Pinto, A. F.; Trésaugues, L.; Moche, M.; Cohen, M. S.; Schüler, H. Structural Basis for Potency and Promiscuity in Poly(ADP-Ribose) Polymerase (PARP) and Tankyrase Inhibitors. *J. Med. Chem.* **2017**, *60*, 1262–1271.

(55)   Mahendar, L.; Satyanarayana, G. Substitution Controlled Functionalization of Ortho-Bromobenzylic Alcohols via Palladium Catalysis: Synthesis of Chromenes and Indenols. *J. Org. Chem.* **2014**, *79*, 2059–2074.

(56)   Molander, G. A.; Trice, S. L. J.; Kennedy, S. M.; Dreher, S. D.; Tudge, M. T. Scope of the Palladium-Catalyzed Aryl Borylation Utilizing Bis-Boronic Acid. *J. Am. Chem. Soc.* **2012**, *134*, 11667–11673.

(57)   Dowlut, M.; Hall, D. G. An Improved Class of Sugar-Binding Boronic Acids, Soluble and Capable of Complexing Glycosides in Neutral Water. *J. Am. Chem. Soc* **2006**, *128*, 4226–4227.

(58)   Bartholome, D.; Klemm, E. Novel Polyarylene−Triarylmethane Dye Copolymers. *Macromolecules* **2006**, *39*, 5646–5651.

(59)   Ling, F.; Hou, H.; Chen, J.; Nian, S.; Yi, X.; Wang, Z.; Song, D.; Zhong, W. Highly Enantioselective Synthesis of Chiral Benzhydrols via Manganese Catalyzed Asymmetric Hydrogenation of Unsymmetrical Benzophenones Using an Imidazole-Based Chiral PNN Tridentate Ligand. *Org. Lett.* **2019**, *21*, 3937–3941.

(60)   He, B.; Nie, H.; Chen, L.; Lou, X.; Hu, R.; Qin, A.; Zhao, Z.; Tang, B. Z. High Fluorescence Efficiencies and Large Stokes Shifts of Folded Fluorophores Consisting of a Pair of Alkenyl-Tethered, π-Stacked Oligo-p-Phenylenes. *Org. Lett.* **2015**, *17*, 6174–6177.

(61)   Li, J.-S.; Yang, Q.; Yang, F.; Chen, G.-Q.; Li, Z.-W.; Kuang, Y.-J.; Zhang, W.-J.; Huang, P.-M. Aerobic Oxidative Acylation of Nitroarenes with Arylacetic Esters under

Mild Conditions: Facile Access to Diarylketones. *Org. Biomol. Chem.* **2018**, *16*, 140–145.

(62)   Ishiyama, T.; Murata, M.; Miyaura, N. Palladium(0)-Catalyzed Cross-Coupling Reaction of Alkoxydiboron with Haloarenes: A Direct Procedure for Arylboronic Esters. *J. Org. Chem.* **1995**, 60*3*, 7508–7510.

(63)   Corey, E. J.; Shibata, S.; Bakshi, R. K. An Efficient and Catalytically Enantioselective Route to (S)-(-)-Phenyloxirane. *J. Org. Chem.* **1988**, *53*, 2861–2863.

(64)   Liu, Y.-Y.; Yang, J.; Song, R.-J.; Li, J.-H. Synthesis of 5-(Fluoromethyl)-4,5-Dihydroisoxazoles by Silver- Catalyzed Oxyfluorination of Unactivated Alkenes. *Adv. Synth. Catal.* **2014**, *356*, 2913–2918.

(65)   Zeynizadeh, B.; Kouhkan, M. A Rapid and Practical Protocol for Solvent-Free Reduction of Oximes to Amines with NaBH$_4$/ZrCl$_4$/Al$_2$O$_3$ System. *Bull. Korean Chem. Soc.* **2011**, *32*, 3448–3452.

(66)   Fujita, M.; Hiyama, T. Erythro-Directive Reduction of Alpha-Substituted Alkanones by Means of Hydrosilanes in Acidic Media. *J. Org. Chem.* **1988**, *53*, 5415–5421.

(67)   Chelouan, A.; Recio, R.; Borrego, L. G.; Álvarez, E.; Khiar, N.; Fernández, I. Sulfinamide Phosphinates as Chiral Catalysts for the Enantioselective Organocatalytic Reduction of Imines. *Org. Lett.* **2016**, *18*, 3258–3261.

(68)   Wang, C.; Chen, H.-Y. T.; Bacsa, J.; Catlow, C. R. A.; Xiao, J. Synthesis and X-Ray Structures of Cyclometalated Iridium Complexes Including the Hydrides. *Dalton Trans.* **2013**, *42*, 935–940.

(69)   Le, T. G.; et al. Structure−Activity Relationship Studies of Tolfenpyrad Reveal Subnanomolar Inhibitors of Haemonchus contortus Development. *J. Med. Chem.* **2019**, *62*, 1036–1053.

(70)   Taeufer, T.; Pospech, J. Palladium-Catalyzed Synthesis of N,N-Dimethylanilines via Buchwald–Hartwig Amination of (Hetero)Aryl Triflates. *J. Org. Chem.* **2020**, *85*, 7097–7111.

Chapter 5: Conclusion and Future Objectives

5.1 Summary and Research Proposals

Boron-containing Lewis acids, particularly boron trihalides, have been used in different chemistry applications for a number of decades, such as in catalysis and organic synthesis.[1,2] On the other hand, as described in Chapter 1 organoboron compounds have also gained prominence in medicinal chemistry in the past decade. This thesis described research on the innovative application of boron trihalides on a plant biomass, as well as exploration into the design, synthesis, properties, and applications of boron heterocycles.

The application of boron trihalides in ether cleavage reactions is well precedented.[3] Lignocellulose, a plant biomass consisting of a complex heteropolymeric lignin connected to cellulose, contains a variety of ether and acetal linkages.[4] The process to separate lignin and cellulose often uses harsh reaction conditions and adversely alters the lignin product (see Chapter 2 for details). Boron trihalides have never been applied towards lignocellulose for the cleavage of ether linkages. The work described in Chapter 2 demonstrates the utility of boron trihalides for the separation of cellulose and lignin from lignocellulose under mild reaction conditions. The lignin obtained after the reaction provided evidence that minimal unwanted condensation had occurred. This process served as a proof of concept for the usage of boron trihalides for obtaining lignin from lignocellulose in a potentially native state. In the future, efficient methods will be explored for converting boron lignin to its prospective monomers of high utility. For example, recently it was shown that a Ru/NbOPO$_4$ catalytic system exhibited high monomer yield for the hydrogenolysis of Kraft lignin, which is itself highly modified.[5,6] Since the boron lignin obtained in Chapter 2 indicated less modifications, the aforementioned catalyst system potentially can produce a higher yield of monomers. Sustainable methods for the boron lignin depolymerization, such as enzymatic cleavage, could also be explored.[7,8]

In Chapter 3, the properties of C=C/B—X isosteric naphthoid compounds, benzoxazaborines and benzodiazaborines, were comprehensively studied. The

decades-long controversy regarding their aromatic character and acidic nature was rectified using a combination of experimental, crystallographic, and computational studies. As a result, benzoxazaborines and benzodiazaborines were found unambiguously to be Lewis acids, with benzoxazaborine and *N*-sulphonyl (EWG) containing benzodiazaborine being the most acidic heterocycles, while benzodiazaborines devoid of EWGs (NH or NMe substituted benzodiazaborines) the least acidic. Moreover, the aromatic character correlated well with the acidic character, where the aromaticity in the boron-containing ring was more pronounced in benzodiazaborines with EDGs, while benzoxazaborine and *N*-sulphonyl benzodiazaborine displayed negligible aromatic character. Furthermore, most of the studied heterocycles exhibited good stability in aqueous conditions, which could be useful in biological applications.

An $H_2{}^{18}O$ labelling experiment was carried out to demonstrate the exchange of the boranol (B—OH) hydroxy moiety, but the results were unreliable due to the reverse hydrolysis with the adventitious $H_2{}^{16}O$ in the ESI-MS chamber. In the future, this problem could be remedied by utilizing the direct analysis in real time (DART) or liquid injection field desorption ionization (LIFDI) technology, which does not involve the use of any solvent system. Another way to visualize the exchange in real time is to use NMR spectroscopy. A solution of the heterocycle in an NMR solvent could be spiked with $H_2{}^{17}O$, and the observation of a new signal in the ^{17}O NMR spectrum would indicate that B—^{16}OH to B—^{17}OH exchange was occurring (Scheme 5.1). The drawback to this approach is the very low sensitivity of the ^{17}O nucleus (magnetogyric ratio ($\gamma/10^7$ rad s^{-1}T^{-1}) of ^{17}O = –3.628 vs for ^1H = 26.752), and that molecules are usually not labelled with 100% efficiency.[9] In addition, the resonances for ^{17}O tend to be broad (nuclear quantum spin = 5/2).[10] These issues could make it difficult to obtain well-resolved spectra, and distinguish between two closely located peaks.
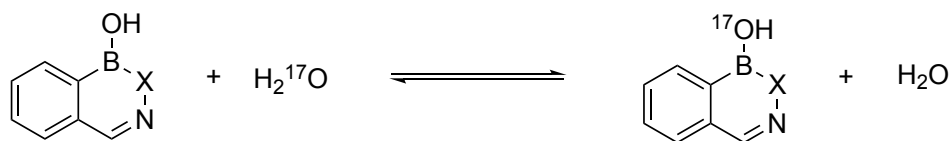
Scheme 5.1. Hydroxy group exchange with an NMR active ^{17}O labelled H_2O.

Knowledge of the aforementioned properties of boron heterocycles, benzoxazaborines and benzodiazaborines, led to the conclusion that benzoxazaborine is a good isostere of benzoxaborole, with a Lewis acidic boron center and non-aromatic character in the boron-containing ring. On the other hand, as a result of its pronounced aromatic character in the boron-containing ring, the NH-containing benzodiazaborine is a reasonable mimic of 4-hydroxyisoquinoline and 1-naphthol. Chapter 4 described the sugar binding capability of these heterocycles, as well as the different synthetic pathways that were used to obtain a variety of their derivatives, highlighting both early-stage and late-stage approaches. Late-stage approaches featured orthogonal reactions, such as amidation, Chan-Lam, and Suzuki-Miyaura reactions, which led to a diversity of analogs. Moreover, numerous isosteric analogs of medicinally relevant molecules, such as tavaborole, crisaborole, and acoziborole were synthesized. Select molecules from the derivative library were also screened for their biological activity, wherein the benzoxazaborine analogs (specifically aryl ketoximes) demonstrate great potential as antibacterial compounds. Furthermore, a bioisostere of a commercial anticancer drug, olaparib, was developed, partially verifying the hypothesis that boranol (B—OH) moiety can serve as an isostere of C=O and confirming the potential of this approach in the field of drug discovery.

There is much potential for the studied boron heterocycles to act as bioisosteres for carbon-based drugs or drug-candidates. For example, Mirati therapeutics recently developed a candidate, **MRTX1719**, for the treatment of methylthioadenosine phosphorylase (MTAP)-deleted cancers (Figure 5.1a).[11] Introduction of the corresponding boron heterocycle could potentially lead to a novel class of anticancer molecules, where the H-bond interactions (C=O/B—OH interactions with Lys333 or Ser578 or N—H interaction with Glu435) and $\pi-\pi$ interactions (aromatic framework with Phe327 and Trp579) could still be maintained within the core scaffold (Figure 5.1b). Based on the precedence of B—OH exchange with alcohols (Chapter 3), there could potentially be additional interactions, such as covalent or dative interactions with Ser578, converting B—OH to B—OSer. Moreover, the B—OH hydrogen could serve

as a H-bond donor, such as with the carbonyl backbone of adjacent residues in the catalytic site (e.g., with Lys333).
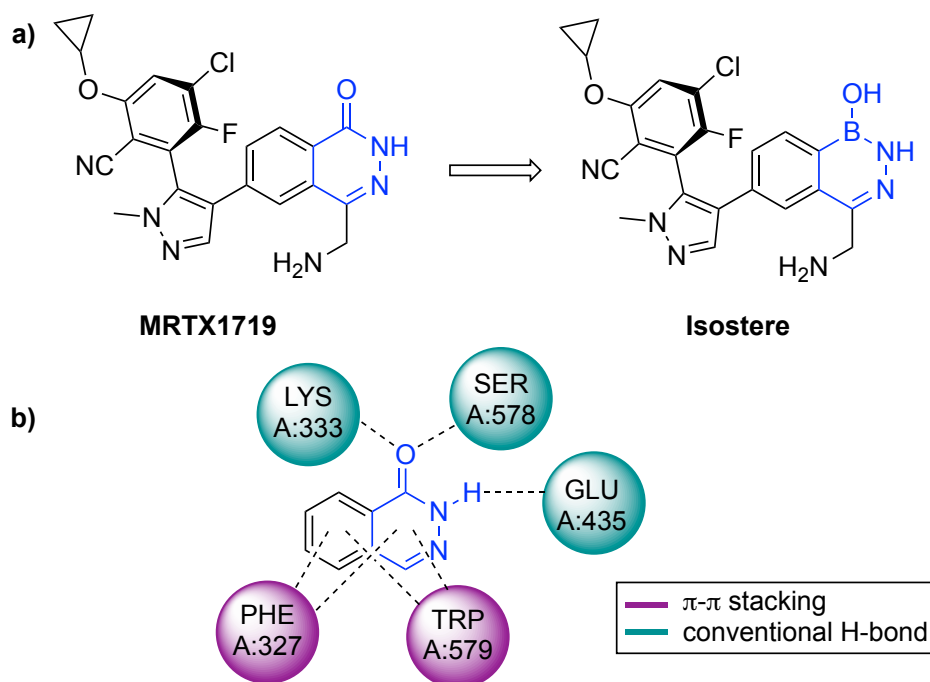
Figure 5.1. a) Isosteric resemblance of **MRTX1719** and benzodiazaborine analog. **b)** Partial receptor-ligand interactions map.[11]

Since benzoxazaborines contain a highly Lewis acidic boron center (pK_a = 5.5) and a boranol (B—OH) moiety able to undergo exchange with alcohols (Chapter 3), they can also be applied towards catalysis, such as in dipolar cycloaddition reactions in an effort to increase the electrophilicity of the alkyne coupling partner (Figure 5.2).[12]
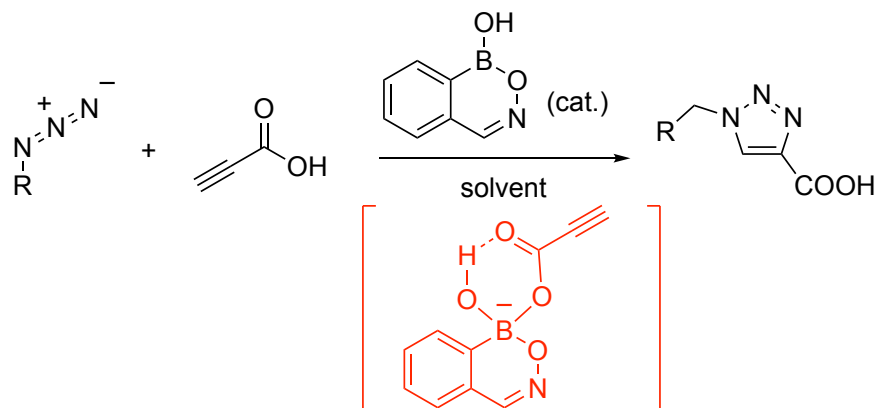
Figure 5.2. Proposed catalytic cycloaddition reaction using a benzoxazaborine catalyst.

Altogether, this thesis presents the first investigation for the use of boron trihalides for separating the components of lignocellulose, as well as describes the properties, design, synthesis, and applications of naphthoid boron-containing heterocycles. This work provides new conclusions that can be applied for the use of boron-containing heterocycles in the fields of catalysis and medicinal chemistry.

5.2 References

(1)   Yao, M.-L.; Kabalka, G. W. Organic Synthesis Using Boron and Organoboron Halides. In *Boron Science*; Hosmane, N. S., Ed.; CRC Press, 2012; pp 579–611.

(2)   Fraile, J. M.; Mayoral, J. A.; Salvatella, L. Theoretical Study on the BF3-Catalyzed Meinwald Rearrangement Reaction. *J. Org. Chem.* **2014**, *79*, 5993–5999.

(3)   Ranu, B. C.; Bhar, S. Dealkylation of Ethers. A Review. *Org. Prep. Proced. Int.* **1996**, *28*, 371–409.

(4)   Leisola, M.; Pastinen, O.; Axe, D. Lignin-Designed Randomness. *BIOcomplexity* **2012**, *3*, 1–11.

(5)   Lange, H.; Decina, S.; Crestini, C. Oxidative Upgrade of Lignin – Recent Routes Reviewed. *Eur. Polym. J.* **2013**, *49*, 1151–1173.

(6)   Dong, L.; Lin, L.; Han, X.; Si, X.; Liu, X.; Guo, Y.; Lu, F.; Rudić, S.; Parker, S. F.; Yang, S.; Wang, Y. Breaking the Limit of Lignin Monomer Production via Cleavage of Interunit Carbon–Carbon Linkages. *Chem.* **2019**, *5*, 1521–1536.

(7)   Marinović, M.; Nousiainen, P.; Dilokpimol, A.; Kontro, J.; Moore, R.; Sipilä, J.; de Vries, R. P.; Mäkelä, M. R.; Hildén, K. Selective Cleavage of Lignin β-O-4 Aryl Ether Bond by β-Etherase of the White-Rot Fungus Dichomitus Squalens. *ACS Sustain. Chem. Eng.* **2018**, *6*, 2878–2882.

(8)   Reiter, J.; Strittmatter, H.; Wiemann, L. O.; Schieder, D.; Sieber, V. Enzymatic Cleavage of Lignin β-O-4 Aryl Ether Bonds via Net Internal Hydrogen Transfer. *Green Chem.* **2013**, *15*, 1373–1381.

(9)   Harris, R. K.; Becker, E. D.; Cabral de Menezes, S. M.; Goodfellow, R.; Granger, P. NMR Nomenclature: Nuclear Spin Properties and Conventions for Chemical Shifts: IUPAC Recommendations 2001. *Solid State Nucl. Magn. Reson.* **2002**, *22*, 458–483.

(10)   Palmer, J.; Wu, G. Chapter One - Recent Developments in ^{17}O NMR Studies of Organic and Biological Molecules in the Solid State. In *Annual Reports on NMR Spectroscopy*; Webb, G. A., Ed.; Academic Press, 2021; Vol. 103, pp 1–46.

(11)   Smith, C. R.; Aranda, R.; Bobinski, T. P.; Briere, D. M.; Burns, A. C.; Christensen, J. G.; Clarine, J.; Engstrom, L. D.; Gunn, R. J.; Ivetac, A.; Jean-Baptiste, R.; Ketcham, J. M.; Kobayashi, M.; Kuehler, J.; Kulyk, S.; Lawson, J. D.; Moya, K.; Olson, P.; Rahbaek, L.; Thomas, N. C.; Wang, X.; Waters, L. M.; Marx, M. A. Fragment-Based Discovery of MRTX1719, a Synthetic Lethal Inhibitor of the PRMT5•MTA Complex for the Treatment of MTAP-Deleted Cancers. *J. Med. Chem.* **2022**, *65*, 1749–1766.

(12)   Zheng, H.; McDonald, R.; Hall, D. G. Boronic Acid Catalysis for Mild and Selective [3+2] Dipolar Cycloadditions to Unsaturated Carboxylic Acids. *Chem. Eur. J.* **2010**, *16*, 5454–5460.

Bibliography

(1)   Shriver, D. F.; Swanson, B. Nature of the Donor-Acceptor Interaction in Boron Trihalide Complexes. Vibrational Spectra and Vibrational Analysis of Acetonitrile-Boron Trichloride and Acetonitrile-Boron Tribromide. *Inorg. Chem* **1971**, *10*, 1354–1365.

(2)   Brinck, T.; Murray, J. S.; Politzer, P. A Computational Analysis of the Bonding in Boron Trifluoride and Boron Trichloride and Their Complexes with Ammonia. *Inorg. Chem.* **1993**, *32*, 2622–2625.

(3)   Miller, J. M.; Onyszchuk, M. The Relative Acceptor Power of Boron Trihalides and Borane Toward Trimethylamine by proton N.M.R. Measurements. *Can. J. Chem.* **1964**, *42*, 1518–1523.

(4)   Bessac, F.; Frenking, G. Why Is BCl$_3$ a Stronger Lewis Acid with Respect to Strong Bases than BF$_3$? *Inorg. Chem.* **2003**, *42*, 7990–7994.

(5)   Silva, D. R.; Santos, L. de A.; Freitas, M. P.; Guerra, C. F.; Hamlin, T. A. Nature and Strength of Lewis Acid/Base Interaction in Boron and Nitrogen Trihalides. *Chem. Asian J.* **2020**, *15*, 4043–4054.

(6)   Naganaboina, R. T.; Peddinti, R. K. BF$_3$·Etherate-Mediated Friedel–Crafts Arylation of 2-Hydroxy-1,4-Benzoxazines: Synthesis of 2-Aryl-1,4-Benzoxazine Derivatives. *J. Org. Chem.* **2013**, *78*, 12819–12824.

(7)   Ranu, B. C.; Bhar, S. Dealkylation of Ethers. A review. *Org. Prep. Proced. Int.* **1996**, *28*, 371–409.

(8)   Lappert, M. F.; Litzow, M. R.; Pedley, J. B.; Tweedale, A. Bonding Studies of Compounds of Boron and the Group IV Elements. Part V. Boron-11 Nuclear Magnetic Resonance Data for the Boron Trihalides and Mixed Trihalides. *J. Chem. Soc. A: Inorg., Phys., Theor.* **1971**, 2426–2428.

(9)   Boyd, P. D. W.; Taylor, M. J. Halogen Exchange in Boron Trihalides: The BCl$_3$-BI$_3$ Reaction. *Inorganica Chim Acta* **1992**, *193*, 1–3.

(10)   Atienza, B. J. P.; Truong, N.; Williams, F. J. Reliably Regioselective Dialkyl Ether Cleavage with Mixed Boron Trihalides. *Org. Lett.* **2018**, *20*, 6332–6335.

(11)   Mayer, U.; Gutmann, V.; Gerger, W. The Acceptor Number — A Quantitative Empirical Parameter for the Electrophilic Properties of Solvents. *Monatshefte für Chemie / Chemical Monthly* **1975**, *106*, 1235–1257.

(12)   Beckett, M. A.; Strickland, G. C.; Holland, J. R.; Sukumar Varma, K. A Convenient NMR Method for the Measurement of Lewis Acidity at Boron Centres: Correlation of Reaction Rates of Lewis Acid Initiated Epoxide Polymerizations with Lewis Acidity. *Polymer* **1996**, *37*, 4629–4631.

(13)   Childs, R. F.; Mulholland, D. L.; Nixon, A. The Lewis Acid Complexes of α,β-Unsaturated Carbonyl and Nitrile Compounds. A Nuclear Magnetic Resonance Study. *Can. J. Chem.* **1982**, *60*, 801–808.

(14)   Dowlut, M.; Hall, D. G. An Improved Class of Sugar-Binding Boronic Acids, Soluble and Capable of Complexing Glycosides in Neutral Water. *J. Am. Chem. Soc.* **2006**, *128*, 4226–4227.

(15)   Bérubé, M.; Dowlut, M.; Hall, D. G. Benzoboroxoles as Efficient Glycopyranoside-Binding Agents in Physiological Conditions: Structure and Selectivity of Complex Formation. *J. Org. Chem.* **2008**, *73*, 6471–6479.

(16)   Bhangu, J.; Whittal, R. M.; Hall, D. G. Design, Synthesis and Structure of a Frustrated Benzoxaborole and Its Applications in the Complexation of Amines, Amino Acids, and Protein Modification. *Org. Biomol. Chem.* **2020**, *18*, 3492–3500.

(17)   James, T. D.; Phillips, M. D.; Shinkai, S. The Molecular Recognition of Saccharides. Complexation of Boronic Acids with Saccharides. Fluorescent Sensors. Modular Fluorescent Sensors. Other Types of Sensor. Other Systems for Saccharide Recognition. RSC, **2006**, 3–176.

(18)   Kuivila, H. G.; Keough, A. H.; Soboczenski, E. J. Areneboronates from Diols and Polyols. *J. Org. Chem.* **1954**, *19*, 780–783.

(19)   Shin, S. B. Y.; Almeida, R. D.; Gerona-Navarro, G.; Bracken, C.; Jaffrey, S. R. Assembling Ligands in Situ Using Bioorthogonal Boronate Ester Synthesis. *Chem. Biol.* **2010**, *17*, 1171–1176.

(20)   Akgun, B.; Hall, D. G. Fast and Tight Boronate Formation for Click Bioorthogonal Conjugation. *Angew. Chem. Int. Ed.* **2016**, *55*, 3909–3913.

(21)   Sun, X.; Odyniec, M. L.; Sedgwick, A. C.; Lacina, K.; Xu, S.; Qiang, T.; Bull, S. D.; Marken, F.; James, T. D. Reaction-Based Indicator Displacement Assay (RIA) for the Colorimetric and Fluorometric Detection of Hydrogen Peroxide. *Org. Chem. Front.* **2017**, *4*, 1058–1062.

(22)   Kubo, Y.; Ishida, T.; Kobayashi, A.; James, T. D. Fluorescent Alizarin–Phenylboronic Acid Ensembles: Design of Self-Organized Molecular Sensors for Metal Ions and Anions. *J. Mater. Chem.* **2005**, *15*, 2889–2895.

(23)   Duggan, P. J.; Offermann, D. A. The Preparation of Solid-Supported Peptide Boronic Acids Derived from 4-Borono-L-Phenylalanine and Their Affinity for Alizarin. *Aust. J. Chem.* **2007**, *60*, 829–834.

(24)   Richardson, P. G.; Hideshima, T.; Anderson, K. C. Bortezomib (PS-341): A Novel, First-in-Class Proteasome Inhibitor for the Treatment of Multiple Myeloma and Other Cancers. *Cancer Control* **2003**, *10*, 361–369.

(25)   Fernandes, G. F. S.; Denny, W. A.; Santos, J. L. D. Boron in Drug Design: Recent Advances in the Development of New Therapeutic Agents. *Eur. J. Med. Chem.* **2019**, *179*, 791–804.

(26)   Richardson, P. G.; Zweegman, S.; O'Donnell, E. K.; Laubach, J. P.; Raje, N.; Voorhees, P.; Ferrari, R. H.; Skacel, T.; Kumar, S. K.; Lonial, S. Ixazomib for the Treatment of Multiple Myeloma. *Expert Opin. Pharmacother.* **2018**, *19*, 1949–1968.

(27)   Vshyvenko, S.; Clapson, M. L.; Suzuki, I.; Hall, D. G. Characterization of the Dynamic Equilibrium between Closed and Open Forms of the Benzoxaborole Pharmacophore. *ACS Med. Chem. Lett.* **2016**, *7*, 1097–1101.

(28)   Adamczyk-Woźniak, A.; Borys, K. M.; Sporzyński, A. Recent Developments in the Chemistry and Biological Applications of Benzoxaboroles. *Chem. Rev.* **2015**, *115*, 5224–5247.

(29)   Rock, F. L.; Mao, W.; Yaremchuk, A.; Tukalo, M.; Crépin, T.; Zhou, H.; Zhang, Y.-K.; Hernandez, V.; Akama, T.; Baker, S. J.; Plattner, J. J.; Shapiro, L.; Martinis, S. A.; Benkovic, S. J.; Cusack, S.; Alley, M. R. K. An Antifungal Agent Inhibits an Aminoacyl-TRNA Synthetase by Trapping TRNA in the Editing Site. *Science* **2007**, *316*, 1759–1761.

(30)   Akama, T.; Baker, S. J.; Zhang, Y.-K.; Hernandez, V.; Zhou, H.; Sanders, V.; Freund, Y.; Kimura, R.; Maples, K. R.; Plattner, J. J. Discovery and Structure–Activity Study of a Novel Benzoxaborole Anti-Inflammatory Agent (AN2728) for the Potential Topical Treatment of Psoriasis and Atopic Dermatitis. *Bioorg. Med. Chem. Lett.* **2009**, *19*, 2129–2132.

(31)   Freund, Y. R.; Akama, T.; Alley, M. R. K.; Antunes, J.; Dong, C.; Jarnagin, K.; Kimura, R.; Nieman, J. A.; Maples, K. R.; Plattner, J. J.; Rock, F.; Sharma, R.; Singh, R.; Sanders, V.; Zhou, Y. Boron-Based Phosphodiesterase Inhibitors Show Novel Binding of Boron to PDE4 Bimetal Center. *FEBS Lett.* **2012**, *586*, 3410–3414.

(32) Nocentini, A.; Supuran, C. T.; Winum, J.-Y. Benzoxaborole Compounds for Therapeutic Uses: A Patent Review (2010- 2018). *Expert. Opin. Ther. Pat.* **2018**, *28*, 493–504.

(33) Gardner, S. D.; Kim, J.; Baptiste-Brown, S.; Lopez, V.; Hamatake, R.; Gan, J.; Edwards, S.; Elko-Simms, L.; Dumont, E. F.; Leivers, M.; Hong, Z.; Paff, M. T. GSK2878175, a Pan-Genotypic Non-Nucleoside NS5B Polymerase Inhibitor, in Healthy and Treatment-Naïve Chronic Hepatitis C Subjects. *J. Viral. Hepat.* **2018**, *25*, 19–27.

(34) Langmuir, I. Isomorphism, Isosterism and Covalence. *J. Am. Chem. Soc.* **1919**, *41*, 1543–1559.

(35) Friedman, H. L. *First Symposium on Chemical-Biological Correlation, May 26-27, 1950*; National Academies Press: Washington, D.C., 1951.

(36) Burger, A. Isosterism and Bioisosterism in Drug Design. In *Progress in Drug Research / Fortschritte der Arzneimittelforschung / Progrès des recherches pharmaceutiques*; Salmon, J. A., Garland, L. G., Hoyle, B. D., Costerton, J. W., Seiler, N., Raeburn, D., Karlsson, J.-A., Polak, A., Hartman, P. G., Rohmer, M., Bisseret, P., Sutter, B., Burger, A., Jucker, E., Eds.; Birkhäuser Basel: Basel, 1991, pp. 287–371.

(37) Patani, G. A.; LaVoie, E. J. Bioisosterism: A Rational Approach in Drug Design. *Chem. Rev.* **1996**, *96*, 3147–3176.

(38) Stepan, A. F.; Subramanyam, C.; Efremov, I. v; Dutra, J. K.; O'Sullivan, T. J.; DiRico, K. J.; McDonald, W. S.; Won, A.; Dorff, P. H.; Nolan, C. E.; Becker, S. L.; Pustilnik, L. R.; Riddell, D. R.; Kauffman, G. W.; Kormos, B. L.; Zhang, L.; Lu, Y.; Capetta, S. H.; Green, M. E.; Karki, K.; Sibley, E.; Atchison, K. P.; Hallgren, A. J.; Oborski, C. E.; Robshaw, A. E.; Sneed, B.; O'Donnell, C. J. Application of the Bicyclo[1.1.1]Pentane Motif as a Nonclassical Phenyl Ring Bioisostere in the Design of a Potent and Orally Active γ-Secretase Inhibitor. *J. Med. Chem.* **2012**, *55*, 3414–3424.

(39) Chalmers, B. A.; Xing, H.; Houston, S.; Clark, C.; Ghassabian, S.; Kuo, A.; Cao, B.; Reitsma, A.; Murray, C.-E. P.; Stok, J. E.; Boyle, G. M.; Pierce, C. J.; Littler, S. W.; Winkler, D. A.; Bernhardt, P. v; Pasay, C.; De Voss, J. J.; McCarthy, J.; Parsons, P. G.; Walter, G. H.; Smith, M. T.; Cooper, H. M.; Nilsson, S. K.; Tsanaktsidis, J.; Savage, G. P.; Williams, C. M. Validating Eaton's Hypothesis: Cubane as a Benzene Bioisostere. *Angew. Chem. Int. Ed.* **2016**, *55*, 3580–3585.

(40) Baranac-Stojanović, M. Aromaticity and Stability of Azaborines. *Chem. Eur. J.* **2014**, *20*, 16558–16565.

(41) Liu, L.; Marwitz, A. J. V.; Matthews, B. W.; Liu, S.-Y. Boron Mimetics: 1,2-Dihydro-1,2-Azaborines Bind inside a Nonpolar Cavity of T4 Lysozyme. *Angew. Chem. Int. Ed.* **2009**, *48*, 6817–6819.

(42) Lee, H.; Fischer, M.; Shoichet, B. K.; Liu, S.-Y. Hydrogen Bonding of 1,2-Azaborines in the Binding Cavity of T4 Lysozyme Mutants: Structures and Thermodynamics. *J. Am. Chem. Soc.* **2016**, *138*, 12021–12024.

(43) Rombouts, F. J. R.; Tovar, F.; Austin, N.; Tresadern, G.; Trabanco, A. A. Benzazaborinines as Novel Bioisosteric Replacements of Naphthalene: Propranolol as an Example. *J. Med. Chem.* **2015**, *58*, 9287–9295.

(44) Zhao, P.; Nettleton, D. O.; Karki, R. G.; Zécri, F. J.; Liu, S.-Y. Medicinal Chemistry Profiling of Monocyclic 1,2-Azaborines. *ChemMedChem.* **2017**, *12*, 358–361.

(45) Stegemann, S.; Leveiller, F.; Franchi, D.; de Jong, H.; Lindén, H. When Poor Solubility Becomes an Issue: From Early Stage to Proof of Concept. *Eur. J. Pharm. Sci.* **2007**, *31*, 249–261.

(46) Snyder, H. R.; Reedy, A. J.; Lennarz, Wm. J. Synthesis of Aromatic Boronic Acids. Aldehydo Boronic Acids and a Boronic Acid Analog of Tyrosine. *J. Am. Chem. Soc.* **1958**, *80*, 835–838.

(47) Dewar, M. J. S.; Dougherty, R. C. Boron-Containing Analogs of Isoquinoline. *J. Am. Chem. Soc.* **1962**, *84*, 2648–2649.

(48) Das, B. C.; Adil Shareef, M.; Das, S.; Nandwana, N. K.; Das, Y.; Saito, M.; Weiss, L. M. Boron-Containing Heterocycles as Promising Pharmacological Agents. *Bioorg. Med. Chem.* **2022**, *63*, 116748.

(49) Högenauer, G.; Woisetschläger, M. A Diazaborine Derivative Inhibits Lipopolysaccharide Biosynthesis. *Nature* **1981**, *293*, 662–664.

(50) Grassberger, M. A.; Turnowsky, F.; Hildebrandt, J. Preparation and Antibacterial Activities of New 1,2,3-Diazaborine Derivatives and Analogs. *J. Med. Chem.* **1984**, *27*, 947–953.

(51) Hicks, J. W.; Kyle, C. B.; Vogels, C. M.; Wheaton, S. L.; Baerlocher, F. J.; Decken, A.; Westcott, S. A. Synthesis, Characterization, and Antifungal Activity of Boron-Containing Thiosemicarbazones. *Chem. Biodivers.* **2008**, *5*, 2415–2422.

(52) Baldock, C.; Rafferty, J. B.; Sedelnikova, S. E.; Baker, P. J.; Stuitje, A. R.; Slanas, A. R.; Hawkes, T. R.; Rice, D. W. A Mechanism of Drug Action Revealed by Structural Studies of Enoyl Reductase. *Science* **1996**, *274*, 2107–2110.

(53) António, J. P. M.; Gonçalves, L. M.; Guedes, R. C.; Moreira, R.; Gois, P. M. P. Diazaborines as New Inhibitors of Human Neutrophil Elastase. *ACS Omega* **2018**, *3*, 7418–7423.

(54) Dukes, A. O.; Carroll, X. B.; Groziak, M. P. Design, Development, Synthesis, and Crystal Structure of the Prototype of a New Class of Deep Blue-Fluorescing Boron Heterocycle Estrogen Mimics. *Bioorg. Med. Chem. Lett.* **2022**, *72*, 128864–128870.

(55) Adamczyk-Woźniak, A.; Cyrański, M. K.; Żubrowska, A.; Sporzyński, A. Benzoxaboroles – Old Compounds with New Applications. *J. Organomet. Chem.* **2009**, *694*, 3533–3541.

(56) Zhang, Y.-K.; Plattner, J. J.; Freund, Y. R.; Easom, E. E.; Zhou, Y.; Gut, J.; Rosenthal, P. J.; Waterson, D.; Gamo, F.-J.; Angulo-Barturen, I.; Ge, M.; Li, Z.; Li, L.; Jian, Y.; Cui, H.; Wang, H.; Yang, J. Synthesis and Structure–Activity Relationships of Novel Benzoxaboroles as a New Class of Antimalarial Agents. *Bioorg. Med. Chem. Lett.* **2011**, *21*, 644–651.

(57) Zhang, Y.-K.; Plattner, J. J.; Freund, Y. R.; Easom, E. E.; Zhou, Y.; Ye, L.; Zhou, H.; Waterson, D.; Gamo, F.-J.; Sanz, L. M.; Ge, M.; Li, Z.; Li, L.; Wang, H.; Cui, H. Benzoxaborole Antimalarial Agents. Part 2: Discovery of Fluoro-Substituted 7-(2-Carboxyethyl)-1,3-Dihydro-1-Hydroxy-2,1-Benzoxaboroles. *Bioorg. Med. Chem. Lett.* **2012**, *22*, 1299–1307.

(58) Ye, L.; Ding, D.; Feng, Y.; Xie, D.; Wu, P.; Guo, H.; Meng, Q.; Zhou, H. Convenient and Versatile Synthesis of Formyl-Substituted Benzoxaboroles. *Tetrahedron* **2009**, *65*, 8738–8744.

(59) Zhao, J.; Chen, J.; Xu, Q.; Li, H. Synthesis of Benzoxaboroles by Ortho-Oxalkylation of Arylboronic Acids with Aldehydes/Ketones in the Presence of Brønsted Acids. *Org. Lett.* **2021**, *23*, 1986–1990.

(60) Wu, P. H.; Meng, Q. Q.; Zhou, H. C. Synthesis of a Novel Pyrrolo-Benzoxaborole Scaffold and Its Derivatization via Friedel–Crafts Reaction Catalyzed by Anhydrous Stannic Chloride. *Chin. Chem. Lett.* **2011**, *22*, 1411–1414.

(61) Li, X.; Zhang, Y.-K.; Liu, Y.; Zhang, S.; Ding, C. Z.; Zhou, Y.; Plattner, J. J.; Baker, S. J.; Liu, L.; Bu, W.; Kazmierski, W. M.; Wright, L. L.; Smith, G. K.; Jarvest, R. L.; Duan, M.; Ji, J.-J.; Cooper, J. P.; Tallant, M. D.; Crosby, R. M.; Creech, K.; Ni, Z.-J.; Zou, W.; Wright, J. Synthesis of New Acylsulfamoyl Benzoxaboroles as Potent Inhibitors of HCV NS3 Protease. *Bioorg. Med. Chem. Lett.* **2010**, *20*, 7493–7497.

(62) Kumar, J. S.; Bashian, C. M.; Corsello, M. A.; Jonnalagadda, S. C.; Mereddy, V. R. Development of Practical Methodologies for the Synthesis of Functionalized Benzoboroxoles. *Tetrahedron Lett.* **2010**, *51*, 4482–4485.

(63) Fuscaldo, R. S.; Vontobel, P. H. V.; Boeira, E. O.; Moro, A. V.; Costa, J. S. da. Synthesis of Amino- and Hydroxymethyl Benzoxaboroles: Prominent Scaffolds for Further Functionalization. *Eur. J. Org. Chem.* **2019**, *2019*, 2050–2055.

(64) Akama, T.; Zhang, Y.-K.; Freund, Y. R.; Berry, P.; Lee, J.; Easom, E. E.; Jacobs, R. T.; Plattner, J. J.; Witty, M. J.; Peter, R.; Rowan, T. G.; Gillingwater, K.; Brun, R.; Nare, B.; Mercer, L.; Xu, M.; Wang, J.; Liang, H. Identification of a 4-Fluorobenzyl l-Valinate Amide Benzoxaborole (AN11736) as a Potential Development Candidate for the Treatment of Animal African Trypanosomiasis (AAT). *Bioorg. Med. Chem. Lett.* **2018**, *28*, 6–10.

(65) Dewar, M. J. S.; Kubba, V. P. New Heteroaromatic Compounds—IV: The Nitration and Chlorination of 10-Methyl-10:9- Borazarophenanthrene. *Tetrahedron* **1959**, *7*, 213–222.

(66) Dewar, M. J. S.; Dietz, R.; Kubba, V. P.; Lepley, A. R. New Heteroaromatic Compounds. Part X. Grignard Reactions and Hydride Reductions of B-Oxides Derived from 10,9-Borazarophenanthrene and 2,1-Borazaronaphthalene. *J. Am. Chem. Soc.* **1961**, *83*, 1754–1756.

(67) Ashe, A. J.; Fang. A Synthesis of Aromatic Five- and Six-Membered B−N Heterocycles via Ring Closing Metathesis. *Org. Lett.* **2000**, *2*, 2089–2091.

(68) Campbell, P. G.; Marwitz, A. J. V.; Liu, S.-Y. Recent Advances in Azaborine Chemistry. *Angew. Chem. Int. Ed.* **2012**, *51*, 6074–6092.

(69) Brown, A. N.; Li, B.; Liu, S.-Y. Negishi Cross-Coupling Is Compatible with a Reactive B–Cl Bond: Development of a Versatile Late-Stage Functionalization of 1,2-Azaborines and Its Application to the Synthesis of New BN Isosteres of Naphthalene and Indenyl. *J. Am. Chem. Soc.* **2015**, *137*, 8932–8935.

(70) Kanichar, D.; Roppiyakuda, L.; Kosmowska, E.; Faust, M. A.; Tran, K. P.; Chow, F.; Buglo, E.; Groziak, M. P.; Sarina, E. A.; Olmstead, M. M.; Silva, I.; Xu, H. H. Synthesis, Characterization, and Antibacterial Activity of Structurally Complex 2-Acylated 2,3,1-Benzodiazaborines and Related Compounds. *Chem. Biodivers.* **2014**, *11*, 1381–1397.

(71) Nunes, C. S.; Kunamneni, A. Chapter 7 - Laccases—Properties and Applications. In *Enzymes in Human and Animal Nutrition*; Nunes, C. S., Kumar, V., Eds.; Academic Press, 2018; pp 133–161.

(72) Klemm, D.; Heublein, B.; Fink, H.-P.; Bohn, A. Cellulose: Fascinating Biopolymer and Sustainable Raw Material. *Angew. Chem. Int. Ed.* **2005**, *44*, 3358–3393.

(73) Boerjan, W.; Ralph, J.; Baucher, M. Lignin Biosynthesis. *Annu. Rev. Plant Biol.* **2003**, *54*, 519–546.

(74) Ciriminna, R.; Fidalgo, A.; Meneguzzo, F.; Parrino, F.; Ilharco, L. M.; Pagliaro, M. Vanillin: The Case for Greener Production Driven by Sustainability Megatrend. *ChemistryOpen* **2019**, *8*, 660–667.

(75) Arevalo-Gallegos, A.; Ahmad, Z.; Asgher, M.; Parra-Saldivar, R.; Iqbal, H. M. N. Lignocellulose: A Sustainable Material to Produce Value-Added Products with a Zero Waste Approach—A Review. *Int. J. Biol. Macromol.* **2017**, *99*, 308–318.

(76) Adler, Erich. Structural Elements of Lignin. *Ind. Eng. Chem.* **1957**, *49*, 1377–1383.

(77) Lange, H.; Decina, S.; Crestini, C. Oxidative Upgrade of Lignin – Recent Routes Reviewed. *Eur. Polym. J.* **2013**, *49*, 1151–1173.

(78) Renders, T.; van den Bosch, S.; Koelewijn, S.-F.; Schutyser, W.; Sels, B. F. Lignin-First Biomass Fractionation: The Advent of Active Stabilisation Strategies. *Energy Environ. Sci.* **2017**, *10*, 1551–1557.

(79) Sturgeon, M. R.; Kim, S.; Lawrence, K.; Paton, R. S.; Chmely, S. C.; Nimlos, M.; Foust, T. D.; Beckham, G. T. A Mechanistic Investigation of Acid-Catalyzed Cleavage of Aryl-Ether Linkages: Implications for Lignin Depolymerization in Acidic Environments. *ACS Sustain. Chem. Eng.* **2014**, *2*, 472–485.

(80) Chung, H.; Washburn, N. R. 2 - Extraction and Types of Lignin. In *Lignin in Polymer Composites*; Faruk, O., Sain, M., Eds.; William Andrew Publishing, 2016; pp 13–25.

(81) Gratzl, J. S.; Chen, C.-L. Chemistry of Pulping: Lignin Reactions. In *Lignin: Historical, Biological, and Materials Perspectives*; ACS Symposium Series; American Chemical Society, 1999; Vol. 742, pp 392–421.

(82) See, A.; Salleh, A.; Bakar, F.; Yusof, N.; Abdulamir, A.; yook heng, L. Risk and Health Effect of Boric Acid. *Am. J. Appl. Sci.* **2010**, *7*, 620–627.

(83) Kosak, T. M.; Conrad, H. A.; Korich, A. L.; Lord, R. L. Ether Cleavage Re-Investigated: Elucidating the Mechanism of BBr$_3$-Facilitated Demethylation of Aryl Methyl Ethers. *Eur. J. Org. Chem.* **2015**, *2015*, 7460–7467.

(84) Benton, F. L.; Dillon, T. E. The Cleavage of Ethers with Boron Bromide. I. Some Common Ethers. *J. Am. Chem. Soc.* **1942**, *64*, 1128–1129.

(85) Bhatt, M. V.; Kulkarni, S. U. Cleavage of Ethers. *Synthesis* **1983**, *1983*, 249–282.

(86) Ding, T.; Wu, Y.; Zhu, X.; Lin, G.; Hu, X.; Sun, H.; Huang, Y.; Zhang, S.; Zhang, H. Promoted Production of Phenolic Monomers from Lignin-First Depolymerization of Lignocellulose over Ru Supported on Biochar by N,P-Co-Doping. *ACS Sustain. Chem. Eng.* **2022**, *10*, 2343–2354.

(87) Kazmi, M. Z. H.; Karmakar, A.; Michaelis, V. K.; Williams, F. J. Separation of Cellulose/Hemicellulose from Lignin in White Pine Sawdust Using Boron Trihalide Reagents. *Tetrahedron* **2019**, *75*, 1465–1470.

(88) Buchanan, M. Solvent extractives of wood and pulp, Technical Association of the Pulp and Paper Industry, *T204cm-97*, **2007**, 1–6.

(89) Wiselogel, A.; Tyson, J.; Johnsson, D. Biomass Feedstock Resources and Composition. In *Handbook on Bioethanol: Production and Utilization*; Wyman, C. E., Ed.; Taylor & Francis: New York, 1996; pp 105–118.

(90) Risanto, L.; Hermiati, E.; Sudiyani, Y. Properties of Lignin from Oil Palm Empty Fruit Bunch and Its Application for Plywood Adhesive. *Makara J. Technol.* **2014**, *18*, 67.

(91) Wood, P. J. Specificity in the Interaction of Direct Dyes with Polysaccharides. *Carbohydr. Res.* **1980**, *85*, 271–287.

(92) Mitra, P. P.; Loqué, D. Histochemical Staining of Arabidopsis Thaliana Secondary Cell Wall Elements. *J. Vis. Exp.* **2014**, *87*, 51381.

(93) O'Brien, T. P.; Feder, N.; McCully, M. E. Polychromatic Staining of Plant Cell Walls by Toluidine Blue O. *Protoplasma* **1964**, *59*, 368–373.

(94) Li, S.; Talebi, A. M.; M, Q.-S. Y.; Florent, H.; Yanding, L.; Hoon, K.; Richard, M.; Clint, C.; John, R.; S, L. J. Formaldehyde Stabilization Facilitates Lignin Monomer Production during Biomass Depolymerization. *Science* **2016**, *354*, 329–333.

(95) Vékey, K. Mass Spectrometry and Mass-Selective Detection in Chromatography. *J. Chromatogr. A* **2001**, *921*, 227–236.

(96) Scanlon, J. T.; Willis, D. E. Calculation of Flame Ionization Detector Relative Response Factors Using the Effective Carbon Number Concept. *J. Chromatogr. Sci.* **1985**, *23*, 333–340.

(97) Li, X.; He, J.; Zhang, Y. BBr3-Assisted Preparation of Aromatic Alkyl Bromides from Lignin and Lignin Model Compounds. *J. Org. Chem.* **2018**, *83*, 11019–11027.

(98) Hämäläinen, V.; Grönroos, T.; Suonpää, A.; Heikkilä, M. W.; Romein, B.; Ihalainen, P.; Malandra, S.; Birikh, K. R. Enzymatic Processes to Unlock the Lignin Value. *Front. Bioeng. Biotechnol.* **2018**, *6*.

(99)   Hackney, H. E.; Paladino, M.; Fu, H.; Hall, D. G. Diazaboryl-Naphthyl-Ketone: A New Scaffold with Bright Fluorescence, Aggregation-Induced Emission, and Application in the Quantitation of Trace Boronic Acids in Drug Intermediates. *Chem. Eur. J.* **2020**, *26*, 14324–14329.

(100) Estrada, C. D.; Ang, H. T.; Vetter, K.-M.; Ponich, A. A.; Hall, D. G. Enantioselective Desymmetrization of 2-Aryl-1,3-Propanediols by Direct O-Alkylation with a Rationally Designed Chiral Hemiboronic Acid Catalyst That Mitigates Substrate Conformational Poisoning. *J. Am. Chem. Soc.* **2021**, *143*, 4162–4167.

(101) Wang, B. J.; Groziak, M. P. Chapter Two - Recent Developments in the Chemistry of Boron Heterocycles. In *Advances in Heterocyclic Chemistry*; Scriven, E. F. V., Ramsden, C. A., Eds.; Academic Press, 2016; Vol. 118, pp 47–90.

(102) Akgun, B.; Li, C.; Hao, Y.; Lambkin, G.; Derda, R.; Hall, D. G. Synergic "Click" Boronate/Thiosemicarbazone System for Fast and Irreversible Bioorthogonal Conjugation in Live Cells. *J. Am. Chem. Soc.* **2017**, *139*, 14285–14291.

(103) Palvai, S.; Bhangu, J.; Akgun, B.; Moody, C. T.; Hall, D. G.; Brudno, Y. In Vivo Targeting Using Arylboronate/Nopoldiol Click Conjugation. *Bioconjug. Chem.* **2020**, *31*, 2288–2292.

(104) Baldock, C.; Boer, G-J. d.; Rafferty, J. B.; Stuitje, A. R.; Rice, D. W. Mechanism of Action of Diazaborines. *Biochem. Pharmacol.* **1998**, *55*, 1541–1550.

(105) Dewar, M. J. S.; Dougherty, R. C. New Heteroaromatic Compounds. XX. Derivatives of 4,3-Borazaroisoquinoline. *J. Am. Chem. Soc.* **1964**, *86*, 433–436.

(106) Dewar, M. J. S.; Jones, Richard. New Heteroaromatic Compounds. XXV. Studies of Salt Formation in Boron Oxyacids by Boron-11 Nuclear Magnetic Resonance. *J. Am. Chem. Soc.* **1967**, *89*, 2408–2410.

(107) Dunn, H. E.; Catlin, J. C.; Snyder, H. R. Arylboronic Acids. Imino Derivatives from O-Formylbenzeneboronic Acid. *J. Org. Chem.* **1968**, *33*, 4483–4486.

(108) Groziak, M. P.; Chen, L.; Yi, L.; Robinson, P. D. Planar Boron Heterocycles with Nucleic Acid-Like Hydrogen-Bonding Motifs. *J. Am. Chem. Soc.* **1997**, *119*, 7817–7826.

(109) Dilek, O.; Lei, Z.; Mukherjee, K.; Bane, S. Rapid Formation of a Stable Boron–Nitrogen Heterocycle in Dilute, Neutral Aqueous Solution for Bioorthogonal Coupling Reactions. *Chem. Comm.* **2015**, *51*, 16992–16995.

(110) Stress, C. J.; Schmidt, P. J.; Gillingham, Dennis. G. Comparison of Boron-Assisted Oxime and Hydrazone Formations Leads to the Discovery of a Fluorogenic Variant. *Org. Biomol. Chem.* **2016**, *14*, 5529–5533.

(111) Gu, H.; Chio, T. I.; Lei, Z.; Staples, R. J.; Hirschi, J. S.; Bane, S. Formation of Hydrazones and Stabilized Boron–Nitrogen Heterocycles in Aqueous Solution from Carbohydrazides and Ortho-Formylphenylboronic Acids. *Org. Biomol. Chem.* **2017**, *15*, 7543–7548.

(112) Kazmi, M. Z. H.; Rygus, J. P. G.; Ang, H. T.; Paladino, M.; Johnson, M. A.; Ferguson, M. J.; Hall, D. G. Lewis or Brønsted? A Rectification of the Acidic and Aromatic Nature of Boranol-Containing Naphthoid Heterocycles. *J. Am. Chem. Soc.* **2021**, *143*, 10143–10156.

(113) Shao, Y.; et al. Advances in molecular quantum chemistry contained in the Q-Chem 4 program package. *Mol. Phys.* **2015**, *113*, 184−215.

(114) Ishibashi, J. S. A.; Dargelos, A.; Darrigan, C.; Chrostowska, A.; Liu, S.–Y. BN Tetracene: Extending the Reach of BN/CC Isosterism in Acenes *Organometallics* **2017**, *36*, 2494–2497.

(115) Mottishaw, J. D.; Erck, A. R.; Kramer, J. H.; Sun, H.; Koppang, M. Electrostatic Potential Maps and Natural Bond Orbital Analysis: Visualization and Conceptualization of Reactivity in Sanger's Reagent. *J. Chem. Educ.* **2015**, *92*, 1846–1852.

(116) Gershoni-Poranne, R.; Stanger, A. Chapter 4 - NICS—Nucleus-independent Chemical Shift. In *Aromaticity: Modern Computational Methods and Applications*; Fernandez, I., Ed.; Elsevier, 2021; pp 99–154.

(117) Mikhailov, B. M.; Kuimova, M. E. Organoboron Compounds: CCCXVIII. On the Problem of the Aromatic Character of Boron Heterocyclic Compounds. *J. Organomet. Chem.* **1976**, *116*, 123–133.

(118) Rettig, S. J.; Trotter, J. Crystal and Molecular Structure of Phenylboronic Acid, $C_6H_5B(OH)_2$. *Can. J. Chem.* **1977**, *55*, 3071–3075.

(119) Tanjaroon, C.; Daly, A.; Marwitz, A. J. V.; Liu, S.-Y.; Kukolich, S. Microwave Measurements and Ab Initio Calculations of Structural and Electronic Properties of N-Et-1,2-Azaborine. *J. Chem. Phys.* **2009**, *131*, 224312.

(120) Wrackmeyer, B. Carbon-13 NMR Spectroscopy of Boron Compounds. *Progress in NMR Spectroscopy* **1978**, *12*, 227–259.

(121) Gantt, R. W.; Peltier-Pain, P.; Cournoyer, W. J.; Thorson, J. S. Using Simple Donors to Drive the Equilibria of Glycosyltransferase-Catalyzed Reactions. *Nat. Chem. Biol* **2011**, *7*, 685– 691.

(122) Ribeiro, C. J. A.; Nunes, R. C.; Amaral, J. D.; Gonçalves, L. M.; Rodrigues, C. M. P.; Moreira, R.; Santos, M. M. M. Spirotriazoline Oxindoles: A Novel Chemical Scaffold With *In vitro* Anticancer Properties. *Eur. J. Med. Chem*. **2017**, *140*, 494–509.

(123) Martzel, T.; Lohier, J-F.; Gaumont, A-C.; Brière, J-F.; Perrio, S. Sulfinate-Organocatalyzed (3+2) Annulation Reaction of Propargyl or Allenyl Sulfones with Activated Imines. *Eur. J. Org. Chem.* **2018**, *36*, 5069–5073.

(124) Ricardo, C. L.; Mo, X.; McCubbin, J. A.; Hall, D. G. A Surprising Substituent Effect Provides a Superior Boronic Acid Catalyst for Mild and Metal-Free Direct Friedel–Crafts Alkylations and Prenylations of Neutral Arenes. *Chem. Eur. J.* **2015**, *21*, 4218–4223.

(125) Cammidge, A. N.; Goddard, V. H. M.; Gopee, H.; Harrison, N. L.; Hughes, D. L.; Schubert, C. J.; Sutton, B. M.; Watts, G. L.; Whitehead, A. J. Aryl Trihydroxyborates: Easily Isolated Discrete Species Convenient for Direct Application in Coupling Reactions. *Org. Lett.* **2006**, *8*, 4071–4074.

(126) Poole, K. Resistance to β-Lactam Antibiotics. *Cell. Mol. Life Sci.* **2004**, *61*, 2200–2223.

(127) Worthington, R. J.; Melander, C. Overcoming Resistance to β-Lactam Antibiotics. *J. Org. Chem.* **2013**, *78*, 4207–4213.

(128) Heravi, M. M.; Zadsirjan, V. Prescribed Drugs Containing Nitrogen Heterocycles: An Overview. *RSC Adv*. **2020**, *10*, 44247–44311.

(129) Serafini, M.; Cargnin, S.; Massarotti, A.; Pirali, T.; Genazzani, A. A. Essential Medicinal Chemistry of Essential Medicines. *J. Med. Chem.* **2020**, *63*, 10170–10187.

(130) O'Donovan, M. R.; Mee, C. D.; Fenner, S.; Teasdale, A.; Phillips, D. H. Boronic Acids—A Novel Class of Bacterial Mutagen. *Mutat. Res. Genet. Toxicol. Environ. Mutagen* **2011**, *724*, 1–6.

(131) Hansen, M. M.; Jolly, R. A.; Linder, R. J. Boronic Acids and Derivatives—Probing the Structure–Activity Relationships for Mutagenicity. *Org. Process Res. Dev.* **2015**, *19*, 1507–1516.

(132) Masuda-Herrera, M. J.; et al. *In Vivo* Mutagenicity Testing of Arylboronic Acids and Esters. *Environ. Mol. Mutagen.* **2019**, *60*, 766–777.

(133) Baker, S. J.; Ding, C. Z.; Akama, T.; Zhang, Y.-K.; Hernandez, V.; Xia, Y. Therapeutic Potential of Boron-Containing Compounds. *Future Med. Chem.* **2009**, *1*, 1275–1288.

(134) Das, B. C.; Thapa, P.; Karki, R.; Schinke, C.; Das, S.; Kambhampati, S.; Banerjee, S. K.; Van Veldhuizen, P.; Verma, A.; Weiss, L. M.; Evans, T. Boron Chemicals in Diagnosis and Therapeutics. *Future Med. Chem.* **2013**, *5*, 653–676.

(135) Trippier, P. C.; McGuigan, C. Boronic Acids in Medicinal Chemistry: Anticancer, Antibacterial and Antiviral Applications. *MedChemComm.* **2010**, *1*, 183–198.

(136) Baker, S. J.; Zhang, Y.-K.; Akama, T.; Lau, A.; Zhou, H.; Hernandez, V.; Mao, W.; Alley, M. R. K.; Sanders, V.; Plattner, J. J. Discovery of a New Boron-Containing Antifungal Agent, 5-Fluoro-1,3-Dihydro-1-Hydroxy-2,1- Benzoxaborole (AN2690), for the Potential Treatment of Onychomycosis. *J. Med. Chem.* **2006**, *49*, 4447–4450.

(137) Novelli, A.; del Giacomo, P.; Rossolini, G. M.; Tumbarello, M. Meropenem/Vaborbactam: A next Generation β-Lactam β-Lactamase Inhibitor Combination. *Expert Rev Anti Infect Ther* **2020**, *18*, 643–655.

(138) Lutje, V.; Probyn, K.; Seixas, J.; Bergman, H.; Villanueva, G. Chemotherapy for Second-Stage Human African Trypanosomiasis: Drugs in Use. *Cochrane Database Syst. Rev.* **2021**, *2021*.

(139) Trial Number: NCT03087955.

(140) Cummings, W. M.; Cox, C. H.; Snyder, H. R. Arylboronic Acids. Medium-Size Ring-Containing Boronic Ester Groups. *J. Org. Chem.* **1969**, *34*, 1669–1674.

(141) Mothana, S.; Grassot, J.-M.; Hall, D. G. Multistep Phase-Switch Synthesis by Using Liquid–Liquid Partitioning of Boronic Acids: Productive Tags with an Expanded Repertoire of Compatible Reactions. *Angew. Chem. Int. Ed.* **2010**, *49*, 2883–2887.

(142) VanVeller, B.; Aronoff, M. R.; Raines, R. T. A Divalent Protecting Group for Benzoxaboroles. *RSC Adv.* **2013**, *3*, 21331–21334.

(143) Gamrat, J. M.; Mancini, G.; Burke, S. J.; Colandrea, R. C.; Sadowski, N. R.; Figula, B. C.; Tomsho, J. W. Protection of the Benzoxaborole Moiety: Synthesis and Functionalization of Zwitterionic Benzoxaborole Complexes. *J. Org. Chem.* **2018**, *83*, 6193–6201.

(144) Gravel, M.; Thompson, K. A.; Zak, M.; Bérubé, C.; Hall, D. G. Universal Solid-Phase Approach for the Immobilization, Derivatization, and Resin-to-Resin Transfer Reactions of Boronic Acids. *J. Org. Chem.* **2002**, *67*, 3–15.

(145) Hinkes, S. P. A.; Klein, C. D. P. Virtues of Volatility: A Facile Transesterification Approach to Boronic Acids. *Org. Lett.* **2019**, *21*, 3048–3052.

(146) Wurst, J. M.; Liu, G.; Tan, D. S. Hydrogen-Bonding Catalysis and Inhibition by Simple Solvents in the Stereoselective Kinetic Epoxide-Opening Spirocyclization of Glycal Epoxides to Form Spiroketals. *J. Am. Chem. Soc.* **2011**, *133*, 7916–7925.

(147) Chen, X.-L.; Ai, B.-R.; Dong, Y.; Zhang, X.-M.; Wang, J.-Y. Hexafluoro-2-Propanol-Assisted Quick and Chemoselective Nitro Reduction Using Iron Powder as Catalyst under Mild Conditions. *Tetrahedron Lett.* **2017**, *58*, 3646–3649.

(148) Mas-Roselló, J.; Smejkal, T.; Cramer, N. Iridium-Catalyzed Acid-Assisted Asymmetric Hydrogenation of Oximes to Hydroxylamines. *Science* **2020**, *368*, 1098–1102.

(149) Brown, D. G.; Boström, J. Analysis of Past and Present Synthetic Methodologies on Medicinal Chemistry: Where Have All the New Reactions Gone? *J. Med. Chem.* **2016**, *59*, 4443–4458.

(150) Pattabiraman, V. R.; Bode, J. W. Rethinking Amide Bond Synthesis. *Nature* **2011**, *480*, 471–479.

(151) Kaspar, A. A.; Reichert, J. M. Future Directions for Peptide Therapeutics Development. *Drug Discov. Today* **2013**, *18*, 807–817.

(152) Shi, M.; Ye, N.; Chen, W.; Wang, H.; Cheung, C.; Parmentier, M.; Gallou, F.; Wu, B. Simple Synthesis of Amides via Their Acid Chlorides in Aqueous TPGS-750-M. *Org. Process Res. Dev.* **2020**, *24*, 1543–1548.

(153) Liu, M. G. H. Preparation Method of 4-Aminophenylboronic Acid Derivative from 4-Nitrophenylboronic Acid via Hydrogenation Reduction and Acylation. CN 106946920 A, July 14, 2017.

(154) Gillis, E. P.; Eastman, K. J.; Hill, M. D.; Donnelly, D. J.; Meanwell, N. A. Applications of Fluorine in Medicinal Chemistry. *J. Med. Chem.* **2015**, *58*, 8315–8359.

(155) King, A. E.; Brunold, T. C.; Stahl, S. S. Mechanistic Study of Copper-Catalyzed Aerobic Oxidative Coupling of Arylboronic Esters and Methanol: Insights into an Organometallic Oxidase Reaction. *J. Am. Chem. Soc.* **2009**, *131*, 5044–5045.

(156) King, A. E.; Ryland, B. L.; Brunold, T. C.; Stahl, S. S. Kinetic and Spectroscopic Studies of Aerobic Copper(II)-Catalyzed Methoxylation of Arylboronic Esters and Insights into Aryl Transmetalation to Copper(II). *Organometallics* **2012**, *31*, 7948–7957.

(157) Lam, P. Y. S.; Bonne, D.; Vincent, G.; Clark, C. G.; Combs, A. P. N-Arylation of α-Aminoesters with p-Tolylboronic Acid Promoted by Copper(II) Acetate. *Tetrahedron Lett.* **2003**, *44*, 1691–1694.

(158) Jalalian, N.; Petersen, T. B.; Olofsson, B. Metal-Free Arylation of Oxygen Nucleophiles with Diaryliodonium Salts. *Chem. Eur. J.* **2012**, *18*, 14140–14149.

(159) Quach, T. D.; Batey, R. A. Copper(II)-Catalyzed Ether Synthesis from Aliphatic Alcohols and Potassium Organotrifluoroborate Salts. *Org. Lett.* **2003**, *5*, 1381–1384.

(160) Burgos, C. H.; Barder, T. E.; Huang, X.; Buchwald, S. L. Significantly Improved Method for the Pd-Catalyzed Coupling of Phenols with Aryl Halides: Understanding Ligand Effects. *Angew. Chem. Int. Ed.* **2006**, *45*, 4321–4326.

(161) Marcoux, D.; Charette, A. B. Palladium-Catalyzed Synthesis of Functionalized Tetraarylphosphonium Salts. *J. Org. Chem.* **2008**, *73*, 590–593.

(162) Ertl, P.; Altmann, E.; McKenna, J. M. The Most Common Functional Groups in Bioactive Molecules and How Their Popularity Has Evolved over Time. *J. Med. Chem.* **2020**, *63*, 8408–8418.

(163) Zhen, X.; Lundborg, C. S.; Sun, X.; Hu, X.; Dong, H. Economic Burden of Antibiotic Resistance in ESKAPE Organisms: A Systematic Review. *Antimicrob. Resist. Infect. Control* **2019**, *8*, 137.

(164) Hamada, Y.; Kiso, Y. The Application of Bioisosteres in Drug Design for Novel Drug Discovery: Focusing on Acid Protease Inhibitors. *Expert Opin. Drug Discov.* **2012**, *7*, 903–922.

(165) Morales, J.; Li, L.; Fattah, F. J.; Dong, Y.; Bey, E. A.; Patel, M.; Gao, J.; Boothman, D. A. Review of Poly (ADP-Ribose) Polymerase (PARP) Mechanisms of Action and Rationale for Targeting in Cancer and Other Diseases. *Crit. Rev. Eukaryot. Gene Expr.* **2014**, *24*, 15–28.

(166) Yelamos, J.; Farres, J.; Llacuna, L.; Ampurdanes, C.; Martin-Caballero, J. PARP-1 and PARP-2: New Players in Tumour Development. *Am. J. Cancer Res.* **2011**, *1*, 328–346.

(167) Thorsell, A.-G.; Ekblad, T.; Karlberg, T.; Löw, M.; Pinto, A. F.; Trésaugues, L.; Moche, M.; Cohen, M. S.; Schüler, H. Structural Basis for Potency and Promiscuity in Poly(ADP-Ribose) Polymerase (PARP) and Tankyrase Inhibitors. *J. Med. Chem.* **2017**, *60*, 1262–1271.

(168) Mahendar, L.; Satyanarayana, G. Substitution Controlled Functionalization of Ortho-Bromobenzylic Alcohols via Palladium Catalysis: Synthesis of Chromenes and Indenols. *J. Org. Chem.* **2014**, *79*, 2059–2074.

(169) Molander, G. A.; Trice, S. L. J.; Kennedy, S. M.; Dreher, S. D.; Tudge, M. T. Scope of the Palladium-Catalyzed Aryl Borylation Utilizing Bis-Boronic Acid. *J. Am. Chem. Soc.* **2012**, *134*, 11667–11673.

(170) Bartholome, D.; Klemm, E. Novel Polyarylene−Triarylmethane Dye Copolymers. *Macromolecules* **2006**, *39*, 5646–5651.

(171) Ling, F.; Hou, H.; Chen, J.; Nian, S.; Yi, X.; Wang, Z.; Song, D.; Zhong, W. Highly Enantioselective Synthesis of Chiral Benzhydrols via Manganese Catalyzed

Asymmetric Hydrogenation of Unsymmetrical Benzophenones Using an Imidazole-Based Chiral PNN Tridentate Ligand. *Org. Lett.* **2019**, *21*, 3937–3941.

(172) He, B.; Nie, H.; Chen, L.; Lou, X.; Hu, R.; Qin, A.; Zhao, Z.; Tang, B. Z. High Fluorescence Efficiencies and Large Stokes Shifts of Folded Fluorophores Consisting of a Pair of Alkenyl-Tethered, π-Stacked Oligo-p-Phenylenes. *Org. Lett.* **2015**, *17*, 6174–6177.

(173) Li, J.-S.; Yang, Q.; Yang, F.; Chen, G.-Q.; Li, Z.-W.; Kuang, Y.-J.; Zhang, W.-J.; Huang, P.-M. Aerobic Oxidative Acylation of Nitroarenes with Arylacetic Esters under Mild Conditions: Facile Access to Diarylketones. *Org. Biomol. Chem.* **2018**, *16*, 140–145.

(174) Ishiyama, T.; Murata, M.; Miyaura, N. Palladium(0)-Catalyzed Cross-Coupling Reaction of Alkoxydiboron with Haloarenes: A Direct Procedure for Arylboronic Esters. *J. Org. Chem.* **1995**,*603*, 7508–7510.

(175) Corey, E. J.; Shibata, S.; Bakshi, R. K. An Efficient and Catalytically Enantioselective Route to (S)-(-)-Phenyloxirane. *J. Org. Chem.* **1988**, *53*, 2861–2863.

(176) Liu, Y.-Y.; Yang, J.; Song, R.-J.; Li, J.-H. Synthesis of 5-(Fluoromethyl)-4,5-Dihydroisoxazoles by Silver- Catalyzed Oxyfluorination of Unactivated Alkenes. *Adv. Synth. Catal.* **2014**, *356*, 2913–2918.

(177) Zeynizadeh, B.; Kouhkan, M. A Rapid and Practical Protocol for Solvent-Free Reduction of Oximes to Amines with NaBH$_4$/ZrCl$_4$/Al$_2$O$_3$ System. *Bull. Korean Chem. Soc.* **2011**, *32*, 3448–3452.

(178) Fujita, M.; Hiyama, T. Erythro-Directive Reduction of Alpha-Substituted Alkanones by Means of Hydrosilanes in Acidic Media. *J. Org. Chem.* **1988**, *53*, 5415–5421.

(179) Chelouan, A.; Recio, R.; Borrego, L. G.; Álvarez, E.; Khiar, N.; Fernández, I. Sulfinamide Phosphinates as Chiral Catalysts for the Enantioselective Organocatalytic Reduction of Imines. *Org. Lett.* **2016**, *18*, 3258–3261.

(180) Wang, C.; Chen, H.-Y. T.; Bacsa, J.; Catlow, C. R. A.; Xiao, J. Synthesis and X-Ray Structures of Cyclometalated Iridium Complexes Including the Hydrides. *Dalton Trans.* **2013**, *42*, 935–940.

(181) Le, T. G.; et al. Structure−Activity Relationship Studies of Tolfenpyrad Reveal Subnanomolar Inhibitors of *Haemonchus contortus* Development. *J. Med. Chem.* **2019**, *62*, 1036–1053.

(182) Taeufer, T.; Pospech, J. Palladium-Catalyzed Synthesis of N,N-Dimethylanilines via Buchwald–Hartwig Amination of (Hetero)Aryl Triflates. *J. Org. Chem.* **2020**, *85*, 7097–7111.

(183) Yao, M.-L.; Kabalka, G. W. Organic Synthesis Using Boron and Organoboron Halides. In *Boron Science*; Hosmane, N. S., Ed.; CRC Press, 2012; pp 579–611.

(184) Fraile, J. M.; Mayoral, J. A.; Salvatella, L. Theoretical Study on the BF3-Catalyzed Meinwald Rearrangement Reaction. *J. Org. Chem.* **2014**, *79*, 5993–5999.

(185) Leisola, M.; Pastinen, O.; Axe, D. Lignin-Designed Randomness. *BIOcomplexity* **2012**, *3*, 1–11.

(186) Dong, L.; Lin, L.; Han, X.; Si, X.; Liu, X.; Guo, Y.; Lu, F.; Rudić, S.; Parker, S. F.; Yang, S.; Wang, Y. Breaking the Limit of Lignin Monomer Production via Cleavage of Interunit Carbon–Carbon Linkages. *Chem.* **2019**, *5*, 1521–1536.

(187) Marinović, M.; Nousiainen, P.; Dilokpimol, A.; Kontro, J.; Moore, R.; Sipilä, J.; de Vries, R. P.; Mäkelä, M. R.; Hildén, K. Selective Cleavage of Lignin β-O-4 Aryl Ether Bond by β-Etherase of the White-Rot Fungus Dichomitus Squalens. *ACS Sustain. Chem. Eng.* **2018**, *6*, 2878–2882.

(188) Reiter, J.; Strittmatter, H.; Wiemann, L. O.; Schieder, D.; Sieber, V. Enzymatic Cleavage of Lignin β-O-4 Aryl Ether Bonds via Net Internal Hydrogen Transfer. *Green Chem.* **2013**, *15*, 1373–1381.

(189) Harris, R. K.; Becker, E. D.; Cabral de Menezes, S. M.; Goodfellow, R.; Granger, P. NMR Nomenclature: Nuclear Spin Properties and Conventions for Chemical Shifts: IUPAC Recommendations 2001. *Solid State Nucl. Magn. Reson.* **2002**, *22*, 458–483.

(190) Palmer, J.; Wu, G. Chapter One - Recent Developments in ^{17}O NMR Studies of Organic and Biological Molecules in the Solid State. In *Annual Reports on NMR Spectroscopy*; Webb, G. A., Ed.; Academic Press, 2021; Vol. 103, pp 1–46.

(191) Smith, C. R.; Aranda, R.; Bobinski, T. P.; Briere, D. M.; Burns, A. C.; Christensen, J. G.; Clarine, J.; Engstrom, L. D.; Gunn, R. J.; Ivetac, A.; Jean-Baptiste, R.; Ketcham, J. M.; Kobayashi, M.; Kuehler, J.; Kulyk, S.; Lawson, J. D.; Moya, K.; Olson, P.; Rahbaek, L.; Thomas, N. C.; Wang, X.; Waters, L. M.; Marx, M. A. Fragment-Based Discovery of MRTX1719, a Synthetic Lethal Inhibitor of the PRMT5•MTA Complex for the Treatment of MTAP-Deleted Cancers. *J. Med. Chem.* **2022**, *65*, 1749–1766.

(192) Zheng, H.; McDonald, R.; Hall, D. G. Boronic Acid Catalysis for Mild and Selective [3+2] Dipolar Cycloadditions to Unsaturated Carboxylic Acids. *Chem. Eur. J.* **2010**, *16*, 5454–5460.

Appendices

Appendix 1: Chromatographic Plot of the Monomers Obtained After Hydrogenolysis Reaction and a Plot for Commercial Standards (Chapter 2)

Chromatogram plot of the monomers obtained from B lignin hydrogenolysis

Chromatogram plot of the monomers obtained from FA lignin hydrogenolysis

Chromatogram plot of the monomers obtained from Klason lignin hydrogenolysis

File: c:\brukerws\data\williams\zain\s3 (11-29-2019, 11-52-04 pm).xms
Sample: S3
Scan Range: 1 - 4772 Time Range: 4.00 - 24.67 min.

Operator: MassSpec Lab
Date: 2019-11-29 11:53 PM

TIC; S3 (11-29-2019, 11-52-04 PM).xms; Filtered

Apex: 5.457 min.
Area: 3.321e+9

1A

Apex: 10.012 min.
Area: 2.079e+8

GCps

5.0   7.5   10.0   12.5   minutes
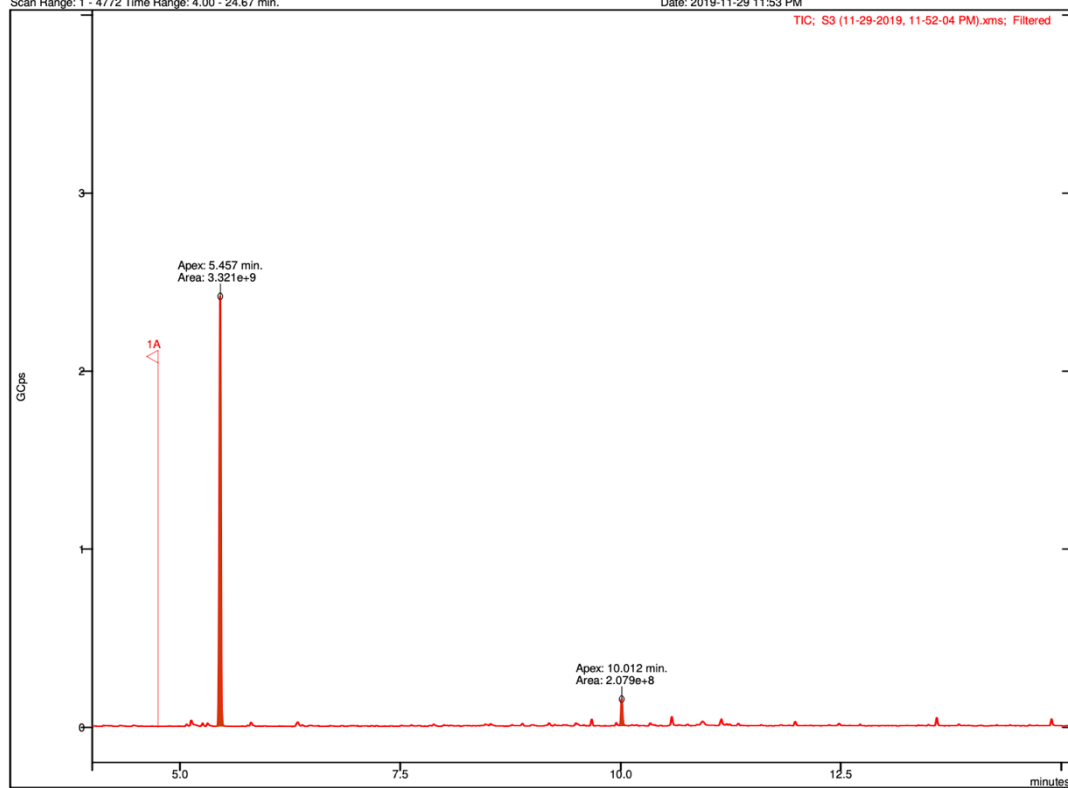
Chromatogram plot of the commercial monomers using GC-MS for the validation of R_t. From left to right: propyl benzene, n-decane, guaiacol (**M1**), 2,6-dimethoxyphenol, 3-(4-methoxyphenyl)-1-propanol, 2-methoxy-4-methyl phenol (**M2**), and 2-methoxy-4-ethyl phenol (**M3**).
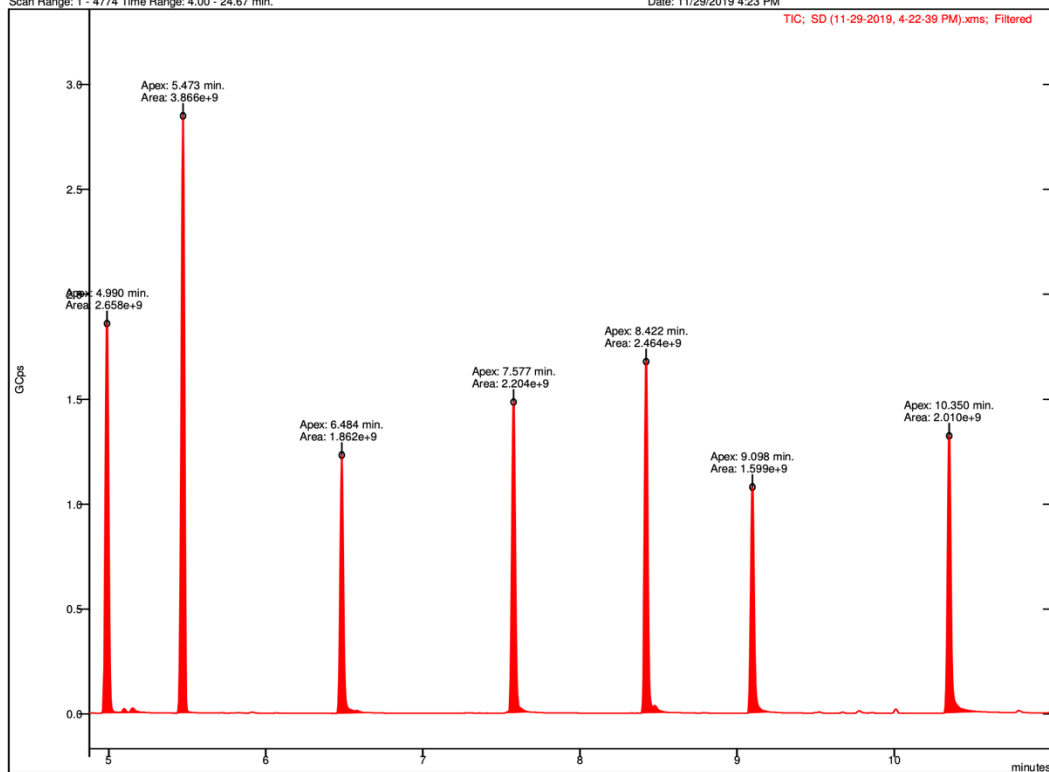
Appendix 2: Selected Copies of NMR Spectra (Chapter 4)

^{1}H NMR spectrum of a benzoxazaborine analog (**4-7f**) synthesized by the early-stage approach (*d₆*-acetone + 1 drop D_2O, 400 MHz)

^{11}B NMR spectrum of a benzoxazaborine analog (**4-7f**) synthesized by the early-stage approach (*d₆*-acetone + 1 drop D_2O, 128 MHz)
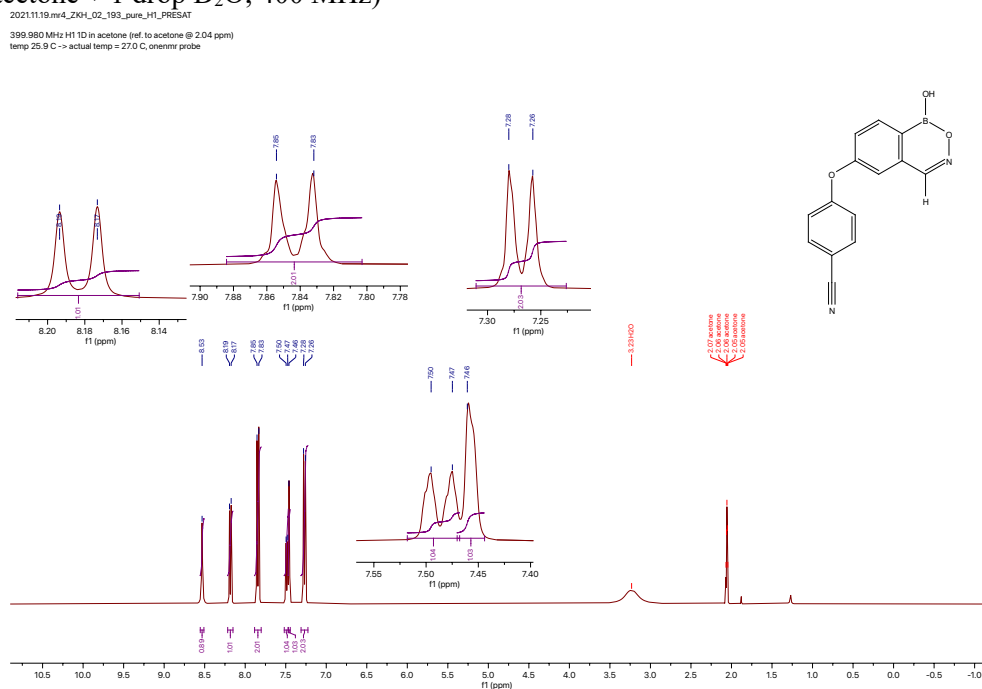
^{13}C NMR spectrum of a benzoxazaborine analog (**4-7f**) synthesized by the early-stage approach (d_6-acetone + 1 drop D$_2$O, 126 MHz)
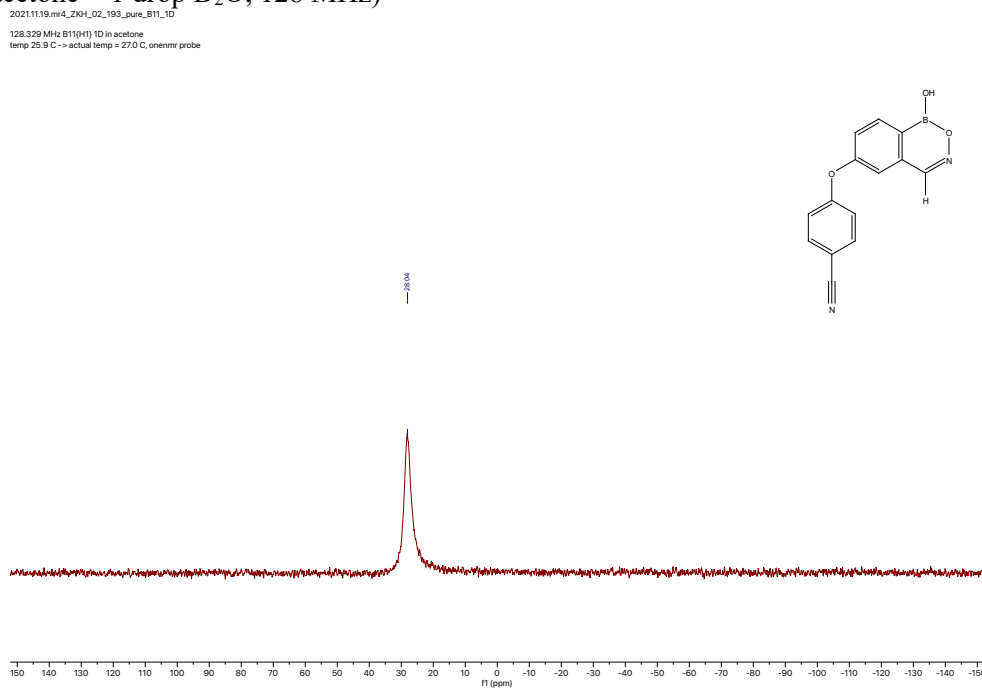
^{1}H NMR spectrum of a benzodiazaborine analog (**4-8d**) synthesized by the early-stage approach (d_6-acetone + 1 drop D$_2$O, 400 MHz)
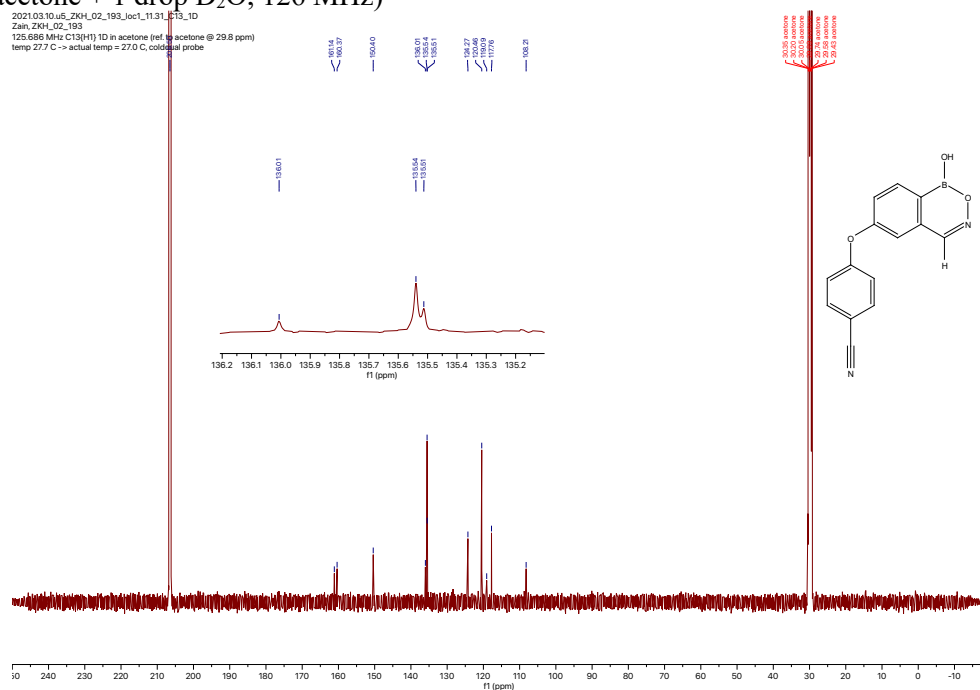
¹¹B NMR spectrum of a benzodiazaborine analog (**4-8d**) synthesized by the early-stage approach (d_6-acetone + 1 drop D_2O, 128 MHz)
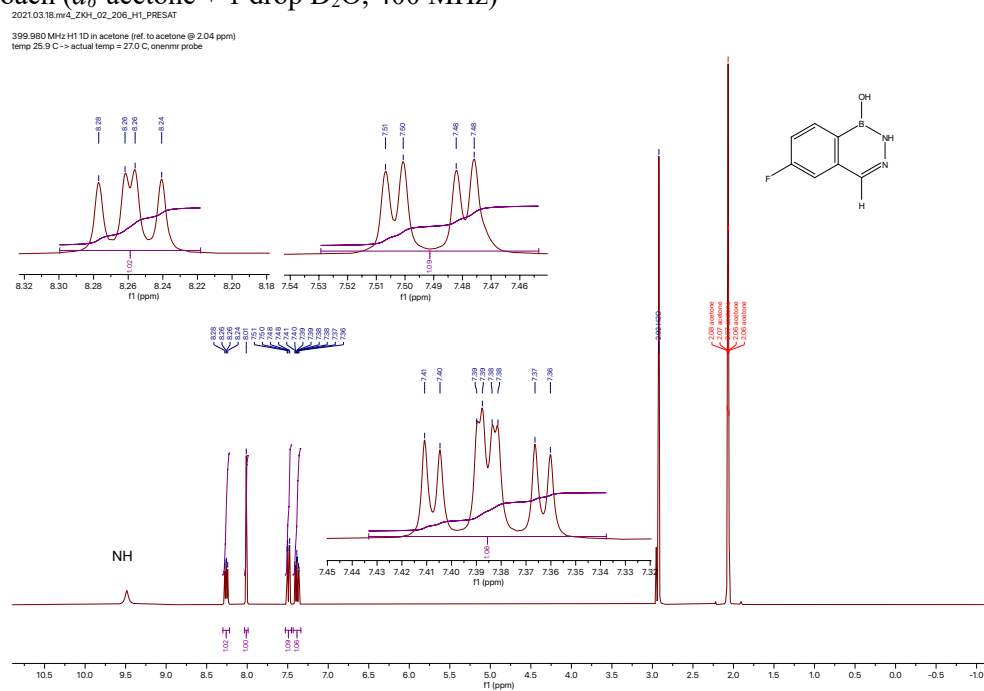
2021.03.18.mr4_ZKH_02_206_B11_1D

128.329 MHz B11{H1} 1D in acetone
temp 25.9 C -> actual temp = 27.0 C, onenmr probe

¹⁹F NMR spectrum of a benzodiazaborine analog (**4-8d**) synthesized by the early-stage approach (d_6-acetone + 1 drop D_2O, 126 MHz)
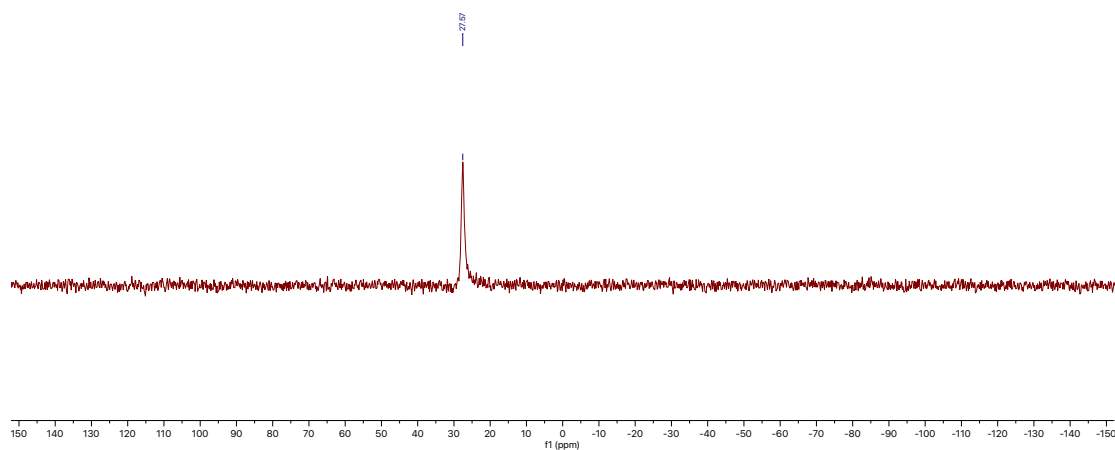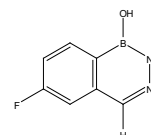
2021.03.18.mr4_ZKH_02_206_F19_1D

376.308 MHz F19 1D in acetone
temp 25.9 C -> actual temp = 27.0 C, onenmr probe

298

^{13}C NMR spectrum of a benzodiazaborine analog (**4-8d**) synthesized by the early-stage approach (d_6-acetone + 1 drop D$_2$O, 126 MHz)

^{1}H NMR spectrum of a benzoxazaborine analog (**4-22a**) obtained after amidation reaction using the late-stage approach (d_6-acetone + 1 drop D$_2$O, 400 MHz)

^{11}B NMR spectrum of a benzoxazaborine analog (**4-22a**) obtained after amidation reaction using the late-stage approach (d_6-acetone + 1 drop D$_2$O, 128 MHz)

^{13}C NMR spectrum of a benzoxazaborine analog (**4-22a**) obtained after amidation reaction using the late-stage approach (d_6-acetone + 1 drop D$_2$O, 126 MHz)

¹H NMR spectrum of a benzodiazaborine analog (**4-23b**) obtained after amidation reaction using the late-stage approach (*d₆*-acetone + 1 drop D₂O, 600 MHz)

¹¹B NMR spectrum of a benzodiazaborine analog (**4-23b**) obtained after amidation reaction using the late-stage approach (*d₆*-acetone + 1 drop D₂O, 160 MHz)

^{13}C NMR spectrum of a benzodiazaborine analog (**4-23b**) obtained after amidation reaction using the late-stage approach (d_6-acetone + 1 drop D$_2$O, 126 MHz)
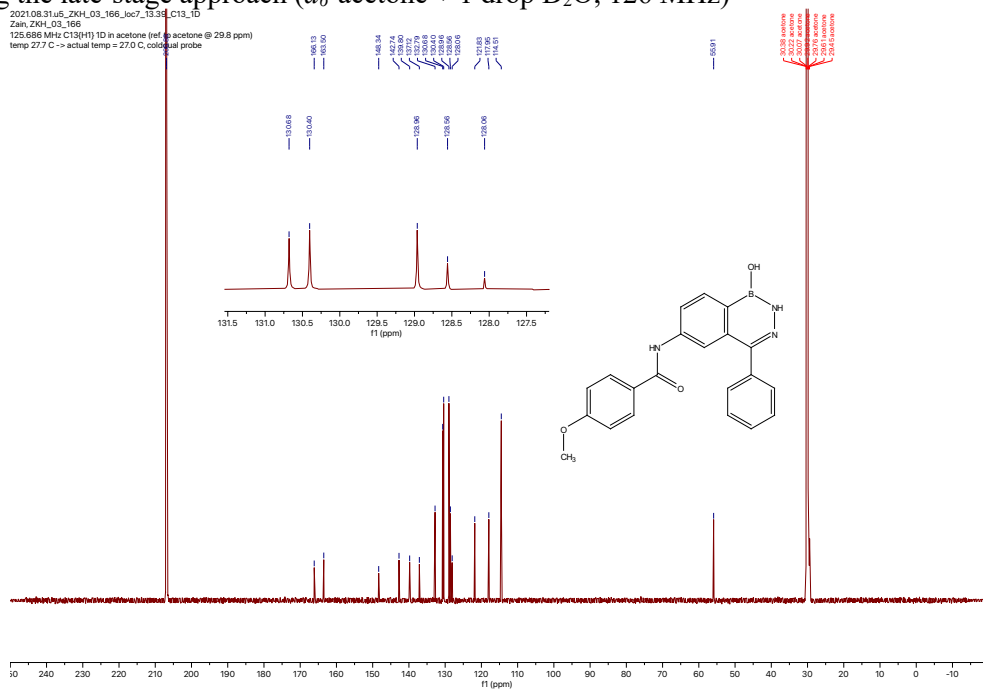
^{1}H NMR spectrum of a benzodiazaborine analog (**4-25a**) obtained after Chan-Lam reaction using the late-stage approach (d_6-acetone + 1 drop D$_2$O, 400 MHz)

^{11}B NMR spectrum of a benzodiazaborine analog (**4-25a**) obtained after Chan-Lam reaction using the late-stage approach (d_6-acetone + 1 drop D_2O, 128 MHz)

2022.01.27.mr4_ZKH_04_98_after_crystallization_B11_1D

128.329 MHz B11{H1} 1D in acetone
temp 25.9 C -> actual temp = 27.0 C, onenmr probe
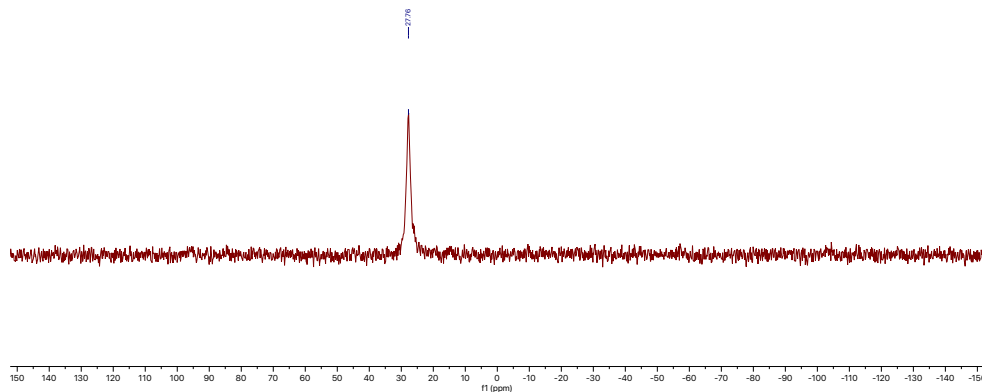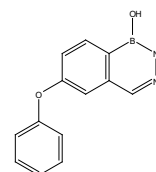
^{13}C NMR spectrum of a benzodiazaborine analog (**4-25a**) obtained after Chan-Lam reaction using the late-stage approach (d_6-acetone + 1 drop D_2O, 126 MHz)

2022.01.27.u5_ZKH_04_98_loc1_18.58_C13_1D
Zain, ZKH_04_98
125.686 MHz C13{H1} 1D in acetone (ref. to acetone @ 29.8 ppm)
temp 27.7 C -> actual temp = 27.0 C, coldqual probe
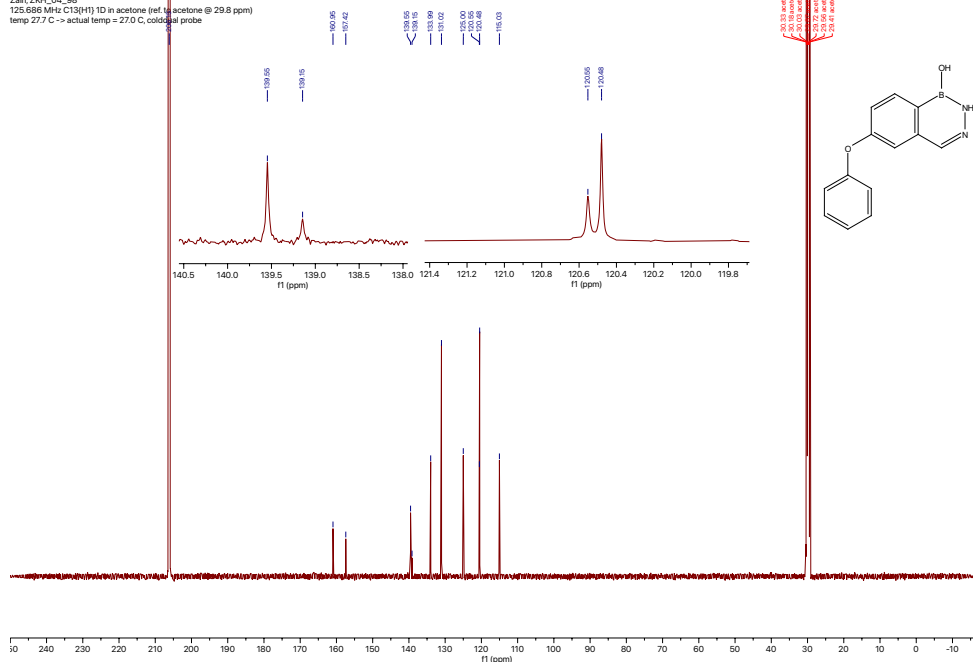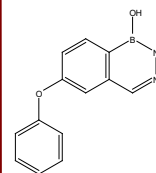
¹H NMR spectrum of a benzoxazaborine analog (**4-31c**) obtained after Suzuki-Miyaura cross-coupling using the late-stage approach (*d₆*-acetone + 1 drop D₂O, 500 MHz)

¹¹B NMR spectrum of a benzoxazaborine analog (**4-31c**) obtained after Suzuki-Miyaura cross-coupling using the late-stage approach (*d₆*-acetone + 1 drop D₂O, 160 MHz)

¹³C NMR spectrum of a benzoxazaborine analog (**4-31c**) obtained after Suzuki-Miyaura cross-coupling using the late-stage approach (*d₆*-acetone + 1 drop D₂O, 126 MHz)

¹H NMR spectrum of a benzodiazaborine analog (**4-32j**) obtained after Suzuki-Miyaura cross-coupling using the late-stage approach (*d₆*-acetone + 1 drop D₂O, 400 MHz)
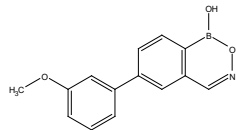
<superscript>11</superscript>B NMR spectrum of a benzodiazaborine analog (**4-32j**) obtained after Suzuki-Miyaura cross-coupling using the late-stage approach (*d₆*-acetone + 1 drop D₂O, 128 MHz)

2022.05.05.mr4_ZKH_04_149_B11_1D
128.329 MHz B11{H1} 1D in acetone
temp 25.9 C -> actual temp = 27.0 C, onenmr probe
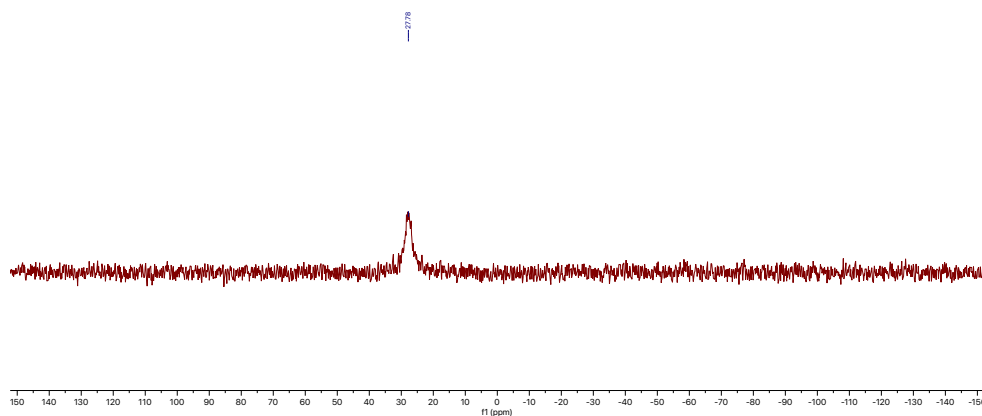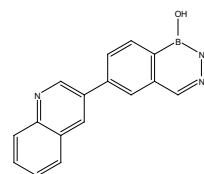
<superscript>13</superscript>C NMR spectrum of a benzodiazaborine analog (**4-32j**) obtained after Suzuki-Miyaura cross-coupling using the late-stage approach (*d₆*-acetone + 1 drop D₂O, 126 MHz)

2022.05.05.u5_ZKH_04_149_loc2_14.45_C13_1D
Zain, ZKH_04_149
125.686 MHz C13{H1} 1D in acetone (ref. to acetone @ 29.8 ppm)
temp 27.7 C -> actual temp = 27.0 C, colddual probe
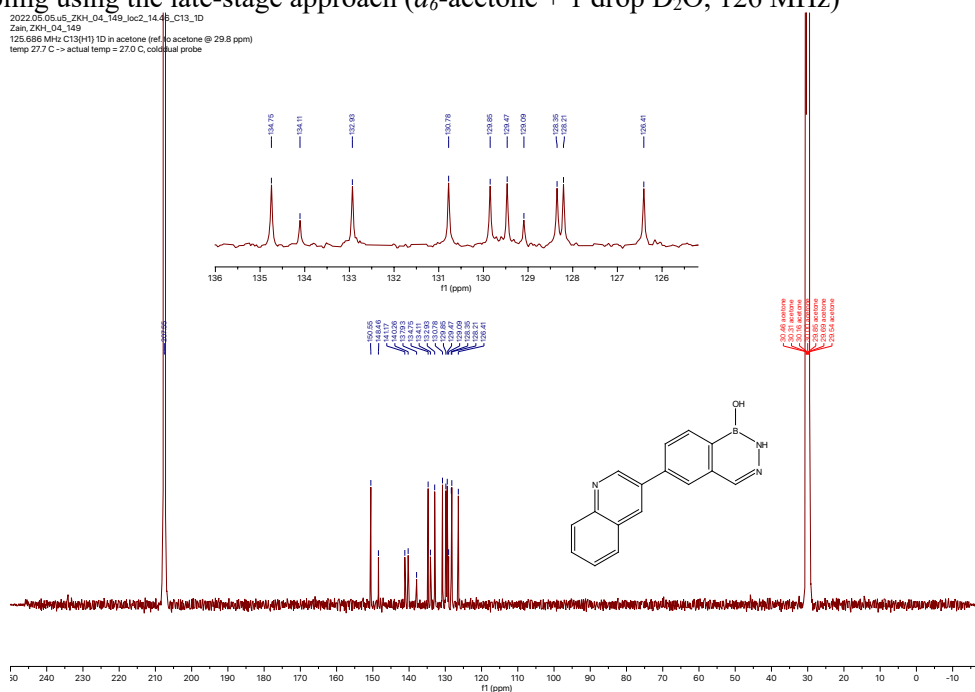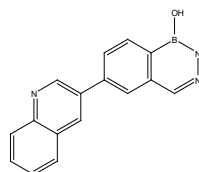
¹H NMR spectrum of a benzodiazaborine analog of olaparib (**4-37**) (*d₆*-acetone + 1 drop D₂O, 400 MHz)
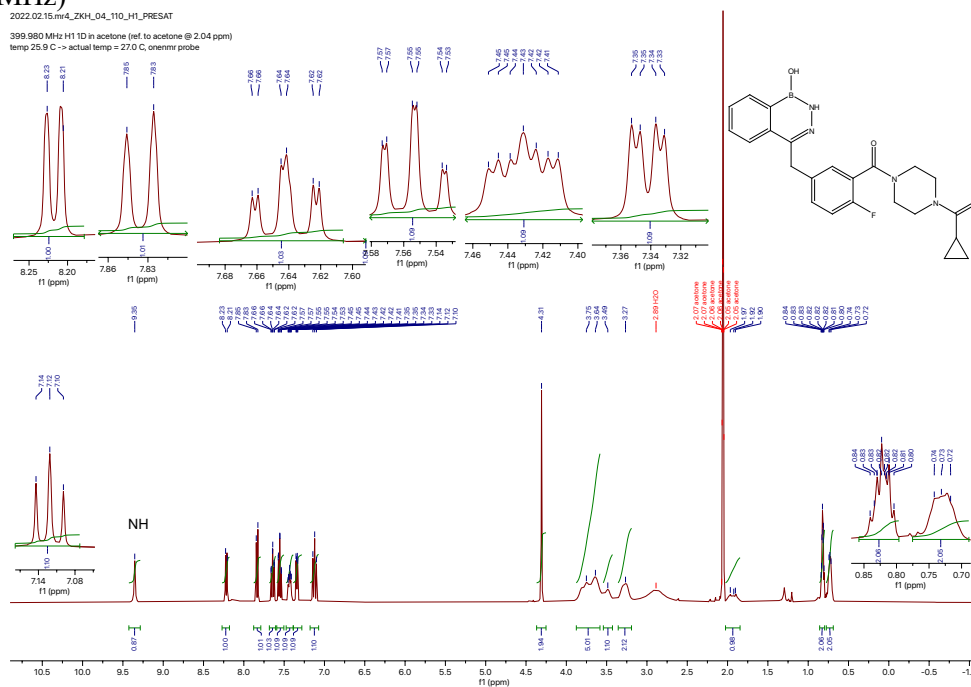
¹¹B NMR spectrum of a benzodiazaborine analog of olaparib (**4-37**) (*d₆*-acetone + 1 drop D₂O, 128 MHz)
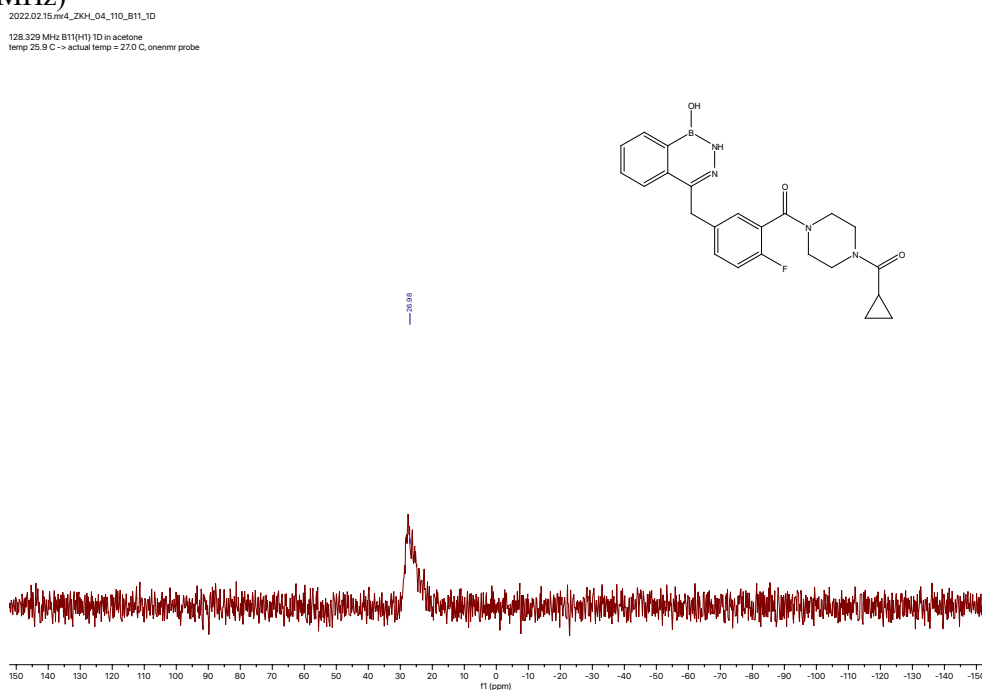
¹⁹F NMR spectrum of a benzodiazaborine analog of olaparib (**4-37**) (*d₆*-acetone + 1 drop D₂O, 376 MHz)
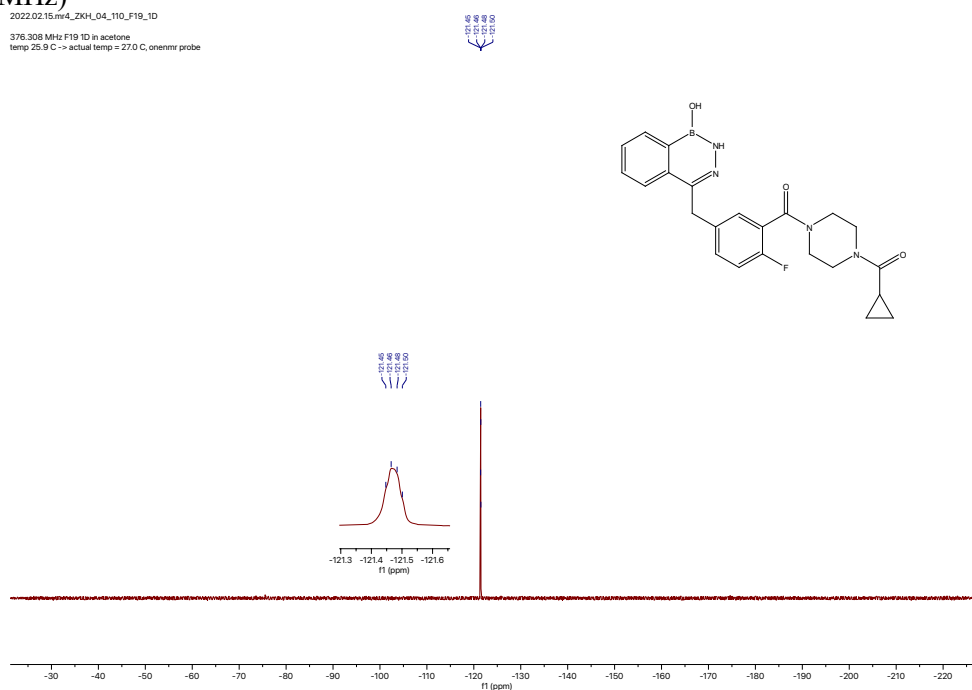
¹³C NMR spectrum of a benzodiazaborine analog of olaparib (**4-37**) (*d₆*-acetone + 1 drop D₂O, 176 MHz)
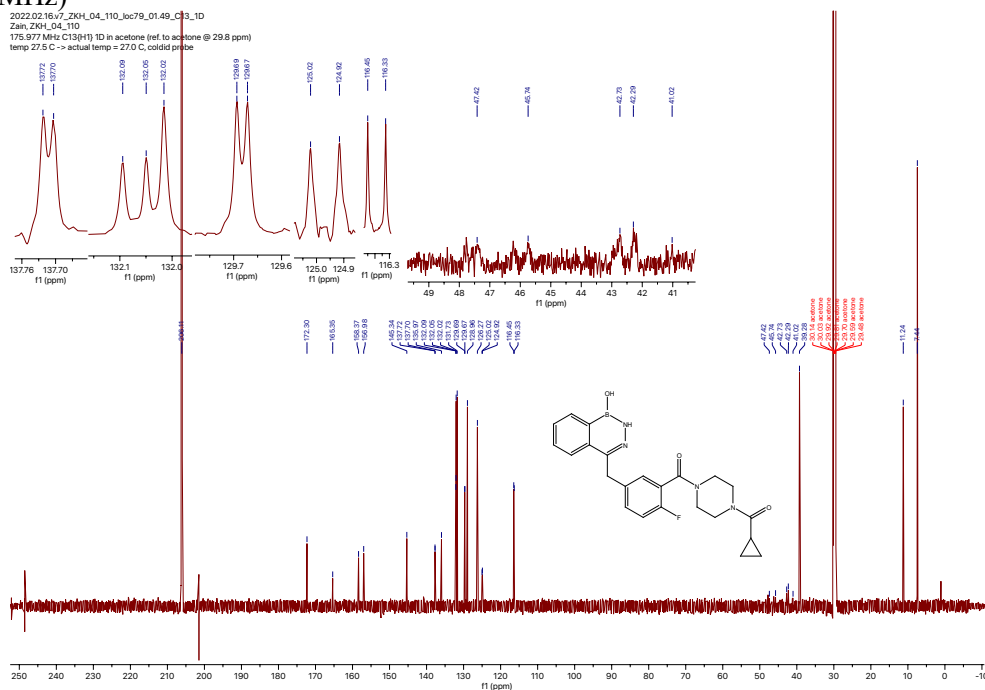
Assay Report

6405 Mira Mesa Blvd. Suite 100
San Diego, CA 92121
Tel: 1.858.829.3082
Fax: 1.858.481.8694
Email: info@bpsbioscience.com

Poly (ADP-ribose) Polymerases (PARPs) Inhibitor Assays
Enzymatic Study of Two Compounds from University of Alberta.

UnivA_PARP_220309

PARP Inhibitor Assays

Study Sponsor: University of Alberta

Attention: Dennis Hall
                        Zain Kazmi

Address: University of Alberta, Department of Chemistry
                        11227 Saskatchewan Dr NW, Edmonton, AB
T6G 2N4

Study Director: Henry Zhu, Ph.D.

Testing Facility: BPS Bioscience Inc.
                        6405 Mira Mesa Blvd. Suite 100
                        San Diego, CA 92121
                        USA

Study Period:

Report Version: 1

Report Date: March 09, 2022

Study Director

Katarzyna Zientara-Rytter, Ph.D.
Sr. Scientist I

03-09-2022

Date

Henry Zhu, Ph.D.
President

1. **Purpose of the Study**

The purpose of the study is to determine the effects of two compounds from University of Alberta, on the enzymatic activities of recombinant human PARP1 and PARP2 enzymes by using *in vitro* enzymatic assays.

2. Materials and Methods

2.1 Materials

BPS PARP1 and PARP2 assay kits are used in the assay (Catalog #80551, 80552).
AZD-5305 was purchased from MedChemExpress (Catalog #HY-132167).
Olaparib was purchased from LC Laboratories (Cat# O-9201)

2.2 Compounds

Compound I.D.	Compound Supplied	Stock Concentration	Dissolving Solvent	Test Range (nM)	Intermediate Dilution
FR17390868	Solid	10 mM	DMSO	0.0038 – 1000	10 % DMSO in Assay Buffer
FR17390908	Solid	10 mM	DMSO	0.0038 – 1000	10 % DMSO in Assay Buffer
AZD-5305*	Solution	10 mM	DMSO	0.0038 – 1000	10 % DMSO in Assay Buffer
Olaparib*	Solution	10 mM	DMSO	0.0038 – 1000	10 % DMSO in Assay Buffer

* Reference Compounds.

2.3 Experimental Conditions

2.3.1 Enzymes and Substrates

Assay	Catalog # (Lot #)	Enzyme Used (nM)/ Reaction	Substrate
			Activated DNA
PARP1	80501 (210223)	1	13.5 µM NAD$^+$/1.5 µM NAD$^+$-Biotin
			625 ng/ml
PARP2	80502 (210317-2)	1	27 µM NAD$^+$/3 µM NAD$^+$-Biotin
			625 ng/ml

2.3.1 Assay Conditions

In general, all assays were done by following the BPS PARP1 or PARP2 assay kit protocols with some modifications.

The enzymatic reactions were conducted in duplicate at room temperature for 1 hour in a 96 well plate pre-coated with histone substrate. The 50 µl reaction mixtures in PARP Assay Buffer containing substrate (see **2.3.1**), enzyme (see **2.3.1**) and the test compound (see **2.2**) were incubated at room temperature for 60 min. The wells were washed five times with PBST. Next, 50 µl of Streptavidin-horseradish peroxidase (prepared with Blocking Buffer 3) was added to each well and the plate was incubated at room temperature for an additional 30 min. The wells were washed again and 100 µl ELISA ECL substrate was added to each well. Luminescence was measured using a BioTek Synergy™ 2 microplate reader.

2.3.2 Data Analysis

PARP activity assays were performed in duplicates. The luminescence data were analyzed using the computer software, Graphpad Prism. In the absence of the compound, the luminescence (L_t) in each data set was defined as 100% activity. In the absence of the PARP, the luminescence (L_b) in each data set was defined as 0% activity. The percent activity in the presence of each compound was calculated according to the following equation: % activity = $[(L - L_b)/(L_t - L_b)] \times 100$, where L= the luminescence in the presence of the compound, L_b = the luminescence in the absence of the PARP, and L_t = the luminescence in the absence of the compound. The percent inhibition was calculated according to the following equation: % inhibition = 100 - % activity.

The values of % activity versus a series of compound concentrations were then plotted using non-linear regression analysis of Sigmoidal dose-response curve generated with the equation $Y = B + (T-B)/1 + 10^{((LogEC50-X) \times Hill\ Slope)}$, where Y=percent activity, B=minimum percent activity, T=maximum percent activity, X= logarithm of compound and Hill Slope=slope factor or Hill coefficient. The IC_{50} value was determined by the concentration causing a half-maximal percent activity. pIC_{50} values were determined using the following equation: $pIC_{50} = -log_{10}(N)$, where N= the IC_{50} concentration of the compound in molar (M) units.

3. Assay Results

3.1 Summary of the effects of the compounds on PARP Activities

The IC_{50} values of the compounds against PARP1 and PARP2 are summarized in Table 3.1. Approximate values are assigned for IC_{50} when only one plateau for curve fit is available. If IC_{50} is higher than 1000 nM percentage inhibition of the compound at that concentration is calculated.

Table 3.1   Inhibitory Effects of the Compounds on PARP Activities

| Compound I.D. | IC$_{50}$ (nM) | |
| | PARP1 | PARP2 |
	IC$_{50}$	IC$_{50}$
FR17390868	~539	122
FR17390908	> 1000 nM No inhib. @ 1000 nM	> 1000 nM 18% inhib. @ 1000 nM
AZD-5305*	1.0	11
Olaparib*	0.51	0.13

3.2 Results of effects of the compounds on individual PARP Activity

3.2.1 PARP1

3.2.1.1 FR17390868

Table 3.2.1.1. Data for the Effect of FR17390868 on PARP1 Activity

| FR17390868 (nM) | PARP1 Activity [(Luminescence Signal)] | | % Activity | |
	Repeat 1	Repeat 2	Repeat 1	Repeat 2
No Compound	55640	51846	104	96
0.0038	53623	55352	100	103
0.015	52687	51542	98	96
0.061	51341	49732	96	93
0.24	49490	48363	92	90
0.98	47884	48330	89	90
3.9	49924	50472	93	94
16	47508	47492	88	88
63	46176	46474	86	86
250	37360	38773	69	72
1000	16013	19902	30	37
Background	30	40		

PARP1
(13.5 µM NAD/1.5 µM NAD-biotin)

IC$_{50}$ ~ 539 nM

FR17390868, [Log(nM)]
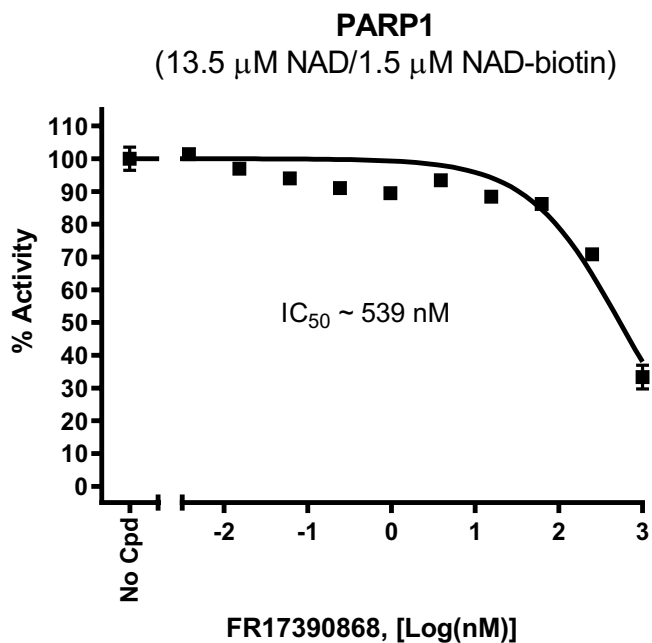
3.2.1.2 FR17390908

Table 3.2.1.2. Data for the Effect of FR17390908on PARP1 Activity

FR17390908 (nM)	PARP1 Activity [(Luminescence Signal)]		% Activity	
	Repeat 1	Repeat 2	Repeat 1	Repeat 2
No Compound	52117	48180	104	96
0.0038	48093	51099	96	102
0.015	53834	52604	107	105
0.061	45340	48637	90	97
0.24	46842	46727	93	93
0.98	47805	48481	95	97
3.9	48769	46668	97	93
16	44387	46951	89	94
63	46499	50195	93	100
250	47156	51589	94	103
1000	48857	48459	97	97
Background	28	25		

PARP1
(13.5 µM NAD/1.5 µM NAD-biotin)

IC$_{50}$ > 1000 nM
No inhib @ 1000 nM

FR17390908, [Log(nM)]
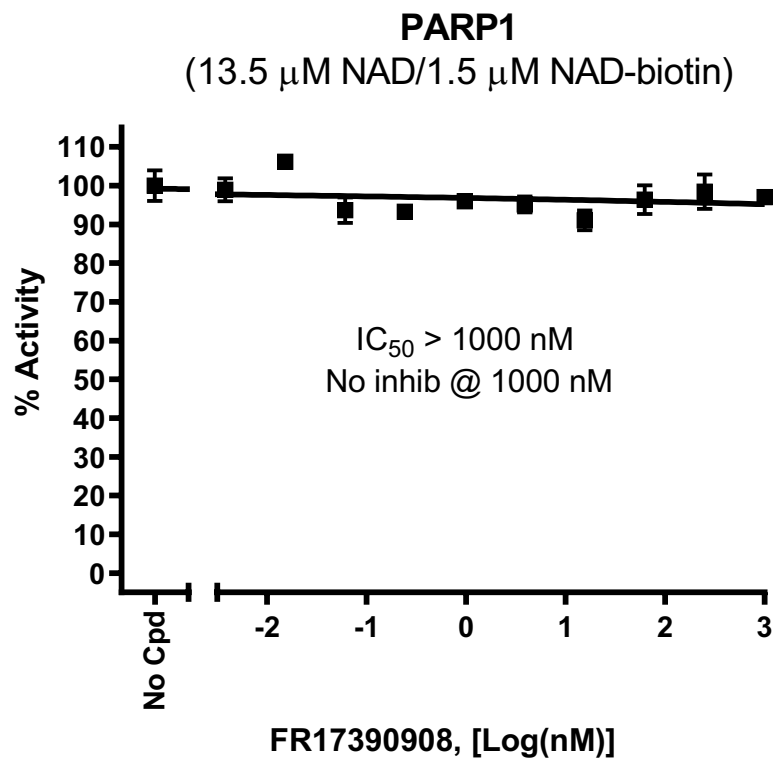
3.2.1.3 AZD5305

Table 3.2.1.3. Data for the Effect of AZD5305 on PARP1 Activity

AZD5305 (nM)	PARP1 Activity [(Luminescence Signal)]		% Activity	
	Repeat 1	Repeat 2	Repeat 1	Repeat 2
No Compound	55475	55946	100	100
0.0038	53676	51256	96	92
0.015	53848	52785	97	95
0.061	54478	50186	98	90
0.24	45469	38932	82	70
0.98	34206	29668	61	53
3.9	10825	9542	19	17
16	790	1017	1	2
63	56	47	0	0
250	25	23	0	0
1000	13	16	0	0
Background	38	39		

PARP1
(13.5 μM NAD/1.5 μM NAD-biotin)

IC$_{50}$ = 1.0 nM

% Activity (y-axis)

AZD5305, [Log(nM)] (x-axis)

No Cpd
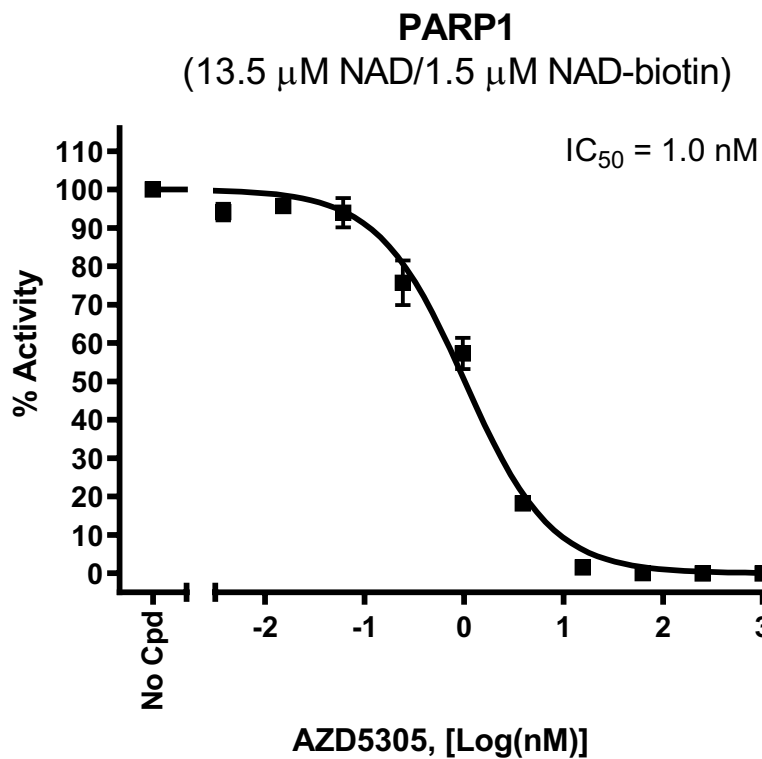
3.2.1.4 Olaparib

Table 3.2.1.4. Data for the Effect of Olaparib on PARP1 Activity

Olaparib (nM)	PARP1 Activity [(Luminescence Signal)]		% Activity	
	Repeat 1	Repeat 2	Repeat 1	Repeat 2
No Compound	52768	51217	101	99
0.0038	56669	53504	109	103
0.015	53361	49788	103	96
0.061	47279	45862	91	88
0.24	36258	35427	70	68
0.98	14496	14438	28	28
3.9	11860	11172	23	21
16	1866	1601	3	3
63	95	110	0	0
250	26	132	0	0
1000	21	20	0	0
Background	75	47		

PARP1

(13.5 μM NAD/1.5 μM NAD-biotin)

IC$_{50}$ = 0.51 nM

Olaparib, [Log(nM)]
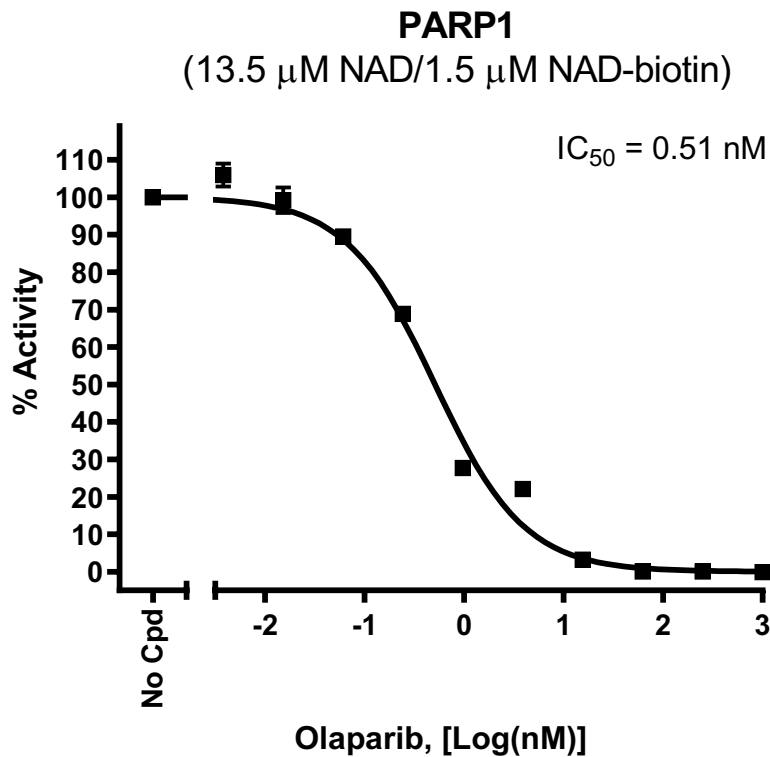
3.2.2 PARP2

3.2.2.1 FR17390868

Table 3.2.2.1. Data for the Effect of FR17390868 on PARP2 Activity

FR17390868 (nM)	PARP2 Activity [(Luminescence Signal)]		% Activity	
	Repeat 1	Repeat 2	Repeat 1	Repeat 2
No Compound	69165	66308	102	98
0.0038	67334	65278	99	96
0.015	70799	64470	105	95
0.061	68757	64217	102	95
0.24	65016	61213	96	90
0.98	63326	62467	93	92
3.9	64058	63531	95	94
16	59255	62077	87	92
63	49224	52295	73	77
250	20044	14585	29	21
1000	4093	2962	6	4
Background	98	201		

PARP2

(27 μM NAD/3 μM NAD-biotin)

IC$_{50}$ = 122 nM

FR17390868, [Log(nM)]
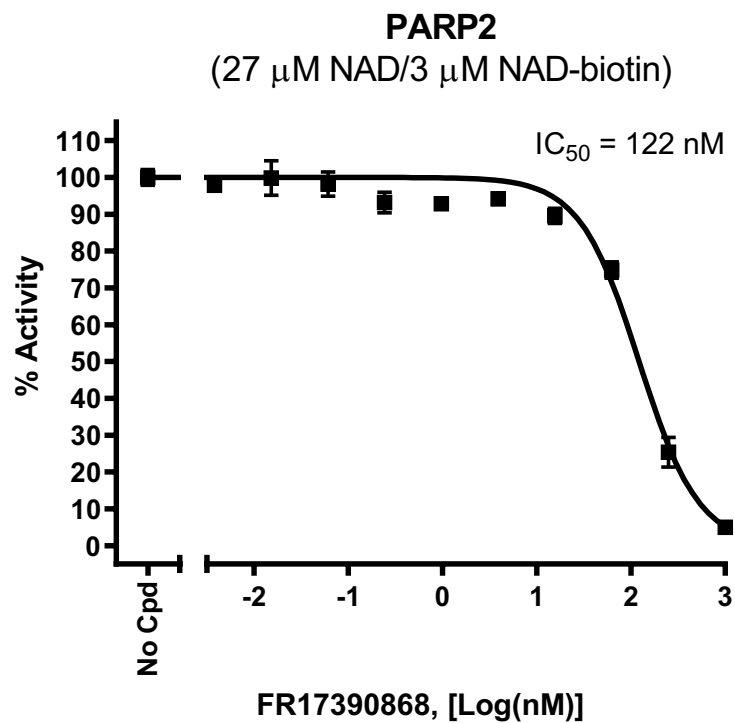
3.2.2.2 FR17390908

Table 3.2.2.2. Data for the Effect of FR17390908 on PARP2 Activity

FR17390908 (nM)	PARP2 Activity [(Luminescence Signal)]		% Activity	
	Repeat 1	Repeat 2	Repeat 1	Repeat 2
No Compound	66410	63473	102	98
0.0038	61105	65334	94	101
0.015	64950	63461	100	98
0.061	65636	61638	101	95
0.24	63427	62581	98	96
0.98	64297	65617	99	101
3.9	66863	69333	103	107
16	66528	64260	102	99
63	64505	67469	99	104
250	63283	66886	97	103
1000	52903	53102	81	82
Background	44	52		

PARP2
(27 μM NAD/3 μM NAD-biotin)

IC$_{50}$ > 1000 nM
18% inhib @ 1000 nM

FR17390908, [Log(nM)]
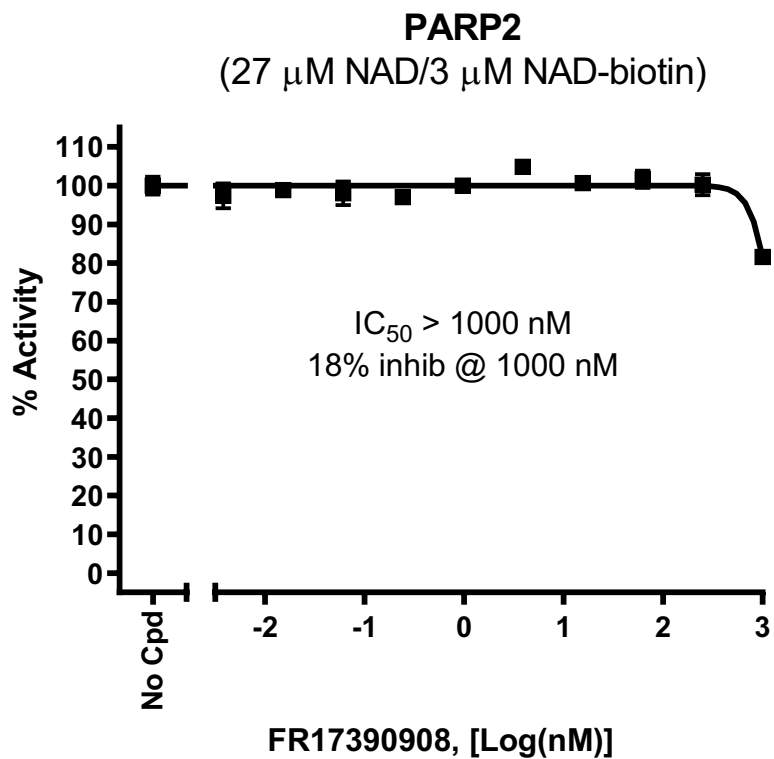
3.2.2.3 AZD5305

Table 3.2.2.3. Data for the Effect of AZD5305 on PARP2 Activity

AZD5305 (nM)	PARP2 Activity [(Luminescence Signal)]		% Activity	
	Repeat 1	Repeat 2	Repeat 1	Repeat 2
No Compound	66103	67682	99	101
0.0038	69211	66358	103	99
0.015	65383	65390	98	98
0.061	66859	62654	100	94
0.24	64710	65233	97	98
0.98	62581	66516	94	99
3.9	55330	57358	83	86
16	25772	25376	38	38
63	4693	5192	7	8
250	456	244	1	0
1000	29	42	0	0
Background	33	33		

PARP2
(27 μM NAD/3 μM NAD-biotin)

IC_{50} = 11 nM
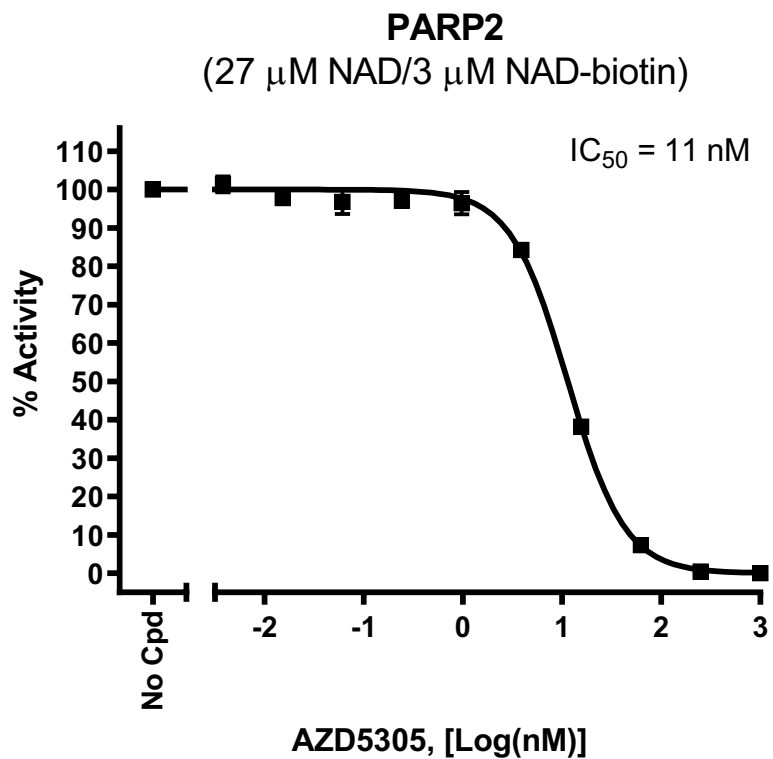
3.2.2.4 Olaparib

Table 3.2.2.4. Data for the Effect of Olaparib on PARP2 Activity

Olaparib (nM)	PARP2 Activity [(Luminescence Signal)]		% Activity	
	Repeat 1	Repeat 2	Repeat 1	Repeat 2
No Compound	71825	67658	103	97
0.0038	71210	73069	102	105
0.015	69173	71743	99	103
0.061	52852	58296	76	84
0.24	16676	14479	24	21
0.98	950	473	1	0
3.9	914	407	1	0
16	109	104	0	0
63	387	1043	0	1
250	57	28	0	0
1000	89	1102	0	1
Background	347	69		

PARP2
(27 μM NAD/3 μM NAD-biotin)

$IC_{50} = 0.13$ nM
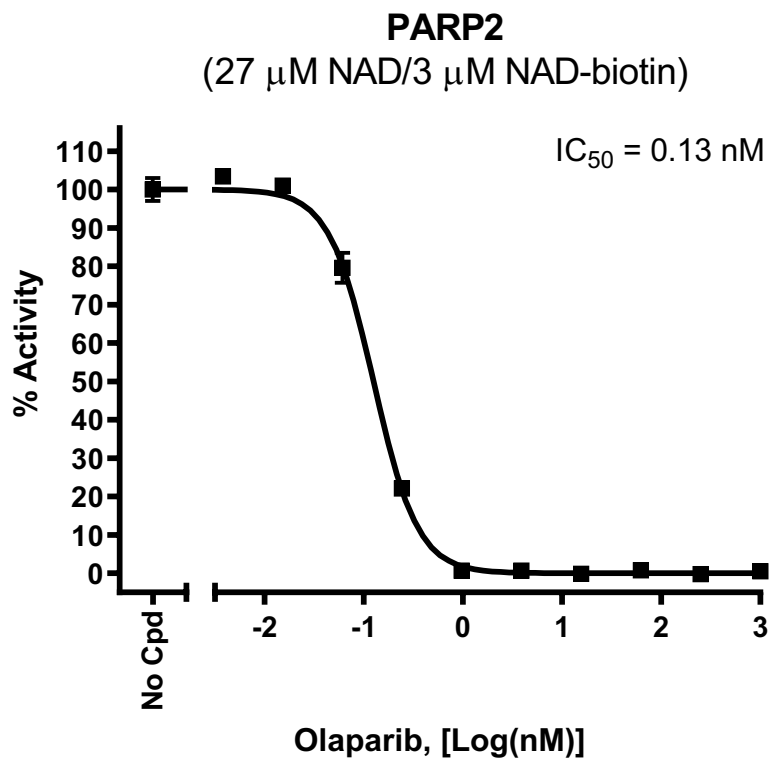
4. Quality Assurance Statement

I certify that the results presented in this report were generated using the materials and methods mentioned and that these results reflect the Raw Data.

(signature)

Henry Zhu, Ph.D.
President

03-09-2022

Date

X-ray crystallographic data of compound 4-11

XCL Code: DGH2021 **Date:** 12 December 2020

Compound: (4-bromophenyl)(1-hydroxy-4-methyl-1,4-dihydro-3*H*-2,3,1-
benzoxazaborinin-3-yl)methanone

Formula: $C_{15}H_{13}BBrNO_3$

Supervisor: D.G. Hall **Crystallographer:** M. J. Ferguson
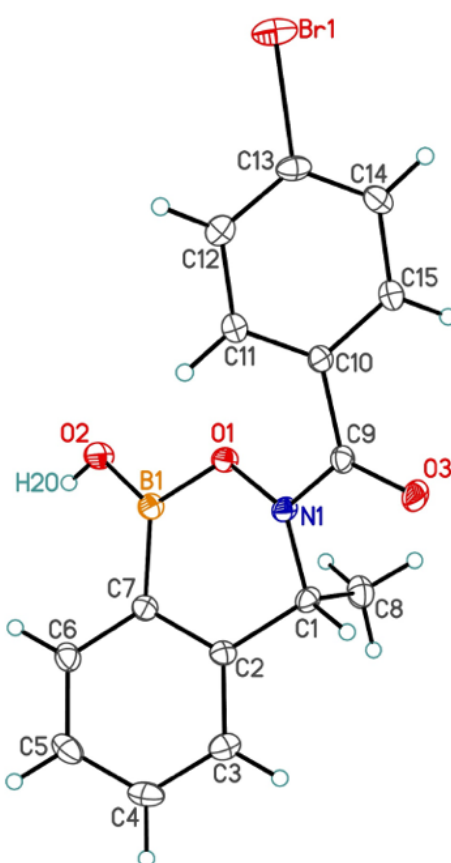
Perspective view of the (4-bromophenyl)(1-hydroxy-4-methyl-1,4-dihydro-3*H*-2,3,1-benzoxazaborinin-3-yl)methanone molecule showing the atom labelling scheme. Non-hydrogen atoms are represented by Gaussian ellipsoids at the 30% probability level. Hydrogen atoms are shown with arbitrarily small thermal parameters.

X-ray crystallographic data of compound 4-22a

XCL Code: DGH2114   **Date:** 20 July 2021

Compound: *N*-(1-hydroxy-4-phenyl-1*H*-2,3,1-benzoxazaborinin-6-yl)benzamide, acetonitrile hemisolvate

Formula: $C_{21}H_{16.50}BN_{2.50}O_3$ ($C_{20}H_{15}BN_2O_3 \cdot 0.5C_2H_3N$)

Supervisor: D. G. Hall   **Crystallographer:**   M. J. Ferguson
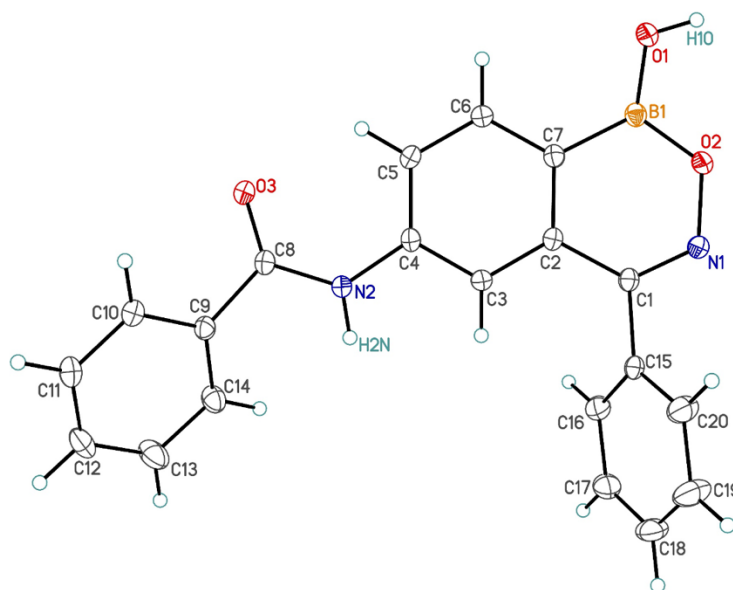
Perspective view of the first of two crystallographically independent *N*-(1-hydroxy-4-phenyl-1*H*-2,3,1-benzoxazaborinin-6-yl)benzamide molecules (molecule A) showing the atom labelling scheme.   Non-hydrogen atoms are represented by Gaussian ellipsoids at the 30% probability level.   Hydrogen atoms are shown with arbitrarily small thermal parameters.

Appendix 5: Computational Studies (Chapter 3)

Optimized Structures and Molecular Orbitals for Neutral Boron Heterocycles and Comparators

Density functional theory calculations (DFT) were performed with Q-Chem 5.1 using the Spartan 18 suite (Wavefunction, Irvine, California). Structures were pre-optimized by molecular mechanics (MMFF) then minimized with DFT using the ωB97X-D method with the 6-31G* basis set, in the gas phase, starting with a syn conformer where the boranol OH bond is aligned synperiplanar with the endocyclic B–O or B–N bond. The resulting structures were not confirmed to be global minima, however in all cases the syn conformer is lower or similar in energy compared to the anti-isomer, thus it was employed for the comparison of molecular orbitals depicted in Figure 3.11 and Table 3.1. Energy values are self-consistent field (SCF) electronic energy values without thermochemical correction. Entropy differences for these structurally similar compounds are expected to be very small.

Compound 3-1
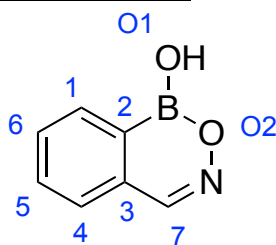
Formula:	$C_7H_6BNO_2$
Job type:	Equilibrium Geometry
Method:	ωB97X-D
Basis set:	6-31G*
Energy:	–500.298034 hartrees

Molecular Orbital Energies

Label	Energy (ev)	Sym. Lab.
LUMO{+2}	3.21	A"
LUMO{+1}	0.98	A"
LUMO	0.45	A"
HOMO	–8.75	A"
HOMO{–1}	–9.32	A"
HOMO{–2}	–9.72	A'

Atomic Charges

Atom Label	Natural Charge	Atom Label	Natural Charge
B1	+1.136	H2	+0.507
C1	–0.189	H3	+0.243
C2	–0.390	H4	+0.246
C3	–0.091	H5	+0.249
C4	–0.215	H6	+0.249
C5	–0.223	N1	–0.093
C6	–0.231	O1	–0.895
C7	+0.009	O2	–0.569

H1	+0.256

Calculated Bond Orders

Bond	Löwdin		Bond	Löwdin
B1 – C2	1.041		**C4 – C5**	1.542
B1 – O1	1.512		**C4 – H4**	0.894
B1 – O2	1.357		**C5 – C6**	1.462
C1 – C2	1.414		**C5 – H5**	0.899
C1 – C6	1.537		**C6 – H6**	0.898
C1 – H1	0.892		**C7 – H3**	0.881
C2 – C3	1.365		**C7 – N1**	2.004
C3 – C4	1.394		**N1 – O2**	1.217
C3 – C7	1.127		**O1 – H2**	0.818

LUMO	HOMO	ELECTROSTATIC
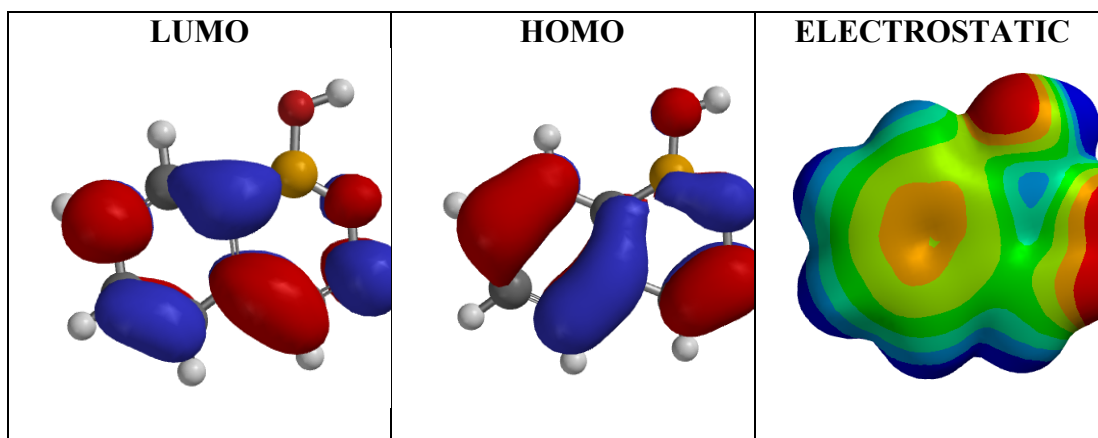
Compound 3-2a
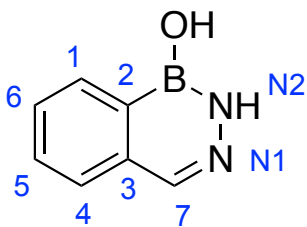
Formula: $C_7H_7BN_2O$

Job type: Equilibrium Geometry

Method: ωB97X-D

Basis set: 6-31G*

Energy: –480.455105 hartrees

Molecular Orbital Energies

Label	Energy (ev)	Sym. Lab.
LUMO{+2}	3.50	A"
LUMO{+1}	1.36	A"
LUMO	0.95	A"
HOMO	–8.02	A"
HOMO{–1}	–8.94	A"
HOMO{–2}	–9.45	A'

Atomic Charges

Atom Label	Natural Charge	Atom Label	Natural Charge
B1	+1.014	H2	+0.416
C1	−0.192	H3	+0.230
C2	−0.372	H4	+0.243
C3	−0.085	H5	+0.245
C4	−0.219	H6	+0.245
C5	−0.228	H10	+0.494
C6	−0.238	N1	−0.244
C7	+0.007	N2	−0.678
H1	+0.252	O1	−0.889

Calculated Bond Orders

Bond	Löwdin	Bond	Löwdin
B1 – C2	1.056	C4 – H4	0.895
B1 – N2	1.325	C5 – C6	1.445
B1 – O1	1.456	C5 – H5	0.900
C1 – C2	1.397	C6 – H6	0.899
C1 – C6	1.556	C7 – H3	0.889
C1 – H1	0.892	C7 – N1	1.931
C2 – C3	1.360	N1 – N2	1.319
C3 – C4	1.376	N2 – H2	0.848
C3 – C7	1.153	O1 – H10	0.831
C4 – C5	1.562		

LUMO	HOMO	ELECTROSTATIC
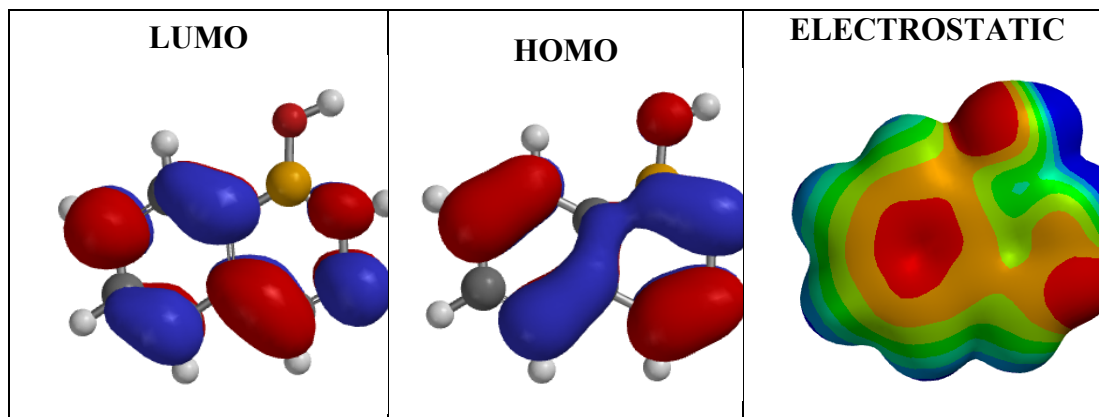
Compound 3-2b
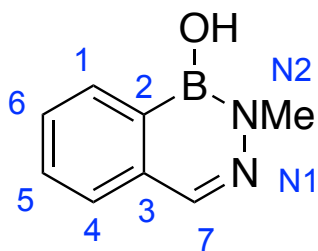
Formula: $C_8H_9BN_2O$

Job type: Equilibrium Geometry

Method: ωB97X-D

Basis set: 6-31G*

Energy: –519.753912 hartrees

Molecular Orbital Energies

Label	Energy (ev)
LUMO{+2}	3.52
LUMO{+1}	1.37
LUMO	0.99
HOMO	–7.84
HOMO{–1}	–8.89
HOMO{–2}	–9.40
HOMO{–3}	–9.45

Atomic Charges

Atom Label	Natural Charge	Atom Label	Natural Charge
B1	+1.029	H4	+0.242
C1	–0.191	H5	+0.245
C2	–0.371	H6	+0.244
C3	–0.083	H7	+0.225
C4	–0.220	H8	+0.225
C5	–0.228	H9	+0.265
C6	–0.239	H10	+0.497
C7	+0.009	N1	–0.249
C8	–0.495	N2	–0.497
H1	+0.252	O1	–0.889
H3	+0.231		

Calculated Bond Orders

Bond	Löwdin	Bond	Löwdin
B1 – C2	1.062	C5 – C6	1.441
B1 – N2	1.276	C5 – H5	0.900
B1 – O1	1.452	C6 – H6	0.899
C1 – C2	1.391	C7 – H3	0.888
C1 – C6	1.560	C7 – N1	1.914
C1 – H1	0.892	C8 – H7	0.935
C2 – C3	1.359	C8 – H8	0.935
C3 – C4	1.371	C8 – H9	0.924
C3 – C7	1.158	C8 – N2	1.079

C4 – C5	1.566		N1 – N2	1.293
C4 – H4	0.895		O1 – H10	0.827

LUMO	HOMO	ELECTROSTATIC
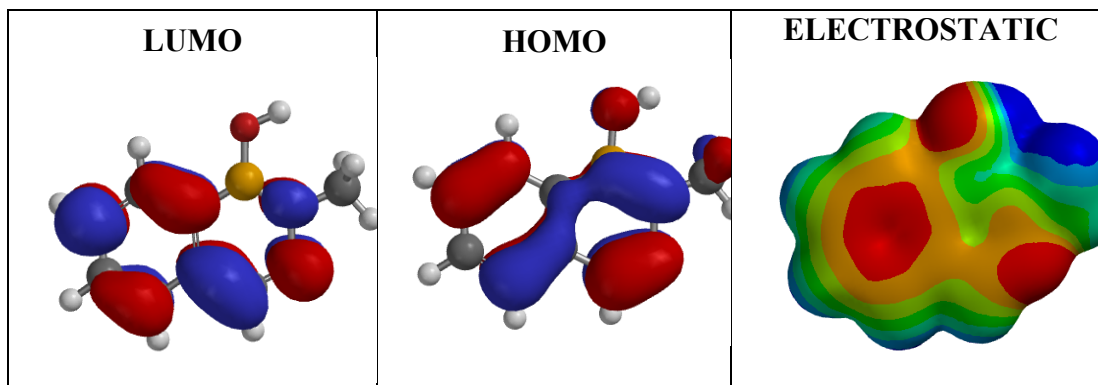
Compound 3-2c
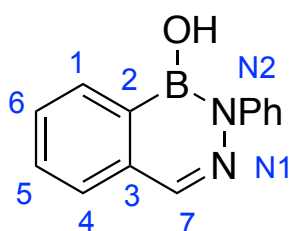
Formula: $C_{13}H_{11}BN_2O$

Job type: Equilibrium Geometry

Method: ωB97X-D

Basis set: 6-31G*

Energy: –711.429913 hartrees

Molecular Orbital Energies

Label	Energy (ev)
LUMO{+2}	1.65
LUMO{+1}	1.20
LUMO	0.76
HOMO	−7.79
HOMO{−1}	−8.86
HOMO{−2}	−9.03

Atomic Charges

Atom Label	Natural Charge		Atom Label	Natural Charge
B1	+1.038		H1	+0.254
C1	−0.189		H2	+0.262
C2	−0.372		H3	+0.232
C3	−0.085		H4	+0.243
C4	−0.219		H5	+0.246
C5	−0.227		H6	+0.245
C6	−0.238		H7	+0.506
C7	+0.021		H8	+0.256
C8	+0.156		H9	+0.248

C9	–0.249	**H10**	+0.248
C10	–0.238	**H11**	+0.246
C11	–0.289	**N1**	–0.248
C12	–0.230	**N2**	–0.498
C13	–0.228	**O1**	–0.892

Calculated Bond Orders

Bond	Löwdin	Bond	Löwdin
B1 – C2	1.057	**C7 – N1**	1.929
B1 – N2	1.232	**C8 – C10**	1.420
B1 – O1	1.472	**C8 – C11**	1.428
C1 – C2	1.396	**C8 – N2**	1.077
C1 – C6	1.555	**C9 – C12**	1.513
C1 – H1	0.891	**C9 – C13**	1.488
C2 – C3	1.361	**C9 – H11**	0.900
C3 – C4	1.378	**C10 – C13**	1.522
C3 – C7	1.150	**C10 – H2**	0.888
C4 – C5	1.560	**C11 – C12**	1.495
C4 – H4	0.894	**C11 – H8**	0.887
C5 – C6	1.446	**C12 – H9**	0.898
C5 – H5	0.900	**C13 – H10**	0.898
C6 – H6	0.899	**N1 – N2**	1.263
C7 – H3	0.887	**O1 – H7**	0.810

LUMO	HOMO

ELECTROSTATIC

Compound 3-2d

Formula: $C_{14}H_{13}BN_2O_3S$

Job type: Equilibrium Geometry

Method: ωB97X-D

Basis set: 6-31G*

Energy: −1299.247020 hartrees

Compound 3-3
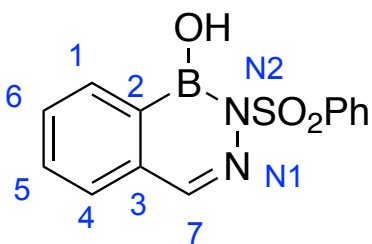
Formula: $C_{13}H_{11}BN_2O_3S$

Job type: Equilibrium Geometry

Method: ωB97X-D

Basis set: 6-31G*

Energy: −1259.942513 hartrees

Molecular Orbital Energies

Label	Energy (ev)
LUMO{+2}	1.08

LUMO{+1}	0.65
LUMO	0.38
HOMO	−8.53
HOMO{−1}	−9.22
HOMO{−2}	−9.46

Atomic Charges

Atom Label	Natural Charge	Atom Label	Natural Charge
B1	+1.050	H3	+0.237
C1	−0.186	H4	+0.245
C2	−0.367	H5	+0.248
C3	−0.091	H6	+0.248
C4	−0.216	H7	+0.528
C5	−0.224	H8	+0.280
C6	−0.231	H9	+0.271
C7	+0.047	H10	+0.251
C8	−0.348	H11	+0.254
C9	−0.214	N1	−0.266
C10	−0.199	N2	−0.750
C11	−0.213	O1	−0.894
C12	−0.238	O2	−0.922
C13	−0.238	O3	−0.988
H1	+0.258	S1	+2.413
H2	+0.254		

Calculated Bond Orders

Bond	Löwdin	Bond	Löwdin
B1 – C2	1.043	C8 – C11	1.449
B1 – N2	1.172	C8 – S1	0.903
B1 – O1	1.551	C9 – C12	1.500
C1 – C2	1.407	C9 – C13	1.500
C1 – C6	1.544	C9 – H10	0.899
C1 – H1	0.888	C10 – C13	1.506
C2 – C3	1.361	C10 – H8	0.881
C3 – C4	1.390	C11 – C12	1.506
C3 – C7	1.138	C11 – H9	0.883
C4 – C5	1.548	C12 – H2	0.897
C4 – H4	0.893	C13 – H11	0.896
C5 – C6	1.455	N1 – N2	1.251
C5 – H5	0.899	N2 – S1	0.914
C6 – H6	0.898	O1 – H7	0.768
C7 – H3	0.884	O2 – S1	1.851
C7 – N1	1.951	O3 – H7	0.075
C8 – C10	1.444	O3 – S1	1.699

LUMO	HOMO

ELECTROSTATIC

Compound 3-4

Formula: C$_9$H$_7$NO

Job type: Equilibrium Geometry

Method: ωB97X-D

Basis set: 6-31G*

Energy: –476.982172 hartrees

Molecular Orbital Energies

Label	Energy (ev)	Sym. Lab.
LUMO{+2}	3.00	A"
LUMO{+1}	1.25	A"
LUMO	0.62	A"
HOMO	–7.76	A"
HOMO{–1}	–9.11	A'
HOMO{–2}	–9.13	A"

Atomic Charges

Atom Label	Natural Charge	Atom Label	Natural Charge

C1	–0.215	H1	+0.261
C2	–0.085	H2	+0.499
C3	–0.095	H3	+0.224
C4	–0.207	H4	+0.246
C5	–0.239	H5	+0.248
C6	–0.229	H6	+0.248
C7	+0.039	H8	+0.222
C9	–0.104	N1	–0.439
C10	+0.323	O1	–0.697

Calculated Bond Orders

Bond	Löwdin	Bond	Löwdin
C1 – C2	1.303	C5 – H5	0.899
C1 – C6	1.638	C6 – H6	0.899
C1 – H1	0.890	C7 – H3	0.891
C2 – C3	1.300	C7 – N1	1.765
C2 – C10	1.231	C9 – C10	1.528
C3 – C4	1.309	C9 – H8	0.891
C3 – C7	1.273	C9 – N1	1.461
C4 – C5	1.636	C10 – O1	1.280
C4 – H4	0.894	O1 – H2	0.831
C5 – C6	1.370		

LUMO HOMO ELECTROSTATIC

Nucleus Independent Chemical Shift (NICS) Calculations

Method: Geometries were optimized at the B3LYP level of theory using the 6-311+G(2d,p) basis set. Nucleus independent chemical shift (NICS) were found using the GIAO-B3LYP/6-311+G(2d,p) level of theory. Molecular structures were visualized using GaussView 5. All calculations were performed using the Gaussian 16 a03 software package accessed on the Graham supercluster via Compute Canada.
Coordinates:

Compound 3-1

C	2.73228147	–0.20843047	0.36972807
C	1.81985854	–1.21116652	0.08867049
C	0.51230819	–0.87162442	–0.28357961
C	0.12238536	0.47628519	–0.37319280
C	1.05960481	1.47371604	–0.08505976
C	2.35341963	1.13501318	0.28325960
H	3.74475829	–0.46495628	0.65808630
H	2.11182440	–2.25332003	0.15519013
H	0.76684178	2.51477259	–0.15184655
H	3.07586846	1.91142055	0.50549238
C	–0.47446437	–1.89100641	–0.58643833
H	–0.19368884	–2.93893541	–0.52333462
O	–2.14374341	–0.39306512	–1.04347414
B	–1.34079490	0.70170092	–0.79244086
O	–1.89400864	1.93904530	–0.93123947
H	–2.81986778	1.90848591	–1.19953550
N	–1.69759189	–1.72379639	–0.93727970

Compound 3-2a

C	2.77992200	–0.23399900	0.00001100
C	1.81068200	–1.21834600	0.00006900
C	0.44985200	–0.86582200	0.00005200
C	0.07164200	0.49502800	–0.00002400
C	1.07552600	1.47483300	–0.00008300
C	2.41297900	1.11804700	–0.00006500
H	3.82863300	–0.50747900	0.00002400
H	2.09370200	–2.26536500	0.00012700
H	0.79220800	2.52088300	–0.00014000
H	3.18066900	1.88297200	–0.00010900
C	–0.57962800	–1.88235600	0.00011300
H	–0.28868100	–2.92836200	0.00016500
B	–1.43839500	0.78547500	–0.00002800
O	–1.93366200	2.06881500	–0.00012700
H	–2.89202600	2.14661400	–0.00015000
N	–1.85335700	–1.67413800	0.00009400
N	–2.27454900	–0.37110200	0.00002100
H	–3.28375000	–0.33478900	0.00000200

Compound 3-2b

0 1			
C	3.14979400	–0.31333100	0.00113600
C	2.15179100	–1.26764300	0.00396100
C	0.80234000	–0.87175000	0.00205100
C	0.46451300	0.49796600	–0.00271900
C	1.49812600	1.44767400	–0.00492200
C	2.82349100	1.05005700	–0.00346300
H	4.18994100	–0.61788200	0.00265600
H	2.40202000	–2.32300700	0.00764900
H	1.24659500	2.50179500	–0.00775800
H	3.61436200	1.79105000	–0.00553200
C	–0.26365900	–1.84450100	0.00408700
H	–0.01699900	–2.90184800	0.00730100
B	–1.03388700	0.83568600	–0.00154100
O	–1.46995100	2.14163300	0.00939700
H	–2.42343100	2.26087100	0.01935800
N	–1.53008500	–1.58759600	–0.00115400
N	–1.93302800	–0.27927300	–0.01019000
C	–3.38562000	–0.13584000	–0.00038900
H	–3.74822700	0.21091500	0.97238100
H	–3.71127600	0.56633200	–0.77296400
H	–3.82680100	–1.10743500	–0.20960300

Compound 3-2c

0 1			
C	–4.57975000	0.28525900	–0.04947500
C	–3.58925700	1.23368300	–0.21764200
C	–2.23805900	0.85396900	–0.14952000
C	–1.88790200	–0.49002600	0.08937200
C	–2.91227000	–1.43317100	0.26130700
C	–4.24165600	–1.05295100	0.19156300
H	–5.62239200	0.57621600	–0.10224600
H	–3.84803000	2.27075100	–0.40165200
H	–2.65109800	–2.46789700	0.44937700
H	–5.02592600	–1.78907300	0.32393200
C	–1.17835000	1.82251200	–0.30776700
H	–1.43557600	2.86521600	–0.46982500
B	–0.38681200	–0.81867100	0.14959500
O	0.04319900	–2.08699500	0.44309600
H	1.00012600	–2.18255600	0.50380000
N	0.08906500	1.58377200	–0.27927100
N	0.51054600	0.28548700	–0.09495300
C	1.93452700	0.16439200	–0.06279400
C	2.56951300	–0.81566600	–0.82656400
C	2.69679900	1.02086700	0.73174900

C	3.95384700	–0.95542600	–0.77143400
H	1.98493800	–1.44313900	–1.48876300
C	4.07774500	0.88463800	0.77099400
H	2.19780000	1.79116300	1.30435300
C	4.71175400	–0.10816500	0.02751400
H	4.43795200	–1.71656800	–1.37161900
H	4.66261400	1.55405000	1.39060500
H	5.78914900	–0.21315400	0.06504400

Compound 3-3

0 1			
C	–4.88547000	–1.38270300	0.24565100
C	–3.73786300	–1.80600000	–0.40009000
C	–2.59134800	–0.99760500	–0.38491500
C	–2.60053800	0.24153300	0.28309400
C	–3.77457500	0.64927800	0.92976000
C	–4.90489300	–0.15263500	0.91231100
H	–5.77286100	–2.00448400	0.23506700
H	–3.71955700	–2.75834300	–0.91845700
H	–3.78954400	1.60262900	1.44423300
H	–5.80863700	0.17157100	1.41470300
C	–1.37519400	–1.41567300	–1.04972700
H	–1.35522300	–2.37374100	–1.56113500
B	–1.30867900	1.08609600	0.25925100
O	–1.23923300	2.28951300	0.87545100
H	–0.37285200	2.71291800	0.76459300
N	–0.27108400	–0.76013300	–1.10597900
N	–0.20666900	0.46544100	–0.47688300
S	1.34433100	1.15985200	–0.73263700
O	1.32948200	2.38841300	0.04830800
O	1.61290700	1.19326200	–2.14559700
C	2.46708400	0.00940400	0.03582600
C	3.07875800	–0.96363100	–0.74639800
C	2.72480000	0.12137100	1.39847300
C	3.96542400	–1.84764700	–0.14326900
H	2.86207700	–1.01660700	–1.80399900
C	3.61310800	–0.76864300	1.98876700
H	2.25036000	0.90096000	1.97937700
C	4.23006700	–1.75170000	1.21965700
H	4.45115700	–2.60987500	–0.73984000
H	3.82818700	–0.68968600	3.04720800
H	4.92385100	–2.44220700	1.68409100

Compound 3-4

```
0 1
 C          2.72753800     0.25226500     0.00000200
 C          1.77962300     1.24367500     0.00000300
 C          0.40256800     0.91831800    –0.00001000
 C          0.01689800    –0.45061000    –0.00000500
 C          1.01163500    –1.45653800     0.00000400
 C          2.33861100    –1.10595700     0.00000300
 H         –0.33963500     2.95678900     0.00003300
 H          3.78076100     0.50589900    –0.00000100
 H          2.07191000     2.28756900     0.00000300
 C         –0.61724100     1.90552000    –0.00001200
 C         –1.37595300    –0.72088500     0.00000300
 H          0.71076500    –2.49546100     0.00002000
 H          3.09985800    –1.87698900     0.00000500
 C         –2.26935300     0.32339200     0.00001500
 H         –3.33957000     0.12929300     0.00000400
 O         –1.75817000    –2.03199500    –0.00002300
 H         –2.72123200    –2.08724900     0.00010400
 N         –1.89763500     1.62586100    –0.00000200
```